University of Glasgow

Development and Use of an *in vitro* Air-Liquid Interface Model of the Bovine Respiratory Tract and Multifaceted Proteomic Approaches to Investigate Host-Pathogen Interactions of *Mannheimia haemolytica*

A thesis submitted to the University of Glasgow for the degree of Doctor of Philosophy

Edward Grahame Bsc. (Hons) MRes.

Institute of Infection, Immunity and Inflammation

College of Medical, Veterinary and Life Sciences

University of Glasgow

Declaration

I hereby declare that the work presented in this thesis is my own, except where otherwise cited or acknowledged. No part of this thesis has been presented for any other degree. The research for this thesis was performed between

October 2012 and October 2015.

Edward Grahame

Acknowledgements

First and foremost I would like to thank my principal supervisor Dr Robert Davies. The advice and guidance provided throughout the project was invaluable and for this I am very grateful. I would also like to thank my other supervisors, Dr Catherine Berry and Dr Richard Burchmore. Only with their expertise in cell culturing and proteomics was the project a success and for this I am very grateful, thank you. I would also like to thank Dr Geraldine Taylor and Dr Becky Herbert who helped me out in the early phases of the project, thank you.

I would like to thank the members of my group, both past and present whom I have had the pleasure to work alongside for the past four years. You have made the experience of completing this project all the more enjoyable, so much so that the past four years have flown by. I would like to extend this acknowledgement to everyone who has worked in 'level 2' microbiology over the course of my time here, as with the members of my group you have made working here a pleasure and I look forward to seeing where everyone ends up in the future.

I would like to extend special thanks to a number of individuals. I would like to thank Dr Michael Ormsby who completed his PhD during the same period me, your sense of humour kept me going when things weren't exactly going to plan and without you around I might have packed this in a long time ago; it was a pleasure to work alongside you. I would like to thank Dr Nicky O'Boyle whom I worked closely with on the development of the epithelial cell model, I enjoyed working with you and particularly valued all the input when I had ideas to bounce about, and I wish you all the best in the future. I am also grateful to Dr Nicky O'Boyle for the extraction of DNA for use in the whole genome sequencing experiments, thank you. I would like to thank Miss Erin Sutherland for your help with aspects of the project, particularly in capturing the vast number of images accociated with this project. I would like to thank Dr Daniel Cozens who succeeded me in the development of the bovine airway epithelial cell model, it has been very enjoyable to see you bring together aspects of the project that

were out with the scope of this PhD and it has been equally enjoyable getting to know you.

Finally, I would like to thank Miss Maranda Thomson for her enduring support and belief in me. To say you inspire me is an understatement; there aren't words to convey how grateful I am to you, thank you.

Presentations and Publications

1. Grahame, E., Hounsome, J. D A., Burchmore, R., Berry, C. & Davies R. L. Comparative Outer Membrane Proteomic Analyses of *Mannheimia haemolytica* Isolates Recovered from Cattle and Sheep. Poster presentation at the 115th General Meeting of the American Society for Microbiology. 30th May – 2nd June 2015, New Orleans, Louisiana, USA.

2. Grahame, E., Hounsome, J. D. A., Burchmore, R., Berry, C. & Davies R. L. Comparative Outer Membrane Proteomic Analyses of *Mannheimia haemolytica* Isolates Recovered from Cattle and Sheep. Poster presentation at The Society for General Microbiology Annual Conference 2015. 30th March – 2nd April 2015, Birmingham, UK.

3. Grahame, E., Berry, C., Burchmore, R., & Davies R. L. Respiratory Tract Modelling of *Mannheimia haemolytica* Colonisation. Poster presentation at the Young Microbiologists Symposium on Microbe Signalling, Organisation and Pathogenesis. 2nd June – 3rd June 2014, Dundee, UK.

Summary

In the present study, an air-liquid interface culture system was optimised for the use of bovine airway epithelial cells. This culture system has been adopted for other species, where a pseudostratified epithelium comprising multiple cell types and resembling the *in vivo* environment is produced. Several aspects of the epithelial culture process were optimised, including (i) the cell harvesting process and the expansion of cells in submerged culture, (ii) the substrate material used for air-liquid interface culture, the effects of collagen-coating of the substrate, and the substrate porosity, (iii) the oxygen tension (iv) growth factor (retinoic acid and epidermal growth factor) concentration used during culture and (v) the anatomical region of the respiratory tract from which the epithelial cells were harvested. The optimisation of the aforementioned conditions resulted in the production of an *in vitro* respiratory tract model that was more than 40% ciliated, pseudostratified with a layer of P63-expressing basal cells and capable of mucus and CC10 (Clara cell secretory protein) production. Thus, an *in vitro* model of the bovine respiratory tract was established to determine the host-pathogen interactions of *M. haemolytica* with the respiratory epithelium.

A rigorous proteomic characterisation was carried out on the outer membrane of *M. haemolytica*. The Sarkosyl insoluble fractions of seven *M. haemolytica* and one *M. glucosida* isolates, representing a range of serotypes and host species, were prepared in triplicate. Tryptic digests of each sample were prepared using gel-based and gel-free proteomic digests before analysis by LC-MS/MS. Data was searched against the NCBI Uniprot database using MSCOT (Matrix Science). Assembly of the data revealed that a total of 83 unique outer membrane proteins were distributed amongst the eight Mannheimia spp. isolates. Fifty seven of the 83 OMPs were identified using both gel-free and gel-based methodologies with a further 18 and eight identified with a single methodology alone. Several proteins were identified in an isolate specific manner; two OMPs exhibited a strong pattern of serotype-specific identification. The YadA-like trimeric autotransporter was identified with full reproducibility in A2 serotype strains yet not in strains of different serotype. Conversely, the lipoprotein, plpD

was identified in at least two replicates of all isolates except those of serotype A2 where it was not identified at all.

The air-liquid interface culture system was used to study the adherence and colonisation of *Mannheimia haemolytica* to the bovine respiratory tract. In a pilot study, pathogenic bovine and ovine isolates *M. haemolytica* isolates were studied with bovine and ovine air-liquid interface airway epithelial cells. Bovine and ovine *M. haemolytica* isolates were found to adhere to the epithelial cells, six hours post-infection in the case of an ovine isolate and 24 hours in the case of a bovine isolate. Bovine isolates of *M. haemolytica* were predominantly found to invade and adhere to the sub-apical regions of the epithelium with relatively few bacteria found on the apical face. Adherence to the sub-apical epithelium represents the first description of *M. haemoyltica* causing invasive disease. Microscopic evidence of outer membrane vesicle production and exopolymeric material were also noted for one of the ovine isolates during infection.

Following optimisation of the bovine air-liquid interface culture system, an experiment was conducted that examined the ability of *M. haemolytica* to adhere and colonise air-liquid interface cultures with epithelial cells derived from different anatomical regions of the respiratory tract. Cells derived from the nasopharynx, the mid-trachea and the secondary/tertiary bronchi were differentiated at ALI and infected with pathogenic and non-pathogenic bovine isolates of *M. haemolytica*. The non-pathogenic *M. haemolytica* isolate was found to adhere and colonise the nasopharyngeal derived cells better than either the bronchial or tracheal derived cells. Conversely, the pathogenic *M. haemolytica* isolate was found to have significantly greater adherence to the bronchial derived epithelial cultures and significantly higher adherence ($P>0.0001$) than the non-pathogenic isolate. The pathogenic *M. haemolytica* isolate was also found to colonise the nasopharyngeal-derived epithelial culture albeit with lower frequency than was observed for the bronchial-derived epithelial cells.

The results presented herein demonstrate the development of a novel *in vitro* tool for studying the infection process of respiratory pathogens. The use of this tool to study the infection properties of *M. haemolytica* in combination with characterisation of the outer membrane proteome provides new insight into the

process of colonisation and highlights the protein machinery that likely contributes to the process.

Table of Contents

List of Figures

List of Tables

Abbreviations

°C	Degrees Celsius
Ø	Diameter
µg	Microgram
µl	Microliter
µM	Micromolar
µm	Micrometre
3D	Three dimensional
Å	Angstrom
ABC	ATP-binding cassette
AEC	Airway epithelial cell
AEGM	Airway epithelial growth medium™
ALI	Air liquid interface
ATP	Adenosine triphosphate
BAL	Bronchoalveolar lavage
BAM	Beta barrel assembly machinery
BBEC	Bovine bronchial epithelial cell
BEGM	Bronchial epithelial growth medium™
BIL	Bacteria intein-like
BHIB	Brain heart infusion broth
BHIA	Brain heart infusion agar
BHV	Bovine herpes virus
BNEC	Bovine nasopharyngeal epithelial cells
BPI3	Bovine parainfluenza 3
BRD	Bovine respiratory disease complex
BRSV	Bovine respiratory syncytial virus
BSA	Bovine serum albumen
BTEC	Bovine tracheal epithelial cell
BVDV	Bovine viral diarrhoea virus
CEACAM	Carcinoembryonic antigen cell adhesion molecule
CF	Cystic fibrosis
CFTR	Cystic fibrosis transmembrane conductance regulator
CFU	Colony forming unit
CID	Collision induced dissociation
CS	Culture supernatant
CSF	Cerebral spinal fluid
cAMP	Cyclic adenosine monophosphate
DAPI	4',6-diamidino-2-phenylindole
DC	Dendritic cell
DMEM	Dulbecco's modified eagles' medium
DNA	Deoxyribonucleic acid
DTT	Dithiotheritol
ECM	Extracellular matrix
EGF	Epidermal growth factor
EGFR	Epidermal growth factor receptor
EPS	Extracellular polymeric substance
ESI	Electrospray ionisation
ESC	Embryonic stem cells
ET	Electrophoretic type
FASP	Filter aided sample preparation
FHA	Filamentous hemagglutinin
FTICR	Fourier transform ion cyclotron resonance
GAG	Glycosaminoglycan
GlcNAc	N-acetylglucosamine
H&E	Haematoxylin and eosin

HBMEC	Human brain microvascular endothelial cells
HKO	Heat killed organisms
HEPES	4-(2-hydroxyethyl)-1-piperazineethanesulfonic acid
HGT	Horizontal gene transfer
HMDS	hexamethyldisilazane
ICAM	Intracellular adhesion molecule
IFA	Immunofluorescence
Ig	Immunoglobulin
IHC	Immunohistochemistry
IM	Inner membrane
IROMP	Iron regulated outer membrane protein
LAP	Lingual antimicrobial peptide
LC	Liquid chromatography
LPS	Lipopolysaccharide
Lpt	Lipopolysaccharide transport system
LOS	Lipooligosaccharide
LRT	Lower respiratory tract
MALDI	Matrix assisted laser desorption ionisation
mg	Milligram
MHC	Major histocompatibility complex
ml	Millilitre
MLEE	Multilocus enzyme electrophoresis
mM	Millimolar
min	Minutes
mm	Millimetre
MOWSE	Molecular weight search
mRNA	Messenger ribonucleicacid
MS	Mass spectrometry
MSCRAMM	Microbial surface components recognising adhesive matrix molecules
MurNAc	N-acetylmuramic acid
NTHi	Nontypeable *Haemophilus influenzae*
OD_{600}	Optical density at 600 nm
OM	Outer membrane
OMP	Outer membrane protein
OTEC	Ovine tracheal epithelial cell
PAGE	Polyacrylamide gel electrophoresis
PAS	Periodic acid shiffs
PBS	Phosphate buffered saline
PET	Polyethylene terephthalate
PG	Peptidoglycan
PGE_2	Prostaglandin E_2
PMF	Peptide mass fingerprint
POTRA	Polypeptide transport associated
PTFE	Polytetrafluoroethylene
RA	Retinoic acid
RAR	Retinoic acid receptor
RARE	Retinoic acid response element
RND	Resistance nodulation driven
RPMI	Roswell Park Memorial Institute medium
RXR	Retinoid receptor
SDS	Sodium dodecyl sulphate
SEC	General secretory pathway
SEM	Scanning electron microscope
SLPI	Secretory leukocyte protease inhibitor
SSE	Sodium salicylate extract
STWS	Scotts tap water substitute
s	Seconds

T1SS	Type 1 secretion system
T2SS	Type 2 secretion system
T3SS	Type 3 secretion system
T4SS	Type 4 secretion system
T5SS	Type 5 secretion system
T6SS	Type 6 secretion system
T7SS	Type 7 secretion system
T8SS	Type 8 secretion system
T3	Triiodothyronine
TAM	Translocation assembly module
TAP	Tracheal antimicrobial peptide
TAT	Twin arginine translocation pathway
TEER	Trans epithelial electrical resistance
TEM	Transmission electron microscope
TOF	Time of flight
TPS	Two partner secretion system
UDP	Uridine diphosphate
URT	Upper respiratory tract
v/v	Volume per volume
w/v	Weight per volume
ZO-1	Zona Occludin 1

Chapter 1 Introduction

1.1 Bovine respiratory disease complex

Bovine respiratory disease (BRD) complex is a major disease syndrome of cattle that contributes significant economic loss to the agricultural industry annually (Griffin, 1997; Jim, 2009). The disease is multifaceted and is usually associated with environmental stress and viral infection (Fig 1.1). Bovine respiratory disease is the leading cause of disease in the cattle industry, causing 70-80% of feedlot morbidity and 40-50% of feedlot mortality (Edwards, 2010). The disease is brought on by transport owing to the stressful conditions and enhanced viral transmissibility. This has resulted in the name 'shipping fever' being used informally to describe BRD. The demise of the infected cattle results from opportunistic bacterial pathogens, that ordinarily reside in the upper respiratory tract (URT) but under the predisposing viral infection and combined stress can colonise and expand into the lungs producing fatally acute pneumonia (Ellis, 2009; Rice *et al.*, 2007). However, the aetiology is complicated and experimental challenge with the bacterial pathogens is sufficient to propagate the infection (Gånheim *et al.*, 2003, 2005). The bacterial species involved in BRD include *Mannheimia haemolytica*, *Pasteurella multocida*, *Histophilus somni* and *Mycoplasma bovis* (Srikumaran *et al.*, 2007). Of these, *M. haemolytica* is the most frequently isolated bacterial pathogen in cases of BRD (Griffin *et al.*, 2010; Klima *et al.*, 2014b).

Several viruses have been implicated in perpetrating the conditions that allow for opportunistic pathogens to establish colonisation. The viruses achieve this by impairing the condition of the respiratory epithelium and weakening the host's immune defences. The primary viruses identified in BRD include bovine herpesvirus-1 (BHV-1), bovine respiratory syncytial virus (BRSV), bovine viral diarrhoea virus (BVDV) and bovine parainfluenza-3 virus (BPI3) (Srikumaran *et al.*, 2007). The combined effect that these viruses have on innate and adaptive host immunity provides the necessary alterations to the host respiratory tract that allow for colonisation of the secondary bacterial pathogens.

The gross pathology of each virus involved in BRD is well characterised. BHV-1 is characterised by lung consolidation with scattered areas of necrosis and

atelectasis (Gershwin *et al.*, 2015). BRSV is characterised by lung consolidation and lung tissue necrosis (Gershwin *et al.*, 2015). BVDV exhibits milder clinical symptoms than either BRD and BHV-1 with only small areas of the bovine lung showing consolidation (Gershwin *et al.*, 2015). However, several pathological lesions are more characteristic of BVDV than are of BHV-1 or BRSV. These include ulcerative rhinitis, laryngeal ulceration, tracheal ulceration and intranuclear inclusion bodies (Gershwin *et al.*, 2015). The pathology of BPI-3 infection has been characterised in a guinea pig model and found to comprise lung consolidation and atelectasis (Shi *et al.*, 2014).

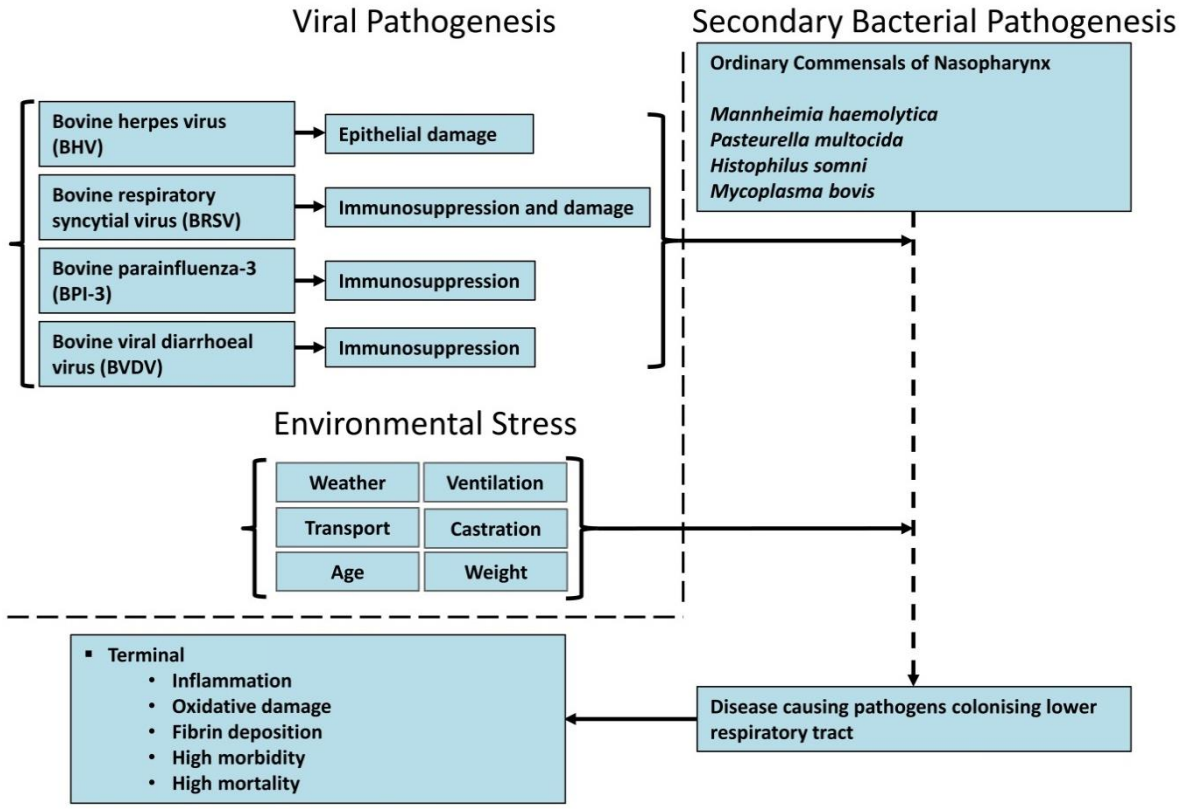

Fig 1.1 Bovine respiratory disease complex overview
Displayed are the various respiratory viruses and environmental factors that can contribute to opportunistic bacterial infection.

The precise chain of events that allow bacterial colonisation of the respiratory tract is not known. What is understood is that viral infection predisposes ruminants to secondary bacterial infection. Several studies have examined the factors that might allow for secondary bacterial infection. Destruction of ciliated epithelial and goblet cells have been attributed to BHV-1, the result of which includes rhinotracheitis lesions and an impaired epithelial barrier (Srikumaran *et al.*, 2007). BHV-1 has also been shown to require access to the basolateral side of the epithelium for replication to occur (Kirchhoff *et al.*,

2014). Early research also implicated BPI-3 in causing damage to the cilia of the respiratory tract (Tsai & Thomson, 1975). More recent studies have confirmed that BPI-3 causes damage to the ciliated epithelium (Goris *et al.*, 2008; Kirchhoff *et al.*, 2014).

In addition to physical damage, the immune system is another factor influenced by the viruses of BRD. BHV1 impairs host defences, as it has been shown to down regulate MHC class I molecules in infected cells including $CD4^+$ T cells (Ellis, 2009). BPI-3 is known to inhibit alveolar macrophages from generating superoxide anions (Dyer *et al.*, 1994) and BVDV is known to replicate in lymphocyte cell populations during bovine respiratory disease inducing apoptosis in B cells and a reduction in T cell proliferation. The co-infection of BRSV with BVDV has been shown to be more potent and destructive than with either virus in isolation (Srikumaran *et al.*, 2007). This serves to demonstrate the synergism of the viruses, which in turn makes the understanding of BRD a challenge.

Several studies have looked directly at the link between immunosuppression and secondary bacterial colonisation. Challenge experiments of calves with either BVDV, *M. haemolytica* or both demonstrated that BVDV and *M. haemolytica* elicited more severe clinical symptoms than challenge with either pathogen alone (Gånheim *et al.*, 2003). Furthermore, only one of six calves from the *M. haemolytica* group could produce cultured bacteria versus four of six from the lungs of the BVDV and *M. haemolytica* group. This suggests that BVDV might impair the mucociliary escalator resulting in an ineffective bacterial clearance. Further work by the authors showed that BVDV suppresses the serum leukocyte count (Gånheim *et al.*, 2005). This impairment in immune function may contribute to secondary *M. haemolytica* infection. This theme of immune suppression extends to the antibody response generated towards the leukotoxin of *M. haemolytica*. Pre-infection of calves with BVDV results in a lower anti-leukotoxin antibody titre following *M. haemolytica* challenge as compared to *M. haemolytica* challenge alone (Burciaga-Robles *et al.*, 2010), indicating that the immune system is suppressed. Deducing the necessary changes to the host respiratory tract that allow for secondary bacterial infection would constitute a major advance in the understanding of the disease process.

Aside from immunosuppression, physical damage may also contribute to the colonisation process. For example, BHV-1 creates lesions and disrupts the surface-exposed epithelial barrier, this might create an entry route to the basal cells which would be normally inaccessible (Schuh *et al.*, 1992). The intracellular adhesion molecule (ICAM) receptor is known to be over expressed in the lung tissue following *M. haemolytica* infection (Ackermann & Brogden, 2000) and the phylogenetically related bacterium *Haemophilus influenzae* is known to adhere to ICAM-1 (Sajjan *et al.*, 2008). Basal cells in the healthy epithelium are normally inaccessible to bacteria and show a higher expression of ICAM-1 than other respiratory epithelial cells (Jakiela *et al.*, 2008). This example serves to highlight the complexity of interactions between the viral and bacterial elements of BRD.

Unlike colonisation, more is known about the primary virulence factors that *M. haemolytica* uses when proliferation has occurred in the lower respiratory tract. *M. haemolytica* is known to produce a lymphocyte-lysing RTX toxin, referred to as leukotoxin (Deshpande *et al.*, 2002; Li *et al.*, 1999). Similarly, for *P. multocida* several virulence factors are accociated with disease causing isolates, for example *pfhA* which encodes filamentous haemagglutinin (Ewers *et al.*, 2006; Katsuda *et al.*, 2013; Verma *et al.*, 2013). Other minor factors are also implicated in the virulence for each bacterial pathogen associated with BRD. Ultimately, *M. haemolytica* remains the most important of the bacterial pathogens in BRD owing to the high prevalence compared with the other pathogens (Griffin *et al.*, 2010; Klima *et al.*, 2014b). Understanding how *M. haemolytica* colonises the respiratory tract would be a major leap in understanding and controlling BRD.

1.1.1 Mannheimia haemolytica

1.1.2 The organism

Mannheimia haemolytica is a Gram-negative aerobic bacterium of the Pasteurellaceae family. The organism described by Newsom & Cross (1932), was placed within the genus *Pasteurella* until DNA-DNA hybridisation experiments led to its reclassification in the genus *Mannheimia*. Seventeen serotypes, based on polysaccharide capsule typing were originally attributed to

P. haemolytica. However, some strains of *P. haemolytica* are untypeable (Donachie *et al.*, 1984). A means of biotyping was also used to distinguish the 13 arabinose-fermenting, and the four trehalose-fermenting serotypes (Smith, 1961). Designation was applied by means of an A or T preceding the serotype number. Of the 17 serotypes, 12 of the arabinose-fermenting types (A1, A2, A5-A9, A12-A14, A16 and A17) were reclassified as *M. haemolytica* (Angen *et al.*, 1999a). Serotype A11 organisms were reclassified as *Mannheimia glucosida* (Angen *et al.*, 1999a) and the remaining four serotypes (T3, T4, T10 and T15) were reclassified as *Pasteurella trehalosi* (later renamed *Bibersteinia trehalosi*) (Sneath & Stevens, 1990). The closest relatives of *M. haemolytica* based on 16S sequencing are *B. trehalosi*, *Actinobacillus capsulatus* and *Haemophilus parainfluenzae* (Highlander, 2001).

1.1.3 The disease

M. haemolytica is the etiological agent of pneumonic pasteurellosis of cattle, sheep and other ruminants. In cattle, symptoms include depression, anorexia, fever, serous or mucoid cough and elevated shallow respiration (Blowey & Weaver, 2003). The latter of these has been shown to be the best clinical marker for identification of the disease (Reve-Johnson, 2001). The gross pathology of *M. haemolytica* infection is characterised by fibrous bronchopneumonic lung lesions (Gershwin *et al.*, 2015; Singh *et al.*, 2011), as shown in Fig 1.2.

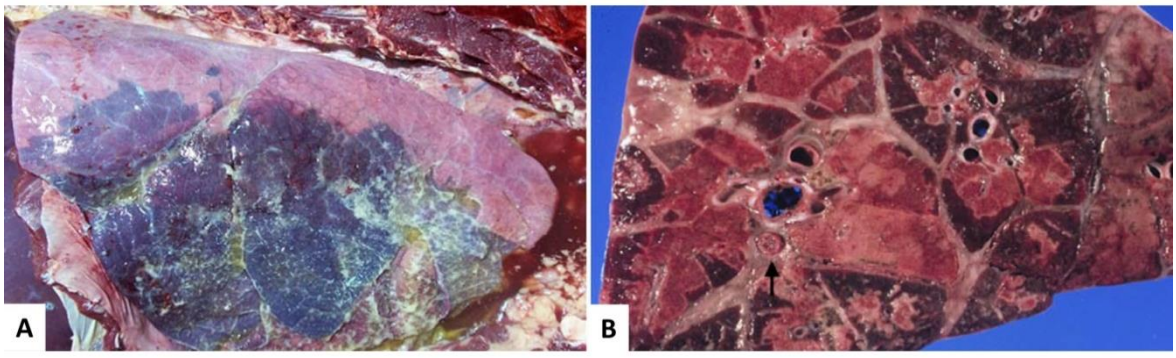

Fig 1.2 Gross pathology of the bovine lung following *M. haemolytica* infection
Shown is a large patch of bovine lung necrosis with fibrin deposits (A). A cross section through an infected lung reveals extensive bronchopnemoic lung lesions (B). Adapted from (Singh *et al.*, 2011).

These lung lesions occur following mobilisation of the pro-inflammatroy cytokine response which leads to mass infiltration of neutrophils into the lung. Subsequently, the secreted leukotoxin of *M. haemolytica* causes neutrophil lysis which results in the release of reactive oxygen species and causes the observed damage to the lung (Ackermann & Brogden, 2000; Singh *et al.*, 2011). Although *M. haemolytica* is primarily associated with respiratory disease it is also recovered from cases of bovine abortion (Ward, 1990).

In sheep the clinical symptoms for diagnosing pneumonic pasteurellosis include fever, depression, anorexia, weight loss, mucopurulent nasal discharge, tachypnoea and coughing (Plummer *et al.*, 2012). As in cattle, the gross pathology of the lung in sheep following infection is characterised by acute fibrinopurulent bronchopneumonia (Plummer *et al.*, 2012). Additionally, *M. haemolytica* can cause mastitis in sheep, although *M. glucosida* is more commonly recovered from mastitis cases (Omaleki *et al.*, 2010). Recent epidemiological analysis of mastitis concluded that a diverse array of *M. haemolytica* and *M. glucosida* strains are responsible for mastitis in sheep (Omaleki *et al.*, 2012).

In cattle presenting with pneumonic pasteurellosis the most frequently recovered *M. haemolytica* serotype from the lungs is A1 (Al-Ghamdi *et al.*, 2000; Purdy *et al.*, 1998). Serotype characterisation of *M. haemolytica* recovered from different geographic locations has revealed an increase in the recovery of A6 serotype strains from cases of pasteurellosis (Al-Ghamdi *et al.*, 2000; Jaramillo-Arango *et al.*, 2008; Katsuda *et al.*, 2008; Purdy *et al.*, 1997). The A1 and the A6 serotype strains of *M. haemolytica* are genetically similar. Multilocus enzyme electrophoresis (MLEE) analysis of 178 *M. haemolytica* and 16 *M. glucosida* isolates demonstrated that A1 and A6 pathogenic cattle isolates occupy a single electrophoretic type (ET) (Davies *et al.*, 1997). In contrast to the pneumonic lung, the A2 serotype is more frequently recovered from the nasopharynx, where serotype A1 is recovered with low frequency (Frank & Smith, 1983; Frank, 1985). Similarly, A2 isolates occupy a different genetic lineage to that of bovine A1 and A6 serotypes (Davies *et al.*, 1997).

In contrast to cattle, the most commonly recovered serotype of *M. haemolytica* from sheep exhibiting signs of pneumonic pasteurellosis is A2 (Davies &

Donachie, 1996; Kirkan & Kaya, 2005; Odugbo *et al.*, 2003). Serotypes A7 and A9 are also recovered to a lesser extent. Serotype A1 is frequently recovered from the nasopharynx of healthy sheep.

All ruminants are susceptible to *M. haemolytica* infection although cattle are noted as being of particular risk owing to several factors. Cattle have one of the lowest lung volume to body mass ratios in the animal kingdom (Veit & Farrell, 1978). This ratio not only dictates the required respiration rate but consequently means even small losses of functional lung tissue may compromise the animal. Cattle also show impaired lung immune defence that make them more susceptible to respiratory infection including low numbers of alveolar macrophages and a low tissue concentration of lysozyme (Veit & Farrell, 1978), both of which contribute to an elevated infection risk relative to other mammals. Thus, the stringent requirement for lung tissue preservation and the impaired host defences leave cattle more susceptible to respiratory infection than other livestock.

1.1.4 Molecular phylogenetics

Within *M. haemolytica*, population diversity studies have given rise to the hypothesis that horizontal gene transfer (HGT) has occurred in ancestral strains. Evidence of host switching has been observed in the *tbpBA* operon, *lktA* and *ompA* gene (Davies & Lee, 2004; Davies *et al.*, 2001; Lee & Davies, 2011). These genetic studies provide evidence to suggest that the pathogenic A2 serotype of sheep and the pathogenic serotype A1 and A6 of cattle originated in cattle and sheep, respectively. It is theorised that the advent of domestication allowed for exchange of A2 isolates from cattle to sheep and A1 and A6 isolates from sheep to cattle. Acquisition of new genetic material via horizontal gene transfer from resident strains provided the genetic material that allowed for adaptation to their new host environment. It is hypothesised that modern pathogenic isolates of *M. haemolytica* descend from these ancestral events.

1.1.5 Virulence factors of *M. haemolytica*

M. haemolytica possesses many virulence factors that contribute to the disease aetiology. While some, such as the secreted leukotoxin are well characterised, the contribution of others to the disease is poorly understood.

1.1.5.1 Leukotoxin

Leukotoxin is the primary virulence factor of *M. haemolytica*. It is a 104 kDa secreted toxin belonging to the RTX (repeats-in-toxin) family which is characterised by glycine-rich C-terminal nonapetide repeats (Burrows & Lo, 1992; Coote, 1992). The toxin is encoded as an operon, *lktABCD* (Highlander *et al.*, 1989), proteins encoded by *lktB* and *lktD* are responsible for secretion (Strathdee & Lo, 1989), *lktA* encodes the pre-toxin which is acetylated by the product of *lktC* to achieve activation into of the active form of the toxin (Highlander *et al.*, 1990; Jeyaseelan *et al.*, 2002; Lo *et al.*, 1987). The RTX toxins of other bacterial species have been shown to be delivered to the extracellular environment through use of the TolC protein in combination with an inner membrane transporter and a periplasmic fusion protein (Balakrishnan *et al.*, 2001; Crosby & Kachlany, 2007; Wandersman & Delepelaire, 1990). Thus, it is very likely that the transport proteins LktB and LktD function similarly, along with TolC, in delivering LktA.

The mature toxin functions as a pore-forming toxin in the plasma membrane of leukocytes where it causes necrotic cell death upon binding to the CD18 integrin subunit (Deshpande *et al.*, 2002). The leukotoxin also causes apoptosis at sub-lytic concentrations (Atapattu & Czuprynski, 2005), this occurs via internalisation at lipid rafts in a clatherin-dependent manner (Atapattu & Czuprynski, 2007; Atapattu *et al.*, 2008). More recently leukotoxin has been shown to bind cyclophilin D on the the mitochondrial membrane (Aulik *et al.*, 2011), and the targeting of leukotoxin to the mitochondira has been shown to be the result of a signal sequence in the N-terminal part of the protein (Kisiela *et al.*, 2010). Aditionally, stimulation of neutrophil and macrophage extracellular trap formation by leukotoxin has been demonstrated (Aulik *et al.*, 2010, 2012). *M. haemolytica* mutants that cannot produce the activated toxin are partially attenuated (Highlander *et al.*, 2000). Higher morbidity occurred in calves

challenged with the wild type compared to the mutant. Also, in the surviving calves (day 4), there was a reduction in clinically-determined lung pathology of animals infected with the mutant as compared with the wild type. The retained pathogenicity of the mutant, although reduced, indicates that either the pre-toxin or other virulence factors elicit at least some of the attributed lung damage and morbidity.

Nucleotide sequence analysis of the leukotoxin operon has revealed that the *lktD* gene is highly conserved amongst *M. haemolytica*, *M. glucosida* and *B. trehalosi* (Davies *et al.*, 2002). Contary to lktD, the other genes of the operon exhibit evidence of recombinant exchange giving rise to a mosaic structure in the nucleotide sequence of the operon. In *lktA*, the pre-toxin gene, allelic diversity amongst ovine *M. haemolytica* isolates is greater than in bovine isolates (Davies *et al.*, 2001). This suggests that selective pressures conferred on lktA have been more influential in driving the diversity observed in sheep compared to cattle. The effect the active toxin from various strains has on bovine and ovine neutrophils supports the nucleotide sequence analysis (Davies & Baillie, 2003). Of all ovine isolates tested, higher activity, of at least four-fold, was observed against ovine neutrophils compared with bovine neutrophils. In contrast, the cytotoxic activity of bovine isolates was comparable against neutrophils of either species.

1.1.5.2 Lipopolysaccharide

Lipopolysaccharide, unique to Gram negative bacteria, is a major contributor to the host recognition of Gram-negative pathogens. Toll-like receptor 4 (TLR4) of host cells recognises LPS and engages the adaptive immune response. Structurally, LPS is composed of three well defined regions; (1) lipid A, which anchors the molecule in the OM, (2) a highly conserved core polysaccharide adjoined to lipid A and (3) a highly variable O-antigen chain that protrudes away from the cell surface. The diversity of O-antigens is generally greater amongst enteric bacteria where species such as *E. coli* exhibit more than 170 O-serotypes, although some respiratory bacteria can vary their core structure through phase variation (Raetz & Whitfield, 2002). *M. haemolytica* is known to produce only a single type of O-antigen but displays either rough or smooth LPS on its cell surface (Davies & Donachie, 1996). The *losB* gene of *M. haemolytica*

has been shown to encode the enzyme responsible for transfer of the first outer core residue, D-glycero-D-manno-heptose, onto the inner core (Logan *et al.*, 2006). Assessment of virulence in *M. haemolytica* isolates with similar core structures but the presence or absence of an O-antigen chain revealed that rough LPS isolates were more virulent than their smooth counterparts when subjected to challenge in sheep (Hodgson *et al.*, 2003). Thus, the presence or absence of an O-antigen is a major contributor to the virulence of a particular *M. haemolytica* strain.

The employment of immunohistochemistry after *M. haemolytica* infection has revealed that LPS localises to the cytoplasms of neutrophils, alveolar macrophages, endothelial cells, pulmonary intravascular macrophages, and to the surface of epithelial cells (Whiteley *et al.*, 1990). Studies looking at the involvement of LPS in pneumonic pasteurellosis have demonstrated that LPS can increase the membrane permeability of endothelial cells but not of pneumocytes (McClenahan *et al.*, 2008). However, increased membrane permeabillity of pneumocytes has been demonstrated to occur after treatment with LPS-activated neutrophils (McClenahan *et al.*, 2008). More recently LPS from *M. haemolytica* has been shown to stimulate the release of ATP as determined by the bronchoalveolar larvage (BAL) of calves (Craddick *et al.*, 2012). Importantly, ATP has been shown *in vitro* to reversibly increase the permeability of pulmonary epithelial cell monolayers (McClenahan *et al.*, 2009), this bears relevance to *M. haemolytica* infection where leakage of vascular products into the lumen of the airways is noted (Slocombe *et al.*, 1985). Thus, in the gross pathology where leukotoxin results in the necrosis and apoptosis of neutrophils in the lung, LPS may contribute to the influx of these along with other vascular products. In addition, lipopolysaccharide has been shown to complex with leukotoxin (Li & Clinkenbeard, 1999), where LPS augments the activity of leukotoxin increasing its cytotoxicity (Lafleur *et al.*, 2001). Thus, in terms of *M. haemoytica* virulence LPS is arguably the most important contributor to the aetiology of the disease after leukotoxin.

1.1.5.3 O-sialoglycoprotein endopeptidase

M. haemolytica produces a secreted glycoprotease (Gcp) that targets proteins post-translationally modified with sialic acid. This 35 kDa metalloprotease

targets glycoproteins containing O-linked sialic acid (Abdullah *et al.*, 1992; Sutherland *et al.*, 1992). Glycoproteins containing exclusively N-linked sialic acid are not subjected to proteolytic cleavage. Activity of the protein has been linked to the metal cofactors Ca^{2+} and Mg^{2+} (Cladman *et al.*, 1996). A role for the protein in pathogenesis has been proposed to involve the secreted enzyme digesting cell-surface receptors on platelets, activating them, and contributing to the fibrin deposits observed during infection (Nyarko *et al.*, 1998).

1.1.5.4 Polysaccharide capsule

A polysaccharide capsule is a constituent of many pathogenic Gram-negative bacteria including *M. haemolytica*. Capsules normally consist of secreted carbohydrate material that loosely associates with the outer membrane to form a sheath on the order of several hundred nanometres thick. Virulence has been noted in bacterial pathogens to arise from several factors. The shielding of immunogenic surface antigens to prevent antibody binding is a recognised defence mechanism of the capsule (Nelson *et al.*, 2007).

In *M. haemolytica* the molecular makeup of the A1 serotype capsule has been demonstrated to be similar to that of the enterobacterial common antigen (Adlam *et al.*, 1984), with the A2 similar to that of *N. meningitidis* serogroup B and *E. coli* K1 (Adlam *et al.*, 1987), and the A7 similar to that of *N. meningitidis* serogroup L and *H. influenzae* type F (Adlam *et al.*, 1986). The role of the capsule in the pathogenesis of *M. haemolytica* has been investigated in several studies. The capsule has been shown to confer resistance to complement mediated killing (Chae *et al.*, 1990) and neutrophil mediated killing (Czuprynski *et al.*, 1989). A study of *M. haemolytica* grown in subcutaneous tissue chambers has revealed that bacteria produce capsular material *in vivo* (Brogden & Clarke, 1997). Additionally microcolonies of *M. haemolytica* in the bovine lung have been shown to be encapsulated (Morck *et al.*, 1989). Thus the capsule may be involved in adherence to these tissues, such is the case for *S. pneumoniae* (Schrager *et al.*, 1998). However, an acapsular mutant constructed from a serotype A1 *M. haemolytica* isolate demonstrated greater binding to fibronectin as well a greater sensitivity to immune bovine serum (Lo & Sorensen, 2007; Mckerral & Lo, 2002). The capsule is noted as impairing adherence in other respiratory pathogens. For example, in *K. pneumoniae* the capsule is noted as

causing impaired adhesion to epithelial cells, most likely because of its outer membrane protein (OMP) masking effect but also as a result of negative surface charge enhancement (Sahly *et al.*, 2000). Both *S. pneumoniae* and *N. meningitidis* have been shown to decrease capsule production when contact is made with epithelial cells (Deghmane *et al.*, 2002; Hammerschmidt *et al.*, 2005). In *N. meningitidis* the decrease in capsule production follows the initial binding of the CD46 glycoprotein by pili. This activates the Crg repressor which binds the promoter region of the *sia* genes involved in capsule production (Deghmane *et al.*, 2002). Similarly, in *M. haemolytica* regulation of the capsule may be used to control exposure of OMPs.

1.1.5.5 Pili

The *M. haemolytica* genome contains the locus *pilABCD* necessary for the formation of type IV pili (Gioia *et al.*, 2006). However, experimental evidence of pili expression in *M. haemolytica* is limited to two electron microscopy studies of infected cattle lungs from the 1980's (Morck *et al.*, 1987, 1988). Pili expression has not been described since and the role of pili in *M. haemolytica's* infection remains unclear.

1.1.5.6 Superoxide dismutase

The enzyme superoxide dismutase (SOD) is widely distributed across the various kingdoms of life. The function of SOD is in the conversion of the superoxide anion (O_2^-)to either molecular oxygen (O_2) or hydrogen peroxide (H_2O_2), thus preventing the build-up of damaging reactive oxygen species (ROS) (Sheng *et al.*, 2014). In Gram-negative bacteria, cytoplasmic forms of SOD utilise iron and manganese as a cofactor and function in the dismutation of superoxide from aerobic metabolism. Another type of SOD that has been found to be present in the periplasm of Gram-negative bacteria utilises copper and zinc as a cofactor (Kroll *et al.*, 1995). In *M. haemolytica* the characterisation of a wide variety of serotypes isolated from sheep revealed that all the A2 and some of the A7 serotype organism tested had activity for the Cu-Zn cofactor form of SOD (Lainson *et al.*, 1996). As the hallmark of pneumonic pasteurellosis is the influx of neutrophils into the lung, and their subsequent lysis by the activity of the leukotoxin, the role that SOD plays in survival during these events may be crucial

to the virulence of the organism. Further characterisation demonstrated the presence of SOD in the periplasm of A1 and A2 *M. haemolytica* but not T10 *B. trehalosi* (Rowe *et al.*, 1997). Additionally, it was shown that the A1 strain, isolated from a calf lung, could not survive 30 minutes in the presence of superoxide where the A2 strain, isolated from an ovine lung could. Much remains to be determined for the role of SOD during infection.

1.1.5.7 Outer membrane proteins

M. haemolytica encodes many OMPs with as of yet undefined roles in pathogenicity (Gioia *et al.*, 2006; Lawrence *et al.*, 2010). Certain OMPs are somewhat characterised with demonstratable roles in virulence including the OmpA protein which has been shown to bind fibronectin (Lo & Sorensen, 2007) or the transferrin receptor (TbpA and TbpB) which confer immunogenic protection against *M. haemolytica* (Potter *et al.*, 1999) (covered in more detail in 1.1.6). However, many OMPs are uncharacterised, some share homology with well-defined virulence factors of other organisms, including a homologue of the *B. pertussis* filamentous hemagglutinin, numerous iron uptake systems, a high molecular weight (MW) neuraminidase of the subtilize family and several proteins with homology to the trimeric autotransporter adhesins of *N. meningitidis* and *H. influenzae* . Because little is known of the contribution to pathogenicity that these OMPs confer, these proteins represent a knowledge-gap in the understanding of the aetiology of the disease. However, many of these have been shown to elicit an immune response (Ayalew *et al.*, 2011a; Pandher *et al.*, 1998), thus implicating these under-characterised proteins in the disease aetiology. An overview of the outer membrane of Gram-negative bacteria is presented in section 1.2.3 and further information relating to the OMPs *of M. haemolytica* is provided.

1.1.6 Vaccination

Efforts in *M. haemolytica* vaccine design have been driven by the economic losses experienced from livestock production. Commercial vaccines against *M. haemolytica* are available based on whole cell preparations, recombinant leukotoxin, cell surface antigens and combinations of these strategies (Bowland & Shewen, 2000). Research into improved vaccine design has been driven by the

ineffectiveness of *M. haemolytica* vaccines and the requirement of recurrent administration. Collective assessment of 18 commercial vaccine trials against *M. haemolytica* challenge demonstrated that only three out of 18 displayed a statistically significant reduction in morbidity versus control (Larson & Step, 2012).

Vaccines that make use of *M. haemolytica* leukotoxin are currently used in disease prevention. Leukotoxin is the primary virulence factor of *M. haemolytica*. Administration of culture supernatant (CS) confers protection against A1 isolates in cattle where antibody titres towards leukotoxin and capsular polysaccharide are observed in the serum of vaccinated animals (Hodgins & Shewen, 2000). Similarly in sheep, protection against challenge with *M. haemolytica* is afforded through the administration of CS (Subramaniam *et al.*, 2011). Indeed, administration of purified recombinant leukotoxin alone confers protection against *M. haemolytica* A1 (Conlon *et al.*, 1991). However, much greater protection was afforded via the administration of a vaccine containing the recombinant leukotoxin as well the *M. haemolytica* culture supernatant. More recently, Briggs *et al.* (2012) constructed an in-frame leukotoxin mutant that displayed cytotoxic attenuation and was able to protect cattle against challenge when administered orally in feedlot. However, CS and other cellular antigens were not included in the trial. Thus, supplementation of additional factors may aid in improving the formulation.

Immunogenic outer membrane (OM) surface antigens are another target of vaccine development. Sarkosyl insoluble OM fractions have been shown to increase resistance to *M. haemolytica* challenge (Morton *et al.*, 1995). Immunogenicity has been demonstrated for 21 surface-exposed OMPs of *M. haemolytica* A1 (Pandher *et al.*, 1999). Amongst these, identities have been given to serotype specific antigen 1 (Ssa1), OmpA, OmpP2, BamA, PlpE and PlpF (Ayalew *et al.*, 2011b; Pandher *et al.*, 1998). Early work examining the immunogenicity of iron–regulated OMPs (IROMPs) identified that three OMPs induced under low iron growth conditions were immunogenic to convalescent sera (Deneer & Potter, 1989). More recent work has trialled the transferrin binding proteins, TbpA and TbpB (covered in detail in 1.2.2.3.1) for their immunogenic protection in cattle (Potter *et al.*, 1999). Antibody titres were

observed for TbpB but not for TbpA. However, the best protection was conferred when both proteins were administered together resulting in only a single loss (n=10) within ten days of *M. haemolytica* challenge.

Similar to cattle, sheep vaccinated with OMPs have demonstrated protection to *M. haemolytica* infection. Both convalescent sera and sera from lambs vaccinated with a mixture of heat killed-organisms (HKO) and sodium salicylate cell extracts were able to confer protection to lambs challenged with *M. haemolytica* A2 (Jones *et al.*, 1989). This demonstrates that cell-surface antigens confer protection to sheep when administered in a vaccine.

Research into the immunogenicity of IROMPs in sheep identified two IROMPs of 70 and 100 kDa which were immunogenic (Donachie & Gilmour, 1988). However, only the 70 KDa band was expressed in isolates recovered from the pleural fluid of lambs challenged with *M. haemolytica* A2. The inclusion of iron regulated proteins has also been demonstrated to improve the efficacy of vaccination in lambs challenged with *M. haemolytica* A2 (Gilmour *et al.*, 1991). Comparison was made between *M. haemolytica* grown in the presence of the iron chelator dipyridyl, which induces IROMPs, and *M. haemolytica* grown in the absence of the chelator. Sodium salicylate extract (SSE) was used to extract the cell envelope. When subjected to challenge, lambs vaccinated with the IROMP-SSE conferred greater protection compared with SSE vaccinated lambs. Thus, SSE extract of A2 *M. haemolytica*, which had been shown in earlier studies to be relatively poor in conferring protection was improved through the stimulation of IRP expression (Gilmour *et al.*, 1983, 1991). In summary, for both cattle and sheep, OMPs confer immunogenic protection and represent an important consideration in vaccine design.

Studies have employed approaches that target leukotoxin as well as OMPs. Ayalew *et al.* (2008) constructed a recombinant chimeric protein vaccine consisting of 55 amino acids of PlpE adjoined to 133 amino acids of LktA. Use of a mouse model demonstrated a greater effectiveness of the chimeric vaccine as compared to challenge with either protein alone (Ayalew *et al.*, 2008). The LktA-PlpE recombinant vaccine has since been assessed in cattle and has been shown to produce higher PlpE and LktA IgG titres as compared with a bacterin vaccine (Confer *et al.*, 2009). However, in response to *M. haemolytica*

challenge, a significantly greater reduction in lung lesions were observed in cattle vaccinated with both bacterin and LktA-PlpE recombinant vaccine as compared with either vaccine alone. More recently, another chimeric protein comprising a domain of LktA flanked by two immunogenic domains of PlpE was constructed (Batra *et al.*, 2016). Mice immunised with this chimeric protein raised antibodies that recognised LktA and PlpE. Similarly, Shewen *et al.* (2003) examined the protection conferred by the secreted Gcp endopeptidase. In this study it was found that Gcp conferred protection against *M. haemolytica* challenge. However, maximal coverage, minimal clinical score and minimal necrotic lung damage was afforded when Gcp was administered along with recombinant leukotoxin and culture supernatant as compared with administration of these alone. Although the finding was not statistically significant it does suggest that the best coverage is afforded through the use of multiple antigens.

Similar findings have been demonstrated for vaccination in sheep. An SSE preparation of *M. haemolytica* was shown to be relatively ineffective in protecting lambs against *M. haemolytica* challenge. Inclusion of the *M. haemolytica* culture supernatant into the vaccine formula raised the percent protection from 47 to 98 % (Sutherland *et al.*, 1989). Coverage afforded through cultured supernatant alone was 86 %. These results, for both cattle and sheep, show that protection against *M. haemolytica* is afforded through the use of complementary strategies that encompass multiple antigens.

1.2 The outer membrane of Gram-negative bacteria

The Gram-negative bacterial cell envelope comprises a double membrane structure that separates the cytoplasm of the cell from the extracellular space. The inner membrane (IM) is a symmetrical phospholipid bilayer that separates the cytoplasm from the periplasm. The periplasm represents the intermembrane space and contains the peptidoglycan (PG) layer which is composed of N-acetylglucosamine (GlcNAc) and N-acetylmuramic acid (MurNAc). The outer membrane, unique to Gram-negative bacteria, separates the periplasm from the extracellular space. This membrane is an asymmetric structure comprised of a phospholipid inner leaflet and mixed lipopolysaccharide-phospholipid outer leaflet (Fig 1.3).

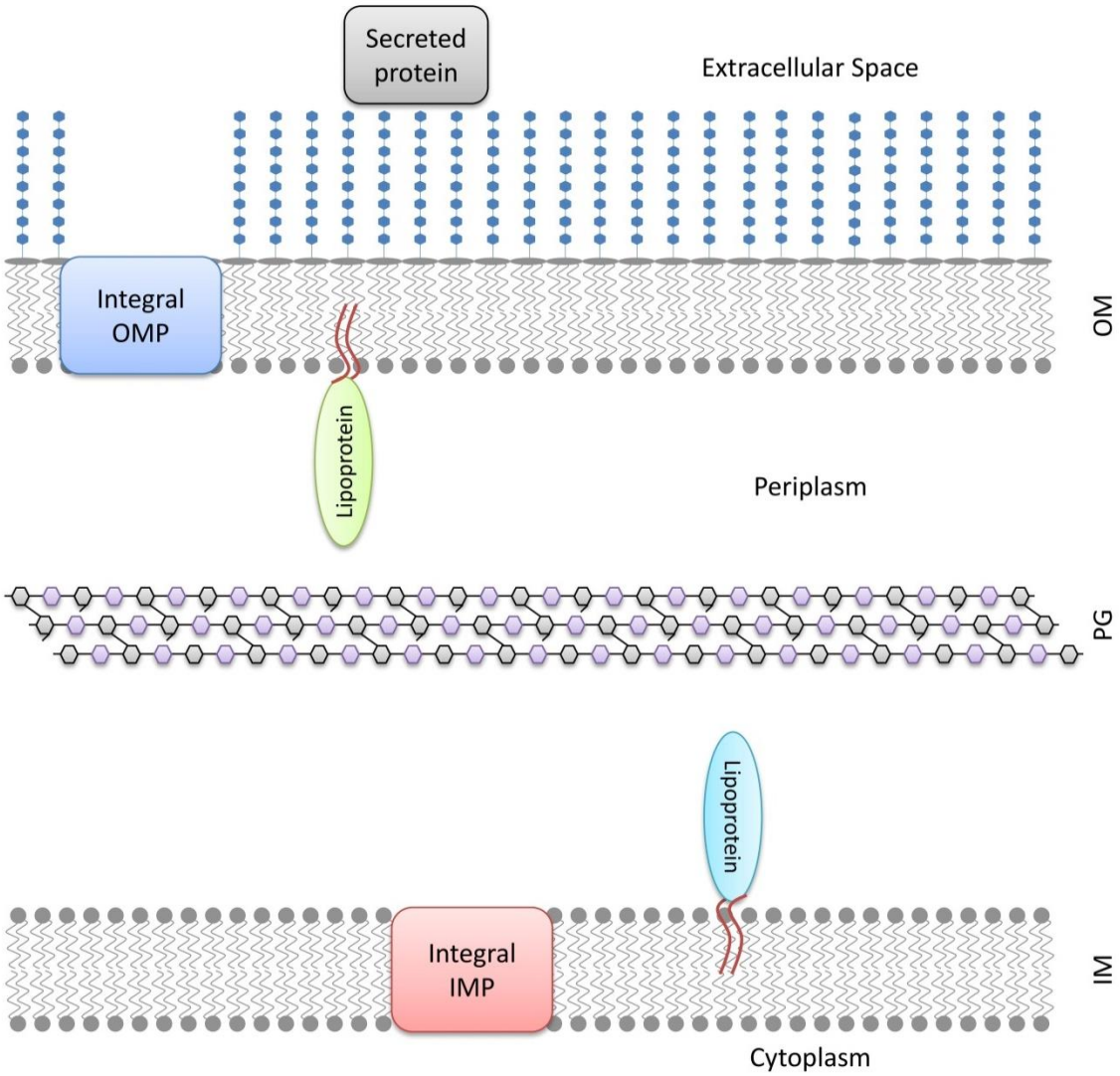

Fig 1.3 The Gram-negative cell envelop.
Diagram of the cell envelope of Gram-negative bacteria. Abbreviations, Outer membrane: OM, peptidoglycan: PG, Inner membrane: IM.

The OM represents the interface between a microbe and its environment. Processes at the OM are responsible for outer membrane biogenesis and integrity, transport and receptor activities, adherence and enzymatic activity. Specialised protein machinery is adapted to control these processes and involves interaction with periplasmic, IM and extracellular components, the details of which are discussed in the following sections.

1.2.1 Biogenesis and integrity

Homeostasis at the OM involves the correct transport, folding and insertion of various OMPs into the asymmetric lipid bilayer. Two distinct classes of proteins; integral OMPs and lipoproteins, represent the bulk protein machinery at the OM.

Integral OMPs consist of a transmembrane β-barrel. This structure comprises a mixture of polar and hydrophobic residues that orientate via β-sheets to create a hydrophilic inner channel and a hydrophobic outer surface (Wimley, 2003). Large aromatic residues are found predominantly at the lipid interface, whereas the internal barrel strands comprises small polar and non-polar residues (Wimley, 2003). The other class of OMP, the lipoprotein, does not contain transmembrane domains but is post translationally modified to contain a lipid anchor.

Certain proteins of the OM contribute to the structure and integrity of the OM. OmpA, one of the most abundant proteins in the OM, is non-covalently linked to the PG cell wall (Confer & Ayalew, 2013). Similarly, murein (Braun's) lipoprotein tethers the OM to the PG, although unlike OmpA it is covalently bound to the PG cell wall (Kovacs-Simon *et al.*, 2011). Along with murein-lipoprotein is the peptidoglycan-associated-lipoprotein (Pal), which links with other proteins including the periplasmic protein TolB and the IM proteins TolA, TolQ and TolR, to form complexes (Cascales *et al.*, 2002; Godlewska *et al.*, 2009). Altogether these complexes provide integrity to the OM and prevent the leakage of periplasmic contents out of the bacterial cell.

1.2.1.1 β-barrel assembly and insertion

The two types of protein that function at the OM are integral membrane proteins and lipoproteins. Integral membrane proteins contain transmembrane spanning domains and are assembled at the OM via the aid of the β-barrel assembly machinery (BAM) complex. The BAM complex functions to fold, assemble and insert β-barrel proteins into the OM. The complex is formed by five distinct protein subunits, BamA-E (Fig 1.4).

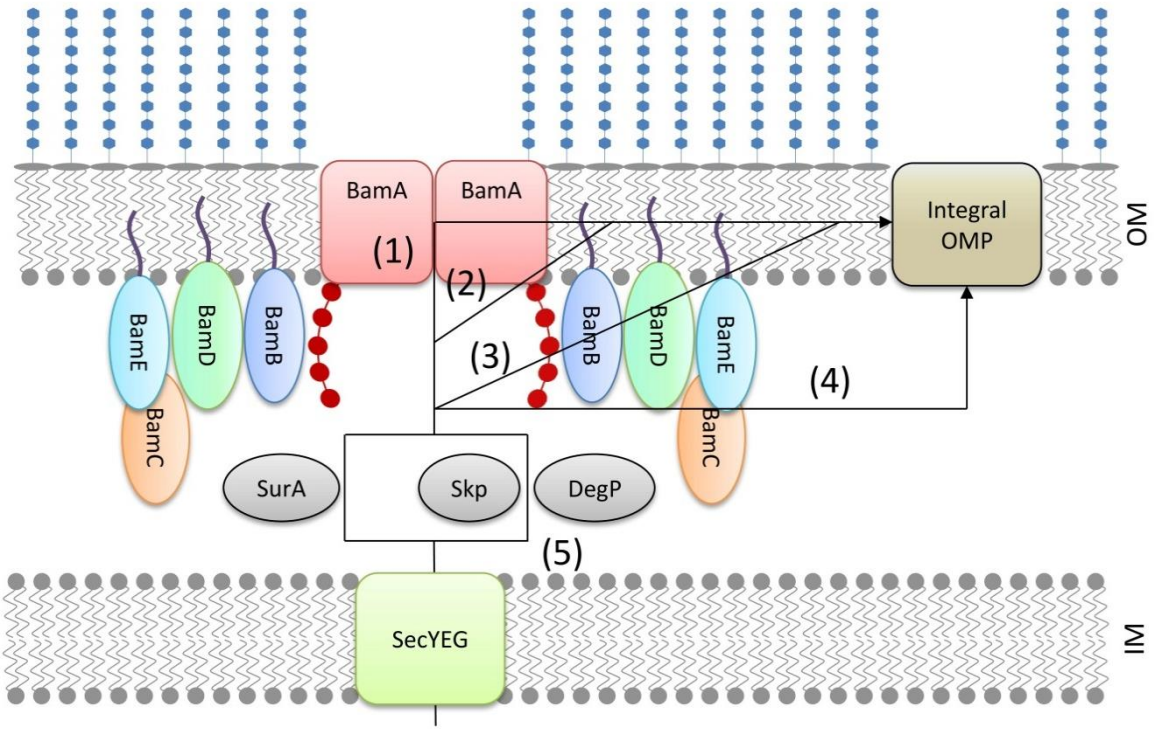

Fig 1.4 BAM complex machinery.
A schematic representation of the BAM complex (BamABCDE) together with the periplasmic chaperone proteins (SurA, Skp and DegP). Numbers reflect the five potential routes to OMP assembly as discussed in the text.

BamA constitutes the main component in assembly and is a member of the Omp85 family of protein which are architecturally characterised by an integral OM β-barrel and periplasmic polypeptide-transport-associated (POTRA) domains (Gentle *et al.*, 2005). BamA contains five POTRA domains. The other proteins of the complex, BamB, BamC, BamD and BamE are lipoproteins that act as accessories to BamA (Knowles *et al.*, 2009). Of the protein subunits, only 'knockouts' of BamA and BamD result in cell death, although 'knockouts' of the other subunits result in miss-folding of β-barrel OMPs (Genevrois *et al.*, 2003; Malinverni *et al.*, 2006; Palmer *et al.*, 2003; Sklar *et al.*, 2007).

While it is currently unknown how the BAM complex assembles β-barrel proteins, studies based on deducing the function have provided several hypotheses. Most of these hypotheses postulate that OMPs interact with the five POTRA domains of BamA. It has been proposed that the POTRA domain binds the OMP via C-terminal recognition motifs that can initiate the folding and insertion (Kim *et al.*, 2007a; Robert *et al.*, 2006). Mutation of the POTRA domains has been

shown to compromise insertion but not assembly of the β-barrel. Analysis of which of the five domains is necessary for folding and insertion has produced conflicting results with one study proposing only domain five was necessary (Bos *et al.*, 2007), and another reporting that all domains were needed (Kim *et al.*, 2007a).

Altogether, five potential models have been proposed that account for the BAM complex functioning (Knowles *et al.*, 2009) (Fig 1.4). The first (1) of these involves all subunits functioning to fold the β-barrel before membrane insertion and translocation. The second (2) involves the use of the POTRA domains to specifically thread the polypeptide chain into the BamA pore, where assembly occurs *de novo*. The third (3) model proposes that the BamA β-barrel provides a template for the assembly of the β-barrel of inserted proteins. The fourth (4) postulates that the chaperones, SurA, Skp, and DegP are involved in folding and the BAM complex only functions in insertion of the folded OMP. The final model (5) is contrary to the fourth, postulating that that the BAM complex folds the β-barrel before delivery to the periplasmic chaperones for insertions.

For the specific case of autotransporter β-barrels, a second assembly system has been discovered called the translocation and assembly module (TAM). This system consists of two proteins, TamA, an OM Omp85 family protein with three periplasmic POTRA domains, and an IM component, TamB (Gruss *et al.*, 2013; Selkrig *et al.*, 2012). Initial characterisation found an accumulation of unfolded autotransporters in the periplasm following TamA and TamB deletion; this led to their designation as autotransporter assemblers (Selkrig *et al.*, 2012). Further work has led to a proposed model of folding whereby unfolded autotransporters are delivered to TamA, recognition is made by the POTRA domains which begin to thread the C-terminal. As this occurs, the TamA barrel opens to accommodate folding of the new β-barrel and insertion of the passenger domain (Gruss *et al.*, 2013). Reversion of TamA to the closed state results in ejection of the now folded autotransporter into the OM. More recently TamB has been shown to dock to TamA via insertion of the POTRA domains. In this model TamB is proposed to drive the conformational changes needed in OM insertion (Selkrig *et al.*, 2015). Whether the TAM complex is the only component needed in autotransporter assembly is not fully understood. Studies have reported a lack

of autotransporter assembly following deletion of BamA or BamD (Lehr *et al.*, 2010; Rossiter *et al.*, 2011). Thus, the exact mechanism of assembly might involve both the BAM and TAM complexes.

1.2.1.2 Lipoprotein synthesis and insertion

Lipoproteins are proteins attached to the IM and OM via post translation addition of fatty acid chains. This chain acts like a tether to anchor the protein to the OM. Most lipoproteins reside on the inner leaflet of the OM although some do face out into the extracellular space (Zückert, 2014). Synthesis and transport of lipoproteins is summarised in Fig 1.5.

Synthesis and insertion begins with recognition of an N-terminal signal peptide that delivers the protein through the general secretory pathway (SecYEG) or twin arginine translocation pathway (TAT) across the IM. Once transported, lipidation occurs via the action of three IM bound enzymes, Lgt, Lsp and Lnt (Buddelmeijer, 2015; Wu *et al.*, 1982). The N-terminal portion which is heavily charged remains on the cytoplasmic side. The transported protein is transferred to Lgt where recognition of a lipobox motif results in addition of a fatty acid chain to the free thiol group of a conserved cysteine residue. .

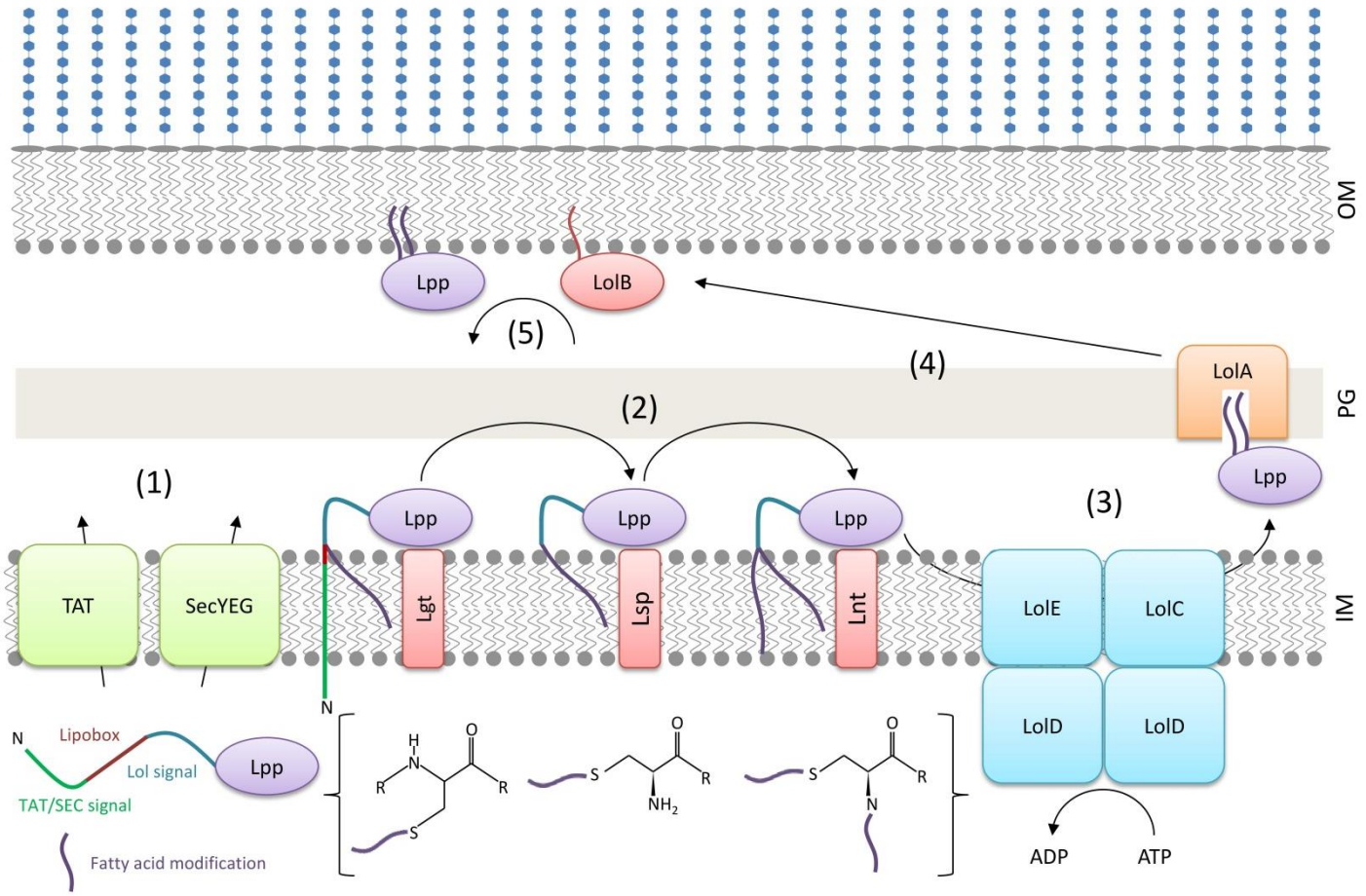

Fig 1.5 Lipoprotein synthesis and location.
Polypeptide chain is targeted for transport across the IM by either the TAT or SecYEG systems (1). The highly charged N-terminus remains in the cytoplasm while Lgt adds the first acyl chain, Lsp then cleaves off the signal peptide up to the new acyl modification (2). Lpp adds another acyl chain. Transport to the OM is accomplished with the LolDCE complex (3) and the periplasmic chaperone LolA (4). Final insertion into the OM is mediated through LolB (5).

Transfer to Lsp then occurs which cleaves the signal peptide up to the cysteine residue generating a new N-terminus. The third protein, Lnt, only present in proteobacteria and actinomyctes, adds another fatty acid residue to the free amino of the new N-terminal cysteine. Transport to the OM occurs via the Lol sorting signals. Recognition of an amino acid positioned two residues along from the new N-terminal cysteine determines the final location of the lipoprotein (Zückert, 2014). If asparagine is present two residues from the N-terminal cysteine then the lipoprotein is retained at the IM, any other amino acid at this position results in the lipoprotein being delivered to the OM. Delivery to the OM begins with the transfer of the lipoprotein to the periplasmic shuttle protein LolA (Zückert, 2014). This occurs when the LolCDE complex hydrolyses adenosine triphosphate (ATP) to facilitate transfer. Transfer to the OM occurs via the LolB protein which contains a binding pocket of higher affinity than that of LolA to facilitate spontaneous transfer from LolA to LolB (Takeda *et al.*, 2003). The process that governs the final transition whereby LolB gives up the lipoprotein is not clearly understood although mutation analysis has pinpointed one residue, leucine 68, of a protruding loop, as a necessary component for transfer to the OM (Hayashi *et al.*, 2014).

1.2.1.3 Lipopolysaccharide synthesis and transport

The outer leaflet of the cell envelope is composed predominantly of lipopolysaccharide (LPS), although phospholipids are present as well. Structurally, LPS is composed of three well defined regions; (1) lipid A, which anchors the molecule in the OM, (2) a highly conserved core polysaccharide adjoined to lipid A and (3) a highly variable O-antigen chain that protrudes away from the cell surface. Synthesis of lipid A occurs through the Raetz pathway that comprises a nine step enzymatic process at the inner leaflet (Whitfield & Trent, 2014). The process is highly conserved amongst Gram-negative bacteria with only a few exceptions. Synthesis begins with UDP-GlcNAc and terminates with the production of Kdo_2^-lipidA. Complete lipid A is then modified with the addition of core polysaccharide via enzymes on the IM inner leaflet. Immature LPS is now transferred from the IM inner leaflet to the IM outer leaflet by MsbA (Fig 1.6), commonly referred to as the 'flipase' (Dawson & Locher, 2006).

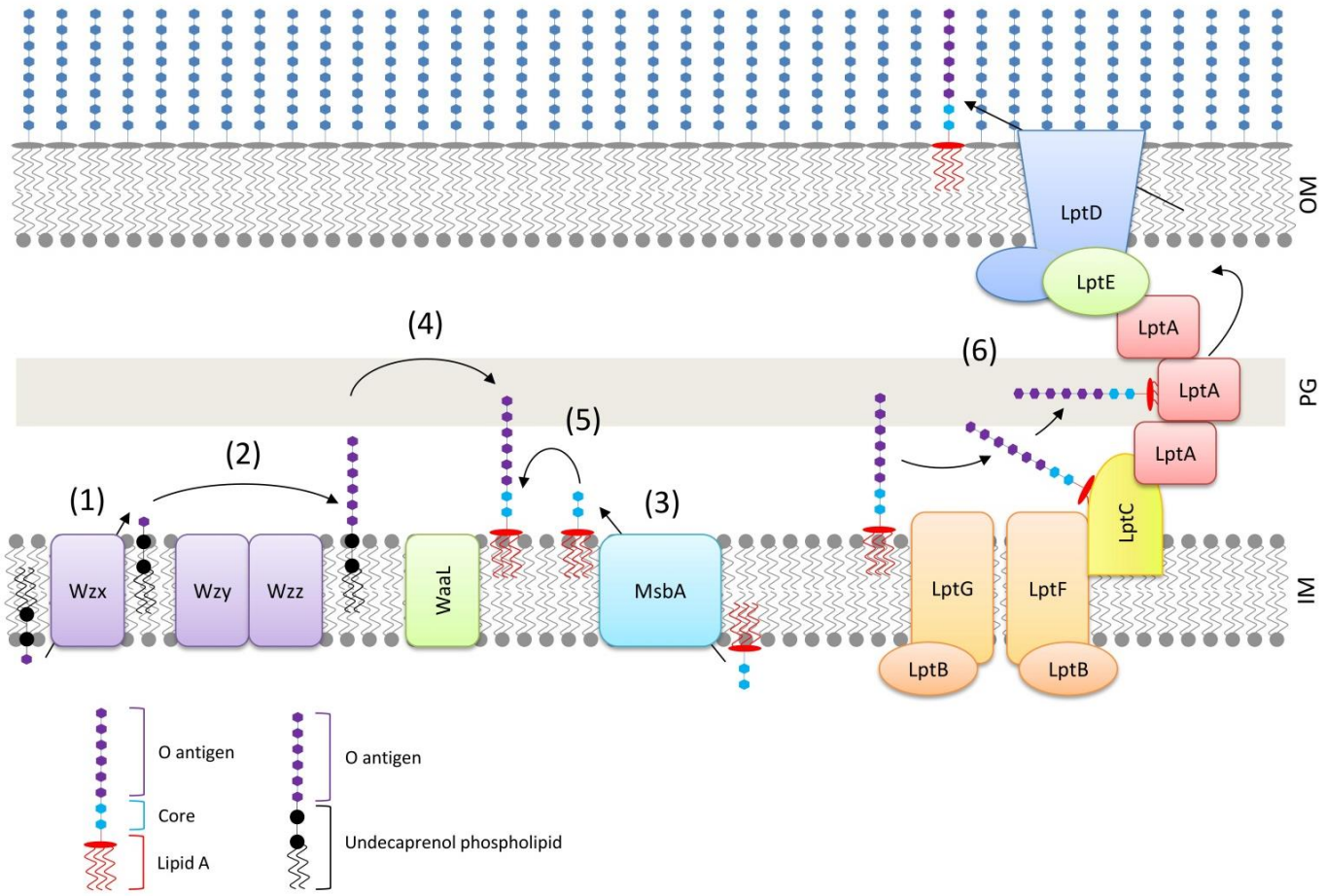

Fig 1.6 LPS assembly and transport.
Displayed is a schematic of Wzy dependent LPS synthesis. O-antigen-undecaprenol is flipped across the IM by Wzy (1). The O-antigen chain elongation is accomplished with Wzy and Wzz (2). The lipid A-core component is flipped across the IM via MsbA (3). Lipid A-core and O-antigen are ligated via WaaL(4 + 5). The LptABCDEFG forms a complex for the final transfer of LPS into the OM (6).

MsbA is a homodimer with a transmembrane domain and a cytosolic nucleotide binding domain. Nucleotide hydrolysis provides the energy to facilitate lipd A-core flipping (Dong *et al.*, 2005).

The O-antigen component of LPS is synthesised separately and combined with the lipidA-core on the outer leaflet of the IM. Unlike lipid A-core synthesis, the machinery for O-antigen production is highly variable amongst Gram-negative bacteria. This segmentation of lipid A-core and O-antigen biosynthesis routes confers a number of biological advantages that promote survival in a host (Cummings *et al.*, 2004). Horizontal acquisition of genes encoding the O-antigen synthesis pathways and phase variation of different sets of O-antigen producing genes both provide routes by which bacteria can evade antibody mediated killing (Cota *et al.*, 2012; Hester *et al.*, 2013).

Synthesis of O-antigen occurs by one of three routes; Wzy dependent, ABC transporter dependent and synthase dependent (Greenfield & Whitfield, 2012). The feature common to all three pathways is the requirement of an undecaprenol phosphate substrate for O-antigen growth. The Wzy pathway (Fig 1.6) involves initially flipping the undecaprenol phosphate substrate for stepwise addition of repeating units by Wzy and final chain length determination by Wzz. The other two pathways involve O-antigen synthesis at the cytoplasmic face before subsequent flipping to the periplasmic side. Little is known of the synthase pathway which is only found in *Salmonella enterica*. It has been postulated to occur via a duel extension flipping complex known as the 'synthase'. In the ABC transporter pathway flipping is achieved via a nucleotide binding flipase. All pathways converge on the protein WaaL, which combines the O-antigen with the lipid A-core region completing the final LPS synthesis step (Abeyrathne & Lam, 2007; Han *et al.*, 2012).

Fully mature LPS can now be exported via the lipopolysaccharide transport (Lpt) system. The system is non-discriminatory and can accept lipid A-core in the absence of O-antigen, thus accounting for the length variation observed at the OM. Two subunits of LptB and one each of LptF and LptG form the energy transducing IM complex (Whitfield & Trent, 2014). Acceptance of LPS into a contiguous helical groove formed through the shuttle proteins LptFGCAD facilitates transport to the OM (Gu *et al.*, 2015). The final portion of the

contiguous groove involves a helical twist of the LPS into the β-barrel portion of LptD which contains a break in the barrel structure allowing for LPS to exit the transport system with the correct orientation (Qiao *et al.*, 2014).

1.2.2 Transport and receptor activities

1.2.2.1 Porin proteins

Classical porins are medium molecular weight proteins that form 16-stranded β-barrels in the OM of Gram-negative bacteria. Classical porins such as OmpC and OmpF of *E. coli* (Fig 1.7) associate as homotrimers and function in the free diffusion of small molecules and ions through the pore formed by the β-barrel architecture (Baslé *et al.*, 2006; Cowanit *et al.*, 1995). The only selectivity conferred by porins is by size, where an upper limit of around 600 Da is imposed, and by charge, where porins can show bias for either cations or anions (Schirmer & Phale, 1999). Porins reside in one of two gated states, open and closed. An external membrane potential provides the stimulus to switch between the two states. This has been shown to involve the negatively charged loop 3 of the porin that resides inside the channel barrel and forms an electric field with the positively charged opposing surface of the barrel wall (Pezeshki *et al.*, 2009). When the critical voltage (V_C) is reached, loop three dislocates upon cation binding exposing a conserved aromatic residue that prevents ion flow (Song *et al.*, 2015).

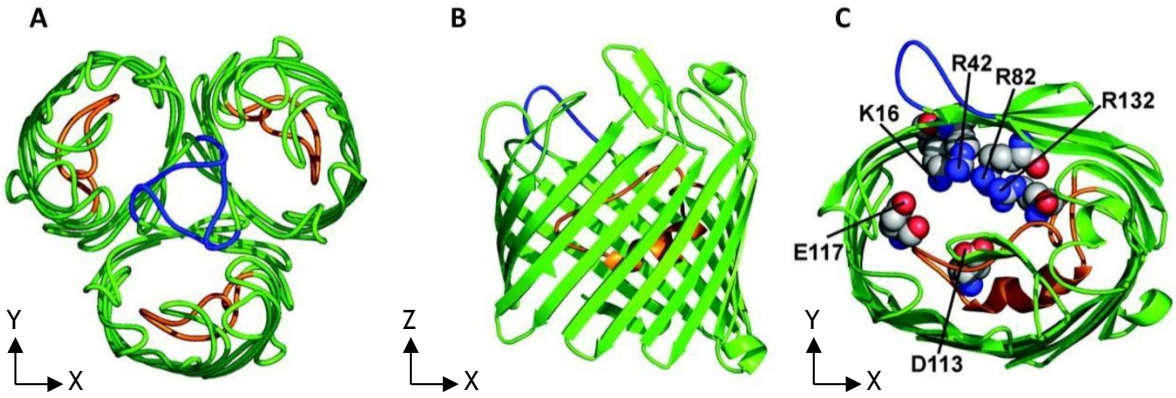

Fig 1.7 Structure of the OmpF porin from *E. coli*
Shown is three orientations of the OmpF porin structure. (A) Shown in the x-y plane is the association of three copies of OmpF forming a trimer. (B) Orthogonal view of a single OmpF copy. (C) View of a single OmpF protein in the x-y plane showing the six amino acids that comprise the constriction zone between loop 3 and the barrel wall. Shown in all views are loop 3 (orange) and loop 2 (blue). Adapted from (Nikaido, 2003).

In addition to the classical porins are substrate-specific porins. Structurally these deviate from classical porins with an additional two β-barrel strands, resulting in an 18-stranded barrel (Schirmer *et al.*, 1995). These still function to provide free diffusion across the OM but they place constraint on the substrate. One of the most extensively characterised substrate-specific porins is the maltose-specific porin LamB. This porin contains a specific binding site for maltose in the C-terminus of the protein which contains a hydrophobic slot (Charbit *et al.*, 1998; Dutzler *et al.*, 1995). This provides a means for the transport of large malto-oligosaccharides which ordinarily cannot pass through free diffusion porins (Benson *et al.*, 1988). Small molecular weight species can pass freely through LamB when the channel is not occupied by a maltose substrate (Schulein & Benz, 1990).

1.2.2.2 TonB dependent uptake

Active transport as compared with free diffusion across the OM requires energy-transducing mechanisms. One of the most heavily conserved mechanisms for active uptake is the TonB dependent system. Structurally, this system comprises a periplasmic protein, TonB, and two IM proteins, ExbB and ExbD. The system couples to various OM receptors through a Ton box motif found on the periplasmic side of the OM receptors. All TonB-dependent receptors are integral OMPs which architecturally comprise a 22-stranded β-barrel (Wimley, 2003). Altogether the system transduces energy via proton flux across the IM to drive OM uptake against a concentration gradient (Noinaj *et al.*, 2010). Most TonB dependent receptors function in the uptake of iron, although others have been identified for the uptake of copper, nickel, manganese and zinc (Porcheron *et al.*, 2013; Schauer *et al.*, 2007; Stork *et al.*, 2010; Yoneyama & Nakae, 1996) as well as for the uptake of coblamin (vitamin B_{12}) (Raux *et al.*, 2000). *M. haemolytica* possess various TonB dependent systems each targeted to a particular host source. These sources include haem, haemopexin, transferrin, haemoglobin and as well siderophore-mediated uptake, all of which are under the control of TonB-dependent acquisition.

1.2.2.3 Iron uptake

Iron is an essential nutrient for bacterial growth because it is utilised as a cofactor in many enzymatic processes. Bacteria that are involved in host colonisation, including *M. haemolytica,* have evolved mechanisms of scavenging this essential nutrient from a variety of host sources. All of these uptake systems involve TonB-dependent transport mechanisms (see 1.2.2.2) and are summarised in Fig 1.8.

1.2.2.3.1 Transferrin uptake

Transferrin uptake in *M. haemolytica* is accomplished via the use of two transferrin binding proteins, TbpA and TbpB, these proteins share homology with the two extensively characterised transferrin binding proteins of *N. meningitidis* and *N. gonorrhoeae*. TbpA is an integral OM TonB-dependent receptor and has been proposed to function as the conduit for iron transport across the OM (Cornelissen *et al.*, 1998). TbpB is an OM lipoprotein that is tethered to the outer leaflet. Structurally, it comprises two ß-barrels and two ß-handles that form a bi-lobed structure on the cell surface (Calmettes *et al.*, 2012; Moraes *et al.*, 2009). The N-terminal barrel and adjacent handle form the transferrin binding region (Calmettes *et al.*, 2011). TbpB is believed to function as a recruitment factor, specifically binding apo-transferrin, this maximises uptake of transferrin, where contrary to TbpB, TbpA is known to bind both holo and apo forms indiscriminately (Retzer *et al.*, 1998).

Unlike many of the *M. haemolytica* OMPs, the TbpA and TbpB proteins are somewhat characterised. Immunogenic cross reactivity can be observed amongst purified TbpB of different serotypes but not in TbpA (Deneer & Potter, 1989; Potter *et al.*, 1999). Both proteins are encoded by the *tbpBA* operon. Genetic analysis of the operon has demonstrated that the alleles of pathogenic bovine A1 and A6 isolates are more similar to the closely related ovine isolates (Lee & Davies, 2011). However, the A2 alleles differ considerably between isolates recovered from cattle and sheep suggesting transferrin sequestration is host specific in *M. haemolytica*.

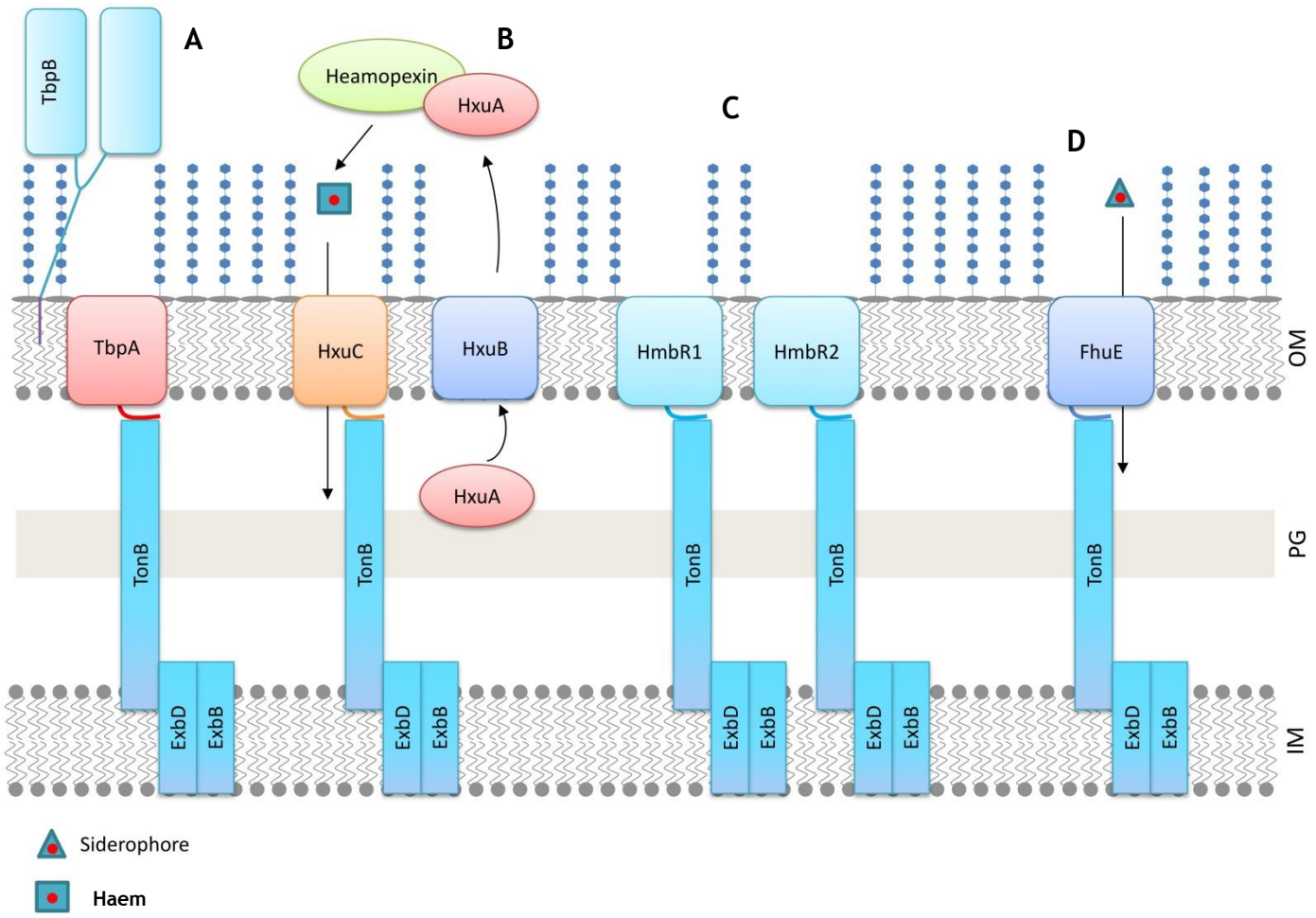

Fig 1.8 Iron uptake systems in *M. haemolytica*
Displayed are the confirmed iron mediated uptake systems including (A) transferrin , (B) haem / haemopexin, (C) haemoglobin, and (D) siderophore mediated uptake (FhuE).

1.2.2.3.2 Haemopexin uptake

The haem/haemopexin HxuABC system is well characterised in *H. influenzae*, where it has been shown to consist of a TPS system of HxuB and HxuA (Baelen *et al.*, 2013). The function of HxuB is to transport HxuA across the outer membrane and into the extracellular milieu. Once out-with the cell HxuA functions to bind host haemopexin and deliver it to the OM for uptake via the TonB-dependent receptor, HxuC (Cope *et al.*, 1995, 1998; Morton *et al.*, 2007). In addition to this primary function, HxuC has been shown to bind free haem and free haemoglobin independently of HxuA (Cope *et al.*, 2001). Little has been demonstrated of this system in *M. haemolytica*.

1.2.2.3.3 Haemoglobin uptake

The acquisition of iron from host haemoglobin can be achieved by *M. haemolytica* through the use of two haemoglobin binding receptors that share homology with the single haemoglobin receptor of *Neisseria spp.* These receptors have been demonstrated to be TonB-dependent (Stojiljkovic & Srinivasan, 1997) and unlike the transferrin binding receptors are believed to function independently of one another as the homologous *N. meningitidis* functions alone (Evans *et al.*, 2010; Jordan & Saunders, 2009). No structural information of these receptors is available at present.

1.2.2.3.4 Siderophore-mediated iron uptake

Siderophores are small molecule iron chelators produced by many bacterial species to scavenge iron for uptake. It is well documented that *M. haemolytica* does not produce siderophores (Gioia *et al.*, 2006). However, encoded within the *M. haemolytica* genome are several TonB-dependent siderophore uptake receptors (Gioia *et al.*, 2006; Lawrence *et al.*, 2010). The process of siderophore uptake in the absence of siderophore production is termed xenosiderophore acquisition (Matzanke *et al.*, 1997). This confers an advantage upon any microorganism that occupies the same niche as another siderophore producing species (Miethke *et al.*, 2013). Energy is conserved through the lack of production yet benefit is maximised when other organisms in close proximity generate siderophores. One prominent example of xenosiderophore acquisition is by the respiratory pathogens *B. pertussis* and *B. bronchiceptica*. Both

organisms produce and utilise the alcaligin siderophore (Brickman *et al.*, 1996; Moore *et al.*, 1995). To accomplish this, they contain machinery for the uptake of enterobactin, ferrichrome and desferrioxamine B siderophores (Beall & Hoenes, 1997; Beall & Sanden, 1995), none of which are produced by *B. pertussis* or *B. bronchiceptica*.

1.2.2.4 Capsular polysaccharide transport

Synthesis and transport of the polysaccharide capsule begins in the cytoplasm with an undecaprenol phosphate substrate. The IM proteins WbaP and Wzx function to flip the substrate from the cytoplasmic face of the IM to the periplasmic face of the IM (Fig 1.9). The substrate is then polymerised on the periplasmic face via the action of Wzy (Fig 1.9). Polymerisation is driven by phosphorylation of a tyrosine residue on the oligomeric protein Wzc and subsequent dephosphorylation of the residue via Wzb which is non covalently docked to Wzc at the cytoplasmic side (Cuthbertson *et al.*, 2009). This ATP-consuming process provides the energy for stepwise growth of the polymer.

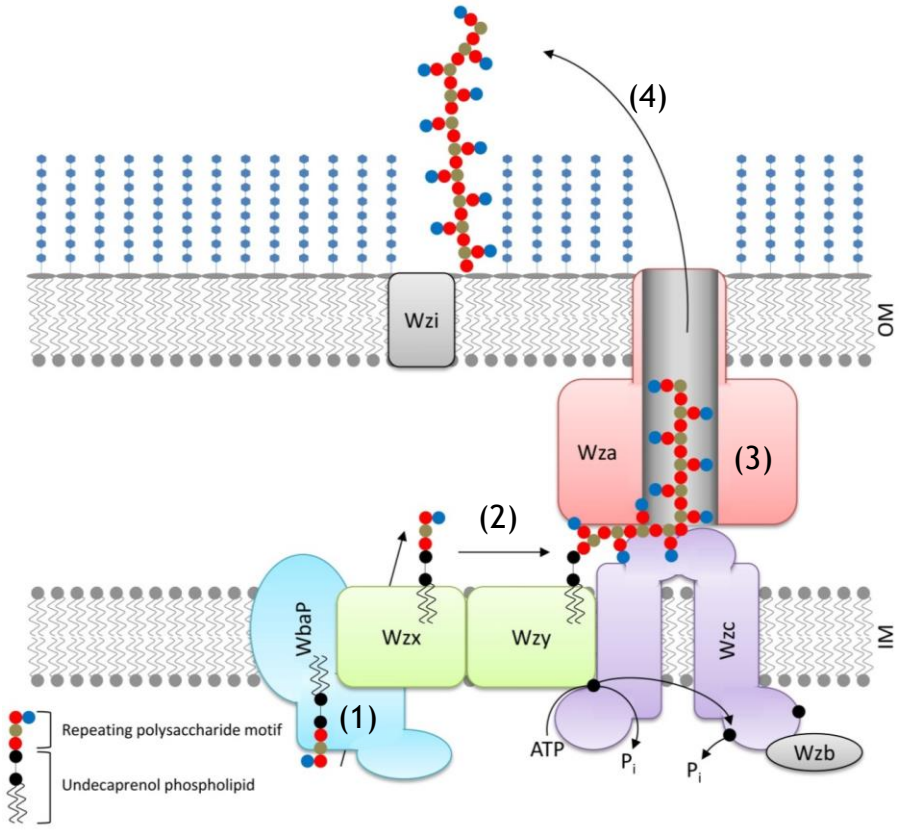

Fig 1.9 Capsular polysaccharide transport
(1) Undecaprenol phospholipid substrate is flipped across the inner membrane. (2) Repeating polysaccharide subunits are then added to the growing chain in a stepwise manner. (3) Transfer to the outer membrane is accomplished via the membrane spanning channel Wza. (4) Association with the OM is maintained through the lectin activity of Wzi.

The translocation into the extracellular space occurs via Wza, which is an octameric membrane spanning channel that threads the growing chain through a 17 Å opening into the extracellular space (Fig 1.9). Structurally Wza is a lipoprotein (Drummelsmith & Whitfield, 2000), anchored to the OM through acyl chains attached to each subunit, yet the subunits build a spiralled α-helical transmembrane channel that resembles the architecture of a β-barrel but with α-helices in place of β-sheets (Dong *et al.*, 2006). Wza represented a completely new paradigm in the understanding of OMPs as it was the first integral OMP to be discovered that did not consist of a β-barrel.

The final process involves the integral OMP Wzi. This protein is an 18-stranded β-barrel that functions as a cell surface lectin (Bushell *et al.*, 2010, 2013). As capsular polysaccharide emerges from the Wza channel the association of the capsular material that keeps it in contact with the bacterial cell is mediated through Wzi. This has been demonstrated in *Klebsiella pneumoniae* where surface plasmon resonance confirmed the high affinity of Wzi for the K30 serotype polysaccharide (Bushell *et al.*, 2013). Mutagenesis in Wzi extracellular loops 3, 5 and 7 mapped the functional binding to these regions of the extracellular face.

1.2.2.5 Secretion systems

To date nine different secretion systems have been identified in bacteria for the export of proteins, DNA and small molecules. They are designated as type I to IX secretion systems.

1.2.2.6 Type I secretion

Type I secretion (T1SS; Fig 1.10 D) involves the outer membrane conduit TolC which can couple to a number of different systems for energy transduction and export. All of the components that TolC couples to include an inner membrane energy transducer and a periplasmic membrane fusion protein that couples TolC to the inner membrane component (Costa *et al.*, 2015).

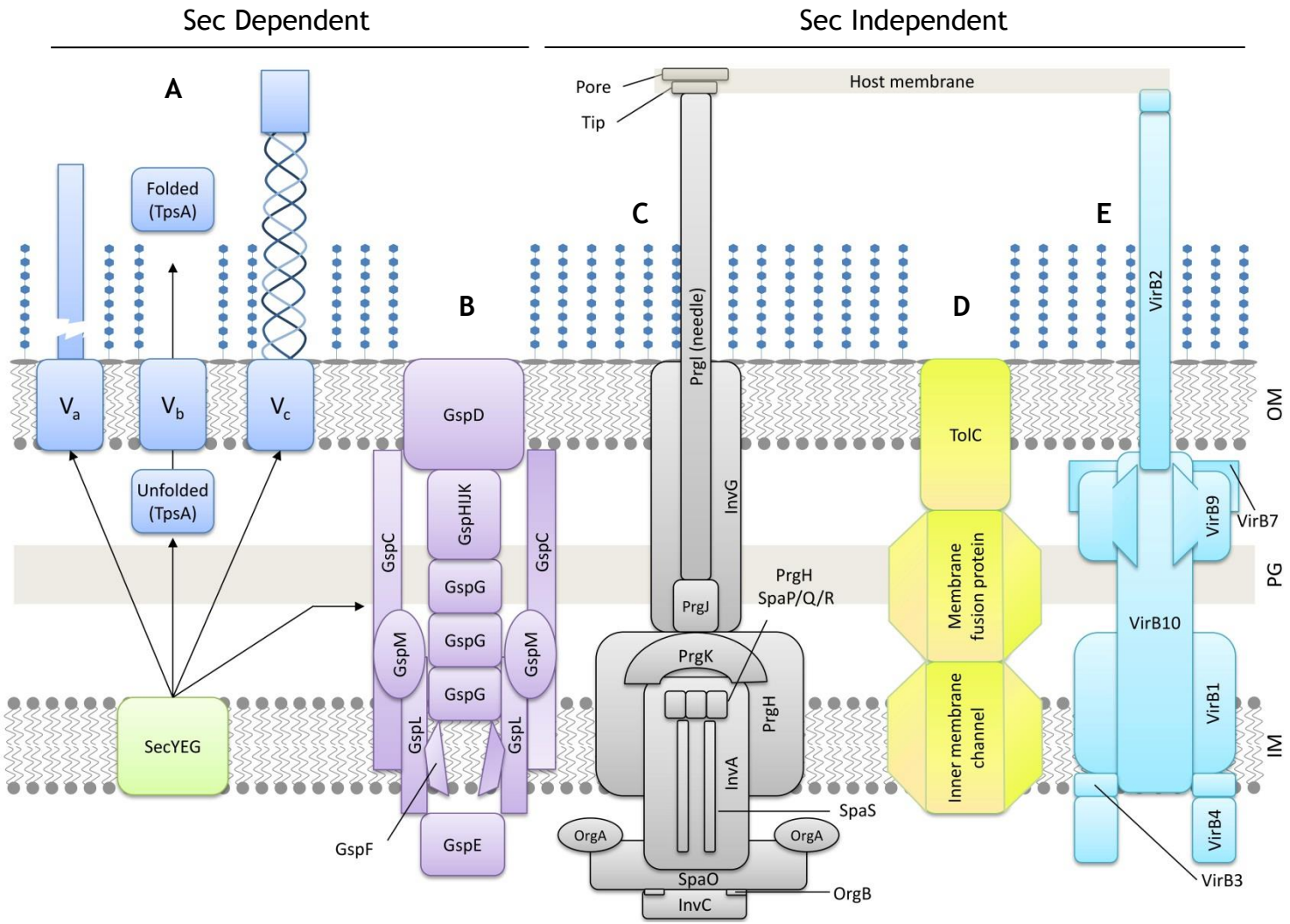

Fig 1.10 Gram negative secretion systems
Schematic diagram of secretion systems I-V. Displayed are type V secretion (A) showing classical (V_a), two partner (V_b) and trimeric ($V_{c)}$ autotransporters, type II secretion (B), type III secretion (C), type I secretion (D) and type IV secretion (E).

Together, these protein complexes form channels that can deliver substrates from the cytoplasm directly into the extracellular space. Of the IM and membrane fusion components that couple to TolC several different energy transducing mechanisms have been identified. These include ABC cassette binding systems that transduce energy from ATP hydrolysis, RND efflux systems that make use of the proton motive force for energy transduction and MF transporters which also make use of the proton motive force (Tikhonova *et al.*, 2009). Structurally, one of the most extensively characterised systems is the TolC-AcrA/B system (Du *et al.*, 2014). This functions as a multidrug efflux pump via an ABC cassette energy transducing mechanism. Three subunits of TolC form an OM β-barrel and a periplasmic coiled-coil of α-helices for the docking of the membrane fusion protein AcrA. AcrA is comprised of six subunits which form an opening of 34 Å at the TolC fusion point, a constriction of 16 Å towards the proteins centre and a 28 Å wide channel where the protein couples to AcrB. The function of AcrB is as the energy transducing ATP cassette and substrate acceptor. The complex comprises three subunits that cycle between three conformations, loose (L), tight (T) and extrusion (O). These function to provide access (L), binding (T) and extrusion (O) where each subunit occupies one conformation at one time cycling between the three states to deliver substrates into the extracellular space (Eicher *et al.*, 2012).

1.2.2.7 Type II secretion

The type II secretion system (T2SS; Fig 1.10 B) is responsible for the delivery of enzymes and toxins into the extracellular environment. The T2SS is a 12-15 component complex consisting of an OM dodecameric secretin, named GspD in *E. coli* and various subunits in the inner membrane (Costa *et al.*, 2015). Secretion by the T2SS is SEC and TAT dependent as substrates are loaded into the complex in the periplasm (Korotkov *et al.*, 2012). Energy transduction for substrate delivery is accomplished with a hexameric ATPase, GspE, which is located in the cytoplasmic portion of the complex (Korotkov *et al.*, 2012). The T2SS is responsible for the delivery of many important virulence factors in various pathogenic bacteria, such as cholera toxin of *Vibrio cholerae* (Reichow *et al.*, 2010), and various toxins and proteases from *Pseudomonas aeruginosa* (Ball *et al.*, 2002).

1.2.2.8 Type III secretion

Type III secretory system (T3SS; Fig 1.10 C), also described as the 'injectisome', is a multimeric protein complex that functions to deliver effector proteins directly from the cytoplasm through a needle-like channel and into the cytoplasm of a host cell. The T3SS shares homology with the flagella apparatus and it is believed that the injectisome evolved from the flagella apparatus (Abby & Rocha, 2012). Sensing of the host plasma membrane is hypothesised to involve conformational changes in the distal end upon contact with the plasma membrane that transduces further conformational changes along the length of the needle (Fujii *et al.*, 2012). Once contact is made the delivery of effectors is accomplished via InvC which is a hexameric, cytoplasmic ATPase that provides the necessary energy for effector delivery (Eichelberg *et al.*, 1994). The T3SS first delivers translocators for pore formation at the host membrane before effectors are injected (Costa *et al.*, 2015). The delivery of effectors into the host cytoplasm is achieved via a mechanism where they are loaded into the T3SS, N terminal first and unfolded during the process (Radics *et al.*, 2014). Delivered effectors preform various functions for the bacterium. In the case of enteropathogenic *E.coli* the T3SS functions to deliver Tir (translocated intamin receptor) which functions as a receptor for the *E. coli* adhesion intimin (Kenny *et al.*, 1997). Other effectors modulate the host environment to polymerise the characteristic actin pedestal observed with enteropathogenic *E.coli* infection.

1.2.2.9 Type IV secretion

The type IV secretion system (T4SS; Fig 1.10 E) is widely distributed amongst the Bacterial and Archaeal Kingdoms. Unique amongst the secretion systems is its ability to delivery DNA as well as protein cargo directly into the cytoplasm of prokaryotic and eukaryotic cells (Costa *et al.*, 2015). The complete structure comprises 12 proteins in *Agrobacterium tumefaciens*, with subunits involved in energy transduction and channel formation as well as accessory structural components. The T4SS components VirD4, VirB11 and VirB4 all have nucleotide binding sites and are responsible for energy transduction (Atmakuri *et al.*, 2004). These three subunits initially recruit and dock DNA for export. Delivery across the OM is achieved through a channel formed by subunits of VirB7, VirB9 and VirB10 (Fronzes *et al.*, 2009; Low *et al.*, 2014). This channel continues into the

VirB2 subunit pilus. The distal tip of the VirB2 delivery pilus comprises the VirB5 subunit (Aly & Baron, 2007; Yeo *et al.*, 2003). In addition to DNA delivery T4SSs are known to be the delivery vehicle for several proteins of pathogenic bacteria including the A/B pertussis toxin of *Bordetella pertussis* (Alvarez-Martinez & Christie, 2009).

1.2.2.10 Type V secretion

Type V secretion system (T5SS; Fig 1.10 A), also termed the autotransporter pathway, involves the delivery of protein cargo by an outer membrane β-barrel translocator. Crucially, these proteins are either joined to their own translocator, or a separate but specific translocator achieves their delivery across the OM (ur Rahman & van Ulsen, 2013). Inner membrane delivery occurs via the SecYEG system. Three broad categories of T5SSs exist. The first system (type Va), described as classical autotransporters, are proteins comprised of a C-terminal β-barrel, a linker region and an adjoining N-terminal functional domain. The linker and functional domain are passed from the periplasm to the extracellular environment through the β-barrel translocator (Wells *et al.*, 2007). A single copy of this protein contains the full translocation and functional capacity. Once translocated, classical autotransporters in some cases undergo autoproteolysis to release the functional portion into the extracellular milieu; such is the case for the IgA1 protease of *N. meningitidis* (Mistry & Stockley, 2006). The second T5SS (type Vb) is known as the two-partner secretion (TPS) system; it consists of separate protein cargo and translocator β-barrel, these are referred to as TpsA and TpsB respectively (Jacob-Dubuisson *et al.*, 2013). TpsB functions to deliver TpsA into the extracellular space where it can either remain tethered to the OM translocator or released into the extracellular space; such is the case for FhaB (Melvin *et al.*, 2014). The third T5SS (type Vc) is the trimeric autotransporter. Like the classical autotransporter the trimeric autotransporter subunits consists of three domains; a translocator β-barrel, a linker region and a functional domain. The discerning feature of the trimeric autotransporter is that three subunits accociate to form a homotrimer (Cotter *et al.*, 2005a). Thus, each individual protein subunit comprises one third of the β-barrel, linker and functional domain. Structurally, the linker of trimeric autotransporters assembles into an α-helical coiled-coil triplet that forms a stalk-like projection away from the outer membrane with the functional head domain presenting on

the end of the stalk (Koretke *et al.*, 2006). The advantage of trimeric over classical autotransporters has been postulated to be the increased number of binding domains that present in the functional head group (Cotter *et al.*, 2005a).

1.2.2.11 Type VI, VII, VIII and IX secretion

The type VI secretion system (T6SS) comprises 13 core proteins and is the newest of the secretion systems to be described (Pukatzki *et al.*, 2006, 2007). The T6SS has been identified across many bacterial species, where large heterogeneity in function exists between different bacterial species. Aspects of type VI secretion are covered in the review by *Coulthurst et al* (2013). The type VII secretion system (T7SS) is a secretion system found almost exclusively in *Mycobacteria* and is not covered in any further detail (Houben *et al.*, 2014). The type VIII secretion system (T8SS) is responsible for curli biogenesis at the OM (Chagnot *et al.*, 2013). The type IX secretion system (T9SS) is restricted to Bacteroidetes and is responsible for the secretion of proteins related to gliding motility (Chagnot *et al.*, 2013).

1.2.3 Adherence

1.2.3.1 Trimeric autotransporter adhesins

The A1 bovine, A2 bovine and A2 ovine genomes of *M. haemolytica* all contain open reading frames encoding four trimeric autotransporters (Gioia *et al.*, 2006; Lawrence *et al.*, 2010). These four proteins show homology with the YadA and Hia/Hsf trimeric autotransporter of *N. meningitidis* and *H. influenzae* respectively. The *Yersinia* adhesin, YadA, is widely considered the archetypal autotransporter adhesion. It contains functional domains for binding the extracellular matrix (ECM) proteins laminin, collagen and fibronectin (Flugel *et al.*, 1994; Nummelin *et al.*, 2004; Tertti *et al.*, 1992). Collagen binding has been structurally determined for the head domain of YadA where a β-roll architecture provides a pocket for the demonstrated binding of collagen triple helices (Nummelin *et al.*, 2004). As well as adhering to ECM proteins, YadA allows for attachment to epithelial cells and in certain species even mediates cellular invasion (Heesemann & Griiter, 1987; Heise & Dersch, 2006). In addition to mediating adherence, YadA is also known to confer serum resistance through the

recruitment of complement factors H and C4bP to the cell surface (Kirjavainen *et al.*, 2008; Schindler *et al.*, 2012).

Hsf and Hia are trimeric autotransporter adhesisns of typeable and non-typeable *H. influenzae,* respectively. The coiled-coil stalk domain of Hia is much shorter than that of Hsf owing to differences in the repeat regions (Geme *et al.*, 1996), this phenomenon is attributed to the difference in polysaccharide capsule thickness between typeable and non typeable *H. influenzae*. A longer stalk segment is proposed as a requirement in typeable *H. influenza* to expose the functional head domains beyond the extent of the capsular reach (Meng *et al.*, 2008). Such a great length is not required in NTHi which lacks a polysaccharide capsule (Cotter *et al.*, 2005b; Geme *et al.*, 1996). All isolates of typeable *H. influenzae* possess the Hsf adhesin. This is contrary to NTHi where only some isolates carry the *hia* gene and of those isolates that do, most do not possess the T5SS (type Vb) high molecular weight adhesins HMW1 and HMW2 (Satola *et al.*, 2008). Functional domain characterisation has revealed that Hia has two binding domains, HiaBD1 and HiaBD2, which mediate cellular attachment to the same receptor (Laarmann *et al.*, 2002; Yeo *et al.*, 2004). Three domains with homology to those in Hia have been identified in Hsf with two of these containing an acidic pocket similar to the HiaBD1 (Cotter *et al.*, 2005b). These two domains, HsfBD1 and HsfBD2, are responsible for epithelial cell attachment, with HsfBD1 displaying a higher receptor affinity than HsfBD2 which is attributed to a single amino acid residue (Radin *et al.*, 2009).

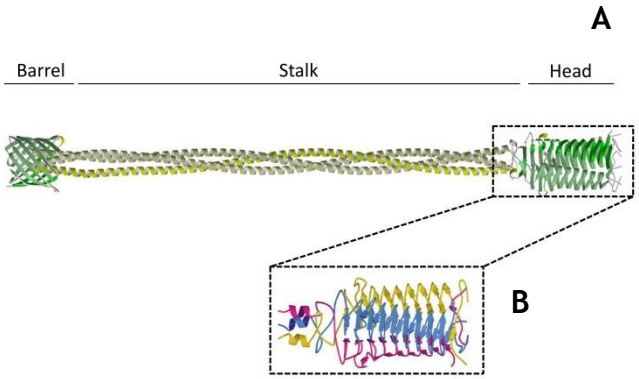

Fig 1.11 Structure of YadA
(A) Molecular model of YadA with α helices and β-sheets coloured yellow and green respectively. (B) Expanded view of the head region of YadA is shown with the three subunits of the trimer coloured yellow, blue and purple respectively.

Only one trimeric autotransporter of *M. haemolytica,* Ahs, has been characterised. This trimeric autotransporter was found to bind collagen and was demonstrated to be immunogenic in cattle (Daigneault & Lo, 2009). Ahs was also demonstrated to be expressed *in vivo* following analysis of the lung washings of challenged calves (Lo *et al.*, 2006). However, the function of this protein in the context of colonisation remains to be elucidated.

1.2.3.2 Filamentous hemagglutinin

M. haemolytica encodes a putative filamentous haemagglutinin (FHA) in its genome (Gioia *et al.*, 2006). While not well characterised in *M. haemolytica*, FHA does however share homology with the FHA of the *Bordetellae* (Gioia *et al.*, 2006). FHA is the major non-pilus adhesin of *Bordetella spp*. Differences in the colonisation properties related to FHA are observed among different Bordetella species. Adhesion is multifaceted and the protein contains domains for binding sulphated glycosaminoglycans, carbohydrates of epithelial cells and the CR3 integrin of macrophages via the RGD (Arg-Gly-Asp) repeat motif (Locht *et al.*, 1993; Menozzi *et al.*, 1994; Relman *et al.*, 1990). In *B. bronchiseptica*, FHA is necessary for the organism to colonise the lower respiratory tract (LRT), where in *B. pertussis* FHA is only necessary for URT colonisation (Cotter *et al.*, 1998; Khelef *et al.*, 1994; Pethe *et al.*, 2001). However, evidence suggests that there is functional interchangeability between the FHA of these two species (Julio *et al.*, 2009).

FHA is part of the TPS (T5SS Vb) system of autotransporters (1.2.2.10), where the functional adhesin, FhaB (TpsA) is delivered to the extracellular side of the OM via secretion through the FhaC (TpsB) translocator (Hodak *et al.*, 2006; Jacob-Dubuisson *et al.*, 1999). The structure of FhaC is that of a 16-stranded β-barrel with two POTRA domains located on the periplasmic side which function similarly to the POTRA domains of BamA in the recognition and assembly of transport cargo (Clantin *et al.*, 2004). The delivery of FhaB to the translocator barrel begins in the cytoplasm where the polypeptide chain is delivered to the periplasm via the SecYEG machinery. The polypeptide chain then undergoes C-terminal cleavage where the 340 kDa precursor is reduced to a smaller 220 kDa fragment (Renauld-monge *et al.*, 1996). The remaining 120 kDa portion of the protein acts in enhancing the secretion of the functional 220 kDa segment

(Mazar & Cotter, 2006; Renauld-monge *et al.*, 1996). The 220 kDa fragment is then inserted through the channel of FhaC in a process that involves the stepwise threading of the protein from its N terminal end. This serves not only to pass the protein across the OM but also to assemble its final structure as it has been shown that the TPS domain, which contains the TpsB signal sequence, must be unfolded for recognition and insertion by FhaC (Hodak *et al.*, 2006). The final structure consists of a long β-helical stalk which is wound with short β-sheets and turns that stack into repeating layers to construct the helical motif (Clantin *et al.*, 2004; Kajava *et al.*, 2001).

M. haemolytica produces a homologue to the FHA of *Bordetella spp.* with two clear distinctions (Gioia *et al.*, 2006). Firstly, the *M. haemolytica* FhaB does not contain a RGD integrin binding domain suggesting the protein might only be involved in carbohydrate and sulphated glycosaminoglycan binding. Secondly, contained within the amino acid sequence is a bacterial intein-like (BIL) domain. These domains function as protein cleavage points and suggest that a portion of the protein might be released to carry out additional functions or in the evasion of the host immune response. The function of FHA in *M. haemolytica* remains to be characterised.

1.2.3.3 OmpA

The OmpA protein of *M. haemolytica* has been shown to act as an adhesin of fibronectin (Lo & Sorensen, 2007). Since this initial discovery, OmpA has been shown to mediate adherence to bovine bronchial epithelial cells (Kisiela & Czuprynski, 2009). Thus, OmpA is a multifunctional protein acting as an adhesin alongside its primary role in the structure and integrity of the OM. The crystal structure of OmpA from *E. coli* reveals it to be an eight-stranded anti-parallel β-barrel with four extracellular loops connecting the transmembrane β-sheets and several short periplasmic turns (Pautsch & Schulz, 2000). The extracellular loops of OmpA in *M. haemolytica* have been shown to constitute the hypervariable portion of the protein as compared to the well conserved transmembrane domain (Davies & Lee, 2004). The loops of OmpA have also been suggested to confer species-specificity as demonstrated through the use of cross absorbed antibodies (Hounsome *et al.*, 2011). In summary, this information suggests that OmpA binds fibronectin and that the extracellular loops are surface exposed,

hypervariable and species specific. It is therefore reasonable to assume that the fibronectin binding domains involve the extracellular loops and that binding reflects adaptation to different hosts.

1.2.3.4 Mam7 / PqiB

Mam7 (originally named PqiB) was first characterised in *Vibrio parahaemolyticus* as a duel functioning constitutively-expressed adhesin that can mediate binding to the ECM protein, fibronectin and the lipid, phosphatidic acid (Krachler *et al.*, 2011). Further to this initial characterisation study it was shown that fibronectin and phosphatidic acid could be bound independently but also simultaneously by Mam7 (Krachler & Orth, 2011). Most recently, the host response to phosphatidic acid binding by Mam7 has been elucidated where it was found that binding activated GTPase causing a rearrangement in the host cytoskeletal actin (Lim *et al.*, 2014). Actin rearrangement was shown in Caco-2 monolayers to consequently cause an increase in epithelial permeability which conclusively pinpoints Mam7 as having a role in the tissue invasion of *V. parahaemolyticus*.

1.2.3.5 Opacity associated protein

The *M. haemolytica* genome encodes one orthologue to the *Neisseria spp* opacity associated proteins (Opa). These proteins are eight-stranded β-barrels that derive their name from changes exhibited in colony morphology. They function in binding to carcinoembryonic antigen cell adhesion molecule 1 (CEACAM1) of epithelial cells and neutrophils as well as binding to epithelial cell proteoglycan receptors (Duensing, 1997; Muenzner *et al.*, 2000). The adhesin has also been demonstrated to initiate the internalisation of *N. gonorrhoeae* into epithelial cells where different routes of internalisation have been mediated through the targeting of different CEACAM receptors (Billker *et al.*, 2002).

1.2.4 Enzymatic processes

Many OMPs function as enzymes contributing to aspects of cell integrity and virulence amongst other. Within *M. haemolytica* this includes the cell wall hydrolases and several virulence factors.

1.2.4.1 Peptidoglycan biogenesis

The process of peptidoglycan synthesis, in construction of the cell wall, is an enzymatic process common to all Gram-negative bacteria. The OM proteins involved include PG hydrolases and the LpoA and LpoB lipoproteins. Peptidoglycan hydrolases are a highly diverse group of enzymes (Vollmer *et al.*, 2008). The commonality between these enzymes is that they cleave various PG bonds. Functionally, this allows for the growth of the cell wall and incorporation of new peptidoglycan material. Lytic murine transglycosylases, for which *M. haemolytica* encodes three, specifically cleave the β1-4-glycosidic bond between MurNAc and GlcNac (Eidam *et al.*, 2013; Vollmer *et al.*, 2008). The other aforementioned proteins, LpoA and LpoB, are another type of OM protein involved in PG synthesis and remodelling. These adopt an elongated structure extending ≈145 Å into the periplasm where they contact with a cognate PG synthase (Jean *et al.*, 2014). LpoA and LpoB function to activate the cognate PG synthase, facilitating the incorporation of new PG material (Paradis-Bleau *et al.*, 2010; Typas *et al.*, 2010).

1.2.4.2 Serotype specific antigen

Serotype specific antigen (Ssa1) is a serine protease of the subtilase family of proteases which derive their name from their homology to the serine protease of *Bacillus subtilis*. Ssa1 was initially discovered in serotype A1 strains and derives its name from these initial studies (Lo *et al.*, 1991). Further characterisation of Ssa1 from a wider range of serotypes confirmed its presence in at least six of twelve *M. haemolytica* serotypes (Gonzalez *et al.*, 1991). Initially the function of Ssa1 was postulated as an adhesin to the URT (Gonzalez *et al.*, 1995). However, subsequent work on homologues of Ssa1 in *Actinobacillus pleuropneumoniae* and *N. meningitidis* revealed the function of these proteins as serine proteases (Ali *et al.*, 2008; Turner *et al.*, 2002). In *N. meningitidis the* NalP serine protease was identified as sharing 30% homology to *M. haemolytica* Ssa1. NalP was characterised as a classical autotransporter with the ability to autocatalytically release a 68-70 kDa fragment from its passenger domain (Turner *et al.*, 2002). In addition, antibodies against NalP were identified in the sera of patients with meningococcal infection. This has similarly been demonstrated for Ssa1 using an immunoproteomic approach with calf sera

(Ayalew *et al.*, 2010). NalP has also been shown to proteolytically process other OMPs. Namely, the App and IgA protease autotransporters (van Ulsen *et al.*, 2003). Thus, Ssa1 may also function in the post-translational processing of other OMPs. Recently, a specific role in virulence for NalP has been demonstrated where the protein was shown to cleave the C3 complement protein resulting in a decrease of C3b surface deposition (Tordello *et al.*, 2014). Even greater homology is shared between *M. haemolytica* Ssa1 and *A. pleuropneumoniae* AasP at 58% similarity (Ali *et al.*, 2008). Therefore, Ssa1 might functionally be more similar to AasP, which instead of cleaving part of its passenger domain, functions to cleave a fragment from the OlmA lipoprotein for release (Ali *et al.*, 2008).

1.2.4.3 Neuraminidase

Neuraminidase (sialidase) functions to cleave the terminal sialic acid from host carbohydrates, glycolipids, glycoproteins and gangliosides (Roggentin *et al.*, 1993). These modulate the host environment in various ways to promote bacterial colonisation of the host. Cholera toxin produced by *Vibro cholerae* requires neuraminidase to desialylate host gangliosides in order to expose the GM1 receptor for toxin binding (Galen *et al.*, 1992). In *S. pneumoniae* the NanA neuraminidase has been demonstrated as mediating the invasion of the pathogen into brain microvascular endothelial cells, a crucial step in crossing the blood brain barrier (Banerjee *et al.*, 2010; Uchiyama *et al.*, 2009). Pathogens have also been shown to decorate their LPS/LOS with sialic acid as a form of host mimicry (see section 1.1.5.2). Consequently neuraminidases can also function to remove bacterial acquired sialic acid. For example, the neuraminidase of *S. pneumoniae* has been shown to desialylate the LPS of *N. meningitidis* and *H. influenzae* (Shakhnovich *et al.*, 2002), highlighting the interspecies competition at play for these organism that colonise a common niche.

Specific roles for the *M. haemolytica* neuraminidase (NanH) have yet to be elicited. Current understanding places the NanH protein as being of the high molecular weight class of neuraminidase (Roggentin *et al.*, 1993; Straus & Purdy, 1994). This class represents neuraminidases that possess lectin domains along with a catalytic site for sialic acid cleavage (Crennell *et al.*, 1994; Moustafa *et al.*, 2004). The activity of NanH has been shown to extend to a variety of substrates with the A1 serotype exhibiting the greatest activity among the 12 *M.*

haemolytica serotypes (Straus *et al.*, 1993). The expression *in vivo* has also been confirmed with challenged goats exhibiting NanH neutralising sera (Straus & Purdy, 1994). However, a specific role in the colonisation process has yet to be reported.

1.2.4.4 IgA1 Protease

The published genomes of *M. haemolytica* have been shown to encode multiple isozymes that share homology with the IgA1 proteases of *N. meningitidis* and *H. influenzae* (Gioia *et al.*, 2006; Lawrence *et al.*, 2010). The IgA1 protease of *N. gonorrhoeae* was the first protein to be discovered as a classical autotransporter (Johannes *et al.*, 1987). These proteases contain a trypsin like domain capable of cleaving serine-proline and serine-threonine peptide bonds within recognition motifs in the hinge region of IgA1 (Mistry & Stockley, 2006). The structure of an IgA1 protease of *H. influenzae* reveals that the protein consists of a β-helical backbone, similar in structure to the β-helix of filamentous hemagglutinin (see section 1.2.3.2), flanked by several domains that amongst them contain the chymotrypsin-like active site (Johnson *et al.*, 2009). A loop occludes access to the active site until IgA is docked conferring the observed specificity of the protease. Like *M. haemolytica*, *N. meningitidis* and *H. influenzae* possess multiple isozymes which are homologous to one another yet function to cleave different peptide bonds of the IgA1 hinge region (Johnson *et al.*, 2009; Mistry & Stockley, 2006). Two key distinctions have been noted between the IgA1 protease of *M. haemolytica* and its respective orthologues in other species (Gioia *et al.*, 2006). Firstly, it has been proposed that the protein likely cleaves IgG instead of IgA as this is the main secretory antibody on the mucosal surfaces of cattle. Secondly, it has been noted that the polypeptide chain contains a domain with homology to the adhesin pertactin of *B. pertussis*. Pertactin is a classical autotransporter which functions in cell adhesion (Leininger *et al.*, 1991; Melvin *et al.*, 2014) . Pertactin's basic structure is that of a β-helix (Emsley *et al.*, 1996) Homology between pertactin and IgA protease may therefore equate to similarities in the structural spine.

1.2.5 Hypothetical proteins

A protein can be defined as 'hypothetical' when three general criteria are met. (1) There is a potential coding region in the nucleotide sequence which defines the translated 'hypothetical' polypeptide chain. (2) No experimental evidence exists to demonstrate that the nucleotide region is transcribed and translated. (3) No putative function can be assigned through homology to other well characterised proteins.

In *M. haemolytica*, the OM proteome has been hypothesised, through a bioinformatic consensus prediction system to comprise 26 (of 93) OMPs of unknown function (Hounsome, 2012). Of these 26, 11 could not be assigned an identity via homology to other proteins. Therefore, a considerable percentage of the *M. haemolytica* OM proteome remains uncharacterised. Revealing the function of these proteins and the role they play in the infection process would constitute a major advance in combatting the disease.

1.3 Modelling host-pathogen interactions within the respiratory tract

The OM represents the interface between a Gram-negative pathogen and its environment. For *M. haemolytica*, this environment is the ruminant respiratory tract. In the URT *M. haemolytica* survives as a commensal yet under certain conditions can colonise the LRT and elicit pathogenesis. Understanding how *M. haemolytica* interacts with the respiratory tract and how it may utilise its repertoire of OMPs would represent a major advance in understanding the aetiology of the disease. To accomplish this requires the use of a biological model. *In vivo* approaches utilising the natural animal host are the most representative conditions for modelling infection. However, *in vivo* modelling does not allow for much user-defined flexibility in the experimental system, and in the case of important livestock species, namely cattle and sheep, the approach is costly. *In vitro* modelling represents an advantageous alternative via a reductionist approach, user-defined flexibility and practicalities of experimentation. Thus, development of an *in vitro* respiratory tract model to study the host-pathogen interactions of *M. haemolytica* would allow for new insight into the disease process.

1.3.1 Structure and function of the respiratory tract

Anatomically the respiratory tract is divided into two sections, the upper and the lower. The URT comprises the larynx, nasopharynx, oropharynx and laryngopharynx. The LRT comprises the trachea, the bronchi, the bronchioles and the alveoli where gas exchange with the cardiovascular system occurs. In the upper regions of the trachea and the bronchi the epithelium is arranged into a pseudo-stratified layer. The smaller bronchi, bronchioles and further sub-divisions are arranged into a simple columnar morphology. This structure represents the interface between the inhaled air of the environment and the body. Various cell types, including basal, ciliated, goblet and Clara, combine to form the epithelial lining. These cells function together to create structural support and a first line of defence against invading microorganisms.

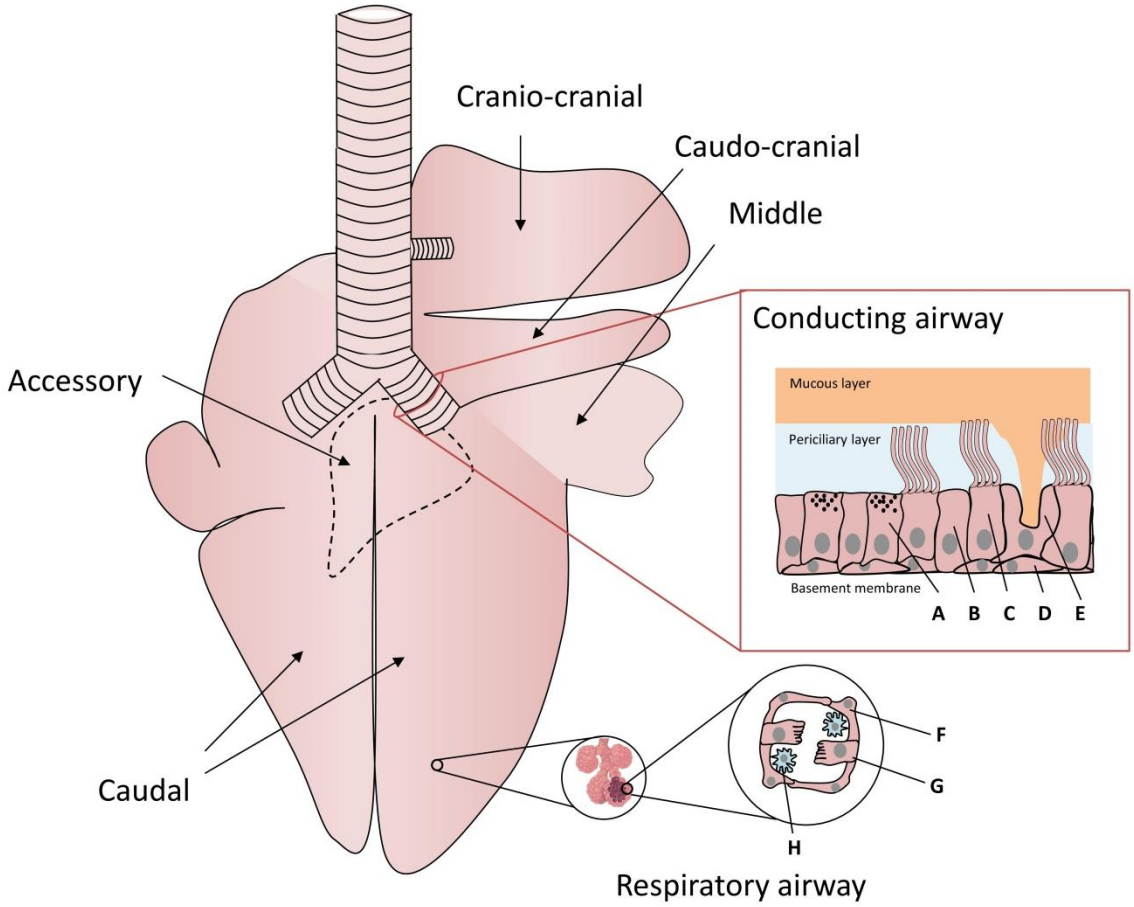

Fig 1.12 Anatomy of the bovine lung.
Labelled with arrows is the lung lobe nomenclature. Expansion panels show conducting and respiratory airways. Cell types are labelled as follows, (A) Clara cell, (B) intermediate cell, (C) ciliated cell, (D) basal cell, (E) goblet cell, (F) type I pneumocytes, (G) type II pneumocytes and (H) alveolar macrophage.

1.3.2 Cell Types of the respiratory epithelium

1.3.2.1 Basal cells

Basal epithelial cells are attached to the basement membrane and are not exposed to the lumen as are ciliated and goblet cells. The columnar cells that protrude into the lumen reach the basement membrane but are tethered to the well-anchored basal cells (Evans *et al.*, 2001). Basal cells make contact on their underlying side with mesenchymal stem cells and neurons underlying the basal lamina. Mouse studies have revealed these cells to function as progenitors to the other cell types in the respiratory epithelium where they act as a source for cell replenishment during development and repair (Hackett *et al.*, 2011; Rock *et al.*, 2009). There is evidence that human basal cells act as progenitors to secretary cell types as well as ciliated cells. This has been inferred by the ability of cultured basal cells to self-renew and form ciliated and secretory cells in a tissue culture model (Rock *et al.*, 2010). During repair basal cells infiltrate damaged epithelium and differentiate to repopulate areas devoid of epithelial tissue (Pardo-Saganta *et al.*, 2015). More recent work has tracked the fate of basal cells in the respiratory tract of mice (Watson *et al.*, 2015). Basal cells were found to differentiate into a short-lived basal-like progenitor followed by differentiation into secretory cell phenotypes. These secretory cells were identified as self-replicating and capable of terminal differentiation into ciliated cells. Thus, the model for differentiation from basal to ciliated cell proceeds via secretory cells.

1.3.2.2 Ciliated cells

Ciliated epithelial cells are a differentiated cell type with long filamentous projections called cilia that extend between 5 and 10 μm into the lumen of the respiratory tract (Lai *et al.*, 2009). The cilia are the defining feature of this cell type. They consist of 9 pairs of microtubules arranged around a central pair; other structural proteins connect the main microtubule framework together Fig 1.13). At the base of each cilium lies the basal body which anchors the cilium to the plasma membrane. The basal body structure is identical to that of a centrosome consisting of 9 triplet microtubules (Vladar & Stearns, 2007). Dynein motor proteins, connected to the 9 outer columns of microtubules, act in synchronisation to pull one microtubule doublet relative to adjacent doublets.

This process allows for the cilium to beat. The entire microtubule structure is covered in the cell membrane and one ciliated cell contains many functional cilia. Ciliated cells are located at the interface between the exposed air of the respiratory tract and the underlying tissue of the body. In the pseudostratified epithelium they make contact with the basal cells and the basement membrane (Hodson, 1977).

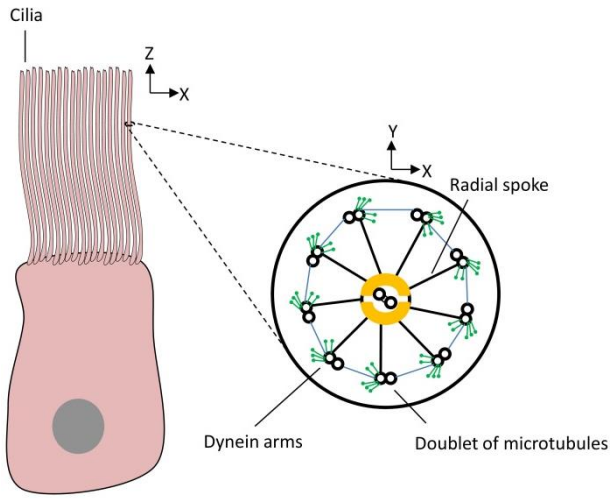

Fig 1.13 Diagram of a ciliated cell
Ciliated epithelial cell orientated along the axis of polarisation where apical cilia face into the luminal space. A cross section of a cilium displays the 9+2 arrangement of microtubule pairs, connected by radial spoke proteins and powered for movement through the dynein motors attached to each of the nine outer microtubule doublets.

1.3.2.3 Goblet cells

Goblet cells, like ciliated cells, are tethered to the basement membrane and protrude towards the lumen of the respiratory tract. Their presence extends from the trachea down into the bronchi but not as far as the bronchioles (Widdicombe, 2002). This cell type contains mucous granules that produce and secrete the mucin glycoproteins that coat the respiratory epithelium.

Mucins are designated MUC with a following number (eg. MUC5, MUC8 etc.). Currently 20 human variants are known and they can be placed in two main categories: Those that are secreted and those that are tethered to the epithelial membrane (Pearson & Brownlee, 2005).

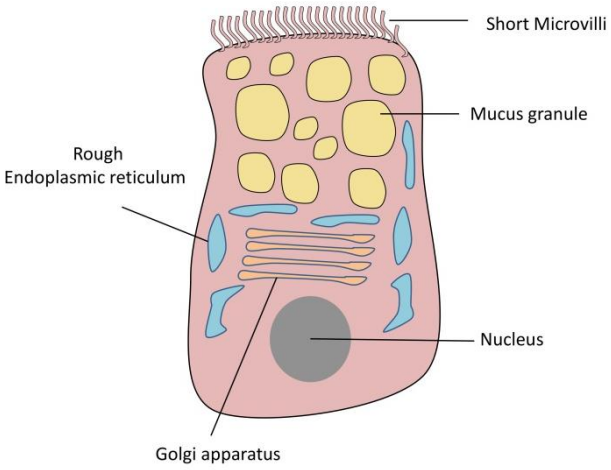

Fig 1.14 Diagram of a goblet cell
Displayed is a basic diagram of a goblet cell orientated along the axis of polarisation. Microvilli cover the apical face (luminal side) of the goblet cell.

Structurally, the mucin glycoproteins consist of a core variable number of tandem repeats (VNTR) that links the amino acid residues serine and threonie via N-acetylgalactosamine to a variety of carbohydrate molecules including N-acetylglucosamine, glactose, fucose, mannose and sialic acid. The VNTR domain is the only feature of these proteins in common with one another (Allen *et al.*, 1998). Goblet cells can regulate their levels of mucous production according to external stimuli such as the presence of bacterial LPS or the proinflammatory cytokines, interleukin-1, interleukin-6, interleukin-8, and TNF-α (Pearson & Brownlee, 2005). These serve to increase the levels of mucin glycoproteins being secreted. As one strategy for bacterial adherence involves binding to surface glycoproteins, the secreted mucin can act as a false surface to bind and trap invading microorganisms in the mucous layer. Recently, it has been shown that secretory cells have the capacity to revert to a basal cell phenotype when the respiratory epithelium is devoid of basal cells (Tata *et al.*, 2013). This demonstrates the plasticity available to respiratory epithelial cells in self-regulating population levels.

1.3.2.4 Clara cells

Clara cells are another type of non-ciliated secretory epithelial cell. Clara cells function to destroy immobilised toxins in the mucosal epithelial cell lining, secrete antimicrobial agents, activate the innate immune system by the release of cytokines and differentiate into other cell types (Reynolds & Malkinson, 2010).

They are the main secretory cell in the bronchioles and terminal bronchioles where goblet cells have little or no presence (Widdicombe, 2002).

The progenitor capacity of Clara cells allow them to reprogram themselves and differentiate into either the mucus-secreting phenotype or into a fully differentiated ciliated cell (Reynolds & Malkinson, 2010). Once fully differentiated their reprogramming capacity is lost. Recently, it has been discovered that the progenitor differentiation ability is attributed to the Foxm1 cell cycle transcriptional factor (Ustiyan *et al.*, 2012). The full picture of Clara cell differentiation remains to be elucidated.

1.3.2.5 Immune cells

The respiratory epithelium contains numerous immune cells that function in fighting invading microorganisms. The alveolar macrophage is a cell of the immune system specifically adapted to the lung. Alveolar macrophages reside in the lumen of the airways and display several markers that differentiate them from interstitial and peritoneal macrophages (Hussell & Bell, 2014). Another resident immune cell of the respiratory epithelium is the dendritic cell (DC). These reside below the respiratory epithelium and serve as antigen-presenting cells (Reis e Sousa, 2004). Thus, DCs represent the interface between the innate and adaptive immune system. Once DCs are activated they purposely prime naïve T-cells to combat invading microorganisms. Indeed, aside from DCs and alveolar macrophages, numerous other immune cells are present in the lung at any one time, particularly following pro-inflammatory stimuli; these include neutrophils, T lymphocytes and B lymphocytes.

1.3.2.6 Other cell types

Although basal, ciliated, goblet and Clara cells represent the main constituents of the respiratory epithelium, more than 40 cell types have been identified in total (Bérubé *et al.*, 2010a). Among these other cell types include intermediate cells and fibroblasts. Intermediate cells are in contact with the basal lamina, but do not reach the surface of the lumen (Bérubé *et al.*, 2010b). Fibroblasts synthesise extracellular matrix. This, in the context of the respiratory

epithelium, involves the construction of the basement membrane upon which the epithelium sits.

The terminal portion of the lung consists of the alveoli which comprise their own unique cell type, the type 1 and type 2 pneumocytes. Type 1 pneumocytes are responsible for gas exchange where their basolateral side is fused to endothelial cells of the circulatory system. Type 2 pneumocytes serve as progenitors and secretory cells in this terminal portion of the lung (Bérubé *et al.*, 2010a).

1.3.3 Junctional complexes

Cells of the respiratory epithelium are joined to one another through four junctional complexes: tight junctions, adherens junctions, desmosomes and gap junctions. These junctional complexes produce barriers, provide mechanical strength and are involved in cell-cell communication.

Proceeding from the apical face, the first kind of junctional complex encountered is the tight junction complex (Fig 1.15 A). Tight junctions serve two main purposes. Firstly, they segregate the membranes of polarised epithelial cells into apical and basolateral portions, preventing the diffusion of integral membrane proteins between these two regions (Hartsock & Nelson, 2008). Secondly, via the adjoining of neighbouring cells they produce an impenetrable barrier between the luminal extracellular space and the underlying tissue (Hartsock & Nelson, 2008). The tight junctional complex comprises several transmembrane proteins including Jam-A, occludin and members of the claudin family (Feldman *et al.*, 2005; Niessen, 2007). These proteins link to one another across the paracellular space resulting in the joining of neighbouring cells. On the cytoplasmic side, these transmembrane proteins contact other proteins of the complex including members of the zona occludin family (ZO-1, ZO-2, ZO-3) and several others. These proteins link to the actin cytoskeleton.

Located below the tight junction level is the adherens junction complex (Fig 1.15 B). Transmembrane cadherins provide the intracellular connection. Catenins α and β form the cytoplasmic link between the transmembrane cadherins and the actin cytoskeleton (Drees *et al.*, 2005). Overall, the function of the adherens junction is less defined compared with the tight junction.

Functional roles include stabilisation of cell adhesion, actin regulation, as well as intercellular and intracellular communication (Hartsock & Nelson, 2008).

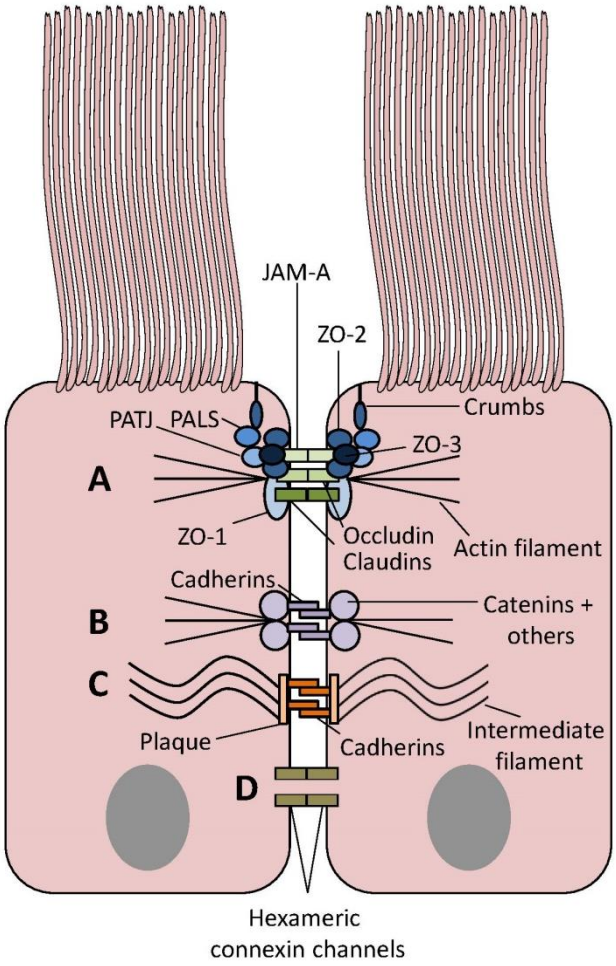

Fig 1.15 Junctional complex overview
Diagrammatic representation of the four types of epithelial junctional complex. (A) tight junction, (B) adherens junction,(C) desmosome and (D) gap junction.

Desmosomes (Fig 1.15 C) are junctional complexes that provide mechanical strength to cells of the respiratory epithelium (Garrod & Chidgey, 2008). Transmembrane cadherin proteins make strong intracellular connections to one another (Garrod & Chidgey, 2008). These are joined to linker proteins that form a dense plaque on the cytoplasmic side and this is, in turn, linked to intermediate filaments (North *et al.*, 1999). The Intermediate filaments involved in desmosomes are keratin-based cytoskeletal structures. Heterodimerisation of acidic and basic keratins allow for the structural assembly

of intermediate filaments (Hatzfeld & Franke, 1985). These confer the mechanical strength upon the cell.

Gap junctions are the most basally located of the junctional complexes (Fig 1.15 D). Structurally, the gap junction consists of a transmembrane channel built from six connexin subunits (Evans & Martin, 2002). The channel creates an opening of 35 Å in diameter and constricts to 14 Å in diameter at the contact point with the gap junction of a neighbouring cell (Maeda *et al.*, 2009). Gap junctions create a cell to cell channel that allows for the free diffusion of ions and small molecules between cell cytoplasms (Kumar & Gilula, 1996).

1.3.4 The mucociliary escalator

The cells of the respiratory epithelium (Fig 1.16) function to provide a barrier between the environment and the underlying tissue. A multitude of inhalants require clearance from the lungs including pollen, dust particles, xenobiotic chemicals and microorganisms. The clearance of these irritants is necessary to preserve the lungs working capacity. A process referred to as mucociliary clearance (Fig 1.16) removes particles and microorganisms that become entrapped in the viscous mucous layer produced by the secretory cells.

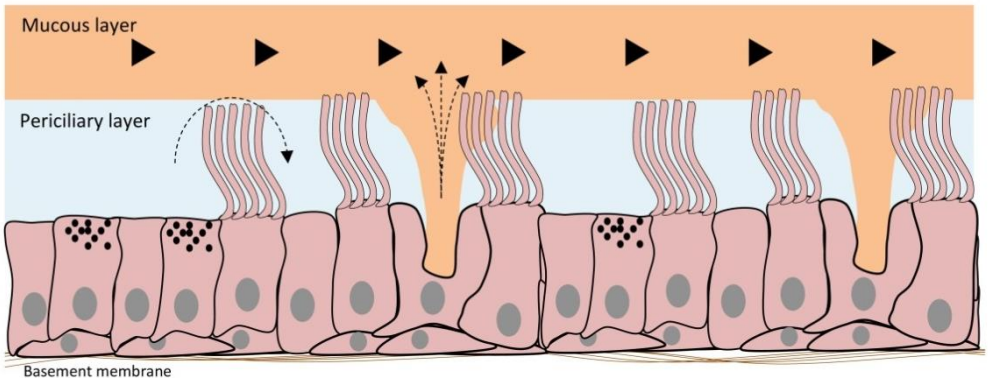

Fig 1.16 Schematic representation of the mucocillary escalator.
Cilia (thin hair like projections) beat in the low viscosity periciliary layer with an asymmetric and cell to cell coordinated beat pattern. The beating action of the cilia serves to drive mucus, produced by goblet cells, up the respiratory tract. Inhalants such as microorganisms and dust particles are trapped in the mucus layer and cleared from the respiratory tract. Separation between the non-Newtonian viscous mucous layer and low viscosity periciliary layer is maintained in order to preserve the transport properties of the escalator

Once trapped, inhalants are carried towards the larynx in the mucous layer by the beating action of the cilia that protrude into the lumen (Cone, 2009). The cilia sweep to a rhythmic synchronicity in the periciliary layer which is less viscous than that of the overlying mucosal layer. The tips of the cilia pass into the mucous at the apex of one beat cycle (Widdicombe, 2002). Mucus, being a non-Newtonian fluid, permits a decrease in local viscosity as the cilia increase the shear stress of the fluid; this allows the cilia to efficiently propel the mucosal layer without impeding their motion (Cone, 2009; Lai *et al.*, 2009). The coordinated action draws the mucous and entrapped inhalants up to the larynx. Mucous containing particulate inhalants and microorganisms can then pass via the oesophagus into the harshly acidic environment of the stomach for breakdown. Separation of mucus and periciliary layers is maintained by the tethered mucins and proteoglycans that create an exclusion mesh (Button *et al.*, 2012). This creates a size selective gradient that allows for deeper penetration of low-molecular-mass versus high-molecular-mass species, consequently preserving layer separation.

The mucosal layer not only provides physical entrapment by its viscosity but chemical entrapment. As the mucin proteins present in this layer can be as much as 80 percent glycosylated by mass (Allen *et al.*, 1998), and many of the bacterial proteins involved in adhesion target the glycosylated cell surface receptors on eukaryotic cells (Virji, 2005), the mucosal layer therefore acts as a false surface to invading bacteria that would otherwise adhere to the epithelial cells (Virji, 2005).

1.3.5 Innate immunology of airway secretions

1.3.5.1 Cationic peptides

Cationic peptides are antimicrobial peptides that stick to the negatively charged outer leaflets of bacterial OMs and form membrane-destroying pores (Zasloff, 2002). In this manner they take advantage of the differences between the membranes of Gram-negative bacteria and multicellular organisms, since the latter lack charge on their membrane outer leaflet. Cationic peptides are subdivided into various classes, designated I-IV, all of which function in a similar manner but are distinguished on the basis of different structural features such as

α-helical or ß-sheet content, amino acid content and cyclisation (Grubor *et al.*, 2006). Expression of cationic peptides following *M. haemolytica* challenge has revealed that the ovine-specific defence peptides, sheep β-defensins 1 and 2, are downregulated 24 h post infection suggesting that they are Nf-κB independent (Ackermann *et al.*, 2004). This is in contrast to the bovine defensins tracheal antimicrobial peptide (TAP) and lingual antimicrobial peptide (LAP), which demonstrate increased expression following *M. haemolytica* challenge (Caverly *et al.*, 2003; Stolzenberg *et al.*, 1997).

1.3.5.2 Lysozyme

Lysozyme is a 14 kDa enzyme found on the mucosal surfaces of multicellular organisms (Grubor *et al.*, 2006). The enzyme functions in hydrolysing the covalent bond between N-acetylmuramic acid and N-acetylglucosamine of the peptidoglycan cell wall (Chipman & Sharon, 1969). Lysozyme is produced by a variety cell types including epithelial cells of the respiratory tract. Here, lysozyme has been shown to contribute directly to host survivability following infection of transgenic mice (Akinbi *et al.*, 2000). Lysozyme alone is sufficient to mediate killing of Gram-positive bacteria. However, for Gram-negative species lyzosyme alone is bacteriostatic and only becomes bactericidal with the cooperative action of lactoferrin (Ellison & Giehl, 1991).

1.3.5.3 Lactoferrin

Lactoferrin is an 80 kDa protein that is found on mucosal surfaces including the respiratory tract and, along with lysozyme, constitutes the most abundant antimicrobial product secreted into the lumen (Lonnerdal & Iyer, 1995; Travis *et al.*, 1999). The predominant function of lactoferrin is as a host iron scavenging protein although it also has an N-terminal antimicrobial domain (Bellamy *et al.*, 1992). Lactoferrin is produced by neutrophils and epithelial cells, the latter of which has been shown to produce lactoferrin following heavy metal binding of cell-surface receptors (Ghio *et al.*, 1999; Masson *et al.*, 1969). Bacteria from the families *Neisseria* and *Moraxella* possess lactoferrin uptake proteins, LbpA and LbpB (Gray-Owen & Schryvers, 1996), that function similarly to the more widely distributed transferrin binding proteins (1.2.2.3.1), highlighting that in some pathogenic bacteria lactoferrin can also constitute a source of iron.

1.3.5.4 Anti-proteases

This class of proteins consists of several low molecular weight cationic proteins that contain numerous disulphide bonds (Grubor *et al.*, 2006). Contained within this class are secretory leukocyte protease inhibitor (SLPI), elafin and the phospholipase A2 family enzymes, all of which broadly function in the inhibition of one or more bacterial proteases (Six & Dennis, 2000; Thompson & Ohlssont, 1986; Wiedow *et al.*, 1990). Of these, SLPI and elafin are secreted by a wide variety of cell types including various epithelial cells of the respiratory epithelium (Grubor *et al.*, 2006). Enzymes of the phospholipase A2 family are known to be secreted by macrophages and have been shown to be secreted from the BEAB-2 cell line *in vitro* (Gimenez *et al.*, 2004; Lindbom *et al.*, 2002).

1.3.5.5 Collectins

Collectins are a large family of proteins that share a common structural theme of a C-terminal lectin domain and an adjacent collagen-like domain (Grubor *et al.*, 2006). Notably, three collectins, CL-43, CL-46 and conglutinin, are found exclusively in bovidae (Hansen & Holmskov, 2002). Surfactant proteins A and D (SP-A and SP-D) are some of the most extensively characterised collectins. Both SP-A and SP-D are expressed by alveolar type II cells and Clara cells (Crouch *et al.*, 1992; Ogasawara *et al.*, 1992). Collectins have a triple functional role of antimicrobial agent, proinflammatory stimulator and anti-inflammatory stimulator (Grubor *et al.*, 2006). Neonatal lambs challenged with PI-3 have statistically significant higher levels of SP-D in their lungs relative to control groups (Grubor *et al.*, 2004a). In contrast, lambs challenged with *M. haemolytica* have shown no increase in SP-D expression at day one post exposure and a stark reduction at day 15 day post exposure (Grubor *et al.*, 2004b). This disparity is indicative of the multiple roles that collectins have in the mucosa.

1.3.6 Microbial colonisation of mucosal surfaces

The respiratory tract provides a strong defence against microorganisms. However it can still succumb to invading bacteria which utilise various mechanisms to establish colony formation. Many bacterial species can cause respiratory disease. Some of the more well-known human pathogens include *Mycobacterium tuberculosis* which causes tuberculosis, accounting for millions

of deaths annually (WHO, 2012), and *B. pertussis* which causes Whooping cough, and is responsible for high mortality in infants (Cherry, 2005). Other bacterial pathogens do not ordinarily colonise the respiratory tract yet are infectious under certain adverse conditions. An example of this is cystic fibrosis (CF). In CF, the early stages of the disease are characterised with common infectious agents such as *H. influenzae* and *P. aeruginosa*. However, during later stages of the disease infection by atypical species such as *Burkholderia cepacia, Stenotrophomonas maltophilia and Alcaligenes xylosoxidans* is observed leading up to the individuals demise (Davies *et al.*, 2007). A parody can be drawn with BRD in cattle. Predisposing viral infection and environmental stress produce changes to the host respiratory mucosa allowing for secondary bacterial infection (Grissett *et al.*, 2015). Understanding the conditions that allow for bacterial colonisation and how *M. haemolytica*, the principal bacterial pathogen in BRD, establishes colonies would greatly enhance the understanding of this important veterinary disease.

1.3.6.1 Microbial targets of adherence

The most important factor in bacterial colonisation of the respiratory tract is the initial adherence to host tissue. Adherence is a requirement for the initiation of the colonisation process and is the preceding factor to many more deleterious effects such as biofilm formation, cellular invasion and toxin secretion (Virji, 2005). Targets of bacterial adhesins include the macromolecular components available in the respiratory tract. These include glycoproteins (Reneer *et al.*, 2006), glycosaminoglycans (GAG) (Menozzi *et al.*, 1994), ECM proteins (Chagnot *et al.*, 2012), integrins (Chagnot *et al.*, 2012; Patti *et al.*, 1994), ICAMs (Avadhanula *et al.*, 2006) and CEACAMs (Gray-Owen & Blumberg, 2006). All these components serve in many pathogens as the targets for attachment often facilitating adhesion during different stages of colonisation whereby different receptors are encountered.

1.3.6.1.1 Glycosaminoglycans

One of the most accessible adhesion targets that many bacterial pathogens exploit is the proteoglycan macromolecules. These serve as targets based on their cell-surface presence and distribution in the void space of the ECM (Virji,

2005). Proteoglycans consist of a glycoprotein backbone decorated heavily with covalently bound GAG side chains (Gandhi & Mancera, 2008). Glycosaminoglycans are ≈100 kDa unbranched hetropolysaccharides, all of which, with the exception of hyaluronic acid (HA), are covalently attached to proteins. Many structural variations exist. However, the common themes can be summarised as follows. The repeating unit is a disaccharide, usually with one unit of uronic acid and one unit of either N-acetyl-D-glucosamine (GlcNAc) or N-acetyl-D-galactosamine (GalNAc). Either unit of the disaccharide can be sulphated (with the exception of HA) and the polymer, as a result, will carry a large negative charge (Gandhi & Mancera, 2008). The functions of GAGs are also rather varied but can be summarised as having roles in chemokine activation, cell-matrix interactions and, most importantly, wound repair where inflammation, thrombin initation and cell matrix interactions all converge (Gandhi & Mancera, 2008; Taylor & Gallo, 2006). Bacterial targeting of GAGs has been described for various respiratory pathogens (Lin *et al.*, 2015a, b; van Putten *et al.*, 1998; Raymond *et al.*, 2015). Specifically, in *M. haemolytica* a protein, *Mannheimia haemolytica* adhesin (Mha), has been identified that demonstrates specific binding to GlcNAc, N-Acetylneuraminic acid (NeuAc) and polymer derivatives of these sugars (Jaramillo *et al.*, 2000). Functional characterisation has shown Mha to induce oxidative bursts in bovine neutrophils (De la Mora *et al.*, 2006). Purification of the receptor from neutrophils has confirmed the target of adherence to be a 165-kDa heterodimeric proteoglycan containing GlcNAc and NeuAc sugars (De la Mora *et al.*, 2007). Whether additional GlcNAc and NeuAc containing targets exist for Mha on other cell types remains unknown.

1.3.6.1.2 Extracellular Matrix

Extracellular matrix proteins represent another large class of bacterial adherence targets. The ECM functions as an intracellular framework for the adhesion of various cell types that comprise a tissue. Within this framework, collagen acts as the main structural component, elastin also acts as a structural component providing elasticity (Mouw *et al.*, 2014). Cells attach to these structural components via membrane integrins. Fibronectin acts as a binding intermediate between a cells integrin and collagen (Mouw *et al.*, 2014). Laminin

also acts as an intermediate in integrin binding and can also form separate networks (Mouw *et al.*, 2014).

Bacterial adhesins that target ECM proteins are collectively referred to as microbial-surface-components-recognising-adhesive-matrix-molecules (MSCRAMM) (Patti *et al.*, 1994). MSCRAMMs, like many adhesins, function in binding multiple host targets. This is the case for the trimeric auto transporter adhesin, YadA, which possesses domains capable of binding to fibronectin, laminin and collagen (Koretke *et al.*, 2006) and the classical autotransporter Hap of *H. influenzae* which can bind collagen IV, laminin and fibronectin through motifs in the C terminus of its passenger domain (Fink *et al.*, 2003). MSCRAMMs that bind multiple targets are not limited to ECM proteins. This is observed for the YadA protein of *Yersinia enterocolitica*, which, in addition to ECM binding has a polymorphic nuclear leukocyte binding domain (Cornelis *et al.*, 1998). Other adhesins can act as MSCRAMMs in addition to GAG binding as is the case for OpaA of *N. gonorrhoeae* (van Putten *et al.*, 1998). The OpaA protein has been demonstrated to mediate initial binding to the proteoglycan – syndecan, followed by a second interaction with the $\alpha\beta_1$ integrin mediated via fibronectin (van Putten & Paul, 1995; van Putten *et al.*, 1998). This secondary interaction then promotes the internalisation of *N. gonorrhoeae* into mucosal epithelial cells. This is a theme that is repeated in other bacterial pathogens, i.e. ECM binding precedes cellular internalisation. For example, YadA, has been demonstrated to preferentially mediate the internalisation of *Y. pseudotuberculosis* over the classical invasion protein, invasin (InV), when fibronectin is available (Hudson *et al.*, 2005). More recently, it has been shown that YadA mediates its fibronectin-based adherence through the ß1-based integrins on fibroblasts and αv-based integrins on epithelial cells, and that this binding initiates T3SS effector delivery (Keller *et al.*, 2015). A similar effect within this pathogenicity theme can be observed with collagen. In *Legionella pneumophila* it has been demonstrated that collagen binding through the macrophage infectivity potentiator (Mip) precedes transmigration through lung epithelial monolayers (Ünal *et al.*, 2011). This extends to Gram positive organisms such as *Streptococcus pyogenes* where it has been shown that fibronectin binding by one domain of the *Streptococcal* fibronectin binding

protein (Sfbl) allows for internalisation via binding of a second domain (Talay *et al.*, 2000).

In the case of *M. haemolytica* several MSCRAMMs have been identified including a YadA homologue (Gioia *et al.*, 2006), a collagen-binding trimeric autotransporter, Ahs (Daigneault & Lo, 2009), and the OmpA protein which has been demonstrated to bind fibronectin (Lo & Sorensen, 2007). How each of these is involved in the colonisation process and whether any contribute to such processes as cellular invasion remains to be characterised.

1.3.6.1.3 Cell surface receptors: CEACAMs, integrins and ICAMs

Eukaryotic cell surface receptors that serve as binding targets for microorganisms principally include CEACAMs, integrins and ICAMs. These classes of proteins are functionally similar in that they serve as eukaryotic adhesins to various targets.

CEACAMS. A principle target of bacterial adherence is the CEACAM family of proteins. This family of molecules are involved in cell-to-cell adherence via non-glycosylated β-sheets present in the extracellular portion of the protein (Gray-Owen & Blumberg, 2006). CEACAMs 1, 5, 6 and 7 are expressed on epithelial cells with CEACAM 1 also being widely distributed amongst endothelial, lymphocytes and myeloid cells and CEACAM 6 is expressed by granulocytes (Gray-Owen & Blumberg, 2006). A single CEACAM type can exist in various isoforms based differences in exon splicing (Gray-Owen & Blumberg, 2006). CEACAMs can associate on the cell surface in the form of cis-homodimers between single CEACAMs. However, association between CEACAMs in cell-to-cell interactions is possible between different CEACAMs (Gray-Owen & Blumberg, 2006). The archetypal family of adhesins that target CEACAMs is the Opa proteins of *Neisseria spp.* Different Opa variants exist in different species of *Neisseria* as well as in organism of other bacterial families (Brooks *et al.*, 2006). Within *N. meningitidis* alone extensive genetic recombination and gene duplication has been identified reflecting the variation in the molecular targets of the Opa proteins (Hobbs *et al.*, 1994). Within *N. meningitidis,* functional characterisation of nine Opa variants served to show that two of the variants could bind multiple CEACAMs, five could bind a single CEACAM and two could

bind no CEACAMs (Muenzner *et al.*, 2000). Cellular invasion could also be attributed to seven of the nine CEACAM-binding Opa variants suggesting the two remaining variants have roles distinct from that of the other Opa adhesins (Muenzner *et al.*, 2000). Further characterisation has revealed that hyper-invasive strains of *N. meningitidis* possess certain variant combinations of Opa proteins (Callaghan *et al.*, 2006). A single Opa variant that confers internalisation can mediate this effect through different mechanistic pathways. This has been demonstrated in *N. gonoroheae* where a single Opa variant can mediate internalisation following binding of either CEACAM1, CEACAM3 or CEACAMs 5/6 (Mccaw *et al.*, 2004). Thus, Opa proteins display functional diversification for targeting different CEACAMs and can exploit different pathways to mediate uptake upon binding.

Integrins. The integrin class of cell-surface receptors comprise many transmembrane proteins. The extracellular portion of integrins connects to the ECM, the cytoplasmic portion couples to the actin cytoskeleton (Giancotti & Ruoslahti, 1999). Thus, integrins function in cell-matrix adherence. The interaction between the ECM and integrins involves recognition and binding through the RGD domain on fibronectin (Leahy *et al.*, 1996). Many different microbial adhesins exploit mimicry of this domain to allow for adherence to cell surface integrins (Barden *et al.*, 2013; Dawid *et al.*, 2001; Huang *et al.*, 2006; Johnson *et al.*, 2011; Zhang *et al.*, 2012a; Zimmermann *et al.*, 2010). The most extensively characterised RGD domain containing adhesin is the FHA protein of *Bordetella spp.* This adhesin allows for the RGD-mediated binding of leukocytes through the surface integrin LRI (leukocyte response integrin) (Ishibashi *et al.*, 1994). This interaction stimulates the upregulation of a second integrin, CR3 ($\alpha_M\beta_2$, CD11b/CD18), which can allow for a second binding through the RGD binding domain of FHA (Ishibashi *et al.*, 1994; Relman *et al.*, 1990). Beyond adherence, integrin binding by the RGD domain can precede cellular invasion. This has been shown for the RGD domain of FHA in *B. pertussis* which can bind the α5β1 integrin, allowing for epithelial invasion (Ishibashi *et al.*, 2001). Not all bacterial integrin binding proceeds through the use of an RGD domain-containing adhesin. The P66 transmembrane porin of *Borrelia burgdorferi* binds β_3 and some β_1 integrins. Binding is not necessary for infection but it has been

shown to facilitate transfer across endothelial cell monolayers (Ristow *et al.*, 2015).

ICAMs. Another target for bacterial adherence is the ICAM family. Five different types of ICAM receptor exist. Of these, ICAM-1 is the most widely distributed (Yang, 2012) and is expressed on the surface of a range of cell types including endothelial cells, epithelial cells and macrophages (Radi *et al.*, 1999). The ICAM-1 receptor is the target for the attachment of two β2 integrin leukocyte receptors, LFA-1 and MAC-1 (Radi *et al.*, 1999). The physiological purpose of ICAM-1 is to tether various immune cells to endothelial and epithelial cells to allow migration through tissue in response to cytokine gradients (Millán *et al.*, 2006; Yang *et al.*, 2005). An example of an ICAM acting as a receptor for bacterial adherence is the attachment of NTHi. In this example, the bacterium mediates attachment to ICAM-1 through the use of P5 fimbriae (Avadhanula *et al.*, 2006). In addition to ICAM-1 mediated attachment, P5 fimbriae of *H. influenzae* have also been shown to utilise CEACAM1 for binding (Hill *et al.*, 2001). Thus, a single adhesin can function in binding these two distinct targets. More recent studies have demonstrated P5 to be the major adhesin to the respiratory tract (Euba *et al.*, 2015), where knockout of the protein results in a statistically-significant decrease in both adherence and invasion of respiratory epithelial cells. As many pathogens, including *M. haemolytica* have been demonstrated to upregulate ICAM-1 during infection (Frick *et al.*, 2000; Ishibashi & Nishikawa, 2002; Krunkosky *et al.*, 2007; N'jai *et al.*, 2013; Radi *et al.*, 1999; Vieira *et al.*, 2007), it is possible that many of these organisms also take advantage of the change in tropism and mediate binding to ICAM receptors.

1.3.6.2 Biofilm formation

Microbes have two distinct growth states, planktonic and biofilm. Which state a microbe survives and replicates in largely depends on the availability of nutrients although other factors are involved. The planktonic state can be defined as microbes replicating autonomously in a liquid medium where free movement is permitted (Marshall, 2006). In the biofilm state microbes form a cooperative multicellular community anchored to a surface. Adhesion is maintained through the secretion of macromolecular material that forms a matrix to hold the bacterial cells together and attach them to the surface

(Flemming & Wingender, 2010). The microbial population can either be homogenous or heterogeneous in the species diversity that composes the biofilm (Cole *et al.*, 2004; Moller *et al.*, 1996). The development of a biofilm is a process that involves multiple stages beginning with adherence to a surface (Fig 1.17).

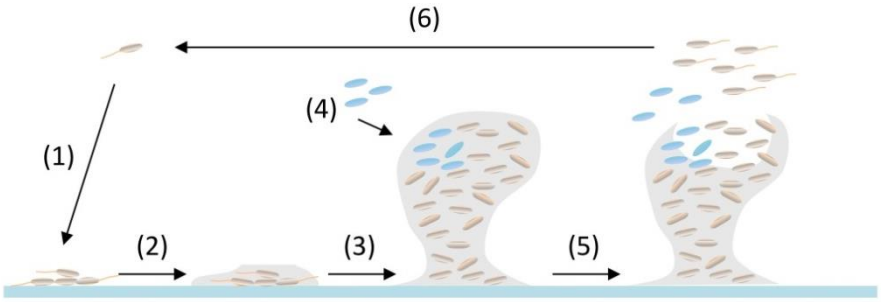

Fig 1.17 Biofilm formation process.
Planktonic bacteria initially adhere to a surface and form a microcolony (1). Bacteria in the microcolony begin to produce EPS material (2). Cooperation amongst individual cells allows the biofilm grow and mature into a complex structure (3). Other bacterial species may colonise the biofilm (4). Biofilm maturation terminates with the dispersal of cells into the planktonic state. The entire process can be repeated (6)

Once bacteria have adhered, a microcolony can form that involves the secretion of extracellular polymeric substance (EPS) that acts as a matrix for the developing biofilm (Bjarnsholt *et al.*, 2013). Maturation of the biofilm involves formation of mushroom-shaped structures. This has been shown to involve motile bacteria climbing a 'stalk' of non-motile cells through the use of pili to form the 'cap' region (Klausen *et al.*, 2003). During growth of the biofilm structure, channels form to allow for diffusion into the central areas of the biofilm (Stanley & Lazazzera, 2004). In *P. aeruginosa*, channel development has been shown to occur through the action of rhamnolipid which acts as a surfactant to reduce surface tension (Davey *et al.*, 2003). The final development stage involves dispersion of bacterial cells from the biofilm back into the planktonic state. This can either occur randomly through shear forces (Bjarnsholt *et al.*, 2013) and following temperature changes (Kaplan & Fine, 2002), or through controlled means such as the secretion of enzymes that allow for release from the matrix (Kaplan *et al.*, 2003).

Microorganisms can produce biofilms in a wide variety of environments, including various tissues of multicellular organisms. Such tissues represent a niche for biofilm formation and certain pathologies are hallmarked by the formation of biofilms on mucosal surfaces. One of the most active areas of biofilm research is in the pathology of cystic fibrosis (CF). The aetiology of the disease is characterised by a defective mutation in the cystic fibrosis transmembrane conductance regulator (CFTR) chloride channel of respiratory airway epithelial cells (Perez *et al.*, 2007). Because of the defective CFTR channel an osmotic imbalance is created that leads to an increase in the epithelial water uptake and consequently a thickening of the mucosal layer. The mucociliary escalator no longer functions in the clearance of microorganisms and many pathogenic bacteria can easily colonise the respiratory epithelium. This colonisation process is marked by the formation of biofilms mainly by *H. influenzae*, *S. aureus* and *P. aeruginosa* that lay the foundations for other less common microorganism to establish colonies (Davies *et al.*, 2007). The pathogens involved in CF that form biofilms display resistance to host immunity as a result of their biofilm state. Examples for *P. aeruginosa* include necrosis of polymophonucear leukocytes by rampholipid (Jensen *et al.*, 2007), macrophage killing by the EPS secretion product alginate (Leid *et al.*, 2005) and the release of bacteria from the biofilm which act as 'sacrificial' decoy targets to neutrophils (Jesaitis *et al.*, 2003). However, host mechanisms exist to deliberately counter biofilm formation. In the case of *P. aeruginosa* infection, it has been shown that lactoferrin can inhibit biofilm formation (Singh *et al.*, 2002) and that human airway epithelial cells can destroy the acetylated quorum messengers used in intra-bacterial communication during biofilm development (Chun *et al.*, 2004). Treatment strategies to combat biofilm infections are also impaired as biofilms demonstrate extensive resistance to antibiotic-mediated killing. In *P. aeruginosa* this has been linked to the physical process of building a barrier that is mediated through transient phenotypic changes (Drenkard & Ausubel, 2002). However, distinct genetic mechanisms also contribute to the process. Mah *et al*. (2003) demonstrated that synthesis of periplasmic glucans can physically impair antibiotic penetration into the bacterial cell.

Research into *M. haemolytica* biofilm formation is in its infancy, although publications in recent years have highlighted this phenotype might be involved in

the disease process. Haig (2011) showed by scanning electron microscopy (SEM) that isolates of *M. haemolytica* are capable of forming EPS-like material during colony formation on ovine epithelial cells. More recent work by Boukahil & Czuprynski (2014) into the biofilm process elucidated several key factors governing the process. Blocking of the OmpA protein with anti-OmpA antibodies resulted in a decrease in biofilm formation, indicating that OmpA adherence might be involved. Biofilm formation was also inhibited by D-mannose and D-galactose, suggesting a potential initiation event *in vivo* is the binding of host polysaccharides. Biofilms were also shown to be resistant to antibiotics of various classes and the composition of the EPS material was determined to be predominantly composed of protein material, rather than polysaccharide or nucleotide. This is unusual considering that most microorganisms produce an EPS composed largely of polysaccharide material. This is the case of the close relative *A. pleuropneumoniae* (Tremblay *et al.*, 2013). However, biofilms comprised mainly of protein are not completely undocumented (Conrad *et al.*, 2003). Identifying the matrix proteins and the sugar-binding adhesins that underpin the process would be a key advancement in understanding the process.

1.3.6.3 Cellular Invasion

Following the initial colonisation of mucosal surfaces, many pathogenic bacteria proceed to invade bodily tissues. One of the best examples of this is the different cellular barriers that *N. meningitidis* overcomes during the pathology of meningococcal meningitis (Miller *et al.*, 2013). Traversal begins with the epithelium of the nasopharynx, followed by the underlying endothelium; a final traversal is then made across the endothelium to emerge into the cerebrospinal fluid of the host (Hammerschmidt *et al.*, 1996; Pujol *et al.*, 1997; Virji *et al.*, 1993; de Vries *et al.*, 1996). The traversal of cellular barriers by bacteria can occur either via internalisation into the host cell cytoplasm, or through extracellular routes where bacteria travel between adjoining cell types. These two pathways are referred to as transcytosis and paracytosis, respectively (Fig 1.18).

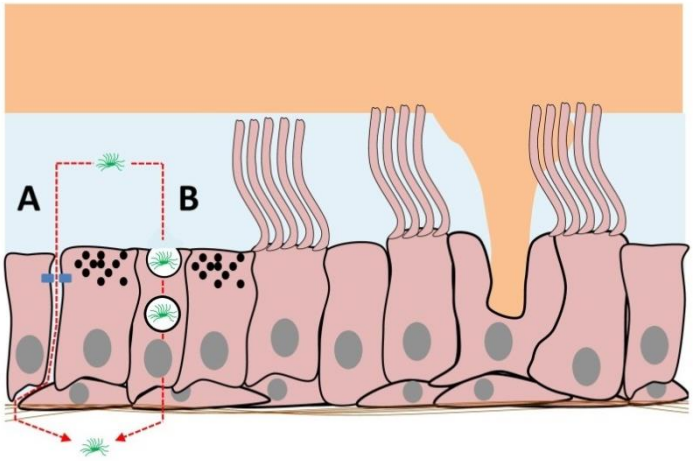

Fig 1.18 Paracytosis and transcytosis of the respiratory epithelium
(A) Paracytosis of bacteria through the epithelium as a result of an increase in epithelial permeability. (B) Transcytosis of the epithelium where bacteria are engulfed into cytoplasmic vacuoles and delivered through the cellular cytoplasm before fusion with the basolateral membrane which allows for release.

1.3.6.3.1 Transcytosis

Transcytosis involves the engulfment of bacteria by endocytosis into cell cytoplasmic vacuoles. Taking the example of *N. meningitidis*, adherence is the first step and involves the use of pili (Bartley *et al.*, 2013). Following initial attachment, the C class of opacity associated proteins (Opc) have been demonstrated to mediate adherence and consequently internalisation into both nasopharyngeal epithelial cells and vascular endothelial cells by transcytosis (Virji *et al.*, 1993). The opacity associated proteins are known to undergo phase variation via a slipped strand mispairing mechanism to control their expression (Hammerschmidt *et al.*, 1996; de Vries *et al.*, 1996) The interaction with epithelial cells involves the binding of cell surface heparin sulphate proteoglycan receptors (de Vries *et al.*, 1998). However, the interaction with endothelial cells involves the binding of Opc to either vitronectin or fibronectin which in turn interact with $\alpha_v\beta_3$ and $\alpha_5\beta_1$ integrins, respectively (Unkmeir *et al.*, 2002; Virji *et al.*, 1994). More recently, a study by Slanina *et al* (2012) sought to underpin the mechanism that leads from adherence to internalisation. In this study of human brain microvascular endothelial cells (HBMEC), the initial integrin binding was found to mediate an enhancement in the FAK/Scr phosphorylation of cortactin, an actin rearranging protein. By this mechanism *N. meningitis* is able to drive actin rearrangement around its cell structure, leading

to vacuole formation. The final crossing made by *N. meningitidis* across the choroid plexus epithelium to reach the cerebral spinal fluid (CSF) has been shown *in vitro* to proceed entirely via transcytosis (Schwerk *et al.*, 2012). In this model no loss of junctional integrity or increase in permeability was observed following infection with *N. meningitidis* onto the basolateral face. Once translocated, bacteria formed microcolonies on the apical surface.

Members of the Pasteurellaceae family that are known to invade cells via macropinocytosis include *P. multocida* and *H. influenzae* (Hotomi *et al.*, 2010; Ketterer *et al.*, 1999; Othman *et al.*, 2012). Whereas both these pathogens are characterised by invasive forms of disease, *M. haemolytica* is not. However, there is some evidence to show *M. haemolytica* inside epithelial cytoplasmic vesicles (Vilela *et al.*, 2004). More work would be needed to determine if *M. haemolytica* has an intracellular role.

1.3.6.3.2 Paracytosis

Paracytosis is a mechanism of cellular invasion that involves crossing an endothelial or epithelial barrier via a route between the membranes of adjacent cells. Again using *N. meningitidis* as an example the process can be illustrated in the crossing of the HBMECs that comprise the blood brain barrier. This has been shown to occur via paracytosis where initial adherence and microcolony formation of *N. meningitidis* allows for the recruitment of junctional components to the host cell membrane directly below the microcolony. This ulterior recruitment diverts components away from their normal role in cell to cell contact resulting in a permeability increase (Coureuil *et al.*, 2009). The entire process is type IV pili dependent. Another paracytotic route of *N. meningitidis* was discovered to be the answer for how certain infections could present with meningitis in the absence of bacteremia (Sjölinder & Jonsson, 2010) In this study, *N. meniningitis* was shown to take an alternative route to the CFS via the olfactory nerves that connect with the nasal cavity. This process involves crossing the nasal epithelium via paracytosis before accessing the underlying nerve.

H. influenzae has been shown to cross respiratory epithelial barriers through in process of paracytosis (van Schilfgaarde *et al.*, 1995). Whether *M. haemolytica* can undergo a similar process is at present unknown.

1.3.7 Three dimensional air liquid interface culture

A great deal remains to be answered as to how *M. haemolytica* colonises the ruminant respiratory tract. Beneficial to the understanding of this process is the use of an *in vitro* model to investigate the complex host-pathogen interactions between the bacterium and the respiratory epithelium.

Although submerged airway epithelial cell culture is a useful tool for studying microbial colonisation, a fundamental flaw is the lack of epithelial differentiation into populations of ciliated, goblet, Clara and basal cells. This fundamental flaw was circumvented by Wu *et al.* (1986) who, in the mid 1980's, made it possible to mimic the *in vivo* environment. This was achieved by supplying media containing nutrients and growth factors to the basolateral side of an epithelial monolayer growing on an artificial membrane, whilst exposing the apical surface of the epithelium to the atmosphere and thus generating an air-liquid interface (ALI). This approach allowed for the differentiation of epithelial cells into the various, specialised cells types of the respiratory tract (described in 1.3.2) (Robinson & Wu, 1993). The similarity of ALI grown cells to the *in vivo* tissue has been confirmed by the similarity of transcript profiles (Dvorak *et al.*, 2011). Increased transcript levels for the ALI cultures were observed for genes relating to proliferation and the cell cycle, genes showing a higher expression in the tissue samples included those involved in cytoskeleton organisation and the humerol immune response. Overall 81 percent of genes showed similar expression levels. Analysis of the secreted glycoproteins showed that there was a high degree of similarity with the only discrepancy being the lack of MUC2 in the ALI model; MUC2 is present at low levels in the airway epithelium. Pathway analysis of all the transcript levels suggested that the ALI cultures have lower levels of xeneobiotic and fatty acid metabolism, an effect likely due to the lack of contaminants under sterile culture. Overall, these differences are easily rationalised. The molecular resemblance of ALI cultures to their *in vivo* origin is a testament to the accuracy by which the native

environment is mimicked. The process involved in culturing cells at ALI is summarised in Fig 1.19.

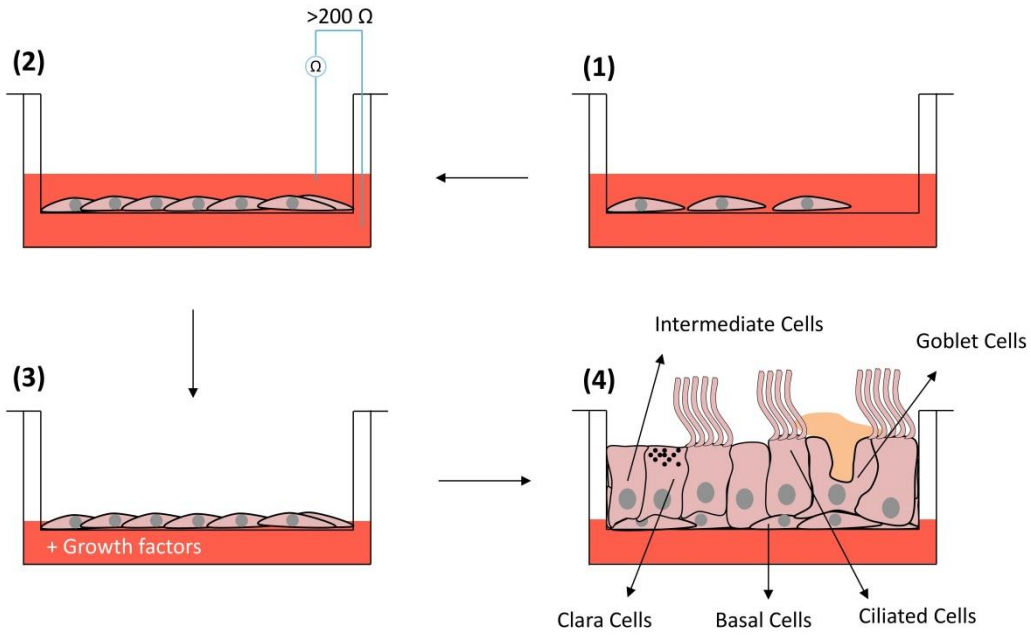

Fig 1.19 ALI culture process
(1) Cells are seeded onto a membrane filter and maintained in submerged conditions. (2) Once an electrically tight monolayer is established, media can be removed (3) from the upper chamber allowing for feeding and growth factor addition from the lower chamber. (4) Maintenance over time allows for the differentiation of cells into the specialised types.

1.3.7.1 Controlling differentiation

The question of how to control differentiation falls on various influential parameters. Consideration must be made for the underlying substrate which mimics the basement membrane (Timpl, 1996). The earliest ALI studies noted the importance of substratum, demonstrating that collagen-coating elicits the mucociliary phenotype (Rearick & Jetten, 1989; Wu *et al.*, 1986). Studies since have continued to show a strong correlation between material properties and differentiation with factors such as ECM coating affecting differentiation (Huang *et al.*, 2010a, b, 2013; Yoon *et al.*, 1997). As a result substrate choice represents a key parameter in controlling differentiation.

Another phenotype-influencing parameter is the choice of base (non-growth factor components) media. Historically, ALI culture media derives from either light harvesting complex (LHC) basal medium which was used prior to the advent

of ALI for defined media culture (Lechner *et al.*, 1982), or the use of HAMs F12 which was used by Wu *et al* (1986) in the development of the first ALI model (Wu & Smith, 1982; Wu *et al.*, 1986). Variations on LHC have evolved into the commercial BEGM™ and AEGM™ (Fulcher *et al.*, 2005); Ham's F12 use has remained unchanged. An added dimension to the use of these culture media is the 1:1 mixing prior to use with DMEM. Studies following on from Lechner *et al.* (1982) adopted a 1:1 mixing (Kaartinen *et al.*, 1993a). Other studies reported that the BEGM basal media yielded better performance in growth and differentiation after 1:1 mixing (Gray *et al.*, 1996). Many studies use variants on either the HAMs F12 or BEGM/AEGM media with little consensus in the literature for which media and which media combinations produce optimal results (Fig 1.20). As a result, media choice represents an important yet relatively unchartered aspect of differentiation that would benefit from further characterisation.

In addition to the availability of soluble nutrients, the influence of air exposure is noted as being necessary with submerged cultures failing to generate pseudostratification and the mucociliary phenotype (Xu *et al.*, 2014). Thus, the partial pressure of oxygen and nitrogen may also affect how these cultures develop.

Differentiation is not simply a product of the air-liquid interface. Many studies have noted that control of pseudostratification and the mucociliary phenotype are heavily influence by retinoic acid (RA) and epidermal growth factor (EGF) (Bernacki *et al.*, 1999; Clark *et al.*, 1995; Gray *et al.*, 1996; Wu *et al.*, 1997; Yoon *et al.*, 1997). These studies have shown that RA is necessary for differentiation and can exhibit a dose dependent effect with regards to mucin production (Gray *et al.*, 2001; Yoon *et al.*, 1997). The influence that EGF has upon cultures is less clear with studies reporting both increases and decreases in mucin production with the inclusion of EGF as a supplement (Clark *et al.*, 1995; Guzman *et al.*, 1995; Wu *et al.*, 1997). Other growth factors that have been demonstrated to have an effect include triiodothyronine (T3) which has been demonstrated in human tracheobronchial cells to produce a decrease in mucin production when included in the culture (Yoon *et al.*, 1997).

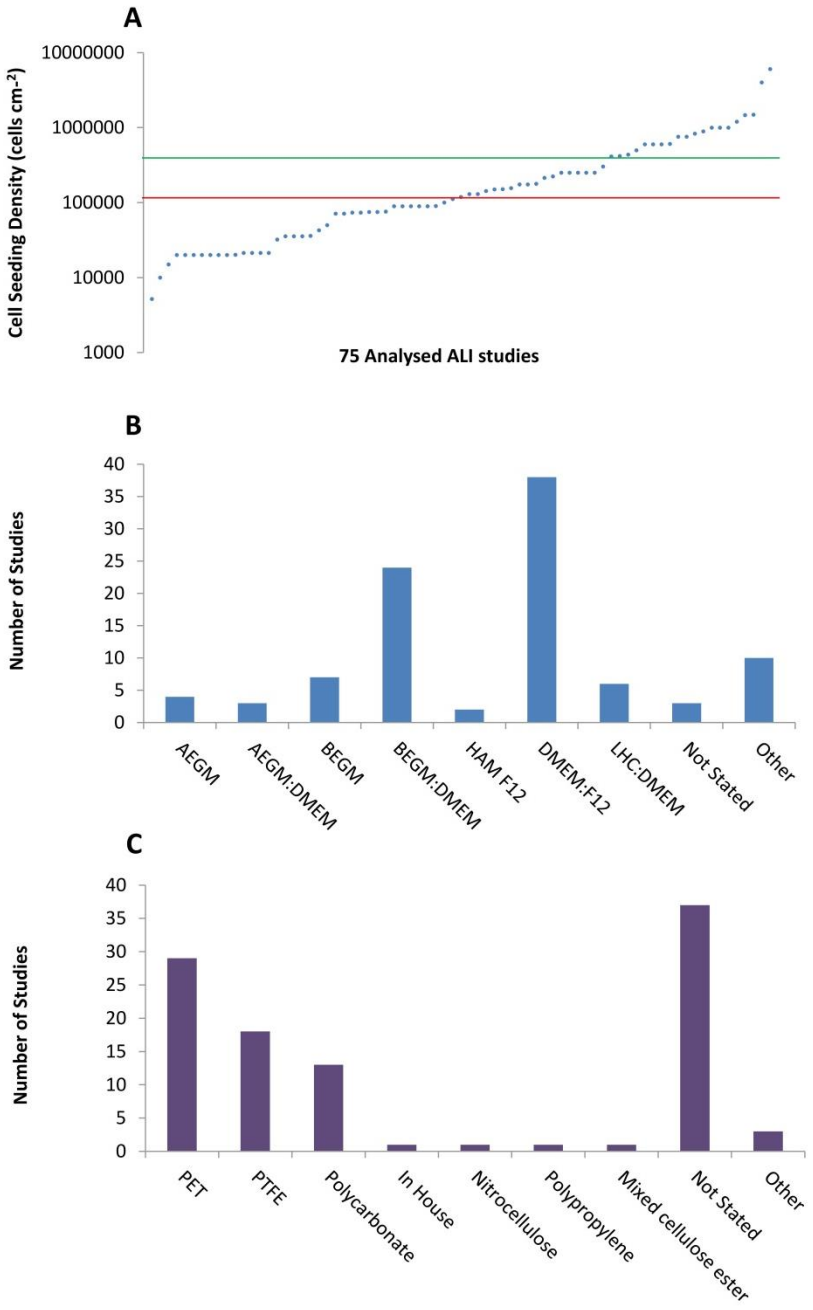

Fig 1.20 Analysis of variable parameters in ALI culture studies
Graphs compile three key parameters from literature analysis of ALI epithelial studies. (A) Cell seeding value of 75 analysed studies including the mean (green line) and median (red line) value of the analysis. Analysis of the media type (B) and substrate material (C) used during ALI culture in 95 different studies. A comprehensive list of all the studies used can be found in Appendicies

Table 7.1.

In addition, the testing of hydrocortisone, epinephrine and transferrin has shown these three growth factors to be redundant in the differentiation process while insulin has been identified as necessary (Yoon *et al.*, 1997).

Many studies have used ALI culture as a technique for recapitulating the respiratory tract *in vivo*. Of all these studies, discrepancies exist in the

parameters used during differentiation as summarised in Fig 1.20. Very few of these studies have used bovine cells (Goris *et al.*, 2008; Kameyama *et al.*, 2003; Kirchhoff *et al.*, 2014; Kondo *et al.*, 1993, 1997) and, although these studies report differentiation into the mucociliary phenotype, none have examined the parameters that control the process.

1.3.7.2 Application of 3D ALI models to study infection

To date, respiratory epithelial cell models at ALI have been developed encompassing a wide variety of species and anatomical location (Abraham *et al.*, 2011; Bals *et al.*, 2004; Brockman-Schneider *et al.*, 2008; Bérubé *et al.*, 2010a; Glorieux *et al.*, 2007; Kaartinen *et al.*, 1993b; Lam *et al.*, 2011; Vandekerckhove *et al.*, 2009). These ALI models are all accurate representations of the *in vivo* mucosa and comprise ciliated, basal and secretory cells. As a result of their mimicry they have been deployed to answer a diverse range of questions concerning the biological functions of the respiratory tract. The study of toxicological effects is one area in which ALI culture has particular benefits over submerged culture. An example of this is a study which examined the effects of cigarette smoke on the respiratory epithelium in the context of pulmonary oedema (Zhang *et al.*, 2011b). By using an ALI system and exposing it to cigarette smoke the authors were able to show that prostaglandin E_2 (PGE_2) levels are decreased in pulmonary oedema-derived epithelial cells as compared to healthy cigarette smokers. The resulting decrease in PGE_2 produced a decrease in the mRNA levels of human ß defensin 2, an antimicrobial peptide of the innate immune system. Exposure of ALI cells to *M. catterhalis* resulted in an increased production of PGE_2. However, pre-treatment of ALI epithelial cells with cigarette smoke abolished the increase in PGE_2 and led to an increase in bacterial titres recovered from the ALI cells. This result would likely have not presented itself in submerged culture owing to the lack of resemblance to the *in vivo* features as well as differences in gas diffusion to the epithelial surface boundary.

Another area in which the ALI system has been applied is in the study of respiratory infections. Bacterial pathogens contribute to a diverse range of pathologies. Respiratory colonisation by pathogens such as those involved in CF including *H. influenzae* (Ren *et al.*, 2012), *P. aeruginosa* (Moreau-Marquis *et al.*,

2009) and *Burkholderia cepacia* (Schwab *et al.*, 2002) is one major area of research where the drive to establish routes of adherence and colonisation has benefited from the use of ALI cultures. In a similar way to that of toxicological studies, bacterial colonisation benefits from the use of a system which mimics the *in vivo* situation more closely than submerged cultures without imposing the ethical issues and research constraints of using an *in vivo* model. A study of *P. aeruginosa* infection (Moreau-Marquis *et al.*, 2009) on ALI-cultured epithelial cells demonstrated that iron-chelating antimicrobial agents were 25 times less effective at disrupting biofilm formation on the ALI model as compared to growth on plastic surfaces. Without the ALI comparison the effectiveness of these drugs would be otherwise overrepresented. Additionally, information was obtained regarding the delivery of these drugs, the results indicating that application to the apical rather than basolateral side was more effective suggesting aerosol delivery would be beneficial. *H. influenzae* is another bacterial species involved in cystic fibrosis and where the use of ALI has been uniquely insightful. The use of this system (Ren *et al.*, 2012) identified that NTHi does not produce major tissue damage in long term culture within the infected ALI model, retaining ciliated cells while increasing relative levels of goblet cells, an effect that would otherwise go unnoticed using submerged epithelial cells. Furthermore, the ALI model was used to show that outer membrane vesicles (OMVs) were produced by NTHi. The genetic elements of CF have also been studied using an ALI system (Perez *et al.*, 2007) in which the use of ALI culture in combination with CFTR protein inhibitors demonstrated a substantial increase in epithelial inflammatory cytokines.

Like the pathogens involved in CF, the host-pathogen interactions *of Mycoplasma pneumoniae* and *Mycoplasma hypopneumoniae* in humans and pigs, respectively, have been studied using an ALI culture system (Krunkosky *et al.*, 2007; Young *et al.*, 2000). The use of ALI culture in studying human airway epithelial infection was successful at showing that *M. pneumonia* adhered to the ciliated cells and localised at the cilia base. The profile of ICAM-1, an immunoglobulin like protein involved in respiratory disease, presented elevated levels in the epithelial cells after bacterial treatment. The treatment of porcine ALI-cultured epithelial cells with *M. hypopneumoniae* revealed extensive damage to the cilia including clumping and a loss of mucocillary clearance for pathogenic strains.

The effect was not observed with non-pathogenic strains and highlights another case where the differentiated features of the ALI system provide new insights into virulence.

The study of inflammatory cytokines have also benefited from the use of ALI systems. It has been demonstrated that receptors for IFN-γ, IL-4 and IL-8 are differentially expressed in epithelial cells with clustering around the basolateral side (Humlicek *et al.*, 2007). By utilising the polarised features of ALI culture it was demonstrated that these molecules could only elicit an immune response when exposed from the basolateral side or in the event of injury to compromise the epithelium. Thus, with the use of submerged epithelial cells this discovery would not be possible owing to the lack of polarisation.

Viral infection has also been studied using ALI culture systems whereby modulation to the epithelial barrier can propagate several diseases. The use of this technique to study BRD allowed for the identification of different infection mechanisms in two of the viruses involved in BRD (Goris *et al.*, 2008). Both BPIV3 and BRSV are involved in modulation of the epithelium of cattle that allows for opportunistic bacterial pathogens to capitalise on the ensuing event. Infection of bovine ALI epithelial cultures with BRSV and BPI-3 demonstrated that BPI-3 primarily infected ciliated cells at MOI of 0.1. However, BRSV was comparably ineffective at this MOI and could only establish infection in non-ciliated cells; an MOI of 3.5 was required to establish infection in ciliated cells. This finding was only possible from *in vitro* culture models that contain cilia, highlighting the advantageous use of ALI over submerged cell culture. Further work by Kirchhoff *et al.* (2014) utilised ALI culture to study BHV-1 as well as BPI3 and BRSV. This approach revealed that BHV-1 can only establish infection from the basolateral side. For BHV-1 to establish infection from the apical side, mechanical damage or chemical disruption of the tight junctions is required to allow the virus to access the underlying cells. Because these results derive from epithelial polarisation, which is absent in submerged culture, these observations are once again only possible *in vitro* through the use of a differentiated model.

Viral co-infection is also important in the colonisation of *H. influenzae* where the rhinovirus has been shown to modulate the epithelium prior to infection (Schroth *et al.*, 1999). The use of ALI systems in two independent studies

(Jakiela *et al.*, 2008; Sajjan *et al.*, 2008) demonstrated that the virus preferentially infects the basal cells due to the presence of higher ICAM-1 receptors. Pre-incubation with a rhinovirus allowed *H. influenzae* to transmigrate the epithelial barrier but only when the virus replicates within the host epithelial tissue.

1.4 Proteomics

Whilst *in vitro* modelling of the respiratory tract provides a platform with which to examine the host-pathogen interactions of *M. haemolytica*, it is not in itself a means to understating the molecular interactions of the bacterium with the epithelium. An experimental strategy that addresses the composition of the *M. haemolytica* OM proteome would provide insight into the molecular machinery used by the organism to facilitate colonisation. Thus, the complementation of *in vitro* modelling alongside characterisation of the *M. haemolytica* OM proteome will provide insight into the mechanism of adherence and colonisation.

The proteome of any biological system is defined as the complete repertoire of proteins expressed under a given set of conditions (Aebersold & Mann, 2003). Conceptually, the proteome is a molecular snapshot of a biological system. Experimentally observing all the proteins in a given system presents many challenges that are, however, outweighed by the benefits. Compared to traditional reductionist approaches that study proteins in isolation, proteomics offers an unbiased approach to examine the molecular makeup of a cell, organelle or any other biological compartment. Thus, as a result, interactions that would otherwise be overlooked or missed altogether are instead made evident. This has important implications, where the researcher can impose a given set of conditions and observe the state of a biological system in its entirety. Experimentally the field of proteomics has become largely mass spectrometry based. Although other technologies such as microarrays have been utilised to great success, mass spectrometry remains at the forefront of proteome characterisation.

1.4.1 Mass spectrometry design

Many different mass spectrometry designs exist all with different purposes. However, they all have two common features: (1) an ionisation source to generate gas phase ions and (2) a mass analyser to separate ions based on their mass to charge (m/z) ratio.

1.4.1.1 Ionisation source

The ionisation source serves to impart a charge on a sample and vaporise it for analysis. Various ionisation techniques have been developed all of which can be broadly classified as either 'hard' or 'soft' based on the preservation of molecular structure (Portolés *et al.*, 2011). Within the field of proteomics ionisation techniques that are employed fall into the soft category for their ability to ionise polypeptides without altering their structural composition. The two most widely used ionisation sources are electrospray ionisation (ESI) and matrix assisted laser desorption ionisation (MALDI) (Hillenkamp *et al.*, 2014; Wilm, 2011; Zenobi & Knochenmuss, 1999). Both these methods function to generate gas phase ions. The ESI method accomplishes this via ejection of solvated sample from a fine capillary. Acceleration in an electric field coincides with solvent evaporation. Charged, solvent free sample is thus ejected into the mass analyser. The MALDI method involves co-crystallisation of sample with a chemical matrix. The purpose of the matrix is to absorb laser light. This results in the transfer of energy to the sample, ionising it, and ejecting into the gas phase ready for measurement by the mass analyser.

1.4.1.2 Mass analyser

The second important component of mass spectrometry is the mass analyser. This functions to measure the mass to charge ratio (m/z) of ions generated by the ionisation source. While proteomics mainly makes use of only a few ionisation sources, the range of mass analysers is much larger offering a range of resolution and ionisation coupling capabilities as well as more practical differences such as cost. The predominantly-used mass analysers include the time-of-flight detector (TOF), the ion trap, the orbitrap and the Fourier transform ion cyclotron resonance (FTICR) mass spectrometer (Church, 1969; Clark *et al.*, 2013; Hu *et al.*, 2005; Makarov *et al.*, 2005; Marshall, 1985;

Marshall *et al.*, 1998; Russell & Edmondson, 1997). In essence, all mass analysers function to measure the m/z ratio.

The two most widely used mass spectrometry configurations in the field of proteomics are the ESI-iontrap and the MALDI-TOF (Fig 1.21).

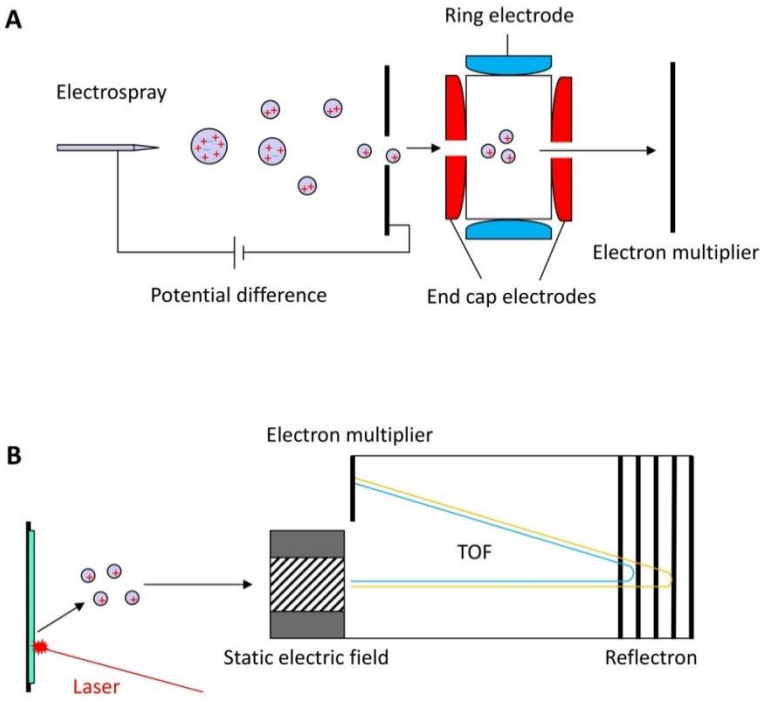

Fig 1.21 Two common mass spectrometry designs used for proteomics
(A) An ESI-iontrap configuration and (B) MALDI-TOF reflectron configuration (B).

1.4.2 Mass spectrometry based proteomics

In order to identify individual proteins amongst a complex mixture using mass spectrometry requires in essence a series of separation steps, mass spectrometry measurements and statistical evaluations in order to successfully identify the proteins from that sample.

1.4.2.1 Sample preparation

Prior to measurement with mass spectrometry is the preparation of a biological sample. Reducing the complexity of a sample often aids in the detection process by reducing the total proteome of a system to a sub-proteome within.

This can take the form of sub-fractionation, for example, where the components of a cell are separated by the use of centrifugation and selective detergent solubilisation to obtain a protein mixture that is representative of a particular organelle rather than the whole cell. Prior to mass spectrometry, separation of a sample can also be performed which commonly involves the separation of proteins by either 1D or 2D sodium dodecyl sulphate-polyacrylamide gel electrophoresis (SDS-PAGE) (Shevchenko *et al.*, 2006). This allows for further compartmentalisation of the proteome into manageable subsets. However, although an aid in reducing complexity, SDS-PAGE does present disadvantages in only selecting for proteins within the set mass and isoelectric limits.

1.4.2.2 Enzymatic digestion

A sample can now be converted to a complex mixture of peptides by proteolytic cleavage. This process is controlled through the use of enzymes that cut polypeptides at defined positions along the amino acid chain. This process generates what is known as a peptide fingerprint from a given protein; that is, a set of peptides that can theoretically be mapped based on the chosen enzyme. By far the most widely used enzyme is trypsin which cleaves the amide bond on the C-terminal side of lysine and arginine residues (Olsen *et al.*, 2004), except when they are flanked by proline. The consequence of this is that a set of peptides, analysed by mass spectrometry, can then be mapped back to the amino acid sequence of the protein.

1.4.2.3 Peptide mass fingerprinting

A complex peptide mixture generated from a complex protein sample can now be experimentally measured by mass spectrometry to produce what is known as a peptide mass fingerprint (PMF) (Pappin *et al.*, 1993). Typically the peptide mixture is first separated with the use of liquid chromatography (LC) before introduction into the mass spectrometer. As peptides elute from the chromatography system they are ionised and their m/z ratios are measured by the mass analyser. Now with the m/z ratios known and the knowledge that an enzyme of particular specificity was used to generate the peptides in the sample, the peptides can be mapped to the amino acid sequence of a protein from a given database. This can be used to confirm the presence of a particular

protein in a sample with consideration for probability of finding false positives (1.4.2.5).

1.4.2.4 Tandem mass spectrometry

The limitations of PMF occur when considering that from the m/z ratios measured for a given peptide, the amino acid composition may be inferred simply based on the differences in amino acid mass (with the exception of leucine and isoleucine). However, the sequential order of amino acids within the peptide remains unknown. This becomes a problem when considering multiple proteins within a given sample might generate tryptic peptides with the same mass yet different amino acid sequences. This problem can be overcome by the use of a fragmentation technique and a second mass analyser in order to identify the break down products (Hunt *et al.*, 1986). Ions are selected for fragmentation and measurement using various gating strategies. Different fragmentation techniques exist that can be used to physically break the covalent bonds of the peptide backbone (Paizs & Suhai, 2005). Introducing these peptide fragments into a second mass spectrometer allows for an amino acid sequence to be deduced from a peptide. Fragmentation techniques, as applied to peptide chemistry, break different bonds along the polypeptide backbone. A popular technique is collision-induced dissociation (CID) which is used for its relative preference in breaking the amine bond over other backbone bonds (Papayannopoulos, 1995). Physically, the technique involves bombarding the peptide with neutral gas phase atoms, usually helium, nitrogen or argon. The ions generated are referred to as b and y, the b ion representing the N-terminal portion of the peptide and the y ion representing the C-terminal portion (Paizs & Suhai, 2005). Thus, much in the way PMF maps a series of peptides to an amino acid sequence, tandem mass spectrometry can be used to map a series of fragments to the peptide in order to deduce the amino acid composition.

1.4.2.5 Database searching and statistical interpretation

With a series of identified peptide masses and corresponding fragment masses, the multitude of data requires a database search. This involves mapping the information to the amino acid sequences of protein records within the database. This usually requires having a sequenced genome that corresponds, at least in

homology if not identity, to the generated protein sample (Shevchenko *et al.*, 2001). A genome can provide all the translated open reading frame sequences and serves as template against which to match the data. The practicality of this involves using software that can match the mass spectrometry data based on a series of user-specified criteria that allow for mass-error tolerances, missed tryptic cleavages as well as biological, user-generated or environmental chemical modifications (Sadygov *et al.*, 2004). Interpreting the matched results involves careful consideration for the generation of false positives (Chen *et al.*, 2009). The use of tandem mass spectrometry in addition to PMF helps to circumvent this problem. However, a common problem is the case where a full series of b-y ions are not obtained for a given peptide and so a range of possible identities may be attributed to a peptide. All the various possibilities might not exist within a given database. However, when more than one does exist, the ambiguity in the identity of the peptide and the protein matches must be accounted for statistically (Li *et al.*, 2009; Mortz *et al.*, 1996). Indeed, even when a full series of b-y ions is obtained some peptides that represent conserved motifs might be found multiple times in a database and must therefore be statistically accounted for. This is achieved by the use of algorithms, such as the MOWSE score (Pappin *et al.*, 1993), that report on the false positive likelihood within a given sample. Data is usually reported with a confidence limit that specifies a protein is considered identified above a false positive threshold.

1.5 Aims

The aims of the project were as follows. Firstly, to develop an *in vitro* ALI model of the bovine respiratory tract. The objective was to optimise the experimental parameters that govern growth and differentiation of the epithelial cells to produce the most accurate mimicry of the native epithelium possible. Characterisation of the *in vitro* ALI airway epithelial cultures involved several assays to measure the percentage ciliation of the cultures, the culture depth and the cellular composition. The latter of which included the identification of Goblet cells by histological staining for mucus, the identification of basal cells via the P63 marker and the identification of Clara cells via the Clara cell secretory protein (CC10) marker.

The second aim was to compare the *M. haemolytica* OM proteomes of representative pathogenic and commensal isolates from cattle and sheep. The objective was to gain insight into the molecular profiles that constitute the host-pathogen interface and understand how the molecular makeup of the OM differed between the selected isolates. Eight isolates of *M. haemolytica*, representing different serotypes and host species, were subjected to a dual proteomic approach of in-gel and in-solution tryptic digestion. Triplicate OM samples were prepared so as to maximise the reliability of the findings.

The third aim was to use the developed ALI *in vitro* model to study the adherence and colonisation of *M. haemolytica* to the respiratory tract. As part of this objective, the interactions of a bovine pathogenic A1 isolate and a bovine non-pathogenic A2 isolate were compared for their ability to colonise *in vitro* ALI cultures generated from epithelial cells derived from different anatomic regions of the respiratory tract. In principle this was to establish if the pathogenic and non-pathogenic isolates have different propensities for colonising the URT and LRT.

The final aim was to establish the OM proteome composition of *M. haemolytica* during colonisation of the ALI airway epithelial cell cultures. Although this aim was not realised as part of this project due to time constraints it nonetheless represents an important component of future studies into the interactions of *M. haemolytica* with the respiratory epithelium.

Chapter 2 Development of an *in vitro* Model of the Bovine Respiratory Tract

2.1 Introduction

Modelling microbial respiratory infections *in vitro* is a powerful way of answering important questions about host-pathogen interactions. Questions addressing the condition of the respiratory tract and the bacterial protein machinery required for colonisation can be effectively answered using *in vitro* modelling. Modelling of respiratory infections necessitates recapitulating the host mucosa in the laboratory setting. In its most basic form this consists of either primary-derived or immortalised epithelial cells grown in submerged culture. These cells, when grown immersed in appropriate media, form a monolayer of homogeneous basal-like epithelial cells (Tata *et al.*, 2013). This is in stark contrast to the *in vivo* environment where the host respiratory mucosa consists of several different cell types, namely ciliated, basal, Clara and goblet cells amongst numerous other specialist cells (Coraux *et al.*, 2008). In addition, these cell types work in unison to create a physiological process known as the mucociliary escalator (Cone, 2009). This process involves the secreted mucus of the respiratory cells being propelled up the conducting airways by the beating action of the cilia. The resulting drive allows for clearance of inhaled microorganisms and particulate matter from the environment. In combination with secreted antimicrobial factors from the epithelial cells, the whole system functions to provide the first defensive barrier in combating respiratory infections.

Significant differences exist between the *in vivo* mucosa and standard monolayer epithelial cell culture. Therefore, it is beneficial to produce a culture system that captures the physiological functions of the respiratory epithelium, complete with cell polarisation (Fig 1.15) and a fully differentiated heterogeneous cell population. Cultured systems aimed at recreating the mucociliary phenotype *in vitro* have focused predominantly on culture of these cells at an ALI. Cells cultured at the ALI have been described for a wide variety of species and different lung anatomies (Abraham *et al.*, 2011; Bals *et al.*, 2004; Clark *et al.*, 1995; Glorieux *et al.*, 2007; Haig, 2011; Jakiela *et al.*, 2008; Kameyama *et al.*, 2003; Prytherch *et al.*, 2011; Vandekerckhove *et al.*, 2009; Yamaya *et al.*, 1992). These studies all report production of the mucociliary phenotype resulting from

the culture of cells at ALI. Studies that have examined the molecular mimicry of these culture systems have found many similarities with the *in vivo* environment. Transcriptome analysis of submerged mono-cellular cultures and ALI-differentiated multicellular cultures reveal that a significantly different molecular signature defines these two cell populations (Hackett *et al.*, 2011). Furthermore, comparison of native basal cells, recovered via bronchial brushing of human subjects, and ALI day 0 basal cells revealed they have similar molecular signatures. However, comparison of these basal cells with differentiated native tissue and day 28 ALI cultures revealed the ALI cultures did exhibit some differences in molecular signature as compared with the native tissue. Differences in the transcriptome of native and ALI-differentiated cultures have been shown to predominantly reflect variation in cytoskeletal organisation, humoral immune response, proliferation and the cell cycle (Dvorak *et al.*, 2011). These major differences can be attributed to the dynamic organisation of the differentiating cultures as well as, in the case of the humoral immune response, the interaction with other cell types *in vivo*. Thus, although ALI cultures are not exact mimics of the native environment they are extremely accurate *in vitro* representations that offer a multitude of advantages over submerged culture and endow an element of user-defined control over the differentiation process.

To develop an ALI culture requires an understanding of the factors that control differentiation. Factors demonstrated to influence the differentiation include media (Gray *et al.*, 1996; Sachs *et al.*, 2003), growth surface (substrate) (Huang *et al.*, 2009, 2010a, b, 2013), growth factor concentration (Bateman *et al.*, 2015; Clark *et al.*, 1995; Wu *et al.*, 1997; Yoon *et al.*, 1997) and the air interface (Kameyama *et al.*, 2003; Kondo *et al.*, 1997; Xu *et al.*, 2014; Yamaya *et al.*, 1992). Examination of the literature reveals that there is much discrepancy in the various parameters that influence differentiation (Fig 1.20). Thus, in order to produce an ALI model, these parameters must be considered when recapitulating the native environment. Therefore, the initial aim of this project was to develop and characterise an *in vitro* model of the bovine respiratory tract that could subsequently be used for the study of adherence and colonisation by *M. haemolytica*. All the differentiation-influencing factors that were examined in the present study are summarised in Fig 2.1. The process of culturing

epithelial cells at ALI, and the nomenclature used to refer to the various growth stages, is summarised in Fig 2.2.

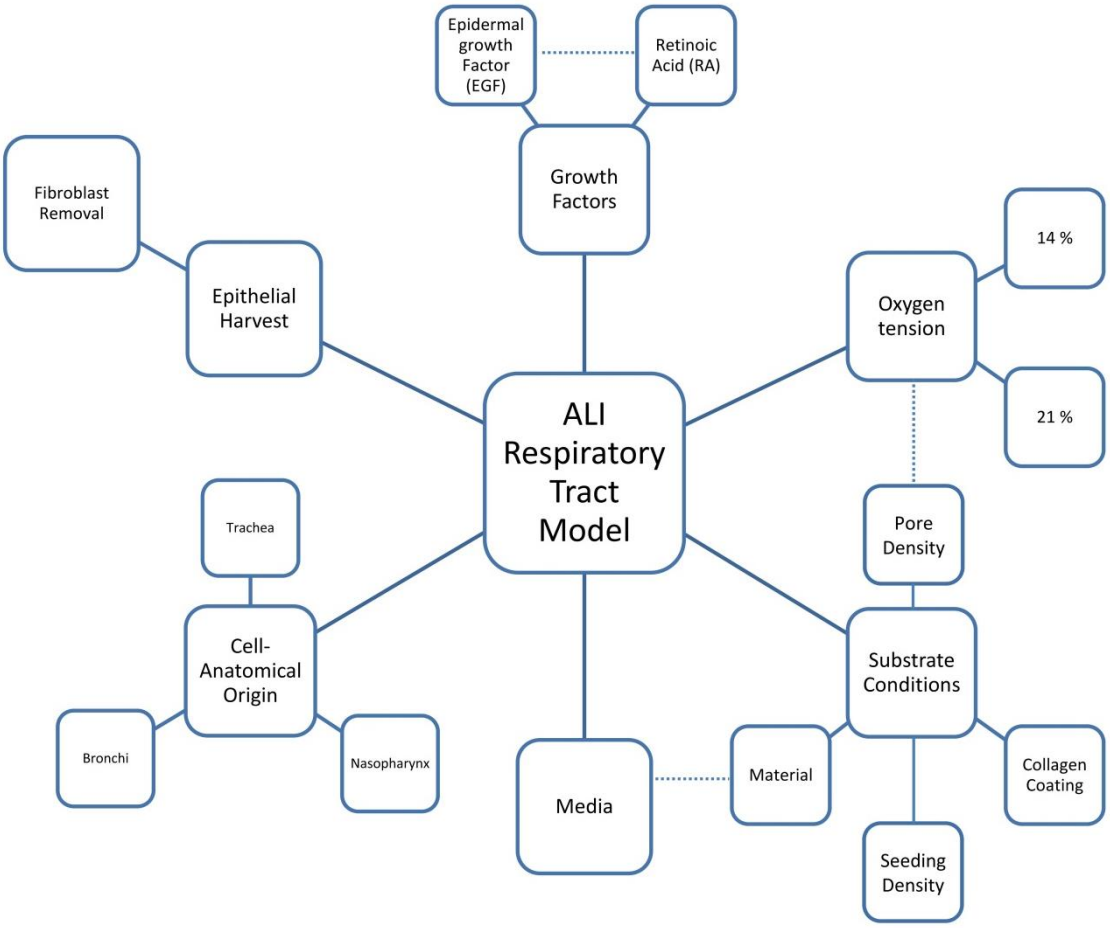

Fig 2.1 Schematic of the ALI culture optimisation process
A summary of the influencing factors that have been optimised to control differentiation of the ALI model. Dotted lines represent areas where interrelation of different parameters was examined.

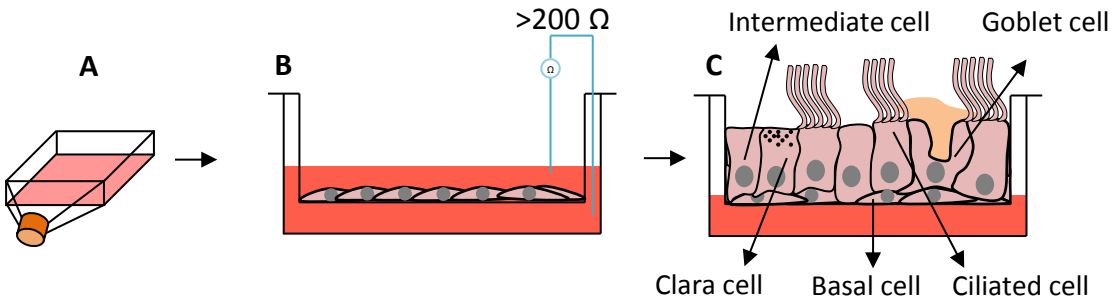

Fig 2.2 Schematic of the ALI culture process
The process of ALI culture can be defined in three stages. (A) Submerged expansion of primary cells in tissue culture plastic-ware, referred to in the text as 'phase one' of culture. (B) Seeding onto membrane filters and subsequent expansion into a confluent monolayer, referred to in the text as 'phase two' of culture. (C) Generation and maintenance of an ALI to achieve differentiation, referred to in the text as 'phase three' culture.

2.2 Materials and methods

2.2.1 Tissue culture

2.2.1.1 Tissue collection and harvesting

Prior to tissue collection a number of different media were prepared. Transport media comprised phosphate buffered saline supplemented with 100 U/ml penicillin/streptomycin and 2.5 µg/ml amphotericin. Processing media comprised a mixture of 50:50 DMEM: Ham's Nutrient Mixture F12 supplemented with 100 U/ml penicillin/streptomycin and 2.5 µg/ml amphotericin B. Incubation media comprised a mixture of 50:50 DMEM: Ham's Nutrient Mixture F12 supplemented with 100 U/ml penicillin/streptomycin, 2.5 µg/ml amphotericin B and 1mg/ml dithiothreitol.

Tissue was obtained courtesy of Sandyford abattoir. Lungs, trachea and heads were obtained from freshly slaughtered cattle. Swabs of the tissue were taken and plated out on BHIA supplemented with 5% blood to check for contamination. Tracheobronchial material was cut into sections, placed in transport medium on ice and immediately transported to the laboratory. All subsequent procedures were performed in a sterile tissue culture hood. Sections of tracheobroncheal tissue were cut along the proximal-distal axis using sterile scissors and pinned down on a dissection board with the epithelium facing upwards. For tracheal tissue, the epithelium was excised using a sterile forceps and scalpel; for bronchial tissue, the epithelium was left attached to the underlying cartilage; for nasopharyngeal tissue, the epithelium was excised directly from the nasal cavity following bisection of the skull. The epithelial tissue was transferred to 125 ml incubation medium. Following transfer of all tissue, the incubation medium was supplemented with 5 mg/ml DNAse, 100 mg/ml Protease XIV and 166.7 mg/ml DTT to give final concentrations of 0.01 mg/ml, 1 mg/ml and 1 mg/ml respectively. The tissue was incubated at 4°C for 24 h.

After 24 h the digested tissue and media were transferred to petri dishes. The tissue was rinsed several times with liquid from the overnight digest in order to remove the epithelial cells. The final cell suspension was filtered through a 70 µm pore cell strainer and centrifuged at 300 x g for 5 min to pellet the cells. The supernatants were discarded, the cells resuspended in 10 ml of processing

media and centrifuged at 300 x g for 5 min to wash the cells. Following this the cells were resuspended in 20 ml of submerged growth media. A 20 µl sample was removed and combined with 20 µl of 1% tryphan blue to assess the number of live cells. Cell populations were adjusted to provide a seeding density of between 5 $x10^5$ cells/ml and 2 $x10^6$ cells/ml unless otherwise stated.

2.2.1.2 Cell maintenance and subculturing

Cells were seeded into T-75 tissue culture flasks and grown in submerged growth medium (SGM) which comprises a 50:50 mixture of DMEM:HAM's F12 supplemented with 100 U/ml penicillin/streptomycin and 2.5 µg/ml amphotericin and 10% filter sterilised foetal calf serum. Cultures were maintained at 37°C and 5% CO_2 during growth. Cells were fed every two to three days with fresh SGM. Once cells were approaching confluency (approximately 90%) they were trypsinised, this was acomplised by rinsing the culture flasks twice with PBS before adding 5 ml (T-75 flask) of 0.25% trypsin-EDTA onto the cells for approximately seven min in order to detach them. Once detached the action of the trypsin was quenched by the addition of 20 ml of SGM per flask. The cells were pelleted by centrifugation at 300 x g for 5 min, resuspended in SGM and adjusted to a viable (using Tryphan blue) seeding density of either 2.5 x 10^5 cell/ml, 5 x 10^5 cells/ml or 1 x 10^6 cells/ml. Surplus cells were cryopreserved by resuspension in cell recovery medium™ (Sigma) at 1 x 10^6 cells/ml by freezing for 24 h at -80°C before transfer to liquid nitrogen.

2.2.1.3 Air liquid interface growth and differentiation

Cultured cells either at P_0 or P_1 were seeded onto membrane inserts at densities of 2.5 $x10^5$ or 5 $x10^5$ cells/ml. The cells were expanded with media present in both the apical and basolateral chambers until a confluent monolayer of epithelial cells was formed. Confluency was assessed by measuring trans-epithelial-electrical-resistance (TEER) of the cultures with an EVOM 2™(world precision instruments) meter, an insert with no cells was also measured and subtracted from the culture readings. Once a TEER value of >200 $\Omega.cm^2$ was reached an ALI was generated with media confined to the basolateral chamber. Several different insert types were used to assess substrate conditions (Table 2.1).

Table 2.1 Membrane substrate information

	Brand Name	Supplier	Product Code	Material	Pore density (cm^{-2})
1	Transwell-COL™	Corning	3493	PTFE	Electrospun matrix
2	Transwell™	Corning	3460	PET	4×10^6
3	Thincert™	Greiner	665641	PET	2×10^6
4	Thincert™	Greiner	665640	PET	1×10^8

Several different media were compared as outlined in section 2.3.2.1. **DMEM:Ham's F12** is a 50:50 ratio of Dulbeco's Modified Eagles Medium and Ham's Nutrient Mixture F12 supplemented with 2% Ultroser G™, 0.1 µg/ml RA (Sigma R2625), 10 ng/ml cholera toxin (Sigma C8052), 100 U/ml penicillin, 100 µg/ml streptomycin, and 2.5 µg/ml Fungizone™ (Life Technologies).

AEGM:DMEM unless otherwise stated is a 50:50 mixture of Airway Epithelial Basal Medium™ (Promocell) and Dulbeco's Modified Eagles Media (Sigma) supplemented with 6.7 ng/ml Triiodothyronine (T3), 5 µg/ml insulin, 0.5 µg/ml hydrocortisone, 10 ng/ml EGF, 4 µl/ml bovine pituitary extract. 10 µg/ml transferrin, 0.1 µg/ml RA (Sigma R2625), 0.5 µg/ml epinephrine, 10 ng/ml cholera toxin (Sigma C8052), 100 U/ml penicillin: 100 µg/ml, streptomycin and 2.5 µg/ml Fungizone® (Life Technologies).

BEGM:DMEM unless otherwise stated is a 50:50 mixture of Bronchial Epithelial Growth Media™ (Lonza) and Dulbecco's Modified Eagles Media (Sigma) supplemented with the following hormones, the concentrations of which are proprietary by the manufacturer: Insulin, T3, hydrocortisone, epidermal growth factor, bovine pituitary extract, transferrin and epinephrine. In addition BEGM:DMEM was supplemented with 0.1 µg/ml RA (Sigma R2625), 10 ng/ml cholera toxin (Sigma C8052), 100 U/ml penicillin, 100µg/ml, streptomycin and 2.5 µg/ml Fungizone® (Life Technologies). From section 2.3.2.4 onward following optimisation of culture conditions, AEGM:DMEM was formulated, as described, but with the omission of cholera toxin. Cultures were maintained at 37°C and 5 % CO_2 and assessed for differentiation by the microscopic observation of beating cilia.

2.2.1.4 Collagen coating of membrane inserts

Bovine type I collagen (Becton Dickinson) was prepared from stock (3.1 mg/ml) to a concentration of 50 µg/ml in 0.01 M HCl. Two hundred and fifty microliters of the working solution was added to each membrane insert and incubated at room temperature for 1 h. The collagen solution was aspirated and the inserts were air-dried at room temperature. The membrane inserts were washed three times in PBS and stored at 4°C for up to 24 h prior to use.

2.2.1.5 Trans epithelial electrical resistance

Trans epithelial electrical resistance (TEER) was performed using an EVOM^{2}™ (World Precision Instruments) ohmmeter. Electrodes were submerged in cultures prepared with fresh media (apically and basally) and a reading was taken once stability was achieved. Three measurements were taken at 120° sectors around the insert and these were averaged to produce an accurate reading. A blank insert containing no epithelial cells was used to take reference readings which were then subtracted from measurements to produce a net value.

2.2.2 Microscopy

2.2.2.1 Light microscopy

Cultures were fixed with 4% formaldehyde (10% neutral buffered formalin) and 2% sucrose for 20 min at 37 °C before staining. A 2% w/v solution of Coomassie brilliant blue was added for 8 mins. Cultures were then washed three times with PBS to remove all residual Coomassie.

2.2.2.2 Scanning electron microscopy

Cultures processed for SEM imaging were fixed in 1.5 % glutaraldehyde (Sigma), 0.1 M sodium cacodulate for 1 h at 4°C before being washed twice in 0.1 M sodium cacodulate buffer. Cells were stained with 0.1 % osmium tetroxide (Sigma) for 1 h at room temperature. Following this, samples were washed three times in dH_2O and negatively stained with 0.5 % uranyl acetate (Sigma) for 1 h in the dark. Samples were then dried in ethanol and hexamethyldisilazane (HMDS)(Sigma) as indicated in Table 2.2; this was achieved by gradual

replacement of the water in the sample with a stepwise increase in ethanol concentration before a final change into HMDS for overnight dehydration in a desiccator.

Table 2.2 SEM dehydration steps

Solution	Incubation Time (Min)	Number of Steps
30% Ethanol	5	2
50% Ethanol	5	2
70% Ethanol	5	2
90% Ethanol	5	2
100% Ethanol	5	4
Dried Absolute Ethanol	5	4
Hexamethyldisilazane	10	2

Following complete dehydration in HMDS, samples were sputter-coated with gold-palladium. Two three-minute treatments were applied with a 20 mA current and a 1.5 kV application to give a coating thickness of 54 nm. Samples were viewed using a JEOL 6400 SEM with an accelerating voltage of 10 kV.

2.2.2.3 Immunofluorescent microscopy

Cells were washed twice in sterile PBS before being fixed in a PBS solution containing either 4 % formaldehyde (10% Formalin) and 2 % sucrose or 4 % paraformaldehyde for 20 min at room temperature. After incubation, cells were washed three times in PBS before being treated with permeabilisation buffer (0.5 % Triton-X 100 in PBS supplemented with 0.3 M sucrose, 0.05 M NaCl, 6.3 mM $MgCl_2$ and 0.02 M HEPES, pH 7.2) for 10 min at room temperature. Samples were washed three times in PBS / 1% bovine serum albumen (BSA) and blocked with 1% BSA / 10 % goat serum in PBS for 1 h at room temperature. Following blocking, samples were incubated for 1 h with either primary antibody or rhodamine phalloidin (Table 2.3) before being washed three times in PBS / 1% BSA and incubated with secondary antibody where necessary (Table 2.3). In the case of dual antibody staining, samples were blocked for a second time between the addition of first secondary and second primary. After all antibody staining, samples were washed a further three times in PBS / 1 % BSA, stained with liquid DAPI for 10 minutes at room temperature, and mounted in fluorescent mounting media (Table 2.3). All images were captured using an Axiovert 200 (Zeiss) microscope.

Table 2.3 Immunofluorescent antibody list

Antibody / Reagent Name	Description	Experimental Purpose	Concentration[a]	Supplier	Product Code
Rhodamine Phalloidin	Actin binding	Actin cell cytoskeleton	1U / sample	Life Tech	R415
Anti β-Tubulin	Primary	Cell cilia	5 µg/ml	Abcam	ab6046
Anti-Pan Cytokeratin	Primary	Epithelial cell marker	1.33 µg/ml	Abcam	[C-11] ab7753
Anti ZO-1 (1)	Primary	Tight junction formation	10 µg/ml	Invitrogen	33-9100/1A12
Alexa 546 anti-rabbit / mouse	Secondary	Identification of primary	5 µg/ml	Life Technology	A11010 / A21123
Alexa 488 anti-rabbit / mouse	Secondary	Identification of primary	5 µg/ml	Life Technology	A11008 / A21121
Biotinylated horse anti mouse	Secondary	Identification of primary	15 µg/ml	Vector Labs	BA-2000
Fluorescein - Streptavidin	Tertiary	Identification of secondary	10 µg/ml	Vector Labs	SA-5001
DAPI	Nuclear Stain	Cell nucleus	300nM	Sigma	D9564
Vectasheild	Mountant	Improve photostabillity	N/A	Vector Labs	H-1000

[a]Final concentration applied to cells

2.2.2.4 Determination of ciliation by fluorescence intensity measurements

In order to semi-quantify the degree of ciliation a system based on the difference between the fluorescence intensity of the background versus cilia was developed. For each sample five images were taken using the 20x objective, corresponding to the centre and the four 90° quadrants of the circular insert surface. To reduce bias, two of these latter four were taken such that they were close to the epithelial edge and the other two so that they were set in about a third the distance to the epithelial centre. The images were loaded into ImageJ and a default intensity threshold calibration was applied such that ciliated areas were distinguished from background. The areas of the ciliated regions were then measured. This was performed on duplicate cultures to produces a total of ten images which were then averaged to produce the final semi-quantification of percent ciliation. It should be noted, the measurement distinguishes cilia rather than ciliated cells from the background, and that the cilia from one cell will not entirely cover the area of that cell. As a result the measurement is an under representation of the number of ciliated cells. Nevertheless, the measurement allows for a direct comparison of ciliation between different culture conditions.

2.2.2.5 Histology and immunohistochemistry

All sample embedding, sectioning and staining was carried out by the Veterinary Diagnostic Service Laboratory at the University of Glasgow. Tissue samples prepared for either histology or immunohistochemistry were fixed in either 4% formaldehyde (10% Formalin) with 2% sucrose or 4% paraformaldehyde for 20 min. Tissue was processed overnight with the Sakura Tissue Tek® VIP vacumn infiltration tissue-processor using a graded ethanol series culminating in the manual addition of Histoclear. Samples were then embedded using the Tissue Tek® TEC® embedding centre and sectioned using the Shandon™ Finesse™ Microtome. For immunohistochemistry 2.5 µm sections were cut, picked up on charged slides and baked at 57 °C for 60 mins. To apply antibodies or stain, slides were deparaffinised using a graded series of ethanol. This consisted of incubating tissue sections for 1 min, twice in histoclear, then twice in absolute ethanol and once in 90% ethanol. This series was reversed in order to dehydrate tissue sections following the application of antibodies and stains.

Immunohistochemistry. For immunohistochemical staining, slides were deparaffinised using a graded series of ethanol. Slides were then washed in Tris buffer (pH 7.5) containing Tween 20. Antigen retrieval was then applied to the tissue sections via heat-induced epitope retrieval. The sections were stained using the DAKO Autostainer; the antibodies used are detailed in Table 2.4. The DAKO Autostainer was programed as follows. Firstly, tissue sections were rinsed in Tris buffer (pH 7.5) for 5 min. Then DAKO Real TM Peroxidase solution was applied for 5 min to block. Slides were treated to another 5 min buffer rinse before application of the primary antibody for 30 min. Two buffer rinses were then applied before incubating slides with the secondary antibody-horse radish peroxidase conjugate for 30 min. Two buffer rinses were then applied to the slides. To colour develop, slides were treated with 3'3-diaminobenzidine (DAB) in two 5 min incubations. Slides were then washed three times with dH_2O and counterstained with Gills haematoxylin for 27 s Slides were then washed in tap water and Scotts tap water substitute (STWS) before dehydration with graded ethanol and mounting with synthetic resin.

Table 2.4 Immunohistochemical Antibody List

Antibody	Description	Experimental Purpose	Concentration	Supplier	Product Code
Anti p63	Primary	Basal cell marker	1.125 µg/ml	Abcam	Ab735
Anti CC10	Primary	Clara cell marker	6.67 µg/ml	Bioss	bs-1487
Anti-mouse	Secondary	P63 identification	1/20 diluted	Dako	K4001
Anti-rabbit	Secondary	CC10 identification	1/20 diluted	Dako	K4003

Histology. For histological staining several different stains were used. Haematoxylin and eosin (H&E) was used as a contrast stain; Periodic acid–Schiff (PAS) was used for the staining of glycoproteins, glycolipids and mucins; alcian blue was used in addition to PAS for carbohydrate staining. Slides were deparaffinised using a graded series of histoclear and ethanol and washed in distilled water. For H&E staining, slides were stained in Gills haematoxylin for 5 min, washed in tap water, differentiated in 1 % acid alcohol, washed in tap water and then again in STWS. Slides were counterstained with Eosin for 5 min, washed in tap water, dehydrated with graded ethanol and mounted.

For PAS staining, slides were washed in water then stained with periodic acid for 5 min. Slides were then washed in water before staining with Schiffs reagent for 10 min. Slides were then washed in tap water for at least 20 min before counter staining with Gills haematoxylin for 1 min. Slides were then washed in STWS, dehydrated with graded ethanol and mounted.

For Alcian blue staining, slides were washed in tap water then stained with Alcain blue (pH 2.5) for 10 min. Slides were then washed in tap water for 10 min before counterstaining with 0.25% Safranin O. Lastly, slides were dehydrated with a graded ethanol series and mounted.

2.2.2.6 Histological 3D tissue assessment

To assess the thickness and cell depth of the epithelial cell layer an image-based system of the H&E sections was developed (Fig 2.3). Five images were taken from each section, equidistant along the length of the section using the 40x objective. These five images were then imported into ImageJ and distance calibrated against the known field of view width. For each individual image, three equidistantly spaced measurements were made of apical to basolateral distance and the number of cells also counted. In total, across duplicate cultures, 30 measurements were made. These 30 measurements were then averaged to produce figures of average cell depth and cell number for comparison of different conditions.

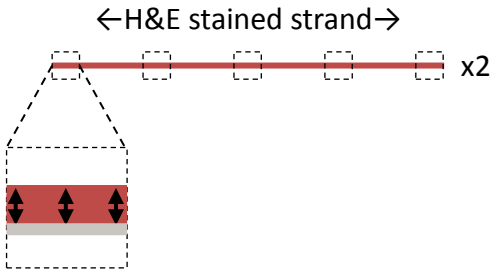

Fig 2.3 Histological measurement scheme
For any single time point and growth condition 30 measurements each of cell number and tissue depth were made. Five equidistant images were captures from two histological sections, each derived from an independent culture. From each image three equidistant measurements of cell number and tissue depth were made.

2.3 Results

2.3.1 Optimisation of cell harvesting and expansion phase

To determine the reliability of extracting and maintaining epithelial cell populations, parameters related to the harvest process and expansion phase were examined.

2.3.1.1 Fibroblast removal (phase 1)

Fibroblasts present a challenge when trying to extract primary populations of cells due to their widespread occurrence and rapid proliferation in culture. The initial phase of development was thus concerned with examining epithelial purity. The epithelium of a fresh bovine trachea was harvested as outlined in section 2.2.1.1 with the following amendments for the purposes of the experiment. An initial cell count was performed to determine the total number of extracted cells before adjusting the cells to a concentration of $7x10^5$ cells/ml and splitting into four flasks. One flask was cultured as normal, whilst the remaining three were incubated for 2, 4 and 6 h at 37 °C to allow fibroblasts to settle out of suspension and attach to the flask (referred to as 'panning'). Following this settling period, cells remaining in suspension were collected by centrifugation at 300 x g for 5 min and re-seeded at $7x10^5$ cells/ml on to coverslips. The total live/dead population was estimated at each of the four time points by Tryphan blue counting at each time point (Fig 2.4 A). The proportion of live cells between t=0 and t=2 decreased substantially with a small, further decrease in live cell numbers at t=4 and t=6. The population of dead cells did not vary with panning time. Thus, with longer panning times, the ratio of live to dead cells is reduced.

To determine the enrichment of epithelial cells at each time point (0, 2, 4 and 6 h) a pan-cytokeratin epithelial marker was employed. This was used to distinguish epithelial cells amongst the total cell population, including fibroblasts, via duel-staining with rhodamine-phalloidin. Thus, cells marked with the pan-cytokeratin antibody are conclusively epithelial, while those only marked with rhodamine-phalloidin represent other cell types, including contaminating fibroblasts.

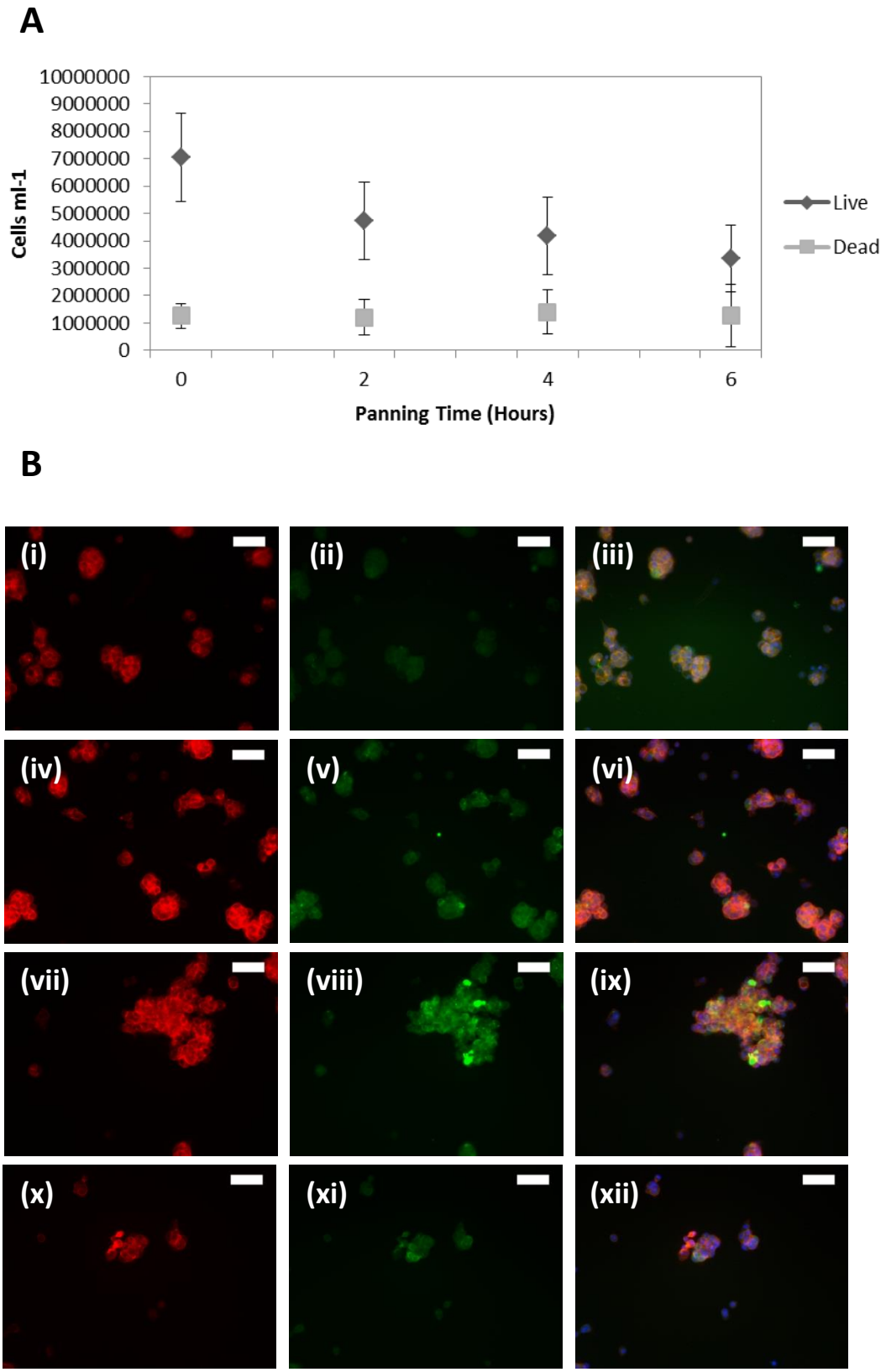

Fig 2.4 Effect of panning on fibroblast depletion.
(A) Graph of total cell counts as a function of panning time. (B) Immunofluorescent images showing actin (red), cytokeratin (green) and the co-localisation (merged) for the three columns of images respectively. Time intervals are as follows, (i), (ii) and (iii), 0 h; (iv), (v) and (vi), 2 h; (vii), (viii) and (ix) 4 h; (x), (xi) and (xii) 6 h. Scale bar represents 50µm.

Cultures panned for different times (0, 2, 4 and 6 h) were allowed to proliferate for 24 h on coverslips before fixation and immunostaining. All visible cells displayed fluorescence for each marker irespective of panning time (Fig 2.4 B). Thus, the cell population extracted was extremely low in fibroblasts with panning offering no further improvement in epithelial purity. **In conclusion, panning or any other measures aimed at removing fibroblasts would confer little benefit on epithelial cell harvesting.**

2.3.1.2 Expansion phase media (phase 1)

The next concern with regards to basic cultivation was the selection of a medium that allows for maximal cell proliferation in submerged culture. Two base media, a 50:50 mixture of DMEM:HAM's F12 and M199 were tested with three different serum concentrations of 0, 5 and 10 %. Harvested cells were resuspended in each medium, then seeded onto coverslips at $5x10^4$ cells/cm^2 and allowed to proliferate for 24 and 72 h. Following proliferation, cells were fixed and enumerated (Fig 2.5). An identical and healthy morphological appearance was observed for cells grown in either base media at serum concentrations of 5 and 10 % (Fig 2.5 A). A serum concentration of 0 % in either media resulted in a morphologically different appearance to that of higher serum concentrations. This included irregular cell borders and the presence of fragmented cell material suggestive of cell death (Fig 2.5 A).

Enumeration of cells revealed cell proliferation was higher in DMEM:HAM's F12 over M199 at equivalent serum concentration and time points (Fig 2.5 B). Serum concentration clearly influenced epithelial cell growth for both media types tested. Increased cell numbers were observed via the use of 5 % serum compared with 0 % serum for both media at 72h. A slight increase in proliferation was observed through the use of 10 % serum compared with 5 % serum for DMEM:HAM's F12. This was not observed for M199. **Ultimately, the condition of DMEM:HAM's F12 with 10% serum gave the greatest proliferation at 72h and was therefore chosen as the base medium for the submerged phase expansion.**

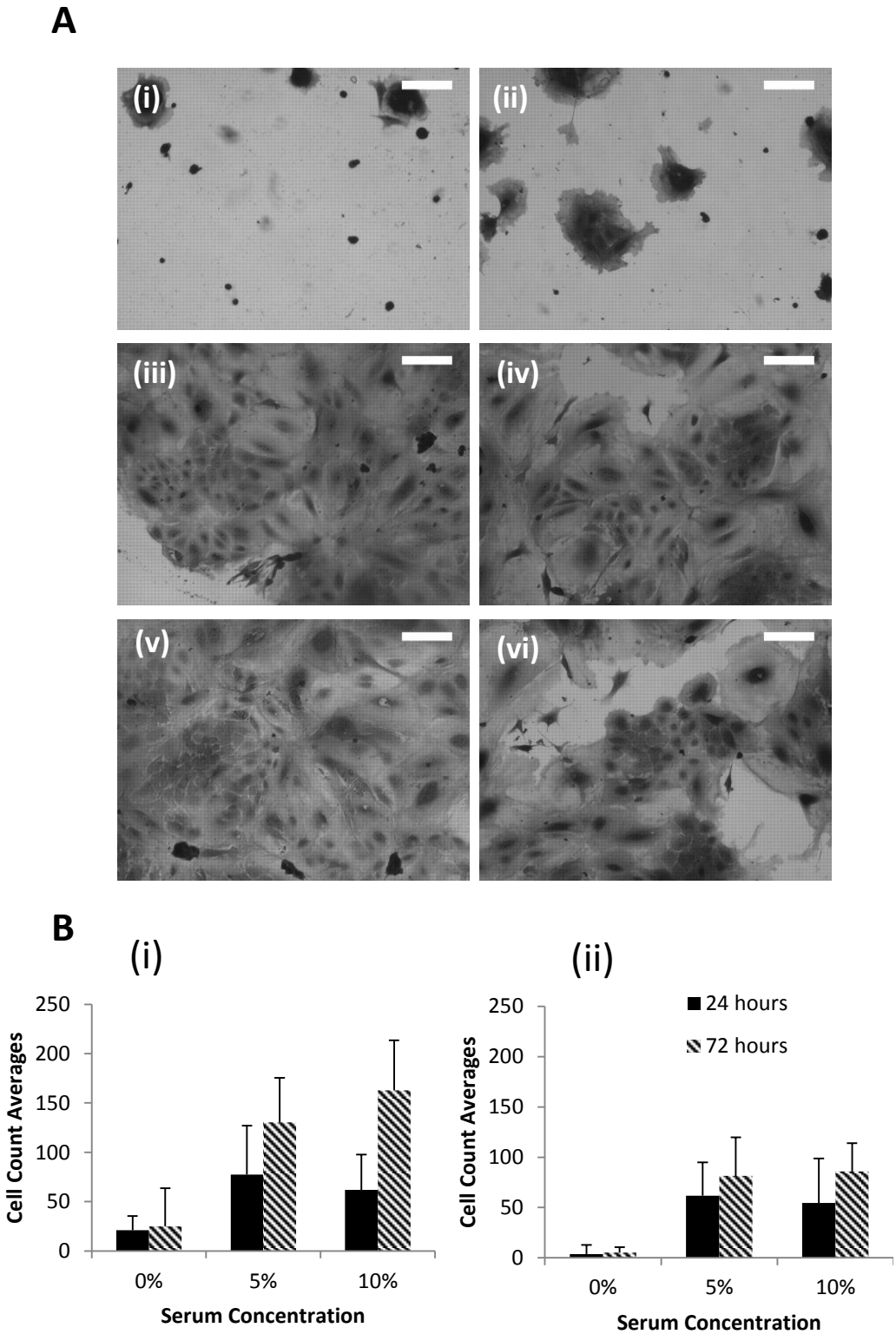

Fig 2.5 Effect of media type and serum concentration on cell proliferation.
(A) Representative images of Coomassie-stained cells grown for 72 h in different media and with different serum concentrations; (i), DMEM:HAM's F12 + 0 % FCS; (ii), M199 + 0 % FCS; (iii), DMEM:HAM's F12 + 5 % FCS; (iv), M199 + 5 % FCS; (v), DMEM:HAM's F12 + 10 % FCS; (vi), M199 + 10 % FCS. Scale bar represents 50 µm. (B) Graphs quantifying six field counts from three independent replicates of cells grown in (i) DMEM:HAM's F12 and (ii) M199, with three concentrations of serum, after 24 and 72 h.

2.3.2 Optimisation of epithelial differentiation

2.3.2.1 Media and substrate optimisation (phases 2 and 3)

The properties of substrate surface and media formulation were examined for their potential to induce differentiation in epithelial cells. Three substrates, polytetrafluoroethylene (PTFE), polyethylene terephthalate (PET), and PET-collagen, were chosen based on their widespread use in the literature (Appendicies; Table 7.1). These surfaces represent entries 1, 2 and 3 of Table 2.1. Three base media were also chosen based on their widespread use in the literature (Appendicies; Table 7.1). These include, BEGM:DMEM, AEGM:DMEM and DMEM:HAM's F12, the details of which are described in section 2.2.1.3. Cells grown on each substrate were compared with growth in each media type resulting in a nine way comparison, each of the substrate-media combinations were examined 14 and 21 days post-ALI.

After 14 days of ALI growth differences in cell morphology were observed and by 21 days post ALI clear differences could be observed by histological assessment (Fig 2.6). Of the nine combinations, six of these (AEGM:DMEM and BEGM:DMEM, each with the three different substrates) appeared to be pseudostratified with an epithelial cell depth of several cells (Fig 2.6 A [i], [ii] & [iii]; B[i], [ii] & [iii]). Of the remaining three conditions, DMEM:HAM's F12 with either PET or PET-collagen appeared to have only achieved growth of between one and two cells deep; this was considerably less than that of the other media used (Fig 2.6 C [i] & [ii]). Regions of the epithelium were considerably thicker, creating islands of increased cell density in localised places. The DMEM:HAM's F12 condition in combination with the PTFE substrate yielded a thicker epithelium. However, cell morphology appeared to comprise a squamous phenotype (Fig 2.6 C [iii]).

Tissue and cell depth analysis of the nine combinations reinforced the morphological observations (Fig 2.7). At 14 days post ALI, cells that had been grown in AEGM:DMEM were similar in thickness to the native tissue yet had a greater number of cells comprising the tissue depth (Fig 2.7 B). Cells grown in BEGM:DMEM produced a thinner tissue than AEGM:DMEM or the native tissue but with a more comparable cell depth number to the native tissue (Fig 2.7 C).

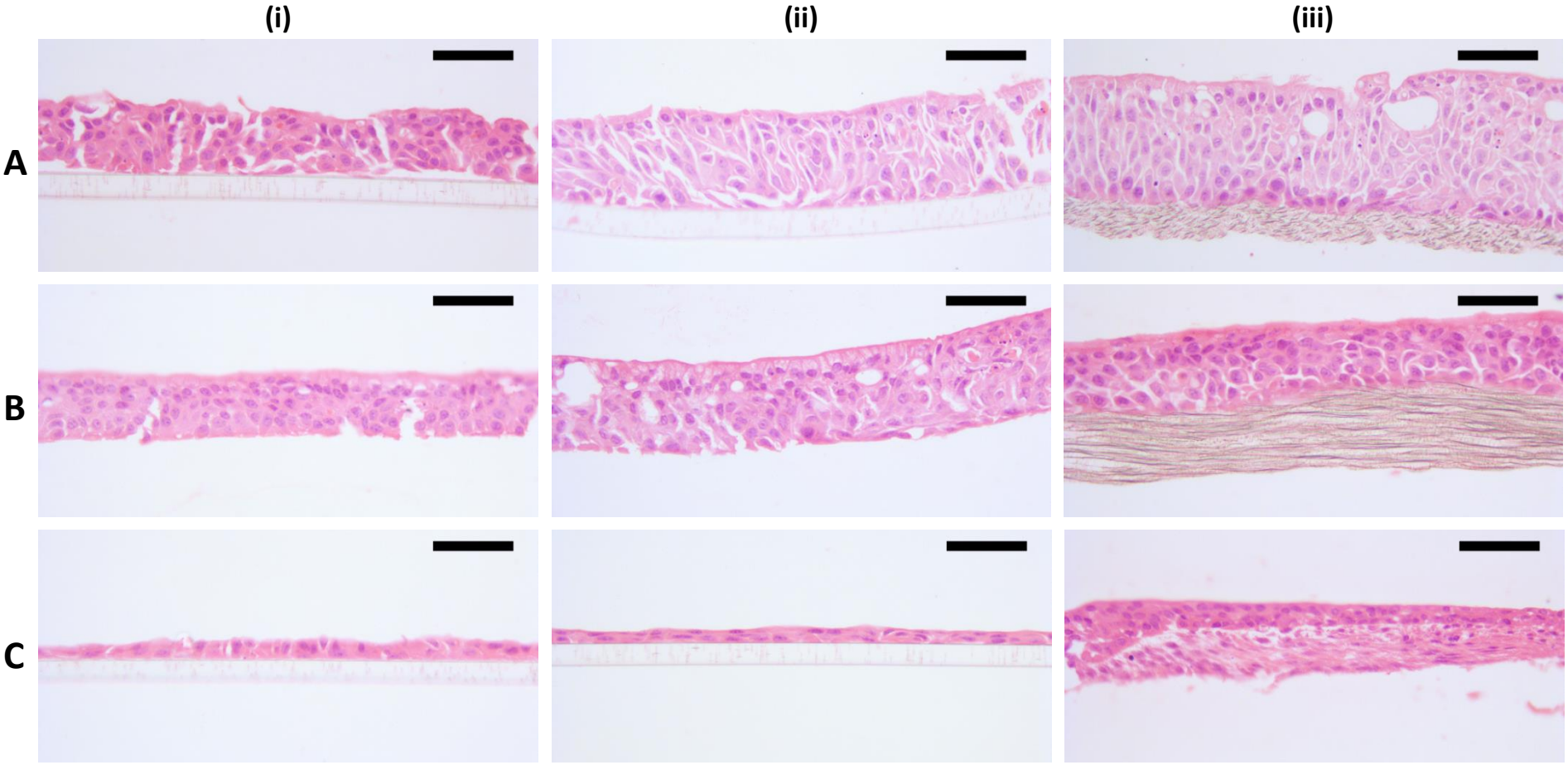

Fig 2.6 Representative H&E stained histological sections of ALI cultures grown using three different substrates and three different base media. Cultures were maintained at ALI for 21 days. Images are labelled in rows as (A) AEGM:DMEM, (B) BEGM:DMEM and (C) DMEM:HAM's F12. Images are labelled in columns as (i) PET, (ii) PET-collagen and (ii) PTFE. Scale bar represents 50µm.

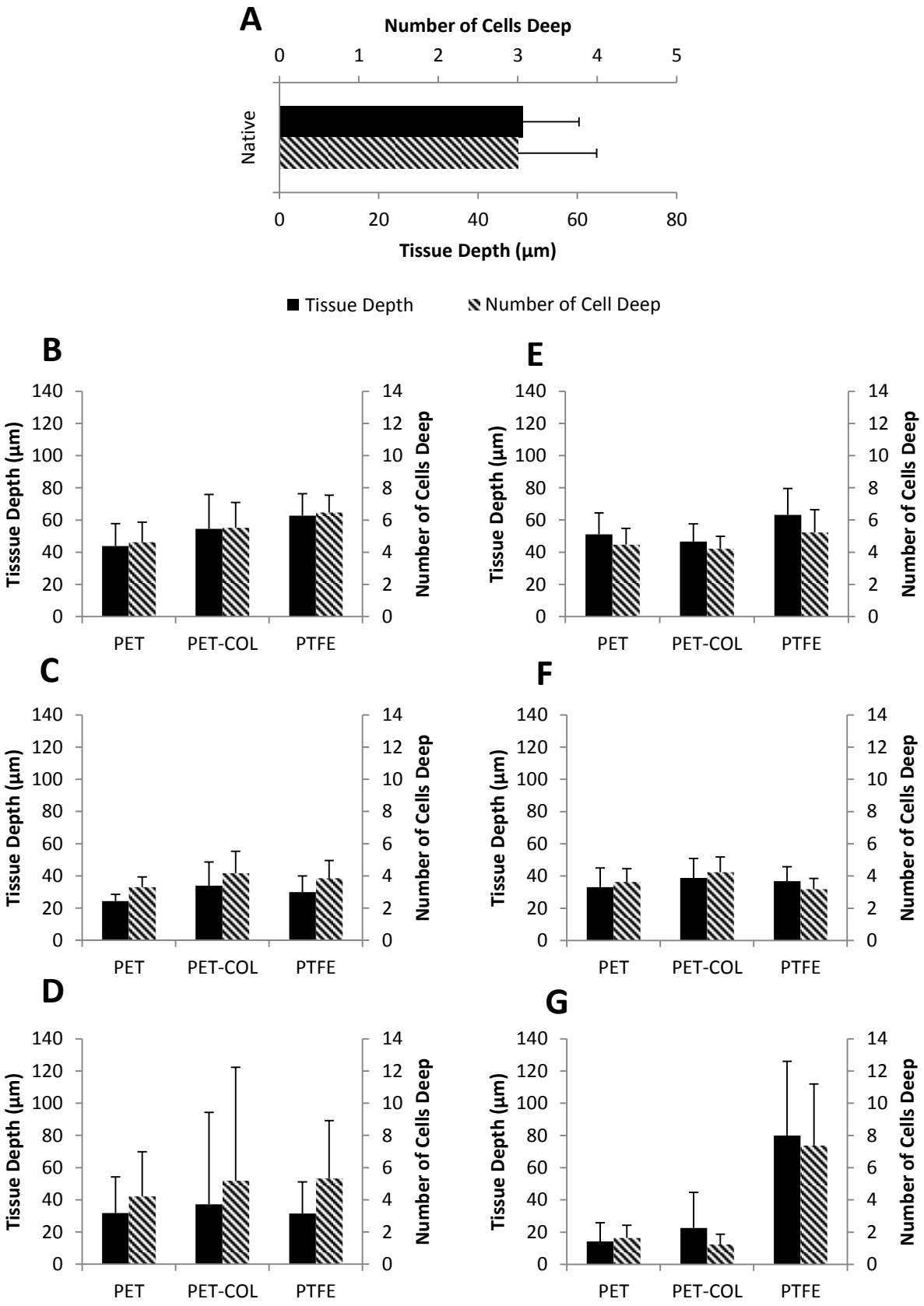

Fig 2.7 Tissue and cell depth analysis of ALI cultures grown using three different substrates and three different media.

Measurements were taken of the native tracheal epithelium (A), and for the in vitro cultures at 14 days (B-D) and 21 days (E-G) post ALI. (B) and (E) represent AEGM:DMEM media, (C) and (F) represent BEGM:DMEM media and (D) and (G) represent DMEM:Ham's F12 media. Details of all media are provided in Materials and Methods (2.2.1.3).

Cells grown in DMEM:HAM's F12 (Fig 2.7 D) produced a similar average cell and tissue depths to the other two media. However, the variability in the histological measurements was greater. This is evident from the standard deviation error bars in Fig 2.7 D. There was little variation in tissue thickness and cell depth amongst any of the substrates tested within a single media condition.

The same histological assessment was carried out on 21 day post-ALI cultures (Fig 2.7, E, F and G). Similar to the 14 day results, cells that had been grown in AEGM:DMEM for 21 days post ALI on any of the three substrates had a tissue depth similar to the native tissue (Fig 2.7 A + E). At 21 days post-ALI, cells of the BEGM:DMEM condition had formed a tissue only slightly thicker than at 14 days, and still slightly thinner than the native tissue (Fig 2.7 A + F). However, the average cell depth was more comparable to the native environment than was measured for the cells of the AEGM:DMEM condition. Both the AEGM:DMEM and BEGM:DMEM conditions produced similar tissue thicknesses for all three of the substrate conditions at 21 days post ALI (Fig 2.7 E + F). Cells of the DMEM:HAM's F12 condition at 21 days post ALI was the only condition that displayed prominent variation in cell and tissue depth amongst the material substrates tested. Cells grown on PET and PET-collagen with HAM's F12:DMEM as the media source yielded an epithelium considerably thinner than the native tissue (Fig 2.7 A + G). As mentioned, this was predominantly a monolayer of cells with no polarisation. Conversely, cells grown on PTFE in DMEM:HAM's F12 produced an epithelium that was on average much thicker than the other two substrates. However, as already mentioned, these cells appeared to be squamous and lacking polarisation.

Analysis of the TEER throughout the culture period demonstrated cells grown under all the conditions tested, except DMEM:HAM's F12 on PTFE, formed a good electrical barrier (Fig 2.8). The eight conditions that maintained an electrically tight epithelial layer all experienced an initial rise in TEER, followed by a decrease in TEER between day three and day nine. All cultures experienced a second peak in TEER at day 11 (four days post-ALI generation) followed by a decrease in TEER to values that remained stable for the duration of the

experiment.

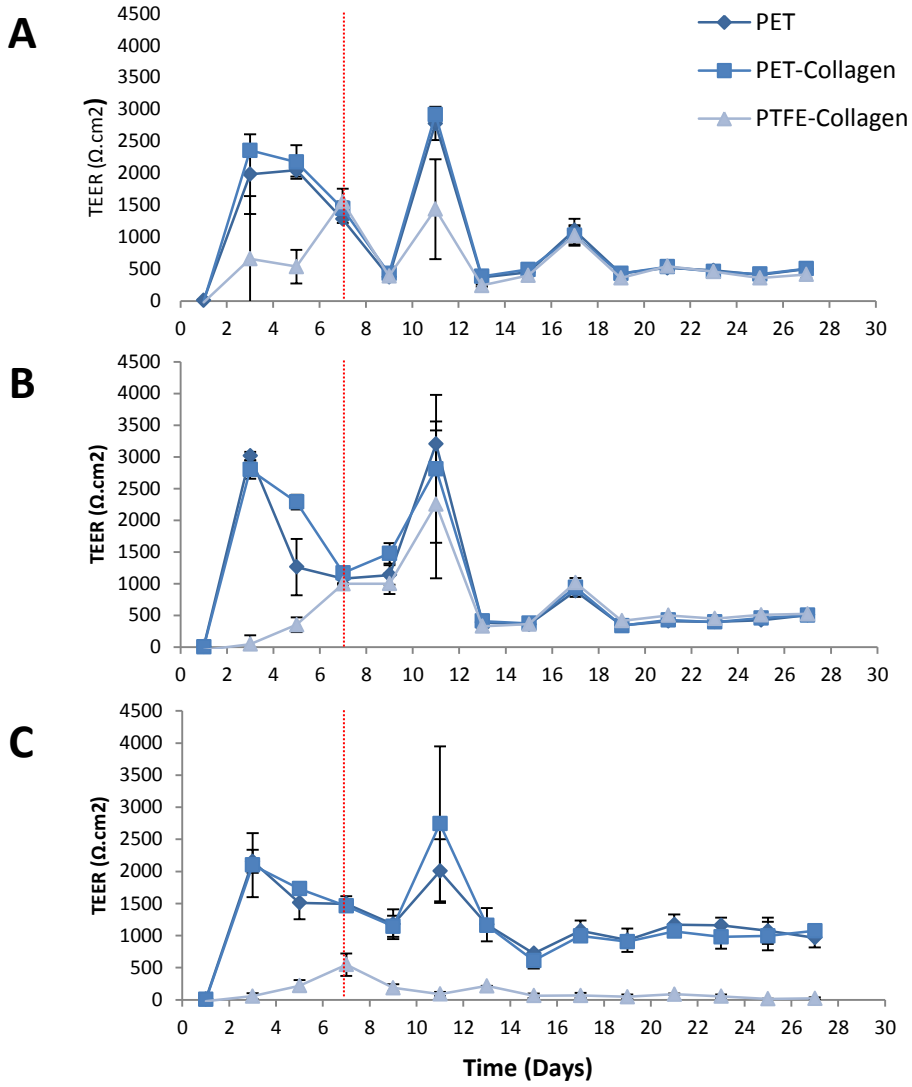

Fig 2.8 TEER measurements of ALI epithelial cultures grown on different substrates and in different media.
(A) BEGM:DMEM; (B), AEGM:DMEM; (C), DMEM: HAM's F12. ALI generation is indicated by the red line. Each measurement was taken three times for three individual cultures; error bars reflect the average of these nine measurements.

The conditions of PET and PET-collagen with DMEM:HAM's F12 as the media source produced cell layers with stabilised TEER values of ≈1000 $\Omega.cm^{-2}$ from day 12 onwards. All other conditions produced stable TEER values of ≈500 $\Omega.cm^{-2}$ from day 12 onwards.

Analysis of 21 day old ALI cultures by SEM revealed all nine conditions supported the formation of ciliated cells (Fig 2.9).

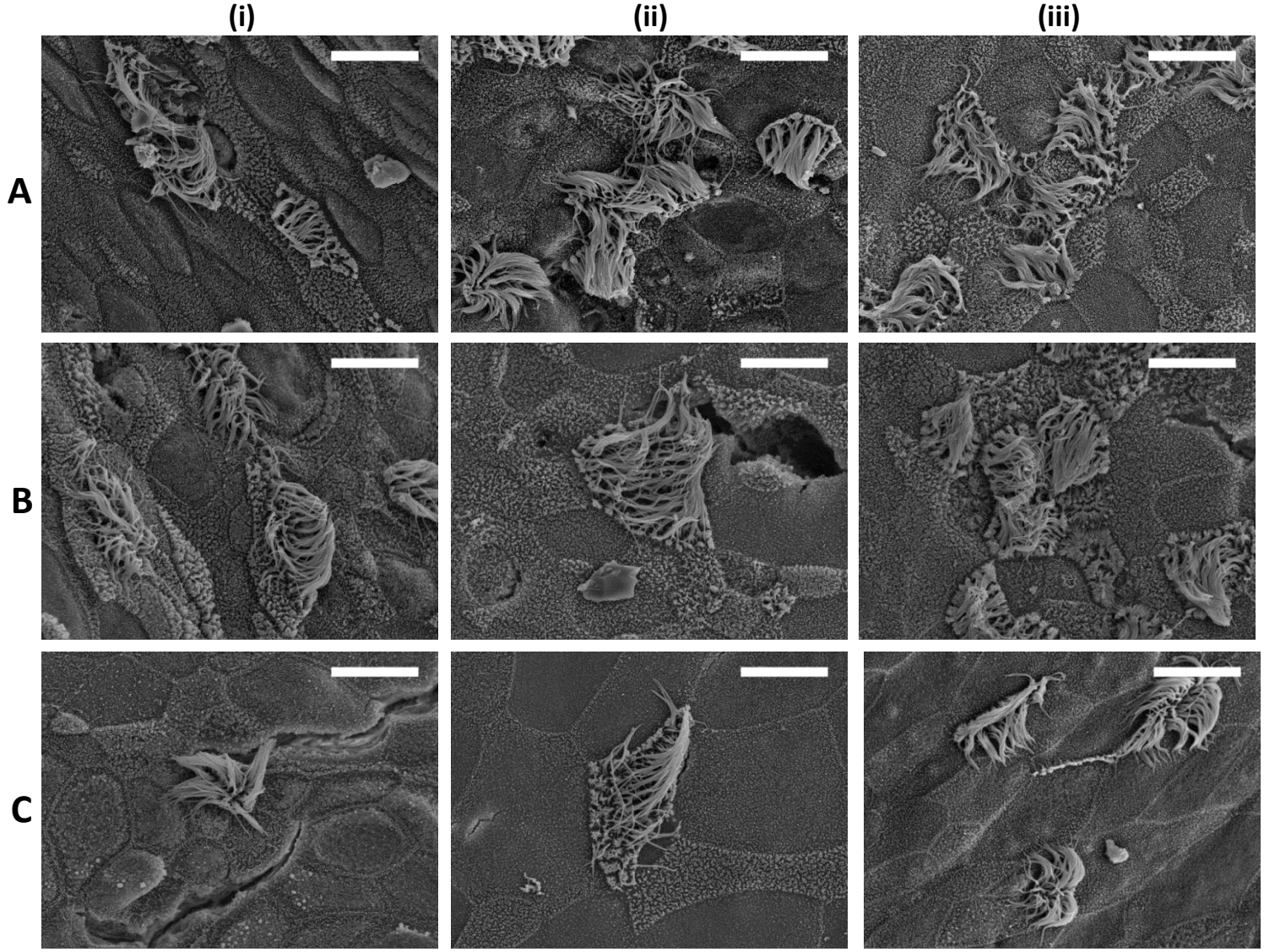

Fig 2.9 Representative SEM imagesof ALI cultures grown using three different substrates and three different base media.
Cultures are 21 days post ALI. Images are labelled in rows as (A) AEGM:DMEM, (B) BEGM:DMEM and (C) DMEM:HAM's F12. Images are labelled in columns as (i) PET, (ii) PET-collagen and (ii) PTFE. Scale bars represents 50µm.

Cultures grown in BEGM:DMEM and AEGM:DMEM and in combination with the PTFE surface appeared to have more ciliated cells than the equivalent cultures grown on PET and PET-collagen substrates (qualitative observations). Few ciliated cells could be found amongst the DMEM:HAM's F12-PET and DMEM:HAM's F12-PET-collagen grown epithelial cells. Cells grown under the DMEM:HAM's F12-PTFE condition exhibited the least cilia of all. The cilia imaged in Fig 2.9 C-(iii) were the only ciliated cells found amongst cells of the DMEM:HAM's F12-PTFE culture condition.

The condition of AEGM:DMEM with a PTFE substrate was selected for further optimisation. This was on the basis of tissue depth similarity to the native environment, formation of an electrically tight barrier and the observed production of ciliated cells.

2.3.2.2 Refinement of media and substrate conditions (phase 2)

Having selected the base conditions it was noted that there was a considerable amount of variation in the performance of cells grown on PTFE inserts. Cells failed to grow to confluency after seeding on the PTFE inserts rendered ALI generation unfeasible. To address this issue, an experiment was designed looking at several factors that might contribute to epithelial growth during phase two of the culture process (Table 2.5). The experiment included the consideration that growth at phase one may affect performance at phase two, so alongside the previously optimised submerged growth media (DMEM:Ham's F12) a specialist media, AEGM™, was tested. The use of retinoic acid (RA) during phase two culture is divided in the literature. The knowledge that RA is used as an inducer of epithelial differentiation, rather than a growth promoter (1.3.7.1), provided the rationale that its involvement in phase two may hamper differentiation. Thus, the effect of RA incorporation or exclusion in the phase 2 culture process was examined. Additional considerations were made for the abrupt change in media environment and so taken into account was a 50:50 change in phase 2 to phase 3 (ALI) media. Cell seeding density was also explored where a cell seeding density lower than used previously was tested. A higher seeding density was also examined under a single condition (PET (A)).

Table 2.5 Experimental plan for comparing different phase two (membrane expansion phase) media during differentiation.

Culture conditions								
Group[a]	Phase1	Phase 2		Phase 3		Membrane insert seeding densities[e]		
	Media[b]	Media[c]	Retinoic Acid[d]	Media[c]	Retinoic Acid[d]	1.25 x 10^5 Cells ml^{-1}	2.5 2.5 x 10^5 Cells ml^{-1}	1x10^6 Cells ml^{-1}
(A)	Serum	AEGM:DMEM (50:50)	+	AEGM:DMEM	+	2	2	1
(B)	Serum	AEGM:DMEM (50:50)	-	AEGM:DMEM	+	2	2	0
(C)	Serum	Serum and Serum:(AEGM:DMEM) (50:(50:50))	+	AEGM:DMEM	+	2	2	0
(D)	Serum	Serum and Serum:(AEGM:DMEM) (50:(50:50))	-	AEGM:DMEM	+	2	2	0
(E)	AEGM	AEGM	-	AEGM:DMEM	+	2	2	0
(F)[f]	AEGM	AEGM and AEGM:Pneuma (50:50)	-	Pneumacult ALI	+	2	2	0
(G)	AEGM	AEGM and AEGM:Pneuma (50:50)	-	Pneumacult ALI	+	0	1	0
PET(A)	Serum	AEGM:DMEM	+	AEGM:DMEM	+	0	2	1
					Total:	**14**	**18**	**2**

[a]Group letter as referred to in the text. Group (A) represents previously used conditions. All groups except PET (A) were cultured on PTFE substrates.
[b]Serum refers to HAM's F12:DMEM containing 10% serum. AEGM refers to the Airway Epithelial Basal Medium (AEBM) with the manufacturers supplements added.
[c]AEGM:DMEM refers to the media previously described (2.2.1.3). Pneumacult™ refers to the media formulated as per the manufacturer's instructions. Mixing 50:50 refers to the mixing of media prior to supplement addition.
[d]Retinoic acid refers to inclusion (+) or exclusion (-) of RA at various phases of growth. Inclusion of RA (+) in each case refers to a concentration of 10 ng/ml (330nM).
[e]Numbers listed in each column refer to the number of culture inserts used for each group of conditions at each seeding density.
[f]Condition (F) was identical to that of condition (G).with the intention of omitting cholera toxin from the media at phase 3, however this was never realised (as discussed in text).

Phase two epithelial growth was assessed seven days post-seeding, a time period where cells would ordinarily be confluent before ALI generation. Differences in cell growth were observed amongst the conditions tested (Table 2.6).

Table 2.6 Confluency assessment after growth under different experimental conditions. Experimental groups refer to the culture conditions described in Table 2.5. Values are displayed as a qualitative assessment of % confluency.

Group	Trachea		
	P1 Transwells[a]		
	1.25 x 10^5 Cells ml^{-1}	2.5 x 10^5 Cells ml^{-1}	1x10^6 Cells ml^{-1}
(A)	++	++	N/A
(B)	+	+	N/A
(C)	+++	+++	N/A
(D)	+++	+++	N/A
(E)	-	-	N/A
(F)	-	-	N/A
(G)	-	-	N/A
PET(A)	N/A	++++	++++

[a] Scoring: (-) no growth beyond seeded cells, (+) minimal growth, (++) at least 80% confluent, (+++) confluent but unable to hold a barrier, (++++) fully confluent and able to hold a barrier

Cells from one of the groups tested reached confluency and sustained an electrically tight barrier, this was the group that utilised the PET substrate (PET(A)). The other groups, all of which used PTFE substrates, failed to produce a compete monolayer of cells. Groups (A) and (B) failed to grow to confluency with growth arrested by day ten with an estimated maximum surface coverage of 75 %. Conditions (C) and (D) grew to confluency indicating a marked improvement over conditions (A) and (B). However, their TEER was poor with values of 35±24 and 77±2 $\Omega.cm^2$ achieved by day ten for (C) and (D) respectively. As a result an ALI could not be generated on these inserts. Conditions (E), (F) and (G) which were grown in AEGM™, failed to grow to any extent when seeded on membrane inserts. Cells grown in the same conditions (Table 2.5 [A-G]) on coverslips reflected this trend (Fig 2.10).

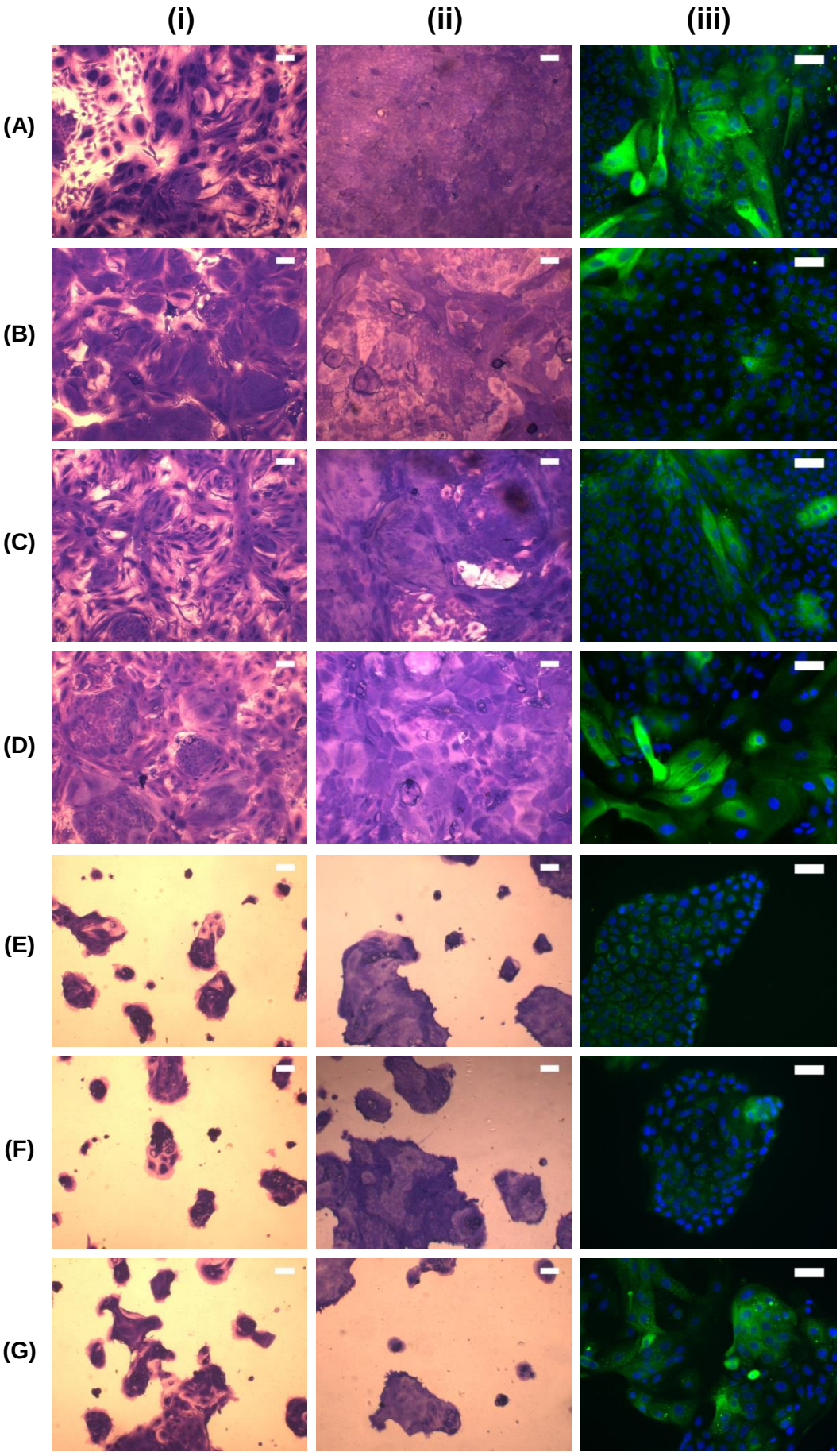

Fig 2.10 Coomassie and cytokeratin stained submerged cultures grown in different media. Growth conditions (A-G) as described in Table 2.5. Coomassie stained cells are displayed four days (i) and seven days (ii) after seeding. (iii) Immunofluorescent cytokeratin (green) and nuclei (blue) stained cells are shown seven days after growth. Cells were seeded at a density of 1.25 x 10^6 cells/cm^2 onto coverslips. Scale bars represent 50 µm for (i) and (ii) and 100 µm for (iii).

Conditions (A) to (D) were close to confluency by day four and fully confluent within seven days. Conditions (E) to (G) failed to achieve any substantial growth by day seven. All conditions resulted in the production of cytokeratin positive cells, ruling out the possibility that non-epithelial cells (including fibroblasts) may be contributing to the lack of growth and poor barrier formation (Fig 2.10 [iii]). **Therefore, as conditions (A) through (G) failed to grow to confluency on PTFE inserts, and the only conditions which could grow to confluency and support barrier formation was PET (A), the conclusion was that the deciding factor in growth performance at phase 2 is the cell culture substrate**.

2.3.2.3 Refinement of material properties (Phase 2 and 3)

To test the hypothesis that substrate material might be influencing the poor growth observed an experiment was designed (Table 2.7).

Table 2.7 Experimental conditions tested to evaluate base condition growth

Condition	Material	Passage	Panning	Trypsin method
(A)	PET	P0	+	N/A
(B)	PET	P0	-	N/A
(C)	PET	P1	+	1
(D)	PET	P1	+	2
(E)	PET	P1	-	1
(F)	PET	P1	-	2
(G)	PTFE	P0	+	N/A
(H)	PTFE	P0	-	N/A
(I)	PTFE	P1	+	1
(J)	PTFE	P1	+	2
(K)	PTFE	P1	-	1
(L)	PTFE	P1	-	2

Properties related to membrane material (PTFE and PET) were examined along with a comparison of cell seeding methodologies, the influence of passage (P0 and P1) and the influence of panning to address fibroblast removal. Of all the combinations tested the only parameter that affected cell growth during phase 2 of culture was the property of substrate material. Cells grown on PET surfaces, irrespective of the other parameters tested, achieved confluency at day seven post-seeding and were cultured at ALI for a further 21 days. Contrary to this, cell growth on PTFE surfaces under all conditions was slow. Conditions (G), (H), (J), (K) and (L) all failed to produce a confluent monolayer. For condition (I),

which had displayed TEER values of greater than 500 $\Omega.cm^2$ at day 12, an attempt at ALI generation was made. This attempt failed to produce a barrier capable of withstanding basal media seepage and thus ALI generation was rendered impossible for condition (I). These results demonstrated that poor growth was a direct result of the membrane material. Only PET substrates could reproducibly achieve adequate growth at phase 2, allowing for the establishment of an ALI.

Together these experiments established a base parameter set of growth conditions from which to examine the properties of differentiation in more detail. SEM and histology analysis of cells cultured on PET substrates highlighted that the differentiated epithelium mainly consisted of two distinct phenotypes under any of the tested culture conditions (Fig 2.11). The first of these phenotypes was characterised by a relatively flat epithelium lacking any markers of differentiation such as ciliation or mucus production (Fig 2.11, 'undifferentiated'). The second of these phenotypes consisted of a thick non-uniform epithelium characterised by an uneven surface topology and a moderate level of ciliation (Fig 2.11 'thick tissue'). The cultures that used PET as the membrane material (A-F) exhibited no variation based on the other parameters tested. **Therefore one condition, (Table 2.7 E), was selected to serve as the culture condition for further optimisation.**

2.3.2.4 Oxygen tension and substrate pore density (phase 3)

Utilising the base condition (E) as described in Table 2.7 the parameters of oxygen tension and membrane pore density were examined to evaluate their effect on epithelial differentiation. To test oxygen tension, values of 21%, representing standard culture conditions, and 14%, representing the average O_2 concentration in the respiratory tract, were compared. To test the influence of membrane pore density upon the epithelial cells a low pore density surface of 2 x 10^6 pores/cm^2 and a high pore density of 1 x 10^8 pores/cm^2 were compared. The four-way comparison was evaluated following 14 and 21 days of ALI culture. Comparative analysis of the degree of ciliation by IFA-intensity (2.2.2.4) revealed a striking difference in the proportion of ciliated cells present between the different conditions (Fig 2.12 A).

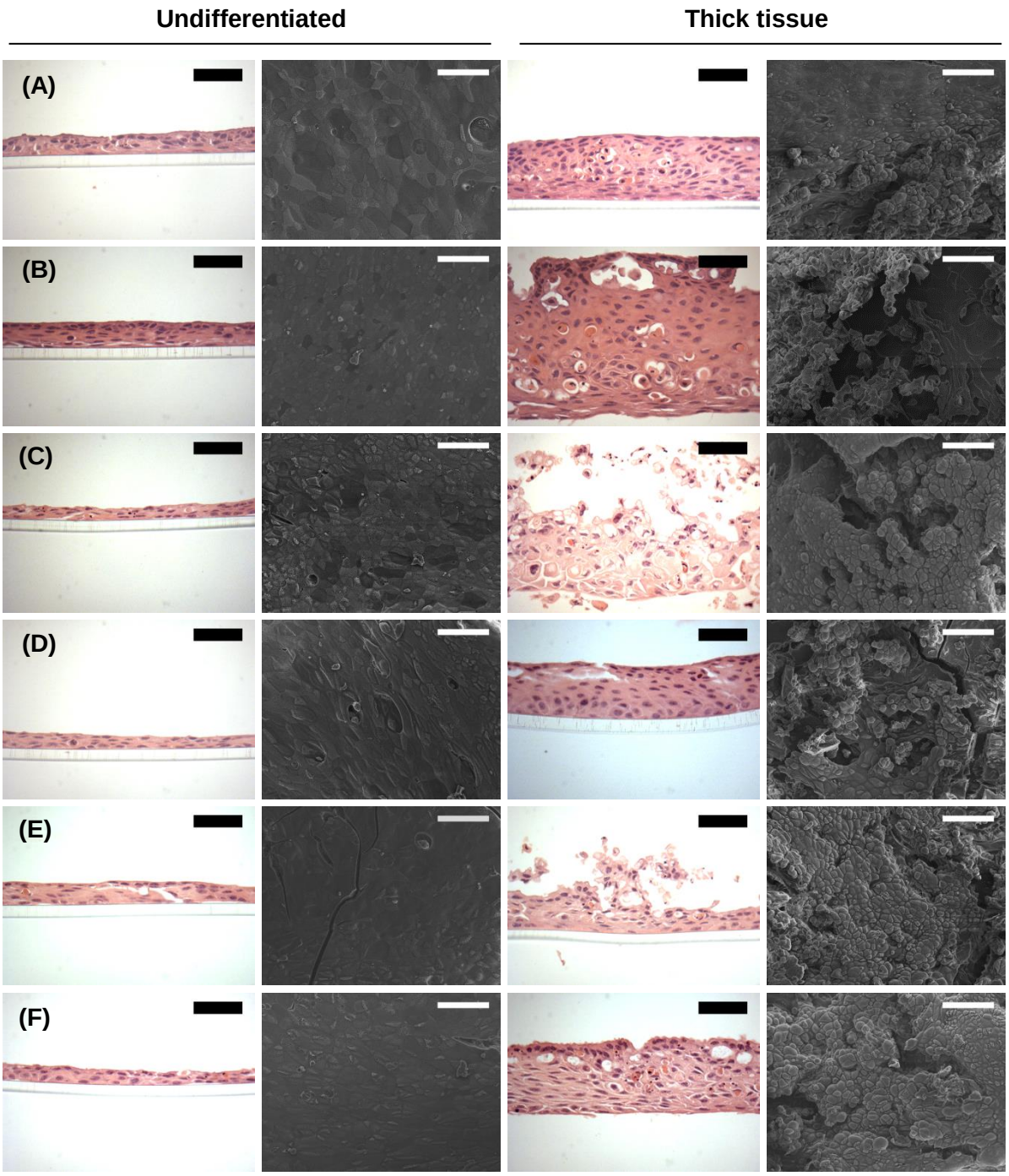

Fig 2.11 Epithelial ALI cultures produced under different harvest and culture conditions. SEM images and H&E stained histological sections from the experimental groups. All images are of 24 day old PET Transwell cultures. (A) to (F) correspond to entries in Table 2.7. (A); P0 + panning; (B); P0 – panning, (C); P1 trypsin method 1 + panning, (D); P1 trypsin method 1 – panning, (E); P1 trypsin method 2 + panning, (F) P1 trypsin method 2 –panning. Each line contains a total of four images from each condition. Scale bars represent 50µm.

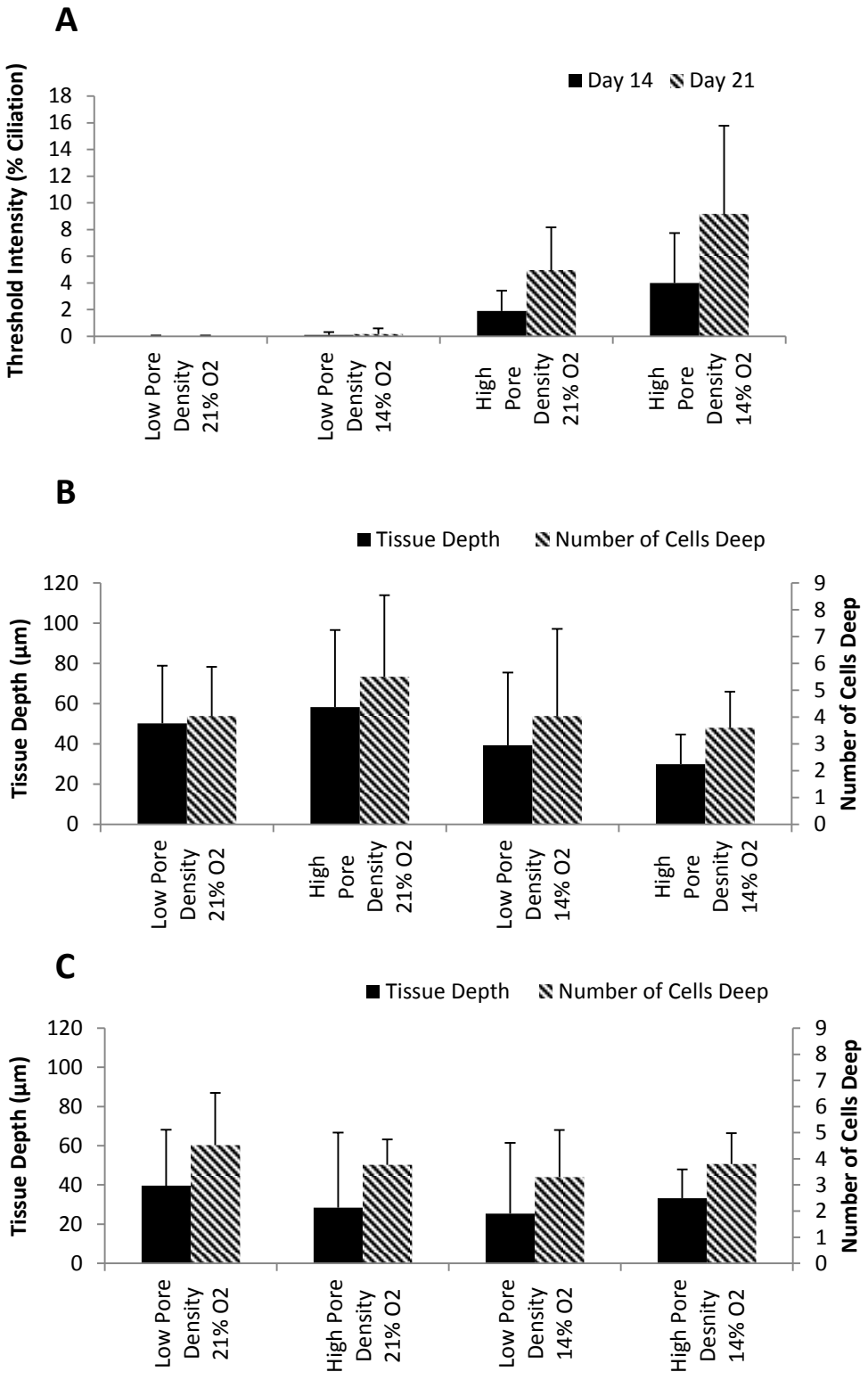

Fig 2.12 Effect of oxygen tension and substrate pore density on differentiation. (A) Percent ciliation of the four tested conditions determined via fluorescence intensity threshold measurement. (B) Day 14 post ALI tissue and cell depth analysis of the four tested conditions. (C) Day 21 post ALI tissue and cell depth analysis of the four tested conditions.

Of the four conditions tested, the two high pore density conditions produced higher levels of ciliation as compared to the low pore density groups at 21 and 14 days post-ALI. Ciliation levels were also higher in cells grown under the 14 % O_2 condition as compared to cells grown under the 21 % O_2 condition.

The marked differences observed in ciliation were reinforced when analysing the number of ciliated cells in histological sections. Ciliated cells counted per section mirrored the values calculated from the fluorescence intensity. Ciliated cells per section length were counted for 14 day post-ALI cultures and determined to be 2, 2, 15 and 2 for the 20 % O_2-high pore density, 14 % O_2-low pore density tension, 21 % O_2 -low pore density and 14 % O_2 -high pore density conditions respectively. Ciliated cells per section length were counted for 21 day post-ALI cultures and determined to be 36, 1, 53 and 2 for the 21 % O_2-high pore density, 14 % O_2-low pore density tension, 21 % O_2 -low pore density and 14 % O_2 -high pore density conditions respectively.

The influence of the four parameters on epithelium thickness was examined. The result revealed that neither oxygen tension nor pore density had any influence on average epithelial thickness at either 14 or 21 days post-ALI (Fig 2.12 B&C). Of the measurements taken, consistency in thickness was improved in the 14% O_2–high pore density condition relative to the other conditions tested. This is evident from the standard deviation values of the thickness measurements. **Collectively, the results indicate that 14 % O_2 and a high pore density are superior to the other conditions tested; as a result, these conditions were taken forward for further optimisation.**

2.3.2.5 Epidermal growth factor and retinoic acid concentration (phase 3)

Epidermal growth factor (EGF) and retinoic acid (RA), which are influential on epithelial differentiation (1.3.7.1), were examined to determine optimal concentrations. A range of concentrations were tested based on their use in the literature; concentrations of 0, 0.5, 2.5, 5 and 10 ng/ml of EGF were tested at a fixed RA concentration of 100 nM and retinoic acid concentrations of 0, 25, 50, 100 and 250 nM were tested at a fixed EGF concentration of 0.5 ng/ml. Cultures were maintained for 14 and 21 days post-ALI before analysis.

During culture, no trend was observed between the concentration of EGF in the culture media and TEER values. Conversely for RA, an inverse relationship between concentration and TEER was observed for the RA variable cultures (Fig 2.13). This RA-dependent TEER pattern emerged at day 19 of culture (10 days post-ALI) and continued to the end of the experiment at day 30 (21 days post-ALI).

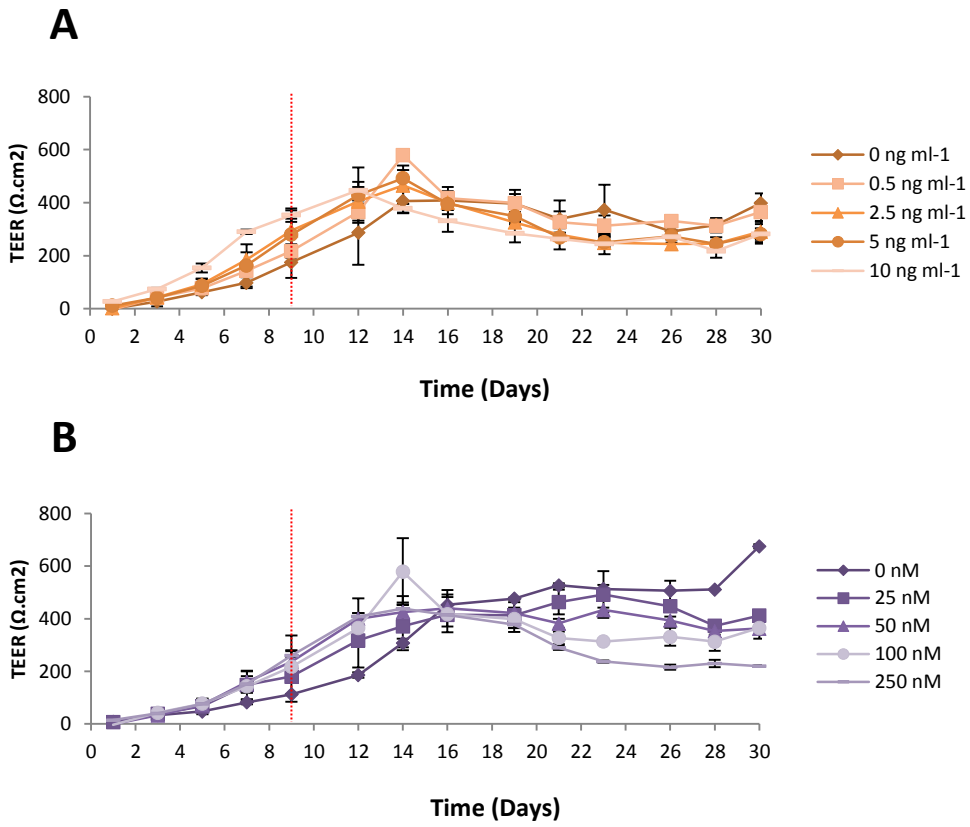

Fig 2.13 TEER graphs of ALI cultures grown in the presence of different EGF and RA concentrations.
Displayed are the TEER measurements of cultures grown with different EGF (A) and RA (B) concentrations. Cells were seeded on day 0, cultured for a further three days in SGM before switching to 50:50 SGM:ALI media containing the respective growth factor alterations. Red line indicates the point at which ALI was generated and cultures were switched completely to ALI media.

Thickness and cell depth measurements for varying concentrations of EGF and RA revealed several concentration-dependent effects. **(1)** At 14 days post-ALI, 10 ng/ml of EGF resulted in thicker tissue than any of the other concentrations tested (Fig 2.14 A). **(2)** At 21 days post-ALI, a greater tissue thickness was measured for 5 and 10 ng/ml EGF as compared with 0.5 and 2.5 ng /ml EGF (Fig 2.14 B). **(3)** At both 14 and 21 days post-ALI, RA over the concentration range of

25 nM to 250 nM exhibited no effect on epithelial cell and tissue depth (Fig 2.14 C & D). **(4)** The complete absence of either RA or EGF resulted in an increase in tissue depth and cell number relative to the inclusion of these growth factors at the lowest concentrations tested (Fig 2.14). However, when either EGF or RA was completely absent the morphology of the epithelial cells was altered resulting in a larger cell size and a lack of columnar shape (supplementary Fig 7.1).

Evaluation of ciliation levels revealed a concentration-dependent increase in ciliation by EGF (Fig 2.15 A). A maximum degree of ciliation was obtained at 5 ng/ml of EGF with no increase in ciliation observed between 5 ng/ml and 10 ng/ml of EGF. No concentration-dependent effect on ciliation was observed for the RA series (Fig 2.15 B). All EGF and RA concentrations tested produced some degree of ciliation except for 0 nM RA which only produced cytoskeletal microtubules (Fig 2.15 C). All EGF and RA concentrations tested displayed ZO-1 localisation to the boundaries of the cell border indicative of tight junction formation and cell polarisation (Fig 2.15). **The conditions of 5 ng/ml EGF and 100nM RA were selected to serve as the optimal growth factor conditions from which further refinements to the model could be made.**

2.3.2.6 Anatomical origin of airway epithelial cells (phase 3)

The structure and cell composition of the respiratory epithelium varies considerably from the upper respiratory tract through to the alveoli (1.3.1). Thus it is reasonable to assume that populations of cells derived from different anatomical regions of the respiratory tract will behave differently in culture. Epithelial cell populations from three anatomic regions were compared for their ability to produce a suitable *in vitro* model. Cell populations were harvested from the nasopharynx, mid-trachea and bronchi and cultured in parallel at ALI to facilitate the differentiation capacity of cells derived from these different anatomical regions. Percentage ciliation varied considerably between the three anatomical regions at day 21 post-ALI (Fig 2.16 A).

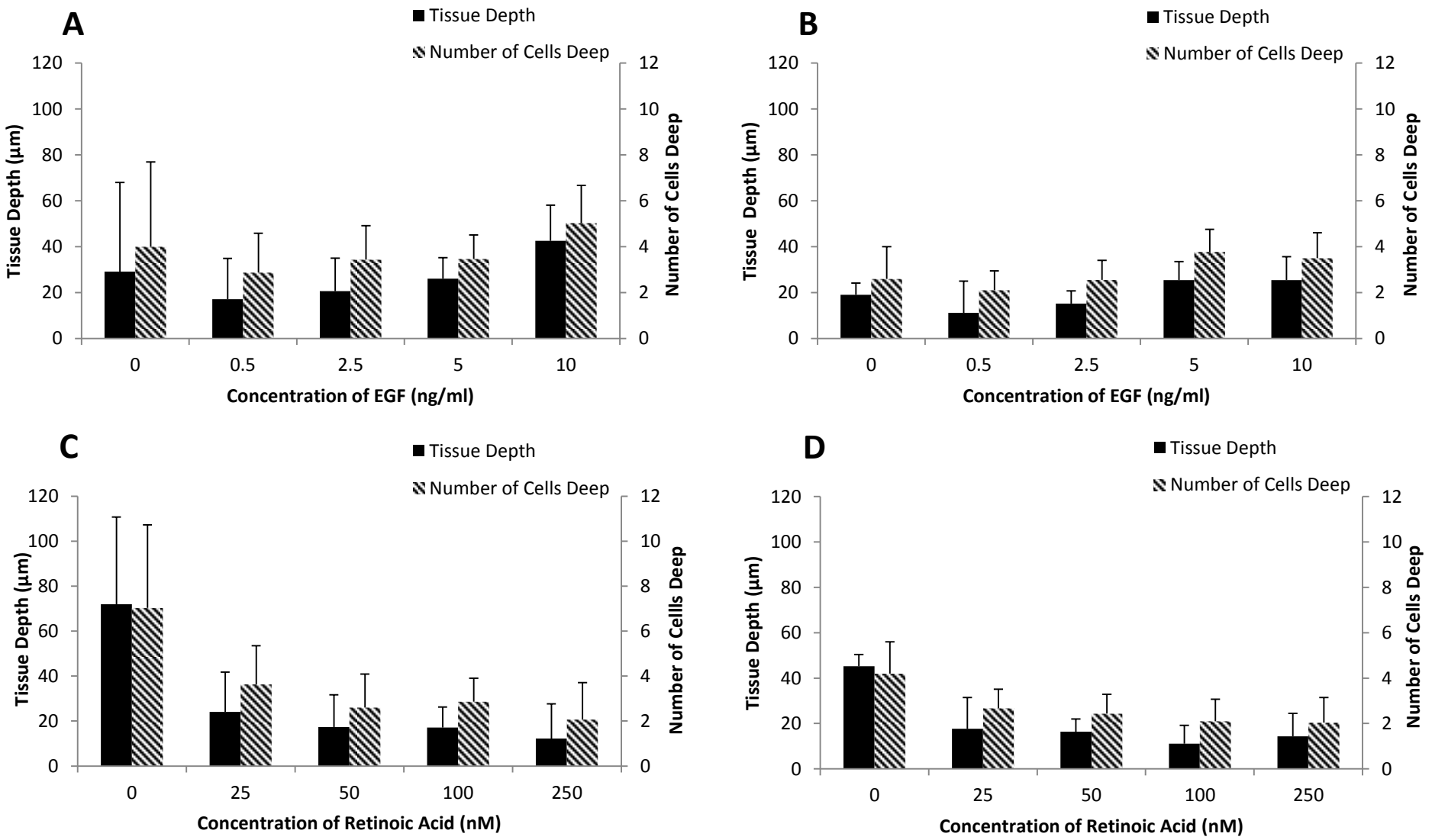

Fig 2.14 Graphs of tissue depth and cell count measurements of cultures grown under varying EGF and RA concentration.
Cultures grown with variable EGF concentrations, assessed after 14 (A) and 21 (B) days post-ALI. Cultures grown with variable RA concentrations, assessed after 14 (C) and 21 (D) days at post-ALI.

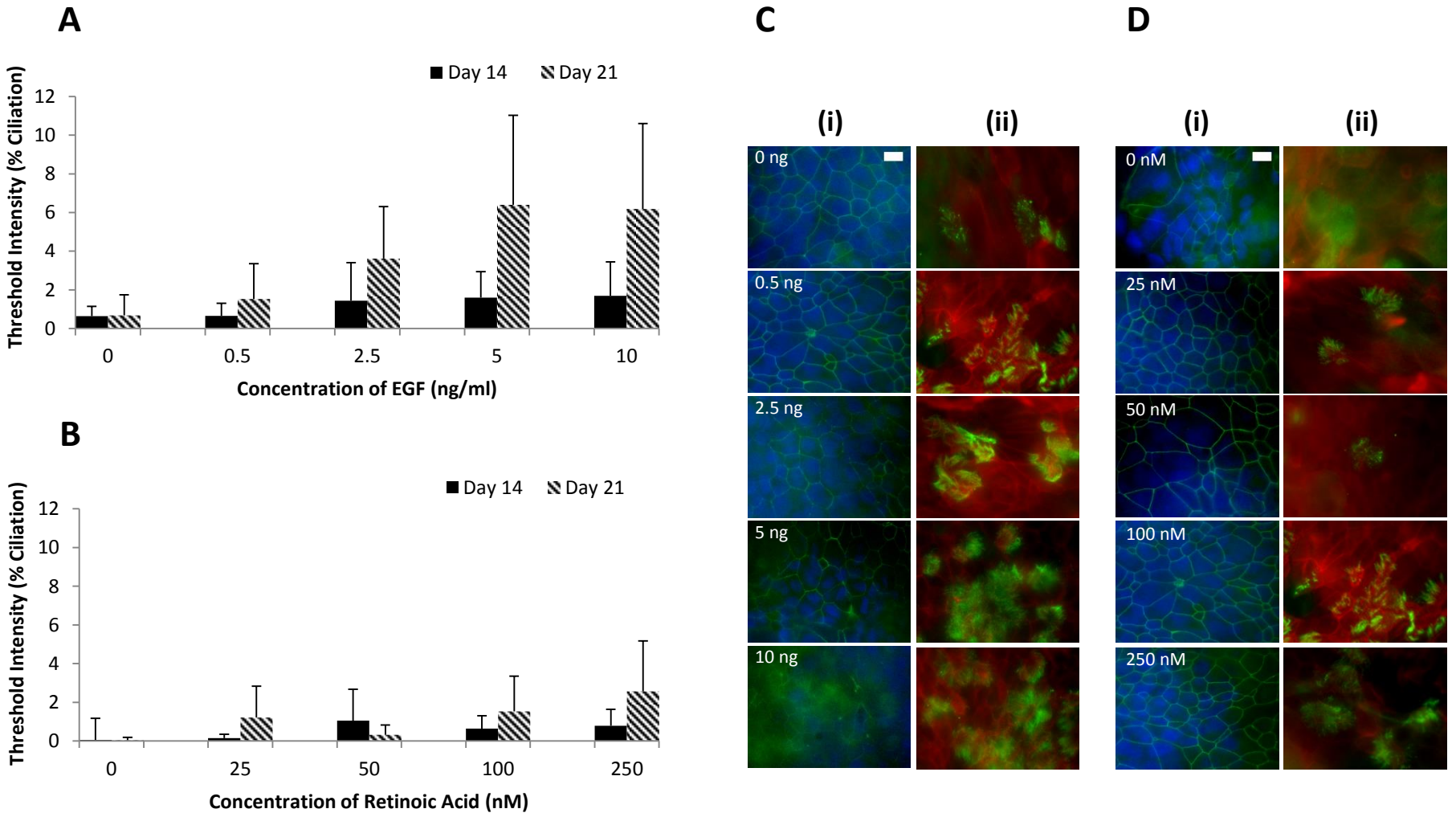

Fig 2.15 Effect of variable EGF and RA on ciliation and tight junction formation.
Percent ciliation measurements for 21 day post-ALI cultures grown with variable EGF (A) and RA (B) concentrations. Representative images of epithelial cells at 21 days post-ALI growth under variable EGF (C) and RA (D). Both (C) and (D) display images showing tight junctions (i) and cilia (ii). Series (i) displays nuclei (blue) and ZO-1 (green) and series (ii) displays β-tubulin (green) and actin (red). Scale bar represents 10 μm.

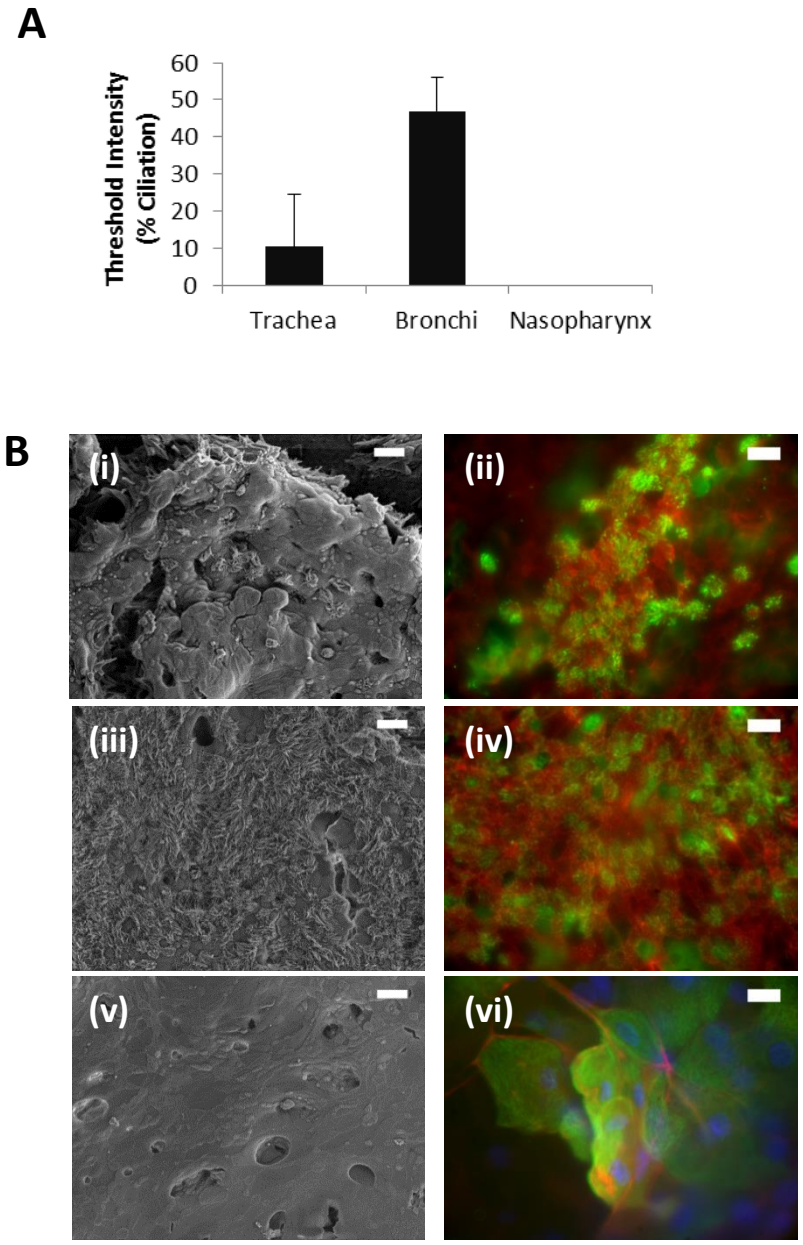

Fig 2.16 Percentage ciliation of ALI cultures derived from tracheal, bronchial and nasopharyngeal cells.
(A) Percentage ciliation across the three anatomically different models. (B) SEM images ([i], [iii] & [v]) and immunofluorescent images ([ii], [iv] and [vi]) of 21 day post-ALI cultures derived from the trachea ([i] & [ii]), bronchi ([iii] & [iv]) and nasopharynx ([v] & [vi]). Immunofluorescent images are stained for β-tubulin (green) to highlight cilia as well as actin (red) and nuclei (blue). All scale bars represent 25 µm.

Cultures derived from the trachea and bronchi produced cilia, whereas cultures derived from the nasopharynx did not produce any cilia. Ciliation was significantly higher in the bronchial cultures as compared to the tracheal cultures. The overall morphology of the tracheal- and bronchial-derived cultures appeared similar (Fig 2.16 B). However, ciliation across the bronchial surface was uniform (Fig 2.16 B [iii] & [iv]), whereas ciliation in the tracheal cultures was localised to intermittent regions (Fig 2.16 B [i] & [ii]). The morphological appearance of the nasopharyngeal cultures differed from the other two sites with a much larger cell size (Fig 2.16 B).

Analysis of the epithelial thickness and cell density numbers were evaluated against the tissue from which the cells were derived (Fig 2.17 A). The bronchial cultures had comparable values of tissue depth and cell depth to the native tissue. Both tracheal and nasopharyngeal derived cultures fell short of their native environments with significantly less tissue depth as compared with the ex-*vivo* tissue. The tracheal ALI culture tissue depth was comparable in thickness to the bronchial ALI culture. However, the tracheal native tissue was much thicker than the bronchial tissue (Fig 2.17 A). Thus, the tracheal ALI culture is a less accurate reflection of the tissue it was derived from.

Morphological assessment of H&E-stained histological sections revealed several differences amongst the ALI cultures (Fig 2.17 B). Both the tracheal and bronchial cultures appeared polarised (Fig 2.17 B [i] & [ii]). Regions devoid of cells within the tissue architecture were noted as more prominent in the bronchial ALI culture as compared with the tracheal-derived and nasopharyngeal-derived ALI cultures (Fig 2.17, B, [vi]-asterisk). These are suspected to be regions of epithelial turnover representing positions where localised cell death has occurred. This was suspected on the basis of their size, ruling them out as intercellular vacuoles and their position, ruling them out as mucus granules. Although these features were noted in tracheal and nasopharyngeal cultures they were more numerous in the bronchial cultures. The nasopharyngeal-derived ALI cultures appeared to have a basal layer of polarised epithelial cells with a squamous layer of epithelial cells atop (Fig 2.17). This was markedly different than either the tracheal- or bronchial-

derived ALI cultures which appeared to have no squamous cells comprising the epithelium.

For the three anatomical sites, native tissue and the corresponding ALI cultures were PAS stained to identify mucus production (Fig 2.18). Immunohistochemical staining was also performed on cultures derived from the three anatomic sites. The basal cell marker P63 (Fig 2.19), and the Clara cell secretory protein, CC10 (Fig 2.20), were probed for using specific antibodies.

Staining with PAS to identify mucus revealed comparative levels of mucus in all three native tissue samples with goblet cell morphology (Fig 2.18 A). Of the ALI cultures, only the bronchial cells displayed any evidence of mucus producing goblet cells (Fig 2.18, B [ii]). Cultures derived from the other two sites only displayed staining in a thin layer on the apical surface (Fig 2.18, B [i] & [iii]). Staining with alcian blue confirmed that the goblet cell identified in the bronchial derived ALI culture was mucus producing (Fig 2.21 [i]).

The ALI cultures derived from each of the three anatomic sites displayed a layer of P63-expressing cells adjacent to the substrate which mimicked the native tissue sections for each anatomical region (Fig 2.19). Deviation of this was only observed in regions of the nasopharyngeal-derived culture which displayed significant cell overgrowth. Within these regions a dual layer of p63-expressing cells was observed, one layer adjacent to the substrate, the other on the apical surface with a phenotypically different mass of cells observed in between (Fig 2.21 [iii]).

Staining with the CC10 marker revealed a diffuse pattern of positive identification throughout the epithelium of both native tissue and ALI cultures (Fig 2.20). Closer inspection revealed that sections of both native tissue and ALI cultures displayed cells with either brown or blue nuclei. This indicated that some, but not all, cells were producing CC10. This phenotype was common to both the ALI cultures and native tissue with no discernible difference between anatomical regions.

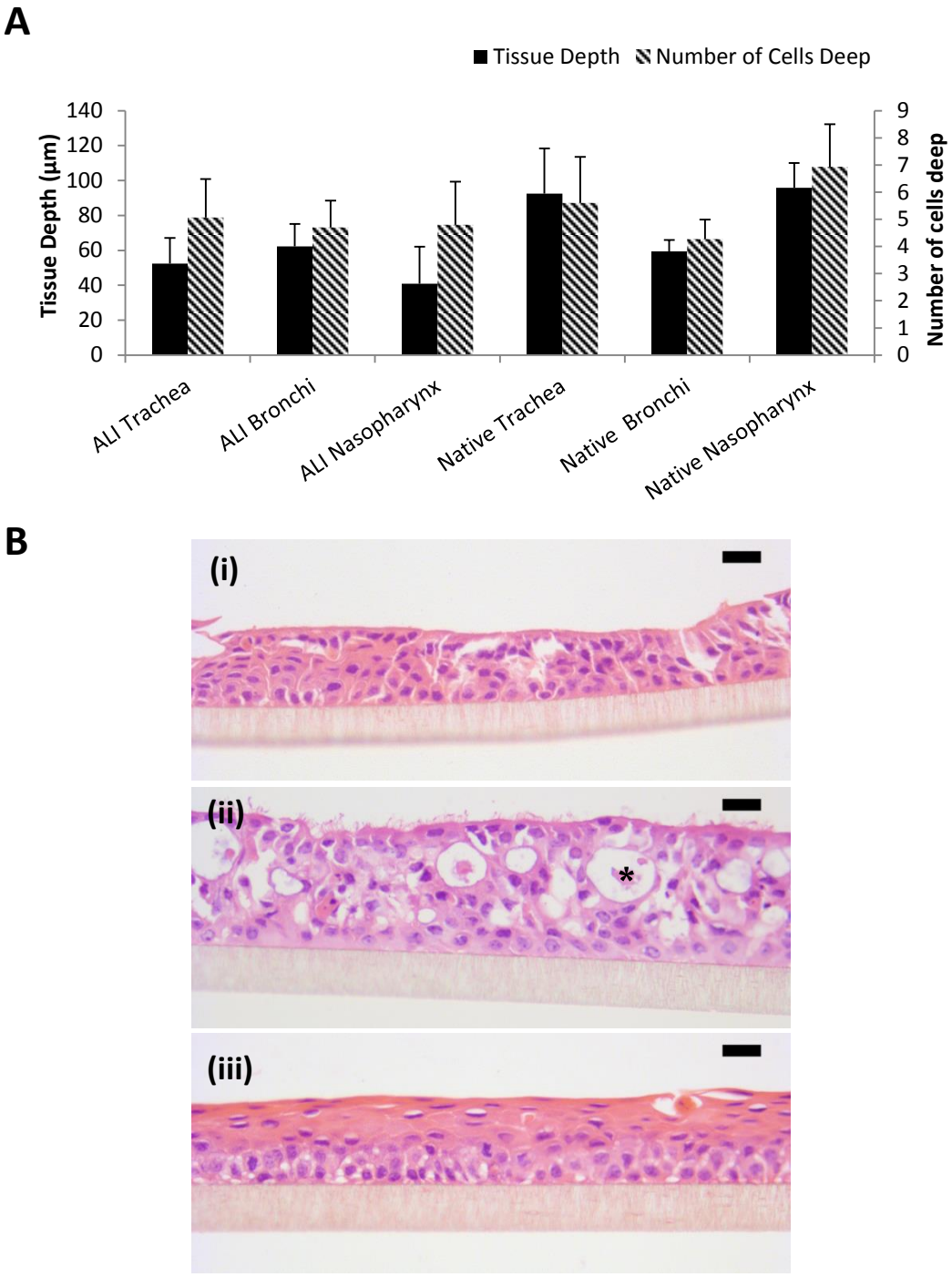

Fig 2.17 Histological analysis of ALI cultures derived from tracheal, bronchial and nasopharyngeal cells.

(A) Tissue depth and cell depth analysis for ALI cultures derived from tracheal, bronchial and nasopharyngeal tissue shown along with the native tissue measurements from each anatomical region. (B) Representative H&E stained histological profiles of 21 day post-ALI cultures grown from epithelial cells of the trachea (i), bronchi (ii) and nasopharynx (iii). Scale bars represent 25µm. Asterisk (panel [ii]) marks a region of epithelium devoid of cells.

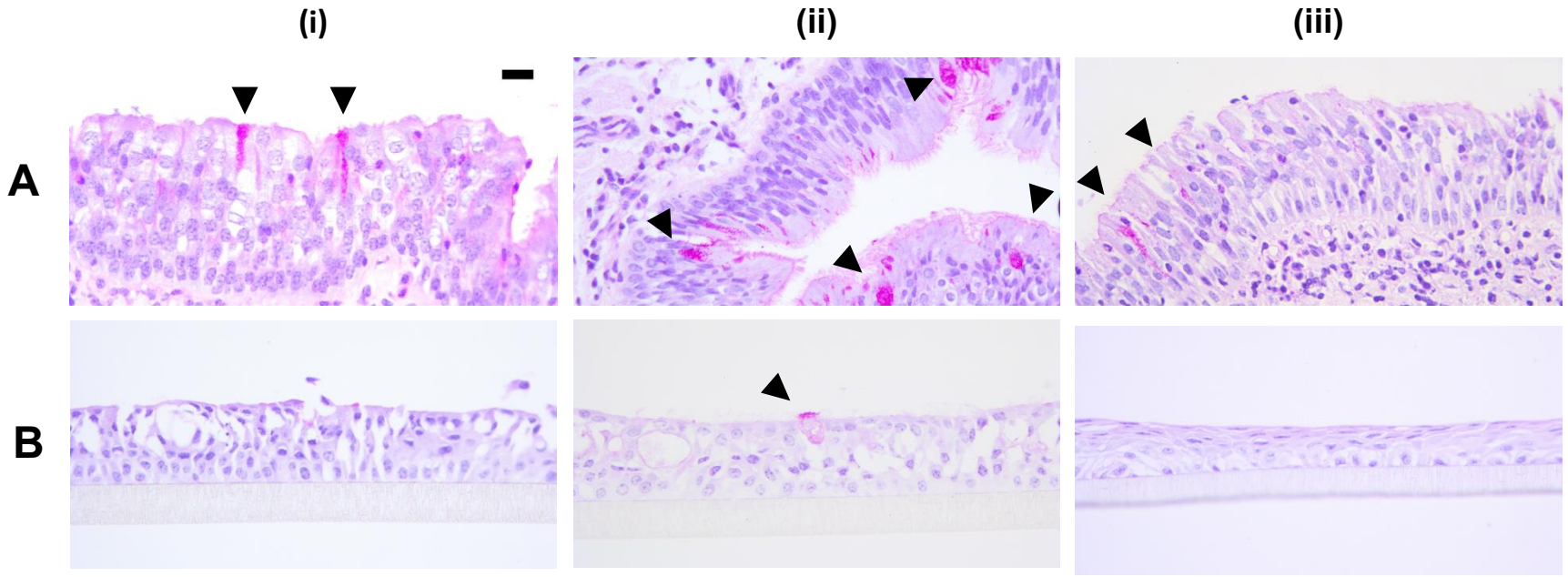

Fig 2.18 PAS stained histological sections of ALI culture and native tissue from three anatomic sites
Displayed alongside each other are (A) native tissue and (B) 21 day post-ALI *in vitro* cultures. Native tissue and ALI cultures are derived from the (i) mid-trachea, (ii) bronchi and (iii) nasopharynx. Scale bar represents 20 µm. Arrows indicate positions of goblet cells.

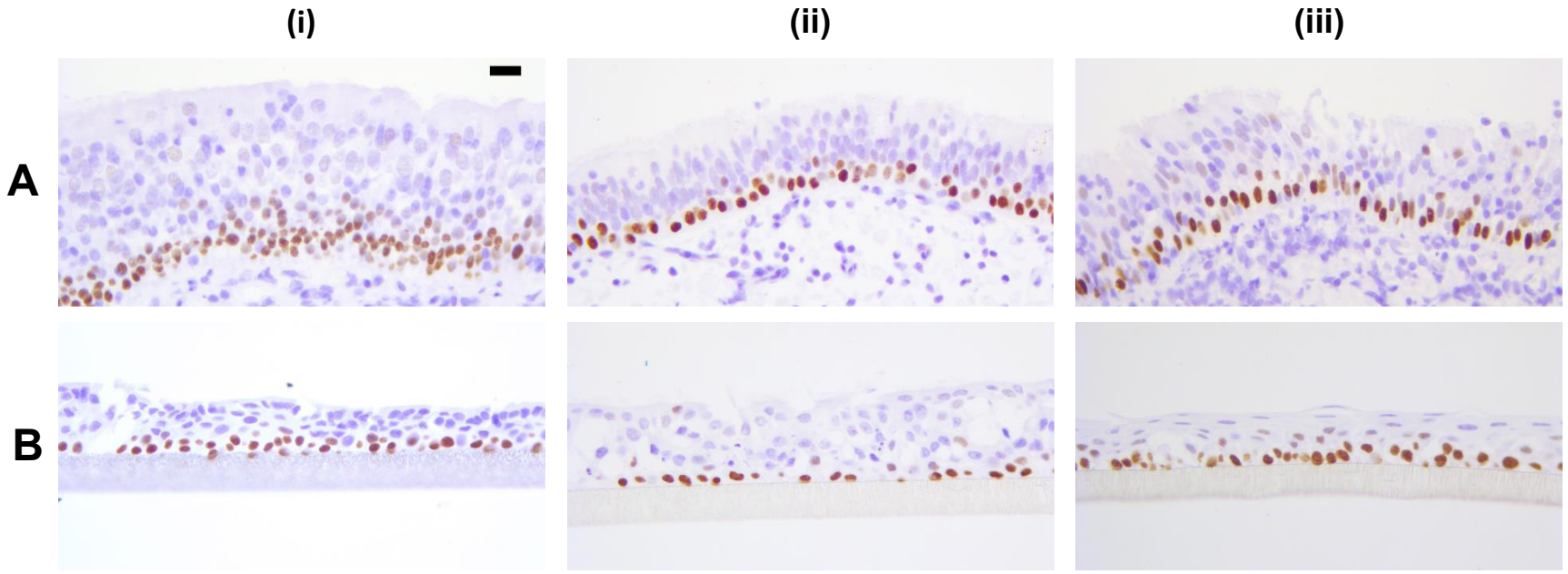

Fig 2.19 P63 immunohistochemical stained sections of ALI cultures and native tissue from three anatomic sites.
Displayed alongside each other are (A) native tissue and (B) 21 day post-ALI *in vitro* cultures. Native tissue and ALI cultures are derived from the (i) mid-trachea, (ii) bronchi and (iii) nasopharynx. Scale bar represents 20 µm.

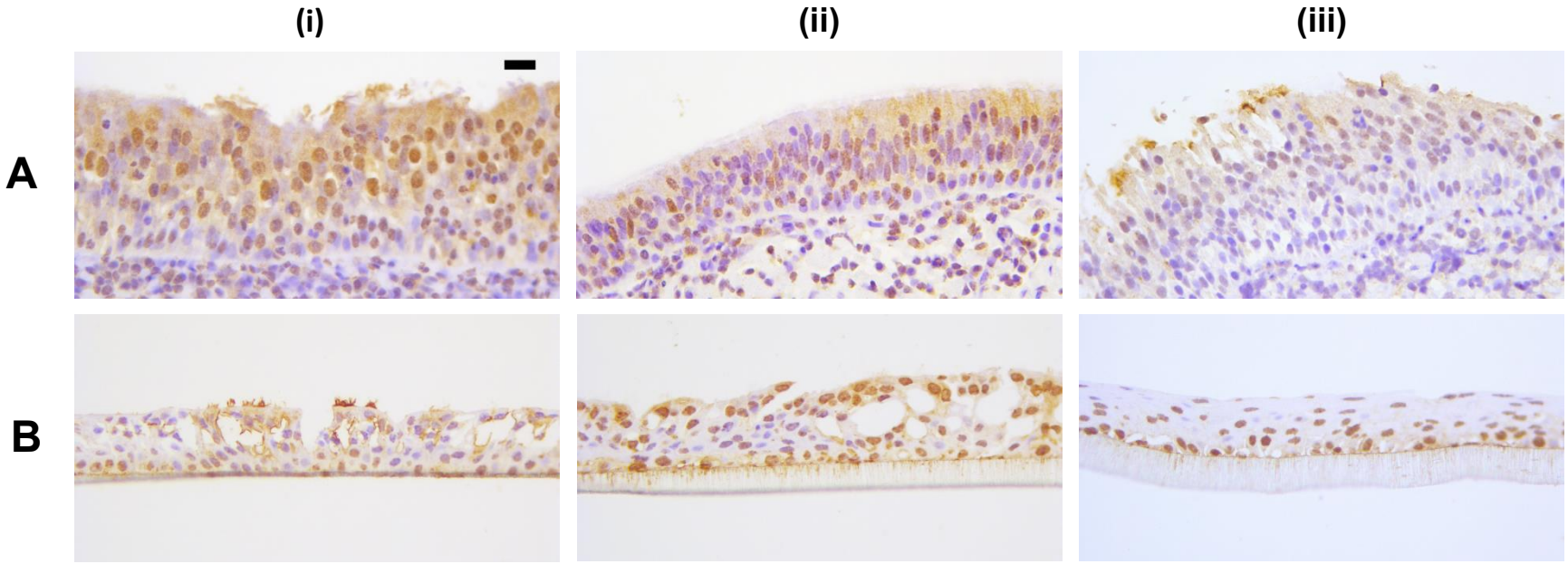

Fig 2.20 CC10 immunohistochemical stained sections of ALI cultures and native tissue from three anatomic sites.
Displayed alongside each other are (A) native tissue and (B) 21 day post-ALI *in vitro* cultures. Native tissue and ALI cultures are derived from the (i) mid-trachea, (ii) bronchi and (iii) nasopharynx. Scale bar represents 20 µm.

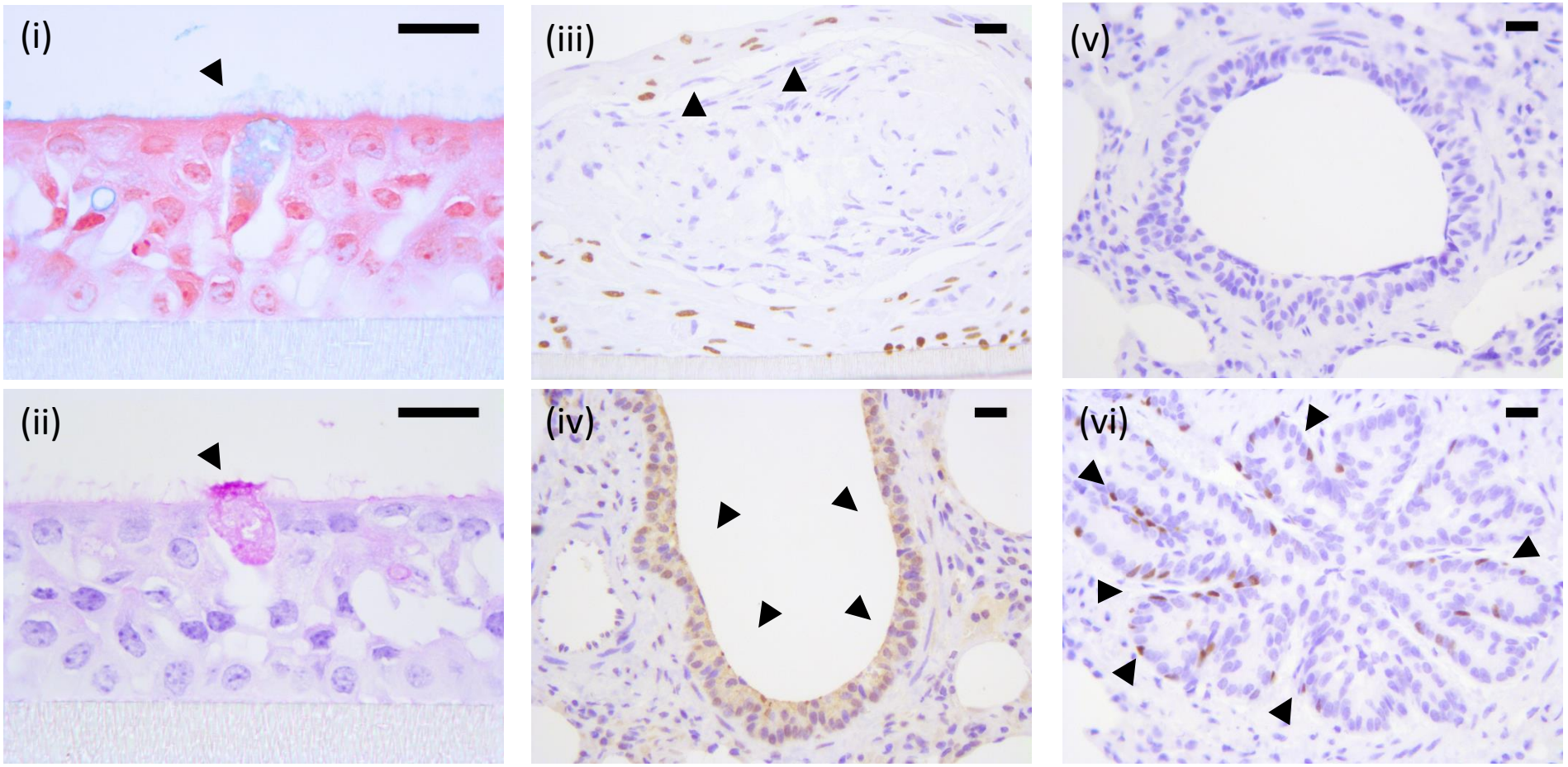

Fig 2.21 Immunohistochemical features of interest in the three anatomic regions.
Shown in panels (i) and (ii) are high magnification images of alcian blue (i) and PAS (ii) stained sections of the bronchial-derived *in vitro* model. Shown in panel (iii) is a p63-stained image of the nasopharyngeal-derived *in vitro* model displaying a large overgrown patch of epithelial cells with apparent concentration of basal cells at the apical as well as basolateral side. Shown in panel (iv) is a CC10-stained images of native lung sections. Shown in panels (v) and (vi) are p63-stained images of native lung sections displaying small (v) and larger (vi) bronchioles. Black arrows highlight areas positively stained with each of the markers used. Scale bar in all images is 20μm.

In addition to the anatomic sites the bronchiolar epithelium was also assessed to produce a comprehensive picture of the epithelium in the lower respiratory tract. Sections of lung tissue were prepared by excision of tissue from the lower right lung and subjected to PAS, P63 and CC10 staining. Observed within the lung sections were small bronchioles which displayed a CC10-expressing phenotype (Fig 2.21 [iv]) but an absence of P63-expressing cells (Fig 2.21 [v]).

Only larger conducting tubes found in the lung sections displayed any P63 positive cells (Fig 2.21 [vi]) and no bronchiolar cells displayed any goblet cell morphology.

Taken together, the results demonstrate that the bronchial-derived ALI cultures are more ciliated and closer in thickness to the native epithelium than either of the other two anatomic sites assessed. All anatomic sites assessed produced a layer of basal cells and could be positively stained for CC10. However, PAS staining revealed that only the bronchial-derived ALI cultures exhibited mucus-producing goblet cells. **Therefore, the bronchial-derived ALI culture offers better mimicry of the native environment than either the tracheal- or nasopharyngeal-derived ALI cultures and of the conditions tested, represents a superior choice to that of the other two.**

2.3.3 Summary of optimal conditions

In conclusion, the most optimal means of culturing bovine airway epithelial cells at ALI to achieve differentiation includes the harvesting of bronchial-derived cells, harvested and grown for phase one in DMEM:HAM's F12 with 10% serum before being seeded onto a high pore density PET membrane at a density of 2.5 x 10^5 cells (1.13 cm^2 culture area) for phase two. Cells should be grown in a 14% oxygen tension environment. Following seeding at phase two, media should be switched to 50:50 ALI:submerged growth media prior to ALI generation. At phase three media should be switched to ALI media for the duration of ALI culture. The optimal composition of ALI media comprises AEGM:DMEM as the base media supplemented with 10ng/ml EGF and 100nM RA, as well as other growth factors (2.2.1.3).

2.4 Discussion

Development of an *in vitro* culture model that accurately mimics the native environment is a challenging process. Here the development of a bovine airway epithelial cell model has been successfully demonstrated. The development process not only encompasses the final product that mimics the native environment, but also provides new insight into parameters that can be varied to produce different environments and further the study of host-microbe interactions.

The final optimised model presented here mimics closely the native environment of the bovine bronchus. With achieved ciliation of greater than 40%, a near 100% reflection in epithelial depth profile, correct anatomical localisation of p63 and CC10-expressing cells and the identification of mucus producing-goblet cells, the epithelium presented here is one of the most representative cell culture models to date of the bovine respiratory epithelium. Since the first human ALI culture systems were developed (Wu *et al.*, 1986), many studies have demonstrated the improved physiological function of ALI culture over conventional submersion (Abraham *et al.*, 2011; Kondo *et al.*, 1993; Neugebauer *et al.*, 2003; Tournier *et al.*, 1998). This advantage is subject to a variety of conditions that affect differentiation including the substrate surface, media composition, air-interface conditions and the anatomic location of recovered epithelial cells. The aim of the work presented here was to examine these conditions in a bovine model in order to refine the culture conditions and increase its mimicry of the native environment.

Substrate choice and base media conditions. Initial considerations focused on the substrate choice and base media that would produce optimal growth and differentiation. The results herein demonstrated differences in epithelial differentiation according to different substrate and base-media combinations (Fig 2.6). Substrate properties are known to influence cell differentiation via mehcanotransduction. In this process, gene transcription is influenced via mechanical forces transmitted through focal adhesions and actin filaments connected between the cell surface and the nuclear lamina (Hamill & Martinac, 2001; Wang *et al.*, 1993). Subsequently, this effect can drive the differentiation of cells down particular lineages (Engler *et al.*, 2006). Thus, material properties

such as stiffness and surface topology can influence differentiation (Dalby *et al.*, 2007; McNamara *et al.*, 2012).

Studies looking at the influence of substrate on the differentiation of epithelial cells at ALI have observed a strong correlation between material properties and differentiation (Huang *et al.*, 2010b, 2013; Yoon *et al.*, 1997). Yoon *et al.* (1997) examined the influence of collagen-coating on the differentiation of ALI-grown epithelial cells and found no morphological differences in the epithelia produced in either coated or non-coated surfaces. However, the study did report increased levels of mucin, lysozyme and leukocyte protease inhibitor measured in the absence of a collagen-coated surface, highlighting the influence substratum has over gene expression. This observation was in contradiction to an earlier study which found increased epithelial thickness and mucus production directly proportional to the thickness of collagen substratum (Robinson & Wu, 1993), although this might be due to the lack of an ALI in the cultures process. Alternatively, the differences involved in these two studies might be accounted for by the differences in surface coating procedure. The former utilised a collagen gel while the latter utilised a thin coating of collagen onto the surface of tissue culture dishes. As the collagen coating used in the present study was applied as a thin layer, this might explain why no change in epithelial thickness was observed. Further attempts at refinement could therefore aim to culture bovine epithelial cells at ALI on a thicker collagen gel.

More recent studies into the effects of substrate on airway epithelial cell differentiation have built upon this early work to further improve differentiation. Studies by Huang *et al* (2010a, b, 2013) reported increases in mucociliary differentiation through the use of different biomaterials. The first of these studies, examining the effect of collagen and esterfied hyaluronan surfaces on ALI culture, revealed a significant increase in ciliation (above 20 percent) as well as increases in mucus production on the hyaluronan versus the collagen surface (Huang *et al.*, 2010b). Increased performance in differentiation was linked to a combined effect of the substrate material and the concentration of RA, a known stimulator of epithelial differentiation (Huang *et al.*, 2010a; Robinson & Wu, 1993). The authors provided evidence for increased ciliation directly via the use of hyaluronan in the substrate. Cells demonstrated greater levels of ciliation when grown in the presence of RA. However, in the absence

of RA, cells grown on the hyaluronan surface had a greater level of ciliation compared with cells grown on collagen. Knockdown of the receptor for hyaluronan-mediated motility (RHAMM) abolished the higher levels of ciliation in hyaluronan vs collagen grown cells, confirming that this effect was a direct response to the membrane material. However, it was noted that the cilia of the hyaluronan-grown cells were shorter and appeared aggregated in the absence of RA compared with its inclusion. Thus, the authors examined the effect of incorporating RA into the hyaluronan matrix (Huang *et al.*, 2013). Incorporation of RA into the matrix produced significantly higher levels of mucus and produced long, non-aggregated cilia. This highlights the relationship between substrate and nutrient requirement; an effect observed in the present study, whereby the combination of media and substrate choice influenced the outcome of the ALI cultures. It is reasonable to conclude that if substrate material properties affect gene transcription, different nutrient requirements will be observed between different substrates.

Substrate pore density. As part of the optimisation procedure the influence of substrate pore density upon ALI epithelial cell differentiation was investigated. *In vivo* the epithelium is supplied by nutrients from the extracellular space beneath the basement membrane. The basement membrane, while providing support to the epithelium, must allow for the adequate passage of nutrients. The substrate surface represents an artificial basement membrane and therefore to function optimally must mimic the diffusion that occurs in the native environment. This provided the rationale for testing different membrane pore densities which produce different diffusion rates. Significantly better ciliation was observed on high pore density versus low pore density substrates after culture at ALI (Fig 2.12). This result might be expected when taking into account the physiological environment of the basement membrane as mentioned. No difference in tissue thickness or TEER was observed for cells grown on membranes of different pore densities.

Previous studies have demonstrated that porosity (material void fraction) and pore size affect cell cultures (Agrawal & Ray, 2001). In static culture, cells grown on a substrate are subject to mass-transfer limited diffusion, which consequently is affected by the substrates porosity (Freed *et al.*, 1993b; Vunjak-Novakovic *et al.*, 1999). Freed *et al.* (1994) stated that substrate designs should

ideally have greater than 90 % porosity. Indeed, the authors evaluated chondrocyte growth on a 91 % poly(L)lactic acid (PLLA) and a 97 % pore density polyglcolic acid (PGA) scaffold (Freed *et al.*, 1993a). The chondrocyte growth rate was found to be twice as high on the PGA scaffold compared with the PLLA scaffold. Thus, as with the results presented herein, higher substrate porosity produced an environment that supported cell proliferation better than that of the low porosity substrate. However, other differences in the material properties of these two scaffolds likely contribute to the effect as well. For example, elasticity has been shown to increase as a function of pore density (Doi *et al.*, 1996). Thus, in addition to influencing mass transfer, elasticity differences may also account for changes in cell behaviour when the substrate porosity is altered. Additionally, it has been shown that chondrocytes cultured on substrates with identical pore density but different connective architectures proliferate differently and exhibit different levels of collagen II production (Miot *et al.*, 2005). Similarly, cultures with identical porosity, yet different pore sizes affect the performance of cultures. This has been demonstrated for osteoblasts in culture, where alkaline phosphatase activity was higher in cells cultured on a high pore size substrate (500-710 μm ø) as compared to a lower pore size substrate (150-300 μm ø) (Ishaug-Riley *et al.*, 1998). Other studies have found the influence of pore size in attachment and proliferation is largely cell type specific (Lee *et al.*, 2004; O'Brien *et al.*, 2005; Salem *et al.*, 2002). Zeltinger *et al.* (2001) examined the interrelation of pore size and pore density in the culture of microvascular epithelial cells and vascular smooth muscle cells. It was found that the high pore density (90 %) culture resulted in higher cell viability than the low pore density (75 %) substrate. Additionally, for the 90 % porous substrate, there was no statistically significant difference in the viability of cells cultured on substrates with different pore sizes (<38 μm – 150 μm).

In summary, evidence in the literature suggests that higher substrate pore densities produce a more favourable culture environment with lower impedance of nutrient and waste diffusion. In the present study, the high and low pore density substrates can be estimated as having 12.5 % and 0.25 % void fractions, respectively. This is based on the assumption that each pore is a straight cylinder through the membrane and that no interconnectivity occurs (in reality these values will be higher). Both the high and low pore density substrate

supported growth, yet differentiation as measured by percent ciliation was significantly improved for epithelial cells grown on the high pore density substrate. It would appear that the mass transfer properties of either pore density tested is enough to support growth. However, the differences exhibited in differentiation suggest mass transfer can influence epithelial cell differentiation. Alternatively, the relationship between porosity and material elasticity may result in different mechanotransductive effects that lead to differentiation. Either way it is clear that the use of the high pore density substrate results in a more differentiated bovine airway epithelium as compared to the use of the low pore density substrate.

Oxygen tension. Coupling the optimisation of pore density to oxygen tension under culture allowed for the interplay between these two parameters to be assessed. Studies have shown that the availability of oxygen influences the cellular uptake of glucose and the production of lactate, with lower levels of available oxygen shifting metabolism away from oxidative phosphorylation towards oxygen-independent glycolysis (Curcio *et al.*, 2010, 2014; Kondo *et al.*, 1997). The interaction of oxygen tension with nutrient diffusion in the experiment presented here revealed an optimal combination of 14 % O_2 and high pore density. However, better ciliation at 14 % vs 21 % O_2 was only observed when the high pore density substrate was used. Use of the low pore density substrate produced poor ciliation irrespective of oxygen tension. Thus, two factors might be assumed, **(1)** that the high pore density substrate will allow for a greater diffusion of glucose and **(2)** that more glucose will be required for growth at a lower oxygen tension due to increased glycolysis in place of oxidative phosphorylation. Thus, perhaps explaining why oxygen tension only influences ciliation when cells are cultured on the high pore density substrate.

Ultimately the question of which oxygen tension produces the best *in vivo* mimicry might involve mimicry not of the adult lung, but of the oxygen gradients experienced during embryonic development. A study by Garreta *et al* (2014) noted that a severely hypoxic environment (5% O_2) was optimal for generating mouse embryonic stem cell (ESC) to endoderm differentiation and subsequent epithelial cell differentiation. A more recent study by Pimton *et al* (2015) identified oxygen tension as low as 1%, mimicking the oxygen tension experienced during early mouse embryo development, was required to increase

the number of ESCs that differentiated into endoderm (Pimton *et al.*, 2015). The process of lung development from the endoderm of the foregut begins with a localised expression of Nkx2-1 in the region that will become the future trachea (Morrisey & Hogan, 2010). This process occurs around day 28 for humans and constitutes the separation into what will become the lung and the oesophagus. The differentiation of progenitor distal tip cells into the specialist cells of the conducting airway epithelium occur later. Although the studies by Garreta *et al* (2014) and Pimton *et al* (2015) examined the influence of oxygen tension on the development of early epithelial progenitors it is not unreasonable to assume that these very low oxygen tensions might also contribute to specialist cell formation. Hence, a valuable future investigation into epithelial cell differentiation could involve examining lower oxygen tensions that mimic early development. Although, studies comparing ALI grown cells to submerged cells note only the ALI cells differentiate (Xu *et al.*, 2014). This suggests that the higher oxygen tension contributes to the differentiation in ALI cultures. However, an alternative explanation, supported by the increase in ciliation of cells cultured at 14 % O_2 versus 21 % O_2, might be that ALI-driven differentiation is a product of cell orientation in the respiratory microenvironment. Thus, the influence of soluble nutrients and growth factors at a single side of the epithelium (the basolateral side) may be the key requirement in epithelial cell differentiation.

Growth factor concentrations (EGF and RA). In order to fully examine the potential differentiation that may be achieved for any given cell system it is necessary to examine the role of specific growth factors that act as triggers and repressors of differentiation. Examination of the literature concerning airway epithelial cell differentiation pinpoints two well-characterised growth factors, EGF and RA, that have a significant role in differentiation (Clark *et al.*, 1995; Gray *et al.*, 1996; Huang *et al.*, 2013; Wu *et al.*, 1997; Yoon *et al.*, 1999, 1997). To investigate the influence of these growth factors on our culture system an experiment looking at a range of concentrations was devised to examine the effect on epithelial differentiation. It was found that the concentration of RA over the range tested did not affect differentiation as long as it was present at the minimum concentration of 25nM. Conversely, it was found that differentiation, as measured by degree of ciliation, exhibited a direct

concentration-dependent effect with EGF, producing higher levels of ciliation at the higher concentrations tested (5ng/ml and above).

Retinoic acid is a metabolite of vitamin A (retinol). The influence of RA on airway epithelia is well documented. The presence of RA maintains a columnar – pseudostratified epithelium while its absence leads to the formation of squamous epithelial cells (Bernacki *et al.*, 1999; Gray *et al.*, 1996; Wu *et al.*, 1997; Yoon *et al.*, 1997). Control over cellular differentiation is exhibited through two nuclear receptors, the RA-specific receptor RAR and the generic retinoid receptor RXR (Luca, 1991). The RARβ receptor, which is expressed exclusively in epithelial cells, has been shown to be necessary in producing epithelial polarisation (Seewaldt *et al.*, 1997). Other studies have demonstrated that the α and γ forms of RAR are the most prolific at inducing mucus production in airway epithelial cells (Gray *et al.*, 2001; Koo *et al.*, 2002). An RA-dose dependent induction of mucin production has been identified in airway epithelial cells and type II pneumocytes (Baybutt *et al.*, 2010; Yoon *et al.*, 1997). Although mucin production as a function of RA concentration was not assessed in the present study, the influence that RA concentration has on ciliation and tissue thickness was examined. RA exhibited no concentration-dependent increase in the ciliation and tissue thickness of bovine tracheal epithelial cells over the range 25 – 250 nM. As the differentiation of basal cells into both ciliated cells and mucus-producing goblet cells are intrinsically linked, whereby the population of cilated cells emerges from that of the self-renewing secretory cell population (Pardo-Saganta *et al.*, 2015; Watson *et al.*, 2015), it is plausible that the lack of a dose-dependent effect on cell ciliation also resulted in no dose dependent increase in mucus production. Therefore, if RA concentration does not have a dose dependent effect on mucus production the results would be in direct contradiction to studies by Baybutt *et al.* (2010) and Yoon *et al.* (1997).

This contradiction might best be explained by examining three pieces of evidence. Firstly, RA and EGF exhibit interplay in their signalling mechanisms. Retinoic acid has been shown to decrease autophosphorylation of the EGF receptor (EGFR) which would augment effects downstream in the signalling cascade (Kim *et al.*, 1992). Changes in mRNA levels of EGFR have also been shown to be under the control of RA, with hepatic and epidermoid cancer cell lines exhibiting increased and decreased synthesis respectively (Raymond *et al.*,

1990; Zheng *et al.*, 1992). Further work within our research group has shown that a dose-dependent relationship between RA and ciliation exists in the range 25 nM – 100nM if 10 ng/ml of EGF is used supplemented in the culture media (unpublished result). Thus, suggesting that the EGF concentration does influence the effect that RA concentration exhibits on cilia development in the ALI cultures.

Secondly, RA is known to promote the mucociliary phenotype through the conventional mechanism of RAR/RXR transcriptional activity, termed RARE, although another non-classical route has been described in the literature (Aggarwal *et al.*, 2006; Hong *et al.*, 2008; Kim *et al.*, 2007b). This mechanism involves RA activating a signalling cascade that results in the activation of the cAMP response element-binding protein (CREB). CREB, when activated functions as a transcription factor for the major secreted airway mucin MUC5AC (Kim *et al.*, 2007b).

Lastly, experiments concerning mucociliary differentiation have observed different effects in different species. Cross-species conservation analysis of RAREs has revealed that these DNA sequences have very low conservation between species with the number of shared RAREs between humans and cattle being around 10% of the total human RAREs (Lalevée *et al.*, 2011). For EGF, rat tracheal epithelial cells have been shown to increase relative ciliation levels and decrease mucin production upon EGF withdrawal from culture (Clark *et al.*, 1995; Guzman *et al.*, 1995). In direct contrast, human epithelial cells have displayed an increase in mucin production following EGF withdrawal (Wu *et al.*, 1997) and swine epithelial cells have been shown to display a decrease in ciliation following EGF withdrawal (Bateman *et al.*, 2015). Furthermore swine epithelial cells have also been shown to exhibit a dose dependent retinoic acid response in ciliation at a low (1 ng/ml) concentration of EGF (Bateman *et al.*, 2015). This is contrast to the results presented here, where no RA concentration-dependent effect on ciliation was observed at an EGF concentration of 0.5 ng/ml.

In summary, different species exhibit different EGF-dependent effects, EGF and RA exhibit cross talk in their signalling mechanisms and RA can influence mucociliary differentiation out-with its classical signalling pathway. Therefore,

it is plausible that the observations made in the experiments presented here might reflect unknown mechanisms of action involving cross talk between EGF and RA that are potentially unique to cattle. Indeed, as previously mentioned, evidence from within our research group would suggest that RA does influence ciiation in a dose dependent manner as long as an EGF concentration of 10 ng/ml is used during ALI culture. Thus, the result of the present study, that RA has no influence on ciliation, most likely reflects the low EGF concentration (0.5 ng/ml) that was used.

Anatomical origin of epithelial cells. The final stage of epithelial cell optimisation concerned the anatomical location from which the epithelial cells are derived. The epithelium throughout the respiratory tract is far from consistent. The epithelium of the upper airways and trachea is relatively thick and pseudostratified. As the epithelium progresses towards the alveoli it thins such that by the bronchioles it is composed of a single-celled columnar epithelium. Changes in cell population of the respiratory epithelium also occur, although this has been noted to vary considerably between different species (Miller *et al.*, 2011). To address these differences, ALI cultures were produced from epithelial cells derived from the nasopharynx, the trachea and the bronchi. The bronchial-derived ALI cultures were found to be superior to cultures derived from the trachea and nasopharynx in producing an epithelium that resembled its tissue of origin in terms of thickness and percentage ciliation. The nasopharyngeal ALI cultures exhibited a lack of ciliation at day 17, in stark contrast to both the tracheal and bronchial ALI cultures. Ciliation was higher in the bronchial cultures compared to the tracheal cultures after 21 days of ALI culture. The thickness of the bronchial ALI cultures was closest to that of the native tissue; this can be explained by examining the tissue origin. Although both tracheal and bronchial ALI cultures were of a similar thickness, the native trachea is naturally thicker than the bronchi resulting in closer mimicry of the native tissue by the bronchial ALI culture. What is less clear is why the bronchial cultures achieved significantly more ciliation compared to the tracheal cultures after 21 days of ALI growth. This implies that the basal cells of the bronchi and the trachea have different propensities to differentiate under the same conditions.

Few studies have examined the spatial distribution of respiratory ciliated cells. Those studies that have done so reveal extensive heterogeneity amongst different cell types and their spatial distribution. Toskala *et al*. (2005) examined the distribution of ciliated cells in the airways of mice and found that there are higher numbers in the trachea compared with the bronchi during post-natal development. Variation in ciliated cell populations also exist in the transverse plane of the respiratory tract. Hoffmann *et al* (2014) examined the ciliated cell distribution in the trachea of common marmosets and discovered that the dorsal side was enriched in ciliated cells and the ventral side was enriched in secretory cells. It has also been shown that differences in anatomical distribution can be influenced by the underlying cartilage. Oliveira *et al* (2003) showed that rat tracheal epithelium is more heavily ciliated passing over cartilage rings than it is in the region of adjoining rings. These studies indicate that ciliated cells of the respiratory epithelium have a highly heterogeneous distribution with multiple modes of spatial variation existing amongst different species. To date, this distribution has not been examined in cattle but, based on the results presented here, it might be expected that the bronchi of cattle are more heavily ciliated than the trachea. Although the native histology sections of trachea and bronchi appear heavily ciliated unknown heterogeneity may exist in the trachea that, when recapitulated *in vitro*, may account for the differences observed.

Other epithelial cell types also exhibit heterogeneous distribution throughout the respiratory epithelium. Goblet cells are numerous in the large airways but diminish in the lower regions of the respiratory tract and are completely absent in the bronchioles; the same is true of basal cells (Miller *et al.*, 2011). Replacing these two cell types in the small airways is the Clara cell which fills the role of a secretory and progenitor cell. The present findings reveal an accurate reflection between the cellular composition of the ALI epithelial cultures and the native tissue. The presence of a single layer of basal cells in each of the nasopharyngeal, tracheal and bronchial cultures reflects the tissue of origin. The presence of CC10-positive cells in cultures derived from each region also reflects the tissue of origin. Considerable species-to-species variation in anatomical distribution of Clara cells is known to occur. Humans are known to possess few Clara cells outwith the bronchioles whereas rodents possess high

numbers in the bronchi (Boers *et al.*, 1999; Bolton *et al.*, 2008; Rock *et al.*, 2010). The data presented here suggests that Clara cells are found in the trachea, bronchi and nasopharynx of cattle, or at the very least cells expressing the CC10 marker. Goblet cells are present in large numbers in the native nasopharynx, trachea and bronchi. This cell type was absent in the ALI epithelial cultures derived from the nasopharynx and trachea but present in small numbers in the bronchial cultures. One explanation for the under representation of goblet cells in the ALI epithelial cultures is the stimulatory effect that environmental exposure plays. Histochemical analysis has revealed that there are relatively few secretory granules in the bronchi of healthy mice, yet an increase in secretory granules is observed following inflammatory stimulus (Fahy & Dickey, 2010). It is therefore plausible that the lack of secretory granules observed in the ALI epithelial cultures relative to the native tissue is a product of the environment; that the *in vitro* culture conditions used does not provide the inflammatory stimulus required to produce comparable levels of secretory granules.

Conclusions. The generation of an epithelial cell model that accurately reflects the environment of the airway epithelium is complex. Considerations for substrate, nutrient requirements, oxygen tension, growth factors and tissue origin must all be taken into account in order to produce the optimum balance of factors that can recreate the bovine airway. The airway epithelial model presented here has been optimised to mimic the native tissue and represents a major advance over the use of conventional submerged culture. This ALI epithelial model will serve as a useful tool for investigations into host-pathogen interactions at the mucosal surface of the bovine respiratory tract.

Chapter 3 The outer membrane proteome of *Mannheimia haemolytica* and *Mannheimia glucosida* recovered from cattle and sheep

3.1 Introduction

The cell envelope of Gram-negative bacteria consists of an inner membrane (IM) separating the cytoplasm from the periplasmic space, a thin peptidoglycan layer located within the periplasm (PP) and an outer membrane (OM) separating the PP from the extracellular environment (Fig 1.3). Thus, the OM functions as the interface between bacteria and their environment and it follows that proteins located in the OM provide the functional interaction of bacteria with their environment. Specific processes with which OMPs are involved include nutrient uptake, adherence to surfaces, enzymatic processes, evasion of the immune system, secretion of various macromolecules and the relaying of information about the environment to the cytoplasm.

The OM of *M. haemolytica* is specialised to interact with the respiratory mucosa of ruminants. Studies have suggested the OM proteome of *M. haemolytica* is adapted to its specific host where phylogenetically similar isolates recovered from cattle and sheep exhibit differences in their OMP profiles (Davies & Donachie, 1996; Davies *et al.*, 1996, 1997). For example, isolates of serotype A1, A2 and A6 exhibit different OMP profiles on the basis of whether the isolate was recovered from cattle or sheep (Davies & Donachie, 1996). Serotypes A1 and A6 are predominantly responsible for the disease in cattle (Al-Ghamdi *et al.*, 2000; Purdy *et al.*, 1998) while serotype A2 is predominantly responsible for disease in sheep (Kirkan & Kaya, 2005). Thus, differences in the OMP profiles may represent examples of adaptation to the host respiratory mucosa.

Certain OMPs of *M. haemolytica*, such as OmpA, display species-specific diversity highlighting potential environmental adaptation at play in the organism. OmpA of *M. haemolytica* can generate a species-specific immune response (Hounsome *et al.*, 2011), due to variation in the hypervariable loop regions of the protein that projects away from the OM into the extracellular space (Davies & Lee, 2004). The OmpA protein is known to be involved in the structure and integrity of the OM but has also been demonstrated to act as an adhesin in *M.*

haemolytica by binding host fibronectin (Lo & Sorensen, 2007), a function which might be host specific. Similar observations have been made with OMPs related to the sequestration of iron from the host. *M. haemolytica* is able to scavenge iron from a number of host sources including transferrin, haem, haemoglobin, haemopexin, and hemin; it is also able to hijack siderophore-bound iron from other bacterial species (Gioia *et al.*, 2006; Roehrig *et al.*, 2007). One of the most extensively characterised systems of iron uptake in *M. haemolytica* involves the transferrin binding proteins TbpA and TbpB (Lee & Davies, 2011; Ogunnariwo & Schryvers, 1996, 2001; Ogunnariwo *et al.*, 1997; Potter *et al.*, 1999; Yu *et al.*, 1992). These proteins share homology with the transferrin binding proteins of other pathogens including *N. meningitidis*, *N. gonorrhoeae*, *H. influenzae* and *A. pleuropneumoniae* (Ogunnariwo *et al.*, 1997). TbpA functions as a TonB-dependent receptor while TbpB acts as an accessory lipoprotein (Cornelissen *et al.*, 1998). Genetic analysis of *M. haemolytica* isolates recovered from cattle and sheep has revealed that serotype A2 strains associated with disease in sheep have a *tbpBA* operon that is genetically distinct from that of serotype A2 strains in cattle (Lee & Davies, 2011). This suggests that TbpA and TbpB have evolved to reflect the host environment of the bacterium.

Studying the complete repertoire of proteins that an organism possesses provides several advantages over studying individual proteins or protein systems in isolation. Looking at the proteome of a cell or cellular compartment provides a snapshot of how the system functions as a whole (Aebersold & Mann, 2003). Consequently, this allows for the identification of patterns that would not be possible though a reductionist approach that targets a small number of proteins. Since the first bacterial genome (*H. influenzae*) was published in 1995 (Fleischmann *et al.*, 1995) the field of bacterial proteomics has emerged to elucidate dynamic changes in an organism's gene repertoire. The study of the OM proteome has emerged from this with considerable success as shown in Table 3.1. These studies reveal information about the function, immunogenicity and environmental adaptation of the OMPs of a wide range of bacterial species (Berven *et al.*, 2006; Blonder *et al.*, 2004; Cho *et al.*, 2014; Kao *et al.*, 2009; Kumar *et al.*, 2010; Schell *et al.*, 2011; Williams *et al.*, 2007; Wu *et al.*, 2014).

Table 3.1 Literature survey of proteomic studies that have identified bacterial OMPs

Bacterial Species	Digest Method[a]	Mass Spectrometry Method	Cellular Location[b]	Protein results[c]	Reference
Lawsonia intracellularis	GB	LC-ESI-MS/MS	OM	19 OMPs	(Watson *et al.*, 2014)
Chlamydiae	GF&GB	MS/MS Linear Trap Quadropole	WC	~1000 proteins (4 methods)	(Aistleitner *et al.*, 2015)
Pseudomonas syringae	GF&GB	MALDI-TOF/TOF and ESI-MS/MS	OMV	42 OMPs	(Kulkarni *et al.*, 2014)
Coxiella burnetii	GB	LC-MS/MS analysis	WC, OM	39 OMPs	(Flores-Ramirez et al., 2014)
Salmonella. Enterica	GB	LC-MS/MS analysis	OMV	162/167 proteins	(Bai *et al.*, 2014)
Escherichia coli	GB	Q-TOF LC/MS	CE	~100 proteins	(Folsom *et al.*, 2014)
Vibrio cholerae	GF	LC-MS/MS analysis	OMV	90 proteins	(Altindis *et al.*, 2014)
Escherichia coli	GB	2D-MS/MS	CE	123 proteins	(Martorana *et al.*, 2014)
Staphylococcus aureus	GF	LC-MS/MS analysis	WC	1302 proteins	(Pförtner *et al.*, 2014)
Campylobacer jejuni	GF	NanoLC-MS/MS analysis	OMV	134 proteins	(Jang *et al.*, 2014)
Bartonella henselae	GF	LTQ-ICR-FT-Ultra MS	WC	74 OMPs	(Stekhoven *et al.*, 2014)
Haemophilus parasuis	GB	2D - MALDI TOF MS/MS	CE	19 proteins	(Zhang *et al.*, 2014)
Edwardsiella tarda	GB	2D - MALDI TOF MS/MS	WC	661 proteins	(Liu *et al.*, 2013)
Escherichia coli	FASP&GB	LC-MS/MS analysis	WC	~1000 proteins (4 methods)	(Tanca *et al.*, 2013)
Neisseria gonorrhoeae	GB	MALDI-TOF-MS	WC	58 proteins	(Nabu *et al.*, 2014)
Staphylococcus aureus	GF	LC-MS/MS	SP	342 proteins	(Diep *et al.*, 2013)
Staphylococcus aureus	GF	Nano-LC-LTQ-Orbitrap Ms	WC	600 proteins	(Pförtner *et al.*, 2013)
Yersinia enterolitica	GB	2D - MALDI TOF MS/MS	WC,OM	~30 proteins	(Gu *et al.*, 2012)
Pseudomonas syringae	GB	1D&2D MALDI & LC-ESI MS/MS	CE	~100 proteins	(Jagannadham *et al.*, 2012)
Borrelia sp.	GF&GB	(LC)-MS/MS or (2D)-LC-MS/MS	CE	286 proteins	(Gesslbauer *et al.*, 2012)
Yersinia pestis	GF&GB	2D-LC-LTQ-FT	WC	1926 proteins	(Zhou *et al.*, 2012)
Edwardsiella tarda	GB	2-DE, MALDI-TOF/TOF	OM	19 proteins	(Wang *et al.*, 2012)
Coxiella burnetti	GB	1D&2D MALDI TOF/TOF	OM	22 OMPs	(Papadioti *et al.*, 2011)
Pseudomonas aeruginosa	GF	LC-MS/MS	OMV	64 OMPs	(Choi *et al.*, 2011)
Salmonella typhimurium	GB	LC-ESI/MS/MS Sequencing	SP	49 proteins	(Sherry *et al.*, 2011)
Actinobac. pleuropneumoniae	GB	MALDI-TOF MS	CL	42 proteins	(Zhang *et al.*, 2011a)
Burkholderia spp.	GB&GF	LTQ (MS/MS) & MALDI TOF (PMF)	OM	>155 proteins	(Schell *et al.*, 2011)
Vibrio parahaemolyticus	GB	2D-LC-ESI-Q-TOF MS/MS	CE	Expression changes	(Chiu *et al.*, 2011)
Protochlamydia amoeba	GB	1D & 2D MALDI-TOF/TOF and nanoLC-ESI	OM	38 OMPs	(Heinz *et al.*, 2010)
Cronobacter turicensis	GF	2-D-LC-MALDI-TOF/TOF-MS	WC, SP	891 proteins	(Carranza *et al.*, 2010)
Mannheimia Haemolytica	GB	2DE MALDI-TOF & LC-MS/MS	OM	55 proteins	(Ayalew *et al.*, 2010)

Bacterial Species	Digest Method	Mass Spectrometry[a]	Cellular location[b]	Protein results[c]	Reference
Mycobacterium tuberculosis	GF	LC-MS/MS analysis	WC	545 proteins	(Kruh *et al.*, 2010)
Azoarcus spp	GB&GF	MALDI-TOF-MS/MS	WC	126 (GB) + 773 (GF)	(Hauberg *et al.*, 2010)
Chlorobaculum tepidum	GB&GF	MALDI–TOF-MS	WC, CE	220 (GF), 202 (GB)	(Kouyianou *et al.*, 2010)
Helicobacter pylori	GB	2D-MALDI TOF/TOF MS	WC, CE.	567 proteins	(Jungblut *et al.*, 2010)
Various	GB	LC-ESI-MS/MS (Ion trap)	various	44 OMPs	(Thein *et al.*, 2010)
Vibrio anguillarum	GB	LC-nano ESI-Q-TOF MS/MS	OM	6 proteins	(Kao *et al.*, 2009)
Edwardsiella tarda	GB	2D-MALDI-TOF MS	OM	21 proteins	(Kumar *et al.*, 2009)
Pasteurella multocida	GB	MALDI-TOF-MS	OM	39 proteins	(Wheeler, 2009)
Legionella pneumophilla	GB	2D-MALDI TOF MS/MS	WC	157 (out of 439 spots used)	(Shevchuk *et al.*, 2009)
Campylobacer jejuni	GF	2D-MALDI-TOF MS & 2DLC MS/MS	SP	77 Proteins & 432 proteins	(Cordwell *et al.*, 2008)
Flavo. columnare	GB	RP-HPLC MS/MS	OM	36 proteins	(Liu *et al.*, 2008)
Helicobacter pylori	GB	Q-TOF MS/MS	OM	42 OMPs	(Kim *et al.*, 2008)
Propionibacterium acnes	GF	Nano-LC-MS/MS analysis	WC	Not discussed	(Nakatsuji *et al.*, 2008)
Flavobacterium psychrophilum	GB	?	OMP	36 Proteins (total)	(Dumetz *et al.*, 2008)
Brucella suis	GB	2D DIGE / MALDI-TOF MS	WC	168 intramacrophagic	(Al Dahouk *et al.*, 2008)
Prevotella intermedia	GB	2D-MALDI-TOF-MS	OM	17 OMPs	(Yu *et al.*, 2007)
Escherichia coli	GB	Nano-LC-ESI-MS/MS	OMV	141 proteins	(Lee *et al.*, 2007)
Neisseria meningitidis	GB	LC-MS/MS	OM, OMV	236 proteins	(Williams *et al.*, 2007)
Brucella abortus	GF&GB	MALDI-TOF MS & LC-MS/MS	CE	163 proteins	(Connolly *et al.*, 2006).
Pasteurella multocida	GB	2D-MALDI-TOF MS & 1D nanoLC-MS/MS	OM	35 OMPs	(Boyce *et al.*, 2006)
Escherichia coli	GB	2D-MALDI-TOF MS	OM	30 OMPs	(Xu *et al.*, 2006)
Shigella flexneri	GB	MALDI-TOF-MS (PMF)	OM	55 OMPs	(Ying *et al.*, 2005)
Vibrio alginolyticus	GB	MALDI-TOF/MS (PMF) & NanoESI-MS/MS	OM	138 proteins (not all OMPs)	(Xu *et al.*, 2005)
Aeromo. salmonicida	GB	2-DE, LC-MS/MS	OM	Unclear	(Ebanks *et al.*, 2004)
Pseudomonas aeruginosa	GB	2D-MALDI-TOF MS	OM	15 proteins	(Peng *et al.*, 2005)
Escherichia coli	GB	2D-MALDI-TOF MS	CE	173 proteins (41 OMPs)	(Lai *et al.*, 2004)
Bartonella henselae	GB	1 and 2D-MALDI-TOF-MS	OM	53 OMPs	(Rhomberg *et al.*, 2004)
Helicobacter pylori	GB	MALDI-TOF-MS	OM	62 proteins (not all OMPs)	(Baik *et al.*, 2004)
Pseudomonas aeruginosa	GB	2D-ESI-MS/MS + GPF	WC	1331 proteins	(Guina *et al.*, 2003)
Caulobacter crescentus	GB	2D-MALDI-TOF-MS	OM	54 proteins (41 OMPs)	(Phadke *et al.*, 2001)
Escherichia coli	GB	MALDI-TOF-MS	OM	25 OMPs	(Molloy *et al.*, 2000)

[a]GB (gel-based), GF (gel-free), FASP (filter aided sample preparation)
[b]OM(outer membrane), IM (Inner membrane), WC (whole cell), CE (cell envelope), SP (supernanatnt), OMV (outer membrane vesicles)
[c]OMP (exclusively outer membrane proteins)

Identifying the complete repertoire of proteins in the OM is crucial to understanding the system as a whole.

Studies of bacterial proteomes have used diverse methodologies in different organisms, the result of which is large variation in the number of proteins identified (Table 3.1). Thus, like-for-like comparison in the literature can be challenging. One aspect that influences proteome coverage is the method used to digest a protein mixture into peptides. Many studies use either a gel-based or in-solution tryptic digest to produce the peptide mixture needed for analysis. Coverage of the proteome can be high with either approach (Stekhoven *et al.*, 2014; Ying *et al.*, 2005) but few studies have used both digestion techniques in complementation of one another. Those that have reveal that each approach has overlapping coverage, yet substantial numbers of proteins are identified with only one technique (Aistleitner *et al.*, 2015; Connolly *et al.*, 2006; Gesslbauer *et al.*, 2012; Hauberg *et al.*, 2010; Kouyianou *et al.*, 2010; Schell *et al.*, 2011; Zhou *et al.*, 2012). Thus, the evidence suggests that to gain a true insight into the full OM proteome complementary techniques are required.

Recently, the OM proteome of *M. haemolytica* was predicted using a bioinformatic consensus approach (Hounsome, 2012). This system employs the use of ten bioinformatic prediction programmes (E-komon *et al.*, 2012). Four predict subcellular localisation, four predict β-barrel motifs and two predict the likelihood of being a lipoprotein. Hounsome (2012) used this system to screen all the encoded ORFs from bovine A1, bovine A2 and ovine A2 *M. haemolytica* genomes. After consensus matching, redundancy elimination and false positive elimination, a total of 93 OMPs were confidently predicted in the three genomes. Eighty-eight proteins were identified in all three genomes, with the remaining five being distributed between either one, or two, of the three genomes.

Although the prediction approach identifies the hypothetical composition of the OM it is, nevertheless, only a prediction. Thus, the objective of the present study was to experimentally determine the *M. haemolytica* OM proteome in selected bovine and ovine isolates with the aim to better understand aspects of host and serotype specificity.

3.2 Materials and methods

3.2.1 Bacterial isolates and growth conditions

Seven isolates of *Mannheimia haemolytica* and one isolate of *Mannheimia glucosida* were used in this study. Properties of these isolates are presented in Table 3.2. All isolates were plated out from -80°C stock cultures (50:50 glycerol:brain heart infusion broth [BHIB]) onto brain hear infusion agar (BHIA) supplemented with 5% defibrinated sheeps blood and incubated overnight at 37°C. For broth grown cultures, a few colonies were taken from a fresh agar plate, inoculated into 15 ml of BHIB, and incubated overnight at 37 °C with shaking at 120 rpm. Eight hundred microliters of culture were used to inoculate 400 ml volumes of BHIB in 2 L Erlenmeyer flasks. The flasks were incubated at 37°C with shaking at 120 rpm until an OD_{660nm} of 0.8 – 0.9 was achieved.

Table 3.2 Properties of *M. haemolytica* and *M. glucosida* isolates used in the proteomic characterisation

Bacterial Isolate	Host Species	Capsular serotype	Electrophoretic type[a]	Disease Status
M. haemolytica				
PH2	Bovine	A1	1	Pneumonia
PH8	Ovine	A1	6	Pneumonia
PH202	Bovine	A2	21	Healthy
PH278	Ovine	A2	21	Pneumonia
PH292	Ovine	A2	22	Pneumonia
PH296	Ovine	A7	12	Pneumonia
PH588	Ovine	A13	15	Pneumonia
M. glucosida				
PH344	Ovine	A11	N/A	Septicaemia

[a]Electrophoretic type Davies *et al.* (1997).

3.2.2 Preparation of OM protein fractions

Each bacterial culture was prepared as described in 3.2.1. Once an OD_{660nm} 0.8-0.9 was reached, growth was halted by chilling on ice. Bacterial suspensions were harvested by centrifugation at 5000 x g for 20 min at 4°C. The supernatants were discarded and the remaining pellets washed by resuspending in 50 ml of 20 mM Tris-HCl (pH 7.2). Bacteria were recovered by centrifugation at 10 000 x g for 30 min at 4°C. The supernatants were discarded and the bacterial cell pellets resuspended in 7 ml of ice cold Tris-HCl (pH 7.2). The bacterial cells were lysed by sonicating for 5 min (at 12 microns) on iced water. Intact bacterial cells were pelleted by centrifugation at 10 000 x g for 30 min at 4°C. The supernatant was centrifuged at 35 000 x g for 1 h at 4°C to recover the cell envelopes. The inner membranes were selectively solubilised by resuspending the pellets in 7 ml of 0.5% n-lauroylsarcosine (Sarkosyl). The gelatinous pellets were thoroughly resuspended by pipetting. The OMs were recovered by centrifugation at 35 000 x g for 1 h at 4°C. The supernatants were discarded and the pellets were washed by resuspending in 20 mM Tris-HCl (pH 7.2) and centrifuging at 35 000 x g for 1 at 4°C. The final OM pellets were resuspended in 200 – 800 µl (depending on the pellet size) of 20mM Tris-HCl (pH 7.2) and stored at -80°C. Fifty microliters were removed for protein assay before freezing. In total, three replicates for each bacterial isolate were prepared.

3.2.3 Protein assay

The OM fractions were assayed for protein concentration using the modified Lowry method (Markwell *et al.*, 1978). A calibration curve of BSA standards was prepared in advance. To 50 µl of each OM sample were added 950 µl of dH_2O. Reagent A (7 mM sodium potassium tartrate, 0.81 M sodium carbonate and 0.5 N NaOH in dH_2O) was mixed with reagent B (70 mM sodium potassium tartrate and 40 mM copper sulphate in dH_2O) in a 1:100 ratio to make reagent C. Three millilitres of reagent C was added to 1ml of each diluted protein sample in a test tube, vortexed and incubated for 1 h at room temperature. Three hundred microliters of Folins reagent were added to each test tube, the samples were vortexed and incubated for 1 hour at room temperature. The absorbance of each sample (λ = 660 nm) was measured against a control that contained no

protein. The protein concentration of each sample was subsequently derived from the standard curve.

3.2.4 SDS-PAGE

One-dimensional SDS-PAGE was performed as follows. A 100 µl aliquot of each sample was adjusted to 2 mg/ml with 20mM Tris-HCl (pH 7.2). Fifty micolitres of each sample were mixed with an equal volume of Laemmli sample buffer and the samples denatured by heating for 5 min in a boiling water bath. Twenty micrograms of total protein were separated in a 12% SDS-polyacrylamide gel using the Laemmli buffer system (Laemmli, 1970). The migration of protein samples through the stacking gel was achieved with a constant current of 20 mA and then resolved in the separating gel with a constant current of 30 mA (Hoefer SE600 electrophoresis system). Once adequate separation had occurred, gels were stained in 1 % Coomassie brilliant blue with shaking overnight. Gels were distained with successive washes in destaining solution (H_2O:methanol:acetic acid 50:40:10 [v/v/v]). Gels were then photographed using a computer scanner.

3.2.5 Preparation of in-gel tryptic digests of proteins

Gel bands were excised from Coomassie blue-stained SDS-PAGE gels and transferred to 96 well microtitre plates for digestion. Gel slices were incubated for 30 min in 300 µl of 100 mM ammonium bicarbonate and subsequently in 300 µl of a 50:50 mixture of 100mM ammonium bicarbonate:acetonitrile. The liquid was discarded and protein bands were reduced by incubating for 30 min at 60 °C with 235 µl of 2.8 mM dithiotheritol (DTT). Protein bands were then alkylated by the addition of 15 µl of 100 mM iodoacetimide to the existing solution followed by 30 min of incubation in the dark. The solution was discarded and protein bands were incubated for 30 min in 300 µl of a 50:50 mixture of 100 mM ammonium bicarbonate: acetonitrile. Protein bands were then dehydrated by submersion in 100 % acetonitrile and 30 min of incubation at room temperature. The remaining liquid was aspirated and the gel bands were allowed to dry fully on the bench. Re-hydration was accomplished with at least 35 µl of 20 µg/ml porcine trypsin (Promega) solution in 25 mM ammonium bicarbonate. Protein bands were incubated at 37°C for 12 to 16 hours to ensure efficient digestion of proteins. After incubation, all remaining liquid was transferred to a fresh 96-

well microtiter plate. Protein bands were incubated for 20 min with 35 µl of 5% formic acid at room temperature. The liquid from each gel piece was removed and added to the microtiter plate containing the aspirated liquid from the overnight digestion. Forty microliters of 100 % acetonitrile were added to each band before incubation of 20 min at room temperature. The liquid from each gel piece was then removed and added to the same microtiter plate containing the overnight digestion liquid and the 5 % formic acid fraction. The final peptide solutions were then dried with a vacuum centrifuge and stored at -20°C until analysis by mass spectrometry.

3.2.6 Preparation of in-solution tryptic digests of proteins

Forty microliters of 2 mg/ml of each OMP sample were combined with 88 µl of 50 mM ammonium bicarbonate and incubated for 20 min in a sonicating bath with periodic vortexing. The samples were heated at 60°C for 20 min and cooled on ice for three min. To each sample were added 32 µl of 20 µg/ml sequencing grade porcine trypsin (Promega) and 48 µl of HPLC grade methanol. Samples were incubated for 12 to 16 h at 37°C to allow full digestion of proteins. The final peptide solutions were then dried with a vacuum centrifuge and stored at -20°C until analysis by mass spectrometry.

3.2.7 LC-MS/MS of tryptic digests

Peptides were solubilized in 2 % acetonitrile with 0.1 % trifluoroacetic acid and fractionated on a nanoflow uHPLC system (Thermo RSLCnano) before online analysis ESI mass spectrometry on an Amazon ion trap MS/MS (Bruker Daltonics). Peptide separation was performed on a Pepmap C18 reversed phase column (LC Packings). Peptides were desalted and concentrated for 4 min on a C18 trap column followed by an acetonitrile gradient (in 0.1 % v/v formic acid) (3.2 to 32 % [v/v], 4 to 27 min; 32 % to 80 % [v/v], 27 - 36 min; held at 80 % [v/v] 36 to 41 min and re-equilibrated at 3.2 %) for a total time of 45 min. A fixed solvent flow rate of 0.3 µl/min was used for the analytical column. The trap column solvent flow rate was fixed at 25 µl/min, using 2 % acetonitrile with 0.1 % v/v trifluoroacetic acid. Mass spectrometric (MS) analysis was performed using a continuous duty cycle of survey MS scan followed by up to ten MS/MS analyses of

the most abundant peptides, choosing the most intense multiply charged ions with dynamic exclusion for 120 s.

3.2.8 MASCOT searching and data analysis

Mass spectra from collected data sets were database searched using MASCOT daemon (Matrix Science). Data sets were searched against NCBI Genbank using a taxonomic restriction of "*Mannheimia haemolytica*" with parent and fragment mass tolerances of ±0.4 Da each and allowing for one missed cleavage. Protein matches with MOWSE scores above a P>0.05 confidence threshold were considered as legitimate matches; protein matches with scores below this threshold were discounted. All information regarding peptide matches and emPAI scores can be found in Table 7.2, Table 7.3 and Table 7.4.

3.2.9 Whole genome sequencing

The eight isolates used for the proteomic study (Table 3.2) were, in addition, prepared for whole genome sequencing (WGS). Extraction was accomplished with the PurElute Bacterial Genomic Kit (Edgebio; 85171). From an overnight culture, 50 µl of bacterial suspension were harvested by centrifugation at 4000 x g for 5 min at 4°C. The pelleted bacteria were resuspended in 2 ml of sterile PBS and centrifuged at 13 000 x g for 1 min at 4°C. The samples had 400 µl of spheroplast buffer added before vortexing for 10 s to resuspend the pellet. Samples were incubation at 37°C for 10 min in a water bath. One hundred microliters of lysis solution 1 were added to each sample and the samples mixed by vortexing for 10 s. One hundred microliters of lysis solution 2 were added to each sample and the samples were mixed by vortexing for 10 s. The samples were incubated at 65°C for 5 min in a water bath. One hundred microliters of extraction buffer were added to each sample and the samples vortexed vigorously for 10 s before centrifugation at 13 000 x g for 3 min at 4°C. The supernatants were transferred to a clean Eppendorf tube and 100 µl of Advamax 2 beads were added to each. The samples were mixed by inversion and the beads were pelleted by centrifugation. The supernatants were collected and an equal volume of isopropanol added. The samples were mixed by inversion and the DNA was pelleted by centrifugation at 13 000 x g for 3 min at 4°C. The supernatants were carefully removed and the DNA was washed by adding 750 µl

70% ethanol. The supernatants were removed and the samples air-dried for 30 min. The DNA was resuspended in 100 µl nuclease free water and stored at -20°C.

Whole genome sequencing was performed using the Illumina Mi-seq system at Glasgow Polyomics. Three hundred base-pair paired-end reads were employed. Reads were trimmed of Illumina adaptor sequences and low quality bases. The CLC genomics workbench was used to *de novo* assemble scaffolds. Annotations were added to scaffolds using the Rapid Annotation using Subsystem Technology (RAST) resource (Aziz *et al.*, 2008).

3.2.10 BLAST analysis

The sequenced genomes of the seven *M. haemolytica isolates* and one *M. glucosida* isolate were subjected to a BLAST search. Nucleotide sequences of the genes encoding the protein matches from the proteomic experiments were used in the BLAST searches. The CLC genomics workbench was used to conduct the BLAST searches. The nucleotide sequences used to conduct the BLAST search were derived from the published genome of an A1 serotype pathogenic bovine isolate (NC_020833). Some genes encoding OMPs were not present in the NC_020833 genome, in these cases an alternative nucleotide sequence had to be used. Details of all the genomes used in the BLAST searches are shown in Table 3.3.

Table 3.3 Genome information from which nucleotide sequences for BLAST were obtained

Genome Accession No.	Assembly No.	BioSample No.	Assembly Level	Serotype	Host
NC_020833	GCA_000349765.1	SAMN02048829	Closed	A1	Bovine
AUNK01	GCA_000443085.1	SAMN02116555	Contig	A2	Bovine
ACZY01	GCA_000176275.1	SAMN02436661	Contig	A2	Bovine
ACZX01	GCA_000176255.1	SAMN02436663	Contig	A2	Ovine
JANJ01	GCA_000584935.1	SAMN02951912	Contig	A1/A6	Cervine

3.3 Results

3.3.1 In gel and In-solution proteomic digest evaluation

To assess the efficiency of proteome coverage a single isolate of *Mannheimia haemolytica* (PH202) was chosen to serve as a reference isolate, this was primarily due to OM sarkosyl preparations of PH202 containing a greater number of coomassie stained protein bands than the other isolates in this study. Analysis of the OM protein fraction was carried out using a duel proteomic approach of in-gel and in-solution (gel-free) tryptic digests, to compare the proteome coverage that each method offers. With the gel-based approach, two methodologies were also employed. One approach, termed 'whole-lane-section', involved the division of the whole gel lane (mini gel format) into 17 equally sized fractions (Fig 3.1 [A]). The other approach, termed 'gel-slice', involved the excision of selected bands from a Coomassie stained gel (Fig 3.1 [B]). These gel-based approaches confer different advantages with the gel-slice method affording greater specificity and the whole-lane-section approach offering greater coverage. Samples were prepared and analysed in triplicate for each method.

Using a combination of all 3 methods (gel-based gel-slice, gel-based whole-lane-section and gel-free methodologies), a total of 64 OMPs were identified in *M. haemolytica* isolate PH202. Outer membrane proteins identified using all three digestion methods amounted to 31 with 8, 3 and 3 proteins identified exclusively by the gel-free, gel-slice and whole-lane-section methods respectively (Fig 3.2 A). Identities to all matched OMPs are shown in Table 3.4.

Two way comparisons of each method as well as comparison between total gel-based and total gel-free methodologies were performed (Fig 3.2 B, C, D and E). Of the gel-based methods, more OMPs were identified with the whole-lane-section method compared to the gel-slice (Fig 3.2 B). More OMPs (42) were identified by both the whole-lane-section and gel-free approaches (Fig 3.2 D) than with the gel-free and the more targeted gel-slice method (35 OMPs) (Fig 3.2 C). The greatest number of unique proteins identified (19 OMPs) was attributed to the gel-free approach when comparing it to the gel-slice approach (Fig 3.2 C).

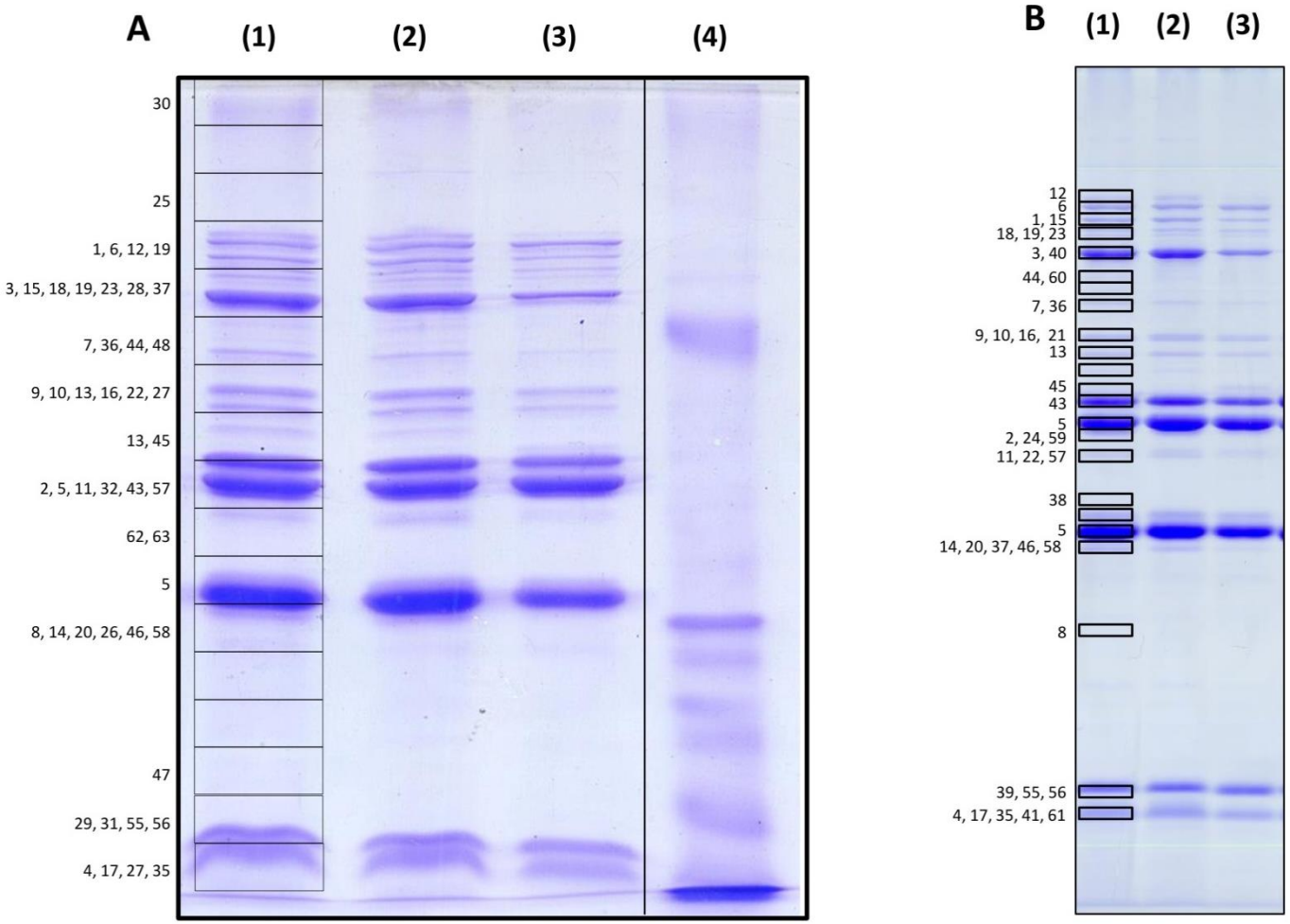

Fig 3.1 Annotated SDS-PAGE gels showing OMP profiles of PH202
A: Whole-lane-section (mini gel format), lanes 1, 2 and 3 all correspond to three independent replicate OMP preparations of isolate PH202 Lane 4 corresponds to the molecular weight standard. Annotated numbers correspond to identified OMPs that match table entries in Table 3.4. B: Gel-slice (large gel format), lanes 1, 2 and 3 correspond to three independent replicate OMP preparations of isolate PH202. Boxes on lane one in both A and B display the excised band positions. Annotated numbers correspond to identified OMPs that match table entries in Table 3.4.

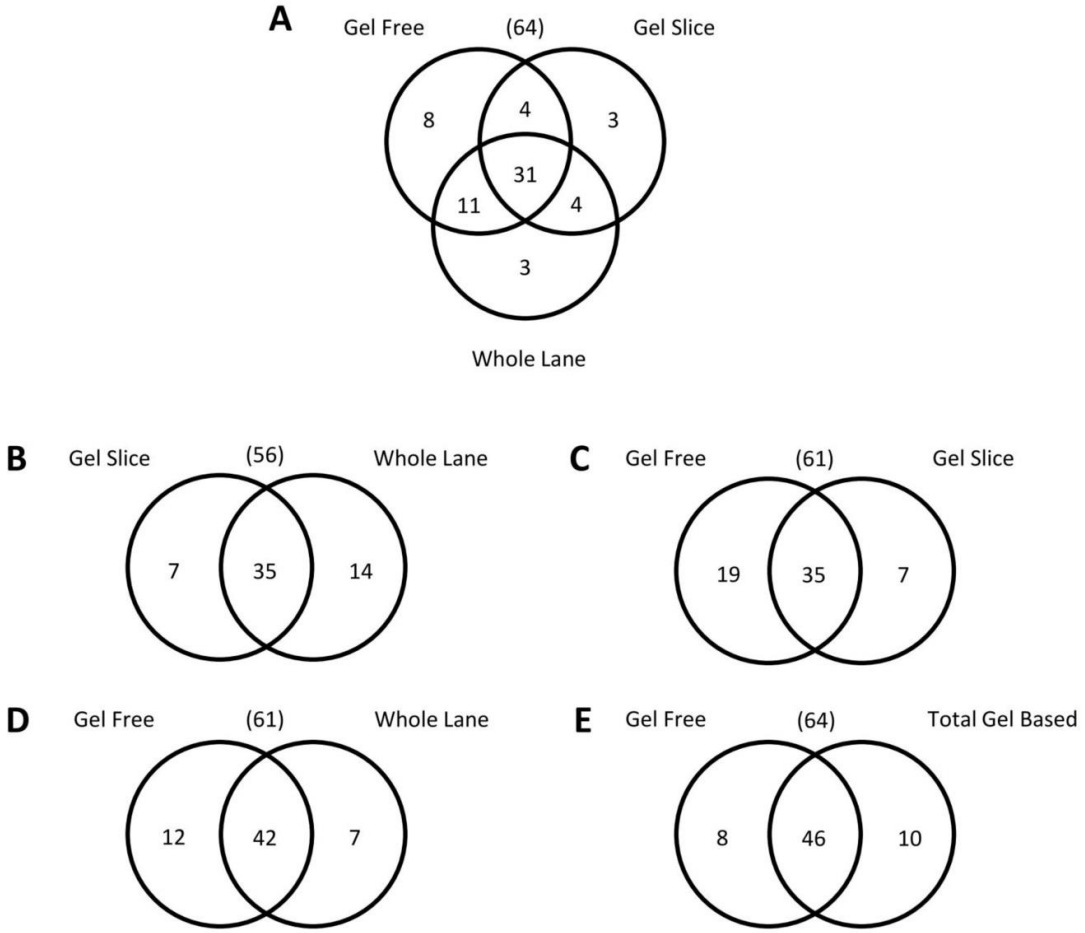

Fig 3.2 Venn diagrams of PH202 OMP identification by three different methods
(A) Total OMP identification-distribution from isolate PH202 between the three methodologies. Two way comparisons of PH202 OMP identification between (B) gel-slice and whole-lane-section, (C) gel-free and gel-slice, (D) gel-free and whole-lane-section methodologies and (E) gel-free and the combination of the two gel-based methods. Numbers in brackets display the total number of OMPs identified by the methods referenced in the diagrams. All samples were prepared in triplicate.

Table 3.4 OMPs identified in isolate PH202 using three different methods of protein digestion
Protein matches (+) are displayed with a superscript indicating the number of replicates (of three) the OMP was found in. No match is marked with (–). Band numbers correspond to the numbers marked on SDS-PAGE gels in Fig 3.1.

Band No.	GI Number	Protein Name	Protein Function	MW (Da)	Gel-Free	Gel Slice	Lane Section
1	gi|472258490	BamA/ YaeT	β barrel assembly	88770	+^{3}	+^{3}	+^{3}
2	gi|472256811	CpxD / Wza	Capsular polysaccharide export	34773	+^{3}	+^{3}	+^{3}
3	gi|472259454	FrpB / FetA	Receptor and transport activities	76672	+^{3}	+^{3}	+^{3}
4	gi|472257701	Omp P6 / Pal	Peptidoglycan anchoring	16534	+^{3}	+^{3}	+^{3}
5	gi|472256940	OmpA	Outer membrane structure and integrity	40461	+^{3}	+^{3}	+^{3}
6	gi|472258673	Ssa1	Serine protease	103701	+^{3}	+^{3}	+^{3}
7	gi|472259236	HbpA	Complement factor H binding	61166	+^{3}	+^{3}	+^{3}
8	gi|472257144	Putative Lipoprotein 1	Unknown function	17598	+^{3}	+^{3}	+^{3}
9	gi|472258540	Omp P1	Hydrophobic compound transport	52791	+^{3}	+^{3}	+^{3}
10	gi|472257531	PlpE	Unknown function	50776	+^{3}	+^{3}	+^{3}
11	gi|472259387	MltC	Peptidoglycan remodelling	40762	+^{3}	+^{3}	+^{3}
12	gi|472257461	TbpA	Transferrin uptake	105517	+^{3}	+^{3}	+^{3}
13	gi|472258822	TolC	Type I secretion system OM channel	51836	+^{3}	+^{3}	+^{3}
14	gi|472258802	PlpA	Unknown function	30200	+^{3}	+^{3}	+^{2}
15	gi|472257731	LptD	LPS assembly	89553	+^{3}	+^{2}	+^{3}
16	gi|472256848	Putative Omp 1	Unknown function	56058	+^{3}	+^{2}	+^{3}
17	gi|472258510	LptE / RlpB	Lipopolysacharride transport	18274	+^{3}	+^{2}	+^{3}
18	gi|472258277	NanH	Cleavage of host sialic acid	89190	+^{3}	+^{2}	+^{2}
19	gi|472257384	HmbR1	Haemoglobin uptake	79431	+^{3}	+^{2}	+^{2}

Band No.	GI Number	Protein Name	Protein Function	MW (Da)	Gel-Free	Gel Slice	Lane Section
20	gi|472258662	OmpP4	Haem acquisition / factor V utilisation	23077	+^{3}	+^{2}	+^{1}
21	gi|472257163	OapA	Cell Adhesion	40883	+^{3}	+^{2}	+^{1}
22	gi|472257142	LppB / NlpD	Cell wall formation and maintenance	44667	+^{3}	+^{1}	+^{2}
23	gi|472259235	HxuC	Siderophore uptake	69601	+^{3}	+^{1}	+^{2}
24	gi|472258419	MltA	Peptidoglycan remodelling	40136	+^{3}	+^{1}	-
25	gi|472258914	IgA1_3	Cleavage of host mucosal IgA	158582	+^{3}	-	+^{3}
26	gi|472258736	BamD / ComL	Accessory lipoprotein of BAM complex	29776	+^{3}	-	+^{2}
27	gi|472257997	Bor / Iss_2	Putative serum resistance function	10287	+^{3}	-	+^{2}
28	gi|472258140	TamA / YtfM	Autotransporter assembly	70662	+^{3}	-	+^{2}
29	gi|472257680	YajG	Unkown function	21179	+^{3}	-	+^{2}
30	gi|472258161	Yad-A like	Trimeric autotransporter adhesin	68188	+^{3}	-	+^{2}
31	gi|472257276	Hly	Haemolysin activity	21059	+^{3}	-	+^{1}
32	gi|472258667	PotD / Lpp38	Unknown function	36042	+^{3}	-	+^{1}
33	gi|472257325	Mam7 / PqiB	Cell adhesion	98151	+^{3}	-	+^{1}
34	gi|472257232	Hypothetical protein 1	Unknown function	20779	+^{3}	-	-
35	gi|472257023	Pcp	Unknown function	15553	+^{2}	+^{3}	+^{3}
36	gi|472259234	CcmD/ HxuB	Haem / haemopexin acquisition	61609	+^{2}	+^{3}	+^{3}
37	gi|472258800	PlpC	Unknown function	28446	+^{2}	+^{3}	+^{1}
38	gi|472258491	OmpH	Outer membrane porin	29201	+^{2}	+^{3}	-
39	gi|472257959	NlpC / P60	Cell wall hydrolysis during growth	19478	+^{2}	+^{2}	-
40	gi|472257460	TbpB	Transferrin binding	60946	+^{2}	+^{1}	+^{1}
41	gi|472257682	NlpE	Stress response transmission	14123	+^{2}	+^{1}	-
42	gi|472258914	IgA1_3 Like	Cleavage of host mucosal IgA	60031	+^{2}	-	-

Band No.	GI Number	Protein Name	Protein Function	MW (Da)	Gel-Free	Gel Slice	Lane Section
43	gi|472258334	Omp P2-like	Outer membrane porin	40229	+[1]	+[3]	+[3]
44	gi|472257273	LpoA	Peptidoglycan synthesis regulation	63533	+[1]	+[3]	+[2]
45	gi|472257424	LamB	Maltose specific porin	44254	+[1]	+[1]	+[3]
46	gi|472258801	PlpB	Unknown function	30224	+[1]	+[1]	+[2]
47	gi|472258478	LemA	Unknown function	19773	+[1]	-	+[2]
48	gi|472258286	FhuE	Siderophore uptake	77881	+[1]	-	+[1]
49	gi|472259186	VacJ-like	Phospholipid homeostasis	14050	+[1]	-	-
50	gi|472257571	Ydcf protein	Putative autotransporter	81196	+[1]	-	-
51	gi|472256863	RlpA	Unknown function	23934	+[1]	-	-
52	gi|472258343	LolB	Outer membrane lipoprotein insertion	24118	+[1]	-	-
53	gi|472259196	Putative Omp 3	Unknown function	37754	+[1]	-	-
54	gi|757542574	TadG-like	Cell adhesion	61134	+[1]	-	-
55	gi|472259098	Omp 18/16	Unknown function	18363	-	+[3]	+[3]
56	gi|493291997	Hypothetical protein 2	Unknown function	18641	-	+[3]	+[3]
57	gi|472256984	Putative Omp 2	Unknown function	37106	-	+[3]	+[2]
58	gi|493290991	fHbp_1	Complement factor H binding	26690	-	+[3]	+[1]
59	gi|472257942	MltB	Peptidoglycan remodelling	40536	-	+[3]	-
60	gi|472257918	FhaC / ShlB	Outer membrane translocator of FhaB	67243	-	+[1]	-
61	gi|472258517	PilA	Type IV pilus subunit	17059	-	+[1]	-
62	gi|493290616	IgA1_2	Outer membrane integrity	79772	-	-	+[1]
63	gi|493292739	IgA1_1	Cleavage of host mucosal IgA	164627	-	-	+[1]
64	gi|472257996	Bor / Iss_1	Putative serum resistance function	10783	-	-	+[1]

Analysis of the gel-free approach against both the gel-based approaches (whole-lane-section and gel-slice) revealed 46 OMPs were identified by a combination of the gel-free approach and both of the gel-based approaches (Fig 3.2 E). However, eight OMPs were solely identified by gel-free and ten OMPs were solely identified using a combination of both gel-based methods (Fig 3.2 E). All the two-way Venn diagrams (Fig 3.2 B, C, D and E) highlighted there were more OMPs identified by both of any two methods than there were with any single method alone. A greater number of OMPs were identified via both techniques when evaluating the gel-free with the whole-lane-section (42) as compared to either of these methodologies in combination with the gel-slice methodology (35). This highlighted the need for at least one method that involves digestion of the entire sample.

Analysis of the protein identities from the gel-free, whole-lane section and gel-slice highlighted differences amongst these three methodologies. Thirty-one OMPs were identified by all three methodologies (Table 3.4). OMP hits from each methodology could be achieved in up to three replicates. Summing the total number of replicate matches for each methodology of the 31 OMPs (derived from Table 3.4) revealed there were almost identical numbers of replicate matches between the gel-slice (76) and whole-lane-section approaches (78) with slightly more being identified in the gel-free approach (81). This serves to show that coverage of the OM proteome is roughly equal amongst the 31 OMPs that were identified by all three methodologies. However, there were cases where some OMPs were matched in one replicate by one methodology, two by another methodology and three by the remaining methodology (Table 3.4); these include the OMPs LppB / NlpD, OmpP4, OapA, PlpC, LpoA and HxuC (Table 3.4). Two of these OMPs (LppB / NlpD and HxuC) were identified in one replicate of the gel-slice, two replicates of the whole-lane-section and three replicates of the gel-free. Two OMPs (OmpP4 and OapA) were identified in two replicates of the gel-slice, one replicate of the whole-lane-section and three replicates of the gel-free. PlpC was identified in three replicates of the gel-slice, one replicate of the whole-lane-section and two replicates of the gel-free. LpoA was identified in three replicates of the gel-slice, two replicates of the whole-lane-section and one replicate of the gel-free. These six OMPs demonstrate that while in sufficient enough abundance to be identified in three replicates with one

technique, they fail to be identified with the same degree of reproducibility by the other methodologies. Thus, there is some bias associated with each method.

Fourteen OMPs were identified by only a single methodology (Table 3.4). However, the majority of these (11 out of 14) were also identified in only a single replicate and the majority (7 out of 11) of these single replicate matches were only identified via one or two peptises (supplementary Table 7.2 and Table 7.4). This suggests that either these OMPs are present in a low copy number per cell and close to the limit of detection by LC-MS/MS, or that biophysical properties of the proteins make detection by mass spectrometry based proteomics challenging. Several OMPs identified in only a single replicate of a single methodology were matched with several peptides including the VacJ-like (3 matched [1 significant]) and Bor/Iss_1 (5 matched [5 significant]) lipoproteins and the IgA1_1 (4 matched [2 significant]) and IgA1_2 (9 matched [3 significant]) autotransporters. Analysis of the number of significant peptides shows that in the cases of IgA1_1, IgA1_2 and VacJ-like it is likely that these are present in a low copy number per cell. Although Bor/Iss_1 was matched via 5 significant peptides these 5 peptides were of the same identity (VTDNIKPTK) and while the identity of the peptide cannot be denied, the assignment to the Bor/Iss_1 may indeed be false.

Three OMPs (IgA_3-like protein, MltB and Hypothetical protein 1) were identified in two or more replicates but only by a single methodology. The IgA_3-like protein was matched in two replicates by the gel-free methodology; MltB and Hypothetical protein 1 were each matched in three replicates by the gel-slice and gel-free methodologies, respectively. The IgA1_3-like protein shares a high degree of homology with IgA1_3; the latter protein was matched in the whole-lane section as well as the gel-free. IgA1_3 has a high molecular mass (~158,000 Da) and, consistent with this, it was identified in the upper most band of the whole-lane-section. The equivalent band position was not excised for the gel-slice methodology (Fig 3.1). Therefore, the likely explanation is that it would have been identified by the gel-slice technique had the upper portion of the gel been subjected to digestion and LC-MS/MS. The same might be applied to the case of Hypothetical protein 1, where identification occurred only by the gel-free method. This protein has a molecular weight of 20,779 Da. A band

equivalent to this molecular weight position was not cut for the gel-slice method (Fig 3.1). However, the whole-lane-section failed to identify this protein even though a band at the corresponding molecular weight position was excised and analysed. As no visible band is present at this molecular weight position, hypothetical protein 1 might be in such low abundance that it cannot be identified by the gel-based methodologies. MltB was only identified in all three biological replicates by the gel-slice method and would have been present in the tryptic digest of the other two methodologies. This suggests MltB is present in all three biological replicates, yet can only be identified by a gel-based tryptic digest and the specific band targeting of the gel-slice methodology is required. Thus, MltB represents a protein that cannot be identified by all tryptic-digest methodologies and highlights the need for complementary methodologies.

Considering all of the above information allowed for two methodologies to be chosen as the basis for analysis of the full repertoire of isolates. Gel-free was chosen as it resulted in the greatest number of OMPs identified and is fundamentally different to the gel-based methods. Of the gel-based approaches, the gel-slice method was chosen. Although more OMPs were identified with the whole-lane-section method, the ability of the gel-slice method to target specific gel bands and the practicalities of running 17 samples per replicate of each isolate rendered whole-lane-sectioning unfeasible.

3.3.2 Gel-free proteomic analysis of the *M. haemolytica* and *M. glucosida* outer membrane

Triplicate OMP extracts were generated for seven isolates *of M. haemolytica* and one isolate of *M. glucosida*. Gel-free proteomic analysis was carried out on the eight isolates from these three independent extractions. A MASCOT search was performed as described in section 3.2.8 and the resulting data sets were exported. Identified proteins were assessed for the likelihood of being an OMP using the bioinformatic list compiled by Hounsome (2012) and literature searching where necessary. Redundancies amongst the OMPs were eliminated to produce a compiled list of OMP hits across the eight isolates (Table 3.5).

Table 3.5 Gel-free proteomic analysis of the OM of *M. haemolytica* and *M. glucosida*
74 OMPs identified in the OM of the eight isolates by gel-free proteomic analysis. Protein matches (+) are displayed with a superscript indicating the number of replicates (of three) the protein was found in. No match is marked with (-).

GI Number	Protein Name	Protein Function	MW (Da)	Protein hits of three replicates								Prediction[a]
				Isolates								
				PH2	PH8	PH202	PH278	PH292	PH296	PH588	PH344	
gi|472258490	BamA/ YaeT	β barrel assembly	88770	+[3]	+[3]	+[3]	+[3]	+[3]	+[3]	+[3]	+[3]	+
gi|472258736	BamD / ComL	Accessory lipoprotein of BAM complex	29776	+[3]	+[3]	+[3]	+[3]	+[3]	+[3]	+[3]	+[3]	+
gi|472257997	Bor / Iss_2	Putative serum resistance function	10287	+[3]	+[3]	+[3]	+[3]	+[3]	+[3]	+[3]	+[3]	+
gi|472256811	CpxD / Wza	Capsular polysaccharide export	34773	+[3]	+[3]	+[3]	+[3]	+[3]	+[3]	+[3]	+[3]	+
gi|472259454	FrpB / FetA	Receptor and transport activities	76672	+[3]	+[3]	+[3]	+[3]	+[3]	+[3]	+[3]	+[3]	+
gi|472257142	LppB / NlpD	Cell wall formation and maintenance	44667	+[3]	+[3]	+[3]	+[3]	+[3]	+[3]	+[3]	+[3]	+
gi|472257731	LptD	LPS transport	89553	+[3]	+[3]	+[3]	+[3]	+[3]	+[3]	+[3]	+[3]	+
gi|472257701	Omp P6 / Pal	Peptidoglycan anchoring	16534	+[3]	+[3]	+[3]	+[3]	+[3]	+[3]	+[3]	+[3]	+
gi|472256940	OmpA	Outer membrane structure and integrity	40461	+[3]	+[3]	+[3]	+[3]	+[3]	+[3]	+[3]	+[3]	+
gi|472258662	OmpP4	Haem acquisition / factor V utilisation	23077	+[3]	+[3]	+[3]	+[3]	+[3]	+[3]	+[3]	+[3]	+
gi|472258673	Ssa1	Serine protease	103701	+[3]	+[3]	+[3]	+[3]	+[3]	+[3]	+[3]	+[3]	+
gi|472257680	YajG	Unknown function	21179	+[3]	+[3]	+[3]	+[3]	+[3]	+[3]	+[3]	+[3]	+
gi|472259236	HbpA	Complement factor H binding	61166	+[3]	+[3]	+[3]	+[3]	+[3]	+[3]	+[3]	+[2]	-
gi|472257144	Putative Lipoprotein 1	Unknown function	17598	+[3]	+[3]	+[3]	+[3]	+[3]	+[3]	+[3]	+[2]	+
gi|472256848	Putative Omp 1	Unknown function	56058	+[3]	+[3]	+[3]	+[3]	+[3]	+[3]	+[3]	+[2]	+
gi|472257276	Hly	Haemolysin activity	21059	+[3]	+[3]	+[3]	+[3]	+[3]	+[3]	+[3]	+[1]	-
gi|472258540	Omp P1	Hydrophobic compound transport	52791	+[3]	+[3]	+[3]	+[3]	+[3]	+[3]	+[3]	-	+
gi|472257531	PlpE	Unknown function	50776	+[3]	+[3]	+[3]	+[3]	+[3]	+[3]	+[3]	-	+
gi|472259387	MltC	Peptidoglycan remodelling	40762	+[3]	+[3]	+[3]	+[3]	+[3]	+[3]	+[2]	+[3]	+
gi|472258510	LptE / RlpB	Lipopolysacharride transport	18274	+[3]	+[3]	+[3]	+[3]	+[3]	+[3]	-	+[1]	+

GI Number	Protein Name	Protein Function	MW (Da)	Protein hits of three replicates								Prediction[a]
				Isolates								
				PH2	PH8	PH202	PH278	PH292	PH296	PH588	PH344	
gi|472257232	Hypothetical protein 1	Unknown function	20779	+3	+3	+3	+3	+3	+2	+3	+3	-
gi|472258277	NanH	Cleavage of host sialic acid	89190	+3	+3	+3	+3	+3	-	+3	-	+
gi|472258667	PotD / Lpp38	Unknown function	36042	+3	+3	+3	+3	+2	+3	+3	-	+
gi|472257461	TbpA	Transferrin uptake	105517	+3	+3	+3	+2	+3	+3	+3	+1	+
gi|472257163	OapA	Cell Adherence	40883	+3	+3	+3	+2	+2	+3	+3	+2	-
gi|472258800	PlpC	Unknown function	28446	+3	+3	+2	+3	+3	+3	+3	+3	+
gi|472257460	TbpB	Transferrin binding	60946	+3	+3	+2	-	+2	+3	+3	-	+
gi|472259186	VacJ-like	Phospholipid homeostasis	14050	+3	+3	+1	+3	+3	+3	+3	+3	+
gi|472257273	LpoA	Peptidoglycan synthesis regulation	63533	+3	+3	+1	+2	+3	+3	+3	-	+
gi|472258068	PlpD	Unknown function	24719	+3	+3	-	-	-	+3	+2	+2	+
gi|472258822	TolC	Type I secretion system OM channel	51836	+3	+2	+3	+3	+3	+3	+3	+3	+
gi|472258140	TamA / YtfM	Autotransporter assembly	70662	+3	+2	+3	+3	+3	+3	+3	-	+
gi|472258802	PlpA	Unknown function	30200	+3	+2	+3	+3	+3	+2	+3	+3	+
gi|472258491	OmpH	Outer membrane porin	29201	+3	+2	+2	+3	+3	+3	+3	+3	+
gi|472257682	NlpE	Stress response transmission	14123	+3	+2	+2	+2	+3	+3	+3	+1	+
gi|472258478	LemA	Unknown function	19773	+3	+2	+1	+2	+2	+2	+3	+1	-
gi|472257023	Pcp	Unknown function	15553	+3	+1	+2	+3	+3	+2	+2	+1	+
gi|472257571	Ydcf-domain protein	Unknown function	81196	+3	+1	+1	+3	+3	+2	-	-	+
gi|472258419	MltA	Peptidoglycan remodelling	40136	+3	-	+3	+2	+3	-	+1	+2	+
gi|472258334	Omp P2-like	Outer membrane porin	40229	+2	+3	+1	+3	+3	+2	+3	+2	+
gi|472257918	FhaC / ShlB	Outer membrane translocator of FhaB	67243	+2	+3	-	+3	+3	-	-	+3	+
gi|472256984	Putative Omp 2	Unknown function	37106	+2	+3	-	+1	-	+1	-	+1	+
gi|472257001	Omp P2	Outer membrane porin	41060	+2	+3	-	-	-	+3	+3	+1	+

GI Number	Protein Name	Protein Function	MW (Da)	Protein hits of three replicates								Prediction[a]
				Isolates								
				PH2	PH8	PH202	PH278	PH292	PH296	PH588	PH344	
gi|472258801	PlpB	Unknown function	30224	+[2]	+[1]	+[1]	+[2]	+[2]	+[2]	+[1]	-	+
gi|472258309	Putative Omp 4	Unknown function	157489	+[2]	+[1]	-	+[2]	+[1]	+[2]	+[1]	-	-
gi|472257384	HmbR1	Haemoglobin uptake	79431	+[1]	-	+[3]	-	+[1]	+[2]	+[3]	-	+
gi|472257911	CirA domain protein	Siderophore uptake	90165	+[1]	-	-	-	+[3]	+[3]	-	-	+
gi|472259235	HxuC	Haem / haemopexin acquisition	69601	-	+[3]	+[3]	+[3]	+[3]	+[3]	+[3]	-	+
gi|472257917	FhaB	Filamentous hemagglutinin (cell adherence)	309018	-	+[3]	-	+[1]	+[3]	-	-	+[3]	+
gi|472257325	Mam7 / PqiB	Cell adherence	98151	-	+[2]	+[3]	+[2]	-	+[1]	+[2]	+[1]	-
gi|472259234	CcmD/ HxuB	Haem / haemopexin acquisition	61609	-	+[2]	+[2]	-	+[3]	+[3]	+[3]	-	+
gi|472256863	RlpA	Unknown function	23934	-	+[2]	+[1]	-	-	-	+[2]	-	-
gi|472258914	IgA1_3	Cleavage of host mucosal IgA	158582	-	+[1]	+[3]	+[3]	-	+[3]	+[1]	-	+
gi|472257617	OmpW	Hydrophobic compound transport	23804	-	+[1]	-	-	-	+[1]	-	+[1]	+
gi|472257086	Hsf	Trimeric autotransporter adhesin	206010	-	+[1]	-	-	-	+[1]	-	-	+
gi|472258161	Yad-A like	Trimeric autotransporter adhesin	68188	-	-	+[3]	+[3]	+[3]	-	-	-	+
gi|472258914	IgA1_3 Like	Cleavage of host mucosal IgA	60031	-	-	+[2]	+[2]	-	+[3]	-	-	+
gi|472257959	NlpC / P60	Cell wall hydrolysis during growth	19478	-	-	+[2]	-	-	-	+[1]	-	+
gi|472257424	LamB	Maltose specific porin	44254	-	-	+[1]	+[1]	-	-	+[1]	-	+
gi|472258343	LolB	Outer membrane lipoprotein insertion	24118	-	-	+[1]	-	-	-	+[2]	+[1]	+
gi|472258286	FhuE	Siderophore uptake	77881	-	-	+[1]	-	-	-	-	-	+
gi|472259196	Putative Omp 3	Unknown function	37754	-	-	+[1]	-	-	-	-	-	+
gi|757542574	TadG-like	Cell adhesion	61134	-	-	+[1]	-	-	-	-	-	-
gi|472258252	BamE	Accessory protein of BAM complex	12986	-	-	-	+[1]	+[1]	-	-	-	+
gi|472258899	FhuA	Siderophore uptake	79395	-	-	-	-	+[2]	-	-	-	+
gi|472259029	Hypothetical protein 3	Unknown function	17890	-	-	-	-	+[1]	-	-	+[1]	+

GI Number	Protein Name	Protein Function	MW (Da)	Protein hits of three replicates								Prediction[a]
				Isolates								
				PH2	PH8	PH202	PH278	PH292	PH296	PH588	PH344	
gi|472258883	BtuB	Vitamin B12 receptor	71229	-	-	-	-	-	+[3]	-	+[3]	+
gi|472256991	WzzB	O-antigen chain length determination	30018	-	-	-	-	-	+[2]	-	-	+
gi|472257912	Hypothetical protein 4	Unknown function	53056	-	-	-	-	-	+[1]	-	-	-
gi|472257084	Putative autotransporter	Unknown function	58835	-	-	-	-	-	+[1]	-	-	+
gi|472258517	PilA	Type IV pilus subunit	17059	-	-	-	-	-	-	+[1]	-	-
gi|472259021	HmbR2	Haemoglobin uptake	92740	-	-	-	-	-	-	-	+[3]	+
gi|261311542	IgA1_4	Cleavage of host mucosal IgA	69224	-	-	-	-	-	-	-	+[1]	+
gi|472257942	MltB	Peptidoglycan remodelling	40536	-	-	-	-	-	-	-	+[1]	+
gi|472259076	TonB-dependednt protein	Unkown function	86387	-	-	-	-	-	-	-	+[1]	+

[a]Predicted OMP (+) or not predicted to be an OMP (-) via the prediction system used by Hounsome, (2012) in conjunction with M. haemolytica as described in the text.

A total of 75 OMPs were identified in one or more replicates amongst the eight isolates. Of these 75 unique OMPs, 12 were considered as 'core' OMPs on the basis of being identified in all three replicates for each of the eight isolates. However, this increased to 22 OMPs by including OMPs that were identified in at least two of three replicates. Additionally, excluding the single *M. glucosida* isolate PH344 from the analysis further increased the core set of OMPs to 29. The remaining 46 OMPs were identified in various numbers of replicate samples in all isolates.

All 75 OMPs were assigned to categories based on their primary functional role (Fig 3.3). The 12 core OMPs comprised six proteins in the functional category of biogenesis and integrity. These included BamA/YaeT and BamD/ComL which are involved in β-barrel assembly, LptD which is involved in LPS transport, LppB/NlpD which is involved in cell wall formation, Omp P6/Pal which is responsible for anchoring the OM to the peptidoglycan layer and OmpA which involved in the structure and integrity of the OM.

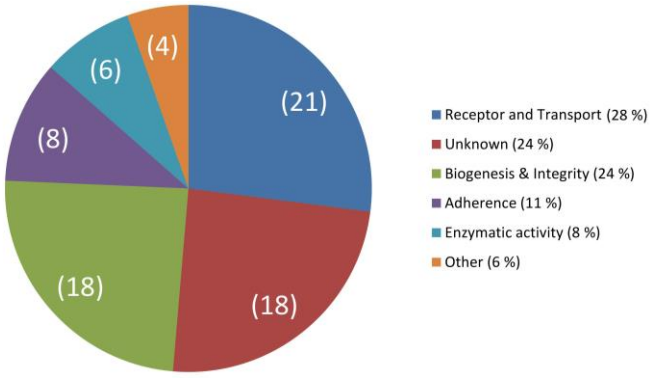

Fig 3.3 Functional categorisation of the 75 gel-free identified proteins
Shown in white on the pie chart are numbers of OMPs that comprise each category.

The 12 core proteins also comprised three OMPs of the transport and receptor category. These included FrpB/FetA which is involved in iron transport, Wza which is involved in capsular polysaccharide export and Omp P4 which is involved in heme acquisition and complement factor V utilisation. Only one OMP from each of the functional categories enzymatic (Ssa1), other (Bor/Iss_2) and unknown (YajG) were represented among the core 12 proteins. No OMPs with adherence related function were identified among the core proteins. Although, when considering OMPs that were matched in at least two of three replicates the core expands to encompass one adherence protein, OapA. Thus, broadly

speaking, the 'core' predominantly comprises proteins with functions essential to the cells integrity and viability.

Non-core OMPs (46) revealed several species-specific and serotype-specific patterns. PlpD was not identified in the serotype A2 strains but was identified in at least two replicates of the other five isolates. Similarly, OmpP2 was not identified in all of the serotype A2 isolates but was present in at least one replicate of each of the other strains. In contrast, the YadA-like trimeric autotransporter was identified in all three serotype A2 isolates, but was absent in all replicates of the other five isolates. The filamentous haemagglutinin protein also displayed isolate-to-isolate variation. FhaB was identified in all replicates of isolates PH8, PH292 and PH344, as well as a single replicate of PH278, but was completely absent from all other isolates; noteably, it was absent from the bovine isolates PH2 and PH202

Within the enzymatic class of OMPs, several proteins were identified with isolate-to-isolate variation. NanH was identified in all replicates of all isolates except PH296 and PH344; in the latter two isolates it was not identifed in any replicates. Of the various IgA-specific metalloendopeptidases that *M. haemolytica* possesses, several were identified with isolate-to-isolate specificity. The endopeptidase designated IgA1_3 was identified in all replicates of isolates PH202, PH278 and PH296 and in a single replicate of isolates PH8 and PH588. However, this protein was not identified in isolates PH2, PH292 and PH344.

Of the iron uptake proteins, HxuB, HxuC, HmbR1, TbpA, TbpB and the CirA domain-containing siderophore receptor exhibited isolate-to-isolate variation. HxuC, involved in heme-hemopexin uptake, was found in all replicates of all isolates except PH2 and PH344 and HxuB was found in two or three replicates of all isolates except PH2, PH278 and PH344. Of the two haemoglobin receptors, HmbR2 was only identified in PH344 while HmbR1 was identified in one, two or three replicates in all isolates except PH8, PH278 and PH588 where it was completely absent. Both of the transferrin binding proteins, TbpA and TbpB. were found to varying degrees amongst the eight isolates. TbpA was identified in three replicates of isolates PH2, PH8, PH202, PH292, PH296 and PH588, two replicates of PH278 and one replicate of PH344. TbpB on the other hand was not identified in any replicates of PH278 and PH344, but was identified in at least

two replicates in the other six isolates. The TonB-dependent siderophore receptor, CirA, was identified in all replicates of isolates PH292 and PH296 and one of three replicates of PH2, but in no replicates of the remaining isolates.

Other OMPs that displayed distinct isolate-to-isolate variation include the TonB-dependent vitamin B12 receptor, BtuB. The BtuB receptor was identified in all replicates of isolates PH296 and PH344 but was completely absent from all replicates of the other six isolates.

Overall it is clear that a large proportion of the identified OMPs are common to all the isolates, as these OMPs are functionally responsible for essential processes. However, 46 OMPs were identified with variation across the eight bacterial isolates; these OMPs may represent differences in host-adaptation and pathogenicity.

3.3.3 Gel-based proteomic analysis of the *M. haemolytica* and *M. glucosida* outer membrane

Based on the evaluation (3.3.1) of the three proteomic methods a gel-based method was used to complement the gel-free analysis. Although whole lane-sectioning identified more OMPs, the greater specificity and lower cost associated with targeting individual bands resulted in the gel-slice method being chosen to complement the gel-free proteomic analysis

Triplicate OM Sarkosyl extracts of the eight isolates were separated on SDS-PAGE gels (Fig 3.4). Fifty-eight bands were excised from the gel in triplicate (174 in total). The bands were selected on the basis that they were at different molecular weight positions to the excised bands of the reference isolate (PH202), or had differences in staining intensity on the SDS-PAGE gel. These included 16 from PH2, five from PH8, five from PH278, seven from PH292, five from PH292, three from PH588 and eight from PH344. Also excised were nine bands from PH202, the reference isolate.

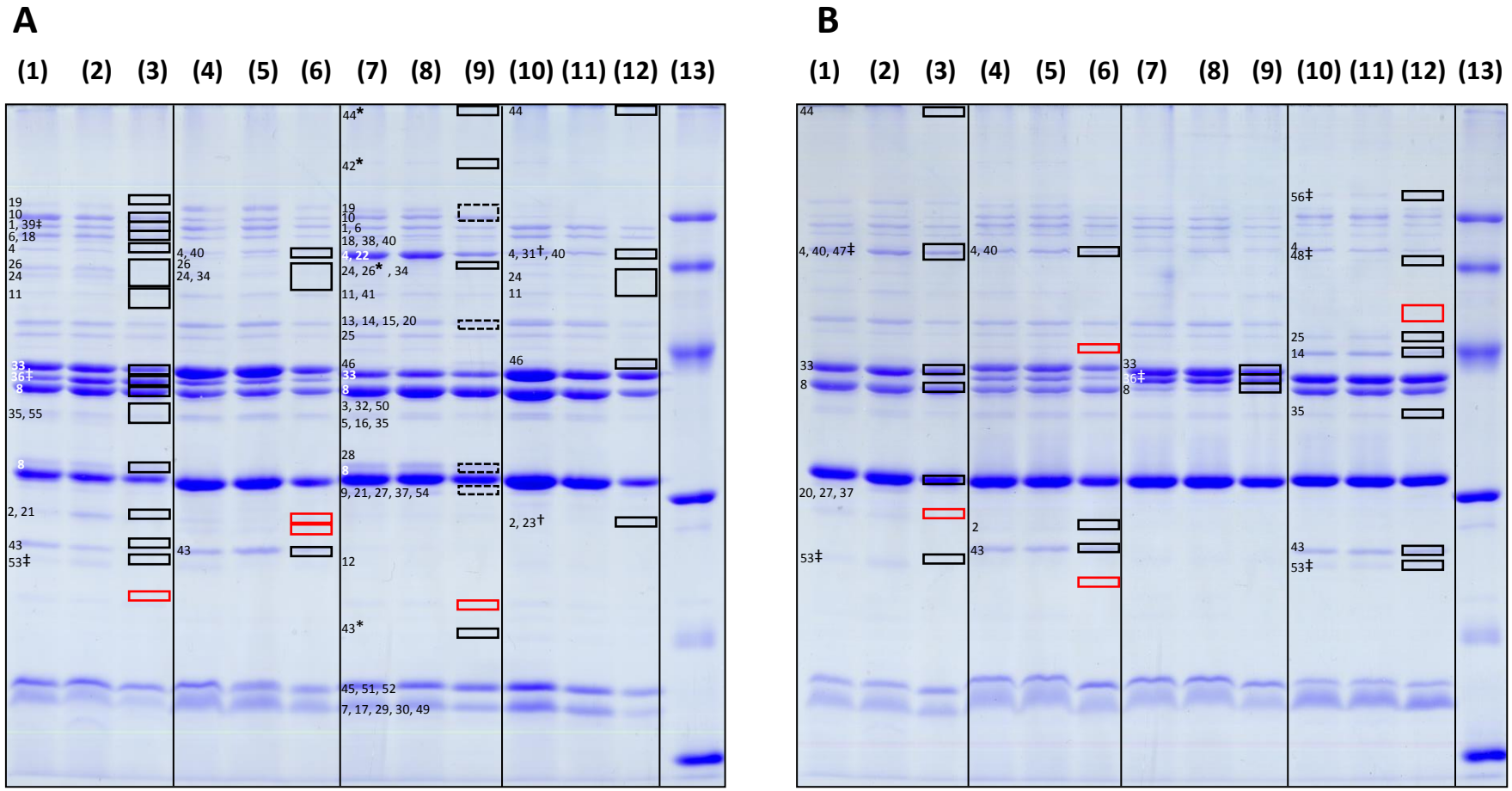

Fig 3.4 Annotated SDS-PAGE separation of OMP fractions

Triplicate OMP preparations of seven *M. haemolytica* isolates and one *M. glucosida* isolate. (A) Lanes 1, 2 and 3 correspond to PH2, 4, 5 and 6 to PH8, 7, 8 and 9 to PH202 and 10, 11 and 12 to PH278. (B) Lanes 1, 2 and 3 correspond to PH292, 4, 5 and 6 to PH296, 7, 8 and 9 to PH588 and 10, 11 and 12 to PH344. Lane 13 of each gel corresponds to the molecular mass standard. Numbers overlaid on replicate 1 of each isolate denote OMP entries in Table 3.6. Boxes overlaid on replicate 3 mark the excised bands. Red boxes correspond to bands where no OMP was identified. Dashed boxes on PH202 correspond to bands that were excised at postions that had previously been excised during the method comparison. Numbers marked with (*) reflect additional proteins identified in PH202 that were not identified during the method comparison (3.3.1). Numbers marked with (†) represent OMPs that were originally only identified in the gel-free method for the reference isolate PH202. Numbers marked with (‡) represent OMPs that were not in the reference isolate PH202 by either gel-based or gel-free methodologies.

Of these nine bands, four were at molecular mass positions the same as bands excised during the method evaluation. The remaining five represented faint band positions that were not included in the method evaluation.

The 174 excised protein bands were subjected to LC-MS/MS (3.2.7) and the resulting data searched using MASCOT (3.2.8) and exported. Protein hits were assessed using literature searching and bioinformatic prediction (Hounsome, 2012) to identify OMPs from amongst the total protein list (Table 3.6). Redundancies amongst the OMP hits were eliminated and the resulting OMPs were mapped to the SDS-PAGE gels (Fig 3.4). The prior identification of OMPs in the reference isolate (PH202) were included and resulted in a total of 56 OMPs identified via the gel-slice methodology. Inclusion of the whole-lane-section of isolate PH202 increased the total to 65 OMPs.

Several proteins exhibited isolate-to-isolate variation when similar excised band positions were compared. Proteins identified exclusively in bovine isolates (PH2 and PH202) include BamA, LptD, Ssa1, NanH and TbpA. No OMPs were identified exclusively in the ovine isolates. This might be expected considering the reference isolate, from which all visible bands were cut, was bovine. Thus, the majority of bands (66 %) excised were from the two bovine isolates (PH2 and PH202).

Several proteins were found only in certain serotypes. For example, TbpA and the YadA-like trimeric autotransporter were found exclusively in the serotype A1 and A2 isolates, respectively. Eight proteins were identified that had not previously been found in the reference isolate PH202 using the gel based methodologies. These included VacJ-like, the YdcF domain-containing protein, Omp P2, the CirA domain-containing protein, FhuA, BtuB, HlpB and Pertactin (Table 3.7). Aside from VacJ-like and the YdcF domain containing protein, the same band positions of these OMPs had been subjected to MS/MS analysis in PH202. Thus, the remaining six OMPs reflect proteins that are either below the limit of detection, not expressed or absent from the PH202 genome.

Table 3.6 Gel-based proteomic analysis of the OM of *M. haemolytica* and *M. glucosida*
56 OMPs identified in the OM of the eight isolates by gel-based proteomic analysis. Protein matches (+) are displayed with a superscript indicating the number of replicates (of three) the protein was found in. No match is marked with (-). If no band was cut at the MW position of the protein then the entry is marked (N/A).

Band No.	GI Number	Protein Name	Protein Function	MW (DA)	Protein Identification								Prediction[a]
					Isolates								
					PH2	PH8	PH202	PH278	PH292	PH296	PH588	PH344	
1	gi|472258490	BamA/ YaeT	β barrel assembly	88770	$+^{3}$	N/A	$+^{3}$	N/A	N/A	N/A	N/A	N/A	+
2	gi|472258736	BamD / ComL	Accessory lipoprotein of BAM complex	29776	$+^{3}$	-	N/A	$+^{2}$	-	$+^{2}$	N/A	N/A	+
3	gi|472256811	CpxD / Wza	Capsular polysaccharide export	34773	N/A	N/A	$+^{3}$	N/A	N/A	N/A	N/A	N/A	+
4	gi|472259454	FrpB / FetA	Receptor and transport activities	76672	$+^{3}$	$+^{2}$	$+^{3}$	$+^{3}$	$+^{3}$	$+^{3}$	N/A	$+^{1}$	+
5	gi|472257142	LppB / NlpD	Cell wall formation and maintenance	44667	N/A	N/A	$+^{1}$	N/A	N/A	N/A	N/A	-	+
6	gi|472257731	LptD	LPS transport	89553	$+^{2}$	N/A	$+^{2}$	N/A	N/A	N/A	N/A	N/A	+
7	gi|472257701	Omp P6 / Pal	Peptidoglycan anchoring	16534	N/A	N/A	$+^{3}$	N/A	N/A	N/A	N/A	N/A	+
8	gi|472256940	OmpA	Outer membrane structure and integrity	40461	$+^{3}$	N/A	$+^{3}$	N/A	$+^{3}$	N/A	$+^{3}$	N/A	+
9	gi|472258662	OmpP4	Heam acquisition / factor V utilisation	23077	-	N/A	$+^{2}$	N/A	N/A	N/A	N/A	N/A	+
10	gi|472258673	Ssa1	Serine protease	103701	$+^{3}$	N/A	$+^{3}$	N/A	N/A	N/A	N/A	N/A	+
11	gi|472259236	HbpA	Complement factor H binding	61166	$+^{1}$	N/A	$+^{3}$	$+^{2}$	N/A	N/A	N/A	-	+
12	gi|472257144	Putative Lipoprotein 1	Unknown function	17598	-	-	$+^{3}$	N/A	-	-	N/A	-	+
13	gi|472256848	Putative Omp 1	Unknown function	56058	N/A	N/A	$+^{3}$*	N/A	N/A	N/A	N/A	N/A	+
14	gi|472258540	Omp P1	Hydrophobic compound transport	52791	N/A	N/A	$+^{3}$	N/A	N/A	N/A	N/A	$+^{3}$	+
15	gi|472257531	PlpE	Unknown function	50776	N/A	N/A	$+^{3}$	N/A	N/A	N/A	N/A	N/A	+
16	gi|472259387	MltC	Peptidoglycan remodelling	40762	-	N/A	$+^{3}$	N/A	N/A	N/A	N/A	-	+
17	gi|472258510	LptE / RlpB	Lipopolysacharride transport	18274	N/A	N/A	$+^{1}$	N/A	N/A	N/A	N/A	N/A	+
18	gi|472258277	NanH	Cleavage of host sialic acid	89190	$+^{3}$	N/A	$+^{2}$	N/A	N/A	N/A	N/A	N/A	+
19	gi|472257461	TbpA	Transferrin uptake	105517	$+^{3}$	N/A	$+^{3}$	N/A	N/A	N/A	N/A	N/A	+
20	gi|472257163	OapA	Cell Adhesion	40883	N/A	N/A	$+^{1}$	N/A	-	N/A	N/A	N/A	-

Band No.	GI Number	Protein Name	Protein Function	MW (DA)	Protein Identification								Prediction[a]
					Isolates								
					PH2	PH8	PH202	PH278	PH292	PH296	PH588	PH344	
21	gi|472258800	PlpC	Unknown function	28446	+[1]	N/A	+[3]	N/A	+[1]	N/A	N/A	N/A	+
22	gi|472257460	TbpB	Transferrin binding	60946	-	-	+[1]	-	-	-	N/A	N/A	+
23	gi|472259186	VacJ-like	Phospholipid homeostasis	14050	-	-	N/A	+[2]	-	-	N/A	N/A	+
24	gi|472257273	LpoA	Peptidoglycan synthesis regulation	63533	+[2]	+[3]	+[2]	+[1]	N/A	N/A	N/A	N/A	+
25	gi|472258822	TolC	Type I secretion system OM channel	51836	N/A	N/A	+[3]	N/A	N/A	N/A	N/A	+[2]	+
26	gi|472258140	TamA / YtfM	Autotransporter assembly	70662	+[2]	+[1]	+[2]*	N/A	-	N/A	N/A	N/A	+
27	gi|472258802	PlpA	Unknown function	30200	N/A	N/A	+[3]	N/A	+[1]	N/A	N/A	N/A	+
28	gi|472258491	OmpH	Outer membrane porin	29201	N/A	N/A	+[3]	N/A	N/A	N/A	N/A	N/A	+
29	gi|472257682	NlpE	Stress response transmission	14123	N/A	N/A	+[1]	N/A	N/A	N/A	N/A	N/A	+
30	gi|472257023	Pcp	Unknown function	15553	N/A	N/A	+[3]	N/A	N/A	N/A	N/A	N/A	+
31	gi|472257571	Ydcf domain protein	Putative autotransporter	81196	N/A	N/A	N/A	+[1]	N/A	N/A	N/A	+[2]	+
32	gi|472258419	MltA	Peptidoglycan remodelling	40136	N/A	N/A	+[1]	N/A	N/A	N/A	N/A	N/A	+
33	gi|472258334	Omp P2-like	Outer membrane porin	40229	+[3]	N/A	+[3]	N/A	+[2]	N/A	+[3]	N/A	+
34	gi|472257918	FhaC / ShlB	Outer membrane translocator of FhaB	67243	-	+[3]	+[1]	-	N/A	N/A	N/A	N/A	+
35	gi|472256984	Putative Omp 2	Unknown function	37106	+[2]	N/A	+[3]	N/A	N/A	N/A	N/A	+[2]	+
36	gi|472257001	Omp P2	Outer membrane porin	41060	+[3]	N/A	-	N/A	-	N/A	+[3]	N/A	+
37	gi|472258801	PlpB	Unknown function	30224	N/A	N/A	+[3]*	N/A	+[1]	N/A	N/A	N/A	+
38	gi|472257384	HmbR1	Haemoglobin uptake	79431	-	N/A	+[2]	N/A	N/A	N/A	N/A	N/A	+
39	gi|472257911	CirA domain protein	Siderophore uptake	90165	+[1]	N/A	-	N/A	N/A	N/A	N/A	N/A	+
40	gi|472259235	HxuC	Haem / haemopexin acquisition	69601	-	+[3]	+[1]	+[3]	+[3]	+[1]	N/A	N/A	+
41	gi|472259234	CcmD/ HxuB	Haem / haemopexin acquisition	61609	-	N/A	+[3]	N/A	N/A	N/A	N/A	N/A	+
42	gi|472258914	IgA1_3	Cleavage of host mucosal IgA	158582	N/A	N/A	+[2]*	N/A	N/A	N/A	N/A	N/A	+
43	gi|472257617	OmpW	Hydrophobic compound transport	23804	+[3]	+[3]	+[1]	N/A	-	+[3]	N/A	+[3]	+

Band No.	GI Number	Protein Name	Protein Function	MW (DA)	Protein Identification								Prediction[a]
					Isolates								
					PH2	PH8	PH202	PH278	PH292	PH296	PH588	PH344	
44	gi|472258161	Yad-A like	Trimeric autotransporter adhesin	68188	N/A	N/A	+[3]	+[2]	+[2]	N/A	N/A	N/A	+
45	gi|472257959	NlpC / P60	Cell wall hydrolysis during growth	19478	N/A	N/A	+[2]	N/A	N/A	N/A	N/A	N/A	+
46	gi|472257424	LamB	Maltose specific porin	44254	N/A	N/A	+[2]	+[3]	N/A	N/A	N/A	N/A	+
47	gi|472258899	FhuA	Siderophore uptake	79395	-	-	-	-	+[1]	-	N/A	-	+
48	gi|472258883	BtuB	Vitamin B12 receptor	71229	-	-	-	N/A	N/A	N/A	N/A	+[3]	+
49	gi|472258517	PilA	Type IV pilus subunit	17059	N/A	N/A	+[1]	N/A	N/A	N/A	N/A	N/A	-
50	gi|472257942	MltB	Peptidoglycan remodelling	40536	N/A	N/A	+[3]	N/A	N/A	N/A	N/A	N/A	+
51	gi|472259098	Omp 18/16	Unknown function	18363	N/A	N/A	+[3]	N/A	N/A	N/A	N/A	N/A	+
52	gi|493291997	Hypothetical protein 2	Unknown function	18641	N/A	N/A	+[3]	N/A	N/A	N/A	N/A	N/A	-
53	gi|493292248	HlpB	Unknown function	20729	+[3]	N/A	-	N/A	+[2]	N/A	N/A	+[1]	+
54	gi|493290991	fHbp_1	Complement factor H binding	26690	N/A	N/A	+[3]	N/A	N/A	N/A	N/A	N/A	+
55	gi|493290616	IgA1_2	Cleavage of host mucosal IgA	79772	+[1]	N/A	-	N/A	N/A	N/A	N/A	-	+
56	gi|589590239	Pertactin	Putative adherence function	80435	-	N/A	-	N/A	N/A	N/A	N/A	+[2]	-

[a]Predicted OMP (+) or not predicted to be an OMP (-) via the prediction system used by Hounsome, (2012) in conjunction with M. haemolytica as described in the text.

[*]Replicate number, out of three, is the maximum taken either from the three excised bands of the method comparison or from three bands excised during the remaining analysis

Table 3.7 Gel-based MS/MS identification of OMPs not found in the reference isolate. Band numbers correspond to the SDS-PAGE gel images in Fig 3.4.

Band Number	GI Number	Protein Name	MW
23	gi|472259186	VacJ-like	14050
31	gi|472257571	Ydcf domain containing protein	81196
36	gi|472257001	Omp P2	41060
39	gi|472257911	CirA domain containing protein	90165
47	gi|472258899	FhuA	79395
48	gi|472258883	BtuB	71229
53	gi|493292248	HlpB	20729
56	gi|589590239	Pertactin	80435

3.3.4 Total Proteomic Analysis

In total 83 unique OMPs were identified using all the complementary techniques (gel-free, gel-based whole-lane-section and gel-based band-slice) of this study (Table 3.8). Of these 83 OMPs, 18 were identified solely by the gel-free method (BamE, RlpA, lolB, HmbR1, IgA1_3-like, IgA1_4 FhaB, Hsf, PlpD, TadG-like, Wzzb, putative Omp3, putative Omp4, putative autotransporter, TonB-dependent protein and hypothetical proteins 1, 3 and 4) and eight by the gel-based method (fHbp_1, IgA1_1, IgA1_2, Bor/Iss_1, Omp 18/16, HlpB, Pertactin and hypothetical protein 2).

Patterns of protein identification between different isolates were confirmed by combining the gel-free and gel-based results. The YadA-like trimeric autotransporter, which was found exclusively in A2 serotype strains PH202, PH278 and PH292, by the gel-free method, was confirmed through the gel-based methodology to be present in these isolates. PlpD, which failed to be identified by the gel-free method in any A2 serotype strains, was similarly not identified in any A2 serotype strains by the gel-based method. The TonB-dependent cobalamin receptor, BtuB, was found only in isolates PH296 and PH344 using the gel-free analysis and only in isolate PH344 using the gel-based analysis. The filamentous haemagglutinin protein, FhaB, was identified in isolates PH8, PH292, PH278 and PH344 using the gel-free method but was not identified in any isolate using the gel-based methodology.

Table 3.8 Combined gel-based and gel-free proteomic analysis of the OM of *M. haemolytica* and *M. glucosida*
OMPs identified in the eight isolates by gel-based and gel-free proteomic analysis. Protein matches (+) are displayed with a superscript indicating the number of replicates (of three) the protein was found in. No match is marked with (-). N/A (not-applicable) applies to the case where band positions were not excised at the corresponding molecular mass i.e. identification cannot be ruled out.

GI Number	Protein Name	Protein Identification																Prediction[a]
		Isolates																
		PH2		PH8		PH202		PH278		PH292		PH296		PH588		PH344		
		Gel-free	Gel-based	Gel-free	Gel-based	Gel-free	Gel-based	Gel-free	Gel-based	Gel-free	Gel-based	Gel-free	Gel-based	Gel-free	Gel-based	Gel-free	Gel-based	
gi|472258490	BamA/ YaeT	+^{3}	+^{3}	+^{3}	N/A	+^{3}	+^{3}	+^{3}	N/A	+^{3}	N/A	+^{3}	N/A	+^{3}	N/A	+^{3}	N/A	+
gi|472258736	BamD / ComL	+^{3}	+^{3}	+^{3}	-	+^{3}	N/A	+^{3}	+^{2}	+^{3}	-	+^{3}	+^{2}	+^{3}	N/A	+^{3}	N/A	+
gi|472257997	Bor / Iss_2	+^{3}	-	+^{3}	-	+^{3}	-	+^{3}	-	+^{3}	-	+^{3}	-	+^{3}	-	+^{3}	-	+
gi|472256811	CpxD / HexD / BexD	+^{3}	N/A	+^{3}	N/A	+^{3}	+^{3}	+^{3}	N/A	+^{3}	N/A	+^{3}	N/A	+^{3}	N/A	+^{3}	N/A	+
gi|472259454	FrpB / FetA	+^{3}	+^{3}	+^{3}	+^{2}	+^{3}	+^{3}	+^{3}	+^{3}	+^{3}	+^{3}	+^{3}	+^{3}	+^{3}	N/A	+^{3}	+^{1}	+
gi|472257142	LppB / NlpD	+^{3}	N/A	+^{3}	N/A	+^{3}	+^{1}	+^{3}	N/A	+^{3}	N/A	+^{3}	N/A	+^{3}	N/A	+^{3}	-	+
gi|472257731	LptD	+^{3}	+^{2}	+^{3}	N/A	+^{3}	+^{2}	+^{3}	N/A	+^{3}	N/A	+^{3}	N/A	+^{3}	N/A	+^{3}	N/A	+
gi|472257701	Omp P6 / Pal	+^{3}	N/A	+^{3}	N/A	+^{3}	+^{3}	+^{3}	N/A	+^{3}	N/A	+^{3}	N/A	+^{3}	N/A	+^{3}	N/A	+
gi|472256940	OmpA	+^{3}	+^{3}	+^{3}	N/A	+^{3}	+^{3}	+^{3}	N/A	+^{3}	+^{3}	+^{3}	N/A	+^{3}	+^{3}	+^{3}	N/A	+
gi|472258662	OmpP4	+^{3}	-	+^{3}	N/A	+^{3}	+^{2}	+^{3}	N/A	+^{3}	N/A	+^{3}	N/A	+^{3}	N/A	+^{3}	N/A	+
gi|472258673	Ssa1	+^{3}	+^{3}	+^{3}	N/A	+^{3}	+^{3}	+^{3}	N/A	+^{3}	N/A	+^{3}	N/A	+^{3}	N/A	+^{3}	N/A	+
gi|472257680	YajG	+^{3}	-	+^{3}	-	+^{3}	-	+^{3}	-	+^{3}	-	+^{3}	-	+^{3}	-	+^{3}	-	+
gi|472259236	HbpA	+^{3}	+^{1}	+^{3}	N/A	+^{3}	+^{3}	+^{3}	+^{2}	+^{3}	N/A	+^{3}	N/A	+^{3}	N/A	+^{2}	-	-
gi|472257144	Putative Lipoprotein 1	+^{3}	-	+^{3}	-	+^{3}	+^{3}	+^{3}	N/A	+^{3}	-	+^{3}	-	+^{3}	N/A	+^{2}	-	+
gi|472256848	Putative Omp 1	+^{3}	N/A	+^{3}	N/A	+^{3}	+^{3*}	+^{3}	N/A	+^{3}	N/A	+^{3}	N/A	+^{3}	N/A	+^{2}	N/A	+
gi|472257276	Hly	+^{3}	-	+^{3}	-	+^{3}	-	+^{3}	-	+^{3}	-	+^{3}	-	+^{3}	-	+^{1}	-	-
gi|472258540	Omp P1	+^{3}	N/A	+^{3}	N/A	+^{3}	+^{3}	+^{3}	N/A	+^{3}	N/A	+^{3}	N/A	+^{3}	N/A	-	+^{3}	+
gi|472257531	PlpE	+^{3}	N/A	+^{3}	N/A	+^{3}	+^{3}	+^{3}	N/A	+^{3}	N/A	+^{3}	N/A	+^{3}	N/A	-	N/A	+

GI Number	Protein Name	Protein Identification																Prediction[a]
		Isolates																
		PH2		PH8		PH202		PH278		PH292		PH296		PH588		PH344		
		Gel-free	Gel-based	Gel-free	Gel-based	Gel-free	Gel-based	Gel-free	Gel-based	Gel-free	Gel-based	Gel-free	Gel-based	Gel-free	Gel-based	Gel-free	Gel-based	
gi|472259387	MltC	+³	-	+³	N/A	+³	+³	+³	N/A	+³	N/A	+³	N/A	+²	N/A	+³	-	+
gi|472258510	LptE / RlpB	+³	N/A	+³	N/A	+³	+¹	+³	N/A	+³	N/A	+³	N/A	-	N/A	+¹	N/A	+
gi|472257232	Hypothetical protein 1	+³	-	+³	-	+³	-	+³	-	+³	-	+²	-	+³	-	+³	-	-
gi|472258277	NanH	+³	+³	+³	N/A	+³	+²	+³	N/A	+³	N/A	-	N/A	+³	N/A	-	N/A	+
gi|472258667	PotD / Lpp38	+³	-	+³	-	+³	-	+³	-	+²	-	+³	-	+³	-	-	-	+
gi|472257461	TbpA	+³	+³	+³	N/A	+³	+³	+²	N/A	+³	N/A	+³	N/A	+³	N/A	+¹	N/A	+
gi|472257163	OapA	+³	N/A	+³	N/A	+³	+¹	+²	N/A	+²	-	+³	N/A	+³	N/A	+²	N/A	-
gi|472258800	PlpC	+³	+¹	+³	N/A	+²	+³	+³	N/A	+³	+¹	+³	N/A	+³	N/A	+³	N/A	+
gi|472257460	TbpB	+³	-	+³	-	+²	+¹	-	-	+²	-	+³	-	+³	N/A	-	N/A	+
gi|472259186	VacJ-like	+³	-	+³	-	+¹	N/A	+³	+²	+³	-	+³	-	+³	N/A	+³	N/A	+
gi|472257273	LpoA	+³	+²	+³	+³	+¹	+²	+²	+¹	+³	N/A	+³	N/A	+³	N/A	-	N/A	+
gi|472258068	PlpD	+³	-	+³	-	-	-	-	-	-	-	+³	-	+²	-	+²	-	+
gi|472258822	TolC	+³	N/A	+²	N/A	+³	+³	+³	N/A	+³	N/A	+³	N/A	+³	N/A	+³	+²	+
gi|472258140	TamA / YtfM	+³	+²	+²	+¹	+³	+²*	+³	N/A	+³	-	+³	N/A	+³	N/A	-	N/A	+
gi|472258802	PlpA	+³	N/A	+²	N/A	+³	+³	+³	N/A	+³	+¹	+²	N/A	+³	N/A	+³	N/A	+
gi|472258491	OmpH	+³	N/A	+²	N/A	+²	+³	+³	N/A	+³	N/A	+³	N/A	+³	N/A	+³	N/A	+
gi|472257682	NlpE	+³	N/A	+²	N/A	+²	+¹	+²	N/A	+³	N/A	+³	N/A	+³	N/A	+¹	N/A	+
gi|472258478	LemA	+³	-	+²	-	+¹	-	+²	-	+²	-	+²	-	+³	-	+¹	-	-
gi|472257023	Pcp	+³	N/A	+¹	N/A	+²	+³	+³	N/A	+³	N/A	+²	N/A	+²	N/A	+¹	N/A	+
gi|472257571	Ydcf domain containing protein	+³	N/A	+¹	N/A	+¹	N/A	+³	+¹	+³	N/A	+²	N/A	-	N/A	-	+²	+
gi|472258419	MltA	+³	N/A	-	N/A	+³	+¹	+²	N/A	+³	N/A	-	N/A	+¹	N/A	+²	N/A	+
gi|472258334	Omp P2-like	+²	+³	+³	N/A	+¹	+³	+³	N/A	+³	+²	+²	N/A	+³	+³	+²	N/A	+

GI Number	Protein Name	Protein Identification																Prediction[a]
		Isolates																
		PH2		PH8		PH202		PH278		PH292		PH296		PH588		PH344		
		Gel-free	Gel-based	Gel-free	Gel-based	Gel-free	Gel-based	Gel-free	Gel-based	Gel-free	Gel-based	Gel-free	Gel-based	Gel-free	Gel-based	Gel-free	Gel-based	
gi|472257918	FhaC / ShlB	+[2]	-	+[3]	+[3]	-	+[1]	+[3]	-	+[3]	N/A	-	N/A	-	N/A	+[3]	N/A	+
gi|472256984	Putative Omp 2	+[2]	+[2]	+[3]	N/A	-	+[3]	+[1]	N/A	-	N/A	+[1]	N/A	-	N/A	+[1]	+[2]	+
gi|472257001	Omp P2	+[2]	+[3]	+[3]	N/A	-	-	-	N/A	-	-	+[3]	N/A	+[3]	+[3]	+[1]	N/A	+
gi|472258801	PlpB	+[2]	N/A	+[1]	N/A	+[1]	+[3]*	+[2]	N/A	+[2]	+[1]	+[2]	N/A	+[1]	N/A	-	N/A	+
gi|472258309	Putative Omp 4	+[2]	-	+[1]	-	-	-	+[2]	-	+[1]	-	+[2]	-	+[1]	-	-	-	-
gi|472257384	HmbR1	+[1]	-	-	N/A	+[3]	+[2]	-	N/A	+[1]	N/A	+[2]	N/A	+[3]	N/A	-	N/A	+
gi|472257911	CirA domain-containing protein	+[1]	+[1]	-	N/A	-	-	-	N/A	+[3]	N/A	+[3]	N/A	-	N/A	-	N/A	+
gi|472259235	HxuC	-	-	+[3]	+[3]	+[3]	+[1]	+[3]	+[3]	+[3]	+[3]	+[3]	+[1]	+[3]	N/A	-	N/A	+
gi|472257917	FhaB	-	-	+[3]	-	-	-	+[1]	-	+[3]	-	-	-	-	-	+[3]	-	+
gi|472257325	Mam7 / PqiB	-	-	+[2]	-	+[3]	-	+[2]	-	-	-	+[1]	-	+[2]	-	+[1]	-	-
gi|472259234	CcmD/ HxuB	-	-	+[2]	N/A	+[2]	+[3]	-	N/A	+[3]	N/A	+[3]	N/A	+[3]	N/A	-	N/A	+
gi|472256863	RlpA	-	-	+[2]	-	+[1]	-	-	-	-	-	-	-	+[2]	-	-	-	-
gi|472258914	IgA1_3	-	N/A	+[1]	N/A	+[3]	+[2]*	+[3]	N/A	-	N/A	+[3]	N/A	+[1]	N/A	-	N/A	+
gi|472257617	OmpW	-	+[3]	+[1]	+[3]	-	+[1]	-	N/A	-	-	+[1]	+[3]	-	N/A	+[1]	+[3]	+
gi|472257086	Hsf	-	-	+[1]	-	-	-	-	-	-	-	+[1]	-	-	-	-	-	+
gi|472258161	Yad-A like	-	N/A	-	N/A	+[3]	+[3]	+[3]	+[2]	+[3]	+[2]	-	N/A	-	N/A	-	N/A	+
gi|472258914	IgA1_3 Like	-	N/A	-	N/A	+[2]	+[2]*	+[2]	N/A	-	N/A	+[3]	N/A	-	N/A	-	N/A	+
gi|472257959	NlpC / P60	-	N/A	-	N/A	+[2]	+[2]	-	N/A	-	N/A	-	N/A	+[1]	N/A	-	N/A	+
gi|472257424	LamB	-	N/A	-	N/A	+[1]	+[2]	+[1]	+[3]	-	N/A	-	N/A	+[1]	N/A	-	N/A	+
gi|472258343	LolB	-	-	-	-	+[1]	-	-	-	-	-	-	-	+[2]	-	+[1]	-	+
gi|472258286	FhuE	-	-	-	-	+[1]	-	-	-	-	-	-	-	-	-	-	-	+
gi|472259196	Putative Omp 3	-	-	-	-	+[1]	-	-	-	-	-	-	-	-	-	-	-	+

GI Number	Protein Name	Protein Identification																Prediction[a]
		Isolates																
		PH2		PH8		PH202		PH278		PH292		PH296		PH588		PH344		
		Gel-free	Gel-based	Gel-free	Gel-based	Gel-free	Gel-based	Gel-free	Gel-based	Gel-free	Gel-based	Gel-free	Gel-based	Gel-free	Gel-based	Gel-free	Gel-based	
gi|757542574	TadG	-	-	-	-	+[1]	-	-	-	-	-	-	-	-	-	-	-	-
gi|472258252	BamE	-	-	-	-	-	-	+[1]	-	+[1]	-	-	-	-	-	-	-	+
gi|472258899	FhuA	-	-	-	-	-	-	-	-	+[2]	+[1]	-	-	-	N/A	-	-	+
gi|472259029	Hypothetical protein	-	-	-	-	-	-	-	-	+[1]	-	-	-	-	-	+[1]	-	+
gi|472258883	BtuB	-	-	-	-	-	-	-	N/A	-	N/A	+[3]	N/A	-	N/A	+[3]	+[3]	+
gi|472256991	WzzB	-	-	-	-	-	-	-	-	-	-	+[2]	-	-	-	-	-	+
gi|472257912	Hypothetical Protein 4	-	-	-	-	-	-	-	-	-	-	+[1]	-	-	-	-	-	-
gi|472257084	Putative Autotransporter	-	-	-	-	-	-	-	-	-	-	+[1]	-	-	-	-	-	+
gi|472258517	PilA	-	N/A	-	N/A	-	+[1]	-	N/A	-	N/A	-	N/A	+[1]	N/A	-	N/A	-
gi|472259021	HmbR2	-	-	-	-	-	-	-	-	-	-	-	-	-	-	+[3]	-	+
gi|261311542	IgA1_4	-	-	-	-	-	-	-	-	-	-	-	-	-	-	+[1]	-	+
gi|472257942	MltB	-	N/A	-	N/A	-	+[3]	-	N/A	-	N/A	-	N/A	-	N/A	+[1]	N/A	+
gi|472259076	TonB-dependednt protein	-	-	-	-	-	-	-	-	-	-	-	-	-	-	+[1]	-	+
gi|472259098	Omp 18/16	-	N/A	-	N/A	-	+[3]	-	N/A	-	N/A	-	N/A	-	N/A	-	N/A	+
gi|493291997	Hypothetical protein 2	-	N/A	-	N/A	-	+[3]	-	N/A	-	N/A	-	N/A	-	N/A	-	N/A	-
gi|493292248	HlpB	-	+[3]	-	N/A	-	-	-	N/A	-	+[2]	-	N/A	-	N/A	-	+[1]	+
gi|493290991	fHbp_1	-	N/A	-	N/A	-	+[3]	-	N/A	-	N/A	-	N/A	-	N/A	-	N/A	+
gi|493290616	IgA1_2	-	+[1]	-	N/A	-	-	-	N/A	-	N/A	-	N/A	-	N/A	-	-	+
gi|493292739	IgA1_1[b]	-	-	-	-	-	-	-	-	-	-	-	-	-	-	-	-	+
gi|472257996	Bor / Iss_1[b]	-	-	-	-	-	-	-	-	-	-	-	-	-	-	-	-	+
gi|589590239	Pertactin	-	-	-	-	-	-	-	-	-	-	-	-	-	-	-	+[2]	-

[a]Predicted OMP (+) or not predicted to be an OMP (-) via the prediction system used by Hounsome, (2012).

[b]OMPs identified only via the whole-lane-sectioning of PH202 and not via gel-slice or gel-free in any of the other seven isolates.

[*]Replicate is the maximum from either the three excised bands of the method comparison or the three excised bands in the subsequent analysis.

Interestingly, the filamentous haemagglutinin transporter, FhaC, was identified in two out of three replicates of PH2 using the gel-free analysis while FhaB was not identified in that strain. Identification of FhaC, by the gel-free methodology, amongst the other isolates corresponded to the same isolates where FhaB was identified. FhaC was also identified, by the gel-based method, in PH8 and PH202.

Of the proteins involved in iron transport, HxuC was identified in three replicates of all isolates except PH2 and PH344 using the gel-free methodology but was only sporadically confirmed by the gel-based method. HxuC was not identified in PH2, PH202 and PH344 using the gel-based methodology. Additionally, HxuB was confirmed by gel-based means in isolate PH202. The haemoglobin uptake protein HmbR1 was identified to varying degrees of reproducibility in all isolates except PH8, PH278 and PH344 using the gel-free methodology. Gel-based analysis confirmed HmbR1 in PH202 and failed to identify it in PH2 where a band of equivalent molecular mass was excised for analysis. Of the transferrin binding uptake proteins, TbpA and TbpB, TbpA was identified to varying degrees of reproducibility in all isolates using the gel-free methodology. In contrast, TbpB was not identified in PH278 and PH344, yet was identified in at least two of three replicates of the other isolates using the gel-free methodology. Using the gel-based methodology confirmed the presence of TbpA in three replicates of PH2 and PH202. For TbpB, an equivalent band position at the molecular weight of TbpB was subjected to LC-MS/MS in all isolates except PH588. However, this failed to identify TbpB in any isolate except PH202. The final iron uptake protein that displayed isolate-to-isolate variation was the FhuA siderophore receptor. This protein was identified in two of three replicates of the gel-free analysis solely in isolate PH292. Gel-based evaluation confirmed the presence of FhuA in isolate PH292, although only in one replicate. This was despite comparative band analysis for all other isolates except PH588. Although FhuA was only identified in PH292 in one and two replicates of the gel-based and gel-free methodologies respectively, the combination of both techniques served to confirm its presence in the OM of that strain. The lack of FhuA identification in any other isolates by either methodology suggests this protein is either specific to isolate PH292, controlled

by a different regulatory mechanism or expressed in lower abundance in other isolates so as to fall below the limit of detection when analysed.

3.3.5 BLAST analysis of the identified outer membrane proteins

MS/MS matched OMPs that exhibit isolate-to-isolate variation can be accounted for by several explanations. Firstly, the expression of OMPs may be different between different isolates grown in BHIB. Thus, the abundance of an OMP might be too low for detection. Alternatively, OMPs might not be detected because a particular strain lacks a gene encoding that OMP. In addition, an isolate can contain a gene encoding a protein with significant homology differences to the proteins sequences in the search database. Thus, even if the full sequence of a peptide is determined via tandem MS, false-negatives may arise if that peptide cannot be matched to a protein in the database owing to substantial differences in homology. To address these considerations for each of the 83 identified OMPs, a BLAST search was performed against the sequenced genomes of the eight isolates. This was accomplished using the nucleotide sequences that encode each of the identified OMPs. For consistency, nucleotide sequences, where possible, were derived from a single publicly available genome (*Mannheimia haemolytica* USDA-ARS-USMARC-183:CP004752.1). If this genome did not contain a locus encoding the OMP another genome was instead used. The complete result of this BLAST search is summarised in Table 3.9.

The results of this search confirm that 13 OMPs are not encoded by one or more of the sequenced genomes. These include HxuB, HxuC, FhaB, hypothetical protein 4, IgA1_4, NanH, Omp P2, Putative Omp 4, TadG-like, Ydcf domain containing protein, fHbp_1, IgA1_2 and Pertactin. Ten of these genes were only absent from one isolate. Seven genes (HxuB / CcmD, HxuC, FhaB, NanH, putative Omp 4, ydcf domain-containing protein and IgA1_2) were missing specifically from the *M. glucosida* isolate PH344.

PlpD and the YadA-like protein had exhibited the most prominent isolate-to-isolate identification pattern in the proteomic experiments. PlpD, which was identified in all isolates except the A2 serotype isolates, was confirmed to be encoded in the genomes of all eight strains.

Table 3.9 Nucleotide BLAST search of proteins identified in proteomic analysis against the individual genomes of eight isolates

Shown in the table are the protein accession numbers and gene loci for '*Mannheimia haemolytica* USDA-ARS-USMARC-183' (NC_020833.1) and the corresponding protein names encoded for at those gene loci. Where a coding sequence from '*Mannheimia haemolytica* USDA-ARS-USMARC-183' could not be obtained an alternative genome was used[b, c, d]

			Results of BLAST Search[a]							
			Isolates							
Nucleotide Gi number	Nucleotide Gene locus	Name	PH2	PH8	PH202	PH278	PH292	PH296	PH588	PH344
gi|472258490	D650_17510	BamA/ YaeT	*	*	*	*	*	*	*	*
gi|472258736	D650_19970	BamD / ComL	*	*	*	*	*	*	*	*
gi|472258252	D650_15130	BamE	*	*	*	*	*	*	*	*
gi|472257997	D650_12580	Bor / Iss_2	*	*	*	*	*	*	*	*
gi|472258883	D650_21440	BtuB	*	*	Δ	Δ	*	*	*	*
gi|472257911	D650_11720	CirA (Major domain)	*	*	*	*	*	*	*	*
gi|472256810	D650_660	CpxC	*	*	*	*	*	*	*	†
gi|472256811	D650_670	CpxD / Wza	*	*	Δ	Δ	*	*	*	*
gi|472257917	D650_11780	FhaB	*	*	*	*	*	Δ†	Δ†	‡
gi|472257918	D650_11790	FhaC / ShlB	*	*	*	*	*	*	*	*
gi|472258899	D650_21600	FhuA	*	*	*	*	*	*	*	*
gi|472259454	D650_27160	FrpB / FetA	*	*	*	*	*	*	†	†
gi|472259236	D650_24980	HbpA	*	*	*	*	*	*	*	†
gi|472257276	D650_5360	Hly (haemolysin/ putative)	*	*	*	*	*	*	*	†
gi|472257384	D650_6440	HmbR1	*	*	*	*	*	*	*	†
gi|472259021	D650_22820	HmbR2	*	*	*	*	*	*	*	*
gi|472257086	D650_3460 / D650_3440	Hsf	*	Δ	Δ†	Δ†	Δ†	*	*	Δ
gi|472259234	D650_24960	HxuB / CcmD	*	*	*	*	*	*	*	‡
gi|472259235	D650_24970	HxuC	*	*	*	*	†	*	*	‡
gi|472257682	D650_9430	NlpE	*	*	*	*	*	*	*	*
gi|472257232	D650_4920	Hypothetical protein 1	*	*	*	*	*	*	*	*
gi|472258973	D650_22340	Hypothetical protein 2	*	*	*	*	*	*	*	*
gi|472259029	D650_22900	Hypothetical protein 3	*	*	*	*	*	*	*	*
gi|472257912	D650_11730	Hypothetical protein 4	*	*	‡	‡	‡	*	‡	†

Nucleotide Gi number	Nucleotide Gene locus	Name	Results of BLAST Search[a] Isolates							
			PH2	PH8	PH202	PH278	PH292	PH296	PH588	PH344
gi|261311542	COK_1281[b]	IgA1_4	‡	*	*	*	*	*	*	*
gi|472258914	D650_21750	IgA1_3	*	*	*	*	*	*	*	*
>gi|528823659	L278_00725[c]	IgA1_3-like	*	*	*	*	*	*	*	*
gi|472257424	D650_6840	LamB	*	*	*	*	*	*	*	†
gi|472258478	D650_17390	LemA	*	*	*	*	*	*	*	*
gi|472258343	D650_16040	LolB	*	*	*	*	*	*	*	*
gi|472257273	D650_5330	LpoA	*	*	*	*	*	*	*	*
gi|472257142	D650_4020	LppB / NlpD	*	*	*	*	*	*	*	*
gi|472257731	D650_9920	LptD	*	*	*	*	*	*	*	*
gi|472258510	D650_17710	LptE / RlpB	*	*	*	*	*	*	*	*
gi|472257325	D650_5850	Mam7 / PqiB	*	*	*	*	*	*	*	*
gi|472258419	D650_16800	MltA	*	*	*	*	*	*	*	*
gi|261307549	COI_2519[d]	MltB-like	*	*	*	*	*	*	*	*
gi|472259387	D650_26490	MltC	*	*	*	*	*	*	*	*
gi|472258277	D650_15380	NanH	*	*	*	*	*	*	*	‡
gi|472257163	D650_4230	OapA	*	*	*	*	*	*	*	*
gi|472258286	D650_15470	FhuE	*	*	*	*	*	*	*	*
gi|472257001	D650_2600	Omp P2	*	*	‡	*	*	*	*	*
gi|472258334	D650_15950	Omp P2-like	*	*	†	†	†	*	†	†
gi|472257701	D650_9620	Omp P6 / Pal	*	*	*	*	*	*	*	*
gi|472256940	D650_1980	OmpA	*	*	*	*	*	*	*	*
gi|472258491	D650_17520	OmpH	*	*	*	*	*	*	*	*
gi|472258540	D650_18010	Omp P1	*	*	*	*	*	*	*	Δ†
gi|472258662	D650_19230	OmpP4	*	*	*	*	*	*	*	*
gi|472257617	D650_8780	OmpW	*	*	†	†	†	*	†	*
gi|472257023	D650_2820	Pcp	*	*	*	*	*	*	*	*
gi|472258517	D650_17780	PilA	*	*	*	*	*	*	*	*
gi|589590239	AK33_04115[e]	Pertactin	‡	‡	‡	‡	‡	‡	‡	Δ†

Gi number	Nucleotide Gene locus	Protein Name	Results of BLAST Search[a]							
			Isolates							
			PH2	PH8	PH202	PH278	PH292	PH296	PH588	PH344
gi|472258802	D650_20630	PlpA	*	*	*	*	*	*	*	*
gi|472258801	D650_20620	PlpB	*	*	*	*	*	*	*	*
gi|472258667	D650_19280	PotD / Lpp38	*	*	*	*	*	*	*	*
gi|472258800	D650_20610	PlpC	*	*	*	*	*	*	*	*
gi|472258068	D650_13290	PlpD	*	*	*	*	*	*	*	*
gi|472257531	D650_7920	PlpE	*	*	*	*	†	*	*	*
gi|472257084	D650_3440	Putative Autotransporter Adhesin	*	Δ	Δ†	Δ†	Δ†	*	*	Δ†
gi|472257959	D650_12200	NlpC / P60	*	*	*	*	*	*	*	*
gi|472258801	D650_20620	PlpB	*	*	*	*	*	*	*	*
gi|472257144	D650_4040	Putative Lipoprotein 1	*	*	*	*	*	*	*	*
gi|472256848	D650_1050	Putative Omp 1	*	*	*	*	*	*	*	*
gi|472256984	D650_2420	Putative Omp 2	*	*	*	*	*	*	*	*
gi|472259196	D650_24580	Putative Omp 3	*	*	*	*	*	*	*	*
gi|472258309	D650_15700	Putative Omp 4	*	*	*	*	*	*	*	‡
gi|472256863	D650_1200	Rlp-like	*	*	*	*	*	*	*	*
gi|472258673	D650_19340	Ssa1	*	*	†	*	*	*	*	*
gi|757542574	AK33_09180[e]	TadG-like	‡	‡	‡	‡	‡	‡	‡	‡
gi|472258140	D650_14010	TamA / YtfM	*	*	*	*	*	*	*	*
gi|472257461	D650_7210	TbpA	*	*	†	*	*	*	*	*
gi|472257460	D650_7200	TbpB	*	*	†	*	*	*	*	†
gi|472258822	D650_20830	TolC	*	*	*	*	*	*	*	*
gi|472259186	D650_24480	VacJ-like	*	*	*	*	*	*	*	*
gi|472256991	D650_2490	WzzB	*	*	*	*	*	*	*	*
gi|472258161	D650_14220	Yad-A like	*	Δ	*	*	*	*	*	*
gi|472257680	COK_2129[b]	YajG	*	*	*	*	*	*	*	*
gi|472257571	D650_8320	Ydcf domain containing protein	*	*	*	*	*	*	*	‡
gi|472259098	D650_23600	Omp 18/16	*	*	*	*	*	*	*	*
gi|472257405	D650_6650	HlpB	*	*	*	*	*	*	*	*

Gi number	Nucleotide Gene locus	Protein Name	Results of BLAST Search[a]							
			Isolates							
			PH2	PH8	PH202	PH278	PH292	PH296	PH588	PH344
gi|472259197	D650_24590	fHbp_1	*	*	*	Δ†	*	‡	Δ†	Δ
gi|472258614	D650_18750	IgA1_2	*	*	*	*	*	*	*	‡
gi|472259150	D650_24120	IgA1_1	*	*	Δ	Δ	Δ	*	*	*
gi|472257996	D650_12570	Bor / Iss_1	*	*	*	*	*	*	*	*
gi|472259076	D650_23380	TonB-dependednt protein	*	*	*	*	*	*	*	*

[a]Key: * Homologous match, † matched with low homology, ‡ no match, Δ truncated match (query coverage)
[b]Alternative genome used: ACZY01
[c]Alternative genome used: AUNK01
[d]Alternative genome used: ACZX01
[e]Alternative genome used: JANJ01

Similarly, the YadA-like protein, which was exclusively identified in the A2 serotype, was confirmed to be encoded in the genomes of all eight strains.

One protein, TadG-like did not return a coding locus for any of the eight genomes when BLAST searched using the coding nucleotide sequence (AK33_09180). This protein was identified in only one isolate, PH202, in the proteomic analyses, and this in only one of three replicates (which was based on two peptides, only one of which was significant). Analysis of the seventeen *M. haemolytica* genomes that comprise the proteomic database reveals that a locus encoding a TadG-like protein is only present in one of the seventeen genomes (JANJ01). Therefore, a likely conclusion is that the TadG-like match identified in PH202 constitutes a false positive and while the identity of the single significant peptide cannot be denied ($P>0.05$), it may have be derived from another protein.

Similarly, for PH344, FhaB was identified in three of three replicates of the gel-free proteomic analyses. However, a homologue to the FhaB nucleotide sequence was not found when BLAST searched against the PH344 genome. All three proteomic matches comprised multiple peptides, many of which were unique to this protein match. Additionally, MOWSE scores were well above the significance cut off ($p>0.05$). The FhaB protein that PH344 matched in the gel-free proteomic experiment (gi|544865382) has a unique amino acid sequence amongst the seventeen FhaB amino acid sequences in the database used for the MASCOT search. The genome encoding the PH344-matched an FhaB sequence (D35; AUNK01) derived from an A2 bovine isolate. The amino acid identity between gi|544865382 (encoded by the D35 genome) and gi|589589614 (the amino acid sequence used in the BLAST searches) share only 63% amino acid identity. Furthermore, a BLAST search of the *fhab* nucleotide sequence from D35 (L278_00010) against the eight *M. haemolytica* genomes yields a match solely to PH344. Therefore, PH344 encodes an FhaB similar to the A2 strain D35, but differing significantly from the other seven isolates analysed and the nucleotide sequence used to test for the presence or absence of FhaB in the eight strains.

Hypothetical protein 4 was found to produce different results on the basis of nucleotide sequence chosen to conduct the BLAST search. Displayed in Table

3.9 is the result of the corresponding BLAST search using the nucleotide sequence derived from the protein matched in the proteomic analysis. Using the nucleotide sequence that encodes the equivalent protein in the A1 genome (D650_11730) identifies a coding locus in the eight analysed genomes. The only match in the proteomic analysis to this hypothetical protein occurred in one replicate of PH292 (Table 3.8). In this instance the protein was matched with a moderately high MOWSE score (46) and via two peptides, only one of which was significant. The genome of PH292 contains a nucleotide sequence with significant sequence differences to the nucleotide sequence encoding the protein matched in the proteomic experiments. However the nucleotide sequence of PH292 is similar to the equivalent nucleotide sequence from an A1 genome. Therefore the protein match in this case must be interpreted with care. It may represent a false positive. Alternatively, it may represent a match to a conserved amino acid motif that simply has significant differences in the gene sequences between the gene encoding the protein and the gene in the PH292 genome.

Noteworthy is the absence of a coding locus for OmpP2, a porin protein, in isolate PH202. While Omp P2 was not identified amongst the A2 serotype strains in the proteomic analysis, only PH202, isolated from a healthy cow, appears to not have the gene encoding Omp P2. The other two A2 strains, both derived from pneumonic sheep lungs, have loci encoding OmpP2. This only differs in one and four nucleotide positions for PH8 and PH278, respectively, as compared to the A1 nucleotide sequence used in the BLAST search.

3.4 Discussion

Introduction. Presented here is a comprehensive study of the *Mannheimia haemolytica* OM proteome. A multifaceted proteomic approach has revealed significant differences in the OM proteome of different isolates of *M. haemolytica*. To date, this represents the most thorough investigation of the cell envelope of this important veterinary pathogen and serves to enhance our understanding of the organisms' adaptation to the ruminant respiratory tract. The *M. haemolytica* OM proteome has been determined hypothetically using a bioinformatic prediction pipeline (E-komon *et al.*, 2012; Hounsome, 2012). The screening of three different genomes, a bovine serotype A1, an ovine serotype

A2 and a bovine serotype A2 predicted 93 OMPs in total, representing 3.3%, 3.4% and 3.6% of the organisms total ORFs, respectively. Although consensus prediction identifies the hypothetical composition of the OM, it is however only a prediction. Thus, the objective of this study was to determine experimentally the *M. haemolytica* OM proteome from isolates recovered from cattle and sheep.

Technical evaluation. Gel-based and gel-free tryptic digest methodologies were employed in order to maximise coverage of the OM proteome. In total, 83 unique OMPs were identified from seven different *M. haemolytica* isolates and one *M. glucosida* isolate; of these 67 had been bioinformatically predicted to be present in the *M. haemolytica* OM by Hounsome (2012). The remaining 16 OMPs (HbpA, Hly, LemA, Mam7 / PqiB, OapA, PilA, IgA1_3 like, putative Omp 4, RlpA, TadG-like, Putative autotransporter, Pertactin and hypothetical proteins 1, 2, 3 and 4) had not been identified via the bioinformatic prediction system. Of these 16 OMPs, four (HbpA, LemA, OapA and RlpA) were noted by Hounsome (2012) as well characterised OMPs that the bioinformatic prediction system failed to identify. One OMP (Mam7 / PqiB) was classified by Hounsome (2012) as being of undeterminate subcellular localisation; more recently the orthologous protein in *V. parahaemolyticus* has been determined to be an adhesin present in the OM (Krachler & Orth, 2011; Krachler *et al.*, 2011). The other 11 OMPs (Hly, PilA, IgA1_3 like, putative Omp 4, TadG-like, putative autotransporter, Pertactin and hypothetical proteins 1, 2, 3 and 4) that were not identified in the bioinformatic prediction by Hounsome (2012) either have transient roles in the OM or are suspected to be present in the OM on the basis of domain analysis and literature searching.

Other studies that have utilised an *in silico* prediction-based system for OM proteome analysis also report identifying only a fraction of the predicted OMPs (Aistleitner *et al.*, 2015; Chung *et al.*, 2007). Aistleitner *et al.* (2015) used the same bioinformatic prediction system as Hounsome (2012) and determined their to be 64, 84 and 50 proteins (β-barrel and lipoprotein) in the OMs of *Parachlamydia acanthamoebae*, *Simkania negevensis* and *Waddlia chondrophila*, respectively. Sarkosyl preparation of membrane fractions and either gel-based mass spectrometry analysis or direct anylsys (gel-free) of *P.acanthamoebae*, *S. negevensis* and *W. chondrophila* resulted in the identification of 61, 77 and 66 %

of the in sillico predicted list, respectively. Thus, comparable to the results of the present study where 72 % of the *in silico* prediction was identified. The 24 putative OMPs that were bioinfomatically predicted but not identified in the proteomic experiments may be expressed under different growth conditions or expressed to levels below the threshold of identification. Additionally, experimental reasons might account for a lack of identification including loss during fractionation, poor solubilisation, poor digestion, poor ionisation, small protein size or if the protein is heavily modified. Many studies have utilised Sarkosyl preparations for the enrichment of OMPs where it has been found to be superior compared to other methods of OMP targeting (Aistleitner *et al.*, 2015; Gesslbauer *et al.*, 2012). Few studies have examined the overlap that complementary proteomic techniques offer on protein coverage; of those that have, coverage in each case has been maximised through the use of complementary techniques (Aistleitner *et al.*, 2015; Connolly *et al.*, 2006; Gesslbauer *et al.*, 2012; Tanca *et al.*, 2013). In each of these studies bias attributed to any of the methodologies tested could be compensated for by the use of a complementary technique.

Of the analysis preformed in this study, eight (fHbp_1, IgA1_1, IgA1_2, Bor/Iss_1, Omp 18/16, HlpB, Pertactin and hypothetical protein 2) and 18 (BamE, RlpA, lolB, HmbR1, IgA1_3-like, IgA1_4 FhaB, Hsf, PlpD, TadG-like, Wzzb, putative Omp3, putative Omp4, putative autotransporter, TonB-dependent protein and hypothetical proteins 1, 3 and 4) OMPs were identified solely by the gel-based and gel-free methodologies respectively. It is easily rationalised that high-molecular-mass OMPs identified solely by the gel-free method might not be identified by the gel-based method owing to the inability of the gels to resolve these proteins. That is, these OMPs are outwith the molecular mass size range of 12% SDS-PAGE gels. However, OMPs that fail to be identified in the gel-based method yet fall within this molecular mass range, or any OMP that fails to be identified via the gel-free method require further consideration. The dynamic range encountered with membrane proteins has been speculated to cross between five and seven orders of magnitude (Jungblut *et al.*, 2010; Van *et al.*, 2008). Therefore, one explanation might be that the extra separation step in the gel-based approach may result in sample loss which, for OMPs of low copy number, could take them below the threshold of detection. Conversely, the

reason why some OMPs were found only with the gel-based method may be due to issues of sample complexity. As the gel-free methodology relies entirely on chromatographic separation prior to mass spectrometry it is plausible that certain peptides, crucial to identification for reasons of specificity, are missed as a result of co-elution with other peptides. If multiple peptides of different abundancies elute from the chromatography column at the same time, peptides in relatively low abundance might not be selected for fragmentation and MS. Therefore, co-elution of peptides with different abundancies may account for the discrepancy.

Core proteome (functional category - biogenesis and integrity). Of the 83 OMPs identified, 12 (BamA/YaeT, BamD/ComL, Bor/Iss_2, Wza/CpxD, FrpB/FetA, LppB/NlpD, LptD, OmpP6/Pal, OmpA, OmpP4, Ssa1 and YajG) were deemed core on the basis of being identified in three replicates of every isolate analysed. A further ten (HbpA, MltC, PlpA, PlpC, OmpH, OapA, TolC, putative lipoprotein 1, putative Omp 1 and hypothetical protein 1) OMPs could be included when allowing for two of three replicates to be matched across the eight isolates and a further seven (Omp P1, PlpE, Hly, TbpA, TamA / Ytfm, PotD / Lpp38 and NlpE) could be included by excluding *M. glucosida*. These mainly represent processes critical to the structure and functioning of the OM. For example, BamA and BamD are involved in the structural assembly of β-barrel proteins within the OM (Knowles *et al.*, 2009), OmpP6 tethers the OM to the peptidoglycan cell wall (Kovacs-Simon *et al.*, 2011) and MltC hydrolyses peptidoglycan to allow for growth of the bacterial cell (Vollmer *et al.*, 2008). However, some of these OMPs are also involved in non-essential processes. For example Wza is responsible for capsular polysaccharide secretion (Dong *et al.*, 2006) and is arguably non-essential on the basis that untypeable strains of *M. haemolytica* persist in the environment (Al-Ghamdi *et al.*, 2000; Angen *et al.*, 1999b; Davies *et al.*, 1996). Nevertheless, these 'core' OMPs largely represent crucial functions at the cell surface.

Serotype-specific OMP identification. Those OMPs that were not identified in all eight isolates potentially represent proteins with more specialised functions. On the basis that they are non-essential, the possibility exists that some of these OMPs are involved in host-adaptation and/or virulence. Examination of these

OMPs reveals several interesting patterns of isolate-to-isolate variation that may be indicative of host adaptation and/or virulence.

Two OMPs were identified in the eight isolates with patterns correlating to serotype. One protein, the YadA-like trimeric autotransporter, was identified only in serotype A2 isolates irrespective of host species. Conversely, the lipoprotein PlpD was present in all isolates except those of serotype A2. However, analysis of the genomes from all eight strains used in this study revealed that all isolates possess a copy of the *yadA*-like and *plpD* genes. Thus, as this cannot be attributed to differences in the gene repertoire of the isolates, the possibility exists that the A2 isolates possess unique regulatory mechanisms responsible for the control the expression of these two proteins that differ from those of other serotypes.

One explanation to why the A2 serotype strains behave similarly in the expression of these proteins (YadA-like and PlpD), irrespective of host species, requires consideration of prior genetic studies. The phylogeny of *M. haemolytica* as assessed by MLEE and 16s ribosomal sequencing has shown the A2 isolates to be phlogenetically distinct (Davies *et al.*, 1996, 1997). Adaptation of *M. haemolytica* to the upper respiratory tract of ruminants, where it exists as a commensal, is well documented. Microbial adaptation to a specific environment involves the specialisation of protein machinery to promote growth and survival within that niche. Thus, differences in OM proteomes amongst isolates of different serotype and host species indicate areas of interspecies tropism. Evidence of host adaptation in *M. haemolytica* is prevalent where comparative nucleotide analysis of the *tbpAB* operon, *lktA* gene and *ompA* gene has provided evidence for host switching amongst isolates of *M. haemolytica* recovered from cattle and sheep (Davies & Lee, 2004; Davies *et al.*, 2001; Lee & Davies, 2011). These studies suggest that serotypes A1 and A6 were transmitted to cattle from sheep, while serotype A2 was transmitted to sheep from cattle. Exchange of genetic material between new and resident isolates allowed for adaptation to their new environment, ultimately giving rise to the pathogenic A1 and A6 serotypes in cattle and the pathogenic A2 serotype in sheep. Thus, as these A2 serotype strains represent isolates recovered from cattle and sheep, and as the A2 serotype strains occupy the same phylogenetic clade then expression of these

OMPs (YadA-like and PlpD) may reflect their ancestral past prior to domestication.

Functional category: Adherence. While the function of PlpD is at present unknown, the homologue PlpA is involved in adherence to BBECs (Kisiela & Czuprynski, 2009). PlpD shares a significant degree of homology with OmpA and can elicit an immune response from challenge *in vivo* (Nardini *et al.*, 1998). Thus, the evidence would suggest that PlpD may be involved in adherence. Contary to PlpD, the YadA trimeric autotransporter has been extensively characterised in several bacterial species. This protein was originally discovered in *Yersinia spp.* and is widely considered the archetypal trimeric autotransporter adhesin. Structurally, it is homotrimer comprised of a translocator ß-barrel, an α-helical coiled-coil stalk segment projecting away from the OM and a functional head domain that interacts with the host (Koretke *et al.*, 2006). Functionally, YadA fulfils multiple roles in host manipulation, the foremost of which is to facilitate adherence to host cells and tissue; YadA has been shown to bind to a multitude of extracellular matrix proteins, epithelial cells and in certain species even to mediate cellular invasion (Heesemann & Griiter, 1987; Heise & Dersch, 2006; Nummelin *et al.*, 2004). YadA has also been shown to inhibit elements of the complement cascade via recruitment of complement factor H and the C4bp protein, conferring serum resistance upon microbes (Kirjavainen *et al.*, 2008; Schindler *et al.*, 2012). Through our analysis, the YadA-like protein was only identified in serotype A2 strains under standard growth conditions. Relating the function of this protein to the hypothesis of host-specificity raises the question of whether the YadA-like protein is constitutively expressed in A2 isolates, which may confer an advantage to the colonisation of the upper respiratory tract. However, why this would only be the case for serotype A2 strains is unclear. The question remains as to what conditions would elicit expression of the protein in isolates of the other serotypes.

Several other adhesins identified in the proteomic analyses exhibited isolate-to-isolate variation. While their identification transcends serotype and species boundaries, they nonetheless pinpoint potential routes of diversification in the OMP repertoire of *M. haemolytica*. Of the remaining adhesins characterised, two proteins, FhaB and the Ydcf domain-containing protein, exhibited variation

in their expression in the eight isolates analysed. FhaB was found in all gel-free replicates of isolates PH8, PH292 and PH344, as well as in a single replicate of PH278. Also identified in all replicates of the same isolates was FhaC. Together, FhaC and FhaB function as a two partner secretion system, where FhaC consists of a 16-strand β-barrel that functions to translocate FhaB through the OM and into the extracellular milieu (Clantin *et al.*, 2004; Hodak *et al.*, 2006). FhaB when assembled on the cell surface represents a potent, multifaceted virulence factor. It projects some 40 nM away from the OM and contains distally located domains responsible for carbohydrate binding and hemagglutinin activity (Guedin *et al.*, 1998; Kajava *et al.*, 2001). Additional domains confer binding to the leukocyte integrin receptor CR3 and the sulphated glycolipids of epithelial cells (Kajava *et al.*, 2001).

The dependence of this important virulence factor, FhaB, on its secretion partner, FhaC, mediates the expectation that either both or neither would be identified. While this is true of the various isolates mentioned previously (PH8, PH278, PH292 and PH344), curiously, FhaC was identified in two out of three replicates of PH2 yet no identification of FhaB was made. Several explanations may account for this. Firstly, serotype A1 strains may possess a regulatory mechanism that allows for expression of FhaC independently of FhaB. This would, however, contradict the well-studied regulation of FhaB and FhaC in *Bordetella spp.*, where both OMPs are under the control of the two component system BvgAS (Beier & Gross, 2006; Boucher *et al.*, 2001). In *Bordetella spp.* both FhaB and FhaC are regulated under the positive virulence phase termed Bvg^{+}. Although it is possible, the current evidence makes independent regulation of FhaC and FhaB unlikely. However, post-translational events might result in the degradation of FhaB or a lack of incorporation into the OM, thus explaining why FhaB was not identified in PH2. Secondly, while it is possible that FhaB in pathogenic cattle isolates became functionally obsolete after host-species switching, this would also be contradictory to findings in *Bordetella spp.* where functional interchangeability between the FhaB of *B. pertussis* and *B. bronchiseptica* has been reported (Julio *et al.*, 2009). Nevertheless, these model organisms still display differences in their ability to colonise host tissue where *B. bronchiseptica* requires FhaB for colonisation of the lower respiratory tract yet *B. pertussis* appears to show no impairment in colonisation with

removal of the protein (Cotter *et al.*, 1998; Khelef *et al.*, 1994; Pethe *et al.*, 2001). Thus, the possibility exists that serotype A1 pathogenic cattle isolates of *M. haemolytica* might possess an FHA that is not required for colonisation in the host.

In isolates PH202, PH296 and PH588 both FhaB and FhaC failed to be identified in the proteomic analysis. However, copies of the genes encoding FhaC and FhaB were identified in all isolates although there were some significant homology differences between the *fhab* gene used to conduct the BLAST search and the *fhab* gene identified in the PH296 and PH588 genomes. Nevertheless, all isolates analysed here possess the apparatus for FHA assembly and thus the question remains as to whether these other isolates produce FHA *in vivo*.

Functional category: Transport and receptor activities. Several proteins, with roles in transport and receptor activities were identified that exhibited isolate-to-isolate variation. The majority of proteins within this class are TonB-dependent receptors. This family of OM receptors consists of 22-stranded ß-barrels that rely on the TonB-ExbB-ExbD energy transducing system for active transport of nutrients against concentration gradients (Noinaj *et al.*, 2010). The proteomic characterisation revealed that several TonB-dependent receptors were identified with isolate-to-isolate variation. Most TonB-dependent receptors function in the role of iron acquisition. Iron is an essential nutrient that participates in the cofactors of many microbial enzymes. As a result bacteria have adapted means to acquiring it from a diverse array of host sources (Krewulak & Vogel, 2008). Of the TonB-dependent iron acquisition systems that *M. haemolytica* possesses, several were identified in an isolate-specific manner including systems involved in transferrin, haemoglobin, haemopexin and siderophore-mediated iron uptake.

The transferrin binding operon of *M. haemolytica*, *tbpAB*, encodes two proteins which function together to acquire iron from host transferrin. TbpA is a typical TonB-dependent receptor with the explicit function of transporting iron, derived from host transferrin, across the OM (Cornelissen *et al.*, 1998). The functionality of TbpB is not well characterised although structural studies have shed light into a potential role for the protein (Calmettes *et al.*, 2011, 2012; Moraes *et al.*, 2009). Structurally, TbpB is an unusual lipoprotein, anchored on

the extracellular face of the OM. It consists of two eight-stranded β-barrels and two β-sheet "handles". Neither of the β-barrels is transmembrane, rather hydrophobic residues face into the barrels interior (Moraes *et al.*, 2009) and the whole structure thus floats in the extracellular milieu from its membrane tether. The transferrin binding region of TbpB has been shown in *Actinobacilluas pleuropneumoniae* to be present on the 'cap' region of the N-terminal β-barrel and adjoining handle (Calmettes *et al.*, 2011). It is hypothesised that TbpB captures transferrin and delivers it to TbpA for iron uptake.

In the findings presented here, TbpA could be identified in every isolate even though the bacteria were grown under iron-replete conditions. In contrast, TbpB was not identified in isolates PH278 and PH344. Nucleotide sequence analysis of the strains presented here have previously demonstrated *tbpB* to be present in the genomes of both PH278 and PH344 (Lee & Davies, 2011). Evidence for intergenic recombination exists in the nucleotide sequence of PH278 *tbpB*. Nucleotide variation in the *tbpAB* operon revealed that the allele of the *tbpAB* operon in PH278 was more similar to that of non A2 isolates than it was of its own serotype suggesting the operon had been horizontally acquired. This evidence is in line with the understanding that TbpA and TbpB are adapted to bind their specific host transferrin (Litt *et al.*, 2000). The exact reason why TbpB was not identified in these two strains is unclear. For PH344, growth in iron-restricted media has been shown to induce the expression of TbpB (Hounsome, 2012). Thus, a simple conclusion is that the growth conditions presented here do not allow for the expression of TbpB in PH344 (Hounsome, 2012). However, for PH278, growth in iron-restricted media still failed to induce expression of TbpB, at least to the point where it could be detected by mass spectrometry. The possibility exists, in PH278 at least, that horizontal acquisition of *tbpBA* did not include the upstream promoter region. This region, in *Neisseria* has been shown to regulate gene expression of *tbpBA* in addition to the ferric uptake regulator (Vélez Acevedo *et al.*, 2014). Further characterisation would be needed to confirm if this is indeed the case.

Another important iron acquisition system in *M. haemolytica* is the uptake of iron from host haemoglobin. This is accomplished by two haemoglobin receptors, HmbR1 and HmbR2, homologues of which in *Neisseria* have been

demonstrated to be TonB-dependent (Stojiljkovic & Srinivasan, 1997). While HmbR2 was found to high levels of reproducibility amongst the isolates examined, HmbR1 was only found in PH344. Unlike the two transferrin-binding proteins discussed, the two haemoglobin receptors are likely to be independent of one another. This is the case for *Neisseria spp* which share a single homologous HmbR receptor capable of functioning alone (Evans *et al.*, 2010; Jordan & Saunders, 2009). Along with this, inspection of the gene loci in the sequenced *M. haemolytica* genomes confirms the two loci to be located in different parts of the chromosome, substantiating their lack of dependency on one another and thus explaining why we were able to identify only one. However, it remains to be seen which growth conditions, would lead to the expression of HmbR1 in PH8, PH278 and PH344 and HmbR2 in the isolates other than PH344. In *N. meningitidis,* phase variation accounts for the differential expression of HmbR via slipped strand mispairing (Lewis *et al.*, 1999; Lucidarme *et al.*, 2013). Whether a similar mechanism governs the haemoglobin receptors of *M. haemolytica* is purely speculation although it does offer a potential answer to the lack of consistent identification between HmbR1 and HmbR2.

Within the remit of TonB-dependent receptors, *M. haemolytica* possesses one further iron acquisition system that displayed interesting isolate–to-isolate variation in the proteomic analyses. The HxuCBA system functions to retrieve iron dually from host haem and haemopexin. HxuA and HxuB form a two-partner secretion system where HxuB can deliver HxuA to the extracellular space (Baelen *et al.*, 2013). Uptake of haemopexin occurs through binding with HxuA which can then deliver its cargo to the TonB-dependent receptor HxuC (Cope *et al.*, 1995, 1998; Morton *et al.*, 2007). In addition to this mechanism, HxuC has been shown to independently bind free haem and free haemoglobin (Cope *et al.*, 2001). In the proteomic results presented here, HxuC was identified in three replicates of all isolates except PH2 and PH344 where it was not identified at all. Similarly, HxuB was found in all isolates except PH2, PH278 and PH344. HxuA, although having a transient role in the OM, was not identified in any isolate; unsurprising considering its final destination is the extracellular space. Although PH2 possesses *hxuB* and *hxuC* genes, the lack of identification of either HxuB or HxuC in PH2, the A1 pathogenic strain, suggests that this system is either regulated differently to the other isolates, has become functionally

obsolete or was not in sufficient enough quantity for mass spectrometry detection. Further characterisation of this system would be required to elucidate the answer.

The BtuB receptor, which is responsible for vitamin B12 uptake, is one of the most extensively studied TonB-dependent receptors. In the present study, BtuB was only identified in isolates PH296 and PH344. Isolates PH296 and PH344 have the same LPS type (4A) (Davies & Donachie, 1996). Other evidence has demonstrated these isolates have undergone horizontal gene transfer of *ompA* and *lktA* and thus a degree of commonality (Davies & Lee, 2004; Davies *et al.*, 2001). The regulatory mechanism governing BtuB is a highly conserved riboswitch (Vitreschak *et al.*, 2003). Riboswitch mechanisms involve the binding of a ligand to the 5' end of transcribed mRNA which in turn induces a conformational change and alters either transcription or translation (Montange & Batey, 2008). Although the riboswitch mechanism is highly conserved, the identification of BtuB only in certain isolates under standard conditions suggests that the picture of regulation in *M. haemolytica* may be more complex than the current knowledge suggests.

Functional category: Enzymatic processes. Of the proteins that carry out enzymatic processes at the OM, the neuraminidase, NanH, displayed interesting patterns of identification in the eight isolates. NanH was identified in three replicates of all isolates in the gel-free analysis except for PH296 and PH344 where it was not identified at all. Additionally, the gel-based method served to reinforce the gel-free identification since NanH was identified in both PH2 and PH202. Neuraminidases are responsible for catalysing the removal of terminal sialic acid from carbohydrates, glycolipids, glycoproteins and gangliosides (Roggentin *et al.*, 1993). In this capacity neuraminidases have been shown to contribute to the virulence of various bacterial pathogens. For example, in *S. pneumoniae,* the NanA neuraminidase has been shown to facilitate entry into brain microvascular endothelial cells (Banerjee *et al.*, 2010; Uchiyama *et al.*, 2009). For *M. haemolytica*, an explicit role in virulence has not been determined. However, in *M. haemolytica* it has been shown to be capable of desialyating a range of carbohydrate substrates and has been shown to be expressed *in vivo* (Straus & Purdy, 1994; Straus *et al.*, 1993). Thus, the

identification of NanH by the gel-free method in all replicates of all isolates except PH292 and PH344 raises the question of why this might be the case. As mentioned previously, isolates PH344 and PH296 have the same LPS type (Davies & Donachie, 1996). However, analysis of the nucleotide BLAST search results (Table 3.9) highlights that a different explanation is needed for each of these isolates. For NanH, the BLAST search returned a nucleotide match for PH296 but not for PH344. It would appear that while PH296 possess the NanH gene PH344 does not. Thus, in PH296, the lack of proteomic identification can be attributed to no or low expression under these conditions, while for PH344, a lack of identification is the result of not possessing the *nanH* gene. How this might translate to the *in vivo* situation is not clear. A role for NanH in the *M. haemolytica* infection process has yet to be determined. However, differences in the origin of these isolates might offer an explanation. While PH296 was isolated from a pneumonic sheep lung, PH344 was isolated from an animal with septicaemia. Therefore, NanH might be essential for colonisation of the lung by *M. haemolytica*. Further characterisation would be required to determine if this is indeed the case.

Functional category: Proteins of unknown function. OMPs of undetermined function represent a critical gap in the understanding of Gram negative bacteria. Furthermore, if these proteins have no orthologues then their functions might be specific to the virulence of the organism. In the proteomic analysis several proteins with unknown function were identified. These include proteins that have been studied to some extent. For example the lipoproteins PlpA, PlpB, PlpC, PlpD, PlpE and PlpF, which share a significant degree of homology to one another (Cooney & Lo, 1993; Murphy & Whitworth, 1993), have been demonstrated to be immunogenic (Ayalew *et al.*, 2004, 2011c; Nardini *et al.*, 1998), and in the case of PlpA, potentially function in adherence (Kisiela & Czuprynski, 2009). However, for other OMPs, functions have not been attributed at all. Several of these OMPs were identified amongst the eight isolates. Putative lipoprotein 1, putative Omp1 and hypothetical protein 1 were identified in at least two of three replicates for each of the isolates analysed. Thus these OMPs represent major constituents of the *M. haemolytica* outer membrane, yet nothing is known of their function. Other OMPs with unknown functions were only identified in certain isolates. Putative Omp2 was identified in PH2, PH8,

PH278, PH296 and PH344 in one or more replicates while putative Omp4 was identified in one or two replicates of all isolates except PH202 and PH344 where it was not identified at all. These OMPs, where nothing related to structure and function is known, may represent undiscovered virulence factors crucial to understanding the pathogenicity of *M. haemolytica*.

Conclusion. In summary, the OM proteomes of seven *M haemolytica* isolates representing a range of serotypes recovered from cattle and sheep and a single *M. glucosida* isolate have been characterised. Through the use of complementary proteomic methodologies, a comprehensive map of the OM composition has been produced. In doing so, 12 proteins (BamA, BamD, Bor / Iss_2, Wza/CpxD, FrpB/FetA, LppB/NlpD, LptD, OmpP6/Pal, OmpA, OmpP4, Ssa1 and YajG) were identified in three replicates of every isolate analysed and a further ten OMPs were identified in at least two out of three replicates of every isolate. These OMPs are generally responsible for essential processes at the OM. Aside from the critical functioning of the OM, several OMPs were identified with isolate-specific patterns including PlpD, YadA-like protein, FhaB, FhaC, TbpB, HmbR2, HxuB and HxuC. Isolate-to-isolate variation in these proteins suggests they play important roles in virulence. Furthermore, these non-essential OMPs may be involved in niche-adaptation and allow for colonisation of the ruminant respiratory tract. However, the question remains what expression patterns exist during colonisation within the host and a natural progression to this study will be the examination of these proteomes under growth conditions that mimic the host environment.

Chapter 4 Adherence and Colonisation of *Mannheimia haemolytica* using ALI Epithelial Cell Cultures

4.1 Introduction

Adherence and colonisation to mucosal surfaces are the first steps by which a microbial pathogen establishes infection. Microbes that cause respiratory disease have evolved virulence mechanisms that allow for survival in this niche. Colonising microbes must overcome the mucociliary escalator, adhere to the host epithelium and sequester nutrients while placating the milieu of host immune responses that threaten to abort this process (section 1.3).

Mannheimia haemolytica undergoes a distinct phenotypic shift from a commensal of the URT to disease-causing pathogen of the LRT (Ackermann & Brogden, 2000). The dependency of the phenotypic shift on the immuno-compromisation of the host and the state of the epithelium raises questions about how this pathogen colonises the ruminant lung.

Analysis of *M. haemolytica* genomes reveals the organism possesses many virulence factors implicated in the colonisation process (Gioia *et al.*, 2006; Lawrence *et al.*, 2010). The organism possesses a repertoire of adhesins that share homology with the adhesins of other respiratory pathogens. Amongst these are trimeric autotransporters including the YadA homologue of *Yersinia spp*, the Hia and Hsf homologues of *H. influenzae*, as well as AhsA and AhsB. The latter two proteins have been demonstrated to mediate collagen binding in *M. haemolytica* (Daigneault & Lo, 2009). Other OMPs identified with an adhesive role include the OmpA protein which has been shown in *M. haemolytica* to bind fibronectin and epithelial cells (Kisiela & Czuprynski, 2009; Lo & Sorensen, 2007), a homologue of the *Neisseria* Opa proteins, type IV pili and a filamentous haemagglutinin with homology to that of *B. pertussis* (Gioia *et al.*, 2006; Morck *et al.*, 1988). How each of these is deployed during the colonisation process remains to be determined. Secreted and cell-surface enzymes that modify the host environment represent other virulence factors involved in colonisation. Homologues of the IgA1-cleaving enzyme of *Neisseria spp*, sialic acid-cleaving NanH, a secreted protease with specificity for O-linked sialic acid glycoproteins

and the serotype specific antigen Ssa1 have been identified within the genomes of *M. haemolytica* (Gioia *et al.*, 2006; Lawrence *et al.*, 2010). Other OMPs with known roles in virulence include various systems dedicated to nutrient uptake, particularly that of iron.

Although the mechanisms by which some of these virulence factors operate has been elucidated, a comprehensive picture of how *M. haemolytica* interacts with the respiratory tract, to establish colonisation, is poorly understood. Questions regarding how the organism utilises its repertoire of adhesins and host modulating enzymes remain unanswered. To date several studies have aimed to address this knowledge gap. Kisiela & Czuprynski (2009) screened biotinylated *M. haemolytica* lysate against bovine bronchial epithelial cells (BBECs) in order to identify bound proteins. Several proteins were identified, including OmpA, PlpA, PlpB, PlpC and Ssa1, with putative roles in adherence. However, Kisiela & Czuprynski (2009) performed this study with submerged monocultures of epithelial cells.

Submerged monolayers are a simple way of assessing bacterial colonisation. However, submerged cultures fail to produce pseudostratification and the mucocillary phenotype and are therefore unrepresentative of the respiratory tract. In addition, the infection process is not accurately mimicked as bacteria are suspended in a liquid medium (RPMI was used by Kisiela & Czuprynski [2009]). As nutrient availability in the lumen of the respiratory tract is poor, submerged monolayers do not mimic the physiological conditions that bacteria encounter (Siegel & Weiser, 2015). Thus, a model that can circumvent the suspension of bacteria in a nutrient rich medium provides a more accurate physiological reflection of *in vivo* infection.

Another consideration of submerged monolayer culture is the growth of bacteria prior to infection. During planktonic growth in BHI media many virulence factors fail to be expressed in different *M. haemolytica* isolates (Chapter 3). As a result, the addition of planktonic bacteria to submerged BBECs will not allow for the identification of virulence factors that might be expressed at mid and late infection stages. This is particularly relevant when considering the formation of biofilms, a process that has been demonstrated to occur in *M. haemolytica*

(Boukahil & Czuprynski, 2014; Haig, 2011), because long incubation periods are required for maturation of the biofilm.

M. haemolytica is a commensal of the URT and serotypes of *M. haemolytica* that are non-pathogenic in cattle or sheep are frequently recovered in low numbers from the URT of healthy animals (Al-Tarazi & Dagnall, 1997; Klima *et al.*, 2014a). Disease-causing serotypes, A1 and A6 in cattle and A2, A7 and A9 in sheep, are recovered from the LRT of infected animals (Al-Ghamdi *et al.*, 2000; Ball *et al.*, 1993; Katsuda *et al.*, 2008; Kirkan & Kaya, 2005; Odugbo *et al.*, 2003; Petersen *et al.*, 2009). Thus, a URT to LRT transition occurs for pathogenic serotypes. The structure of the epithelium is different between different anatomical regions of the respiratory tract (Albertine, 2015; Hoffmann *et al.*, 2014; Miller *et al.*, 2011; Oliveira *et al.*, 2003; Toskala *et al.*, 2005). Therefore, an *in vitro* respiratory tract culture that captures the epithelial phenotypes of the URT and LRT would be advantageous in answering questions related to the serotype-specific colonisation properties of *M. haemolytica* in these anatomically different regions.

Lastly, because colonisation *in vivo* involves the external stimuli of stress and viral infection (Ackermann & Brogden, 2000), an ideal model of colonisation would capture all these influences prior to *M. haemolytica* infection. This point is particularly evident when considering that 517 unique gene expression changes have been shown to occur in BBECs following infection with BHV1 and *M. haemolytica* together (N'jai *et al.*, 2013).

With these considerations in mind, a respiratory tract model that resembles the *in vivo* environment was developed to gain insight into the host-pathogen interactions of *M. haemolytica* colonisation (Chapter 2). The first aim was to conduct preliminary experiments to assess the effectiveness of the model for studying the adherence and colonisation of *M. haemolytica*. In principle this involved a comparison of infection of submerged and ALI-grown epithelial cells. The second aim was to address the ability of *M. haemolytica* to colonise ALI cultures produced with epithelial cells harvested from different anatomical regions of the respiratory tract.

4.2 Materials and methods

4.2.1 Bacteriology

4.2.1.1 Isolates

Details of *M. haemolytica* strains selected for use in the infection studies are presented in Table 4.1. Isolates PH2 and PH376 represent bovine-pathogenic isolates of serotypes A1 and A6, respectively; both were recovered from the lungs of cattle exhibiting symptoms of pneumonic pasteurellosis. Isolates PH278 and PH284 represent ovine-pathogenic isolates of serotypes A2 and A6, respectively; both were recovered from the lungs of sheep displaying clinical sings of pneumonic pasteurellosis. Isolate PH202 is a serotype A2 strain recovered from the nasopharynx of a healthy cow.

Table 4.1 *M. haemolytica* strains used in cellular infection experiments

Strain	Serotype	Host Species	Clinical Status
PH2	A1	Bovine	Pneumonia
PH202	A2	Bovine	Healthy
PH278	A2	Ovine	Pneumonia
PH284	A6	Ovine	Pneumonia
PH376	A6	Bovine	Pneumonia

4.2.1.2 Growth conditions

BHIB growth. Isolates of *M. haemolytica* were stored at -80°C in BHIB in 50 % glycerol (v/v). Isolates were plated out on BHIA containing 5% defibrinated sheeps blood (E&O Laboratories) and grown for 24 h at 37°C. For planktonic growth of bacteria two methods were used. Firstly, three colonies from an agar plate were selected and an emulsion made in 3 ml of BHIB. From this emulsion 250 µl were removed and added to 25 ml of BHIB (1:100 inoculum) in a 100 ml Erlenmeyer flask which was incubated at 37°C with shaking at 120 rpm. Secondly, a starter culture of three colonies from an agar plate were used to inoculate 10 ml of BHIB in a universal and grown overnight at 37 °C with shaking at 120 rpm. Two hundred and fifty microliters of the overnight culture were used to inoculate 250 ml of BHIB in a 1-L Erlenmeyer flask which was incubated

at 37°C with shaking at 120 rpm. All culture flasks were grown until a desired OD_{660nm} (~0.8) was reached.

Serum growth. For the use of serum-grown bacteria, three single colonies from an agar plate were selected and an emulsion was made in 3 ml of FCS (Invitrogen). From this bacterial emulsion, 250 µl were removed and added to 25 ml of FCS (1:100 inoculum) in a 100-ml Erlenmeyer flask. Cultures were grown at 37°C with shaking at 120 rpm.

DMEM growth. For the use of DMEM-grown bacteria, three single colonies from an agar plate were selected and an emulsion was made in 3 ml of DMEM (Sigma) containing 10% FCS. From this bacterial emulsion, 250 µl were removed and added to 25 ml of DMEM containing 10% FCS (1:100 inoculum) in a 100-ml Erlenmeyer flask. Cultures were grown at 37°C with 120 rpm of shaking.

Iron-restricted growth. For the use of bacteria grown under iron-limited conditions, three single colonies from an agar plate were selected and an emulsion was made in 3 ml of BHIB. From this bacterial emulsion, 250 µl were removed and added to 25 ml of BHIB containing 170 µM 2'2-dipyridyl (Sigma) (1:100 inoculum) in a 100-ml Erlenmeyer flask. Cultures were grown at 37°C with 120 rpm of shaking.

4.2.1.3 Production of calibration curves for CFU determination

Enumeration of bacteria was performed using the Miles and Misra method of bacterial CFU determination (Miles *et al.*, 1938). Bacterial suspensions were centrifuged at 5000 x g for 10 min, the pellets resuspended in PBS, centrifuged again (5000 x g for 10 min) and the bacteria resuspended in 20 ml of PBS. Bacteria were doubly-diluted to produce a series of six bacterial dilutions in universals. The OD_{660nm} was measured for each of the six bacterial concentrations. From each of the dilutions, three separate twenty microliter volumes of bacterial suspension were removed independently and combined with three 180 µl volumes of PBS in a microtiter plate. One in ten serial dilutions were then preformed across the microtiter plate. A six concentration range (10^{-3} - 10^{-8}) of the 10-fold dilutions was selected and twenty microliters of each replicate for each concentration were plated onto BHIA with 5 % defibrinated

sheep's blood. Agar plates were grown overnight at 37 °C until colonies were visible. Colonies were enumerated and calibration curves were plotted of $\log_{10}$N CFU against OD_{660nm}.

4.2.1.4 Preparation of inocula for epithelial cell infection

As described in section 4.2.1.3, the Miles and Misra plating method was used for enumeration of bacteria. Using the calibration curves (4.2.1.3), bacterial suspensions were adjusted to an OD value corresponding to the desired inoculum concentration (10^9 CFU/ml was used unless otherwise stated). The inocula used for infecting cultures were enumerated by taking three 20 µl samples and combining each with 180 µl of PBS. Samples were tenfold serially diluted and a range of six concentrations of each replicate was plated onto BHIA with 5% defibrinated sheep's blood. The agar plates were then incubated overnight at 37°C to enumerate bacterial concentration.

4.2.2 Tissue culture

4.2.2.1 Tissue collection and cell harvesting

Tissue collection (bronchi, trachea and nasopharynx) and cell harvesting was performed as described in section 2.2.1.1.

4.2.2.2 Cell maintenance and subculturing

Cell maintenance was performed as described in section 2.2.1.2.

4.2.2.3 Air liquid interface culture

Air-liquid interface culture was performed as described in section 2.2.1.3.

4.2.2.4 Infection of ALI cultures

Cultures were washed twice basolaterally and once apically and changed to antibiotic/antifungal-free media at least two hours prior to infection. Bacteria were grown to mid log phase (OD_{660} 0.6 to 0.8) as described in section 4.2.1. Once an appropriate OD was reached, bacteria were harvested by centrifugation at 5000 x g for 10 min and resuspended in 20 ml of PBS before being centrifuged again at 5000 x g for 10 min. Bacteria were then resuspended in 5 to 10 ml of

PBS depending on the size of the bacterial pellet. The bacterial suspension was adjusted to an OD corresponding to 10^9 CFU ml^{-1} using the calibration curves (4.2.1.3) unless otherwise stated. Twenty five microliters of bacterial suspension were added to the apical surface of each culture. All cultures were incubated at 37°C in a 5 % CO_2 incubator until the infection end point.

4.2.2.5 Submerged epithelial cell Infection

Tracheal epithelial cells were seeded onto coverslips in 12 well tissue culture plates at densities of 2 x 10^5 cells per 13 mm ø coverslip. Coverslips (neuVitro) were either uncoated or coated with rat tail type I collagen or fibronectin. Cells were grown for 24, 48 or 72 h in submered growth media (2.2.1.1). Infection was carried out as described for ALI culture (4.2.2.4) with the exception that 0.5 ml of bacterial suspension in DMEM was added to each culture well and the entire plate was centrifuged at 200 x g for 5 min before incubation at 37°C with 5 % CO_2. After infection, cultures were washed three times with one millilitre of PBS to remove unattatched bacteria prior to fixation for microscopy.

4.2.2.6 Quantitative adherence assay

Infected cultures were washed three times with one millilitre of PBS apically to remove unbound bacteria. Following this, one millilitre of 1 % Triton X-100 in PBS was added to each culture and cells were incubated for 10 min at room temperature. After incubation each cell culture was scraped using the end of a pipette tip to loosen the epithelial cells. The epithelial cells were resuspended and lysed by gently pipetting up-and-down 30 times and a 200 µl volume was removed into a microtitre plate. The lysed cell suspension was serially diluted (10-fold) and plated according to the Miles and Misra method outlined in section 4.2.1.3. Agar plates were incubated at 37 °C overnight for colony enumeration. For any one condition three biological replicates were used. Each biological replicate was assayed in triplicate. Colony numbers and dilution level were accounted for and technical averages were taken for each biological replicate before evaluating average and variation between the three biological replicates.

4.2.3 Microscopy

4.2.3.1 Scanning electron microscopy

Scanning electron microscopy was carried out as previously described in section 2.2.2.2.

4.2.3.2 Histology

Histology was carried out according to section 2.2.2.5.

4.3 Results

4.3.1 *M. haemolytica* adherence to submerged epithelial cells

Preliminary experiments examining the adherence of *M. haemolytica* to BTECs grown on submerged coverslips were conducted. This was performed in three successive experimental stages. Firstly, the infection innoculumn size and infection time were examined. Secondly, bacterial growth conditions prior to infection were analysed. Lastly, the growth confluency of airway epithelial cells was assessed in combination with different coverslip-ECM coatings. Submerged infections were assessed by SEM microscopy (4.2.3.1) and scored according to the observed levels of adherence; (-) no adherence, (+/-) sporadically adhered individual bacterial cells, (+) widespread adherence of individual bacterial cells, (++) sporadic microcolonies, (+++) extensive microcolonies.

4.3.1.1 Submerged adherence for different inocula after different incubation periods

Table 4.2 displays the assessment of adherent *M. haemolytica* after two and four hours of infection at inoculum concentrations of 10^7, 10^8, 10^9 CFU/ml.

Table 4.2 Adherence of *M. haemolytica* to submerged bovine epithelial cells
Semi-quantification of adherence assessed by scoring.[a]

	2 h Post Infection			4 h Post Infection		
	10^9 CFU ml^{-1}	10^8 CFU ml^{-1}	10^7 CFU ml^{-1}	10^9 CFU ml^{-1}	10^8 CFU ml^{-1}	10^7 CFU ml^{-1}
PH2	-	-	-	-	-/+	-/+
PH284	-	-	-	-	-	-
PH376	-	-	-	-	-/+	-/+
Control[b]	-					

[a]Key: (-) No adherence, (-/+) sporadic individual adherent bacterial cells, (+) widespread adherence of individual bacteria cells, (++) sporadic microcolonies, (+++) extensive microcolonies, (++++) early biofilm formation.

[b]Control is an uninfected coverslip assayed for bacterial adherence.

Only dispersed individual bacterial cells of the bovine isolates PH2 and PH376 were found on the epithelial surface after four hours of infection at 10^9 and 10^8 CFU/ml. All other conditions failed to produce any adherent bacteria.

4.3.1.2 Submerged adherence following bacterial growth under different conditions

As a result of few adherent bacteria being found, consideration was made for the influence that growth conditions prior to infection may have on the ability of the bacteria to adhere to the epithelial cells. Using a four-hour infection time and 10^9 CFU/ml inoculum of isolates PH2 and PH376, several different growth conditions were tested to establish if any of these resulted in improved adherence and colonisation. Whilst analysis revealed that all conditions yielded some adherent bacteria, only isolated bacterial cells were observed across the epithelial surface (Table 4.3).

Table 4.3 Adherence *of M. haemolytica* to submerged bovine epithelial cells with different bacterial growth conditions
Semi-quantification of adherence assessed by scoring.[a]

	Growth Condition				
	Broth	Agar	Serum	DMEM + 10% Serum	Broth + 170µm Dipyridyl
PH2	**+**	**+**	**-/+**	**-/+**	**-/+**
PH376	**-/+**	**-/+**	**-/+**	**+**	**-/+**
Control[b]			**-**		

[a]Key: (-) No adherence, (-/+) sporadic individual adherent bacterial cells, (+) widespread adherence of individual bacteria cells, (++) sporadic microcolonies, (+++) extensive microcolonies, (++++) early biofilm formation.

[b]Control is an uninfected coverslip assayed for bacterial adherence.

4.3.1.3 Submerged adherence to epithelial cells grown for different time periods and on different substrate coatings

Again, as no widespread adherence and colonisation was observed (Table 4.3), consideration was given to additional parameters that may influence epithelial colonisation. The rationale that epithelial cells grown on either collagen or

fibronectin may express different cell surface receptors was considered. Additionally, the growth time of the epithelial cells prior to infection was also considered. As a result both of these parameters were tested for their influence on colonisation with ovine tracheal epithelial cells (OTEC) and two strains, PH278 and PH284, recovered from cases of ovine pneumonia (Table 4.4). OTECs were selected for use during this phase to assess whether the low levels of adherence observed on BTECs was a bovine-specific phenomenon. Adherence was broadly greater with PH284 than PH278 when comparing these isolates for any set of the same conditions. Adherence was also greater to epithelial cells grown for 72 h compared with 24 and 48 h grown epithelial cells.

Table 4.4 Adherence of *M. haemolytica* to submerged ovine epithelial cells grown to different confluencies on different extracellular matrix proteins.
Semi-quantification of adherence assessed by scoring.[a]

	24 h Epithelial Growth			48 h Epithelial Growth			72 h Epithelial Growth		
	Uncoated	Collagen	Fibronectin	Uncoated	Collagen	Fibronectin	Uncoated	Collagen	Fibronectin
PH278	-	+/-	+/-	-	-	+/-	++	+/-	-
PH284	+	+/-	+/-	+	+/-	+	+/-	+++	++

[a]Key: (-) No adherence, (-/+) sporadic individual adherent bacterial cells, (+) widespread adherence of individual bacteria cells, (++) sporadic microcolonies, (+++) extensive microcolonies, (++++) early biofilm formation.

The majority of conditions yielded only single-cell attachment of *M. haemolytica* to the epithelial cell surface. However, small microcolonies of PH284 were observed after 72 h of epithelial growth on both the collagen- and fibronectin-coated surfaces. These appeared more numerous on the collagen-grown epithelial cells compared to the fibronectin-grown epithelial cells. Small microcolonies could also be observed for PH278 after 72 h although only on cells grown on the uncoated coverslips. However, Inspection of the SEM images (Fig 4.1) suggested that the microcolonies under these conditions might be artefactual, as in the majority of cases the microcolony was adhered to the coverslip surface as well as a region of the epithelial cells.

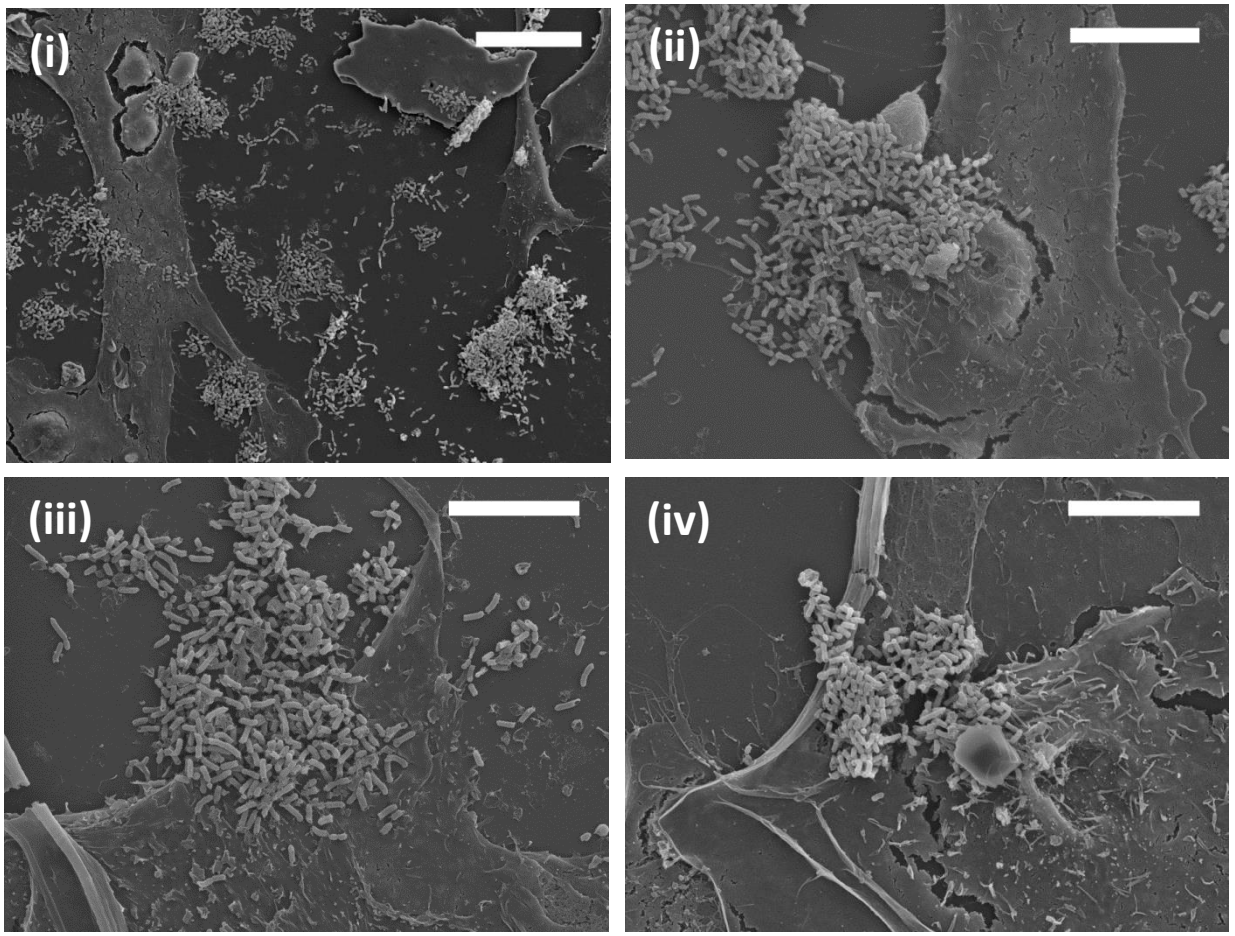

Fig 4.1 SEM images of submerged epithelial cell infection.
Images (i), (ii) and (iii) represent OTECs grown for 72h of growth on collagen coated coverslips and infected with PH284 for four hours. Image (iv) represents OTECs grown for 72h on fibronectin coated coverslips and infected with PH284 for four hours. Scale bars represent 20µm for image (i) and 10µm for images (ii), (iii) and (iv).

4.3.2 Infection of ALI epithelial cell cultures

The inconclusive findings of the submerged infection experiments strengthened the case for the production of an ALI epithelial model. Initial experiments concerned the growth of OTECs and BTECs at ALI in order to establish if infection of these model systems differed to the submerged cultures.

4.3.2.1 Infection of OTECs grown at ALI

Ovine epithelial cultures were differentiated for 20 days at ALI and infected with isolates PH278 and PH284 for 6 and 24 h. The resulting SEM analysis identified several features that were previously unseen in the submerged assays. Six hours post-infection PH278 only exhibited sparsely adherent single cells (Fig 4.2 [i]. However, small pockets of bacteria could be observed beneath the apical face of the epithelium for PH284 (Fig 4.2 [ii]). For PH284, two observations were particularly striking; firstly, the surrounding apical face was devoid of bacteria yet these foci of sub-apical colonisation contained numerous bacteria (Fig 4.2 [ii]) and, secondly, some bacterial cells appeared filamentous with lengths greatly exceeding the normal (~2 μm) bacterial cell length (Fig 4.2 [ii] arrowheads).

Following 24 h of bacterial infection small numbers of microcolonies could be observed for PH278 on the apical surface of the epithelial cells (Fig 4.2 [iii] & [v]). The microcolonies were also associated with material that resembled secreted mucin or exopolysaccharide-like material (Fig 4.2 [v] asterisk). For PH284 after 24 hours, large microcolonies (greater than 100 μm in diameter) were observed across the surface of the epithelium (Fig 4.2 [iv] & [vi]). One example of a small microcolony on the apical surface of the epithelium could be found for PH284 after six hours of infection (Fig 4.3 [i]). However, the large microcolonies observed after 24 h of infection appeared topographically elevated, relative to the epithelial surface (Fig 4.3 [ii] & [iii]). These microcolonies displayed a thick matt of adherent cells with evidence of some secreted EPS-like material adjoining the cells in the colony (Fig 4.3 [iv] arrowheads), indicative of early biofilm formation. More cells were found that were morphologically filamentous (Fig 4.3 [v] arrow heads).

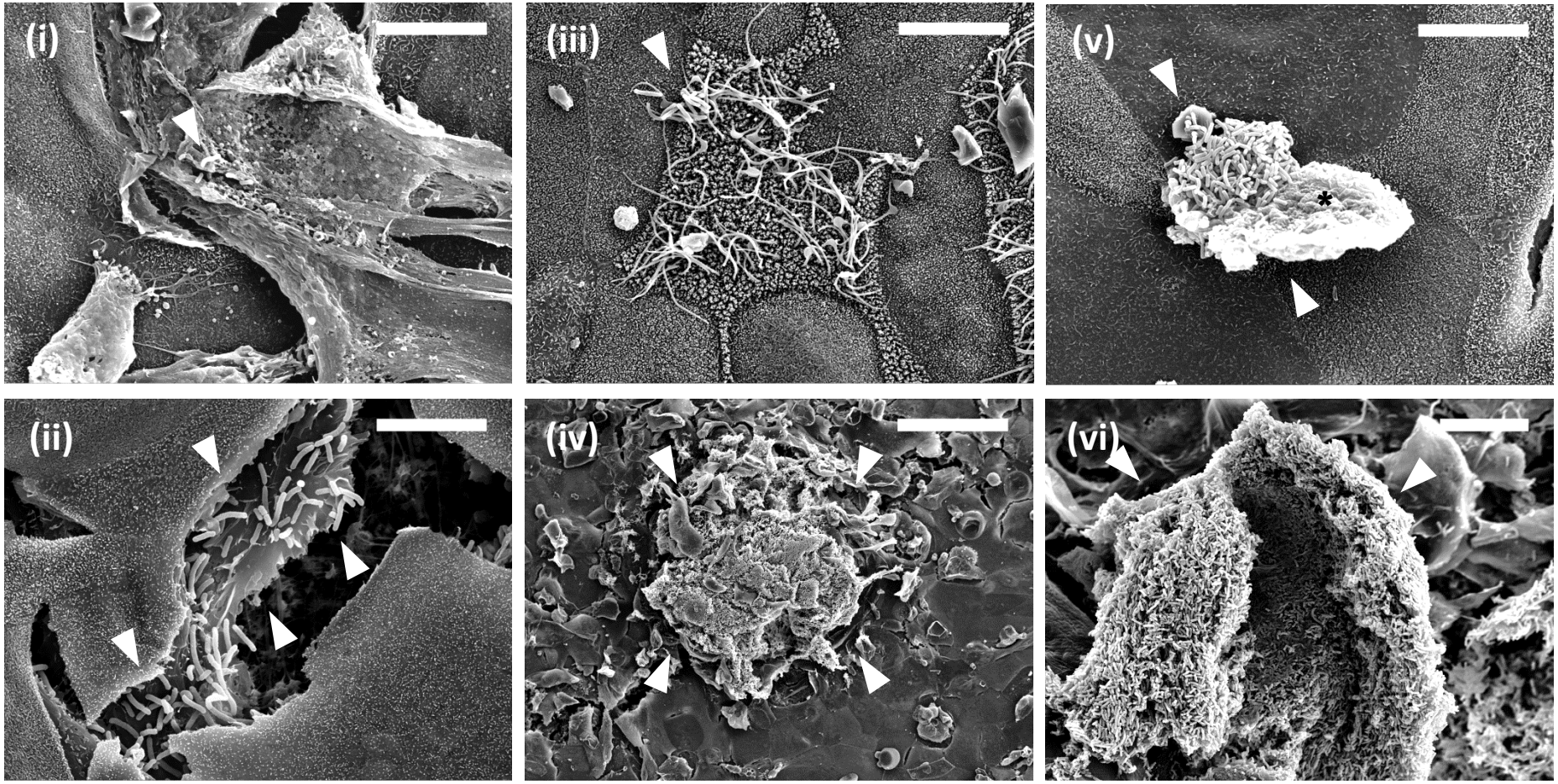

Fig 4.2 SEM images of *M. haemolytica* infecting differentiated ovine ALI cultures
Panels (i), (iii) and (v) represent isolate PH278 at 6 h (i) and 24 h (iii) + (v) post infection. Panels (ii), (iv) and (vi) represent isolate PH284 at 6 h (ii) and 24 h (iv) + (vi) post infection. White arrow heads show foci of bacterial attachment. Scale bars for SEM images are as follows; 10 µm for (i), (ii), (iii), and (iv); 20 µm for (iv); 100 µm for (vi).

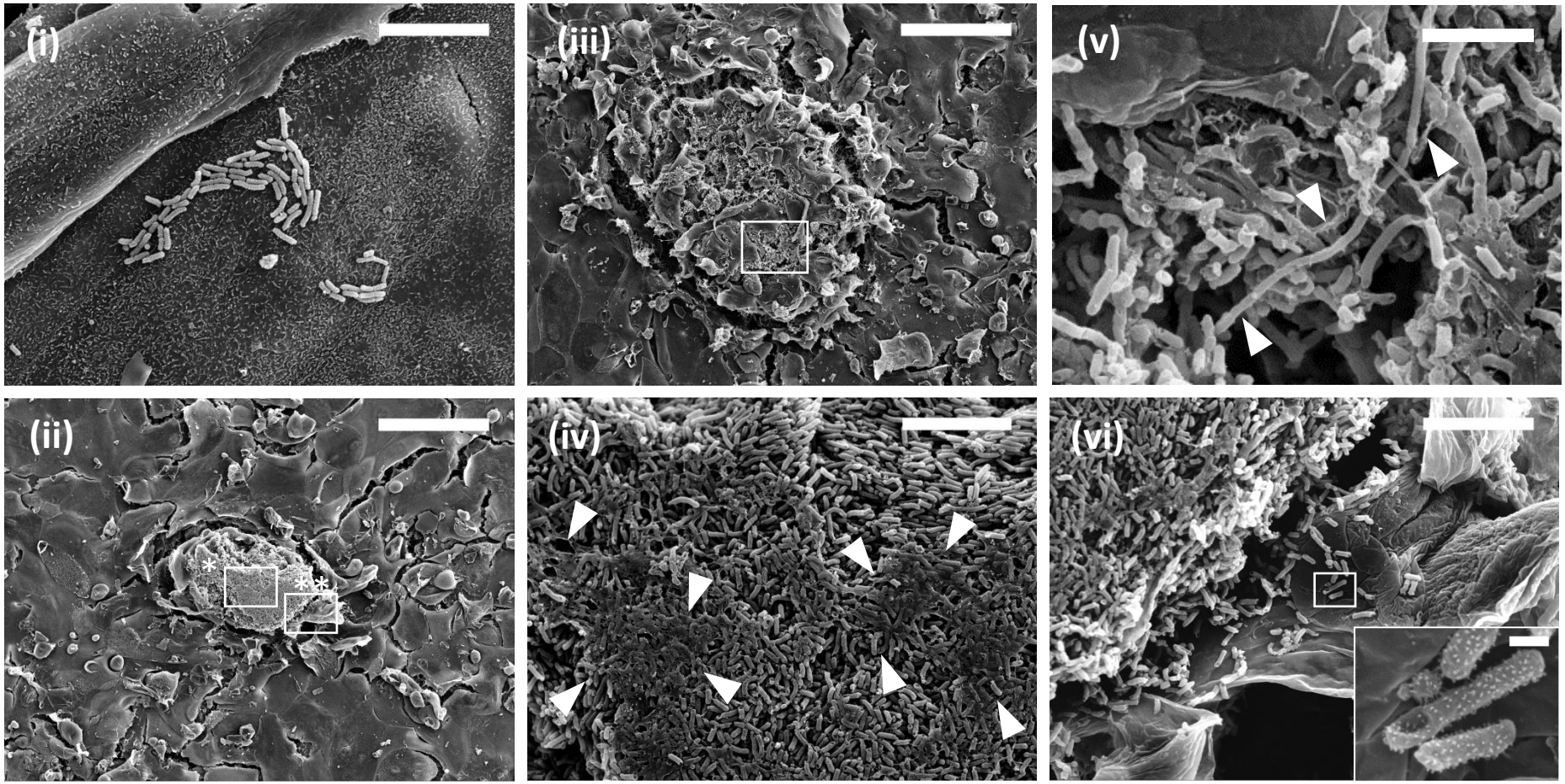

Fig 4.3 SEM images showing the phenotypic properties of *M. haemolytica* isolate PH284 following infection of differentiated ovine ALI cultures
Panel (i) 6 h post infection, panels (ii) – (vi) 24 h post infection. White box in panel (iii) highlights the position of image (iv). White boxes (ii)* and (ii)** highlight the location of panels (iv) and (vi), respectively. Arrow heads represent phenotypic features including EPS-like material (iv) and filamentous bacteria (v). White box in panel (vi) represents the location of the insert. Scale bars for SEM images are as follows; 10 µm for (i), (iii), and (vi); 5 µm for (v); 100 µm for (ii) and (iii); 500nm for the insert in panel (vi).

Closer inspection of individual bacterial cells in the microcolonies revealed that the bacterial cell surface was covered with surface blebs (Fig 4.3 (vi) insert); possibly the formation of microvesicles.

4.3.2.2 Infection of BTECs grown at ALI

Bovine ALI cultures were infected with two pathogenic bovine isolates of *M. haemolytica*. Isolates PH2 and PH376 were selected because they represent the main pathogenic cattle serotypes of A1 and A6, respectively. Bovine epithelial cultures were differentiated at ALI for between 21 and 23 days and infected exactly as the ovine cultures. After six hours of infection the epithelium was relatively free of bacteria for both PH2 and PH376 (Fig 4.4 [i] and [iv]). Only small numbers of individual bacterial cells could be found on the surface and in no instance was the formation of a microcolony noted. After 24 hours of infection with both isolate PH2 and PH376, large numbers of adherent bacteria could be observed across the epithelium. In both isolates, attachment and colonisation was confined almost entirely to the sub-apical regions (Fig 4.4 [ii], [iii], [v] and [vi]); this was similar to what had been observed for PH284 after six hours of infection on OTEC ALI cultures (4.3.2.1). These sub-apical regions likely constitute either the basal cells or the basolateral membrane of the polarised epithelial cells. Apical attachment of bacteria did not consist of microcolonies but rather isolated cases of individual bacteria attached to non-ciliated epithelial cells. The sub-apical foci of attachment for PH2 and PH376 were more numerous than had been observed for PH284 (Fig 4.2 [iv]), occupying the majority of exposed sub-apical regions. Additionally, bacteria appeared more densely clustered in the foci of attachment than had been observed for PH284 after 6 h (Fig 4.2 [iv]). Inspection of individual bacterial cells indicated no surface blebbing and no bacterial cells appeared elongated as was observed with the infection of OTECs with PH284 (Fig 4.2 [vi] insert & [iv]).

4.3.3 TEER analysis of infected BTEC ALI cultures

The observation of *M. haemolytica* in the sub-apical regions of OTEC- and BTEC-derived ALI cultures raised the question of how bacteria were accessing this region. Bacteria could traverse the apical barrier to access the sub-apical region either via paracytosis or transcytosis.

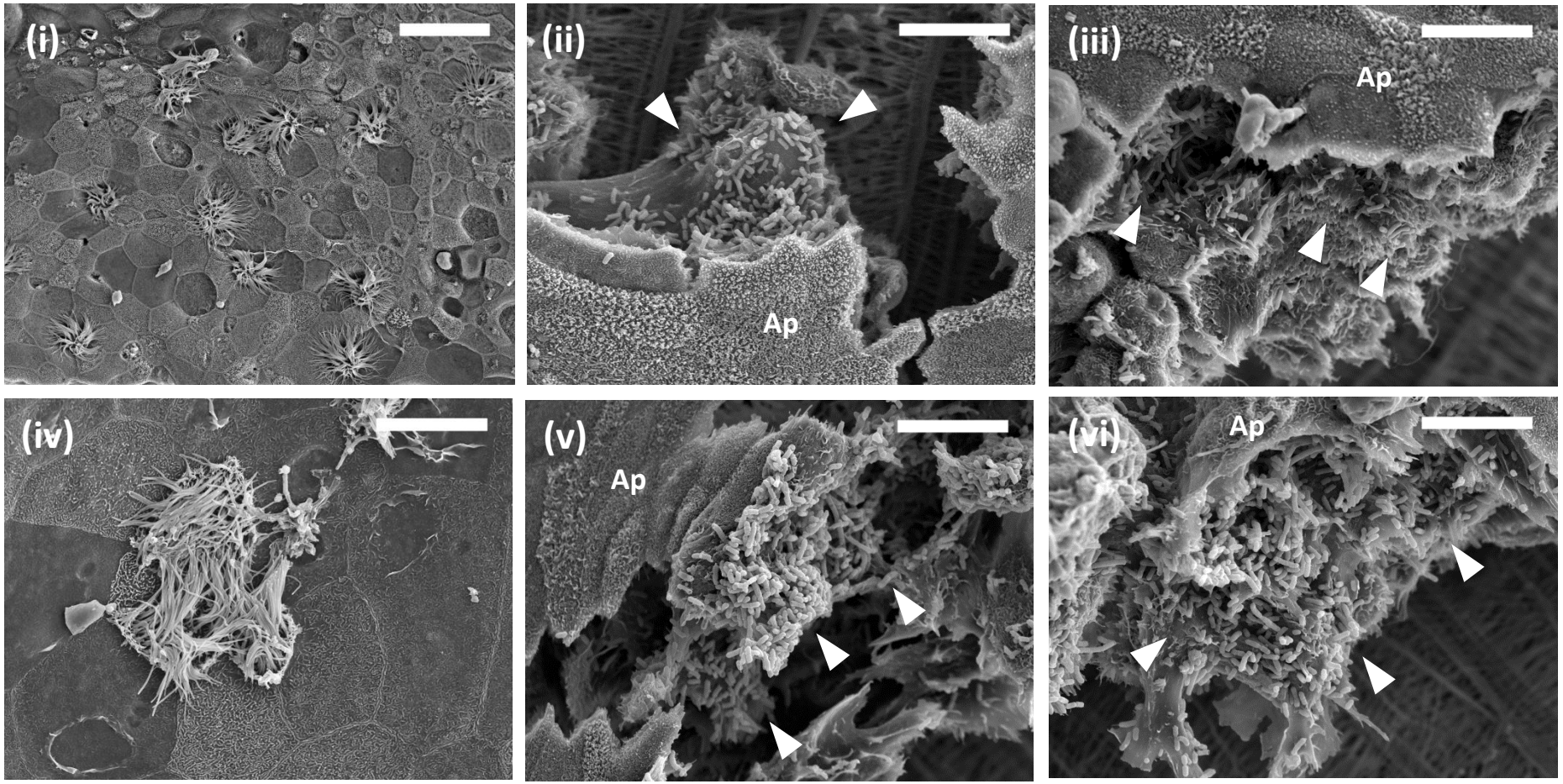

Fig 4.4 SEM images *of M. haemolytica* infecting differentiated bovine ALI cultures.
Panels (i) - (iii) represent isolate PH2 at 6 h (i) and 24 h (ii) + (iii) post infection. Panels (iv) to (vi) represent isolate PH376 at 6 h (iv) and 24 h (v) +(vi) post infection. The letters Ap indicates the apical face of the epithelium and white arrow heads indicate foci of bacterial attachment and colonisation. Scale bars for SEM images are as follows; 20 µm for (i) and 10 µm for (ii), (iii), (iv), (v) and (vi).

Paracytosis would require disruption of the epithelial tight junctions while transcytosis would require engulfment of bacteria into vacuoles for delivery to the sub-apical space. The observation of bacteria in the visible sub-apical space was indicative of paracytosis. However, as the sample processing for SEM introduces cracks in the epithelium, from shrinkage due to dehydration, it is possible that this observation is artefactual. Therefore, cells of *M. haemolytica* may travel to the sub-apical space via transcytosis only to be visible by SEM due to artefactual cracks introduced during the dehydration process.

To assess whether *M. haemolytica* infection causes impairment in barrier integrity the TEER was measured on cultures prior to and during infection with isolate PH2. As can be seen from Fig 4.5, all measured cultures had a net TEER value of >400 $\Omega.cm^{-2}$ prior to *M. haemolytica* infection. Following 15 min, one hour and six hours of infection the TEER values remained unchanged (Fig 4.5). However, after 24 hours of infection a dramatic decrease in TEER of more than 300 $\Omega.cm^{-2}$ was observed (Fig 4.5).

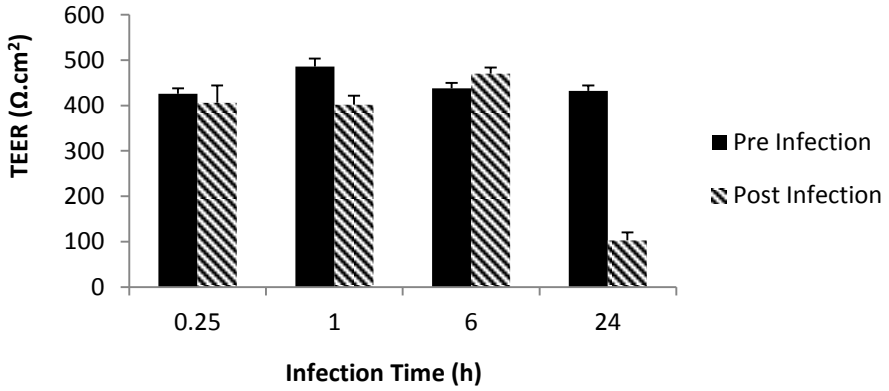

Fig 4.5 Epithelial permeability following *M. haemolytica* infection
Displayed are the triplicate TEER measurements of cultures infected with isolate PH2 at t = 0 (pre-infection, black bars) and one culture each at t = 15 min, 1 h, 6 h and 24 h (post-infection, hatched bars). Infections were carried out 21 days after ALI induction.

The decrease in TEER suggests that by 24 hours post infection permeability of the epithelial barrier increases, although spread plating of samples from the basolateral chambers after each time point failed to yield any colonies on BHI-5% blood agar. Thus, the observation of *M. haemolytica* adherent to the sub-apical regions of the epithelium might therefore occur as a result of paracytosis through the respiratory epithelium.

4.3.4 Colonisation of epithelial cells derived from different anatomical locations

Since *M. haemolytica* is an opportunistic pathogen that can ordinarily be recovered from the URT yet causes infection in the LRT, an experiment was designed that examined the ability of *M. haemolytica* to infect ALI epithelial cultures derived from different anatomical locations of the respiratory tract. Two isolates, PH2 and PH202, were selected based on their differences in pathogenicity. PH2 is a serotype A1 isolate that was recovered from the pneumonic lung of a cow whereas PH202 is a serotype A2 isolate from the nasopharynx of a healthy cow. Both of these isolates were used to infect ALI models derived from tissue harvested from three sites of the respiratory tract of the same animal, i.e. nasopharynx, mid trachea and secondary/tertiary bronchi. Both the BTEC and BBEC ALI cultures produced sufficient TEER to generate an ALI after 7 days of submerged culture and were maintained for a further 21 days at ALI prior to infection. However, the bovine nasopharyngeal epithelial cell (BNEC) cultures displayed a slower increase in TEER and were maintained in submerged culture for 12 days and a further 17 days at ALI prior to infection. Epithelial cultures derived from all three anatomic sites were infected with PH2 and PH202 for 6 and 24 h. After incubation, the infected cultures were assayed for quantitative adherence levels. Cultures were also fixed for histology and SEM.

After 6 h of infection, no adherent bacteria could be observed by either SEM or Giemsa stained histological sections, in cultures derived from any of the three sites. Bacterial quantitation revealed that 1-2 % of the initial inoculums of PH2 and PH202 were adherent to epithelial cultures derived from all three sites (Fig 4.6 A). For each ALI culture investigated (BTEC, BBEC and BNEC), the adherence of PH202 appeared slightly higher, however this represented no statistically significant difference over that of PH2. Similalrly, no statistically significant difference was observed of either isolate between the BTEC, BBEC and BNEC cultures.

After 24 h of infection, large numbers of adherent PH2 were recovered from the BBEC ALI cultures with more than five times the starting inoculum recovered (Fig 4.6 B). Significantly higher numbers of PH2 were recovered from the BBEC ALI

cultures as compared with either the BTEC ALI or BNEC ALI cultures. Furthermore, statistically significant numbers of adherent PH2 were recovered from the BBEC ALI and BTEC ALI cultures as compared with PH202. Slightly more PH202 were recovered from the BNEC ALI cultures as compared to the cultures derived from the other two tissue types. Although the adherence of PH202 was not significantly greater than PH2 on the BNEC ALI cultures, it nonetheless suggests PH202 had a propensity for the BNEC ALI culture. Taken together these results show that (1) PH2 is more efficient at colonising BBEC ALI cultures as compared with either BTEC ALI cultures or BNEC ALI cultures, and (2) that PH202 is more efficient at colonising the BNEC ALI cultures as compared with either of the other two ALI model types.

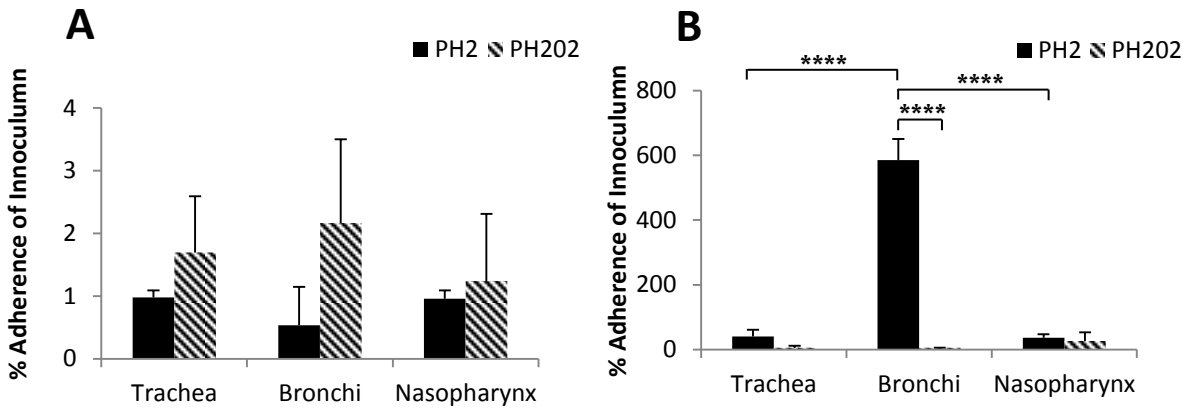

Fig 4.6 Quantitative adherence of *M. haemolytica* on epithelial cultures derived from different anatomical sites.
(A) and (B) display adherence at 2 and 24 h post infection, respectively. Results are the average of three infections on BBEC ALI cultures. Error bars are representative of the standard deviation. Significance determined with two way ANOVA and Tukey Kramer post-test (**** $P < 0.0001$). All cells were harvested from the same animal.

Analysis by SEM of the ALI cultures after 24 h of infection (Fig 4.7 [i] & [ii]) revealed a pattern of PH2 adherence where bacteria attached to and colonised the sub-apical region of the BBEC cultures. This was similar to earlier experiments where sub-apical bacteria (PH2) were observed on ALI cultures with epithelial cells derived from the lower trachea (4.3.2.2). No adherent bacteria could be found on the PH2-infected BTEC ALI cultures by SEM. Adherent bacteria were observed on the nasopharyngeal tissue for both PH2- and PH202-infected ALI cultures (Fig 4.7 [iii], [iv], [v] & [vi]).

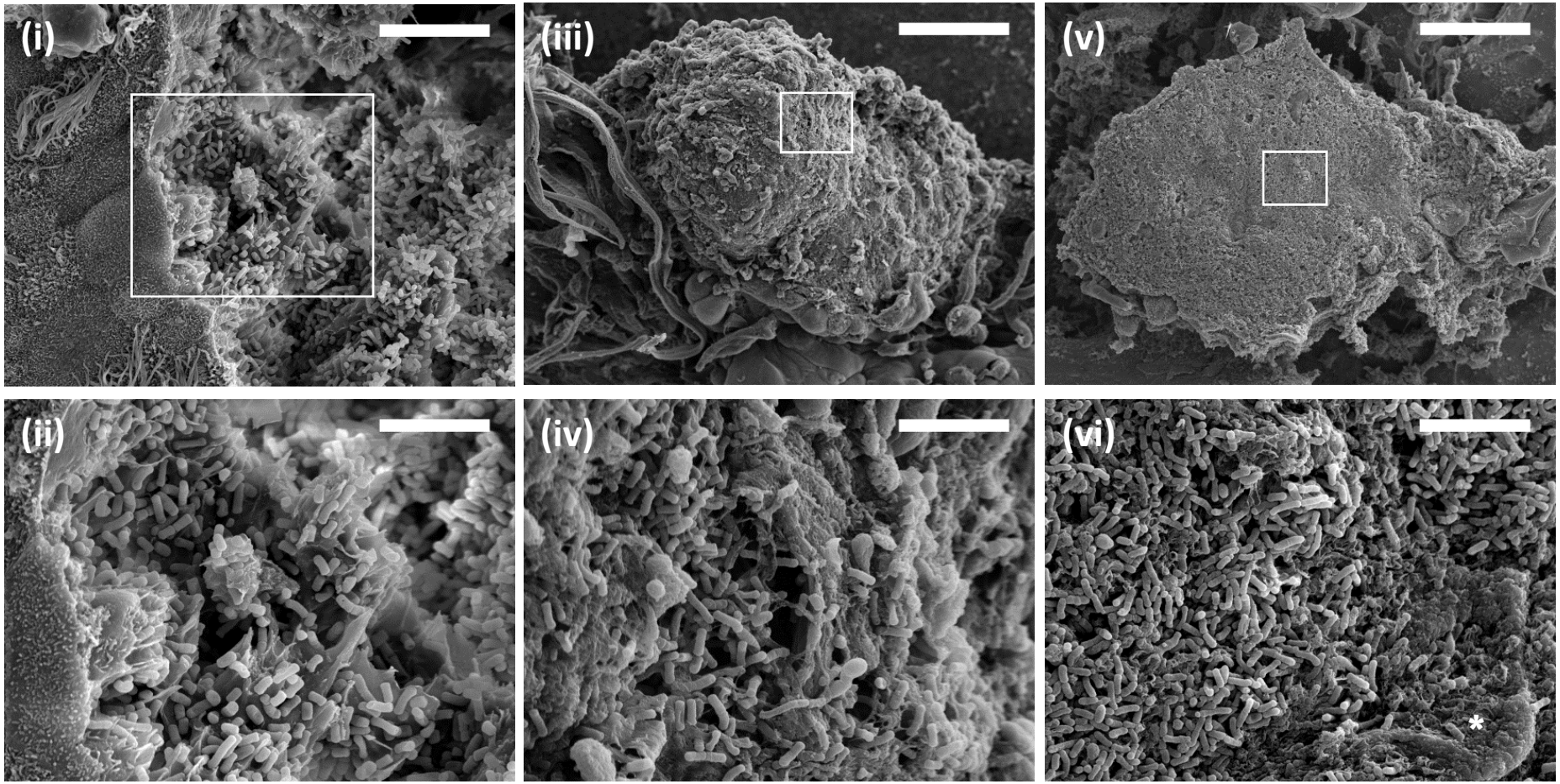

Fig 4.7 SEM images of *M. haemolytica* adhering to epithelial ALI cultures derived from different anatomical sites.
All images are of cultures 24 h post infection. Panels (i) & (ii); PH2 adhering to BBEC cultured at ALI. Panels (iii) & (iv); PH2 adhering to BNEC cultured at ALI. Panels (v) & (vi); PH202 adhering to BNEC cultured at ALI. Scale bars for SEM images are as follows; 5 µm for (ii), (iv) and (vi); 10 µm for (i); and 50 µm for (iii) and (v).

In the case of PH2 colonising the BNEC cultures, small microcolonies of adherent bacteria were located on areas of epithelial tissue that were topographically elevated compared to the surrounding tissue (Fig 4.7 [iii]). In the case of PH202 colonising the BNEC cultures , adherence was non-uniform with only a relatively small region of the total epithelial surface colonised to the extent observed in Fig 4.7 (v). Nevertheless, attachment levels were high in that localised region and the observation of epithelial cells beneath the bacterial mass (Fig 4.7 [vi] asterisk) confirmed the bacteria are adhering to the epithelium (Fig 4.7 [vi]).

Close inspection by SEM of the PH2-infected BBEC and BNEC ALI cultures and the PH202-infected BNEC ALI cultures revealed several phenotypic properties. Where isolate PH2 had infected the BBEC ALI cultures for 24 h, numerous foci of bacterial attachment in the sub-apical regions of the tissue were observed. Analysis of the epithelial surface revealed a small sub-apical area of bacterial adherence which was laterally surrounded by intact tissue (Fig 4.8 [i] and [ii]). This locale of infection possibly represents an early example of bacteria accessing the sub-apical region, as the lesion is relatively small and entirely surrounded by intact tissue. No bacteria were observed on the apical face in the surrounding vicinity.

A property noted for the nasopharyngeal tissue following PH202 infection was the apparent production of mucus (Fig 4.8 [iii]). Although mucus production had been observed on BBEC and BTEC ALI cells, the extrusions appeared more numerous on the BNEC PH202-infected ALI cultures. It should be noted that similar observations were made on control (uninfected) BNEC ALI cultures, albeit less frequent and distinct. It is not possible to determine from these images if PH202 infection has stimulated the release of mucus, further work would be needed to clarify this. Nonetheless, it does reveal that the nasopharyngeal model is capable of producing mucus and with further differentiation possibly cilia.

The observation of microcolonies of PH2 on the BNEC ALI cultures was confined to protrusions in the epithelial surface topography (Fig 4.8 [iv]). However, other epithelial surface protrusions could be found that contained no adherent PH2. Of those that did contain bacterial microcolonies, adherence was widespread.

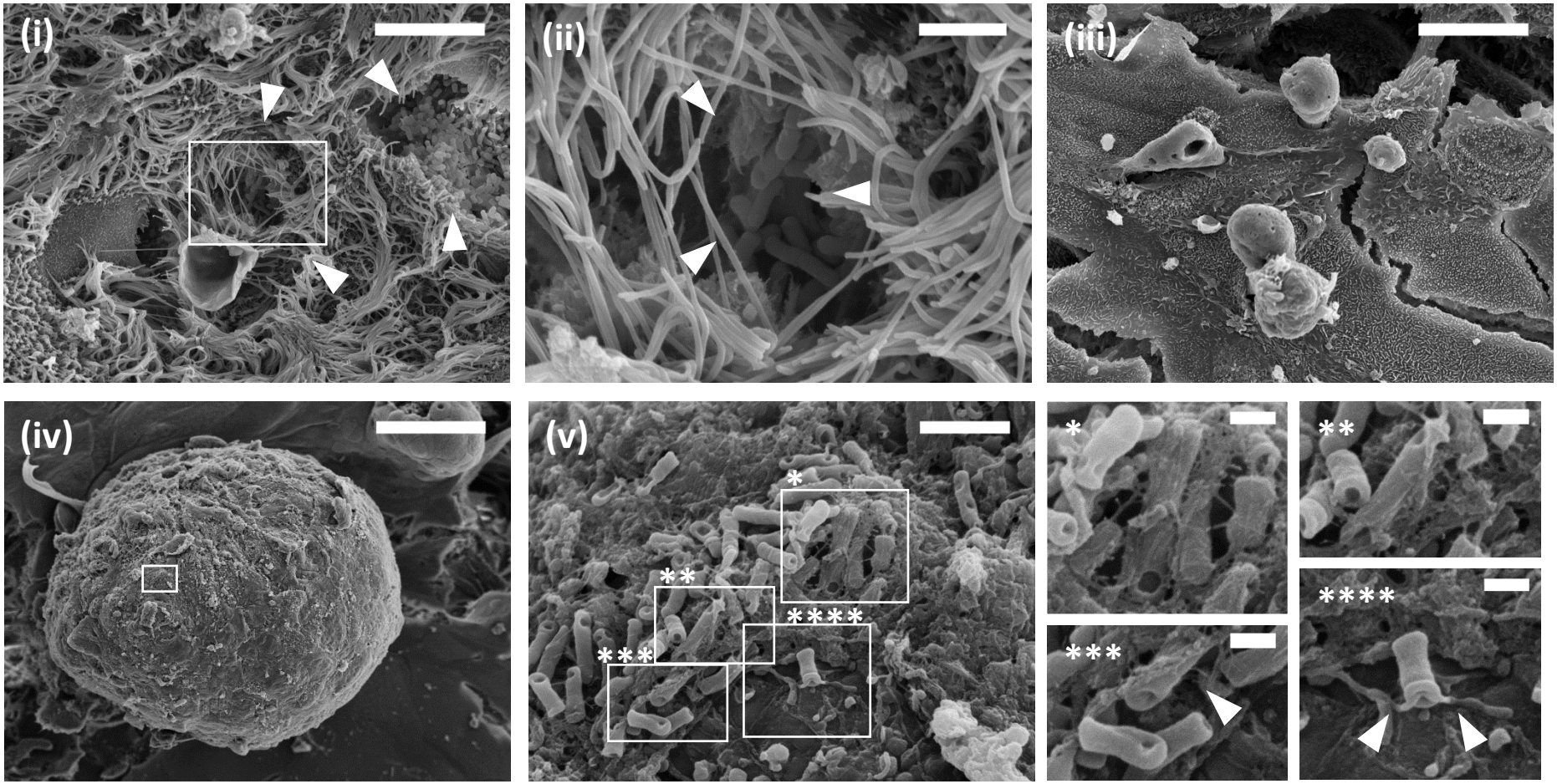

Fig 4.8 Phenotypic observations of infected ALI cultures derived from different anatomical origins.
Panels (i) and (ii) are SEM images of BBEC following infection with PH2. (iii): Surface topography of nasopharyngeal- derived ALI model following PH202 infection. Panels (iv) and (v) represent BNEC ALI cultures following infection with PH2. All images represent cultures 24 h after infection. Asterisk panels reflect corresponding marked areas in image (v). Arrow heads denote foci of bacterial attachment. Scale bars are as follows; 10µm for (i) and (iii); 2µm for (ii) and (v), 50µm for (iv), and 500nm for all asterisk marked panels.

Close inspection of bacteria within these microcolonies revealed several phenotypic properties that were not observed for bacteria infecting the BBEC ALI cultures (Fig 4.8 [v]) and asterisk marked inserts). Properties include the production of an EPS-like material and evidence of distinct interactions with the host epithelium. Another property of note was the appearance of one or more 'dimples' on the bacterial cell surface. While these were observed previously under other conditions they are somewhat prominent in this case. Although well-defined they may reflect an artefact of the SEM process which causes local collapse in some regions of the bacterial cell.

Histological cross sections were taken for PH2-infected and PH202-Infected BTEC, BBEC and BNEC ALI cultures at six and 24 h post-infection. Sections were stained with H&E and Giemsa to identify regions of bacterial colonisation (Fig 4.9). Limited invasion was observed for either of the two tracheal ALI PH2 infected replicates (Fig 4.9 [i]). Multiple foci of bacterial surface penetration were observed in the PH2-infected BBEC ALI cultures (Fig 4.9 [ii]). Considerable foci of bacterial tissue invasion were also observed in PH2-infected BNEC ALI cultures (Fig 4.9 [iii]). No foci could be observed for PH202 infected models regardless of anatomical location (Fig 4.9 [iv], [v] & [vi]). The appearances of PH2 foci were similar in all cases, with bacteria appearing to breach the surface epithelium in one or more locations. Other foci displayed bacteria directly beneath regions of intact epithelium. Contrary to this, some foci appear entirely 'open' from the apical face. This leads to the proposal of a four-stage infection process (Fig 4.10), beginning with small numbers of bacteria gaining access to the sub-apical space (Fig 4.10 [i]). This is followed by traversal of the epithelium by the bacteria in the basal direction (Fig 4.10 [ii]). Replication then occurs which disseminates the bacteria laterally (Fig 4.10 [iii]). Replication continues where bacteria eventually reach the apical face giving rise to the appearance of a large 'chasm' with extensive numbers of bacterial cells and disrupted tissue (Fig 4.10 [iv]).

Large spaces in the tissue structure as indicated by the star in panel [ii] (Fig 4.10) are, as previously mentioned (2.3.2.6), suspected to be localised regions of epithelial cell death. As shown previously they occur in the absence of infection.

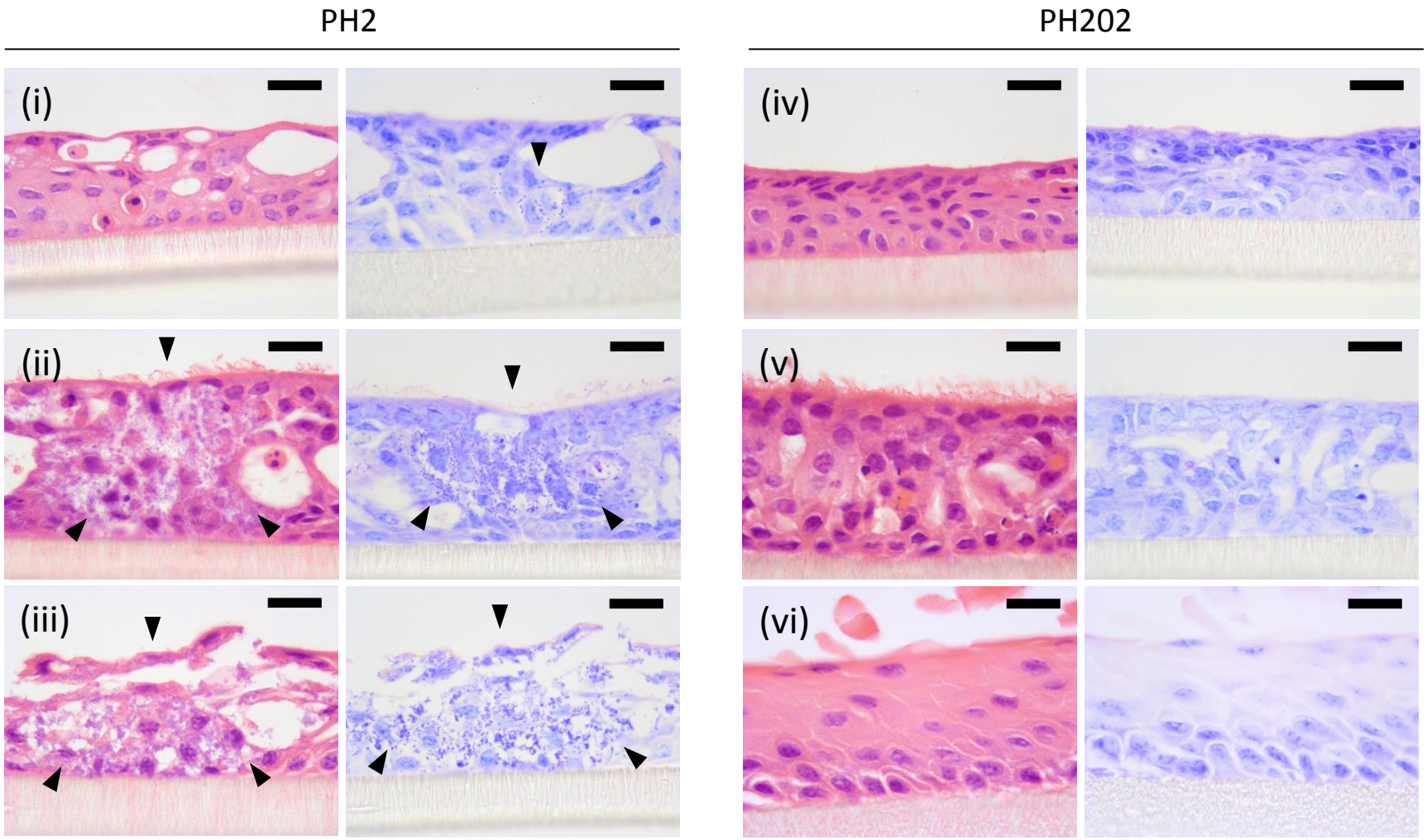

Fig 4.9 Cross sectional analysis of infected ALI cultures derived from different anatomic sites
Paired histological sections stained with H&E and Giemsa. Images show PH2-infected BTEC ALI cells (i), BBEC ALI cells (ii), and BNEC ALI cells (iii) and PH202-infected BTEC ALI cells (iv), BBEC ALI cells (v) and BNEC ALI cells (vi). All scale bars represent 20µm. Black arrows highlight foci of invading bacteria.

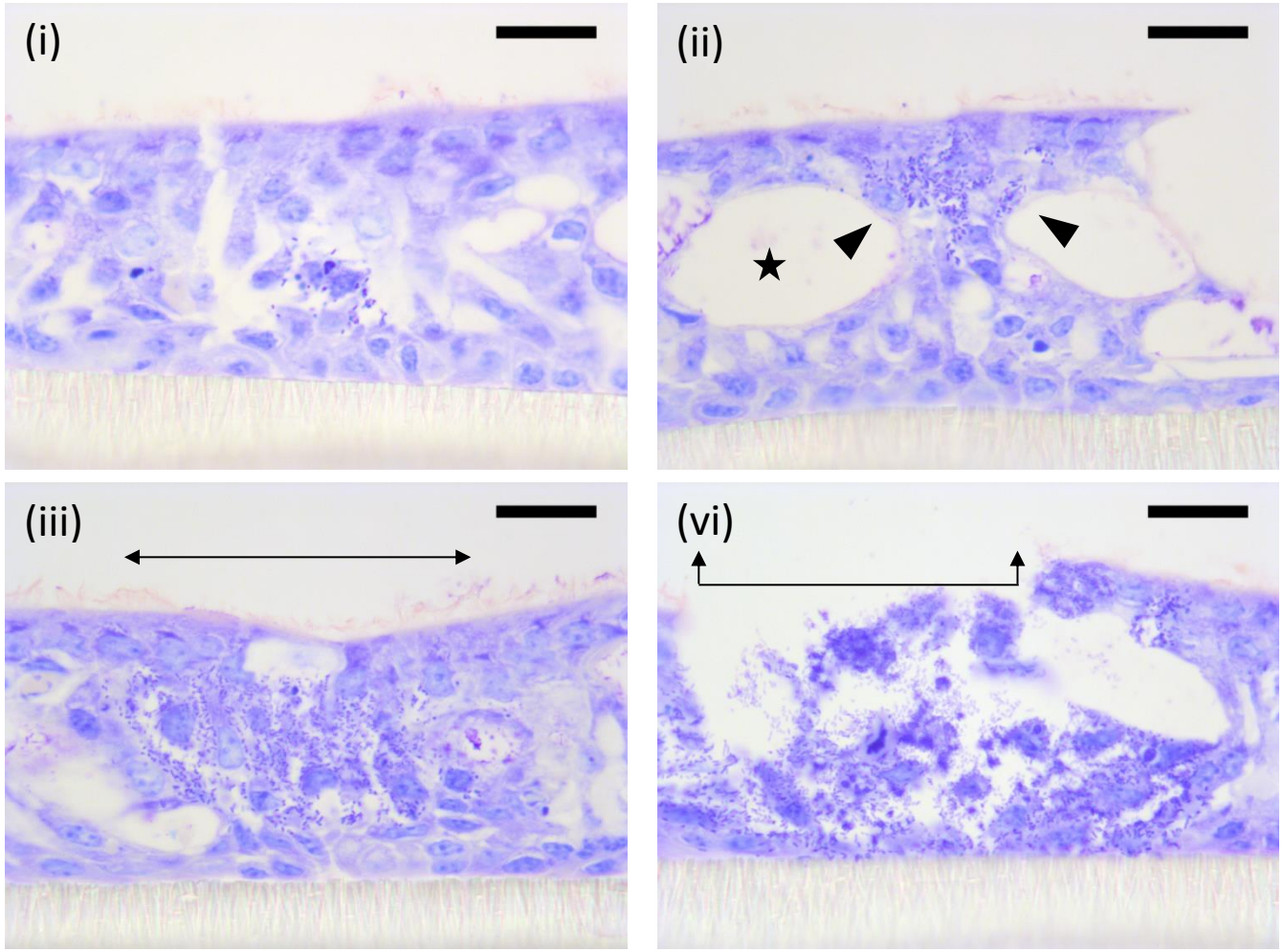

Fig 4.10 Stages of *M. haemolytica* tissue invasion
Foci of bacterial attachment capturing the hypothetical stages of tissue invasion as exemplified by PH2 infecting the bronchial model. Small numbers of bacteria gain access to the sub-apical space. Replication beneath the surface begins (ii), foci are identified by arrows, and starred region highlights an area of missing epithelial cells. Bacteria replicate and disseminate laterally in the x-y plane (iii). As bacteria grow upward they destroy the surrounding tissue creating a void in the epithelial surface (iv). All scale bars represents 20µm.

4.4 Discussion

Introduction. Current understanding of *M. haemolytica* infection presents with a considerable knowledge gap. Extensive research conducted since the organism's discovery has uncovered the mechanisms by which the bacterium elicits lung damage in the host. Arguably, the secretion of the pore-forming leukotoxin is the central perpetrator of the damage. Studies have revealed much about the role of leukotoxin in the disease process including its production, secretion, delivery, mechanism action, molecular evolution and the resulting immune response against it. However, a complete lack of understanding remains over events relating to colonisation of the respiratory tract by *M. haemolytica* and to its subsequent transition from a harmless commensal of the URT to a disease-causing pathogen of the LRT. For these reasons, an ALI epithelial culture system was developed (Chapter 2) that recapitulates the host epithelium in an attempt to address this knowledge gap.

Adherence of M. haemolytica to submerged epithelial cells. The initial characterisation sought to examine whether *M. haemolytica* could adhere to and colonise submerged epithelial cells. Low numbers of adherent *M. haemolytica* were identified under most conditions. However, large numbers of PH284 were observed on the surface of OTEC that had been expanded in culture for 72 h on fibronectin- or collagen-coated coverslips. Several reasons could account for this observation. Collagen and fibronectin coating is a common tissue culture procedure aimed at increasing cell adhesion to surfaces (Cooke *et al.*, 2008; Kleinman *et al.*, 1981; Liberio *et al.*, 2014). However, epithelial cells cultured on collagen or fibronectin have been shown to produce expression changes in various genes (Câmara & Jarai, 2010; Lafrenie *et al.*, 1998; Lam *et al.*, 2001). Thus, the use of coated coverslips in this experiment was on the basis that cell-surface receptor expression might be altered when compared with uncoated coverslips. Consequently, if a particular receptor is required for *M. haemolytica* colonisation, then colonisation of submerged epithelial cells might only occur when the epithelial cells are grown on ECM proteins. Although this is possible, the SEM evidence displaying bacteria bound to the collagen and fibronectin coated coverslips as well as to the epithelial cells suggests these incidences of adherence are artefactual. This idea is enhanced when considering that the OmpA protein of *M. haemolytica* binds fibronectin (Lo & Sorensen, 2007), and

that *M. haemolytica* encodes a YadA orthologue, which in *Yesinia spp*. can bind collagen and fibronectin (Flugel *et al.*, 1994; Gioia *et al.*, 2006; Nummelin *et al.*, 2004; Schulze-Koops *et al.*, 1993). In summary, the conclusion was made that submerged epithelial culture is an ineffective model system.

Kisiela & Czuprynski (2009) have demonstrated that *M. haemolytica* adheres to submerged epithelial cells. The experimental conditions used by these authors for infection included 10^8 CFU/ml of serotype A1 *M. haemolytica* incubated with a monolayer of primary BBEC for a total of two hours. These infection conditions constitute one of the submerged conditions investigated herein (Table 4.2). Thus, the question is raised, as to why so few adherent bacterial cells were observed by SEM under these conditions. One aspect that might account for the discrepancy is the media used for infection. Kisiela & Czuprynski (2009) conducted the infection of BBECs with bacteria suspended in RPMI media whereas in the present study infections were carried out in DMEM. Kisiela & Czuprynski (2009) identified two key adhesins, OmpA and PlpA, as necessary for adherence of *M. haemolytica* to submerged-grown BBECs. PlpA and OmpA were identified in the proteomic analysis of serotype A1 BHIB grown *M. haemolytica*. However, it is possible that expression changes occur following resuspension of *M. haemolytica* in DMEM. While the expression of OmpA is unlikely to change, owing to its essential role in biogenesis and integrity, the expression of PlpA might change when bacteria are suspended in DMEM resulting in a loss of adherence. PlpA was not identified in *M. haemolytica* isolate PH2 grown in DMEM by either gel-based or gel-free proteomic analysis (Hounsome, 2012). However, PlpA also failed to be identified in PH2 when grown in RPMI media (Hounsome, 2012). Therefore, another more pragmatic explanation might be that either the strain of *M. haemolytica* or differences in cell-to-cell variation between different hosts accounts for the discrepancy between the results herein and those of Kisiela & Czuprynski (2009). Either way, additional infections would be needed to establish the true nature of adherence to BBECs.

Advantages of ALI epithelial cells over submerged epithelial cells. Fundamentally, the microenvironment generated in an ALI model is distinctly different from that of submerged culture. Several factors account for this. The main advantage of ALI culture over submerged culture is the production of

multiple cell types that resemble the *in vivo* epithelium (BéruBé *et al.*, 2010, 2011). While ALI culture results in the emergence of ciliated, Clara, basal and mucus-producing goblet cells, submerged culture results in only basal-like cells. Thus, as ALI culture is more representative of the *in vivo* epithelium it represents a more accurate infection model. However, there are other differences between these two culture systems that warrant consideration.

Crucially, differences in gene expression have been noted between ALI and submerged culture (Pezzulo *et al.*, 2011), where primary cells cultured at ALI produce the closest transcriptional match to the native environment. The physiological relevance of culturing cells at an air-interface, something which mimics the natural host, has profound consequences when evaluating these cultures as infection models. Recently, an evaluation of submerged and ALI culture in response to challenge with flagellin demonstrated that ALI cells had a considerably different transcriptional profile in response to flagellin as compared with submerged cells (Clark *et al.*, 2015). The transcription of genes involved in the immune response was found to be much higher in submerged epithelial cells as compared to ALI epithelial cells. This point serves to highlight the physiological differences between the culture systems.

Polarisation represents another fundamental difference between ALI and submerged culture. As ALI cultures develop into a pseudostratified epithelium (Kondo *et al.*, 1993; Yamaya *et al.*, 1992), cells polarise to segregate their membrane into apical and basolateral regions (Fig 1.15). Differential protein sorting follows, where membrane proteins are either targeted towards the apical or basaolateral membranes. Crucially, this creates differences in toll-like receptor (TLR) distribution. TLR5, which recognises flagellin, is understood to localise at the basolateral membrane (Muir *et al.*, 2004), but will mobilise to the apical surface following flagellin challenge within a period of four hours (Adamo *et al.*, 2004). Clark *et al.* (2015) examined the effect of flagellin challenge on ALI-grown and submerged epithelial cells. Four hours after flagellin challenge the transcription of immune-related genes was higher for submerged culture than for ALI culture. However, considering the knowledge that in polarised epithelial cells TLR5 must first be mobilised to the apical surface the discrepancy between these two culture systems becomes apparent; that the

response to flagellin in ALI and *in vivo* might take longer than is observed for submerged culture. Therefore, this is another example where submerged culture could produce artefactual results and serves to highlight an important aspect of ALI culture - time. Submerged infection requires the suspension of bacteria either in tissue culture media, which doesn't reflect the *in vivo* luminal availability of nutrients, or in saline which depletes the epithelial cells of nutrients. Consequently, only short time scales, of the order of a few hours, are feasible for submerged culture. ALI culture circumvents this problem by allowing for the supply of media from the basolateral face while allowing for apical infection of bacteria suspended in a small volume of saline. Consequently, much longer infection times can be tolerated, allowing for the study of processes that fall out-with the ≈4 hour time limit imposed by submerged culture. Studies have used ALI systems to look at bacterial infection of up to one week post infection (Gross *et al.*, 2010). All of these factors, including the production of cilia and mucus, warrant the investigation of *M. haemolytica* colonisation by ALI culture.

Adherence of M. haemolytica to ALI-grown epithelial cells. Initial infection by *M. haemolytica* isolates of OTEC and BTEC ALI cultures revealed multiple phenotypic properties that were unobserved in submerged culture. The use of the ALI models demonstrated that isolate PH284 (after 6 h) and isolates PH2 and PH376 (after 24 h) can be found invading, and adhering to, the sub-apical region of the epithelium. This observation raises several questions relating to the route of entry, the cellular targets, and whether or not the process is passive or actively driven.

The first of these questions, concerning the route of entry, involves one of two possibilities: *M. haemolytica* gains access to the sub-apical space by either transcytosis or paracytosis. Analysis of epithelial permeability (Fig 4.5) during the infection process suggests that the process occurs via paracytosis owing to the decrease in TEER following 24 hours of infection, indicative of tight-junction disruption. Confirmation by a gentamycin protection assay to rule out transcytosis and analysis of the tight junction integrity during infection would substantiate this hypothesis. Other bacteria that invade the respiratory epithelium via paracytosis include *B. cepacia* (Kim *et al.*, 2005; Schwab *et al.*,

2002), *H. influenzae* (Ren *et al.*, 2012; van Schilfgaarde *et al.*, 1995) and *P. aeruginosa* (Zulianello *et al.*, 2006). In the case of *B. cepacia* different genomovars have been shown to mediate paracellular invasion in different ways, where the formation of a biofilm is a prerequisite in some strains but not in others (Schwab *et al.*, 2002). This is important when considering the differences in apparent cell invasion observed with different *M. haemolytica* strains in the present study. Namely, that PH2 and PH376 displayed a widespread tissue invasion 24 hours post infection while isolate PH284 demonstrated this property after as little as 6 hours; isolate PH202, a non-pathogenic bovine isolate showed little to no abillity to colonise BBEC Aside from *B. cepacia,* other bacterial pathogens exhibit a link between biofilm formation and paracellular invasion. *P. aeruginosa* quorum sensing molecules have been shown to interfere with ZO-1 and occludin transcription resulting in a loss of barrier integrity (Vikström *et al.*, 2006). As PH284 was the only isolate which demonstrated widespread secretion of an EPS-like material the possibility exists that biofilm formation and paracytosis are linked in this particular strain. However, in contrast to *P. aeruginosa*, the production of EPS was observed at the latter time point, after the observation of sub-apical bacterial colonisation. Thus, it is possible that in *M. haemolytica* isolate PH284, tissue invasion and sub-apical colonisation is a prerequisite to biofilm formation (Fig 4.11). In this hypothesis, colonisation of the sub-apical space might allow for bacterial growth, upward, into the large bacterial aggregates observed at 24 hours post infection. The result of which is a structure, topographically elevated relative to the epitheliums apical face, yet anchored to the sub-apical region.

The next question with regard to the observed tissue invasion is why *M. haemolytica* was observed predominantly adhering to the sub-apical space yet not the apical surface. One explanation is that the basolateral membrane of polarised cells and the membrane of basal cells contain cell surface receptors distinct from the apical membrane (Rodriguez-Boulan & Macara, 2014). Various signals determine which proteins are sorted to the apical and basolateral membrane, for apical sorting N and O glycosylation as well as the glycosyl phosphatidyl inositol (GPI) anchor are the main determinants (Lisanti *et al.*, 1989; Scheiffele *et al.*, 1995; Yeaman *et al.*, 1997), for basolateral sorting peptide motifs in the cytoplasmic domain of the protein are responsible for

targeting (Rodriguez-Boulan & Macara, 2014). Thus, the target for *M. haemolytica* adherence to the sub-apical space, and the trigger to initiate replication, may be the recognition of a particular receptor that is only present on these membrane locations (Fig 4.12).

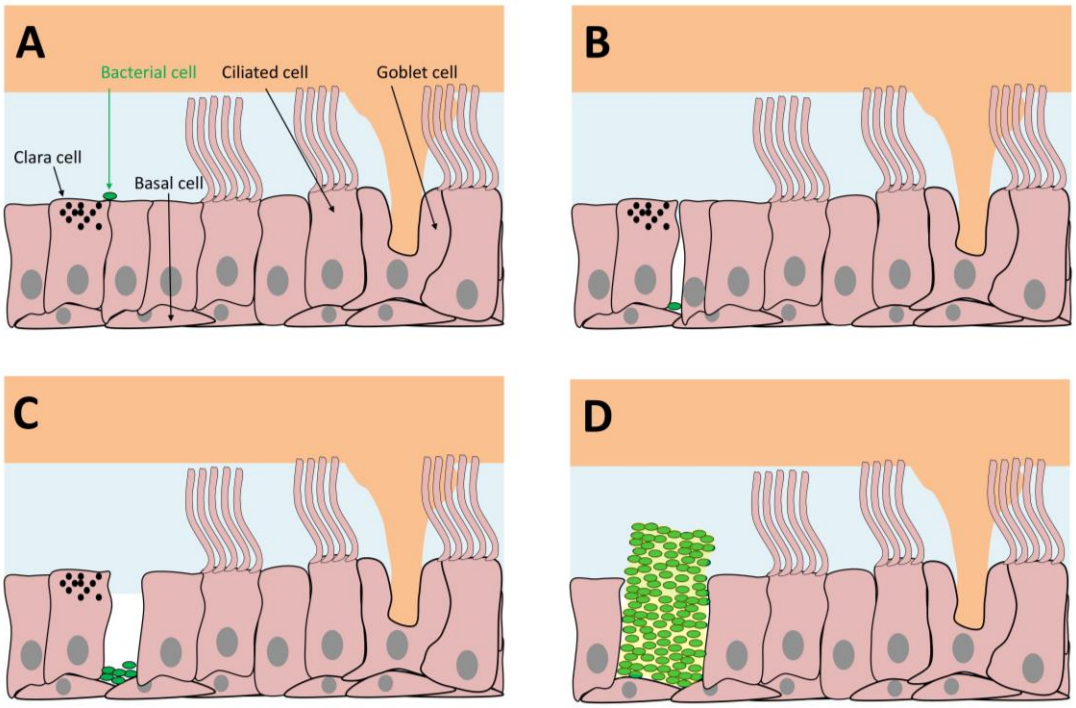

Fig 4.11 Paracytosis is a prerequisite to biofilm formation
On the basis of observing sub-apical colonisation by PH284 after 6 h and, at 24 h, observing the presence of microcolonies displaying signs of early biofilm formation the following mechanism is proposed. (A) A small number of bacteria adhere to the apical surface of the epithelium. (B) Weakening of the tight junctions allows for access to the sub-apical region. (C) Corresponding with the SEM observations at 6 h, bacteria begin to replicate in the sub-apical space. (D) Corresponding with the SEM observation after 24 h, a large microcolony, routed in the sup-apical space and with EPS secretion, is formed that protrudes above the surface epithelium.

Distinct interactions with the apical and basolateral membrane are observed in other respiratory pathogens. For example, *P. aeruginosa* has been shown to target α5β3 integrins in the repairing airway (Roger *et al.*, 1999). This process involves basal cells infiltrating into an epithelial lesion to begin the repair process. As α5β3 is located only on the basaolateral membrane of polarised cells, *P. aeruginosa* can't ordinarily access it except during the repair process. Additionally, *P. aeruginosa* has been shown to specifically target N-linked glycans via type IV pili on the apical membrane and heparan sulphate

proteoglycans via flagella on the basolateral membrane (Bucior *et al.*, 2010, 2012). Recognition of each of these components leads to internalisation via distinct pathways. Thus, it is possible that differences in receptor profiles of different cell membranes within the respiratory epithelium may account for the observation of *M. haemolytica* sub-apical colonisation.

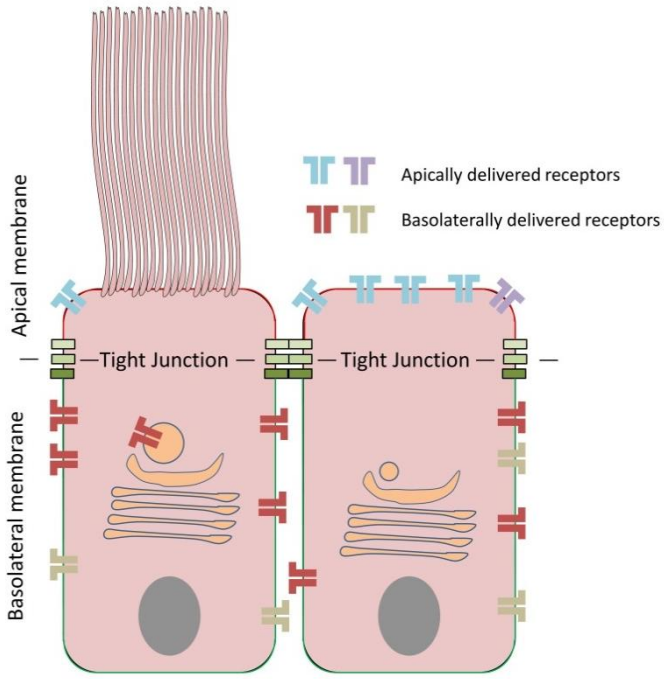

Fig 4.12 Basolateral and apical membrane separation
The 'fence' function of tight junctions serves to separate the membranes of polarised cells into apical and basolateral regions each of which have distinct trafficking routes so as to deliver membrane proteins to one or the other. Thus, the receptor profile for apical and basolateral membranes is different.

What is less clear is how *M. haemolytica* accesses the sub-apical region. Bovine herpes virus-1 (BHV-1) which is associated with BVRD is known to elicit damage to the respiratory epithelium (Srikumaran *et al.*, 2007); this process could expose basal cells to *M. haemolytica in vivo* and allow for the secondary colonisation of bacterium. However, examination of BHV-1 in a bovine ALI airway epithelial model has demonstrated the virus predominantly infects basal cells where the prior opening of the tight junctions was required (Kirchhoff *et al.*, 2014). The possibility exists that one of the other viruses of BRD might be involved in the process. However, as the results presented here involve no pre-

viral challenge the question remains of whether the sub-apical colonisation is opportunistic or pathogen driven.

The opportunistic nature of *M. haemolytica* infection can easily fit the following hypothesis with some consideration. As components of the bacterium will be recognised by TLR and pattern recognition receptors (PRR) an innate pro-inflammatory immune response in the form of cytokine release is likely to be generated in the ALI model (Stadnyk, 1994). One effect of cytokines on the mucosal epithelium is to increase permeability (Coyne *et al.*, 2002; Petecchia *et al.*, 2012). This has been demonstrated to occur following IL-1β (Al-Sadi & Ma, 2007), TNF-α (Poritz *et al.*, 2004) and INF-γ stimulation (Patrick *et al.*, 2006). In the case of INF-γ, the increased permeability conferred upon epithelial cells (T84 and Caco-2) is directly correlated with an increased translocation of commensal *E. coli* across the epithelium (Clark *et al.*, 2005). Clarke *et al.* (2011) demonstrated that direct recognition of *H. influenzae* by TLR4 and *S. pneumoniae* by TLR2 results in a decrease in epithelial barrier integrity facilitating the translocation of bacteria across the epithelium. Claudins 7 and 10 were down-regulated following infection, an effect which was shown to be directly responsible for translocation of bacteria. A mechanism was identified involving the downstream activation of P38 MAPK and TGF-β signalling which led to the upregulation of SNAIL, a transcription factor responsible for repressing the transcription of many tight junction-related genes. As the results by Clarke *et al.* (2011) were shown to occur for both Gram-positive and Gram-negative bacteria the conclusion was made that this mechanism of paracytosis might be generic to many respiratory pathogens. Therefore, in the case of *M. haemolytica* infecting the ALI model, permeability changes resulting from immune engagement may open up the epithelium to allow for *M. haemolytica* to access the sub-apical region. Furthermore, this process might be mechanistically driven in a similar manner as was reported for *H. influenzae* and *S. pneumoniae* by Clarke *et al.* (2011). However, the non-pathogenic A2 serotype strain (PH202) was unable to elicit the same pattern of tissue invasion with relatively few bacteria recovered from ALI grown BBEC after 24 h. The possibility exists that immune recognition of PH202 still occurs and still induces permeability changes in the epithelium; indeed if that is the case the differences observed between PH2 and PH202 might be the result of differences

in the abillity to adhere to the sub-apical portions of the epithelium, more work would be required to examine if this is the case.

Additionally, LPS has been shown to directly increase epithelial permeability (Serikov *et al.*, 2004), and this can be replicated *in vitro* to the effect of reducing barrier integrity (Luyts *et al.*, 2015). The LPS of *M. haemolytica* has been shown to have no effect on the barrier integrity of pneumocytes monolayers (McClenahan *et al.*, 2008), yet ATP which causes a potent reduction in barrier integrity (McClenahan *et al.*, 2009) has been demonstrated to be two fold higher in BAL samples recovered from calves challenged with *M. haemolytica* LPS as compared to control calves (Craddick *et al.*, 2012). Thus, the effects of sub-apical colonisation, demonstrated in the present study, might be initiated following ATP release as a consequence of LPS recognition.

Polymorphonuclear leukocytes (PMNs) contribute to the process of junctional complex degradation and repair *in vivo*. Translocation of PMNs across the respiratory epithelium has been shown to occur in response to TLR2-mediated recognition of microbial targets which leads to IL-8 production and the generation of secondary Ca^{2+} gradients (Chun & Prince, 2006, 2009). Proteolytic degradation of occludin and E-cadherin by Ca^{2+}-dependent enzymes allow for PMN translocation (Chun & Prince, 2009). The translocation of neutrophils has also been shown to cause a transient, reversible decrease in epithelial TEER (Zemans *et al.*, 2011). This reversible trend was attributed to the cleavage of E-cadherin, releasing β-cantenin and activation of the canonical Wnt pathway. The result being the transcription of proteins involved in the repair of the epithelium post-neutrophil translocation. Thus, for these reasons and because *M. haemolytica* infection is intrinsically linked with the infiltration of neutrophils into the bovine lung, the development of a model that incorporates immune cell transmigration might be necessary to fully understand the observed paracytosis.

Recently a new opportunistic mechanism by which *P. aeruginosa* migrates across the respiratory epithelium has been described by Golovkine *et al.* (2016). *P. aeruginosa* was shown to undergo paracytosis across the respiratory epithelium in regions where cells were epithelial barrier integrity was transiently altered (Golovkine *et al.*, 2016). The transient changes included mitosis, apoptosis and surface extrusions. Thus, the possibility exists that *M. haemolytica* crosses the

bovine respiratory epithelium in a similar process, taking advantage of natural fluctuations in epithelial barrier integrity.

The other possibility with regard to the observed sub-apical colonisation is that *M. haemolytica* is actively interfering with junctional complexes in some respect. In this regard *M. haemolytica* might produce a secreted effector protein that targets aspects of tight junction formation. Active targeting of junctional complexes is well documented in certain bacterial species. Enteropathogenic *E. coli* (EPEC) delivers the T3SS effectors NleA, EspF, EspG and Map that interfere with tight junctions of the intestinal epithelium (Dean & Kenny, 2004; McNamara *et al.*, 2001; Thanabalasuriar *et al.*, 2010; Tomson *et al.*, 2005). In the context of respiratory infection, *P. aeuruginosa* produces a virulence factor, elastase, which has been demonstrated to be directly capable of disrupting tight junctions through interference with multiple signalling pathways (Azghani *et al.*, 2000; Clark *et al.*, 2011; Nomura *et al.*, 2014). While no such virulence factor has been reported for *M. haemolytica,* the observed sub-apical colonisation may result from an active targeting of the tight junctions by some yet unknown mechanism. Further investigation would be required.

Filamentation and microvesicle formation. Two additional phenotypic properties were identified in isolate PH284 that were either not observed or were infrequently observed in the other isolates tested. One of these properties was that the sub-apically adhered bacteria exhibited filamentation (Fig 4.2 [iv]). Although isolates PH2 and PH376 displayed small numbers of filamentous bacteria the microcolonies of PH284 appeared to contain more filamentous bacteria. Filamentation has been demonstrated to precede the entry of *L. pneumophila* into airway epithelial cells (Prashar *et al.*, 2012). The formation of a filamentous cell structure correlated with internalisation via a mechanism of actin rearrangement leading to the eventual engulfment into the cytoplasm. Division into multiple progeny could then occur. Other examples of filamentation playing a role in respiratory infection include biofilm formation. For *P. aeruginosa*, it has been demonstrated that the thickened lung mucus of CF patients creates an anaerobic environment and that growth in this oxygen depleted environment triggers filamentation which subsequently leads to biofilm formation (Yoon *et al.*, 2011). Biofilms formed under these conditions were

found to be more robust than aerobically-grown biofilms, a property directly attributed to the increased cell size which allowed for better clumping. The possibility exists that paracytosis or biofilm formation in *M. haemolytica* is linked to the filamentous phenotype. Although purely speculative it would nonetheless be interesting to examine.

The second observation was the presence of what appeared to be OM vesicles or blebs on the cell-surface of isolate PH284 (Fig 4.2 [vi]). Outer membrane vesicles (OMVs) are blebbed fragments of the OM that consist of an asymmetric bilayer comprised of phospholipid in the inner leaflet and LPS in the outer leaflet (Kulp & Kuehn, 2010). Contained within the membrane are OMPs and contained within the vesicle are any periplasmic proteins trapped during formation (Kulp & Kuehn, 2010). Thus, OMVs are essentially nanoscale macromolecular replicas of the cell surface. Roles in virulence of OMVs include effector delivery (Kadurugamuwa & Beveridge, 1996; Li *et al.*, 1996) and allowing for bacterial uptake (Furuta *et al.*, 2009). The production of microvesicles by *M. haemolytica* has been documented previously for A1 and A2 isolates of sheep (Ruiz-Gonzalez *et al.*, 2007). The vesicle composition was determined to be similar to that of the OM protein fraction with some slight differences. The presence of leukotoxin in these microvesicles was also confirmed. Although these results demonstrate that *M. haemolytica* produces microvesicles, they were generated in broth culture via gentamycin spiking, something which has been shown to produce OMVs of different composition and functionality to natural OMVs (Kadurugamuwa & Beveridge, 1996). Furthermore Ruiz-Gonzalez *et al.* (2007) did not examine their role during colonisation. Presented here is the first evidence that *M. haemolytica* microvesicle production may play a role in the pathogenesis of pneumonic pasteurellosis during the early stages of colonisation. Further characterisation would be required to confirm if indeed they are microvesicles and to establish their role in colonisation.

Adherence of *M. haemolytica* to ALI epithelial cells derived from different regions of the bovine respiratory tract. As the pathology of *M. haemolytica* is characteristically opportunistic and because this reflects a transition from URT commensalism to LRT pathogenicity, the abillity of *M. haemolytica* to colonise ALI epithelial cells derived from different regions of the respiratory tract was

investigated. A comparison was made in the ability of a pathogenic serotype A1 strain and a non-pathogenic serotype A2 strain to colonise nasopharyngeal-, tracheal- and bronchial-derived ALI epithelial cultures. It was demonstrated that isolate PH2, the pathogenic A1 strain, had a propensity for colonising bronchial ALI epithelial cultures compared with the tracheal and nasopharyngeal ALI epithelial cultures. Conversely, isolate PH202, the non-pathogenic bovine A2 strain, exhibited no apparent colonisation of the bronchial- and tracheal-derived ALI epithelial cultures yet adherent bacteria could be found on the BNEC ALI cultures.

The cellular composition and anatomical structure of the conducting airways varies spatially within the respiratory tract (Albertine, 2015). Thus, subtly different microenvironments are encountered in different anatomical locations within the respiratory tract. Some prominent factors that contribute to this include cell type composition (Miller *et al.*, 2011; Toskala *et al.*, 2005), mucin production (Kahwa & Purton, 1996), viscoelasticity of mucus (Lai *et al.*, 2009), ciliary beat frequency (Joki & Saano, 1994) as well as differences in immune response (Brand *et al.*, 2012). Consequently, bacteria adapted to these different niches may well exhibit different patterns of colonisation, especially in levels of adherence (Euba *et al.*, 2015), invasion (Euba *et al.*, 2015) and gross pathology (Scheller *et al.*, 2015).

Pathogens of the *Bordetella* genus are some of the most extensively characterised organisms with regards to spatio-temporal colonisation of the lung. *Bordetella pertussis* has been shown to be capable of producing biofilms in both the nasopharynx and trachea of mice, a process that is dependent on FHA expression (Serra *et al.*, 2011). Early research identified that FHA and pertactin were responsible for lung colonisation, with deletion of either resulting in impairment of colonisation (Khelef *et al.*, 1994). However, research contrary to this suggested only deletion of FHA and abolition of the ADP-ribosylating activity of pertussis toxin together produced the observed impairment (Pethe *et al.*, 2001). Other studies on the closely related *B. bronchiseptica* have served to show that colonisation of the larynx and trachea, but not the nasopharynx, are partially dependent on FHA (Cotter *et al.*, 1998). This dependence was pinpointed to the action of the mucocillary escalator as the trachea of

anesthetised animals could be colonised by FHA-deficient *B. broncheceptica*. A similar observation was reported for fimbriae (type I pili) where deletion in *B. bronchiseptica* resulted in decreased colonisation of the larynx and trachea, but not of the nasopharynx (Mattoo *et al.*, 2000). The deletion of pili has since been confirmed not to alter nasopharyngeal colonisation while impairing that of the trachea (Scheller *et al.*, 2015). Deletion was additionally shown to result in bacterial mislocation away from cilia of the conducting airways towards the aveoli (Scheller *et al.*, 2015). Discrepancy in the colonisation of the URT and LRT can also be observed for *B. pertussis*, where a whole-cell *B. pertussis* vaccine was able to reduce the colonisation of *B. bronchiseptica* in the LRT, but crucially not the URT (Goebel et al., 2009). Taken together, these studies highlight differences in the colonisation properties of a bacterium towards different tissues (i.e. tissue tropism).

The *Bordetellae* example also provides an illustration that might explain some of the anatomically distinct colonisation patterns observed with *M. haemolytica*. The observation made that isolate PH2, the pathogenic A1 isolate, can colonise BBEC ALI cultures to a greater extent than cells from either of the other sites, is strongly suggestive that the organism has a propensity for bronchial colonisation. That is not to say that is doesn't colonise the trachea or the nasopharynx; indeed, low levels of adherence were observed for cells from both sites and microcolonies could be observed on the surface of the BNEC ALI epithelial cells (Fig 4.7). But, crucially, no sub-apical attachment was observed in BTEC (mid-trachea) and BNEC ALI cultures. It suggests that a signal is encountered on the BBEC ALI cultures that allows for the ensuing infection. *M. haemolytica* possesses an orthologue of the *Bordetella* FHA along with many other adhesins (Gioia *et al.*, 2006; Lawrence *et al.*, 2010). Thus, it is possible that a receptor-mediated interaction provides the necessary stimulus for the ensuing tissue invasion and that the receptor is potentially not expressed on cells derived from the other sites.

Another consideration may account for the differences in ciliation of the ALI cultures obtained from the three anatomical sites (Fig 2.16). As ciliation increased in the order nasopharyngeal, tracheal and bronchial cells, it might be reasonable to assume this plays a role. Comparison with *Bordetella*, which has

been shown to adhere to the cilia of the respiratory epithelium (Edwards *et al.*, 2005), would offer an explanation for this observation were it not for the fact that *M. haemolytica* adherence is largely confined to non-ciliated areas. However, it is possible that differentiation into the mucociliary phenotype is correlated with the expression of a particular receptor. Thus, the differences in *M. haemolytica* colonisation of BTEC, BBEC and BNEC ALI epithelial cells might be the result of differences in the level of differentiation. Therefore, were the BTEC and BNEC cultures more ciliated, a receptor, required for colonisation, might be expressed in greater abundance, consequently producing comparable levels of adherence as observed herein with the BBEC ALI cultures.

Another possibility considers that increased mucus production coincides with an increase in ciliation. This is considering that ciliated cells are derived from secretory cells (Watson *et al.*, 2015). Mucus production has been observed in many of the ALI cultures analysed and therefore the possibility exists that recognition of mucin glycoproteins may initiate the chain of events leading to the observed levels of adherence, by isolate PH2, to BBEC ALI cultures.

The question is whether the tissue invasion and sub-apical adherence to the BBEC ALI cultures, as compared to cells from the other two anatomical locations, is a reflection of the anatomical origin or due to artefactual differences resulting, perhaps, from differences in differentiation. Production of these cultures (BTEC, BBEC and BNEC) under different culture conditions with the aim to standardise ciliation and mucus production could provide an answer to this problem. However, differences in the culture conditions would not make for an effective comparison either. Therefore, the elucidation of an answer may require a multifaceted approach encompassing *in vivo* as well as *in vitro* infection studies.

Conclusions. In summary, the infection of airway epithelial cells by *M. haemolytica* has revealed several interesting properties of adherence and colonisation that serve as the basis of future study. Sub-apical invasion of *M. haemolytica* into the deeper regions of the epithelium has not, until now, been described. Additional phenotypic observations were made of *M. haemolytica* during colonisation including the production of microvesicles, secretion of EPS-like material and the presence of filamentous bacterial cells. The discovery that

a serotype A1 pathogenic bovine isolate preferentially colonises BBEC ALI cells over BNEC and BTEC ALI cultures strongly supports the hypothesis that this isolate is adapted to colonise the lower regions of respiratory tract. This is further substantiated when considering that a non-pathogenic bovine A2 isolate was incapable of colonising BBEC ALI cultures to any degree. Furthermore, both A1 pathogenic and A2 non-pathogenic bovine isolates could colonise the nasopharyngeal derived ALI cells with low frequency. Together, these results highlight that the use of ALI culture is likely to prove useful in understanding the fundamental differences in pathogenicity between different strains of *M. haemolytica*. In conclusion, the use of ALI culture has the potential to reveal much information about adherence and colonisation of the host respiratory tract. The improved mimicry of the *in vivo* environment over submerged culture and the user-defined control afforded by the culture system will undoubtedly benefit the future understanding of the *M. haemolytica* infection process.

Chapter 5 Final Discussion

Mannheimia haemolytica, responsible for pneumonic pasteurellosis of cattle and sheep, continues to be the number one cause of feedlot morbidity and mortality in the livestock industry (Singh *et al.*, 2011). The consequences of this are large economic losses to the farming industry (Griffin, 1997). While much is understood about the pathology of the disease and the primary virulence factor, leukotoxin, a distinct lack of understanding remains around the colonisation process. Whereas leukotoxin is responsible for the necrotic lung damage, other virulence factors are responsible for the colonisation of the URT and proliferation in the LRT. This point is iterated in the efficacy of current vaccines. Whilst leukotoxin represents the most thoroughly characterised of the *M. haemolytica* virulence factors, vaccination with recombinant leukotoxin alone offers only partial protection against challenge by *M. haemolytica* (Conlon *et al.*, 1991). Furthermore, improved coverage is obtained by supplementation of leukotoxin with other components of the secretome or OM antigens (Ayalew *et al.*, 2008; Confer *et al.*, 2009; Conlon *et al.*, 1991; Shewen *et al.*, 2003; Sutherland *et al.*, 1989). Thus, understanding the role of other virulence factors during the colonisation process would greatly enhance our understanding of pneumonic pasteurellosis and could underpin the development of improved vaccines.

This study aimed to address the knowledge gap surrounding the colonisation process by developing a 3D *in vitro* airway epithelial cell model of the bovine respiratory tract. This was used to characterise the phenotypic properties of *M. haemolytica* during the early stages of colonisation. Simultaneously, a rigorous characterisation of the OM proteome was performed on a selected panel of *M. haemolytica* isolates. Together, these two areas of research have provided new insights into the process of colonisation and identified putative virulence factors likely to be involved.

In vitro respiratory tract modelling involves constructing a cell culture that is representative of the *in vivo* environment. An *in vitro* culture serves as a platform to investigate or 'model' *in vivo* processes. The ALI *in vitro* model is a system in which the basal-like cells of a submerged culture are encouraged to differentiate into the multicellular mucociliary phenotype (Wu *et al.*, 1986).

This produces an accurate reflection of the natural respiratory epithelium while allowing for user-defined control over the experimental system. Therefore, an ALI airway epithelial model of the bovine respiratory tract was developed via a series of optimisation stages.

Refinement of various parameters that influence differentiation was assessed including the base media, substrate material, oxygen tension, growth factor (RA and EGF) concentration and anatomical origin. The combination that produced optimum differentiation required epithelial cells harvested from the bovine bronchus, expanded in tissue culture flasks, seeded onto high pore-density PET membranes, cultured at ALI in a 14 % O_2 environment, supplied with AEGM:DMEM media and supplemented with 5 ng/ml EGF and 10 nM RA. Optimisation resulted in an epithelial cell ALI model with greater than 40% ciliation, containing goblet, Clara and basal cells, and with tissue-depth comparable to the native environment. To date, few studies have constructed ALI models of bovine origin and none have attempted to optimise the process (Goris *et al.*, 2008; Kameyama *et al.*, 2003; Kirchhoff *et al.*, 2014; Kondo *et al.*, 1993, 1997). A recent study by Bateman *et al.* (2015) optimised components of a porcine ALI culture system. Crucially, a broad conclusion was that compared to previously optimised human ALI systems, swine ALI culture required different experimental parameters for optimal growth and differentiation. Thus, the endeavour to produce an optimised ALI model of any species, bovine included, requires individual examination of the parameters that govern differentiation. Consequently, the ALI model developed with bovine-optimised conditions represents one of most accurate *in vitro* representations of the native tissue.

The purpose of AEC ALI model development was to create an experimental system for examining the host-pathogen interactions of *M. haemolytica*. The ALI culture was therefore deployed to identify phenotypic properties and behaviour during colonisation using microscopic approaches. Several novel properties were identified. Firstly, in a pre-optimisation pilot study, ovine ALI cultures were infected with serotype A2 (PH278) and A6 (PH284) *M. haemolytica* isolates and bovine ALI cultures infected with serotype A1 (PH2) and A6 (PH376) strains. Isolates PH2, PH284 and PH376 were found to adhere mainly to regions of the epithelium beneath the apical surface, either attaching to the basal cells or the

basolateral face of apically exposed cells. For PH284 this effect occurred following six hours of infection and for PH2 and PH376 this occurred after 24 hours of infection. To date, studies that have examined the interaction of *M. haemolytica* with respiratory epithelial cells have not reported *M. haemolytica* adhering to the sub-apical epithelium (Kisiela & Czuprynski, 2009). This is easily explained by considering that Kisiela & Czuprynski (2009) used submerged, undifferentiated epithelial cells. Thus, without proper polarisation and the multicellular 3D structure of the ALI epithelium this effect would not be observed. Several other effects were noted from the SEM analysis of infected cells. In isolate PH284 the apparent production of EPS-like material signifies the early stages of biofilm formation on the epithelial cells. While *M. haemolytica* biofilm formation has been described previously on submerged epithelial cells (Haig, 2011), the observation here, that it occurs on polarised epithelial cells, solidifies the idea that it is involved in the disease process. Recently, Boukahil & Czuprynski (2014) studied the *M. haemolytica* EPS matrix material in detail, finding that it mostly comprised protein rather than nucleic acids and carbohydrates. Additionally, biofilm formation could be blocked via the addition of anti-OmpA antibodies, D-Mannose and D-galactose. Thus, the process of biofilm formation in *M. haemolytica* likely involves OmpA and carbohydrate-mediated adherence.

Following optimisation of the ALI model, the adherence and colonisation of *M. haemolytica* was assessed on ALI epithelial cells derived from different anatomical regions of the respiratory tract. A pathogenic A1 serotype strain (PH2) and a non-pathogenic serotype A2 strain (PH202) were compared in the infection of bovine AECs grown at ALI derived from tracheal, bronchial and nasopharyngeal tissue. The aetiology of pneumonic pasteurellosis is characterised by pathogenic isolates first colonising the URT and then proliferating in the LRT (Singh *et al.*, 2011); yet non-pathogenic isolates are recovered from the nasopharynx of healthy animals (Klima *et al.*, 2014b). This experiment sought to address some of the fundamental questions regarding the behaviour of pathogenic and non-pathogenic strains in different regions of the respiratory tract. It was found that PH2, but not PH202, could infiltrate and replicate sub-apically within the epithelium generated from BBECs. Conversely, both isolates were capable of colonising the epithelium generated from BNECs;

adherence was broadly restricted to the apical face in both cases. Whether colonisation of the BNEC reflects a property of the anatomical location or an artefact due to the comparative lack of differentiation (2.3.2.6) is unknown. Whichever is the case, either would represent an important advance in our understanding of *M. haemolytica* pathogenicity.

In addition to optimisation of the ALI AEC cultures and the *M. haemolytica* colonisation study, an investigation into the composition of the *M. haemolytica* OM proteome was also performed. Eight isolates representing pathogenic and non-pathogenic serotypes recovered from cattle and sheep were included in the study. The approach of using complementary proteomic methodologies has been demonstrated to provide better proteome coverage compared to the use of a single technique alone (Aistleitner *et al.*, 2015; Connolly *et al.*, 2006; Gesslbauer *et al.*, 2012; Tanca *et al.*, 2013). Therefore, gel-based and gel-free methodologies were employed to provide maximum coverage of the OM proteome. In total, 83 OMPs were identified with various distribution amongst the eight isolates. Twelve OMPs were identified in three replicates in all eight isolates using the gel-free methodology; this number rose to 22 when considering protein matches in two of three replicates. These proteins represent the 'core' OM proteome and are mostly responsible for essential functions. Other OMPs demonstrated isolate-to isolate-variation that marks them as potential virulence factors involved in the host colonisation process. Two proteins in particular, PlpD, an immunogenic OmpA-like lipoprotein (Ayalew *et al.*, 2010; Nardini *et al.*, 1998), and an autotransporter adhesin similar to the prototypical YadA of *Yersinia spp.*, exhibited serotype-specific identification patterns (Gioia *et al.*, 2006; Hartmann *et al.*, 2012). Whereas PlpD was not identified in the three A2 serotype isolates, the YadA-like protein was identified exclusively in these isolates.

Studies have demonstrated that A2 serotype strains of *M. haemolytica* are genetically different from the other serotypes (Davies *et al.*, 1996, 1997). It was hypothesised that A2 serotype strains share a common ancestor and that the advent of domestication produced a switch in host from cattle to sheep giving rise to the pathogenic A2 serotype strains of sheep. Thus, as the YadA-like protein was identified exclusively in serotype A2 isolates and PlpD was not

identified in A2 isolates, yet identified in all isolates of other serotypes, this provides further evidence to suggest the A2 strains represent a genetically distinct group. This is particularly relevant when considering two A2 serotype strains were isolated from the lungs of sheep exhibiting pneumonic pasteurellosis and the other strain was isolated from the nasopharynx of a healthy cow. Population genetic studies have shown that the alleles of the *tbpBA* operon, *ompA* gene and *lktA* differ in A2 isolates recovered from cattle and sheep, indicating that these genes were horizontally acquired from commensal *M. haemolytica* in the new host, consequently providing adaptation to the new environment (Davies & Lee, 2004; Davies *et al.*, 2001; Lee & Davies, 2011). As the YadA-like protein was identified exclusively in serotype A2 strains and PlpD was identified in all strains except those of serotype A2, irrespective of host species, it suggests that these two OMPs are regulated by a different mechanism to strains of the other serotypes. Furthermore, if the three serotype A2 strains were to possess the same *plpD* and *yadA*-like alleles then it would suggest that selective pressures have preserved the ancestral allele in A2 strains that have transferred from cattle to sheep. As both these genes have putative adherence functions (Keller *et al.*, 2015; Nummelin *et al.*, 2004; Schulze-Koops *et al.*, 1993), it is possible the targets of adherence are conserved between cattle and sheep. However, the alleles for *plpD* and *yadA* need not be identical. Indeed, horizontal acquisition of a gene can still be regulated by an ancestral mechanism (Perez & Groisman, 2009). Whether the alleles of *plpD* and *yadA*-are conserved amongst the A2 serotype strains remains to be determined.

Many questions remain unanswered regarding how *M. haemolytica* colonises the respiratory tract. The reasons for transition from harmless commensal of the URT to a disease-causing pathogen of the LRT is perhaps the biggest unanswered question. In addition, the roles of virulence factors in colonisation, viral pre-infection and environmental stress in the disease process remain poorly understood. Bringing together all the information in this project sheds some light on these unanswered questions.

Several isolates adhered to and colonised the ALI *in vitro* model, exhibiting several phenotypic properties in the process. While AECs grown at ALI exhibit the mucociliary phenotype, differences between the *in vitro* model and the

native respiratory tract might be the key to understanding this process. Ciliation in the bovine respiratory tract is noted as being close to 100% (Al-Shmgani *et al.*, 2012) yet is somewhat less in the ALI model. This could explain some of the ease with which *M. haemolytica* colonises the model. Indeed, BPI-3 and BHV-1 of the BRD complex have been shown to destroy ciliated cells (Goris *et al.*, 2008; Kirchhoff *et al.*, 2014; Srikumaran *et al.*, 2007). Thus, reduction of ciliation below a critical threshold might be one factor in promoting colonisation. This could impact the ability of the mucociliary escalator to clear *M. haemolytica*. As other respiratory pathogens, such as *S. pneumoniae*, can disrupt the mucociliary escalator through rearrangements in the actin cytoskeleton (Fliegauf *et al.*, 2013), the possibility exists that something similar occurs with *M. haemolytica*. Low levels of ciliation might also be crucial for *M. haemolytica* to colonise the sub-apical areas. If viral-pre-infection disrupts the mucociliary escalator, access to the AEC junctional complexes might be enhanced and, in turn, promote the sub-apical colonisation of *M. haemolytica*. Further work would be required to test these hypotheses.

At a molecular level several adhesins are implicated in adherence to the respiratory tract. *M. haemolytica* possess a homologue to the FHA of *Bordetella spp.*, four trimeric autotransporters with homology to the YadA proteins of *Yersinia spp.* and the Hia/Hsf of *H. influenzae*, as well as several others (Gioia *et al.*, 2006; Lawrence *et al.*, 2010). The proteomic results of PH2 indicate that under standard growth conditions in BHIB most of these adhesins are not expressed even though the genome of PH2 encodes them. OMPs with adherence function that were identified in PH2 include the OmpA protein, which binds fibronectin (Lo & Sorensen, 2007), an orthologue to the *N. meningitidis* Opa protein, PlpD, which has been shown previously to bind epithelial cells (Kisiela & Czuprynski, 2009) and a putative Ydcf domain-containing autotransporter. These adherence-related OMPs, expressed under standard growth conditions, represent the adhesin profile of PH2 prior to infection of the AEC ALI cultures. However, addition of PH2 to the AEC ALI cells will inevitably result in changes to the OM proteome on account of the presence of secreted mucus, components of the innate immune system and the scarcer availability of nutrients. After 24 hours of infection, PH2 was observed adhering to the sub-apical epithelial regions. Both the basolateral membrane of polarised epithelial cells and the

membrane of basal cells have a different receptor profile to the apical membrane (Rodriguez-Boulan & Macara, 2014). Thus, it suggests that one or more *M. haemolytica* adhesins are responsible for binding to either the basal cells or the basolateral face of polarised epithelial cells and that the receptor target of the adhesin is not contained on the apical membrane of polarised epithelial cells. Many of the *M. haemolytica* adhesins target components of the ECM including fibronectin in the case of OmpA (Lo & Sorensen, 2007) and collagen in the case of Ahs (Daigneault & Lo, 2009). As these targets aren't ordinarily avalible to *M. haemolytica*, owing to their presence in the sub-apical regions (Alberts *et al.*, 2015), it is perhaps the case that these adhesins contribute to the observed sub-apical binding.

Undoubtedly the role of the immune response will be critical to the understanding of the colonisation process. While the AEC model developed here lacks cells of the immune system various innate immune components, including cationic peptides, lactoferrin, lysozyme, anti-proteases and collectins will be secreted (Grubor *et al.*, 2009). Human differentiated ALI cultures have been shown to display similar transcriptional profiles to the *in vivo* environment for antimicrobial peptides and proteins (Pezzulo *et al.*, 2011). One exception is lysozyme where the concentration has been shown to be different between ALI AECs and the native tissue (Dajani *et al.*, 2005). Furthermore, the amount of secreted lysozyme has been inversely correlated to RA concentration (Yoon *et al.*, 1999, 2000). A lack of RA in AECs is well documented as to produce a squamous phenotype (Bernacki *et al.*, 1999; Gray *et al.*, 1996; Wu *et al.*, 1997; Yoon *et al.*, 1997). If a correlation between the squamous phenotype and lysozyme production is assumed then the BNEC cultures, which exhibited a squamous morphology, would have a higher expression of lysozyme compared with ALI BBEC cultures. Thus, an explanation as to why PH2 was able to colonise the BBEC model with greater efficiency than either the BNEC or BTEC ALI model might be that BBEC ALI cultures produced less lysozyme than either BNEC or BTEC ALI cultures. While this would constitute an artefact of the ALI model, owing to differences in differentiation rather than an inherent property of the different tissue types, this would nonetheless implicate lysozyme, as critical in the prevention of *M. haemolytica* colonisation. An alternative hypothesis is that differences in receptor expression between these cells types account for the

differences in colonisation of PH2 towards cells derived from different respiratory tract regions. Thus, on BBECs, a receptor-mediated interaction may trigger the tissue invasion and replication. It is more likely that multiple differences between BBEC, BTEC and BNEC cells account for the differences in PH2 colonisation of these three tissue types.

The role of cellular immunology in *M. haemolytica* colonisation is at present not well understood. It is well established that the lung pathology attributed to *M. haemolytica* results from the secreted leukotoxin inducing lysis in neutrophils (Atapattu & Czuprynski, 2005; Confer *et al.*, 1990; Thumbikat *et al.*, 2005). So, the question remains how cells of the immune system participate in the colonisation process. Indeed, *M. haemolytica* possesses several virulence factors that target aspects of the cellular immune response including the various IgA protease isoforms. These have been identified in the proteomic characterisation to varying degrees amongst the isolates (Table 3.8). However, whether the IgA proteases are expressed and utilised during colonisation remains to be determined. What can be said is *M. haemolytica* has the means to combat immunoglobulin-based immunity. Immunoglobulins are produced by plasma B cells (Brandtzaeg & Johansen, 2005). Thus, as no immune cells are included in the ALI AEC model no antibodies will be present in the cell cultures. That is not to say the ALI model is irrelevant; the model offers a reductionist approach to look at the interactions of *M. haemolytica* with the respiratory epithelium. However, with an understanding of how *M. haemolytica* behaves in the absence of immune cells, the next step would be the inclusion of one or more immune cells into the model. This would provide insight into the role of components of the immune system in preventing colonisation. Rothen-Rutishauser *et al.* (2005) developed an ALI model that encompassed dendritic cells and macrophages into a differentiated respiratory epithelium. Use of this system would provide insight into the role of these cells in preventing *M. haemolytica* colonisation. Other ALI systems have been used to study the transmigration of neutrophils across the respiratory epithelium (Kidney & Proud, 2000; Klesney-Tait *et al.*, 2013). As neutrophil influx, and their subsequent lysis, is the decisive factor leading to morbidity and mortality in pneumonic pasteurellosis it would be of great benefit to include neutrophils in the ALI epithelial culture model.

The viral component to pneumonic pasteurellosis, noted as interfering with immune regulation, is another factor to consider when interpreting the results of this study. As previously suggested, *M. haemolytica* accessing the sub-apical region may be either an active effect driven by the bacterium or an opportunistic consequential result of inflammatory regulation (4.4). How either of these hypotheses fits the *in vivo* context, where *M. haemolytica* responds opportunistically to take advantage of a change in the host's conditions, requires examination of the viral interactions. BVDV has been shown to upregulate IFN-α and IFN-γ in challenged cattle and human RSV has been shown to upregulate TNF-α, IFN-γ and IL-10 in a lamb model (Palomares *et al.*, 2013; Sow *et al.*, 2011). Considering both TNF-α and INF-γ have been shown to induce permeability changes in the epithelium (Patrick *et al.*, 2006; Poritz *et al.*, 2004), the possibility exists that BVDV and BRSV may perpetrate the conditions that would allow *M. haemolytica* to invade the tissue. The alternative hypothesis is that access to the sub-apical regions is actively driven by the bacteria. In some regard this might be more plausible considering the lack of sub-apical colonisation observed with PH202. However, it may be that PH202 still induces tight junction disruption and simply doesn't have the abillity to colonise the now accessible sub-apical space. Active targeting of the tight junctions would require either a cell-surface interaction or secretion and delivery of an effector. Several hypothetical proteins as well as proteins where the exact function is unknown were identified in the proteomic characterisation. Whether any of these have a role in tight junction disruption is purely speculative although it could nonetheless be a viable alternative. Lawrence *et al.* (2010) proposed that a putative T3SS is encoded within the genomes of serotype A2 bovine and ovine *M. haemolytica* isolates. Most of the supposed effectors were hypothetical proteins. It is tempting to speculate that a T3SS of *M. haemolytica* might be involved in the delivery of an unknown effector that disrupts tight junction formation, particularly as T3SSs of other bacteria are known to secrete effectors that interfere with tight junctions (Dean & Kenny, 2004; Thanabalasuriar *et al.*, 2010; Tomson *et al.*, 2005). However, the A1 genome does not encode a putative T3SS. Thus, although the A1 isolate, PH2, was demonstrated to colonise the sub-apical regions of the ALI epithelium, it is unlikely that T3SS effector delivery is responsible for interfering with tight junction formation. A final consideration involves the secreted proteome or 'secretome' of *M.*

haemolytica. The secretome comprises many of the well-characterised *M. haemolytica* virulence factors such as leukotoxin (Lo *et al.*, 1987; Strathdee & Lo, 1989). Another unknown component of the secretome might be involved in disrupting tight junctions. Clearly, further work into the molecular makeup of the secretome would be required to test this.

Conclusions. In conclusion, the development of an *in vitro* ALI AEC model has revealed several properties of *M. haemolytica* colonisation that were, until now, not recognised. The proteomic characterisation has confirmed the expression of 83 proteins in the OM under standard laboratory conditions. Colonisation of the respiratory tract by *M. haemolytica* is a multifaceted process. Elements involving respiratory viruses, environmental stress and the bacterium make it challenging to understand the colonisation process.

The next challenge will be to identify how and when these OMPs, particularly those involved in virulence, are deployed. This could encompass transcriptomic and proteomic approaches to examine expression during colonisation of the airway epithelium. These approaches would allow for the Identification of virulence factors crucial to the colonisation process. A natural progression to the identification of colonisation-dependent virulence factors would be the construction of gene deletions in the identified virulence factors. Indeed this component of further work could circumvent the prerequisite of colonisation-dependent expression data, be it proteomic or transcriptomic. Creating gene deletions in the putative adhesins that M. haemolytica encodes as well as for other virulence factors identified in the proteomic analysis of the present study would undoubtedly provide deeper insight.

In the specific case of YadA and PlpD, which exhibited serotype specific identification in the proteomic results of the present study, aspects of species specificity could be investigated through gene deletion as well. In this approach, as YadA was only identified in serotype A2 strains it would be interesting to overexpress this adhesin in A1 strains, either using the allele of the A1 serotype strain itself or the allele derived from an A2 serotype strain, this could potentially reveal information regarding aspects of species specificity. These genetically engineered strains could then be tested for their colonisation potential on bovine and ovine derived ALI cultures. Alternatively, as the PlpD

protein was identified in all strains except that of the A2 serotypes it would be interesting to overexpress the PlpD protein, using either the gene sequence derived from an A1 serotype strain or that of the A2 serotype strain itself. Similarly, examining how these strains colonise bovine and ovine derived ALI models could provide insight into the species specificity and the role of resident commensal isolates versus pathogenic disease causing strains.

Examining the effect that pre-infection with the viral agents of BRD has on subsequent *M. haemolytica* colonisation would undoubtedly aid in our understanding of the disease complex. However, all of these approaches would benefit from the inclusion of immune cells. Ultimately the future of research into *M. haemolytica* pathogenesis will require ever more sophisticated approaches to cope with the complex nature of the infection.

Chapter 6 List of References

Abby, S. S. & Rocha, E. P. C. (2012). The non-flagellar type III secretion system evolved from the bacterial flagellum and diversified into host-cell adapted systems. *PLoS Genet* **8**, e1002983.

Abdullah, K. M., Udoh, E. a, Shewen, P. E. & Mellors, A. (1992). A neutral glycoprotease of *Pasteurella haemolytica* A1 specifically cleaves O-sialoglycoproteins. *Infect Immun* **60**, 56–62.

Abeyrathne, P. D. & Lam, J. S. (2007). WaaL of *Pseudomonas aeruginosa* utilizes ATP in in vitro ligation of O antigen onto lipid A-core. *Mol Microbiol* **65**, 1345–59.

Abraham, G., Zizzadoro, C., Kacza, J., Ellenberger, C., Abs, V., Franke, J., Schoon, H.-A., Seeger, J., Tesfaigzi, Y. & Ungemach, F. R. (2011). Growth and differentiation of primary and passaged equine bronchial epithelial cells under conventional and air-liquid-interface culture conditions. *BMC Vet Res* **7**, 26. BioMed Central Ltd.

Ackermann, M. R. & Brogden, K. a. (2000). Response of the ruminant respiratory tract to *Mannheimia (Pasteurella) haemolytica*. *Microbes Infect* **2**, 1079–88.

Ackermann, M. R., Gallup, J. M., Zabner, J., Evans, R. B., Brockus, C. W., Meyerholz, D. K., Grubor, B. & Brogden, K. A. (2004). Differential expression of sheep beta-defensin-1 and -2 and interleukin 8 during acute *Mannheimia haemolytica pneumonia*. *Microb Pathog* **37**, 21–7.

Adamo, R., Sokol, S., Soong, G., Gomez, M. I. & Prince, A. (2004). *Pseudomonas aeruginosa* Flagella Activate Airway Epithelial Cells through asialoGM1 and Toll-Like Receptor 2 as well as Toll-Like Receptor 5. *Am J Respir Cell Mol Biol* **30**, 627–634.

Adlam, C., Knights, J. M., Mugridge, A., Lindon, J. C., Baker, P. R. W., Beesley, J. E., Spcey, B., Craig, G. R. & Nagy, L. K. (1984). Purification, Characterization and Immunological Properties of the Serotype-specific Capsular Polysaccharide of *Pasteurella haemolytica* (Serotype A1) Organisms. *J Gen Microbiol* **130**, 2415–2426.

Adlam, C., Knights, J. M., Mugridge, A., Lindon, J. C., Williams, J. M. & Beesley, J. E. (1986). Purification, characterization and immunological properties of the serotype-specific capsular polysaccharide of *Pasteurella haemolytica* serotype A7 organisms. *J Gen Microbiol* **132**, 1079–87.

Adlam, C., Knights, J. M., Mugridge, A., Williams, J. M. & Lindon, J. C. (1987). Production of colominic acid by *Pasteurella haemolytica* serotype A2 organisms. *FEMS Microbiol Lett* **42**, 23–25.

Aebersold, R. & Mann, M. (2003). Mass spectrometry-based proteomics. *Nature* **422**, 198–207.

Aggarwal, S., Kim, S., Cheon, K., Tabassam, F. H., Yoon, J. & Koo, J. S. (2006). Nonclassical Action of Retinoic Acid on the Activation of the cAMP Response Element-binding Protein in Normal Human Bronchial Epithelial Cells. *Mol Biol Cell* **17**, 566–575.

Agrawal, C. M. & Ray, R. B. (2001). Biodegradable polymeric scaffolds for musculoskeletal tissue engineering. *J Biomed Mater Res*.

Aistleitner, K., Anrather, D., Schott, T., Klose, J., Bright, M., Ammerer, G. & Horn, M. (2015). Conserved features and major differences in the outer membrane protein composition of *chlamydiae*. *Environ Microbiol* **17**, 1397–413.

Akinbi, H. T., Epaud, R., Bhatt, H. & Weaver, T. E. (2000). Bacterial Killing Is Enhanced by Expression of Lysozyme in the Lungs of Transgenic Mice. *J Immunol* **165**, 5760–5766.

Albertine, K. H. (2015). *Anatomy of the Lungs*. *Murray Nadel's Textb Respir Med*, Sixth Edit. Elsevier Inc.

Alberts, B., Johnson, A., David, J. L., Raff, M., Roberts, K., Walter, P., Wilson, J. & Hunt, T. (2015). The Extracellular Matrix of Animals. In *Mol Biol Cell 6th Ed*.

Al-Ghamdi, G. M., Ames, T. R., Baker, J. C., Walker, R., Chase, C. C., Frank, G. H. & Maheswaran, S. K. (2000). Serotyping of *Mannheimia* (*Pasteurella*) *haemolytica* isolates from the upper Midwest United States. *J Vet diagnostic Investig* **12**, 576–8.

Ali, T., Oldfield, N. J., Wooldridge, K. G., Turner, D. P. & Ala'Aldeen, D. a a. (2008). Functional characterization of AasP, a maturation protease autotransporter protein of *Actinobacillus pleuropneumoniae*. *Infect Immun* **76**, 5608–14.

Allen, a, Hutton, D. a & Pearson, J. P. (1998). The MUC2 gene product: a human intestinal mucin. *Int J Biochem Cell Biol* **30**, 797–801.

Alonso, S., Pethe, K., Mielcarek, N., Raze, D. & Locht, C. (2001). Role of ADP-Ribosyltransferase Activity of Pertussis Toxin in Toxin- Adhesin Redundancy with Filamentous Hemagglutinin during *Bordetella pertussis* Infection. *Infect Immun* **69**, 6038–6043.

Al-Sadi, R. M. & Ma, T. Y. (2007). IL-1 Causes an Increase in Intestinal Epithelial Tight Junction Permeability. *J Immunol* **178**, 4641–4649.

Al-Shmgani, H. S., Moate, R. M., Sneyd, J. R., Macnaughton, P. D. & Moody, a J. (2012). Hyperoxia-induced ciliary loss and oxidative damage in an in vitro bovine model: the protective role of antioxidant vitamins E and C. *Biochem Biophys Res Commun* **429**, 191–6. Elsevier Inc.

Al-Tarazi, Y. H. M. & Dagnall, G. J. R. (1997). Nasal Carriage of *Pasteurella Haemolytica* Serotypes By Sheep and Goats in Jordan. *Trop Anim Hlth Prod* **29**, 177–179.

Altindis, E., Fu, Y. & Mekalanos, J. J. (2014). Proteomic analysis of *Vibrio cholerae* outer membrane vesicles. *Proc Natl Acad Sci* **111**, E1548–E1556.

Alvarez-Martinez, C. E. & Christie, P. J. (2009). Biological diversity of prokaryotic type IV secretion systems. *Microbiol Mol Biol Rev* **73**, 775–808.

Aly, K. A. & Baron, C. (2007). The VirB5 protein localizes to the T-pilus tips in *Agrobacterium tumefaciens*. *Microbiology* **153**, 3766–75.

Andrews, K. L., Nettesheim, P., Asai, D. J. & Ostrowski, L. E. (1996). Identification of seven rat axonemal dynein heavy chain genes: expression during ciliated cell differentiation. *Mol Biol Cell* **7**, 71–9.

Angen, Ø., Mutters, R., Caugant, D., Olsen, J. E. & Bisgaard, M. (1999a). Taxonomic relationships of the [Pasteurella] haemolytica complex as evaluated by DNA-DNA hybridizations and 16s rRNA sequencing with proposal

of Mannheimia haemolytica gen . nov ., comb . nov ., Mannheimia granulomatis comb . n. *Int J Syst Bacteriol* **49**, 67–86.

Angen, Ø., Quirie, M., Donachie, W. & Bisgaard, M. (1999b). Investigations on the species specificity of *Mannheimia* (*Pasteurella*) *haemolytica* serotyping. *Vet Microbiol* **65**, 283–290.

Atapattu, D. N. & Czuprynski, C. J. (2007). Mannheimia haemolytica leukotoxin binds to lipid rafts in bovine lymphoblastoid cells and is internalized in a dynamin-2- and clathrin-dependent manner. *Infect Immun* **75**, 4719–27.

Atapattu, D. N., Albrecht, R. M., McClenahan, D. J. & Czuprynski, C. J. (2008). Dynamin-2-dependent targeting of mannheimia haemolytica leukotoxin to mitochondrial cyclophilin D in bovine lymphoblastoid cells. *Infect Immun* **76**, 5357–65.

Atapattu, D. N. & Czuprynski, C. J. (2005). *Mannheimia haemolytica* leukotoxin induces apoptosis of bovine lymphoblastoid cells (BL-3) via a caspase-9-dependent mitochondrial pathway. *Infect Immun* **73**, 5504–5513.

Atmakuri, K., Cascales, E. & Christie, P. J. (2004). Energetic components VirD4, VirB11 and VirB4 mediate early DNA transfer reactions required for bacterial type IV secretion. *Mol Microbiol* **54**, 1199–211.

Aulik, N. a, Hellenbrand, K. M., Klos, H. & Czuprynski, C. J. (2010). *Mannheimia haemolytica* and its leukotoxin cause neutrophil extracellular trap formation by bovine neutrophils. *Infect Immun* **78**, 4454–66.

Aulik, N. a, Hellenbrand, K. M., Kisiela, D. & Czuprynski, C. J. (2011). *Mannheimia haemolytica* leukotoxin binds cyclophilin D on bovine neutrophil mitochondria. *Microb Pathog* **50**, 168–78. Elsevier Ltd.

Aulik, N. a, Hellenbrand, K. M. & Czuprynski, C. J. (2012). *Mannheimia haemolytica* and its leukotoxin cause macrophage extracellular trap formation by bovine macrophages. *Infect Immun* **80**, 1923–33.

Avadhanula, V., Rodriguez, C. A., Ulett, G. C., Bakaletz, L. O. & Adderson, E. E. (2006). Nontypeable *Haemophilus influenzae* Adheres to Intercellular Adhesion Molecule 1 (ICAM-1) on Respiratory Epithelial Cells and Upregulates ICAM-1 Expression. *Infect Immun* **74**, 830–838.

Ayalew, S., Confer, A. W. & Blackwood, E. R. (2004). Characterization of Immunodominant and Potentially Protective Epitopes of *Mannheimia haemolytica* Serotype 1 Outer Membrane Lipoprotein PlpE. *Infect Immun* **72**, 7265–7274.

Ayalew, S., Confer, A. W., Payton, M. E., Garrels, K. D., Shrestha, B., Ingram, K. R., Montelongo, M. a & Taylor, J. D. (2008). *Mannheimia haemolytica* chimeric protein vaccine composed of the major surface-exposed epitope of outer membrane lipoprotein PlpE and the neutralizing epitope of leukotoxin. *Vaccine* **26**, 4955–61.

Ayalew, S., Confer, A. W., Hartson, S. D. & Shrestha, B. (2010). Immunoproteomic analyses of outer membrane proteins of *Mannheimia haemolytica* and identification of potential vaccine candidates. *Proteomics* **10**, 2151–64.

Ayalew, S., Shrestha, B., Montelongo, M., Wilson, A. E. & Confer, A. W. (2011a). Immunogenicity of *Mannheimia haemolytica* recombinant outer membrane proteins serotype 1-specific antigen, OmpA, OmpP2, and OmpD15. *Clin vaccine Immunol* **18**, 2067–74.

Ayalew, S., Shrestha, B., Montelongo, M., Wilson, A. E. & Confer, A. W. (2011b). Immunogenicity of *Mannheimia haemolytica* recombinant outer membrane proteins serotype 1-specific antigen, OmpA, OmpP2, and OmpD15. *Clin vaccine Immunol* **18**, 2067–74.

Ayalew, S., Shrestha, B., Montelongo, M., Wilson, A. E. & Confer, A. W. (2011c). Identification and immunogenicity of *Mannheimia haemolytica* S1 outer membrane lipoprotein PlpF. *Vaccine* **29**, 8712–8. Elsevier Ltd.

Azghani, a. O., Miller, E. J. & Peterson, B. T. (2000). Virulence Factors from *Pseudomonas aeruginosa* Increase Lung Epithelial Permeability. *Lung* **178**, 261–269.

Aziz, R. K., Bartels, D., Best, A. A., DeJongh, M., Disz, T., Edwards, R. A., Formsma, K., Gerdes, S., Glass, E. M. & other authors. (2008). The RAST Server: Rapid Annotations using Subsystems Technology. *BMC Genomics* **9**, 75.

Bacallao, R., Antony, C., Dotti, C., Karsenti, E., Stelzer, E. H. & Simons, K. (1989). The subcellular organization of Madin-Darby canine kidney cells during the formation of a polarized epithelium. *J Cell Biol* **109**, 2817–32.

Baelen, S., Dewitte, F., Clantin, B. & Villeret, V. (2013). Structure of the secretion domain of HxuA from *Haemophilus influenzae*. *Acta Crystallogr Sect F Struct Biol Cryst Commun* **69**, 1322–7. International Union of Crystallography.

Bai, J., Kim, S. I., Ryu, S. & Yoon, H. (2014). Identification and Characterization of Outer Membrane Vesicle-Associated Proteins in Salmonella enterica *Serovar Typhimurium*. *Infect Immun* **82**, 4001–4010.

Baik, S., Kim, K.-M., Song, S.-M., Kim, D., Jun, J., Lee, S.-G., Song, J., Park, J., Kang, H. & other authors. (2004). Proteomic analysis of the sarcosine-insoluble outer membrane fraction of *Helicobacter pylori* strain 26695. *J Bacteriol* **186**, 949–55.

Balakrishnan, L., Hughes, C. & Koronakis, V. (2001). Substrate-triggered recruitment of the TolC channel-tunnel during type I export of hemolysin by *Escherichia coli*. *J Mol Biol* **313**, 501–10.

Balder, R., Krunkosky, T. M., Nguyen, C. Q., Feezel, L. & Lafontaine, E. R. (2009). Hag mediates adherence of *Moraxella catarrhalis* to ciliated human airway cells. *Infect Immun* **77**, 4597–608.

Ball, G., Durand, É., Lazdunski, A. & Filloux, A. (2002). A novel type II secretion system in *Pseudomonas aeruginosa*. *Mol Microbiol* **43**, 475–485.

Ball, H. J., Connolly, M. & Cassidy, J. (1993). *Pasteurella haemolytica* Serotypes Isolated in Northern Ireland during 1989-1991. *Br Veterinanry Journals* **149**, 561–570.

Bals, R., Beisswenger, C., Blouquit, S. & Chinet, T. (2004). Isolation and air-liquid interface culture of human large airway and bronchiolar epithelial cells. *J Cyst Fibros* **3 Suppl 2**, 49–51.

Banerjee, A., Van Sorge, N. M., Sheen, T. R., Uchiyama, S., Mitchell, T. J. & Doran, K. S. (2010). Activation of brain endothelium by pneumococcal neuraminidase NanA promotes bacterial internalization. *Cell Microbiol* **12**, 1576–88.

Barden, S., Lange, S., Tegtmeyer, N., Conradi, J., Sewald, N., Backert, S. &

Niemann, H. H. (2013). A helical RGD motif promoting cell adhesion: crystal structures of the *Helicobacter pylori type* IV secretion system pilus protein CagL. *Structure* **21**, 1931–41. Elsevier Ltd.

Bartley, S. N., Tzeng, Y.-L., Heel, K., Lee, C. W., Mowlaboccus, S., Seemann, T., Lu, W., Lin, Y.-H., Ryan, C. S. & other authors. (2013). Attachment and invasion of *Neisseria meningitidis* to host cells is related to surface hydrophobicity, bacterial cell size and capsule. *PLoS One* **8**, e55798.

Baslé, A., Rummel, G., Storici, P., Rosenbusch, J. P. & Schirmer, T. (2006). Crystal structure of osmoporin OmpC from *E. coli* at 2.0 A. *J Mol Biol* **362**, 933–42.

Bateman, A. C., Karasin, A. I. & Olsen, C. W. (2015). Differentiated swine airway epithelial cell cultures for the investigation of influenza A virus infection and replication. *Influenza Other Respi Viruses* **7**, 139–150.

Batra, S. A., Shanthalingam, S., Donofrio, G. & Srikumaran, S. (2016). A chimeric protein comprising the immunogenic domains of Mannheimia haemolytica leukotoxin and outer membrane protein PlpE induces antibodies against leukotoxin and PlpE. *Vet Immunol Immunopathol* **175**, 36–41. Elsevier B.V.

Baybutt, R. C., Smith, B. W., Donskaya, E. V, Hu, L., Li, T. & Wang, W. (2010). The proliferative effects of retinoic acid on primary cultures of adult rat type II pneumocytes depend upon cell density. *In Vitro Cell Dev Biol Anim* **46**, 20–7.

Beall, B. & Hoenes, T. (1997). An iron-regulated outer-membrane protein specific to *Bordetella bronchiseptica* and homologous to ferric siderophore receptors. *Microbiology* **143**, 135–145.

Beall, B. & Sanden, G. N. (1995). A *Bordetella pertussis fepA* homologue required for utilization of exogenous ferric enterobactin. *Microbiology* **141**, 3193–3205.

Beier, D. & Gross, R. (2006). Regulation of bacterial virulence by two-component systems. *Curr Opin Microbiol* **9**, 143–152.

Bellamy, W., Takase, M., Yamauchi, K., Wakabayashi, H., Kawase, K. & Tomita, M. (1992). Identification of the bactericidal domain of lactoferrin. *Biochim Biophys Acta* **121**, 130–136.

Benson, S. A., Occi, J. L. L. & Sampson, B. A. (1988). Mutations that Alter the Pore Function of the OmpF Porin of *Escherichia coli* K12. *J Mol Biol* **203**, 961–970.

Bernacki, S. H., Nelson, a L., Abdullah, L., Sheehan, J. K., Harris, a, Davis, C. W. & Randell, S. H. (1999). Mucin gene expression during differentiation of human airway epithelia in vitro. Muc4 and muc5b are strongly induced. *Am J Respir Cell Mol Biol* **20**, 595–604.

Bérubé, K., Prytherch, Z., Job, C. & Hughes, T. (2010). Human primary bronchial lung cell constructs: the new respiratory models. *Toxicology* **278**, 311–8.

BéruBé, K., Pitt, A., Hayden, P., Prytherch, Z. & Job, C. (2010). Filter-well technology for advanced three-dimensional cell culture: perspectives for respiratory research. *Altern to Lab Anim* **38 Suppl 1**, 49–65.

BéruBé, K., Gibson, C., Job, C. & Prytherch, Z. (2011). Human lung tissue

engineering: a critical tool for safer medicines. *Cell Tissue Bank* **12**, 11–3.

Berven, F. S., Karlsen, O. A., Straume, A. H., Flikka, K., Murrell, J. C., Fjellbirkeland, A., Lillehaug, J. R., Eidhammer, I. & Jensen, H. B. (2006). Analysing the outer membrane subproteome of *Methylococcus capsulatus* (Bath) using proteomics and novel biocomputing tools. *Arch Microbiol* **184**, 362–77.

Billker, O., Popp, A., Brinkmann, V., Wenig, G., Schneider, J., Caron, E. & Meyer, T. F. (2002). Disrinct mechanisms of internalisation of *Neisseria gonorrhoeae* by members of the CEACAM receptor family involving Rac1- and Cdc42-dependent and -independent pathways. *EMBO J* **21**, 560–71.

Bjarnsholt, T., Alhede, M., Alhede, M., Eickhardt-Sørensen, S. R., Moser, C., Kühl, M., Jensen, P. Ø. & Høiby, N. (2013). The in vivo biofilm. *Trends Microbiol* **21**, 466–74.

Blonder, J., Goshe, M. B., Xiao, W., Ii, D. G. C., Wingerd, M., Davis, R. W. & Smith, R. D. (2004). Global Analysis of the Membrane Subproteome of *Pseudomonas aeruginosa* Using Liquid Chromatography-Tandem Mass Spectrometry. *J Proteome Res* **3**, 434–444.

Blowey, R. W. & Weaver, a D. (2003). *Chapter 5 - Respiratory disorders*. *Color Atlas Dis Disord Cattle*.

Boers, J. E., Ambergen, a W. & Thunnissen, F. B. (1999). Number and proliferation of clara cells in normal human airway epithelium. *Am J Respir Crit Care Med* **159**, 1585–91.

Bolton, S. J., Pinnion, K., Marshall, C. V, Wilson, E., Barker, J. E., Oreffo, V. & Foster, M. L. (2008). Changes in Clara cell 10 kDa protein (CC10)-positive cell distribution in acute lung injury following repeated lipopolysaccharide challenge in the rat. *Toxicol Pathol* **36**, 440–8.

Bos, M. P., Robert, V. & Tommassen, J. (2007). Functioning of outer membrane protein assembly factor Omp85 requires a single POTRA domain. *EMBO Rep* **8**, 1149–54.

Boucher, P. E., Yang, M. & Stibitz, S. (2001). Mutational analysis of the high-affinity BvgA binding site in the *fha* promoter of Bordetella pertussis. *Mol Microbiol* **40**, 991–999.

Boukahil, I. & Czuprynski, C. J. (2014). Characterization of *Mannheimia haemolytica* biofilm formation in vitro. *Vet Microbiol*. Elsevier B.V.

Bowland, S. L. & Shewen, P. E. (2000). Bovine respiratory disease : Commercial vaccines currently available in Canada. *Can Vet J* **41**, 33–48.

Boyce, J. D., Cullen, P. a, Nguyen, V., Wilkie, I. & Adler, B. (2006). Analysis of the *Pasteurella multocida* outer membrane sub-proteome and its response to the in vivo environment of the natural host. *Proteomics* **6**, 870–80.

Brand, J. D., Ballinger, C. a, Tuggle, K. L., Fanucchi, M. V, Schwiebert, L. M. & Postlethwait, E. M. (2012). Site-specific dynamics of CD11b+ and CD103+ dendritic cell accumulations following ozone exposure. *Am J Physiol Lung Cell Mol Physiol* **303**, L1079–86.

Brandtzaeg, P. & Johansen, F. E. (2005). Mucosal B cells: Phenotypic characteristics, transcriptional regulation, and homing properties. *Immunol Rev* **206**, 32–63.

Brickman, T. J., Hansel, J. G., Miller, M. J. & Armstrong, S. K. (1996). Purification, spectroscopic analysis and biological activity of the macrocyclic dihydroxamate siderophore alcaligin produced by *Bordetella pertussis* and *Bordetella bronchiseptica*. *Biometals* **9**, 191–203.

Briggs, R. E., Tabatabai, L. B. & Tatum, F. M. (2012). Mucosal and parenteral vaccination against pneumonic pasteurellosis in cattle with a modified-live in-frame lktA deletion mutant of *Mannheimia haemolytica*. *Microb Pathog* **52**, 302–9. Elsevier Ltd.

Brockman-Schneider, R. a, Amineva, S. P., Bulat, M. V & Gern, J. E. (2008). Serial culture of murine primary airway epithelial cells and ex vivo replication of human rhinoviruses. *J Immunol Methods* **339**, 264–9. Elsevier B.V.

Brockman-Schneider, R. a, Pickles, R. J. & Gern, J. E. (2014). Effects of vitamin D on airway epithelial cell morphology and rhinovirus replication. *PLoS One* **9**, e86755.

Brogden, K. & Clarke, C. (1997). Increase of glycocalyx and altered lectin agglutination profiles of *Pasteurella haemolytica* A1 after incubation in bovine subcutaneous tissue chambers in vivo or in ruminant serum in vitro. *Infect Immun* **65**, 957–963.

Brooks, M. J., Laurence, C. a., Hansen, E. J. & Gray-Owen, S. D. (2006). Characterization of the *Moraxella catarrhalis* Opa-Like Protein, OlpA, Reveals a Phylogenetically Conserved Family of Outer Membrane Proteins. *J Bacteriol* **189**, 76–82.

Bucior, I., Mostov, K. & Engel, J. N. (2010). *Pseudomonas aeruginosa*-mediated damage requires distinct receptors at the apical and basolateral surfaces of the polarized epithelium. *Infect Immun* **78**, 939–53.

Bucior, I., Pielage, J. F. & Engel, J. N. (2012). *Pseudomonas aeruginosa* pili and flagella mediate distinct binding and signaling events at the apical and basolateral surface of airway epithelium. *PLoS Pathog* **8**, e1002616.

Buddelmeijer, N. (2015). The molecular mechanism of bacterial lipoprotein modification--how, when and why? *FEMS Microbiol Rev* **39**, 246–61.

Burciaga-Robles, L. O., Step, D. L., Krehbiel, C. R., Holland, B. P., Richards, C. J., Montelongo, M. a, Confer, a W. & Fulton, R. W. (2010). Effects of exposure to calves persistently infected with bovine viral diarrhea virus type 1b and subsequent infection with *Mannheima haemolytica* on clinical signs and immune variables: model for bovine respiratory disease via viral and bacterial in. *J Anim Sci* **88**, 2166–78.

Burrows, L. L. & Lo, R. Y. C. (1992). Molecular Characterization of an RTX Toxin Determinant from *Actinobacillus suis*. *Infect Immun* **60**, 2166–2173.

Bushell, S. R., Lou, H., Wallat, G. D., Beis, K., Whitfield, C. & Naismith, J. H. (2010). Crystallization and preliminary diffraction analysis of Wzi, a member of the capsule export and assembly pathway in *Escherichia coli*. *Acta Crystallogr Sect F Struct Biol Cryst Commun* **66**, 1621–5. International Union of Crystallography.

Bushell, S. R., Mainprize, I. L., Wear, M. a, Lou, H., Whitfield, C. & Naismith, J. H. (2013). Wzi is an outer membrane lectin that underpins group 1 capsule assembly in *Escherichia coli*. *Structure* **21**, 844–53. Elsevier Ltd.

Button, B., Cai, L.-H., Ehre, C., Kesimer, M., Hill, D. B., Sheehan, J. K.,

Boucher, R. C. & Rubinstein, M. (2012). A periciliary brush promotes the lung health by separating the mucus layer from airway epithelia. *Science (80-)* **337**, 937–41.

Callaghan, M. J., Jolley, K. A. & Maiden, M. C. J. (2006). Opacity-Associated Adhesin Repertoire in Hyperinvasive *Neisseria meningitidis*. *Infect Immun* **74**, 5085–5094.

Calmettes, C., Yu, R., Silva, L. P., Curran, D., Schriemer, D. C., Schryvers, A. B. & Moraes, T. F. (2011). Structural variations within the transferrin binding site on transferrin-binding protein B, TbpB. *J Biol Chem* **286**, 12683–92.

Calmettes, C., Alcantara, J., Yu, R.-H., Schryvers, A. B. & Moraes, T. F. (2012). The structural basis of transferrin sequestration by transferrin-binding protein B. *Nat Struct Mol Biol* **19**, 358–60.

Câmara, J. & Jarai, G. (2010). Epithelial-mesenchymal transition in primary human bronchial epithelial cells is Smad- dependent and enhanced by fibronectin and TNF- a. *Fibrogenes Tissue Repair* **3**, 1–11.

Carranza, P., Grunau, A., Schneider, T., Hartmann, I., Lehner, A., Stephan, R., Gehrig, P., Grossmann, J., Groebel, K. & other authors. (2010). A gel-free quantitative proteomics approach to investigate temperature adaptation of the food-borne pathogen *Cronobacter turicensis* 3032. *Proteomics* **10**, 3248–3261.

Cascales, E., Bernadac, A., Gavioli, M., Lazzaroni, J.-C. & Lloubes, R. (2002). Pal lipoprotein of *Escherichia coli* plays a major role in outer membrane integrity. *J Bacteriol* **184**, 754–759.

Caverly, J. M., Diamond, G., Gallup, J. M., Brogden, K. A., Dixon, R. A. & Ackermann, M. R. (2003). Coordinated Expression of Tracheal Antimicrobial Peptide and Inflammatory-Response Elements in the Lungs of Neonatal Calves with Acute Bacterial Pneumonia. *Infect Immun* **71**, 2950–2955.

Chae, C. H., Gentry, M. J., Confer, a W. & Anderson, G. a. (1990). Resistance to host immune defense mechanisms afforded by capsular material of *Pasteurella haemolytica*, serotype 1. *Vet Microbiol* **25**, 241–251.

Chagnot, C., Listrat, A., Astruc, T. & Desvaux, M. (2012). Bacterial adhesion to animal tissues: protein determinants for recognition of extracellular matrix components. *Cell Microbiol* **14**, 1687–96.

Chagnot, C., Zorgani, M. a, Astruc, T. & Desvaux, M. (2013). Proteinaceous determinants of surface colonization in bacteria: bacterial adhesion and biofilm formation from a protein secretion perspective. *Front Microbiol* **4**, 303.

Charbit, A., Wang, J., Michel, V. & Hofnung, M. (1998). A cluster of charged and aromatic residues in the C-terminal portion of maltoporin participates in sugar binding and uptake. *Mol Gen Genet* **260**, 185–192.

Chen, Y., Zhang, J., Xing, G. & Zhao, Y. (2009). Mascot-Derived False Positive Peptide Identifications Revealed by Manual Analysis of Tandem Mass Spectra. *J Proteome Res* **8**, 3141–3147.

Cherry, J. D. (2005). The epidemiology of pertussis: a comparison of the epidemiology of the disease pertussis with the epidemiology of *Bordetella pertussis* infection. *Pediatrics* **115**, 1422–7.

Chipman, D. M. & Sharon, N. (1969). Mechanism of Lysozyme Action. *Science (80-)* **165**, 454–465.

Chiu, Y., Kuo, T. Y., Lin, C. C. & Chen, W. J. (2011). Proteomic analysis reveals responsive proteins of *Vibrio parahaemolyticus* on exposure to cationic antimicrobial peptides. *J Appl Microbiol* **110**, 80–89.

Cho, Y., Sun, J., Han, J. H., Jang, J. H., Kang, Z. W. & Hahn, T.-W. (2014). An immunoproteomic approach for characterization of the outer membrane proteins of *Salmonella Gallinarum*. *Electrophoresis* **35**, 888–94.

Choi, D.-S., Kim, D.-K., Choi, S. J., Lee, J., Choi, J.-P., Rho, S., Park, S.-H., Kim, Y.-K., Hwang, D. & Gho, Y. S. (2011). Proteomic analysis of outer membrane vesicles derived from *Pseudomonas aeruginosa*. *Proteomics* **11**, 3424–3429.

Chu, H. W., Balzar, S., Seedorf, G. J., Westcott, J. Y., Trudeau, J. B., Silkoff, P. & Wenzel, S. E. (2004). Transforming growth factor-beta2 induces bronchial epithelial mucin expression in asthma. *Am J Pathol* **165**, 1097–106.

Chun, C. K., Ozer, E. A., Welsh, M. J., Zabner, J. & Greenberg, E. P. (2004). Inactivation of a *Pseudomonas aeruginosa* quorum-sensing signal by human airway epithelia. *Proc Natl Acad Sci* **101**, 3587–3590.

Chun, J. & Prince, a. (2006). Activation of Ca2+-Dependent Signaling by TLR2. *J Immunol* **177**, 1330–1337.

Chun, J. & Prince, A. (2009). TLR2-Induced Calpain Cleavage of Epithelial Junctional Proteins Facilitates Leukocyte Transmigration. *Cell Host Microbe* **5**, 47–58. Elsevier Inc.

Chung, J. W., Ng-Thow-Hing, C., Budman, L. I., Gibbs, B. F., Nash, J. H. E., Jacques, M. & Coulton, J. W. (2007). Outer membrane proteome of *Actinobacillus pleuropneumoniae*: LC-MS/MS analyses validate in silico predictions. *Proteomics* **7**, 1854–65.

Church, D. A. (1969). Storage-Ring Ion Trap Derived from the Linear Quadrupole Radio-Frequency Mass Filter. *J Appl Phys* **40**, 3127.

Cladman, W. M., Watt, M. V, Dini, J. & Mellors, A. (1996). The *Pasteurella haemolytica* O -Sialoglycoprotein Endopeptidase Is Inhibited by Zinc Ions and Does Not Cleave Fetuin. *Biochem Biophys Res Commun* **146**, 141–146.

Clantin, B., Hodak, H., Willery, E., Locht, C., Jacob-Dubuisson, F. & Villeret, V. (2004). The crystal structure of filamentous hemagglutinin secretion domain and its implications for the two-partner secretion pathway. *Proc Natl Acad Sci* **101**, 6194–6199.

Clark, A. B., Randell, S. H., Nettesheim, P., Gray, T. E., Bagnell, B. & Ostrowski, L. E. (1995). Regulation of ciliated cell differentiation in cultures of rat tracheal epithelial cells. *Am J Respir Cell Mol Biol* **12**, 329–38.

Clark, a. E., Kaleta, E. J., Arora, a. & Wolk, D. M. (2013). Matrix-Assisted Laser Desorption Ionization-Time of Flight Mass Spectrometry: a Fundamental Shift in the Routine Practice of Clinical Microbiology. *Clin Microbiol Rev* **26**, 547–603.

Clark, C. a., Thomas, L. K. & Azghani, A. O. (2011). Inhibition of Protein Kinase C Attenuates *Pseudomonas aeruginosa* Elastase–Induced Epithelial

Barrier Disruption. *Am J Respir Cell Mol Biol* **45**, 1263–1271.

Clark, E., Hoare, C., Tanianis-Hughes, J., Carlson, G. L. & Warhurst, G. (2005). Interferon γ Induces Translocation of Commensal *Escherichia coli* Across Gut Epithelial Cells via a Lipid Raft--Mediated Process. *Gastroenterology* **128**, 1258–1267.

Clark, J. G., Kim, K.-H., Basom, R. S. & Gharib, S. a. (2015). Plasticity of Airway Epithelial Cell Transcriptome in Response to Flagellin. *PLoS One* **10**, e0115486.

Clarke, T. B., Francella, N., Huegel, A. & Weiser, J. N. (2011). Invasive bacterial pathogens exploit TLR-mediated downregulation of tight junction components to facilitate translocation across the epithelium. *Cell Host Microbe* **9**, 404–414. Elsevier Inc.

Cole, S. P., Harwood, J., Lee, R., She, R. & Guiney, D. G. (2004). Characterization of Monospecies Biofilm Formation by *Helicobacter pylori*. *J Bacteriol* **186**, 3124–3132.

Cone, R. a. (2009). Barrier properties of mucus. *Adv Drug Deliv Rev* **61**, 75–85. Elsevier B.V.

Confer, a W., Ayalew, S., Montelongo, M., Step, D. L., Wray, J. H., Hansen, R. D. & Panciera, R. J. (2009). Immunity of cattle following vaccination with a *Mannheimia haemolytica* chimeric PlpE-LKT (SAC89) protein. *Vaccine* **27**, 1771–1776.

Confer, A. W., Simons, K. R., Barrie, M. T. & Clinkenbeard, K. D. (1990). Effects of *pasteurella haemolytica* leukotoxin on neutrophils from white-tailed deer and several exotic ruminant species. *Vet Res Commun* **14**, 175–180.

Confer, A. W. & Ayalew, S. (2013). The OmpA family of proteins: roles in bacterial pathogenesis and immunity. *Vet Microbiol* **163**, 207–22. Elsevier B.V.

Conlon, J. a, Shewen, P. E. & Lo, R. Y. (1991). Efficacy of recombinant leukotoxin in protection against pneumonic challenge with live *Pasteurella haemolytica* A1. *Infect Immun* **59**, 587–91.

Connolly, J. P., Comerci, D., Alefantis, T. G., Walz, A., Quan, M., Chafin, R., Grewal, P., Mujer, C. V, Ugalde, R. a & DelVecchio, V. G. (2006). Proteomic analysis of *Brucella abortus* cell envelope and identification of immunogenic candidate proteins for vaccine development. *Proteomics* **6**, 3767–80.

Conrad, A., Kontro, M., Keinänen, M. M., Cadoret, A., Faure, P., Mansuy-huault, L. & Block, J. (2003). Fatty Acids of Lipid Fractions in Extracellular Polymeric Substances of Activated Sludge Flocs. *Lipids* **38**, 1093–1105.

Cooke, M. J., Phillips, S. R., Shah, D. S. H., Athey, D., Lakey, J. H. & Przyborski, S. a. (2008). Enhanced cell attachment using a novel cell culture surface presenting functional domains from extracellular matrix proteins. *Cytotechnology* **56**, 71–79.

Cooney, B. J. & Lo, R. Y. (1993). Three contiguous lipoprotein genes in *Pasteurella haemolytica* A1 which are homologous to a lipoprotein gene in Haemophilus influenzae type b. *Infect Immun Immun* **61**, 4682–4688.

Coote, J. G. (1992). Structural and functional relationships among the RTX toxin

determinants of Gram-negative bacteria. *FEMS Microbiol Rev* **8**, 137–161.

Cope, L. D., Yogev, R. A. M., Muller-eberhard, U. & Hansen, E. J. (1995). A Gene Cluster Involved in the Utilization of Both Free Heme and Heme : Hemopexin by *Haemophilus influenzae* Type b. *J Bcteriology* **177**, 2644–2653.

Cope, L. D., Thomas, S. E., Hrkal, Z. & Hansen, E. J. (1998). Binding of Heme-Hemopexin Complexes by Soluble HxuA Protein Allows Utilization of This Complexed Heme by *Haemophilus influenzae*. *J Bacteriol* **66**, 4511–4516.

Cope, L. D., Love, R. P., Guinn, S. E., Gilep, A., Usanov, S., Estabrook, R. W., Hrkal, Z. & Hansen, E. J. (2001). Involvement of HxuC Outer Membrane Protein in Utilization of Hemoglobin by *Haemophilus influenzae*. *Infect Immun* **69**, 2353–2363.

Coraux, C., Roux, J., Jolly, T. & Birembaut, P. (2008). Epithelial cell-extracellular matrix interactions and stem cells in airway epithelial regeneration. *Proc Am Thorac Soc* **5**, 689–94.

Cordwell, S. J., Len, A. C. L., Touma, R. G., Scott, N. E., Falconer, L., Jones, D., Connolly, A., Crossett, B. & Djordjevic, S. P. (2008). Identification of membrane-associated proteins from *Campylobacter jejuni* strains using complementary proteomics technologies. *Proteomics* **8**, 122–139.

Cornelis, G. R., Boland, A., Boyd, A. P., Iriarte, M., Neyt, C., Sory, M., Cornelis, G. U. Y. R., Geuijen, C., Neyt, C. & Stainier, I. (1998). The Virulence Plasmid of *Yersinia* an Antihost Genome. *Microbiol Mol Biol Rev* **62**, 1315–1352.

Cornelissen, C. N., Kelley, M., Marcia, M., Anderson, J. E., Cannon, J. G., Cohen, M. S. & Sparling, P. F. (1998). The transferrin receptor expressed by gonococcal strain FA1090 is required for the experimental infection of human male volunteers. *Mol Microbiol* **27**, 611–616.

Costa, T. R. D., Felisberto-Rodrigues, C., Meir, A., Prevost, M. S., Redzej, A., Trokter, M. & Waksman, G. (2015). Secretion systems in Gram-negative bacteria: structural and mechanistic insights. *Nat Rev Microbiol* **13**, 343–359. Nature Publishing Group.

Cota, I., Blanc-Potard, A. B. & Casadesús, J. (2012). STM2209-STM2208 (opvAB): a phase variation locus of *Salmonella enterica* involved in control of O-antigen chain length. *PLoS One* **7**, e36863.

Cotter, P. A., Yuk, M. H., Mattoo, S., Akerley, B. J., Boschwitz, J., Relman, D. A. & Miller, J. F. (1998). Filamentous Hemagglutinin of *Bordetella bronchiseptica* Is Required for Efficient Establishment of Tracheal Colonization. *Infect Immun* **66**, 5921–5929.

Cotter, S. E., Surana, N. K. & St Geme, J. W. (2005a). Trimeric autotransporters: a distinct subfamily of autotransporter proteins. *Trends Microbiol* **13**, 199–205.

Cotter, S. E., Yeo, H., Juehne, T., Iii, W. S. G., St, J. W. & Iii, G. (2005b). Architecture and Adhesive Activity of the *Haemophilus influenzae* Hsf Adhesin Architecture and Adhesive Activity of the Haemophilus influenzae Hsf Adhesin. *J Bacteriol* **187**, 4656–4664.

Coulthurst, S. J. (2013). The Type VI secretion system - a widespread and versatile cell targeting system. *Res Microbiol* **164**, 640–54. Elsevier Masson SAS.

Coureuil, M., Mikaty, G., Miller, F., Lecuyer, H., Bernard, C., Bourdoulous, S., Dumenil, G., Merge, R.-M., Weskler, B. B. & other authors. (2009). Meningococcal Type IV Pili Recruit the Polarity Complex to Cross the Brain Endothelium. *Science (80-)* **325**, 83–88.

Cowanit, S. W., Garavito, R. M., Jansonius, J. N., Jenkinsit, J. A., Karlsson, R., Konig, N., Pai, E. F., Pauptit, R. A., Rizkallah, P. J. & other authors. (1995). The structure of OmpF porin in a tetragonal crystal form. *Structure* **3**, 1041–1050.

Coyne, C. B., Vanhook, M. K., Gambling, T. M., Carson, J. L., Boucher, R. C. & Johnson, L. G. (2002). Regulation of Airway Tight Junctions by Proinflammatory Cytokines. *Mol Biol Cell* **13**, 3218–3234.

Craddick, M., Patel, R., Lower, A., Highlander, S., Ackermann, M. & McClenahan, D. (2012). Adenosine-5'-triphosphate release by *Mannheimia haemolytica*, lipopolysaccharide, and interleukin-1 stimulated bovine pulmonary epithelial cells. *Vet Immunol Immunopathol* **149**, 58–65. Elsevier B.V.

Crennell, S., Garman, E., Laver, G., Vimr, E. & Taylor, G. (1994). Crystal structure of *Vibrio cholerae* neuraminidase reveals dual lectin-like domains in addition to the catalytic domain. *Structure* **2**, 535–544.

Crosby, J. a & Kachlany, S. C. (2007). TdeA, a TolC-like protein required for toxin and drug export in *Aggregatibacter* (*Actinobacillus*) *actinomycetemcomitans*. *Gene* **388**, 83–92.

Crouch, E., Parghi, D., Kuan, S. & Persson, A. (1992). Surfactant protein D : subcellular localization in nonciliated bronchiolar epithelial cells. *Am J Physiol* **263**, L60–6.

Cummings, C. A., Brinig, M. M., Lepp, P. W., Pas, S. Van De & Relman, D. A. (2004). *Bordetella* Species Are Distinguished by Patterns of Substantial Gene Loss and Host Adaptation. *J Bacteriol* **186**, 1484–1492.

Curcio, E., Macchiarini, P. & De Bartolo, L. (2010). Oxygen mass transfer in a human tissue-engineered trachea. *Biomaterials* **31**, 5131–6. Elsevier Ltd.

Curcio, E., Piscioneri, A., Morelli, S., Salerno, S., Macchiarini, P. & De Bartolo, L. (2014). Kinetics of oxygen uptake by cells potentially used in a tissue engineered trachea. *Biomaterials* **35**, 6829–37. Elsevier Ltd.

Cuthbertson, L., Mainprize, I. L., Naismith, J. H. & Whitfield, C. (2009). Pivotal roles of the outer membrane polysaccharide export and polysaccharide copolymerase protein families in export of extracellular polysaccharides in gram-negative bacteria. *Microbiol Mol Biol Rev* **73**, 155–77.

Czuprynski, C. J., Noel, E. J. & Adlam, C. (1989). Modulation of bovine neutrophil antibacterial activities by *Pasteurella haemolytica* A1 purified capsular polysaccharide. *Microb Pathog* **6**, 133–141.

Al Dahouk, S., Jubier-Maurin, V., Scholz, H. C., Tomaso, H., Karges, W., Neubauer, H. & Köhler, S. (2008). Quantitative analysis of the intramacrophagic *Brucella suis* proteome reveals metabolic adaptation to late stage of cellular infection. *Proteomics* **8**, 3862–70.

Daigneault, M. C. & Lo, R. Y. C. (2009). Analysis of a collagen-binding trimeric autotransporter adhesin from *Mannheimia haemolytica* A1. *FEMS Microbiol Lett* **300**, 242–8.

Dajani, R., Zhang, Y., Taft, P. J., Travis, S. M., Starner, T. D., Olsen, A., Zabner, J., Welsh, M. J. & Engelhardt, J. F. (2005). Lysozyme secretion by submucosal glands protects the airway from bacterial infection. *Am J Respir Cell Mol Biol* **32**, 548–552.

Dalby, M. J., Gadegaard, N., Tare, R., Andar, A., Riehle, M. O., Herzyk, P., Wilkinson, C. D. W. & Oreffo, R. O. C. (2007). The control of human mesenchymal cell differentiation using nanoscale symmetry and disorder. *Nat Mater* **6**, 997–1003.

Davey, M. E., Caiazza, N. C. & Toole, G. A. O. (2003). Rhamnolipid Surfactant Production Affects Biofilm Architecture in *Pseudomonas aeruginosa* PAO. *J Bacteriol* **185**, 1027–1036.

Davidson, D. J., Kilanowski, F. M., Randell, S. H., Sheppard, D. N., Dorin, J. R., Donald, J., Scott, H. & A, J. R. D. (2000). A primary culture model of differentiated murine tracheal epithelium. *Am J Physiol Lung Cell Mol Physiol* **279**, 766–778.

Davies, J. C., Alton, E. W. F. W. & Bush, A. (2007). Cystic fibrosis. *BMJ* **335**, 1255–1259.

Davies, R. L. & Donachie, W. (1996). Intra-specific diversity and host specificity within *Pasteurella haemolytica* based on variation of capsular polysaccharide, lipopolysaccharide and outer-membrane proteins. *Microbiology* **142**, 1895–907.

Davies, R. L., Paster, B. J. & Dewhirst, F. E. (1996). Phylogenetic relationships and diversity within the *Pasteurella haemolytica* complex based on 16S rRNA sequence comparison and outer membrane protein and lipopolysaccharide analysis. *Int J Syst Bacteriol* **46**, 736–744.

Davies, R. L. & Baillie, S. (2003). Cytotoxic activity of *Mannheimia haemolytica* strains in relation to diversity of the leukotoxin structural gene lktA. *Vet Microbiol* **92**, 263–79.

Davies, R. L. & Lee, I. (2004). Sequence Diversity and Molecular Evolution of the Heat-Modifiable Outer Membrane Protein Gene (ompA) of *Mannhemia (pasteurella) haemolytica*, Mannheimia glucosida, and Pasteurella trehalosi. *J Bacteriol* **186**, 5741–5752.

Davies, R. L., Arkinsaw, S. & Selander, R. K. (1997). Evolutionary Genetics of *Pasteurella haemolytica* Isolates Recovered from Cattle and Sheep. *Infect Immun* **65**, 3585–3593.

Davies, R. L., Whittam, T. S. & Robert, K. (2001). Sequence Diversity and Molecular Evolution of the Leukotoxin (lktA) Gene in Bovine and Ovine Strains of *Mannheimia (Pasteurella) haemolytica*. *J Bacteriol* **183**, 1394–1404.

Davies, R. L., Campbell, S. & Whittam, T. S. (2002). Mosaic Structure and Molecular Evolution of the Leukotoxin Operon (lktCABD) in *Mannheimia* (*Pasteurella*) *haemolytica* , *Mannheimia glucosida* , and *Pasteurella trehalosi*. *J Bacteriol* **184**, 266–277.

Dawid, S., Grass, S., St, J. W. & Iii, G. (2001). Mapping of Binding Domains of Nontypeable *Haemophilus influenzae* HMW1 and HMW2 Adhesins. *Infect Immun* **69**, 307–314.

Dawson, R. J. P. & Locher, K. P. (2006). Structure of a bacterial multidrug ABC transporter. *Nature* **443**, 180–5.

Dean, P. & Kenny, B. (2004). Intestinal barrier dysfunction by enteropathogenic *Escherichia coli* is mediated by two effector molecules and a bacterial surface protein. *Mol Microbiol* **54**, 665–675.

Deghmane, A.-E., Giorgini, D., Larribe, M., Alonso, J.-M. & Taha, M.-K. (2002). Down-regulation of pili and capsule of *Neisseria meningitidis* upon contact with epithelial cells is mediated by CrgA regulatory protein. *Mol Microbiol* **43**, 1555–64.

Delgado-Ortega, M., Olivier, M., Sizaret, P.-Y., Simon, G. & Meurens, F. (2014). Newborn pig trachea cell line cultured in air-liquid interface conditions allows a partial in vitro representation of the porcine upper airway tissue. *BMC Cell Biol* **15**, 14.

Deneer, H. G. & Potter, A. A. (1989). Iron- repressible Outer -membrane Proteins of *Pasteurella haemolytica*. *J Gen Microbiol* **135**, 435–443.

Deshpande, M. S., Ambagala, T. C., Ambagala, A. P. N., Kehrli, M. E. & Srikumaran, S. (2002). Bovine CD18 Is Necessary and Sufficient To Mediate Mannheimia (Pasteurella) *haemolytica* Leukotoxin-Induced Cytolysis. *Infect Immun* **70**, 5058–5064.

Didon, L., Zwick, R. K., Chao, I. W., Walters, M. S., Wang, R., Hackett, N. R. & Crystal, R. G. (2013). RFX3 modulation of FOXJ1 regulation of cilia genes in the human airway epithelium. *Respir Res* **14**, 70. Respiratory Research.

Diep, B. A., Phung, Q., Date, S., Arnott, D., Bakalarski, C., Xu, M., Nakamura, G., Swem, D. L., Alexander, M. K. & other authors. (2013). Identifying Potential Therapeutic Targets of Methicillin-resistant *Staphylococcus aureus* Through in Vivo Proteomic Analysis. *J Infect Dis* **209**, 1–9.

Doi, K., Nakayama, Y. & Matsuda, T. (1996). Novel compliant and tissue-permeable microporous polyurethane vascular prosthesis fabricated using an excimer laser ablation technique. *J Biomed Mater Res* **31**, 27–33.

Donachie, W., Fraser, J., Quirie, M. & Gilmour, N. J. (1984). Studies on strains of *Pasteurella haemolytic*a not typable by the indirect haemagglutination test. *Res Vet Sci* **37**, 188–193.

Donachie, W. & Gilmour, N. J. L. (1988). Sheep antibody response to cell wall antigens expressed in vivo by *Pasteurella haemolytica* serotype A2. *FEMS Microbiol Lett* **56**, 271–276.

Dong, C., Beis, K., Nesper, J., Brunkan-Lamontagne, A. L., Clarke, B. R., Whitfield, C. & Naismith, J. H. (2006). Wza the translocon for *E. coli* capsular polysaccharides defines a new class of membrane protein. *Nature* **444**, 226–9.

Dong, J., Yang, G. & Machaourab, H. S. (2005). Structural Basis of Energy Transduction in the Transport Cycle of MsbA. *Science (80-)* **308**, 1023–1029.

Drees, F., Pokutta, S., Yamada, S., Nelson, W. & Weis, W. (2005). α-catenin is a molecular switch that binds E-cadherin-β-catenin and regulates actin-filament assembly. *Cell* **123**, 903–915.

Drenkard, E. & Ausubel, F. M. (2002). *Pseudomonas* biofilm formation and antibiotic resistance are linked to phenotypic variation. *Nature* **416**, 200–203.

Drummelsmith, J. & Whitfield, C. (2000). Translocation of group 1 capsular polysaccharide to the surface of *Escherichia coli* requires a multimeric

complex in the outer membrane. *EMBO J* **19**, 57–66.

Du, D., Wang, Z., James, N. R., Voss, J. E., Klimont, E., Ohene-Agyei, T., Venter, H., Chiu, W. & Luisi, B. F. (2014). Structure of the AcrAB-TolC multidrug efflux pump. *Nature* **509**, 512–5. Nature Publishing Group.

Duensing, T. D. (1997). Natural Proteoglycan Receptor Analogs Determine the Dynamics of Opa Adhesin-Mediated Gonococcal Infection of Chang Epithelial Cells. *Infect Immun* **65**, 5028–5034.

Dumetz, F., Duchaud, E., Claverol, S., Orieux, N., Papillon, S., Lapaillerie, D. & Le Hénaff, M. (2008). Analysis of the *Flavobacterium psychrophilum* outer-membrane subproteome and identification of new antigenic targets for vaccine by immunomics. *Microbiology* **154**, 1793–801.

Dutzler, R., Wang, Y., Rizkallah, P. J., Rosenbusch, J. P. & Schirmer, T. (1995). Crystal structures of various maltooligosaccharides bound to maltoporin reveal a specific sugar translocation pathway. *Structure* **4**, 127–134.

Dvorak, A., Tilley, A. E., Shaykhiev, R., Wang, R. & Crystal, R. G. (2011). Do airway epithelium air-liquid cultures represent the in vivo airway epithelium transcriptome? *Am J Respir Cell Mol Biol* **44**, 465–73.

Dyer, R. M., Majumdar, S., Douglas, S. D. & Korchak, H. M. (1994). Bovine parainfluenza-3 virus selectively depletes a calcium-independent, phospholipid-dependent protein kinase C and inhibits superoxide anion generation in bovine alveolar macrophages. *J Immunol* **153**, 1171–9.

Ebanks, R. O., Dacanay, A., Goguen, M., Pinto, D. M. & Ross, N. W. (2004). Differential proteomic analysis of *Aeromonas salmonicida* outer membrane proteins in response to low iron andin vivo growth conditions. *Proteomics* **4**, 1074–1085.

Edwards, J. A., Groathouse, N. A. & Boitano, S. (2005). *Bordetella bronchiseptica* adherence to cilia is mediated by multiple adhesin factors and blocked by surfactant protein A. *Infect Immun* **73**, 3618–26.

Edwards, T. A. (2010). Control methods for bovine respiratory disease for feedlot cattle. *Vet Clin North Am Food Anim Pr* **26**, 273–284. Elsevier Ltd.

Eichelberg, K., Ginocchio, C. C. & Galan, J. E. (1994). Molecular and Functional Characterization of the *Salmonella typhimurium* Invasion Genes invB and invC : Homology of InvC to the FoF1 ATPase Family of Proteins. *J Bacteriol* **176**, 4501–4510.

Eicher, T., Cha, H. -j., Seeger, M. a., Brandstatter, L., El-Delik, J., Bohnert, J. a., Kern, W. V., Verrey, F., Grutter, M. G. & other authors. (2012). Transport of drugs by the multidrug transporter AcrB involves an access and a deep binding pocket that are separated by a switch-loop. *Proc Natl Acad Sci* **109**, 5687–5692.

Eidam, C., Poehlein, A., Brenner Michael, G., Kadlec, K., Liesegang, H., Brzuszkiewicz, E., Daniel, R., Sweeney, M. T., Murray, R. W. & other authors. (2013). Complete genome sequence of *Mannheimia haemolytica* strain 42548 from a case of bovine respiratory disease. *Genome Announc* **1**, 1–2.

E-komon, T., Burchmore, R., Herzyk, P. & Davies, R. (2012). Predicting the outer membrane proteome of *Pasteurella multocida* based on consensus prediction enhanced by results integration and manual confirmation. *BMC*

Bioinformatics **13**, 63. BioMed Central Ltd.

Ellis, J. a. (2009). Update on viral pathogenesis in BRD. *Anim Health Res Rev* **10**, 149–53.

Ellison, R. T. I. & Giehl, T. J. (1991). Killing of Gram-negative Bacteria by Lactofernn and Lysozyme. *J Clin Invest* **88**, 1080–1091.

Emsley, P., Charles, I. G., Fairweather, N. F. & Isaacs, N. W. (1996). Structure of *Bordetella pertussis* virulence factor P.69 pertactin. *Nature* **381**, 90–92.

Engler, A. J., Sen, S., Sweeney, H. L. & Discher, D. E. (2006). Matrix Elasticity Directs Stem Cell Lineage Specification. *Cell* **126**, 677–689.

Euba, B., Moleres, J., Viadas, C., Ruiz de los Mozos, I., Valle, J., Bengoechea, J. A. & Garmendia, J. (2015). Relative Contribution of P5 and Hap Surface Proteins to Nontypable *Haemophilus influenzae* Interplay with the Host Upper and Lower Airways. *PLoS One* **10**, e0123154.

Evans, M. J., Winkle, L. S. Van, Fanucchi, M. V & Plopper, G. (2001). Cellular and Molecular Characteristics of Basal Cells. *Exp Lung Res* **27**, 401–415.

Evans, N. J., Harrison, O. B., Clow, K., Derrick, J. P., Feavers, I. M. & Maiden, M. C. J. (2010). Variation and molecular evolution of HmbR, the *Neisseria meningitidis* haemoglobin receptor. *Microbiology* **156**, 1384–93.

Evans, W. H. & Martin, P. E. M. (2002). Gap junctions: structure and function (Review). *Mol Membr Biol* **19**, 121–136.

Even-Tzur, N., Jaffa, A., Gordon, Z., Gottlieb, R., Kloog, Y., Einav, S., Wolf, M. & Elad, D. (2010). Air-Liquid Interface Culture of Nasal Epithelial Cells on Denuded Amniotic Membranes. *Cell Mol Bioeng* **3**, 307–318.

Everett, R. S., Vanhook, M. K., Barozzi, N., Toth, I. & Johnson, L. G. (2006). Specific Modulation of Airway Epithelial Tight Junctions by Apical Application of an Occludin Peptide. *Mol Pharmacol* **69**, 492–500.

Ewers, C., Lübke-Becker, A., Bethe, A., Kießling, S., Filter, M. & Wieler, L. H. (2006). Virulence genotype of Pasteurella multocida strains isolated from different hosts with various disease status. *Vet Microbiol* **114**, 304–317.

Fahy, J. V & Dickey, B. F. (2010). Airway mucus function and dysfunction. *N Engl J Med* **363**, 2233–47.

Feldman, G., Mullin, J. & Ryan, M. (2005). Occludin: Structure, function and regulation. *Adv Drug Deliv Rev* **57**, 883–917.

Fink, D. L., Buscher, A. Z., Green, B., Fernsten, P., St, J. W. & Iii, G. (2003). The *Haemophilus influenzae* Hap autotransporter mediates microcolony formation and adherence to epithelial cells and extracellular matrix via binding regions in the C-terminal end of the passenger domain. *Cell Microbiol* **5**, 175–186.

Fleischmann, R. D., Adams, M. D., White, O., Clayton, R. A., Kirkness, E. F., Kerlavage, A. R., Bult, C. J., Tomb, J., Dougherty, B. A. & other authors. (1995). Whole-Genome Random Sequencing and Assembly of *Haemophilus influenzae* Rd. *Science (80-)* **269**, 496–512.

Flemming, H.-C. & Wingender, J. (2010). The biofilm matrix. *Nat Rev Microbiol* **8**, 623–33. Nature Publishing Group.

Fliegauf, M., Sonnen, A. F.-P., Kremer, B. & Henneke, P. (2013). Mucociliary clearance defects in a murine in vitro model of pneumococcal airway

infection. *PLoS One* **8**, e59925.

Flores-Ramirez, G., Jankovicova, B., Bilkova, Z., Miernyk, J. a & Skultety, L. (2014). Identification of *Coxiella burnetii* surface-exposed and cell envelope associated proteins using a combined bioinformatics plus proteomics strategy. *Proteomics* **14**, 1868–81.

Flugel, A., Schulze-koopsh, H., Heesemannll, J., Kuhn, K., Sorokin, L., Burkhardts, H., Mark, K. Von Der & Emmrichs, F. (1994). Interaction of Enteropathogenic *Yersinia enterocolitica* with Complex Basement Membranes and the Extracellular Matrix. *J Biol Chem* **269**, 29732–29738.

Folsom, J. P., Parker, A. E. & Carlson, R. P. (2014). Physiological and proteomic analysis of *Escherichia coli* iron-limited chemostat growth. *J Bacteriol* **196**, 2748–2761.

Frank, G. H. (1985). Serotype-specific resistance to nasal colonization by *Pasteurella haemolytica* in cattle. *Am J Vet Res* **46**, 2245–2248.

Frank, G. H. & Smith, P. C. (1983). Prevalence of *Pasteurella haemolytica* in transported calves. *Am J Vet Res* **44**, 981–985.

Freed, L. E., Marquis, J. C., Nohria, A., Emmanual, J., Mikos, A. G. & Langer, R. (1993a). Neocartilage formation *in vitro* and *in vivo* using cells cultured on synthetic biodegradable polymers. *J Biomed Mater Res* **27**, 11–23.

Freed, L. E., Vunjak-Novakovic, G. & Langer, R. (1993b). Cultivation of cell-polymer cartilage implants in bioreactors. *J Cell Biochem* **51**, 257–264.

Freed, L. E., Vunjak-Novakovic, G., Biron, R. J., Eagles, D. B., Lesnoy, D. C., Barlow, S. K. & Langer, R. (1994). Biodegradable Polymer Scaffolds for Tissue Engineering. *Nat Biotechnol* **12**, 689–693.

Frick, A. G., Joseph, T. D., Pang, L., Rabe, a. M., St. Geme III, J. W. & Look, D. C. (2000). *Haemophilus influenzae* Stimulates ICAM-1 Expression on Respiratory Epithelial Cells. *J Immunol* **164**, 4185–4196.

Fronzes, R., Schäfer, E., Wang, L., Saibil, H. R., Orlova, E. V & Waksman, G. (2009). Structure of a Type IV Secretion System Core Complex. *Science (80-)* **323**, 266–268.

Fujii, T., Cheung, M., Blanco, A., Kato, T., Blocker, A. J. & Namba, K. (2012). Structure of a type III secretion needle at 7-Å resolution provides insights into its assembly and signaling mechanisms. *Proc Natl Acad Sci* **109**, 4461–6.

Fulcher, M. L., Gabriel, S., Burns, K. A., Yankaskas, J. R. & Randell, S. H. (2005). Well-Differentiated Human Airway Epithelial Cell Cultures. In *Hum Cell Cult Protoc*, pp. 183–206.

Furuta, N., Takeuchi, H. & Amano, A. (2009). Entry of *Porphyromonas gingivalis* Outer Membrane Vesicles into Epithelial Cells Causes Cellular Functional Impairment. *Infect Immun* **77**, 4761–4770.

Galen, J. E., Ketley, J. M., Fasano, A., Richardson, S. H., Wasserman, S. S. & Kaperl, J. B. (1992). Role of *Vibrio cholerae* Neuraminidase in the Function of Cholera Toxin. *Infect Immun* **60**, 406–415.

Gandhi, N. S. & Mancera, R. L. (2008). The Structure of Glycosaminoglycans and their Interactions with Proteins. *Chem Biol Drug Des* **72**, 455–482.

Gånheim, C., Hulten, C., Carlsson, U., Kindahl, H., Niskanen, R. & Waller, K. P. (2003). The Acute Phase Response in Calves Experimentally Infected with Bovine Viral Diarrhoea Virus and/or *Mannheimia haemolytica*. *J Vet Med Ser*

B **50**, 183–190.

Gånheim, C., Johannisson, A., Ohagen, P. & Persson Waller, K. (2005). Changes in peripheral blood leucocyte counts and subpopulations after experimental infection with BVDV and/or *Mannheimia haemolytica*. *J Vet Med B Infect Dis Vet Public Health* **52**, 380–5.

Garreta, E., Melo, E., Navajas, D. & Farré, R. (2014). Low oxygen tension enhances the generation of lung progenitor cells from mouse embryonic and induced pluripotent stem cells. *Physiol Rep* **2**, 1–14.

Garrod, D. & Chidgey, M. (2008). Desmosome structure, composition and function. *Biochim Biophys Acta - Biomembr* **1778**, 572–587.

Geme, J. W. S. I., Cutter, D. & Barenkamp, S. J. (1996). Characterization of the Genetic Locus Encoding *Haemophilus influenzae* Type b Surface Fibrils. *J Bacteriol* **178**, 6281–6287.

Genevrois, Â., Steeghs, L., Roholl, P., Letesson, J.-J. & Ley, P. Van Der. (2003). The Omp85 protein of *Neisseria meningitidis* is required for lipid export to the outer membrane. *EMBO J* **22**, 1780–1789.

Gentle, I. E., Burri, L. & Lithgow, T. (2005). Molecular architecture and function of the Omp85 family of proteins. *Mol Microbiol* **58**, 1216–1225.

Gershwin, L. J., Van Eenennaam, A. L., Anderson, M. L., McEligot, H. a., Shao, M. X., Toaff-Rosenstein, R., Taylor, J. F., Neibergs, H. L. & Womack, J. (2015). Single Pathogen Challenge with Agents of the Bovine Respiratory Disease Complex. *PLoS One* **10**, e0142479.

Gesslbauer, B., Poljak, A., Handwerker, C., Schüler, W., Schwendenwein, D., Weber, C., Lundberg, U., Meinke, A. & Kungl, A. J. (2012). Comparative membrane proteome analysis of three *Borrelia* species. *Proteomics* **12**, 845–58.

Ghio, A. J., Carter, J. D., Dailey, L. A., Devlin, R. B. & Samet, J. M. (1999). Respiratory epithelial cells demonstrate lactoferrin receptors that increase after metal exposure. *Am J Physiol* **276**, 933–940.

Giancotti, F. G. & Ruoslahti, E. (1999). Integrin Signaling. *Science (80-)* **285**, 1028–1032.

Gilmour, N. J., Martin, W. B., Sharp, J. M., Thompson, D. A., Wells, P. W. & Donachie, W. (1983). Experimental immunisation of lambs against pneumonic pasteurellosis. *Res Vet Sci* **35**.

Gilmour, N. J., Donachie, W., Sutherland, a D., Gilmour, J. S., Jones, G. E. & Quirie, M. (1991). Vaccine containing iron-regulated proteins of *Pasteurella haemolytica* A2 enhances protection against experimental pasteurellosis in lambs. *Vaccine* **9**, 137–40.

Gimenez, a. P., Wu, Y.-Z., Paya, M., Delclaux, C., Touqui, L. & Goossens, P. L. (2004). High Bactericidal Efficiency of Type IIA Phospholipase A2 against *Bacillus anthracis* and Inhibition of Its Secretion by the Lethal Toxin. *J Immunol* **173**, 521–530.

Gioia, J., Qin, X., Jiang, H., Clinkenbeard, K., Lo, R., Liu, Y., Fox, G. E., Yerrapragada, S., McLeod, M. P. & other authors. (2006). The genome sequence of *Mannheimia haemolytica* A1: insights into virulence, natural competence, and Pasteurellaceae phylogeny. *J Bacteriol* **188**, 7257–66.

Glorieux, S., Van den Broeck, W., van der Meulen, K. M., Van Reeth, K.,

Favoreel, H. W. & Nauwynck, H. J. (2007). In vitro culture of porcine respiratory nasal mucosa explants for studying the interaction of porcine viruses with the respiratory tract. *J Virol Methods* **142**, 105–12.

Godlewska, R., Wiśniewska, K., Pietras, Z. & Jagusztyn-Krynicka, E. K. (2009). Peptidoglycan-associated lipoprotein (Pal) of Gram-negative bacteria: Function, structure, role in pathogenesis and potential application in immunoprophylaxis: Minireview. *FEMS Microbiol Lett* **298**, 1–11.

Golovkine, G., Faudry, E., Bouillot, S., Elsen, S., Attrée, I. & Huber, P. (2016). Pseudomonas aeruginosa Transmigrates at Epithelial Cell-Cell Junctions, Exploiting Sites of Cell Division and Senescent Cell Extrusion. *PLoS Pathog* **12**, 1–22.

Gonzalez, C., Murtaugh, M. P. & Maheswaran, S. K. (1991). Genomic Distribution of a Serotype 1-Specific Antigen-Coding DNA Fragment of *Pasteurella Haernolytica*. *J Vet Med Ser B* **38**, 599–609.

Gonzalez, C. T., Maheswaran, S. K. & Murtaugh, M. P. (1995). *Pasteurella haemolytica* Serotype 2 Contains the Gene for a Noncapsular Serotype 1-Specific Antigen. *Infect Immun* **63**, 1340–1348.

Goris, K., Uhlenbruck, S., Schwegmann-Wessels, Christine Kohl, Frank, W., Niedorf, F., Stern, M., Hewicker-Trautwein, M., Bals, R., Taylor, G., Braun, A. & other authors. (2008). Differential Sensitivity of Differentiated Epithelial Cells to Respiratory Viruses Reveals Different Viral Strategies of Host Infection. *Jounal Virol* **83**, 1962–1968.

Gray, T. E., Guzman, K., Davis, C. W., Abdullah, L. H. & Nettesheim, P. (1996). Mucociliary Differentiation of Serially Passaged Normal Human Tracheobronchial Epithelial Cells. *Am J Respir Cell Mol Biol* **14**, 104–112.

Gray, T., Koo, J. & Nettesheim, P. (2001). Regulation of mucous differentiation and mucin gene expression in the tracheobronchial epithelium. *Toxicology* **160**, 35–46.

Gray-Owen, S. D. & Blumberg, R. S. (2006). CEACAM1: contact-dependent control of immunity. *Nat Rev Immunol* **6**, 433–46.

Gray-Owen, S. D. & Schryvers, A. (1996). Bacterial transferrin and lactoferrin receptors. *Trends Microbiol* **4**.

Greenfield, L. K. & Whitfield, C. (2012). Synthesis of lipopolysaccharide O-antigens by ABC transporter-dependent pathways. *Carbohydr Res* **356**, 12–24. Elsevier Ltd.

Griffin, D. (1997). Economic impact associated with respiratory disease in beef cattle. *Vet Clin North Am Food Anim Pract* **13**, 367–377.

Griffin, D., Chengappa, M. M., Kuszak, J. & McVey, D. S. (2010). Bacterial pathogens of the bovine respiratory disease complex. *Vet Clin North Am Food Anim Pract* **26**, 381–94.

Grissett, G. P., White, B. J. & Larson, R. L. (2015). Structured Literature Review of Responses of Cattle to Viral and Bacterial Pathogens Causing Bovine Respiratory Disease Complex. *J Vet Intern Med* **29**, 770–780.

Gross, C. A., Bowler, R. P., Green, R. M., Weinberger, A. R., Schnell, C. & Chu, H. W. (2010). ß2-agonist promote host defense against bacterial infection in primary human bronchial epithelial cells.pdf. *BMC Pulm Med* **10**, 1–9.

Grubor, B., Meyerholz, D. K. & Ackermann, M. R. (2009). Collectins and Cationic Antimicrobial Peptides of the Respiratory Epithelia. *Vet Pathol* **43**, 595–612.

Grubor, B., Meyerholz, D. K. & Ackermann, M. R. (2006). Collectins and Cationic Antimicrobial Peptides of the Respiratory Epithelia. *Vet Pathol* **612**, 595–612.

Grubor, B., Gallup, J. M., Meyerholz, D. K., Crouch, E. C., Evans, R. B., Brogden, K. A., Lehmkuhl, H. D. & Ackermann, M. R. (2004a). Enhanced Surfactant Protein and Defensin mRNA Levels and Reduced Viral Replication during Parainfluenza Virus Type 3 Pneumonia in Neonatal Lambs. *Clin Diagn Lab Immunol* **11**, 599–607.

Grubor, B., Gallup, J. M., Ramírez-Romero, R., Bailey, T. B., Crouch, E. C., Brogden, K. a & Ackermann, M. R. (2004b). Surfactant protein D expression in normal and pneumonic ovine lung. *Vet Immunol Immunopathol* **101**, 235–42.

Gruss, F., Zähringer, F., Jakob, R. P., Burmann, B. M., Hiller, S. & Maier, T. (2013). The structural basis of autotransporter translocation by TamA. *Nat Struct Mol Biol* **20**, 1318–20. Nature Publishing Group.

Gu, W., Wang, X., Qiu, H., Luo, X., Xiao, D., Xiao, Y., Tang, L., Kan, B. & Jing, H. (2012). Comparative antigenic proteins and proteomics of pathogenic *Yersinia enterocolitica* bio-serotypes 1B/O: 8 and 2/O: 9 cultured at 25°C and 37°C. *Microbiol Immunol* **56**, 583–594.

Gu, Y., Stansfeld, P. J., Zeng, Y., Dong, H., Wang, W. & Dong, C. (2015). Lipopolysaccharide is inserted into the outer membrane through an intramembrane hole, a lumen gate, and the lateral opening of LptD. *Structure* **23**, 496–504. The Authors.

Guedin, S., Willery, E., Locht, C., Inserm, U. & Jacod-Dubuisson, F. (1998). Evidence that a globular conformation is not compatible with FhaC-mediated secretion of the *Bordetella pertussis* filamentous haemagglutinin. *Mol Microbiol* **29**, 763–774.

Guina, T., Wu, M., Miller, S. I., Purvine, S. O., Yi, E. C., Eng, J., Goodlett, D. R., Aebersold, R., Ernst, R. K. & Lee, K. a. (2003). Proteomic analysis of *Pseudomonas aeruginosa* grown under magnesium limitation. *J Am Soc Mass Spectrom* **14**, 742–51.

Guzman, K., Randell, S. H. & Netteshiem, P. (1995). Epidermal Growth Factor Regulates Expression of The Mucous Phenotype of Rat Tracheal Epithelial Cells. *Biochem Biophys Res Commun* **217**, 412–418.

Hackett, N. R., Shaykhiev, R., Walters, M. S., Wang, R., Zwick, R. K., Ferris, B., Witover, B., Salit, J. & Crystal, R. G. (2011). The human airway epithelial basal cell transcriptome. *PLoS One* **6**, e18378.

Haig, S.-J. (2011). Adherence of *Mannheimia haemolytica* to ovine bronchial epithelial cells. *Biosci Horizons* **4**, 50–60.

Halldorsson, S., Gudjonsson, T., Gottfredsson, M., Singh, P. K., Gudmundsson, G. H. & Baldursson, O. (2010). Azithromycin maintains airway epithelial integrity during Pseudomonas aeruginosa infection. *Am J Respir Cell Mol Biol* **42**, 62–8.

Hamill, O. P. & Martinac, B. (2001). Molecular Basis of Mechanotransduction in Living Cells. *Physiol Rev* **81**, 685–741.

Hammerschmidt, S., Muller, A., Muhlenhoff, M., Borrow, R., Gerardy-schahn, R. & Frosch, M. (1996). Capsule phase variation in *Neisseria meningitidis* serogroup B by slipped-strand mispairing in the polysialyltransferase gene (siaD): correlation with bacterial invasion and the outbreak of meningococcal disease. *Mol Microbiol* **20**, 1–10.

Hammerschmidt, S., Wolff, S., Hocke, A., Rosseau, S., Müller, E. & Rohde, M. (2005). Illustration of Pneumococcal Polysaccharide Capsule during Adherence and Invasion of Epithelial Cells. *Infect Immun* **73**, 4653–4667.

Han, W., Wu, B., Li, L., Zhao, G., Woodward, R., Pettit, N., Cai, L., Thon, V. & Wang, P. G. (2012). Defining function of lipopolysaccharide O-antigen ligase WaaL using chemoenzymatically synthesized substrates. *J Biol Chem* **287**, 5357–65.

Hansen, S. & Holmskov, U. (2002). Lung Surfactant Protein D (SP-D) and the Molecular Diverted Descendants : Conglutinin , CL-43 and CL-46. *Immunobiology* **205**, 498–517.

Hao, Y., Kuang, Z., Walling, B. E., Bhatia, S., Sivaguru, M., Chen, Y., Gaskins, H. R. & Lau, G. W. (2012). Pseudomonas aeruginosa pyocyanin causes airway goblet cell hyperplasia and metaplasia and mucus hypersecretion by inactivating the transcriptional factor FoxA2. *Cell Microbiol* **14**, 401–15.

Hartmann, M. D., Grin, I., Dunin-Horkawicz, S., Deiss, S., Linke, D., Lupas, A. N. & Hernandez Alvarez, B. (2012). Complete fiber structures of complex trimeric autotransporter adhesins conserved in enterobacteria. *Proc Natl Acad Sci U S A* **109**, 20907–12.

Hartsock, A. & Nelson, W. J. (2008). Adherens and Tight Junctions: Structure, Function and Connection to the Actin Cytoskeleton. *Biochim Biophys Acta* **1778**, 660–669.

Hatzfeld, M. & Franke, W. W. (1985). Pair formation and promiscuity of cytokeratins: formation in vitro of heterotypic complexes and intermediate-sized filaments by homologous and heterologous recombinations of purified polypeptides. *J Cell Biol* **101**, 1826–41.

Hauberg, L., Schmidt, F., Scharf, C., Dörr, J., Völker, U. & Reinhold-Hurek, B. (2010). Proteomic characterization of a pilR regulatory mutant of *Azoarcus* sp. strain BH72 with the aid of gel-based and gel-free approaches. *Proteomics* **10**, 458–69.

Hayashi, Y., Tsurumizu, R., Tsukahara, J., Takeda, K., Narita, S., Mori, M., Miki, K. & Tokuda, H. (2014). Roles of the protruding loop of factor B essential for the localization of lipoproteins (LolB) in the anchoring of bacterial triacylated proteins to the outer membrane. *J Biol Chem* **289**, 10530–9.

Heesemann, J. & Griiter, L. (1987). Genetic evidence that the outer membrane protein YOP1 of. *FEMS Microbiol Lett* **40**, 37–41.

Heinz, E., Pichler, P., Heinz, C., Op den Camp, H. J. M., Toenshoff, E. R., Ammerer, G., Mechtler, K., Wagner, M. & Horn, M. (2010). Proteomic analysis of the outer membrane of *Protochlamydia amoebophila* elementary bodies. *Proteomics* **10**, 4363–76.

Heise, T. & Dersch, P. (2006). Identification of a domain in Yersinia virulence factor YadA that is crucial for extracellular matrix-specific cell adhesion and uptake. *Proc Natl Acad Sci* **103**, 3375–3380.

Hester, S. E., Park, J., Goodfield, L. L., Feaga, H. a, Preston, A. & Harvill, E. T. (2013). Horizontally acquired divergent O-antigen contributes to escape from cross-immunity in the classical bordetellae. *BMC Evol Biol* **13**, 209. BMC Evolutionary Biology.

Highlander, S. K., Engler, M. J. & Weinstock, G. M. (1990). Secretion and expression of the *Pasteurella haemolytica* leukotoxin. *J Bacteriol* **172**, 2343–2350.

Highlander, S. K. (2001). Molecular Genetic Analysis of Virulence in *Mannheimia* (*Pasteurella*) *haemolytica*. *Front Biosci* **6**, D1128–D1151.

Highlander, S. K., Fedorova, N. D., Dusek, D. M., Panciera, R., Alvarez, L. E. & Rinehart, C. (2000). Inactivation of *Pasteurella* (*Mannheimia*) *haemolytica* Leukotoxin Causes Partial Attenuation of Virulence in a Calf Challenge Model. *Infect Immun* **68**, 3916–3922.

Highlander, S. K., Chidambaram, M., Engler, M. J. & Weinstock, G. M. (1989). DNA Sequence of the *Pasteurella haemolytica* Leukotoxin Gene Cluster. *DNA* **8**, 15–28.

Hill, D. J., Toleman, M. A., Evans, D. J., Villullas, S., Alphen, L. Van & Virji, M. (2001). The variable P5 proteins of typeable and non-typeable *Haemophilus influenzae* target human CEACAM1. *Mol Microbiol* **39**, 850–862.

Hillenkamp, F., Jaskolla, T. W. & Karas, M. (2014). The MALDI Process and Method. In *MALDI MS A Pract Guid to Instrumentation, Methods, Appl*, pp. 1–40.

Hirst, R. a, Rutman, A., Williams, G. & O'Callaghan, C. (2010). Ciliated air-liquid cultures as an aid to diagnostic testing of primary ciliary dyskinesia. *Chest* **138**, 1441–1447.

Hobbs, M. M., Seiler, A., Achtman, M. & Planck, M. (1994). Microevolution within a cional population of pathogenic bacteria : recombination , gene duplication and horizontal genetic exchange in the opa gene family of *Neisseria meningitidis*. *Mol Microbiol* **12**, 171–180.

Hodak, H., Clantin, B., Willery, E., Villeret, V., Locht, C. & Jacob-Dubuisson, F. (2006). Secretion signal of the filamentous haemagglutinin, a model two-partner secretion substrate. *Mol Microbiol* **61**, 368–82.

Hodgins, D. C. & Shewen, P. E. (2000). Vaccination of neonatal colostrum-deprived calves against *Pasteurella haemolytica* A1. *Can J Vet Res* **64**, 3–8.

Hodgson, J. C., Moon, G. M., Quirie, M. & Donachie, W. (2003). Association of LPS chemotype of *Mannheimia* (*Pasteurella*) *haemolytica* with disease virulence in an ovine model of pneumonic pasteurellosis. *J Endotoxin Res* **9**, 25–32.

Hodson, A. (1977). *Development of The Lung*, 1st edn. (A. Hodson, Ed.). New York and Basal.

Hoffmann, R., Braun, A., Knauf, S., Kaup, F.-J. & Bleyer, M. (2014). Distribution of ciliated epithelial cells in the trachea of common marmosets (Callithrix jacchus). *J Med Primatol* **43**, 55–58.

Hong, J. S., Kim, S.-W. & Koo, J. S. (2008). Sp1 up-regulates cAMP-response-element-binding protein expression during retinoic acid-induced mucous differentiation of normal human bronchial epithelial cells. *Biochem J* **410**, 49–61.

Hotomi, M., Arai, J., Billal, D. S., Takei, S., Ikeda, Y., Ogami, M., Kono, M., Beder, L. B., Toya, K. & other authors. (2010). Nontypeable *Haemophilus influenzae* isolated from intractable acute otitis media internalized into cultured human epithelial cells. *Auris Nasus Larynx* **37**, 137–44.

Houben, E. N. G., Korotkov, K. V & Bitter, W. (2014). Take five - Type VII secretion systems of *Mycobacteria*. *Biochim Biophys Acta* **1843**, 1707–16. Elsevier B.V.

Hounsome, J. D. A. (2012). *Comparative outer membrane proteomic analyses of bovine and ovine isolates of* Mannheimia haemolytica *and* Mannheimia glucosida. University of Glasgow.

Hounsome, J. D. a, Baillie, S., Noofeli, M., Riboldi-Tunnicliffe, A., Burchmore, R. J. S., Isaacs, N. W. & Davies, R. L. (2011). Outer membrane protein A of bovine and ovine isolates of *Mannheimia haemolytica* is surface exposed and contains host species-specific epitopes. *Infect Immun* **79**, 4332–41.

Hu, Q., Noll, R. J., Li, H., Makarov, A., Hardman, M. & Graham Cooks, R. (2005). The Orbitrap: a new mass spectrometer. *J mass Spectrom* **40**, 430–43.

Huang, T.-W., Young, Y.-H., Cheng, P.-W., Chan, Y.-H. & Young, T.-H. (2009). Culture of nasal epithelial cells using chitosan-based membranes. *Laryngoscope* **119**, 2066–70.

Huang, T.-W., Cheng, P.-W., Chan, Y.-H., Yeh, T.-H., Young, Y.-H. & Young, T.-H. (2010a). Regulation of ciliary differentiation of human respiratory epithelial cells by the receptor for hyaluronan-mediated motility on hyaluronan-based biomaterials. *Biomaterials* **31**, 6701–9. Elsevier Ltd.

Huang, T.-W., Chan, Y.-H., Cheng, P.-W., Young, Y.-H., Lou, P.-J. & Young, T.-H. (2010b). Increased mucociliary differentiation of human respiratory epithelial cells on hyaluronan-derivative membranes. *Acta Biomater* **6**, 1191–9. Acta Materialia Inc.

Huang, T.-W., Chan, Y.-H., Su, H.-W., Chou, Y.-S. & Young, T.-H. (2013). Increased mucociliary differentiation and aquaporins formation of respiratory epithelial cells on retinoic acid-loaded hyaluronan-derivative membranes. *Acta Biomater* **9**, 6783–9. Acta Materialia Inc.

Huang, Y.-J., Wu, C.-C., Chen, M.-C., Fung, C.-P. & Peng, H.-L. (2006). Characterization of the type 3 fimbriae with different MrkD adhesins: possible role of the MrkD containing an RGD motif. *Biochem Biophys Res Commun* **350**, 537–42.

Hudson, K. J., Bliska, J. B. & Bouton, A. H. (2005). Distinct mechanisms of integrin binding by *Yersinia pseudotuberculosis* adhesins determine the phagocytic response of host macrophages. *Cell Microbiol* **7**, 1474–89.

Humlicek, A. L., Manzel, L. J., Chin, C. L., Shi, L., Excoffon, K. J. D. a, Winter, M. C., Shasby, D. M. & Look, D. C. (2007). Paracellular permeability restricts airway epithelial responses to selectively allow activation by mediators at the basolateral surface. *J Immunol* **178**, 6395–403.

Hunt, D. F., Iii, J. R. Y., Shabanowitz, J., Winston, S. & Hauer, C. R. (1986). Protein sequencing by tandem mass spectrometry. *Proc Natl Acad Sci* **83**, 6233–6237.

Hussell, T. & Bell, T. J. (2014). Alveolar macrophages: plasticity in a tissue-specific context. *Nat Rev Immunol* **14**, 81–93. Nature Publishing Group.

Ishaug-Riley, S. L., Crane-Kruger, G. M., Yaszemski, M. J. & Mikos, A. G. (1998). Three-dimensional culture of rat calvarial osteoblasts in porous biodegradable polymers. *Biomaterials* **19**, 1405–1412.

Ishibashi, Y., Relman, D. a & Nishikawa, A. (2001). Invasion of human respiratory epithelial cells by *Bordetella pertussis*: possible role for a filamentous hemagglutinin Arg-Gly-Asp sequence and alpha5beta1 integrin. *Microb Pathog* **30**, 279–88.

Ishibashi, Y. & Nishikawa, A. (2002). *Bordetella pertussis* infection of human respiratory epithelial cells up-regulates intercellular adhesion molecule-1 expression: role of filamentous hemagglutinin and pertussis toxin. *Microb Pathog* **33**, 115–125.

Ishibashi, Y., Claus, S. & Relman, D. A. (1994). *Bordetella pertussis* Filamentous Hemagglutlnln Interacts with a Leukocyte Signal Transduction Complex and Stimulates Bacterial Adherence to Monocyte CR3 (CDllb/CD18). *J Exp Med* **94**, 1225–1233.

Jacob-Dubuisson, F., El-hamel, C., Saint, N., Gue, S., Willery, E., Molle, G. & Locht, C. (1999). Channel Formation by FhaC , the Outer Membrane Protein Involved in the Secretion of the *Bordetella pertussis* Filamentous Hemagglutinin. *J Biol Chem* **274**, 37731–37735.

Jacob-Dubuisson, F., Guérin, J., Baelen, S. & Clantin, B. (2013). Two-partner secretion: as simple as it sounds? *Res Microbiol* **164**, 583–95.

Jagannadham, M. V. & Chowdhury, C. (2012). Differential expression of membrane proteins helps Antarctic *Pseudomonas syringae* to acclimatize upon temperature variations. *J Proteomics* **75**, 2488–2499. Elsevier B.V.

Jain, R., Pan, J., Driscoll, J. a, Wisner, J. W., Huang, T., Gunsten, S. P., You, Y. & Brody, S. L. (2010). Temporal relationship between primary and motile ciliogenesis in airway epithelial cells. *Am J Respir Cell Mol Biol* **43**, 731–9.

Jakiela, B., Brockman-Schneider, R., Amineva, S., Lee, W.-M. & Gern, J. E. (2008). Basal cells of differentiated bronchial epithelium are more susceptible to rhinovirus infection. *Am J Respir Cell Mol Biol* **38**, 517–23.

Jang, K.-S., Sweredoski, M. J., Graham, R. L. J., Hess, S. & Clemons, W. M. (2014). Comprehensive proteomic profiling of outer membrane vesicles from *Campylobacter jejuni*. *J Proteomics* **98**, 90–98. Elsevier B.V.

Jaramillo, L., Díaz, F., Hernández, P., Debray, H., Trigo, F., Mendoza, G. & Zenteno, E. (2000). Purification and characterization of an adhesin from *Pasteurella haemolytica*. *Glycobiology* **10**, 31–7.

Jaramillo-Arango, C. J., Hernández-Castro, R., Suárez-Güemes, F., Martínez-Maya, J. J., Aguilar-Romero, F., Jaramillo-Meza, L. & Trigo, F. J. (2008). Characterisation of *Mannheimia* spp. strains isolated from bovine nasal exudate and factors associated to isolates, in dairy farms in the Central Valley of Mexico. *Res Vet Sci* **84**, 7–13.

Jean, N. L., Bougault, C. M., Lodge, A., Derouaux, A., Callens, G., Egan, A. J. F., Ayala, I., Lewis, R. J., Vollmer, W. & Simorre, J.-P. (2014). Elongated structure of the outer-membrane activator of peptidoglycan synthesis LpoA: Implications for PBP1A stimulation. *Structure* **22**, 1047–1054. Elsevier Ltd.

Jensen, P. Ø., Bjarnsholt, T., Phipps, R., Rasmussen, T. B., Calum, H., Christoffersen, L., Moser, C., Williams, P., Pressler, T. & other authors. (2007). Rapid necrotic killing of polymorphonuclear leukocytes is caused by quorum-sensing-controlled production of rhamnolipid by *Pseudomonas aeruginosa*. *Microbiology* **153**, 1329–38.

Jesaitis, a. J., Franklin, M. J., Berglund, D., Sasaki, M., Lord, C. I., Bleazard, J. B., Duffy, J. E., Beyenal, H. & Lewandowski, Z. (2003). Compromised Host Defense on *Pseudomonas aeruginosa* Biofilms: Characterization of Neutrophil and Biofilm Interactions. *J Immunol* **171**, 4329–4339.

Jeyaseelan, S., Sreevatsan, S. & Maheswaran, S. K. (2002). Role of *Mannheimia haemolytica* leukotoxin in the pathogenesis of bovine pneumonic pasteurellosis. *Anim Heal Res Rev* **3**, 69–82.

Jim, K. (2009). Impact of bovine respiratory disease (BRD) from the perspective of the Canadian beef producer. *Anim Heal Res Rev* **10**, 109–110.

Johannes, P., Halter, R., Beyreuther, K. & Meyer, T. F. (1987). Gene structure and extracellular secretion of *Neisseria gonorroeae* IgA protease. *Nature* **325**, 458–462.

Johnson, M. D. L., Garrett, C. K., Bond, J. E., Coggan, K. a, Wolfgang, M. C. & Redinbo, M. R. (2011). *Pseudomonas aeruginosa* PilY1 binds integrin in an RGD- and calcium-dependent manner. *PLoS One* **6**, e29629.

Johnson, T. A., Qiu, J., Plaut, A. G. & Holyoak, T. (2009). Active-site gating regulates substrate selectivity in a chymotrypsin-like serine protease the structure of *Haemophilus influenzae* immunoglobulin A1 protease. *J Mol Biol* **389**, 559–74. Elsevier Ltd.

Joki, S. & Saano, V. (1994). Ciliary Beat Frequency at Six levels of the respiratory tract in Cow, Dog, Guinea-Pig, Pig, Rabbit and Rat. *Clin Exp Pharmacol Physiol* **21**, 427–434.

Jones, G. E., Donachie, W., Sutherland, A. D., Knox, D. P. & Gilmour, J. S. (1989). Protection of Lambs Against Experimental Pneumonic Pasteurellosis by Transfer of Immune Serum. *Vet Microbiolgy* **20**, 59–71.

Jordan, P. W. & Saunders, N. J. (2009). Host iron binding proteins acting as niche indicators for *Neisseria meningitidis*. *PLoS One* **4**, e5198.

Julio, S. M., Inatsuka, C. S., Mazar, J., Dieterich, C., Relman, D. A. & Cotter, P. A. (2009). Natural-host animal models indicate functional interchangeability between the filamentous haemagglutinins of Bordetella pertussis and Bordetella bronchiseptica and reveal a role for the mature C-terminal domain, but not the RGD motif, during. *Mol Microbiol* **71**, 1574–90.

Jungblut, P. R., Schiele, F., Zimny-Arndt, U., Ackermann, R., Schmid, M., Lange, S., Stein, R. & Pleissner, K.-P. (2010). *Helicobacter pylori* proteomics by 2-DE/MS, 1-DE-LC/MS and functional data mining. *Proteomics* **10**, 182–93.

Kaartinen, L., Nettesheim, P., Adler, K. B., Randell, S. H., Medicine, V. & A, N. C. K. B. (1993). Rat Tracheal Epithelial Cell Differentiation *in vitro*. *In Vitro Cell Dev Biol Anim* **29(A)**, 481–492.

Kadurugamuwa, J. L. & Beveridge, T. J. (1996). Bacteriolytic effect of membrane vesicles from *Pseudomonas aeruginosa* on other bacteria including pathogens: conceptually new antibiotics. *J Bacteriol* **178**, 2767–2774.

Kahwa, C. K. B. & Purton, M. (1996). Histological and histochemical study of epithelial lining of the respiratory tract in adult goats. *Small Rumin Res* **20**, 181–186.

Kajava, A. V, Cheng, N., Cleaver, R., Kessel, M., Simon, M. N., Willery, E., Jacob-dubuisson, F., Locht, C. & Steven, A. C. (2001). Beta-helix model for the filamentous haemagglutinin adhesin of Bordetella pertussis and related bacterial secretory proteins. *Mol Microbiol* **42**, 279–292.

Kameyama, S., Kondo, M., Takeyama, K. & Nagai, A. (2003). Air Exposure Causes Oxidative Stress in Cultured Bovine Tracheal Epithelial Cells And Produces a Change In Cellular Glutathione Systems. *Exp Lung Res* **29**, 567–583.

Kanoh, S., Tamaoki, J., Kondo, M. & Nagai, A. (2001). New quinolone, grepafloxacin, inhibits Cl- secretion across bovine airway epithelium in culture. *Respirology* **6**, 51–6.

Kao, D.-Y., Cheng, Y.-C., Kuo, T.-Y., Lin, S.-B., Lin, C.-C., Chow, L.-P. & Chen, W.-J. (2009). Salt-responsive outer membrane proteins of *Vibrio anguillarum* serotype O1 as revealed by comparative proteome analysis. *J Appl Microbiol* **106**, 2079–85.

Kaplan, J. B. & Fine, D. H. (2002). Biofilm Dispersal of *Neisseria subflava* and Other Phylogenetically Diverse Oral Bacteria. *J Bacteriol* **68**, 4943–4950.

Kaplan, J. B., Ragunath, C., Ramasubbu, N. & Fine, D. H. (2003). Detachment of *Actinobacillus actinomycetemcomitans* Biofilm Cells by an Endogenous ß-Hexosaminidase Activity. *J Bacteriol* **185**, 4693–4698.

Katsuda, K., Hoshinoo, K., Ueno, Y., Kohmoto, M. & Mikami, O. (2013). Virulence genes and antimicrobial susceptibility in Pasteurella multocida isolates from calves. *Vet Microbiol* **167**, 737–741. Elsevier B.V.

Katsuda, K., Kamiyama, M., Kohmoto, M., Kawashima, K., Tsunemitsu, H. & Eguchi, M. (2008). Serotyping of *Mannheimia haemolytica* isolates from bovine pneumonia: 1987-2006. *Vet J* **178**, 146–8.

Keller, B., Mühlenkamp, M., Deuschle, E., Siegfried, A., Mössner, S., Schade, J., Griesinger, T., Katava, N., Braunsdorf, C. & other authors. (2015). *Yersinia enterocolitica* exploits different pathways to accomplish adhesion and toxin injection into host cells. *Cell Microbiol* **17**, 1179–204.

Kenny, B., Devinney, R., Stein, M., Reinscheid, D. J., Frey, E. A. & Finlay, B. B. (1997). Enteropathogenic E . coli (EPEC) Transfers Its Receptor for Intimate Adherence into Mammalian Cells. *Cell* **91**, 511–520.

Ketterer, M. R., Shao, J. Q., Hornick, D. B., Buscher, B., Bandi, V. K. & Apicella, M. a. (1999). Infection of primary human bronchial epithelial cells by *Haemophilus influenzae:* macropinocytosis as a mechanism of airway epithelial cell entry. *Infect Immun* **67**, 4161–70.

Kettle, R., Simmons, J., Schindler, F., Jones, P., Dicker, T., Dubois, G., Giddings, J., Van Heeke, G. & Jones, C. E. (2010). Regulation of neuregulin 1beta1-induced MUC5AC and MUC5B expression in human airway epithelium. *Am J Respir Cell Mol Biol* **42**, 472–81.

Khelef, N., Bachelet, C., Vargaftig, B. B. & Guisol, N. (1994). Characterization of Murine Lung Inflammation after Infection with Parental *Bordetella pertussis* and Mutants Deficient in Adhesins or Toxins. *Infect Immun* **62**, 2893–2900.

Kidney, J. C. & Proud, D. (2000). Neutrophil Transmigration across Human Airway Epithelial Monolayers. *Am J Respir Cell Mol Biol* **23**, 389–395.

Kim, J. Y., Sajjan, U. S., Krasan, G. P. & Lipuma, J. J. (2005). Disruption of Tight Junctions during Traversal of the Respiratory Epithelium by *Burkholderia cenocepacia*. *Infect Immun* **73**, 7107–7112.

Kim, J., Steck, P., Gallick, G., Lee, J., Blick, M., Hong, W. & Lotan, R. (1992). Suppression by retinoic acid of epidermal growth factor receptor autophosphorylation and glycosylation in cultured human head and neck squamous carcinoma cells. *JNCI Monogr* **131**, 101–10.

Kim, K.-M., Lee, S.-G., Joo, J.-S., Kwon, Y.-C., Bea, D.-W., Song, J.-Y., Kang, H.-L., Lee, W.-K., Cho, M.-J. & other authors. (2008). Proteomic analysis of *Helicobacter pylori* J99 outer membrane protein by tandem mass spectrometry. *J Bacteriol Virol* **38**, 53.

Kim, S., Malinverni, J. C., Sliz, P., Silhavy, T. J., Harrison, S. C. & Kahne, D. (2007a). Structure and Function of an Essential Component of the Outer Membrane Protein Assembly Machine. *Science (80-)* **317**, 961–965.

Kim, S.-W., Hong, J. S., Ryu, S.-H., Chung, W.-C., Yoon, J.-H. & Koo, J. S. (2007b). Regulation of mucin gene expression by CREB via a nonclassical retinoic acid signaling pathway. *Mol Cell Biol* **27**, 6933–47.

Kirchhoff, J., Uhlenbruck, S., Goris, K., Keil, G. M. & Herrler, G. (2014). Three viruses of the bovine respiratory disease complex apply different strategies to initiate infection. *Vet Res* **45**, 20.

Kirjavainen, V., Jarva, H., Biedzka-Sarek, M., Blom, A. M., Skurnik, M. & Meri, S. (2008). *Yersinia enterocolitica* serum resistance proteins YadA and ail bind the complement regulator C4b-binding protein. *PLoS Pathog* **4**, e1000140.

Kirkan, S. & Kaya, O. (2005). Serotyping of *Mannheimia haemolytica* Strains Isolated from Pneumonic Lungs of Sheep in the Ayd › n Region of Turkey *. *Turkish J Vet Anim Sci* **29**, 491–494.

Kisiela, D. I. & Czuprynski, C. J. (2009). Identification of *Mannheimia haemolytica* adhesins involved in binding to bovine bronchial epithelial cells. *Infect Immun* **77**, 446–55.

Kisiela, D. I., Aulik, N. a, Atapattu, D. N. & Czuprynski, C. J. (2010). N-terminal region of *Mannheimia haemolytica* leukotoxin serves as a mitochondrial targeting signal in mammalian cells. *Cell Microbiol* **12**, 976–87.

Klausen, M., Aaes-Jørgensen, A., Molin, S. & Tolker-Nielsen, T. (2003). Involvement of bacterial migration in the development of complex multicellular structures in *Pseudomonas aeruginosa* biofilms. *Mol Microbiol* **50**, 61–68.

Kleinman, H. K., Klebe, R. J. & Martin, G. R. (1981). Role of collagenous matrices in the adhesion and growth of cells. *J Cell Biol* **88**, 473–85.

Klesney-Tait, J., Keck, K., Li, X., Gilfillan, S., Otero, K., Baruah, S., Meyerholz, D. K., Varga, S. M., Knudson, C. J. & other authors. (2013). Transepithelial migration of neutrophils into the lung requires TREM-1. *J Clin Invest* **123**, 138–149.

Klima, C. L., Alexander, T. W., Hendrick, S. & McAllister, T. A. (2014a).

Characterization of *Mannheimia haemolytica* isolated from feedlot cattle that were healthy or treated for bovine respiratory disease. *Can J Vet Res* **78**, 38–45.

Klima, C. L., Zaheer, R., Cook, S. R., Booker, C. W., Hendrick, S., Alexander, T. W. & McAllister, T. a. (2014b). Pathogens of bovine respiratory disease in North American feedlots conferring multidrug resistance via integrative conjugative elements. *J Clin Microbiol* **52**, 438–448.

Knowles, T. J., Scott-Tucker, A., Overduin, M. & Henderson, I. R. (2009). Membrane protein architects: the role of the BAM complex in outer membrane protein assembly. *Nat Rev Microbiol* **7**, 206–14.

Kolesnikova, L., Heck, S., Matrosovich, T., Klenk, H.-D., Becker, S. & Matrosovich, M. (2013). Influenza virus budding from the tips of cellular microvilli in differentiated human airway epithelial cells. *J Gen Virol* **94**, 971–6.

Kondo, M., Finkbeiner, W. E. & Widdicombe, J. H. (1993). Cultures of Bovine Tracheal Epithelium with Differentiated Ultrastructure and Ion Transport. *Vitr Cell Dev Biol* **29A**, 19–24.

Kondo, M., Tamaoki, J., Sakai, a, Kameyama, S., Kanoh, S. & Konno, K. (1997). Increased oxidative metabolism in cow tracheal epithelial cells cultured at air-liquid interface. *Am J Respir Cell Mol Biol* **16**, 62–8.

Koning, H., Sayers, I., Stewart, C. E., de Jong, D., Ten Hacken, N. H. T., Postma, D. S., van Oosterhout, A. J. M., Nawijn, M. C. & Koppelman, G. H. (2012). Characterization of protocadherin-1 expression in primary bronchial epithelial cells: association with epithelial cell differentiation. *FASEB J* **26**, 439–48.

Koo, J. S., Jetten, A. M., Belloni, P., Yoon, J., Kim, Y. & Nettesheim, P. (2002). Role of retinoid receptors in the regulation of mucin gene expression by retinoic acid in human tracheobronchial epithelial cells. *Biochem J* **357**, 351–357.

Koretke, K. K., Szczesny, P., Gruber, M. & Lupas, A. N. (2006). Model structure of the prototypical non-fimbrial adhesin YadA of *Yersinia enterocolitica*. *J Struct Biol* **155**, 154–61.

Korotkov, K. V, Sandkvist, M. & Hol, W. G. J. (2012). The type II secretion system: biogenesis, molecular architecture and mechanism. *Nat Rev Microbiol* **10**, 336–51. Nature Publishing Group.

Kouyianou, K., Aivaliotis, M., Gevaert, K., Karas, M. & Tsiotis, G. (2010). Membrane proteome of the green sulfur bacterium *Chlorobium tepidum* (syn. *Chlorobaculum tepidum*) analyzed by gel-based and gel-free methods. *Photosynth Res* **104**, 153–62.

Kovacs-Simon, A., Titball, R. W. & Michell, S. L. (2011). Lipoproteins of bacterial pathogens. *Infect Immun* **79**, 548–61.

Krachler, A. M. & Orth, K. (2011). Functional characterization of the interaction between bacterial adhesin multivalent adhesion molecule 7 (MAM7) protein and its host cell ligands. *J Biol Chem* **286**, 38939–47.

Krachler, A. M., Ham, H. & Orth, K. (2011). Outer membrane adhesion factor multivalent adhesion molecule 7 initiates host cell binding during infection by Gram-negative pathogens. *Proc Natl Acad Sci* **108**, 11614–11619.

Krewulak, K. D. & Vogel, H. J. (2008). Structural biology of bacterial iron uptake. *Biochim Biophys Acta* **1778**, 1781–804.

Kroll, J. S., Langford, P. R., Wilks, K. E. & Keil, a. D. (1995). Bacterial [Cu,Zn]-superoxide dismutase: Phylogenetically distinct from the eukaryotic enzyme, and not so rare after all! *Microbiology* **141**, 2271–2279.

Kruh, N. a, Troudt, J., Izzo, A., Prenni, J. & Dobos, K. M. (2010). Portrait of a pathogen: the *Mycobacterium tuberculosis* proteome in vivo. *PLoS One* **5**, e13938.

Krunkosky, T. M., Jordan, J. L., Chambers, E. & Krause, D. C. (2007). *Mycoplasma pneumoniae* host-pathogen studies in an air-liquid culture of differentiated human airway epithelial cells. *Microb Pathog* **42**, 98–103.

Kulkarni, H. M. & Jagannadham, M. V. (2014). Molecular Characterization and Functional Analysis of Outer Membrane Vesicles from the Antarctic Bacterium *Pseudomonas syringae* Suggest a Possible Response to Environmental Conditions. *J Proteome Res* **13**, 1345–1358.

Kulp, A. & Kuehn, M. J. (2010). Biological Functions and Biogenesis of Secreted Bacterial Outer Membrane Vesicles. *Annu Rev Microbiol* **64**, 163–184.

Kumar, G., Sharma, P., Rathore, G., Bisht, D. & Sengupta, U. (2009). Proteomic analysis of outer membrane proteins of *Edwardsiella tarda*. *J Appl Microbiol* **108**, 2214–21.

Kumar, N. M. & Gilula, N. B. (1996). The Gap Junction Communication Channel. *Cell* **56**, 1751–1765.

De la Mora, A., Trigo, F., Jaramillo, L., Garfias, Y., Solórzano, C., Agundis, C., Pereyra, A., Lascurain, R., Zenteno, E. & Suárez-Güemes, F. (2006). The N-acetyl-D-glucosamine specific adhesin from *Mannheimia haemolytica* activates bovine neutrophils oxidative burst. *Vet Immunol Immunopathol* **113**, 148–56.

De la Mora, A., Suárez-Güemes, F., Trigo, F., Gorocica, P., Solórzano, C., Slomianny, M.-C., Agundis, C., Pereyra, M. A. & Zenteno, E. (2007). Purification of the receptor for the N-acetyl-D-glucosamine specific adhesin of *Mannheimia haemolytica* from bovine neutrophils. *Biochim Biophys Acta* **1770**, 1483–9.

Laarmann, S., Cutter, D., Juehne, T., Barenkamp, S. J. & Geme, J. W. S. (2002). The *Haemophilus influenzae* Hia autotransporter harbours two adhesive pockets that reside in the passenger domain and recognize the same host cell receptor. *Mol Microbiol* **46**, 731–743.

Laemmli, U. K. (1970). Cleavage of structural proteins during the assembly of the head of bacteriophage T4. *Nature* **227**, 680–685.

Lafleur, R. L., Malazdrewich, C., Jeyaseelan, S., Bleifield, E., Abrahamsen, M. S. & Maheswaran, S. K. (2001). Lipopolysaccharide enhances cytolysis and inflammatory cytokine induction in bovine alveolar macrophages exposed to*Pasteurella* (*Mannheimia*) *haemolytica* leukotoxin. *Microb Pathog* **30**, 347–357.

Lafrenie, R. M., Bernier, S. M. & Yamada, K. M. (1998). Adhesion to Fibronectin or Collagen I Gel Induces Rapid , Extensive , Biosynthetic Alterations in Epithelial Cells. *J Cell Physiol* **173**, 163–173.

Lai, E.-M., Nair, U., Phadke, N. D. & Maddock, J. R. (2004). Proteomic

screening and identification of differentially distributed membrane proteins in *Escherichia coli*. *Mol Microbiol* **52**, 1029–1044.

Lai, S. K., Wang, Y.-Y., Wirtz, D. & Hanes, J. (2009). Micro- and macrorheology of mucus. *Adv Drug Deliv Rev* **61**, 86–100. Elsevier B.V.

Lainson, F. A., Thomson, N., Rowe, H. A., Langford, P. R., Aitchison, K. D., Donachie, W. & Kroll, J. S. (1996). Occurence of [copper, zinc]-cofactored superoxide dismutase in *Pasteurella haemolytica* and its serotype distribution. *FEMS Microbiol Lett* **142**, 11–17.

Lalevée, S., Anno, Y. N., Chatagnon, A., Samarut, E., Poch, O., Laudet, V., Benoit, G., Lecompte, O. & Rochette-Egly, C. (2011). Genome-wide in silico identification of new conserved and functional retinoic acid receptor response elements (direct repeats separated by 5 bp). *J Biol Chem* **286**, 33322–34.

Lam, E., Ramke, M., Groos, S., Warnecke, G. & Heim, a. (2011). A differentiated porcine bronchial epithelial cell culture model for studying human adenovirus tropism and virulence. *J Virol Methods* **178**, 117–23. Elsevier B.V.

Lam, K., Zhang, L., Yamada, K. M. & Lafrenie, R. M. (2001). Adhesion of Epithelial Cells to Fibronectin or Collagen I Induces Alterations in Gene Expression via a Protein Kinase C-Dependent Mechanism. *J Cell Physiol* **90**, 79–90.

Larson, R. L. & Step, D. L. (2012). Evidence-based effectiveness of vaccination against *Mannheimia haemolytica*, *Pasteurella multocida*, and *Histophilus somni* in feedlot cattle for mitigating the incidence and effect of bovine respiratory disease complex. *Vet Clin North Am Food Anim Pract* **28**, 97–106, 106e1–7, ix. Elsevier.

Lawrence, P. K., Kittichotirat, W., McDermott, J. E. & Bumgarner, R. E. (2010). A three-way comparative genomic analysis of *Mannheimia haemolytica* isolates. *BMC Genomics* **11**.

Leahy, D. J., Aukhil, I. & Erickson, H. P. (1996). Crystal Structure of a Four-Domain Segment 2 . 0 A of Human Fibronectin Encompassing the RGD Loop and Synergy Region. *Cell* **84**, 155–164.

Lechner, J. N., Huagen, A., McClendon, I. A. & Pettis, E. W. (1982). Clonal Growth of Normal Adult Human Bronchial Epithelial Cells in a Serum-Free Medium. *In Vitro* **18**, 633–642.

LeDizet, M., Beck, J. C. & Finkbeiner, W. E. (1998). Differential regulation of centrin genes during ciliogenesis in human tracheal epithelial cells. *Am J Physiol* **275**, L1145–56.

Lee, E.-Y., Bang, J. Y., Park, G. W., Choi, D.-S., Kang, J. S., Kim, H.-J., Park, K.-S., Lee, J.-O., Kim, Y.-K. & other authors. (2007). Global proteomic profiling of native outer membrane vesicles derived from *Escherichia coli*. *Proteomics* **7**, 3143–3153.

Lee, I. & Davies, R. L. (2011). Evidence for a common gene pool and frequent recombinational exchange of the tbpBA operon in *Mannheimia haemolytica*, *Mannheimia glucosida* and *Bibersteinia trehalosi*. *Microbiology* **157**, 123–35.

Lee, S. J., Choi, J. S., Park, K. S., Khang, G., Lee, Y. M. & Lee, H. B. (2004). Response of MG63 osteoblast-like cells onto polycarbonate membrane surfaces with different micropore sizes. *Biomaterials* **25**, 4699–4707.

Lehr, U., Schütz, M., Oberhettinger, P., Ruiz-Perez, F., Donald, J. W., Palmer, T., Linke, D., Henderson, I. R. & Autenrieth, I. B. (2010). C-terminal amino acid residues of the trimeric autotransporter adhesin YadA of *Yersinia enterocolitica* are decisive for its recognition and assembly by BamA. *Mol Microbiol* **78**, 932–46.

Leid, J. G., Willson, C. J., Shirtliff, M. E., Hassett, D. J., Parsek, M. R. & Jeffers, a. K. (2005). The Exopolysaccharide Alginate Protects *Pseudomonas aeruginosa* Biofilm Bacteria from IFN- -Mediated Macrophage Killing. *J Immunol* **175**, 7512–7518.

Leininger, E., Robertso, M., Kenimer, J. G., Charles, I. A. N. G., Fairweather, N., Novotny, P. & Brennan, M. J. (1991). Pertactin , an Arg-Gly-Asp-containing *Bordetella pertussis* surface protein that promotes adherence of mammalian cells. *Proc Natl Acad Sci* **88**, 345–349.

Lewis, L. A., Gipson, M., Hartman, K., Ownbey, T. & Dyer, D. W. (1999). Phase variation of HpuAB and HmbR , two distinct haemoglobin receptors of *Neisseria meningitidis* DNM2. *Mol Microbiol* **32**, 977–989.

Li, G.-Z., Vissers, J. P. C., Silva, J. C., Golick, D., Gorenstein, M. V & Geromanos, S. J. (2009). Database searching and accounting of multiplexed precursor and product ion spectra from the data independent analysis of simple and complex peptide mixtures. *Proteomics* **9**, 1696–719.

Li, J., Clinkenbeard, K. D. & Ritchey, J. W. (1999). Bovine CD18 identified as a species specific receptor for *Pasteurella haemolytica* leukotoxin. *Vet Microbiol* **67**, 91–7.

Li, J. & Clinkenbeard, K. D. (1999). Lipopolysaccharide complexes with *Pasteurella haemolytica* leukotoxin. *Infect Immun* **67**, 2920–2927.

Li, S., Intini, G. & Bobek, L. a. (2006). Modulation of MUC7 mucin expression by exogenous factors in airway cells in vitro and in vivo. *Am J Respir Cell Mol Biol* **35**, 95–102.

Li, Z., Clarke, A. J. & Beveridge, T. J. (1996). A major autolysin of *Pseudomonas aeruginosa*: subcellular distribution, potential role in cell growth and division and secretion in surface membrane vesicles. *J Bacteriol* **178**, 2479–88.

Liberio, M. S., Sadowski, M. C., Soekmadji, C., Davis, R. a & Nelson, C. C. (2014). Differential effects of tissue culture coating substrates on prostate cancer cell adherence, morphology and behavior. *PLoS One* **9**, e112122.

Lim, J., Stones, D. H., Hawley, C. A., Watson, C. A. & Krachler, A. M. (2014). Multivalent adhesion molecule 7 clusters act as signaling platform for host cellular GTPase activation and facilitate epithelial barrier dysfunction. *PLoS Pathog* **10**, e1004421.

Lin, H., Li, H., Cho, H., Bian, S., Roh, H., Lee, M., Kim, J. S. U. N., Chung, S., Shim, C. & Kim, D. (2007). Air-Liquid Interface (ALI) Culture of Human Bronchial Epithelial Cell Monolayers as an In Vitro Model for Airway Drug Transport Studies. *J Pharm Sci* **96**, 341–350.

Lin, Y.-P., Bhowmick, R., Coburn, J. & Leong, J. M. (2015a). Host cell heparan sulfate glycosaminoglycans are ligands for OspF-related proteins of the Lyme disease spirochete. *Cell Microbiol* **Ahead of P**.

Lin, Y.-P., Chen, Q., Ritchie, J. a, Dufour, N. P., Fischer, J. R., Coburn, J. & Leong, J. M. (2015b). Glycosaminoglycan binding by *Borrelia burgdorferi*

adhesin BBK32 specifically and uniquely promotes joint colonization. *Cell Microbiol* **17**, 860–75.

Lindbom, J., Ljungman, A. G., Lindahl, M. & Tagesson, C. (2002). Increased Gene Expression of Novel Cytosolic and Secretory Phospholipase A 2 Types in Human Airway Epithelial Cells Induced by Tumor Necrosis Factor- a and IFN-g. *J Interf Cytokine Res* **22**, 947–955.

Linderholm, A. L., Onitsuka, J., Xu, C., Chiu, M., Lee, W.-M. & Harper, R. W. (2010). All-trans retinoic acid mediates DUOX2 expression and function in respiratory tract epithelium. *Am J Physiol Lung Cell Mol Physiol* **299**, L215–21.

Lisanti, M. P., Caras, I. W., Davitz, M. A. & Rodriguez-Boulan, E. (1989). A Glycophospholipid Membrane Anchor Acts as an Apical Targetkng Signal in Polarized Epithelial Cells. *Proc Natl Acad Sci* **109**, 2145–2156.

Litt, D. J., Palmer, H. M. & Borriello, P. S. (2000). *Neisseria meningitidis* Expressing Transferrin Binding Proteins of Actinobacillus pleuropneumoniae Can Utilize Porcine Transferrin for Growth. *Infect Immun* **68**, 550–557.

Liu, G. Y., Nie, P., Zhang, J. & Li, N. (2008). Proteomic analysis of the sarcosine-insoluble outer membrane fraction of *Flavobacterium columnare*. *J Fish Dis* **31**, 269–276.

Liu, X.-J., Kang, L.-Q., Liu, Y.-J., Li, H. & Peng, X. (2013). Characterization of the *Edwardsiella tarda* proteome in response to different environmental stresses. *J Proteomics* **80**, 320–33. Elsevier B.V.

Liu, X., Luo, M., Zhang, L., Ding, W., Yan, Z. & Engelhardt, J. F. (2007). Bioelectric properties of chloride channels in human, pig, ferret, and mouse airway epithelia. *Am J Respir Cell Mol Biol* **36**, 313–23.

Lo, R. Y., Strathdee, C. a, Shewen, P. E. & Cooney, B. J. (1991). Molecular studies of Ssa1, a serotype-specific antigen of *Pasteurella haemolytica* A1. *Infect Immun* **59**, 3398–406.

Lo, R. Y. C., Strathdee, C. a. & Shewen, P. E. (1987). Nucleotide sequence of the leukotoxin genes of *Pasteurella haemolytica* A1. *Infect Immun* **55**, 1987–1996.

Lo, R. Y. C. & Sorensen, L. S. (2007). The outer membrane protein OmpA of *Mannheimia haemolytica* A1 is involved in the binding of fibronectin. *FEMS Microbiol Lett* **274**, 226–31.

Lo, R. Y. C., Sathiamoorthy, S. & Shewen, P. E. (2006). Analysis of in vivo expressed genes in *Mannheimia haemolytica* A1. *FEMS Microbiol Lett* **265**, 18–25.

Locht, C., Bertin, P., Franco, D. & Renauld, G. (1993). The filamentous haemagglutinin, a multifaceted adhesin produced by virulent *Bordetella spp*. *Mol Microbiol* **9**, 653–660.

Logan, S. M., Chen, W., Aubry, A., Gidney, M. A. J., Lacelle, S., St. Michael, F., Kuolee, R., Higgins, M., Neufeld, S. & Cox, A. D. (2006). Production of a d-glycero-d-manno-heptosyltransferase mutant of *Mannheimia haemolytica* displaying a veterinary pathogen specific conserved LPS structure; development and functionality of antibodies to this LPS structure. *Vet Microbiol* **116**, 175–186.

Lonnerdal, B. & Iyer, S. (1995). Lacoferrin: Molecular Structure and Biological

Function. *Annu Rev Nutr* **15**, 93–110.

Low, H. H., Gubellini, F., Rivera-Calzada, A., Braun, N., Connery, S., Dujeancourt, A., Lu, F., Redzej, A., Fronzes, R. & other authors. (2014). Structure of a type IV secretion system. *Nature* **508**, 550–3.

Luca, M. D. E. (1991). Retinoids and their receptors in differentiation. *FASEB J* **5**, 2924–2933.

Lucidarme, J., Findlow, J., Chan, H., Feavers, I. M., Gray, S. J., Kaczmarski, E. B., Parkhill, J., Bai, X., Borrow, R. & Bayliss, C. D. (2013). The Distribution and 'In Vivo' Phase Variation Status of Haemoglobin Receptors in Invasive Meningococcal Serogroup B Disease: Genotypic and Phenotypic Analysis. *PLoS One* **8**, e76932 (Y.-F. Chang, Ed.).

Luyts, K., Napierska, D., Dinsdale, D., Klein, S. G., Serchi, T. & Hoet, P. H. M. (2015). A coculture model of the lung–blood barrier: The role of activated phagocytic cells. *Toxicol Vitr* **29**, 234–241. Elsevier Ltd.

Maeda, S., Nakagawa, S., Suga, M., Yamashita, E., Oshima, A., Fujiyoshi, Y. & Tsukihara, T. (2009). Structure of the connexin 26 gap junction channel at 3.5 Å resolution. *Nature* **458**, 597–602. Nature Publishing Group.

Mah, T., Pitts, B., Pellock, B., Walker, G. C., Stewart, P. S. & Toole, G. A. O. (2003). A genetic basis for *Pseudomonas aeruginosa* biofilm antibiotic resistance. *Nature* **426**, 1–5.

Makarov, A., Hardman, M., Schwarz, J. & Senko, M. W. (2005). Injection of sample ions into electrostatic trap by supplying trapping and release voltages to storage device with sample ions, and trapping the received sample ions in electrostatic trap by applying potential to electrodes.

Malinverni, J. C., Werner, J., Kim, S., Sklar, J. G., Kahne, D., Misra, R. & Silhavy, T. J. (2006). YfiO stabilizes the YaeT complex and is essential for outer membrane protein assembly in *Escherichia coli*. *Mol Microbiol* **61**, 151–64.

Mao, H., Wang, Y., Yuan, W. & Wong, L. B. (2009). Ciliogenesis in cryopreserved mammalian tracheal epithelial cells cultured at the air-liquid interface. *Cryobiology* **59**, 250–7. Elsevier Inc.

Markwell, M. A., Haas, S. M., Bieber, L. L. & Tolbert, N. E. (1978). A modification of the Lowry procedure to simplify protein determination in membrane and lipoprotein samples. *Anal Biochem* **87**, 206–210.

Marshall, A. G. (1985). Fourier transform ion cyclotron resonance mass spectrometry. *Acc Chem Res* **18**, 316–322.

Marshall, A. G., Hendrickson, C. L. & Jackson, G. S. (1998). Fourier Transform Ion Cyclotron Resonance Mass Spectromeyry: A Primer. *Mass Spectrom Rev* **17**, 1–35.

Marshall, K. C. (2006). Planktonic Versus Sessile Life of Prokaryotes. In *The Prokaryotes*, pp. 191–201. Edited by E. Rosenberg, E. F. DeLong, S. Lory, E. Stackebrandt & F. Thompson. Berlin, Heidelberg: Springer Berlin Heidelberg.

Martin, W. R., Brown, C., Zhang, Y. J. & Wu, R. (1991). Growth and differentiation of primary tracheal epithelial cells in culture: regulation by extracellular calcium. *J Cell Physiol* **147**, 138–48.

Martorana, A. M., Motta, S., Di Silvestre, D., Falchi, F., Dehò, G., Mauri, P.,

Sperandeo, P. & Polissi, A. (2014). Dissecting *Escherichia coli* outer membrane biogenesis using differential proteomics. *PLoS One* **9**, e100941.

Masson, P. L., Heremans, J. F. & Schonne, E. (1969). Lactoferrin, an Iron-Binding Protein in Neutrophilic Leukocytes. *J Exp Med* **130**, 643–658.

Matrosovich, M. N., Matrosovich, T. Y., Gray, T., Roberts, N. a & Klenk, H.-D. (2004). Human and avian influenza viruses target different cell types in cultures of human airway epithelium. *Proc Natl Acad Sci U S A* **101**, 4620–4.

Mattoo, S., Miller, J. F. & Cotter, P. a. (2000). Role of *Bordetella bronchiseptica* Fimbriae in Tracheal Colonization and Development of a Humoral Immune Response. *Infect Immun* **68**, 2024–2033.

Matzanke, B. F., Böhnke, R., Möllmann, U., Reissbrodt, R., Schünemann, V. & Trautwein, A. X. (1997). Iron uptake and intracellular metal transfer in mycobacteria mediated by xenosiderophores. *Biometals* **10**, 193–203.

Mazar, J. & Cotter, P. a. (2006). Topology and maturation of filamentous haemagglutinin suggest a new model for two-partner secretion. *Mol Microbiol* **62**, 641–54.

McCaw, S. E., Liao, E. H. & Gray-owen, S. D. (2004). Engulfment of *Neisseria gonorrhoeae*: Revealing Distinct Processes of Bacterial Entry by Individual Carcinoembryonic Antigen-Related Cellular Adhesion Molecule Family Receptors. *Infect Immun* **72**, 2742–2752.

McClenahan, D., Hillenbrand, K., Kapur, a., Carlton, D. & Czuprynski, C. (2009). Effects of Extracellular ATP on Bovine Lung Endothelial and Epithelial Cell Monolayer Morphologies, Apoptoses, and Permeabilities. *Clin Vaccine Immunol* **16**, 43–48.

McClenahan, D., Hellenbrand, K., Atapattu, D., Aulik, N., Carlton, D., Kapur, A. & Czuprynski, C. (2008). Effects of lipopolysaccharide and *Mannheimia haemolytica* leukotoxin on bovine lung microvascular endothelial cells and alveolar epithelial cells. *Clin vaccine Immunol* **15**, 338–47.

McKerral, L. J. & Lo, R. Y. C. (2002). Construction and Characterization of an Acapsular Mutant of Mannheimia haemolytica A1. *Infect Immun* **70**, 2622–2629.

McNamara, B. P., Koutsouris, A., O'Connell, C. B., Nougayréde, J.-P., Donnenberg, M. S. & Hecht, G. (2001). Translocated EspF protein from enteropathogenic *Escherichia coli* disrupts host intestinal barrier function. *J Clin Invest* **107**, 621–9.

McNamara, L. E., Burchmore, R., Riehle, M. O., Herzyk, P., Biggs, M. J. P., Wilkinson, C. D. W., Curtis, A. S. G. & Dalby, M. J. (2012). The role of microtopography in cellular mechanotransduction. *Biomaterials* **33**, 2835–47. Elsevier Ltd.

Melvin, J. a, Scheller, E. V, Miller, J. F. & Cotter, P. a. (2014). *Bordetella pertussis* pathogenesis: current and future challenges. *Nat Rev Microbiol* **12**, 274–88. Nature Publishing Group.

Meng, G., St. Geme, J. W. & Waksman, G. (2008). Repetitive Architecture of the *Haemophilus influenzae* Hia Trimeric Autotransporter. *J Mol Biol* **384**, 824–836. Elsevier Ltd.

Menozzi, F. D., Mutombo, R., Renauld, G., Gantiez, C., Hannah, J. H., Leininger, E., Brennan, M. J. & Lochti, C. (1994). Heparin-Inhibitable

Lectin Activity of the Filamentous Hemagglutinin Adhesin of Bordetella pertussis. *Infect Immun* **62**, 769–778.

Miethke, M., Kraushaar, T. & Marahiel, M. a. (2013). Uptake of xenosiderophores in *Bacillus subtilis* occurs with high affinity and enhances the folding stabilities of substrate binding proteins. *FEBS Lett* **587**, 206–13. Federation of European Biochemical Societies.

Miles, A. A., Misra, S. S. & Irwin, J. O. (1938). The estimation of the bactericidal power of the blood. *J Hyg (Lond)* **38**, 732–749.

Millán, J., Hewlett, L., Glyn, M., Toomre, D., Clark, P. & Ridley, A. J. (2006). Lymphocyte transcellular migration occurs through recruitment of endothelial ICAM-1 to caveola- and F-actin-rich domains. *Nat Cell Biol* **8**, 113–123.

Miller, F., Lécuyer, H., Join-Lambert, O., Bourdoulous, S., Marullo, S., Nassif, X. & Coureuil, M. (2013). Neisseria meningitidis</i> colonization of the brain endothelium and cerebrospinal fluid invasion. *Cell Microbiol* **15**, 512–9.

Miller, F. J., Kimbell, J. S., Preston, R. J., Overton, J. H., Gross, E. a & Conolly, R. B. (2011). The fractions of respiratory tract cells at risk in formaldehyde carcinogenesis. *Inhal Toxicol* **23**, 689–706.

Miot, S., Woodfield, T., Daniels, A. U., Suetterlin, R., Peterschmitt, I., Heberer, M., Van Blitterswijk, C. a., Riesle, J. & Martin, I. (2005). Effects of scaffold composition and architecture on human nasal chondrocyte redifferentiation and cartilaginous matrix deposition. *Biomaterials* **26**, 2479–2489.

Mistry, D. & Stockley, R. a. (2006). IgA1 protease. *Int J Biochem Cell Biol* **38**, 1244–8.

Moller, S., Pedersen, A. R., Poulsen, L. K., Arvin, E. & Molin, S. (1996). Activity and Three-Dimensional Distribution of Toluene-Degrading *Pseudomonas putida* in a Multispecies Biofilm Assessed by Quantitative In Situ Hybridization and Scanning Confocal Laser Microscopy. *Appl Environ Microbiol* **62**, 4632–4640.

Molloy, M. P., Herbert, B. R., Slade, M. B., Rabilloud, T., Nouwens, A. S., Williams, K. L. & Gooley, A. A. (2000). Proteomic analysis of the *Escherichia coli* outer membrane. *Eur J Biochem* **267**, 2871–2881.

Montange, R. K. & Batey, R. T. (2008). Riboswitches: emerging themes in RNA structure and function. *Annu Rev Biophys* **37**, 117–33.

Moore, C. H., Foster, L. a., Gerbig, D. G., Dyer, D. W. & Gibson, B. W. (1995). Identification of alcaligin as the siderophore produced by *Bordetella pertussis* and *B. bronchiseptica*. *J Bacteriol* **177**, 1116–1118.

Moraes, T. F., Yu, R., Strynadka, N. C. J. & Schryvers, A. B. (2009). Insights into the bacterial transferrin receptor: the structure of transferrin-binding protein B from *Actinobacillus pleuropneumoniae*. *Mol Cell* **35**, 523–33. Elsevier Ltd.

Morck, D. W., Raybould, T. J., Acres, S. D., Babiuk, L. a, Nelligan, J. & Costerton, J. W. (1987). Electron microscopic description of glycocalyx and fimbriae on the surface of *Pasteurella haemolytica*-A1. *Can J Vet Res* **51**, 83–8.

Morck, D. W., Watts, T. C., Acres, S. D. & Costerton, J. W. (1988). Electron microscopic examination of cells of *Pasteurella haemolytica*-A1 in experimentally infected cattle. *Can J Vet Res* **52**, 343–8.

Morck, D. W., Olson, M. E., Acres, S. D., Daoust, P. & Costerton, J. W. (1989). Presence of Bacterial Glycocalyx and Fimbriae on *Pasteurella haemolytica* in Feedlot Cattle with Pneumonic Pasteurellosis. *Can J Vet Res* **4**, 167–171.

Moreau-Marquis, S., O'Toole, G. a & Stanton, B. a. (2009). Tobramycin and FDA-approved iron chelators eliminate *Pseudomonas aeruginosa* biofilms on cystic fibrosis cells. *Am J Respir Cell Mol Biol* **41**, 305–13.

Morrisey, E. E. & Hogan, B. L. M. (2010). Preparing for the first breath: genetic and cellular mechanisms in lung development. *Dev Cell* **18**, 8–23. Elsevier.

Morton, D. J., Seale, T. W., Madore, L. L., VanWagoner, T. M., Whitby, P. W. & Stull, T. L. (2007). The haem-haemopexin utilization gene cluster (hxuCBA) as a virulence factor of *Haemophilus influenzae*. *Microbiology* **153**, 215–224.

Morton, R. J., Panciera, R. J., Fulton, R. W., Frank, G. H., Ewing, S. A., Homer, J. T. & Confer, A. W. (1995). Vaccination of cattle with outer membrane protein-enriched fractions of *Pasteurella haemolytica* and resistance against experimental challenge exposure. *Am J Vet Res* **56**, 875–879.

Mortz, E., Connor, P. B. O., Roepstorff, P., Kelleher, N. L., Wood, T. D., Mclafferty, F. W. & Mannt, M. (1996). Sequence tag identification of intact proteins by matching tandem mass spectral data against sequence data bases. *Proc Natl Acad Sci* **93**, 8264–8267.

Moustafa, I., Connaris, H., Taylor, M., Zaitsev, V., Wilson, J. C., Kiefel, M. J., von Itzstein, M. & Taylor, G. (2004). Sialic acid recognition by *Vibrio cholerae* neuraminidase. *J Biol Chem* **279**, 40819–26.

Mouw, J. K., Ou, G. & Weaver, V. M. (2014). Extracellular matrix assembly: a multiscale deconstruction. *Nat Rev Mol Cell Biol* **15**, 771–785.

Muenzner, P., Dehio, C., Fujiwara, T., Meyer, T. F., Gray-owen, S. D. & Achtman, M. (2000). Carcinoembryonic Antigen Family Receptor Specificity of *Neisseria meningitidis* Opa Variants Influences Adherence to and Invasion of Proinflammatory. *Infect Immun* **68**, 3601–3607.

Muir, A., Soong, G., Sokol, S., Reddy, B., Gomez, M. I., van Heeckeren, A. & Prince, A. (2004). Toll-Like Receptors in Normal and Cystic Fibrosis Airway Epithelial Cells. *Am J Respir Cell Mol Biol* **30**, 777–783.

Müller, L., Brighton, L. E., Carson, J. L., Fischer, W. a & Jaspers, I. (2013). Culturing of human nasal epithelial cells at the air liquid interface. *J Vis Exp* 1–7.

Murphy, G. L. & Whitworth, L. C. (1993). Analysis of tandem, multiple genes encoding 30-kDa membrane proteins in *Pasteurella haemolytica* A1. *Gene* **129**, 107–111.

N'jai, A. U., Rivera, J., Atapattu, D. N., Owusu-Ofori, K. & Czuprynski, C. J. (2013). Gene expression profiling of bovine bronchial epithelial cells exposed in vitro to bovine herpesvirus 1 and *Mannheimia haemolytica*. *Vet Immunol Immunopathol* **155**, 182–9. Elsevier B.V.

Nabu, S., Lawung, R., Isarankura-Na-Ayudhya, P., Isarankura-Na-Ayudhya, C.,

Roytrakul, S. & Prachayasittikul, V. (2014). Reference map and comparative proteomic analysis of *Neisseria gonorrhoeae* displaying high resistance against spectinomycin. *J Med Microbiol* **63**, 371–85.

Nakatsuji, T., Shi, Y., Zhu, W., Huang, C.-P., Chen, Y.-R., Lee, D.-Y., Smith, J. W., Zouboulis, C. C., Gallo, R. L. & Huang, C.-M. (2008). Bioengineering a humanized acne microenvironment model: proteomics analysis of host responses to *Propionibacterium acnes* infection in vivo. *Proteomics* **8**, 3406–15.

Nardini, P. M., Mellors, A. & Lo, R. Y. C. (1998). Characterization of a fourth lipoprotein from *Pasteurella haemolytica* A1 and its homology to the OmpA family of outer membrane proteins. *FEMS Microbiol Lett* **165**, 71–77.

Nelson, A. L., Roche, A. M., Gould, J. M., Chim, K., Ratner, A. J. & Weiser, J. N. (2007). Capsule enhances pneumococcal colonization by limiting mucus-mediated clearance. *Infect Immun* **75**, 83–90.

Neugebauer, P., Endepols, H., Mickenhagen, A. & Walger, M. (2003). Ciliogenesis in submersion and suspension cultures of human nasal epithelial cells. *Eur Arch Otorhinolaryngol* **260**, 325–30.

Newsome, I. E. & Cross, F. (1932). Some bipolar organisms found in pneumonia of sheep. *J Am Vet Med Assoc* **80**, 711–719.

Niessen, C. M. (2007). Tight Junctions / Adherens Junctions : Basic Structure and Function. *J Invest Dermatol* 2525–2532.

Nikaido, H. (2003). Molecular Basis of Bacterial Outer Membrane Permeability Revisited. *Microbiol Mol Biol Rev* **67**, 593–656.

Noinaj, N., Guillier, M., Barnard, T. J. & Buchanan, S. K. (2010). TonB-dependent transporters: regulation, structure, and function. *Annu Rev Microbiol* **64**, 43–60.

Nomura, K., Obata, K., Keira, T., Miyata, R., Hirakawa, S., Takano, K., Kohno, T., Sawada, N., Himi, T. & Kojima, T. (2014). *Pseudomonas aeruginosa* elastase causes transient disruption of tight junctions and downregulation of PAR-2 in human nasal epithelial cells. *Respir Res* **15**, 21. Respiratory Research.

North, a J., Bardsley, W. G., Hyam, J., Bornslaeger, E. a, Cordingley, H. C., Trinnaman, B., Hatzfeld, M., Green, K. J., Magee, a I. & Garrod, D. R. (1999). Molecular map of the desmosomal plaque. *J Cell Sci* **112 (Pt 2**, 4325–4336.

Nossol, C., Diesing, a-K., Walk, N., Faber-Zuschratter, H., Hartig, R., Post, a, Kluess, J., Rothkötter, H.-J. & Kahlert, S. (2011). Air-liquid interface cultures enhance the oxygen supply and trigger the structural and functional differentiation of intestinal porcine epithelial cells (IPEC). *Histochem Cell Biol* **136**, 103–15.

Nummelin, H., Merckel, M. C., Leo, J. C., Lankinen, H., Skurnik, M. & Goldman, A. (2004). The *Yersinia* adhesin YadA collagen-binding domain structure is a novel left-handed parallel beta-roll. *EMBO J* **23**, 701–11.

Nyarko, K. a, Coomber, B. L., Mellors, A. & Gentry, P. a. (1998). Bovine platelet adhesion is enhanced by leukotoxin and sialoglycoprotease isolated from *Pasteurella haemolytica* A1 cultures. *Vet Microbiol* **61**, 81–91.

O'Brien, F. J., Harley, B. A., Yannas, I. V. & Gibson, L. J. (2005). The effect

of pore size on cell adhesion in collagen-GAG scaffolds. *Biomaterials* **26**, 433–441.

Odugbo, M. O., Odama, L. E., Umoh, J. U. & Makinde, a. a. (2003). Serotypes of *Pasteurella haemolytica* from pneumonic lungs of sheep in northern Nigeria. *Small Rumin Res* **48**, 239–243.

Ogasawara, Y., Golde, L. M. G. V. A. N. & Geuze, H. J. (1992). Immunocytochemical Localization of Surfactant Protein D (SPD) in Type I1 Cells , Clara Cells , and Alveolar Macrophages of Rat Lung. *J Histochem Cytochem* **40**, 1589–1597.

Ogunnariwo, J. A. & Schryvers, A. B. (1996). Rapid Identification and Cloning of Bacterial Transferrin and Lactoferrin Receptor Protein Genes. *J Bacteriol* **178**, 7326–7328.

Ogunnariwo, J. A. & Schryvers, A. B. (2001). Characterization of a Novel Transferrin Receptor in Bovine Strains of *Pasteurella multocida*. *J Bacteriol* **183**, 890 – 896.

Ogunnariwo, J. A., Woo, T. K. W., Lo, R. Y. C., Gonzalez, G. C. & Schryvers, A. B. (1997). Characterization of the *Pasteurella haemolytica* transferrin receptor genes and the recombinant receptor proteins. *Microb Pathog* **23**, 273–284.

Oliveira, M. J. R., Pereira, a. S., Guimaraes, L., Grande, N. R., Moreira de Sa, C. & Aguas, a. P. (2003). Zonation of Ciliated Cells on the Epithelium of the Rat Trachea. *Lung* **181**, 275–282.

Olsen, J. V, Ong, S.-E. & Mann, M. (2004). Trypsin cleaves exclusively C-terminal to arginine and lysine residues. *Mol Cell Proteomics* **3**, 608–14.

Omaleki, L., Barber, S. R., Allen, J. L. & Browning, G. F. (2010). *Mannheimia* species associated with ovine mastitis. *J Clin Microbiol* **48**, 3419–3422.

Omaleki, L., Browning, G. F., Allen, J. L. & Barber, S. R. (2012). Molecular epidemiology of *Mannheimia haemolytica* and *Mannheimia glucosida* associated with ovine mastitis. *J Vet Diagnostic Investig* **24**, 730–734.

Ostrowski, L. E., Andrews, K., Potdar, P., Matsuura, H., Jetten, a & Nettesheim, P. (1999). Cloning and characterization of KPL2, a novel gene induced during ciliogenesis of tracheal epithelial cells. *Am J Respir Cell Mol Biol* **20**, 675–83.

Ostrowski, L. E., Stewart, D. & Hazucha, M. (2012). Interferon γ stimulates accumulation of gas phase nitric oxide in differentiated cultures of normal and cystic fibrosis airway epithelial cells. *Lung* **190**, 563–71.

Othman, S., Parton, R. & Coote, J. (2012). Interaction between mammalian cells and *Pasteurella multocida* B:2. Adherence, invasion and intracellular survival. *Microb Pathog* **52**, 353–8. Elsevier Ltd.

Paizs, B. & Suhai, S. (2005). Fragmentation pathways of protonated peptides. *Mass Spectrom Rev* **24**, 508–48.

Palermo, L. M., Porotto, M., Yokoyama, C. C., Palmer, S. G., Mungall, B. a, Greengard, O., Niewiesk, S. & Moscona, A. (2009). Human parainfluenza virus infection of the airway epithelium: viral hemagglutinin-neuraminidase regulates fusion protein activation and modulates infectivity. *J Virol* **83**, 6900–8.

Palmer, E., Ono, B. I., Wilhelm, J. M., Ziegelhoffer, T., Nicolet, C., Craig, E.

A., Cristofano, A. Di, Jiao, M. S., Manova, K. & Salomoni, P. (2003). Role of a Highly Conserved Bacterial Protein in Outer Membrane Protein Assembly. *Science (80-)* **299**, 262–266.

Palomares, R. A., Walz, H. G. & Brock, K. V. (2013). Expression of type I interferon-induced antiviral state and pro-apoptosis markers during experimental infection with low or high virulence bovine viral diarrhea virus in beef calves. *Virus Res* **173**, 260–9. Elsevier B.V.

Pandher, K., Confer, a W. & Murphy, G. L. (1998). Genetic and immunologic analyses of PlpE, a lipoprotein important in complement-mediated killing of *Pasteurella haemolytica* serotype 1. *Infect Immun* **66**, 5613–9.

Pandher, K., Murphy, G. L. & Confer, a W. (1999). Identification of immunogenic, surface-exposed outer membrane proteins of *Pasteurella haemolytica* serotype 1. *Vet Microbiol* **65**, 215–26.

Papadioti, A., Markoutsa, S., Vranakis, I., Tselentis, Y., Karas, M., Psaroulaki, A. & Tsiotis, G. (2011). A proteomic approach to investigate the differential antigenic profile of two *Coxiella burnetii* strains. *J Proteomics* **74**, 1150–1159. Elsevier B.V.

Papayannopoulos, I. (1995). The Interpretation of Collision-Induced Dissociation Tandem Mass Spectra of Peptides. *Mass Spectrom Rev* **14**, 49–73.

Pappin, C., Hojrupt, P. & Bleasbyl, A. J. (1993). Rapid Identification of proteins by peptide-mass fingerprinting. *Cell* **3**, 327–332.

Paradis-Bleau, C., Markovski, M., Uehara, T., Lupoli, T. J., Walker, S., Kahne, D. E. & Bernhardt, T. G. (2010). Lipoprotein Cofactors Located in the Outer Membrane Activate Bacterial Cell Wall Polymerases. *Cell* **143**, 1110–1120. Elsevier Inc.

Pardo-Saganta, A., Law, B. M., Tata, P. R., Villoria, J., Saez, B., Mou, H., Zhao, R. & Rajagopal, J. (2015). Injury Induces Direct Lineage Segregation of Functionally Distinct Airway Basal Stem/Progenitor Cell Subpopulations. *Cell Stem Cell* **16**, 184–197. Elsevier Inc.

Parker, J., Sarlang, S., Thavagnanam, S., Williamson, G., O'donoghue, D., Villenave, R., Power, U., Shields, M., Heaney, L. & Skibinski, G. (2010). A 3-D well-differentiated model of pediatric bronchial epithelium demonstrates unstimulated morphological differences between asthmatic and nonasthmatic cells. *Pediatr Res* **67**, 17–22.

Parker, J. C., Thavagnanam, S., Skibinski, G., Lyons, J., Bell, J., Heaney, L. G. & Shields, M. D. (2013). Chronic IL9 and IL-13 Exposure Leads to an Altered Differentiation of Ciliated Cells in a Well-Differentiated Paediatric Bronchial Epithelial Cell Model. *PLoS One* **8**.

Patrick, D. M., Leone, A. K., Shellenberger, J. J., Dudowicz, K. a & King, J. M. (2006). Proinflammatory cytokines tumor necrosis factor-alpha and interferon-gamma modulate epithelial barrier function in Madin-Darby canine kidney cells through mitogen activated protein kinase signaling. *BMC Physiol* **6**, 2.

Patti, J. M., Allen, B. L., McGavin, M. J. & Höök, M. (1994). MSCRAMM-mediated adherence of microorganisms to host tissues. *Annu Rev Microbiol* **48**, 585–617.

Pautsch, a & Schulz, G. E. (2000). High-resolution structure of the OmpA membrane domain. *J Mol Biol* **298**, 273–82.

Pearson, J. P. & Brownlee, I. A. (2005). Structure and Function of Mucosal Surfaces. In *Colon Mucosal Surfaces*, pp. 6–10. Edited by J. Nataro, P. Cohen, H. Mobley & J. Weiser. ASM Press.

Peng, X., Xu, C., Ren, H., Lin, X., Wu, L. & Wang, S. (2005). Proteomic analysis of the sarcosine-insoluble outer membrane fraction of *Pseudomonas aeruginosa* responding to ampicilin, kanamycin, and tetracycline resistance. *J Proteome Res* **4**, 2257–2265.

Perez, A., Issler, A. C., Cotton, C. U., Kelley, T. J., Verkman, A. S. & Davis, P. B. (2007). CFTR inhibition mimics the cystic fibrosis inflammatory profile. *Am J Physiol Lung Cell Mol Physiol* **292**, L383–95.

Perez, J. C. & Groisman, E. A. (2009). Evolution of Transcriptional Regulatory Circuits in Bacteria. *Cell* **138**, 233–244.

Petecchia, L., Sabatini, F., Usai, C., Caci, E., Varesio, L. & Rossi, G. a. (2012). Cytokines induce tight junction disassembly in airway cells via an EGFR-dependent MAPK/ERK1/2-pathway. *Lab Investig* **92**, 1140–1148. Nature Publishing Group.

Petersen, A., Christensen, H., Kodjo, A., Weiser, G. C. & Bisgaard, M. (2009). Development of a multilocus sequence typing (MLST) scheme for *Mannheimia haemolytica* and assessment of the population structure of isolates obtained from cattle and sheep. *Infect Genet Evol* **9**, 626–32.

Pezeshki, S., Chimerel, C., Bessonov, A. N., Winterhalter, M. & Kleinekathöfer, U. (2009). Understanding ion conductance on a molecular level: an all-atom modeling of the bacterial porin OmpF. *Biophys J* **97**, 1898–906.

Pezzulo, A. a, Starner, T. D., Scheetz, T. E., Traver, G. L., Tilley, A. E., Harvey, B.-G., Crystal, R. G., McCray, P. B. & Zabner, J. (2011). The air-liquid interface and use of primary cell cultures are important to recapitulate the transcriptional profile of in vivo airway epithelia. *Am J Physiol Lung Cell Mol Physiol* **300**, L25–L31.

Pförtner, H., Wagner, J., Surmann, K., Hildebrandt, P., Ernst, S., Bernhardt, J., Schurmann, C., Gutjahr, M., Depke, M. & other authors. (2013). A proteomics workflow for quantitative and time-resolved analysis of adaptation reactions of internalized bacteria. *Methods* **61**, 244–50.

Pförtner, H., Burian, M. S., Michalik, S., Depke, M., Hildebrandt, P., Dhople, V. M., Pané-Farré, J., Hecker, M., Schmidt, F. & Völker, U. (2014). Activation of the alternative sigma factor SigB of *Staphylococcus aureus* following internalization by epithelial cells - an in vivo proteomics perspective. *Int J Med Microbiol* **304**, 177–87. Elsevier GmbH.

Phadke, N. D., Molloy, M. P., Steinhoff, S. a, Ulintz, P. J., Andrews, P. C. & Maddock, J. R. (2001). Analysis of the outer membrane proteome of *Caulobacter crescentus* by two-dimensional electrophoresis and mass spectrometry. *Proteomics* **1**, 705–20.

Pickles, R. J., Mccarty, D., Matsui, H., Hart, J., Randell, S. H., Boucher, R. C., Hart, D. J. & Carty, D. M. C. (1998). Limited Entry of Adenovirus Vectors into Well-Differentiated Airway Epithelium Is Responsible for Inefficient Gene Transfer. *Jounal Virol* **72**, 6014–6023.

Pimton, P., Lecht, S., Stabler, C. T., Johannes, G., Schulman, E. S. & Lelkes, P. I. (2015). Hypoxia enhances differentiation of mouse embryonic stem

cells into definitive endoderm and distal lung cells. *Stem Cells Dev* **24**, 663–76.

Plummer, P. J., Plummer, C. L. & Still, K. M. (2012). *Chapter 7 - Diseases of the Respiratory System. Sheep Goat Med (Second Ed*, Second Edi. Elsevier.

Pohl, C., Hermanns, M. I., Uboldi, C., Bock, M., Fuchs, S., Dei-Anang, J., Mayer, E., Kehe, K., Kummer, W. & Kirkpatrick, C. J. (2009). Barrier functions and paracellular integrity in human cell culture models of the proximal respiratory unit. *Eur J Pharm Biopharm* **72**, 339–49. Elsevier B.V.

Porcheron, G., Garénaux, A., Proulx, J., Sabri, M. & Dozois, C. M. (2013). Iron, copper, zinc, and manganese transport and regulation in pathogenic Enterobacteria: correlations between strains, site of infection and the relative importance of the different metal transport systems for virulence. *Front Cell Infect Microbiol* **3**, 90.

Poritz, L. S., Garver, K. I., Tilberg, A. F. & Koltun, W. a. (2004). Tumor necrosis factor alpha disrupts tight junction assembly. *J Surg Res* **116**, 14–18.

Portolés, T., Pitarch, E., López, F. J., Hernández, F. & Niessen, W. M. a. (2011). Use of soft and hard ionization techniques for elucidation of unknown compounds by gas chromatography/time-of-flight mass spectrometry. *Rapid Commun mass Spectrom* **25**, 1589–99.

Potter, A. A., Schryvers, A. B., Ogunnariwo, J. A., Hutchins, W. A., Lo, R. Y. & Watts, T. (1999). Protective capacity of the *Pasteurella haemolytica* transferrin-binding proteins TbpA and TbpB in cattle. *Microb Pathog* **27**, 197–206.

Prashar, A., Bhatia, S., Tabatabaeiyazdi, Z., Duncan, C., Garduño, R. a, Tang, P., Low, D. E., Guyard, C. & Terebiznik, M. R. (2012). Mechanism of invasion of lung epithelial cells by filamentous *Legionella pneumophila*. *Cell Microbiol* **14**, 1632–55.

Prytherch, Z., Job, C., Marshall, H., Oreffo, V., Foster, M. & BéruBé, K. (2011). Tissue-Specific stem cell differentiation in an in vitro airway model. *Macromol Biosci* **11**, 1467–77.

Pujol, L., Euge, E., Nassif, X., Of, I., With, N. M. & Cells, E. (1997). Interactions of *Neisseria meningitidis* with a Polarised Monolayer of Epithelial cells. *Infect Immun* **65**, 4836–4842.

Pukatzki, S., Ma, A. T., Sturtevant, D., Krastins, B., Sarracino, D., Nelson, W. C., Heidelberg, J. F. & Mekalanos, J. J. (2006). Identification of a conserved bacterial protein secretion system in Vibrio cholerae using the Dictyostelium host model system. *Proc Natl Acad Sci U S A* **103**, 1528–33.

Pukatzki, S., Ma, A. T., Revel, A. T., Sturtevant, D. & Mekalanos, J. J. (2007). Type VI secretion system translocates a phage tail spike-like protein into target cells where it cross-links actin. *Proc Natl Acad Sci U S A* **104**, 15508–15513.

Purdy, C. W., Raleigh, R. H., Collins, J. K., Watts, J. L. & Straus, D. C. (1997). Serotyping and enzyme characterization of *Pasteurella haemolytica* and *Pasteurella multocida* isolates recovered from pneumonic lungs of stressed feeder calves. *Curr Microbiol* **34**, 244–9.

Purdy, C. W., Cooley, J. D. & Straus, D. C. (1998). Cross-Protection Studies with Three Serotypes of *Pasteurella haemolytica* in the Goat Model. *Curr*

Microbiol **36**, 207–211.

van Putten, J. P. M. & Paul, S. M. (1995). Binding of syndecan-like cell surface proteoglycan receptors is required for *Neisseria gonorrhoeae* entry into human mucosal cells. *EMBO J* **14**, 2144–2154.

van Putten, J. P. M., Duensing, T. D. & Cole, R. L. (1998). Entry of OpaA þ gonococci into HEp-2 cells requires concerted action of glycosaminoglycans , fibronectin and integrin receptors. *Mol Microbiol* **29**, 369–379.

Qiao, S., Luo, Q., Zhao, Y., Zhang, X. C. & Huang, Y. (2014). Structural basis for lipopolysaccharide insertion in the bacterial outer membrane. *Nature* **511**, 108–11.

Quintana, A. M., Landolt, G. a, Annis, K. M. & Hussey, G. S. (2011). Immunological characterization of the equine airway epithelium and of a primary equine airway epithelial cell culture model. *Vet Immunol Immunopathol* **140**, 226–36. Elsevier B.V.

Radi, Z. a., Register, K. B., Lee, E.-K., Kehrli, M. E., Brogden, K. a., Gallup, J. M. & Ackermann, M. R. (1999). In Situ Expression of Intercellular Adhesion Molecule-1 (ICAM-1) mRNA in Calves with Acute *Pasteurella haemolytica* Pneumonia. *Vet Pathol* **36**, 437–444.

Radics, J., Königsmaier, L. & Marlovits, T. C. (2014). Structure of a pathogenic type 3 secretion system in action. *Nat Struct Mol Biol* **21**, 82–7. Nature Publishing Group.

Radin, J. N., Grass, S. a, Meng, G., Cotter, S. E., Waksman, G. & St Geme, J. W. (2009). Structural basis for the differential binding affinities of the HsfBD1 and HsfBD2 domains in the *Haemophilus influenzae* Hsf adhesin. *J Bacteriol* **191**, 5068–75.

Raetz, C. R. H. & Whitfield, C. (2002). Lipopolysaccharide endotoxins. *Annu Rev Biochem* **71**, 635–700.

Randell, S. H., Walstad, D. I., Schwab, U., Grubb, B. R. & Yankaskas, J. R. (2001). Isolation and Culture of Airway Epithelial Cells from Chronically Infected Human Lungs. *Vitr Cell Dev Biol* **37**, 480–489.

Ransford, G. a, Fregien, N., Qiu, F., Dahl, G., Conner, G. E. & Salathe, M. (2009). Pannexin 1 contributes to ATP release in airway epithelia. *Am J Respir Cell Mol Biol* **41**, 525–34.

Raux, E., Schubert, H. L. & Warren, M. J. (2000). Biosynthesis of cobalamin (vitamin B 12): a bacterial. *Cell Mol Life Sci* **57**, 1880–1893.

Raymond, B. B. a, Jenkins, C., Seymour, L. M., Tacchi, J. L., Widjaja, M., Jarocki, V. M., Deutscher, A. T., Turnbull, L., Whitchurch, C. B. & other authors. (2015). Proteolytic processing of the cilium adhesin MHJ_0194 (P123J) in *Mycoplasma hyopneumoniae* generates a functionally diverse array of cleavage fragments that bind multiple host molecules. *Cell Microbiol* **17**, 425–44.

Raymond, V. W., Grisham, J. W. & Earp, H. S. (1990). Charcterisation of Epidermal Growth Factor Receptor Induction by Retinoic Acid in a Chemically Transformed Rat Liver Cell Line. *Cell Growth Differ* **1**, 393–399.

Rearick, J. I. & Jetten, a M. (1989). Effect of substratum and retinoids upon the mucosecretory differentiation of airway epithelial cells in vitro. *Environ Health Perspect* **80**, 229–37.

Reichow, S. L., Korotkov, K. V, Hol, W. G. J. & Gonen, T. (2010). Structure of the cholera toxin secretion channel in its closed state. *Nat Struct Mol Biol* **17**, 1226–32. Nature Publishing Group.

Reis e Sousa, C. (2004). Activation of dendritic cells: translating innate into adaptive immunity. *Curr Opin Immunol* **16**, 21–25.

Relman, D., Tuomanen, E., Falkow, S., Golenbock, D. T., Saukkonen, K. & Wrighp, S. D. (1990). Recognition of a Bacterial Adhesin by an Integrin : Macrophage CR3 (αMß2, CD1 lb / CD18) Binds Filamentous Hemagglutinin of Bordetella pertussis. *Cell* **61**, 1375–1382.

Ren, D., Nelson, K. L., Uchakin, P. N., Smith, A. L., Gu, X.-X. & Daines, D. a. (2012). Characterization of extended co-culture of non-typeable *Haemophilus influenzae* with primary human respiratory tissues. *Exp Biol Med* **237**, 540–7.

Renauld-monge, G., Cornette, J., Mielcarek, N., Menozzi, F. D. & Locht, C. (1996). Distinct Roles of the N-Terminal and C-Terminal Precursor Domains in the Biogenesis of the *Bordetella pertussis* Filamentous Hemagglutinin. *J Bacteriol* **178**, 1053–1060.

Reneer, D. V, Kearns, S. a, Yago, T., Sims, J., Cummings, R. D., McEver, R. P. & Carlyon, J. a. (2006). Characterization of a sialic acid- and P-selectin glycoprotein ligand-1-independent adhesin activity in the granulocytotropic bacterium *Anaplasma phagocytophilum*. *Cell Microbiol* **8**, 1972–84.

Retzer, M. D., Yu, R., Zhang, Y., Gonzalez, G. C. & Schryvers, A. B. (1998). Discrimination between apo and iron-loaded forms of transferrin by transferrin binding protein B and its N-terminal subfragment. *Microb Pathog* **25**, 175–180.

Reve-Johnson, L. (2001). Relationships between clinical and pathological signs of disease in calves infected with *Mannheimia* (*Pasteurella*) *haemolytka* type A1. *Vet Rec* **149**, 549–542.

Reynolds, S. D. & Malkinson, A. M. (2010). Clara cell: progenitor for the bronchiolar epithelium. *Int J Biochem Cell Biol* **42**, 1–4.

Rhomberg, T. a., Karlberg, O., Mini, T., Zimny-Arndt, U., Wickenberg, U., Röttgen, M., Jungblut, P. R., Jenö, P., Andersson, S. G. E. & Dehio, C. (2004). Proteomic analysis of the sarcosine-insoluble outer membrane fraction of the bacterial pathogen *Bartonella henselae*. *Proteomics* **4**, 3021–3033.

Rice, J. a, Carrasco-Medina, L., Hodgins, D. C. & Shewen, P. E. (2007). *Mannheimia haemolytica* and bovine respiratory disease. *Anim Health Res Rev* **8**, 117–28.

Ristow, L. C., Bonde, M., Lin, Y.-P., Sato, H., Curtis, M., Wesley, E., Hahn, B. L., Fang, J., Wilcox, D. a & other authors. (2015). Integrin binding by *Borrelia burgdorferi* P66 facilitates dissemination but is not required for infectivity. *Cell Microbiol* **17**, 1021–36.

Robert, V., Volokhina, E. B., Senf, F., Bos, M. P., Gelder, P. Van & Tommassen, J. (2006). Assembly Factor Omp85 Recognizes Its Outer Membrane Protein Substrates by a Species-Specific C-Terminal Motif. *PLoS Biol* **4**.

Robinson, C. B. & Wu, R. (1993). Mucin Synthesis and Sectretion by Cultured Tracheal Cells: Effects of Collagen Gel Substartum Thickness. *In Vitr Cell*

Dev Biol **29**, 469–477.

Rock, J. R., Onaitis, M. W., Rawlins, E. L., Lu, Y., Clark, C. P., Xue, Y., Randell, S. H. & Hogan, B. L. M. (2009). Basal cells as stem cells of the mouse trachea and human airway epithelium. *Proc Natl Acad Sci U S A* **106**, 12771–5.

Rock, J. R., Randell, S. H. & Hogan, B. L. M. (2010). Airway basal stem cells: a perspective on their roles in epithelial homeostasis and remodeling. *Dis Model Mech* **3**, 545–56.

Rodriguez-Boulan, E. & Macara, I. G. (2014). Organization and execution of the epithelial polarity programme. *Nat Rev Mol Cell Biol* **15**, 225–242.

Roehrig, S. C., Tran, H. Q., Spehr, V., Gunkel, N., Selzer, P. M. & Ullrich, H. J. (2007). The response of *Mannheimia haemolytica* to iron limitation: implications for the acquisition of iron in the bovine lung. *Vet Microbiol* **121**, 316–29.

Roger, P., Puchelle, E., Bajolet-Laudinat, O., Tournier, J. M., Debordeaux, C., Plotkowski, M. C., Cohen, J. H., Sheppard, D. & de Bentzmann, S. (1999). Fibronectin and alpha5beta1 integrin mediate binding of *Pseudomonas aeruginosa* to repairing airway epithelium. *Eur Respir J* **13**, 1301–9.

Roggentin, P., Schauer, R., Lois, L. & Vimr, E. R. (1993). The sialidase superfamily and its spread by horizontal gene transfer. *Mol Microbiol* **9**, 915–921.

Ross, A. J., Dailey, L. a, Brighton, L. E. & Devlin, R. B. (2007). Transcriptional profiling of mucociliary differentiation in human airway epithelial cells. *Am J Respir Cell Mol Biol* **37**, 169–85.

Rossiter, A. E., Leyton, D. L., Tveen-Jensen, K., Browning, D. F., Sevastsyanovich, Y., Knowles, T. J., Nichols, K. B., Cunningham, A. F., Overduin, M. & other authors. (2011). The essential ß-barrel assembly machinery complex components BamD and BamA are required for autotransporter biogenesis. *J Bacteriol* **193**, 4250–3.

Rothen-Rutishauser, B. M., Kiama, S. G. & Gehr, P. (2005). A three-dimensional cellular model of the human respiratory tract to study the interaction with particles. *Am J Respir Cell Mol Biol* **32**, 281–9.

Rowe, H. a, Knox, D. P., Poxton, I. R. & Donachie, W. (1997). Divergent activity and function of superoxide dismutases in *Pasteurella haemolytica* serotypes A1 and A2 and *Pasteurella trehalosi serotype* T10. *FEMS Microbiol Lett* **150**, 197–202.

Ruiz-Gonzalez, C., Tenorio-Gutierrez, V., Trigo-Tavera, F., Reyes-Lopez, M., Leon-Sicairos, N., Godinez-Vargas, D. & Garza-Amaya, M. (2007). Characterization of Microvesicles of *Mannhemia hamemolytica* serotype A1 (Reference Strain and Serotype A2 (Field isolate). *J Anim Veterinanry Adv* **6**, 1172–1182.

Russell, D. H. & Edmondson, R. D. (1997). High-resolution Mass Spectrometry and Accurate Mass Measurements with Emphasis on the Characterization of Peptides and Proteins by Matrix-assisted Laser Desorption / Ionization Time-of-Fight Mass Spectrometry. *J mass Spectrom* **32**, 263–276.

Sachs, L. a, Finkbeiner, W. E. & Widdicombe, J. H. (2003). Effects of media on differentiation of cultured human tracheal epithelium. *In Vitro Cell Dev*

Biol Anim **39**, 56–62.

Sadygov, R. G., Cociorva, D. & Iii, J. R. Y. (2004). Large-scale database searching using tandem mass spectra : Looking up the answer in the back of the book. *Nat Methods* **1**, 195–202.

Sahly, H., Podschun, R., Oelschlaeger, T. a, Greiwe, M., Parolis, H., Hasty, D., Kekow, J., Ullmann, U., Ofek, I. & Sela, S. (2000). Capsule impedes adhesion to and invasion of epithelial cells by *Klebsiella pneumoniae*. *Infect Immun* **68**, 6744–6749.

Sajjan, U., Wang, Q., Zhao, Y., Gruenert, D. C. & Hershenson, M. B. (2008). Rhinovirus disrupts the barrier function of polarized airway epithelial cells. *Am J Respir Crit Care Med* **178**, 1271–81.

Salem, a. K., Stevens, R., Pearson, R. G., Davies, M. C., Tendler, S. J. B., Roberts, C. J., Williams, P. M. & Shakesheff, K. M. (2002). Interactions of 3T3 fibroblasts and endothelial cells with defined pore features. *J Biomed Mater Res* **61**, 212–217.

Satola, S. W., Napier, B. & Farley, M. M. (2008). Association of IS1016 with the hia adhesin gene and biotypes V and I in invasive nontypeable *Haemophilus influenzae*. *Infect Immun* **76**, 5221–7.

Schauer, K., Gouget, B., Carrière, M., Labigne, A. & de Reuse, H. (2007). Novel nickel transport mechanism across the bacterial outer membrane energized by the TonB/ExbB/ExbD machinery. *Mol Microbiol* **63**, 1054–1068.

Scheiffele, P., Peränen, J. & Simons, K. (1995). N-glycans as apical sorting signals in epithelial cells. *Nature* **378**, 96–98.

Schell, M. A., Zhao, P. & Wells, L. (2011). Outer Membrane Proteome of *Burkholderia pseudomallei* and Burkholderia mallei From Diverse Growth Conditions. *J Proteome Res* **10**, 2417–2424.

Scheller, E. V, Melvin, J. a, Sheets, A. J. & Cotter, P. a. (2015). Cooperative Roles for Fimbria and *Filamentous Hemagglutinin* in Bordetella Adherence and Immune Modulation. *MBio* **6**, 1–11.

van Schilfgaarde, M., Alphen, L. V. A. N., Eijk, P., Everts, V. & Dankert, J. (1995). Paracytosis of Haemophilus influenzae through Cell Layers of NCI-H292 Lung Epithelial Cells. *Infect Immun* **63**, 4729–4737.

Schindler, M. K. H., Schütz, M. S., Mühlenkamp, M. C., Rooijakkers, S. H. M., Hallström, T., Zipfel, P. F. & Autenrieth, I. B. (2012). *Yersinia enterocolitica* YadA mediates complement evasion by recruitment and inactivation of C3 products. *J Immunol* **189**, 4900–8.

Schirmer, T. & Phale, P. S. (1999). Brownian Dynamics Simulation of Ion Flow Through Porin Channels. *J Mol Biol* **294**, 1159–1167.

Schirmer, T., Keller, T. A., Wang, Y. & Rosenbusch, J. P. (1995). Structural Basis for Sugar Translocation Through Maltoporin Channels at 3 . 1 A Resolution. *Science (80-)* **267**, 1–3.

Schrager, H. M., Albertí, S., Cywes, C., Dougherty, G. J., Wessels, M. R., Stevens, D. & Kaplan, E. (1998). Hyaluronic Acid Capsule Modulates M Protein – mediated Adherence and Acts as a Ligand for Attachment of Group A Streptococcus to CD44 on Human Keratinocytes This study. *J Clin Invest* **101**, 1708–1716.

Schroth, M. K., Grimm, E., Frindt, P., Galagan, D. M., Konno, S. I., Love, R. &

Gern, J. E. (1999). Rhinovirus replication causes RANTES production in primary bronchial epithelial cells. *Am J Respir Cell Mol Biol* **20**, 1220–8.

Schuh, J. C., Bielefeldt Ohmann, H., Babiuk, L. a & Doige, C. E. (1992). Bovine herpesvirus-1-induced pharyngeal tonsil lesions in neonatal and weanling calves. *J Comp Pathol* **106**, 243–53.

Schulein, K. & Benz, R. (1990). LamB (maltoporin) of *Saimoneiia typhimurium*: isolation, purification and comparison of sugar binding with LamB of Escherichia coii. *Mol Microbiol* **4**, 625–632.

Schulze-Koops, H., Burkhardt, H., Heesemann, J., Kirsch, T., Swoboda, B., Bull, C., Goodman, S. & Emmrich, F. (1993). Outer membrane protein YadA of enteropathogenic yersiniae mediates specific binding to cellular but not plasma fibronectin. *Infect Immun* **61**, 2513–2519.

Schwab, U., Leigh, M., Ribeiro, C., Burns, K., Gilligan, P., Sokol, P., Boucher, R. & Yankaskas, J. (2002). Patterns of Epithelial Cell Invasion by Different Species of the *Burkholderia cepacia* Complex in Well-Differentiated Human Airway Epithelia. *Infect Immun* **70**, 4547–4555.

Schwerk, C., Papandreou, T., Schuhmann, D., Nickol, L., Borkowski, J., Steinmann, U., Quednau, N., Stump, C., Weiss, C. & other authors. (2012). Polar invasion and translocation of *Neisseria meningitidis* and *Streptococcus suis* in a novel human model of the blood-cerebrospinal fluid barrier. *PLoS One* **7**, e30069.

Seewaldt, V. L., Caldwell, L. E., Johnson, B. S., Swisshelm, K., Collins, S. J. & Tsai, S. (1997). Inhibition of retinoic acid receptor function in normal human mammary epithelial cells results in increased cellular proliferation and inhibits the formation of a polarized epithelium in vitro. *Exp Cell Res* **236**, 16–28.

Selkrig, J., Mosbahi, K., Webb, C. T., Belousoff, M. J., Perry, A. J., Wells, T. J., Morris, F., Leyton, D. L., Totsika, M. & other authors. (2012). Discovery of an archetypal protein transport system in bacterial outer membranes. *Nat Struct Mol Biol* **19**, 506–10, S1. Nature Publishing Group.

Selkrig, J., Belousoff, M. J., Headey, S. J., Heinz, E., Shiota, T., Shen, H.-H., Beckham, S. a, Bamert, R. S., Phan, M.-D. & other authors. (2015). Conserved features in TamA enable interaction with TamB to drive the activity of the translocation and assembly module. *Sci Rep* **5**, 12905. Nature Publishing Group.

Serikov, V. B., Choi, H., Schmiel, K., Skaggs, C., Fleming, N. W., Wu, R. & Widdicombe, J. H. (2004). Endotoxin induces leukocyte transmigration and changes in permeability of the airway epithelium via protein-kinase C and extracellular regulated kinase activation. *J Endotoxin Res* **10**, 55–65.

Serra, D. O., Conover, M. S., Arnal, L., Sloan, G. P., Rodriguez, M. E., Yantorno, O. M. & Deora, R. (2011). FHA-mediated cell-substrate and cell-cell adhesions are critical for *Bordetella pertussis* biofilm formation on abiotic surfaces and in the mouse nose and the trachea. *PLoS One* **6**, e28811.

Shakhnovich, E. A., King, S. J. & Weiser, J. N. (2002). Neuraminidase Expressed by Streptococcus pneumoniae Desialylates the Lipopolysaccharide of *Neisseria meningitidis* and *Haemophilus influenzae*: a Paradigm for Interbacterial Competition among Pathogens of the Human Respiratory

Tract. *Infect Immun* **70**, 7161–7164.

Shaykhiev, R., Zuo, W., Chao, I., Fukui, T., Witover, B., Brekman, A. & Crystal, R. G. (2013). EGF shifts human airway basal cell fate toward a smoking-associated airway epithelial phenotype. *Proc Natl Acad Sci* **110**, 12102–12107.

Sheng, Y., Abreu, I. a., Cabelli, D. E., Maroney, M. J., Miller, A. F., Teixeira, M. & Valentine, J. S. (2014). Superoxide dismutases and superoxide reductases. *Chem Rev* **114**, 3854–3918.

Sherry, A. E., Inglis, N. F., Stevenson, A., Fraser-Pitt, D., Everest, P., Smith, D. G. E. & Roberts, M. (2011). Characterisation of proteins extracted from the surface of *Salmonella Typhimurium* grown under SPI-2-inducing conditions by LC-ESI/MS/MS sequencing. *Proteomics* **11**, 361–370.

Shevchenko, A., Sunyaev, S., Loboda, A., Shevchenko, A., Bork, P., Ens, W. & Standing, K. G. (2001). Charting the Proteomes of Organisms with Unsequenced Genomes by MALDI-Quadrupole Time-of-Flight Mass Spectrometry and BLAST Homology Searching. *Anal Chem* **73**, 1917–1926.

Shevchenko, A., Tomas, H., Havlis, J., Olsen, J. V & Mann, M. (2006). In-gel digestion for mass spectrometric characterization of proteins and proteomes. *Nat Protoc* **1**, 2856–60.

Shevchuk, O., Batzilla, C., Hägele, S., Kusch, H., Engelmann, S., Hecker, M., Haas, A., Heuner, K., Glöckner, G. & Steinert, M. (2009). Proteomic analysis of *Legionella*-containing phagosomes isolated from Dictyostelium. *Int J Med Microbiol* **299**, 489–508.

Shewen, P. E., Lee, C. W., Perets, A., Hodgins, D. C., Baldwin, K. & Lo, R. Y. C. (2003). Efficacy of recombinant sialoglycoprotease in protection of cattle against pneumonic challenge with *Mannheimia* (*Pasteurella*) *haemolytica* A1. *Vaccine* **21**, 1901–1906.

Shi, H., Zhu, Y., Dong, X., Cai, H., Ma, L., Wang, S., Yan, H., Wang, X. & Xue, F. (2014). Pathogenesis of a genotype C strain of bovine parainfluenza virus type 3 infection in albino guinea pigs. *Virus Res* **188**, 1–7. Elsevier B.V.

Siegel, S. J. & Weiser, J. N. (2015). Mechanisms of Bacterial Colonization of the Respiratory Tract. *Annu Rev Microbiol* **69**, 425–444.

Singh, K., Ritchey, J. W. & Confer, a W. (2011). *Mannheimia haemolytica*: bacterial-host interactions in bovine pneumonia. *Vet Pathol* **48**, 338–48.

Singh, P. K., Parsek, M. R., Greenberg, E. P. & Welsh, M. J. (2002). A component of innate immunity prevents bacterial biofilm development. *Nature* **417**, 4–7.

Six, D. A. & Dennis, E. A. (2000). The expanding superfamily of phospholipase A 2 enzymes : classification and characterization. *Biochim Biophys Acta* **1488**, 1–19.

Sjölinder, H. & Jonsson, A.-B. (2010). Olfactory nerve--a novel invasion route of *Neisseria meningitidis* to reach the meninges. *PLoS One* **5**, e14034.

Sklar, J. G., Wu, T., Gronenberg, L. S., Malinverni, J. C., Kahne, D. & Silhavy, T. J. (2007). Lipoprotein SmpA is a component of the YaeT complex that assembles outer membrane proteins in *Escherichia coli*. *Proc Natl Acad Sci* **104**, 6400–6405.

Slanina, H., Hebling, S., Hauck, C. R. & Schubert-Unkmeir, A. (2012). Cell

invasion by *Neisseria meningitidis* requires a functional interplay between the focal adhesion kinase, Src and cortactin. *PLoS One* **7**, e39613.

Slocombe, R. F., Malark, J., Ingersoll, R., Derksen, F. J. & Rob-inson, N. E. (1985). Importance of neutrophils in the pathogenesis of acute pneumonic pasteurellosis in calves. *Am J Vet Res* **46**, 2253–2258.

Smith, G. R. (1961). The characteristics of two types of *Pasteurella haemolytica* associated with different pathological conditions of sheep. *J Pathol Bact* **81**, 431–440.

Sneath, P. H. A. & Stevens, M. (1990). Actinobacillus rossii sp. nov., Actinobacillus seminis sp nov. , noma rev., Pasteurella bettii sp. nov. , Pasteurella lymphangitidis sp. nova., Pasteurella mairi sp. nova, and Pasteurella trehalosi sp. nova. *Int J Syst Bacteriol* **40**, 148–153.

Song, W., Bajaj, H., Nasrallah, C., Jiang, H., Winterhalter, M., Colletier, J.-P. & Xu, Y. (2015). Understanding Voltage Gating of *Providencia stuartii* Porins at Atomic Level. *PLoS Comput Biol* **11**, e1004255.

Sow, F. B., Gallup, J. M., Krishnan, S., Patera, A. C., Suzich, J. & Ackermann, M. R. (2011). Respiratory syncytial virus infection is associated with an altered innate immunity and a heightened pro-inflammatory response in the lungs of preterm lambs. *Respir Res* **12**, 106.

Srikumaran, S., Kelling, C. L. & Ambagala, A. (2007). Immune evasion by pathogens of bovine respiratory disease complex. *Anim Health Res Rev* **8**, 215–29.

Stadnyk, A. W. (1994). Cytokine production by epithelial cells. *FASEB J* **8**, 1041–7.

Stanley, N. R. & Lazazzera, B. a. (2004). Environmental signals and regulatory pathways that influence biofilm formation. *Mol Microbiol* **52**, 917–24.

Stekhoven, D. J., Omasits, U., Quebatte, M., Dehio, C. & Ahrens, C. H. (2014). Proteome-wide identification of predominant subcellular protein localizations in a bacterial model organism. *J Proteomics* **99**, 123–37. Elsevier B.V.

Stewart, C. E., Torr, E. E., Mohd Jamili, N. H., Bosquillon, C. & Sayers, I. (2012). Evaluation of differentiated human bronchial epithelial cell culture systems for asthma research. *J Allergy* **2012**, 943982.

Stojiljkovic, I. & Srinivasan, N. (1997). Neisseria meningitidis tonB, exbB, and exbD Genes: Ton-Dependent Utilization of Protein-Bound Iron in Neisseriae. *J Bacteriol* **179**, 805–812.

Stolzenberg, E. D., Anderson, G. M., Ackermann, M. R., Whitlock, R. H. & Zasloff, M. (1997). Epithelial antibiotic induced in states of disease. *Proc Natl Acad Sci U S A* **94**, 8686–90.

Stork, M., Bos, M. P., Jongerius, I., de Kok, N., Schilders, I., Weynants, V. E., Poolman, J. T. & Tommassen, J. (2010). An outer membrane receptor of *Neisseria meningitidis* involved in zinc acquisition with vaccine potential. *PLoS Pathog* **6**, e1000969.

Strathdee, C. a & Lo, R. Y. (1989). Cloning, nucleotide sequence, and characterization of genes encoding the secretion function of the *Pasteurella haemolytica* leukotoxin determinant. *J Bacteriol* **171**, 916–928.

Straus, D. C. & Purdy, C. W. (1994). In Vivo Production of Neuraminidase by

Pasteurella haemolytica Al in Goats after Transthoracic Challenge. *Infect Immun* **62**, 4675–4678.

Straus, D. C., Jolley, W. L. & Purdy, C. W. (1993). Characterization of Neuraminidases Produced by Various Serotypes of *Pasteurella haemolytica*. *Infect Immun* **61**, 4669–4674.

Subramaniam, R., Shanthalingam, S., Bavananthasivam, J., Kugadas, A., Potter, K. a, Foreyt, W. J., Hodgins, D. C., Shewen, P. E., Barrington, G. M. & other authors. (2011). A multivalent *Mannheimia-Bibersteinia* vaccine protects bighorn sheep against *Mannheimia haemolytica* challenge. *Clin vaccine Immunol* **18**, 1689–94.

Sutherland, A. D., Donachie, W., Jones, G. E. & Quirie, M. (1989). A Crude Cytotoxin Vaccine Protects Sheep Against Experimental *Pasteurella haemolytica* Serotype A2 Infection. *Vet Microbiolgy* **19**, 175–181.

Sutherland, D. R., Abdullah, K. M., Cyopick, P. & Mellors, A. (1992). Cleavage of the cell-surface O-sialoglycoproteins CD34, CD43, CD44, and CD45 by a novel glycoprotease from *Pasteurella haemolytica*. *J Immunol* **148**, 1458–64.

Takeda, K., Miyatake, H., Yokota, N., Matsuyama, S., Tokuda, H. & Miki, K. (2003). Crystal structures of bacterial lipoprotein localization factors , LolA and LolB. *EMBO J* **22**, 3199–3209.

Talay, S. R., Zock, A., Rohde, M., Molinari, G., Oggioni, M., Pozzi, G., Guzman, C. A. & Chhatwal, G. S. (2000). Co-operative binding of human fibronectin to SfbI protein triggers streptococcal invasion into respiratory epithelial cells. *Cell Microbiol* **2**, 521–535.

Tanca, A., Biosa, G., Pagnozzi, D., Addis, M. F. & Uzzau, S. (2013). Comparison of detergent-based sample preparation workflows for LTQ-Orbitrap analysis of the *Escherichia coli* proteome. *Proteomics* **13**, 2597–607.

Tata, P. R., Mou, H., Pardo-Saganta, A., Zhao, R., Prabhu, M., Law, B. M., Vinarsky, V., Cho, J. L., Breton, S. & other authors. (2013). Dedifferentiation of committed epithelial cells into stem cells in vivo. *Nature* **503**, 218–23. Nature Publishing Group.

Taylor, K. R. & Gallo, R. L. (2006). Glycosaminoglycans and their proteoglycans: host-associated molecular patterns for initiation and modulation of inflammation. *FASEB J* **20**, 9–22.

Tertti, R., Skurnik, M., Vartio, T. & Kuusela, P. (1992). Adhesion Protein YadA of *Yersinia* Species Mediates Binding of Bacteria to Fibronectin. *Infect Immun* **60**, 3021–3024.

Thanabalasuriar, A., Koutsouris, A., Weflen, A., Mimee, M., Hecht, G. & Gruenheid, S. (2010). The bacterial virulence factor NleA is required for the disruption of intestinal tight junctions by enteropathogenic *Escherichia coli*. *Cell Microbiol* **12**, 31–41.

Thein, M., Sauer, G., Paramasivam, N., Grin, I. & Linke, D. (2010). Efficient subfractionation of gram-negative bacteria for proteomics studies. *J Proteome Res* **9**, 6135–6147.

Thompson, R. C. & Ohlssont, K. (1986). Isolation, properties , and complete amino acid sequence of human secretory leukocyte protease inhibitor , a potent inhibitor of leukocyte elastase. *Proc Natl Acad Sci* **83**, 6692–6696.

Thumbikat, P., Dileepan, T., Kannan, M. S. & Maheswaran, S. K. (2005). Mechanisms underlying *Mannheimia haemolytica* leukotoxin-induced oncosis and apoptosis of bovine alveolar macrophages. *Microb Pathog* **38**, 161–72.

Tikhonova, E. B., Dastidar, V., Rybenkov, V. V & Zgurskaya, H. I. (2009). Kinetic control of TolC recruitment by multidrug efflux complexes. *Proc Natl Acad Sci* **106**, 16416–16421.

Timpl, R. (1996). Macromolecular organization of basement membranes. *Curr Opin Cell Biol* **8**, 618–624.

Tomei, A. A., Choe, M. M. & Swartz, M. A. (2007). Effects of dynamic compression on lentiviral transduction in an in vitro airway wall model. *Am J Physiol Lung Cell Mol Physiol* **294**, 79–86.

Tomson, F. L., Viswanathan, V. K., Kanack, K. J., Kanteti, R. P., Straub, K. V, Menet, M., Kaper, J. B. & Hecht, G. (2005). Enteropathogenic *Escherichia coli* EspG disrupts microtubules and in conjunction with Orf3 enhances perturbation of the tight junction barrier. *Mol Microbiol* **56**, 447–64.

Del Tordello, E., Vacca, I., Ram, S., Rappuoli, R. & Serruto, D. (2014). *Neisseria meningitidis* NalP cleaves human complement C3, facilitating degradation of C3b and survival in human serum. *Proc Natl Acad Sci U S A* **111**, 427–32.

Toskala, E., Smiley-jewell, S. M., Wong, V. J., King, D., Plopper, C. G. & Temporal, C. G. P. (2005). Temporal and spatial distribution of ciliogenesis in the tracheobronchial airways of mice. *Am J Physiol Lung Cell Mol Physiol* **289**, 454–459.

Tournier, F., Laoukili, J., Giuliani, I., Gendron, M. C., Guennou, C. & Marano, F. (1998). Ciliated differentiation of rabbit tracheal epithelial cells in vitro. *Eur J Cell Biol* **77**, 205–13.

Travis, S. M., Conway, B. D., Zabner, J., Smith, J. J., Anderson, N. N., Singh, P. K., Greenberg, E. P. & Welsh, M. J. (1999). Activity of Abundant Antimicrobials of the Human Airway. *Am J Respir Cell Mol Biol* **20**, 872–879.

Tremblay, Y. D. N., Deslandes, V. & Jacques, M. (2013). *Actinobacillus pleuropneumoniae* genes expression in biofilms cultured under static conditions and in a drip-flow apparatus. *BMC Genomics* **14**, 364. BMC Genomics.

Tsai, K. S. & Thomson, R. G. (1975). Bovine parainfluenza type 3 virus infection: ultrastructural aspects of viral pathogenesis in the bovine respiratory tract. *Infect Immun* **11**, 783–803.

Turner, D. P. J., Wooldridge, K. G., Aldeen, D. A. A. A., Al, T. E. T. & Mmun, I. N. I. (2002). Autotransported Serine Protease A of *Neisseria meningitidis*: an Immunogenic , Surface-Exposed Outer Membrane , and Secreted Protein. *Infect Immun* **70**, 4447–4461.

Turner, J., Roger, J., Fitau, J., Combe, D., Giddings, J., Heeke, G. Van & Jones, C. E. (2011). Goblet cells are derived from a FOXJ1-expressing progenitor in a human airway epithelium. *Am J Respir Cell Mol Biol* **44**, 276–84.

Typas, A., Banzhaf, M., van den Berg van Saparoea, B., Verheul, J., Biboy, J., Nichols, R. J., Zietek, M., Beilharz, K., Kannenberg, K. & other authors. (2010). Regulation of Peptidoglycan Synthesis by Outer-Membrane Proteins. *Cell* **143**, 1097–1109. Elsevier Inc.

Uchiyama, S., Carlin, A. F., Khosravi, A., Weiman, S., Banerjee, A., Quach, D., Hightower, G., Mitchell, T. J., Doran, K. S. & Nizet, V. (2009). The surface-anchored NanA protein promotes pneumococcal brain endothelial cell invasion. *J Exp Med* **206**, 1845–52.

Van Ulsen, P., Van Alphen, L., Ten Hove, J., Fransen, F., Van Der Ley, P. & Tommassen, J. (2003). A Neisserial autotransporter NalP modulating the processing of other autotransporters. *Mol Microbiol* **50**, 1017–1030.

Ünal, C., Schwedhelm, K. F., Thiele, A., Weiwad, M., Schweimer, K., Frese, F., Fischer, G., Hacker, J., Faber, C. & Steinert, M. (2011). Collagen IV-derived peptide binds hydrophobic cavity of *Legionella pneumophila* Mip and interferes with bacterial epithelial transmigration. *Cell Microbiol* **13**, 1558–72.

Unkmeir, A., Latsch, K., Dietrich, G., Wintermeyer, E., Schinke, B., Schwender, S., Kim, K. S., Eigenthaler, M. & Frosch, M. (2002). Fibronectin mediates Opc-dependent internalization of *Neisseria meningitidis* in human brain microvascular endothelial cells. *Mol Microbiol* **46**, 933–946.

ur Rahman, S. & van Ulsen, P. (2013). System specificity of the TpsB transporters of coexpressed two-partner secretion systems of *Neisseria meningitidis*. *J Bacteriol* **195**, 788–97.

Ustiyan, V., Wert, S. E., Ikegami, M., Wang, I.-C., Kalin, T. V, Whitsett, J. a & Kalinichenko, V. V. (2012). Foxm1 transcription factor is critical for proliferation and differentiation of Clara cells during development of conducting airways. *Dev Biol* **370**, 198–212. Elsevier.

Van, P. T., Schmid, A. K., King, N. L., Kaur, A., Pan, M., Whitehead, K., Koide, T., Facciotti, M. T., Goo, Y. A. & other authors. (2008). *Halobacterium salinarum* NRC-1 PeptideAtlas: toward strategies for targeted proteomics and improved proteome coverage. *J Proteome Res* **7**, 3755–64.

Vandekerckhove, A., Glorieux, S., Broeck, W. Van Den, Gryspeerdt, A., van der Meulen, K. M. & Nauwynck, H. J. (2009). In vitro culture of equine respiratory mucosa explants. *Vet J* **181**, 280–7. Elsevier Ltd.

Veit, H. P. & Farrell, R. L. (1978). The Anatomy and Physiology of The Bovine Respiratory System Relating to Pulmonary Disease. *Cornell Vetenarian* **68**, 555–581.

Vélez Acevedo, R. N., Ronpirin, C., Kandler, J. L., Shafer, W. M. & Cornelissen, C. N. (2014). Identification of regulatory elements that control expression of the tbpBA operon in *Neisseria gonorrhoeae*. *J Bacteriol* **196**, 2762–74.

Verma, S., Sharma, M., Katoch, S., Verma, L., Kumar, S., Dogra, V., Chahota, R., Dhar, P. & Singh, G. (2013). Profiling of virulence associated genes of Pasteurella multocida isolated from cattle. *Vet Res Commun* **37**, 83–89.

Vieira, M. L., D'Atri, L. P., Schattner, M., Habarta, A. M., Barbosa, A. S., de Morais, Z. M., Vasconcellos, S. a, Abreu, P. a E., Gómez, R. M. & Nascimento, A. L. T. O. (2007). A novel leptospiral protein increases ICAM-1 and E-selectin expression in human umbilical vein endothelial cells. *FEMS Microbiol Lett* **276**, 172–80.

Vikström, E., Tafazoli, F. & Magnusson, K.-E. (2006). *Pseudomonas aeruginosa*

quorum sensing molecule N-(3 oxododecanoyl)-l-homoserine lactone disrupts epithelial barrier integrity of Caco-2 cells. *FEBS Lett* **580**, 6921–6928.

Vilela, C. L., Fitzpatrick, J. & Morgan, K. L. (2004). In vitro adherence and invasion of ovine mammary epithelium by *Mannheimia* (*Pasteurella*) *haemolytica*. *Vet J* **167**, 211–3.

Villenave, R., Touzelet, O., Thavagnanam, S., Sarlang, S., Parker, J., Skibinski, G., Heaney, L. G., McKaigue, J. P., Coyle, P. V & other authors. (2010). Cytopathogenesis of Sendai virus in well-differentiated primary pediatric bronchial epithelial cells. *J Virol* **84**, 11718–28.

Villenave, R., Thavagnanam, S., Sarlang, S., Parker, J., Douglas, I., Skibinski, G., Heaney, L. G., McKaigue, J. P., Coyle, P. V & other authors. (2012). In vitro modeling of respiratory syncytial virus infection of pediatric bronchial epithelium, the primary target of infection in vivo. *Proc Natl Acad Sci* **109**, 5040–5.

Virji, M. (2005). Bacterial Adherence and Tropism in the Human Respiratory Tract. In *Colon Mucosal Surfaces*, 1st edn., pp. 97–129. Edited by J. Nataro, P. Cohen, H. Mobley & J. Weiser.

Virji, M., Makepeace, K., David, J. P., Achtman, M. & Moxon, E. R. (1993). Meningococcal Opa and Opc proteins : their role in colonization and invasion of human epithelial and endothelial cells. *Mol Microbiol* **10**, 499–510.

Virji, M., Makepeace, K. & Moxon, E. R. (1994). Distinct mechanisms of interactions of Opc-expressing meningococci at apical and basoiateral surfaces of human endothelial celis ; the role of integrins in apical interactions. *Mol Microbiol* **14**, 173–184.

Vitreschak, A. G., Rodionov, D. A., Mironov, A. A. & Gelfand, M. S. (2003). Regulation of the vitamin B 12 metabolism and transport in bacteria by a conserved RNA structural element. *RNA* **9**, 1084–1097.

Vladar, E. K. & Stearns, T. (2007). Molecular characterization of centriole assembly in ciliated epithelial cells. *J Cell Biol* **178**, 31–42.

Vollmer, W., Joris, B., Charlier, P. & Foster, S. (2008). Bacterial peptidoglycan (murein) hydrolases. *FEMS Microbiol Rev* **32**, 259–286.

de Vries, F. P., van der Ende, A., van Putten, J. P. M. & Dankert, J. (1996). Invasion of Primary Nasopharyngeal Epithelial Cells by *Neisseria meningitidis* Is Controlled by Phase Variation of Multiple Surface Antigens. *Infect Immun* **64**, 2998–3006.

de Vries, F. P. De, Cole, R., Dankert, J., Frosch, M. & Putten, J. P. M. Van. (1998). *Neisseria meningitidis* producing the Opc adhesin binds epithelial cell proteoglycan receptors. *Mol Microbiol* **27**, 1203–1212.

Vunjak-Novakovic, G., Martin, I., Obradovic, B., Treppo, S., Grodzinsky, a. J., Langer, R. & Freed, L. E. (1999). Bioreactor cultivation conditions modulate the composition and mechanical properties of tissue-engineered cartilage. *J Orthop Res* **17**, 130–138.

Wakabayashi, Y., Chua, J., Larkin, J. M., Lippincott-Schwartz, J. & Arias, I. M. (2007). Four-dimensional imaging of filter-grown polarized epithelial cells. *Histochem Cell Biol* **127**, 463–72.

Wandersman, C. & Delepelaire, P. (1990). TolC , an *Escherichia coli* outer

membrane protein required for hemolysin secretion. *Proc Natl Acad Sci* **87**, 4776–4780.

Wang, C., Liu, Y., Li, H., Xu, W. J., Zhang, H. & Peng, X. X. (2012). Identification of plasma-responsive outer membrane proteins and their vaccine potential in *Edwardsiella tarda* using proteomic approach. *J Proteomics* **75**, 1263–1275. Elsevier B.V.

Wang, N., Butler, J. P. & Ingber, D. E. (1993). Mechanotransduction Across the Cell Surface and Through the Cytoskeleton. *Science (80-)* **260**, 1124–1127.

Ward, A. C. S. (1990). Isolation of Pasteurellaceae from Bovine Abortions. *J Vet Diagnostic Investig* **2**, 59–62.

Watson, E., Alberdi, M. P., Inglis, N. F., Lainson, A., Porter, M. E., Manson, E., Imrie, L., Mclean, K. & Smith, D. G. E. (2014). Proteomic analysis of *Lawsonia intracellularis* reveals expression of outer membrane proteins during infection. *Vet Microbiol* **174**, 448–455. Elsevier B.V.

Watson, J. K., Rulands, S., Wilkinson, A. C., Wuidart, A., Ousset, M., Van Keymeulen, A., Göttgens, B., Blanpain, C., Simons, B. D. & Rawlins, E. L. (2015). Clonal Dynamics Reveal Two Distinct Populations of Basal Cells in Slow-Turnover Airway Epithelium. *Cell Rep* **12**, 90–101.

Wells, T. J., Tree, J. J., Ulett, G. C. & Schembri, M. a. (2007). Autotransporter proteins: novel targets at the bacterial cell surface. *FEMS Microbiol Lett* **274**, 163–72.

Wheeler, R. (2009). Outer membrane proteomics of *Pasteurella multocida* isolates to identify putative host-specificity determinants. *Biosci Horizons* **2**, 1–12.

Whiteley, L. O., Maheswaran, S. K., Weiss, D. J. & Ames, T. R. (1990). Immunohistochemical localization of Pasteurella haemolytica A1-derived endotoxin, leukotoxin, and capsular polysaccharide in experimental bovine Pasteurella pneumonia. *Vet Pathol* **27**, 150–161.

Whitfield, C. & Trent, M. S. (2014). Biosynthesis and export of bacterial lipopolysaccharides. *Annu Rev Biochem* **83**, 99–128.

WHO. (2012). *Global Tuberculosis Report*.

Widdicombe, J. H. (2002). Regulation of the depth and composition of airway surface liquid. *J Anat* **201**, 313–8.

Wiedow, O., Schroder, J.-M., Young, J. A. & Christophers, E. (1990). Elafin : An Elastase-specific inhibitor of Human. *J Biol Chem* **266**, 14791–14795.

Williams, J. N., Skipp, P. J., Humphries, H. E., Christodoulides, M., O'Connor, C. D. & Heckels, J. E. (2007). Proteomic analysis of outer membranes and vesicles from wild-type serogroup B *Neisseria meningitidis* and a lipopolysaccharide-deficient mutant. *Infect Immun* **75**, 1364–72.

Wilm, M. (2011). Principles of Electrospray Ionization. *Mol Cell proteomics* **10**.

Wimley, W. C. (2003). The versatile ß-barrel membrane protein. *Curr Opin Struct Biol* **13**, 404–411.

Wu, H. C., Lai, J., Hayashi, S. & Giam, C. (1982). Biogenesis of Membrane Lipoproteins in Escherica Coli. *Biophys J* **37**, 307–314.

Wu, R., Sato, G. H. & Whitcutt, M. J. (1986). Developing differentiated epithelial cell cultures: airway epithelial cells. *Fundam Appl Toxicol* **6**, 580–

90.

Wu, R., Zhao, Y. H. & Chang, M. M. J. (1997). Growth and differentiation of conducting airway epithelial cells in culture. *Eur Respir J* **10**, 2398–2403.

Wu, R. & Smith, D. (1982). Continous Multiplication of Rabbit Tracheal Epithelial Cells in a Defined Hormone-Supplemented Medium. *In Vitro* **18**, 800–812.

Wu, Z., Sahin, O., Wang, F. & Zhang, Q. (2014). Proteomic identification of immunodominant membrane-related antigens in *Campylobacter jejuni* associated with sheep abortion. *J Proteomics* **99**, 111–22. Elsevier B.V.

Xu, C., Wang, S., Ren, H., Lin, X., Wu, L. & Peng, X. (2005). Proteomic analysis on the expression of outer membrane proteins of *Vibrio alginolyticus* at different sodium concentrations. *Proteomics* **5**, 3142–52.

Xu, C., Lin, X., Ren, H., Zhang, Y., Wang, S. & Peng, X. (2006). Analysis of outer membrane proteome of *Escherichia coli* related to resistance to ampicillin and tetracycline. *Proteomics* **6**, 462–473.

Xu, W., Janocha, A. J., Leahy, R. a, Klatte, R., Dudzinski, D., Mavrakis, L. a, Comhair, S. a a, Lauer, M. E., Cotton, C. U. & Erzurum, S. C. (2014). A novel method for pulmonary research: Assessment of bioenergetic function at the air-liquid interface. *Redox Biol* **2**, 513–9. Elsevier.

Xue, D., Ma, Y., Li, M., Li, Y., Luo, H., Liu, X. & Wang, Y. (2014). Mycoplasma ovipneumoniae induces inflammatory response in sheep airway epithelial cells via a MyD88-dependent TLR signaling pathway. *Vet Immunol Immunopathol*. Elsevier B.V.

Yamaya, M., Finkbeiner, W. E., Chun, S. Y. & Widdicombe, J. H. (1992). Differentiated structure and function of cultures from human tracheal epithelium. *Am J Physiol* **262**, 713–724.

Yang, H. (2012). Structure, Expression, and Function of ICAM-5. *Comp Funct Genomics* **2012**, 1–11.

Yang, L., Froio, R. M., Sciuto, T. E., Dvorak, A. M., Alon, R. & Luscinskas, F. W. (2005). ICAM-1 regulates neutrophil adhesion and transcellular migration of TNF-alpha-activated vascular endothelium under flow. *Blood* **106**, 584–592.

Yeaman, C., Le Gall, A. H., Baldwin, A. N., Monlauzeur, L., Le Bivic, A. & Rodriguez-Boulan, E. (1997). The O-glycosylated stalk domain is required for apical sorting of neurotrophin receptors in polarized MDCK cells. *J Cell Biol* **139**, 929–940.

Yeo, H., Yuan, Q., Beck, M. R., Baron, C. & Waksman, G. (2003). Structural and functional characterization of the VirB5 protein from the type IV secretion system encoded by the conjugative plasmid pKM101. *Proc Natl Acad Sci* **100**, 15947–15952.

Yeo, H.-J., Cotter, S. E., Laarmann, S., Juehne, T., St Geme, J. W. & Waksman, G. (2004). Structural basis for host recognition by the *Haemophilus influenzae* Hia autotransporter. *EMBO J* **23**, 1245–56.

Ying, T., Wang, H., Li, M., Wang, J., Wang, J., Shi, Z., Feng, E., Liu, X., Su, G. & other authors. (2005). Immunoproteomics of outer membrane proteins and extracellular proteins of *Shigella flexneri* 2a 2457T. *Proteomics* **5**, 4777–93.

Yoneyama, H. & Nakae, T. (1996). Protein C (OprC) of the outer membrane of *Pseudornonas aeruginosa* is a copper-regulated channel protein. *Microbiology* **142**, 2137–2144.

Yoon, J. H., Koo, J. S., Norford, D., Guzman, K., Gray, T. & Nettesheim, P. (1999). Lysozyme expression during metaplastic squamous differentiation of retinoic acid-deficient human tracheobronchial epithelial cells. *Am J Respir Cell Mol Biol* **20**, 573–81.

Yoon, J. H., Kim, K. S., Lee, J. G., Kim, S. S. & Park, I. Y. (2000). Secretory differentiation of serially passaged normal human nasal epithelial cells by retinoic acid: Expression of mucin and lysozyme. *Ann Otol Rhinol Laryngol* **109**, 594–601.

Yoon, J.-H., Gray, T., Karen, G., Koo, J. S. & Netteshiem, P. (1997). Regulation of the secretory phenotype of Human Airway Epithelium by retioic acid, triiodothyronine and Extracellular matrix. *Am J Respir Cell Mol Biol* **16**, 724–731.

Yoon, M. Y., Lee, K. M., Park, Y. & Yoon, S. S. (2011). Contribution of cell elongation to the biofilm formation of *Pseudomonas aeruginosa* during anaerobic respiration. *PLoS One* **6**, 1–11.

You, Y., Richer, E. J., Huang, T. A. O., Brody, S. L., Huang, T., Growth, S. L. B., Physiol, A. J., Cell, L., Physiol, M. & L, L. (2002). Growth and differentiation of mouse tracheal epithelial cells: selection of a proliferative population. *Am J Physiol Lung Cell Mol Physiol* **283**, 1315–1321.

You, Y., Huang, T., Richer, E. J., Schmidt, J. H., Zabner, J., Borok, Z. & Brody, S. L. (2004). Role of f-box factor foxj1 in differentiation of ciliated airway epithelial cells. *Am J Physiol Lung Cell Mol Physiol* **286**, 650–657.

Young, T. F., Thacker, E. L., Erickson, B. Z. & Ross, R. F. (2000). A tissue culture system to study respiratory ciliary epithelial adherence of selected swine mycoplasmas. *Vet Microbiol* **71**, 269–79.

Yu, F., Anaya, C. & Lewis, J. P. (2007). Outer membrane proteome of *Prevotella intermedia* 17: identification of thioredoxin and iron-repressible hemin uptake loci. *Proteomics* **7**, 403–12.

Yu, R. H., Gray-Owen, S. D., Ogunnariwo, J. & Schryvers, A. B. (1992). Interaction of ruminant transferrins with transferrin receptors in bovine isolates of *Pasteurella haemolytica* and *Haemophilus somnus*. *Infect Immun* **60**, 2992–4.

Zasloff, M. (2002). Antimicrobial peptides of multicellual organisms. *Nature* **415**, 389–395.

Zeltinger, J., Sherwood, J. K., Graham, D. A., Müeller, R. & Griffith, L. G. (2001). Effect of Pore Size and Void Fraction on Cellualr Adhesion , Proliferation , and Matrix Deposition. *Tissue Eng* **7**, 557–572.

Zemans, R. L., Briones, N., Campbell, M., McClendon, J., Young, S. K., Suzuki, T., Yang, I. V., De Langhe, S., Reynolds, S. D. & other authors. (2011). Neutrophil transmigration triggers repair of the lung epithelium via ß-catenin signaling. *Proc Natl Acad Sci* **108**, 15990–15995.

Zenobi, R. & Knochenmuss, R. (1999). Ion Formation in MALDI Mass Spectrometry. *Mass Spectrom Rev* **17**, 337–366.

Zhang, L., Zhang, C., Ojcius, D. M., Sun, D., Zhao, J., Lin, X., Li, L., Li, L. &

Yan, J. (2012a). The mammalian cell entry (Mce) protein of pathogenic *Leptospira* species is responsible for RGD motif-dependent infection of cells and animals. *Mol Microbiol* **83**, 1006–23.

Zhang, L., Wen, Y., Li, Y., Wei, X., Yan, X., Wen, X., Wu, R., Huang, X., Huang, Y. & other authors. (2014). Comparative proteomic analysis of the membrane proteins of two *Haemophilus parasuis* strains to identify proteins that may help in habitat adaptation and pathogenesis. *Proteome Sci* **12**, 38.

Zhang, Q., Li, Q., Wang, C., Li, N. & Li, J. (2012b). Redistribution of tight junction proteins during EPEC infection in vivo. *Inflammation* **35**, 23–32.

Zhang, W., Shao, J., Liu, G., Tang, F., Lu, Y., Zhai, Z., Wang, Y., Wu, Z., Yao, H. & Lu, C. (2011a). Immunoproteomic analysis of bacterial proteins of Actinobacillus pleuropneumoniae serotype 1. *Proteome Sci* **9**, 32.

Zhang, W., Case, S., Bowler, R. P., Martin, R. J., Jiang, D. & Chu, H. W. (2011b). Cigarette smoke modulates PGE(2) and host defence against *Moraxella catarrhalis* infection in human airway epithelial cells. *Respirology* **16**, 508–16.

Zhao, K.-Q., Xiong, G., Wilber, M., Cohen, N. a & Kreindler, J. L. (2012). A role for two-pore K^+ channels in modulating Na^+ absorption and Cl^- secretion in normal human bronchial epithelial cells. *Am J Physiol Lung Cell Mol Physiol* **302**, L4–L12.

Zheng, Z.-S., Polakowska, R., Johnson, A. & Goldsmith, L. A. (1992). Transcriptional Control of Epidermal Receptor by Retinoic Acid Growth Factor. *Cell Growth Differ* **3**, 225–232.

Zhou, L., Ying, W., Han, Y., Chen, M., Yan, Y., Li, L., Zhu, Z., Zheng, Z., Jia, W. & other authors. (2012). A proteome reference map and virulence factors analysis of *Yersinia pestis* 91001. *J Proteomics* **75**, 894–907.

Zimmermann, L., Peterhans, E. & Frey, J. (2010). RGD motif of lipoprotein T, involved in adhesion of *Mycoplasma conjunctivae* to lamb synovial tissue cells. *J Bacteriol* **192**, 3773–9.

Zückert, W. R. (2014). Secretion of Bacterial Lipoproteins : Through the Cytoplasmic Membrane , the Periplasm and Beyond. *Biochim Biophys Acta* **1843**, 1509–1516. Elsevier B.V.

Zulianello, L., Canard, C., Kohler, T., Caille, D., Lacroix, J.-S. & Meda, P. (2006). Rhamnolipids Are Virulence Factors That Promote Early Infiltration of Primary Human Airway Epithelia by *Pseudomonas aeruginosa*. *Infect Immun* **74**, 3134–3147.

Chapter 7 Appendicies

Table 7.1 Table of literature-based analysis of studies using ALI AEC culture and the parameters used during ALI culture

Reference	Media	Insert Manufacturer	Pore Size	Membrane material	Coating	Plate Size	Seeding Density[a] (cells/cm2)
(Goris *et al.*, 2008)	DMEM: F12	Greiner	0.4 µm	Not stated	Collagen	24	757576
(Li *et al.*, 2006)	BEGM:DMEM	Corning	Not stated	PTFE	Collagen	6	21413
(Stewart *et al.*, 2012)	BEGM:DMEM	Corning	0.4 µm	Polyester/PET	Not stated (uncoated*)	12	89285
(Abraham *et al.*, 2011)	DMEM:F12	Greiner	0.4 µm	Polyester/PET	Collagen	24	412121
(Bernacki *et al.*, 1999)	BEGM: DMEM	Corning	Not stated	PTFE	Collagen	Not Stated	175000
(Prytherch *et al.*, 2011)	BEGM:DMEM	Millipore	0.4 µm	Polyester/PET	Not stated	24	Not Stated
(Perez *et al.*, 2007)	DMEM:F12	Corning	Not stated	Polyester/PET	Collagen	6 and 12	1470588 / 892857
(Lam *et al.*, 2011)	AEGM:DMEM	Corning	0.4 µm	Polyester/PET	Not state	24	606061 / 303030
(Jakiela *et al.*, 2008)	BEGM:DMEM	Corning	0.4 µm	Polycarbonate	Collagen	12	130000
(Krunkosky *et al.*, 2007)	BEGM:DMEM	Corning	0.4 mm*	Not stated	Collagen	Not Stated	20000
(Bals *et al.*, 2004)	DMEM:F12	Corning	Not stated	Not stated	Collagen	12 and 6	4000000
(Wu *et al.*, 1986)	HAM F12	Home Made	Not stated	Polycarbonate / Nitrocellulose	Collagen	Petri dish	Not Stated
(Li *et al.*, 2006)	BEGM:DMEM	Corning	Not Stated	PTFE	Collagen	6	21413
(Schwab *et al.*, 2002)	LHC:DMEM	Corning	Not stated	Not stated	Collagen	Not Stated	1000000
(Zhang *et al.*, 2011b)	Not stated	Corning	Not stated	Polyester/PET	Collagen	12	35714
(Moreau-Marquis *et al.*, 2009)	Not stated	Corning	Not stated	Not stated	Not stated	6	214133
(Ren *et al.*, 2012)	BEGM	BD / Biocoat	3 µm	Not stated	Not stated	Petri dish	142857
(Linderholm *et al.*, 2010)	LHC:DMEM	Corning	Not stated	Not stated	Not stated	12	15000
(Young *et al.*, 2000)	DMEM:F12	Millipore	0.45 µm	Polypropylene	Collagen	24	437500
(Humlicek *et al.*, 2007)	DMEM:F12	Millipore	Not Stated	Polycarbonate	Collagen	24	500000
(Sajjan *et al.*, 2008)	BEGM:DMEM	Corning	Not Stated	Polyester/PET	Not stated	12	Not Stated
(Quintana *et al.*, 2011)	DMEM:F12	Corning	Not Stated	Not Stated	Collagen	Not Stated	Not Stated
(Mao *et al.*, 2009)	BEGM	Corning	Not Stated	PTFE	Collagen	24	151515

Reference	Media	Insert Manufacturer	Pore Size	Membrane material	Coating	Plate Size	Seeding Density[a] (cells/cm2)
(Pohl *et al.*, 2009)	AEGM / MEM	Corning	0.4 µm	Polycarbonate	Not stated	24	50000
(Yoon *et al.*, 1997)	BEGM:DMEM	Corning	Not Stated	Not stated	Collagen	Not Stated	Not Stated
(Wakabayashi *et al.*, 2007)	MEM	Corning	0.4 µm	Not stated	Not stated	12	20179
(Lin *et al.*, 2007)	BEGM/(F12:DMEM)	Corning	Not stated	Not stated	Not stated	12	223214
(Stewart *et al.*, 2012)	BEGM:DMEM	Corning	0.4 µm	Polyester/PET	Not stated	12	89286
(Matrosovich *et al.*, 2004)	BEGM:DMEM	Corning	0.4 µm	PTFE / PET	Not stated	6	20000
(Palermo *et al.*, 2009)	⌂	⌂	⌂	⌂	⌂	⌂	⌂
(Yamaya *et al.*, 1992)	DMEM:F 12	Millipore	0.45 µm	Mixed cellulose ester / PTFE	Not stated	24	1000000
(Villenave *et al.*, 2012)	AEGM	Corning	0.4 µm	PTFE	Not stated	12	Not Stated
(Didon *et al.*, 2013)	DMEM:F12	Corning	0.4 µm	Not stated	Collagen VI	Not Stated	600000
(Clark *et al.*, 1995)	DMEM:F12	Not stated	Not stated	Not stated	Collagen I	Not Stated	Not Stated
(Gray *et al.*, 1996)	BEGM:DMEM	Corning	0.45 µm	PET / PTFE	Not Stated	6	20000
(Chu *et al.*, 2004)	DMEM:F12	BD / Discovery	Not stated	Not stated	Collagen	12	35714
(Balder *et al.*, 2009)	BEGM:DMEM	Corning	Not stated	Not stated	Not stated	12 and 24	20000
(Hao *et al.*, 2012)	BEGM: (F12:DMEM)	Corning	0.4 µm	Not stated	Not stated	Not Stated	150000
(Fliegauf *et al.*, 2013)	DMEM: F12	Corning	0.4 µm	PET	Collagen	12	Not Stated
(Randell *et al.*, 2001)	BEGM	Corning	Not stated	PTFE	Collagen	12	36000
(Halldorsson *et al.*, 2010)	DMEM:F12	Corning	0.4 µm	Not stated	Not stated	12	Not Stated
(Ketterer *et al.*, 1999)	Widdicombe's Media	Millipore	0.45 µm	Not stated	Not stated	24	Not Stated
(Ostrowski *et al.*, 2012)	BEGM	Millipore	0.4 µm	Not stated	Not Stated	6	Not Stated
(Andrews *et al.*, 1996)	DMEM:F12	Corning	Not Stated	PTFE	Collagen	6	Not Stated
(Bateman *et al.*, 2015)	BEGM:DMEM	Corning	0.4 µm	Polyester/PET	Collagen IV	12	111607
(Brockman-Schneider *et al.*, 2014)	BEGM:DMEM	Corning	0.4 µm	Polycarbonate	Collagen	12	130000
(Button *et al.*, 2012)	LHC:DMEM	Corning	0.4 µm	Not stated	Not stated	12	250000
(Davidson *et al.*, 2000)	DMEM:F12	Corning	0.4 µm	Polyester/PET	Collagen	24	1200000
(Delgado-Ortega *et al.*, 2014)	DMEM:F12 & AEGM	Greiner	Not Stated	Not stated	Not stated	24	75758

Reference	Media	Insert Manufacturer	Pore Size	Membrane material	Coating[a]	Plate Size	Seeding Density[a] (cells/cm2)
(Dvorak *et al.*, 2011)	⌂	⌂	⌂	⌂	⌂	⌂	⌂
(Even-Tzur *et al.*, 2010)	BEGM	Millipore	Not stated	PTFE	Amniotic membrane / Collagen	6	156250
(Everett *et al.*, 2006)	LHC:DMEM	Corning	0.4 µm	PTFE	Not stated	12	178571
(Gray *et al.*, 2001)	BEGM:DMEM	Corning	0.4 µm	PET	Not stated	Not Stated	20000
(Gross *et al.*, 2010)	DMEM:F12	Corning	0.4 µm	Polyester / PET	Collagen	12	35714
(Guzman *et al.*, 1995)	DMEM:F12	Corning	Not stated	PTFE	Collagen	Not Stated	Not Stated
(Hackett *et al.*, 2011)	DMEM:F12	Corning	0.4 µm	Not stated	Collagen		600000
(Hirst *et al.*, 2010)	BEGM:DMEM	Corning	Not Stated	PET	Collagen	12	100000
(Huang *et al.*, 2010b)	DMEM:F12	Corning	Not stated	Chitosan	Collagen	6	32120
(Jain *et al.*, 2010)	DMEM:F12	Corning	0.4 µm	PET**	Collagen I	Not Stated	75000
(Kaartinen *et al.*, 1993)	DMEM:F12	Not stated	0.45 µm	Not stated	Collagen I, III	6**	10000
(Kameyama *et al.*, 2003)	DMEM:F12	Corning	0.4 µm	Polycarbonate	Not stated	24	6060606
(Kanoh *et al.*, 2001)	DMEM:F12	Not stated	0.4 µm	Polycarbonate	Not stated	Not Stated	250000
(Kim *et al.*, 2007b)	BEGM:DMEM	Corning	Not stated	Not stated	Not stated	6	21413
(Kirchhoff *et al.*, 2014)	DMEM: F12	Greiner	0.4 µm	Not stated	Not stated	24	757575
(Kolesnikova *et al.*, 2013)	BEGM:DMEM	Corning	0.4 µm	PTFE / PET	Not stated	6	20000
(Kondo *et al.*, 1993)	DMEM: F12	Corning	0.3 µm	Not stated	Collagen	6	250000
(Kondo *et al.*, 1997)	DMEM: F12	Corning	0.4 µm	Polycarbonate	Collagen	6	250000
(Koning *et al.*, 2012)	Δ	Δ	Δ	Δ	Δ	24	833333
(Koo *et al.*, 2002)	DMEM:F12	Corning	Not Stated	Not stated	Collagen	6	21413
(LeDizet *et al.*, 1998)	DMEM:F12	Not Stated	Not Stated	Not stated	Vitrogen & Collagen	12	1491071
(Liu *et al.*, 2007)	BEGM	Millipore	0.4 µm	Polycarbonate	Not stated	(0.6 cm^2)	416667
(Martin *et al.*, 1991)	HAM F12	Not stated	Not stated	Not stated	Collagen	Dish (35mm Ø)	5200
(Müller *et al.*, 2013)	PneumaCult™	Not stated	0.4 µm	Polyester/PET	Not stated	12	89925
(Nossol *et al.*, 2011)	DMEM:F12	Greiner	1 µm	Polyester/PET	Not stated	15mm diameter	Not Stated
(Ostrowski *et al.*, 1999)	DMEM:F12	Corning	Not stated	Not stated	Collagen	6	Not Stated

Reference	Media	Insert Manufacturer	Pore Size	Membrane material	Coating	Plate Size	Seeding Density[a] (cells/cm2)
(Ostrowski *et al.*, 2012)	DMEM:F12	Corning	Not stated	Not stated	Collagen	6	20000
(Parker *et al.*, 2013)	AEGM:DMEM	Corning	0.4 µm	Polyester/PET**	Collagen	12	71428
(Parker *et al.*, 2010)	AEGM:DMEM	Corning	0.4 µm	Polyester/PET	Collagen	12	71428
(Pickles *et al.*, 1998)	LHC:DMEM	Corning	0.4 µm	PTFE	Not Stated	6	42827
(Ransford *et al.*, 2009)	BEGM: DMEM	Corning	Not stated	Polyester/PET	Not stated	12	175000
(Ross *et al.*, 2007)	BEGM	Corning	0.4 µm	Polyester/PET	Vitrogen	12	89286
(Rothan-Rutishauser et al., 2005)	RPMI 1640	BD / Falcon	3 µm	Polyester/PET	Not stated	6	119047
(Sachs *et al.*, 2003)	DMEM:F12	Corning	Not stated	Polycarbonate	Not stated	12	1000000
(Shaykhiev *et al.*, 2013)	DMEM:F12	Corning	0.4 µm	Not stated	Collagen	Not Stated	600000
(Tomei *et al.*, 2007)	BEGM: DMEM	In-house	In-house	In-house	Collagen I	N/A	250000
(Tournier *et al.*, 1998)	DMEM:F12	Millipore	Not stated	Not stated	Collagen I	Not Stated	75000
(Turner *et al.*, 2011)	BEGM:DMEM	Corning	0.4 µm	Not stated	Not stated	12	73660
(Kettle *et al.*, 2010)	BEGM:DMEM	Corning	Not stated	Not stated	Not stated	12	73660
(Villenave *et al.*, 2010)	AEGM	Corning	Not stated	PTFE	Collagen	12	89285
(Xu *et al.*, 2014)	DMEM:F12	Fisherbrand	Not stated	Not Stated	Not stated	12	Not Stated
(Xue *et al.*, 2014)	Not stated	Millipore	0.4 µm	Polycarbonate / Polyester	Collagen	(0.6 cm^2)	166667
(You *et al.*, 2004)	DMEM:F12	Corning	0.4 µm	Polycarbonate / Polyester	Collagen	Not Stated	75000
(You *et al.*, 2002)	DMEM:F12	Corning	0.4 µm	Polycarbonate / Polyester	Collagen	Not Stated	75000
(Zhang *et al.*, 2012b)	LHC:DMEM	Corning	0.4 µm	PTFE	Collagen	12	Not Stated
(Zhao *et al.*, 2012)	BEGM:DMEM	Corning	0.4 µm	Polyester/PET	Not stated	24	242424

*Suspected miss-print.
**Inferred rather than explicitly stated
[a]cells/cm2 was calculated from parameters listed in the publications unless otherwise stated in cells/cm2.
ΔEpiairway™system
⌂MucilAir™system (Epithelix)

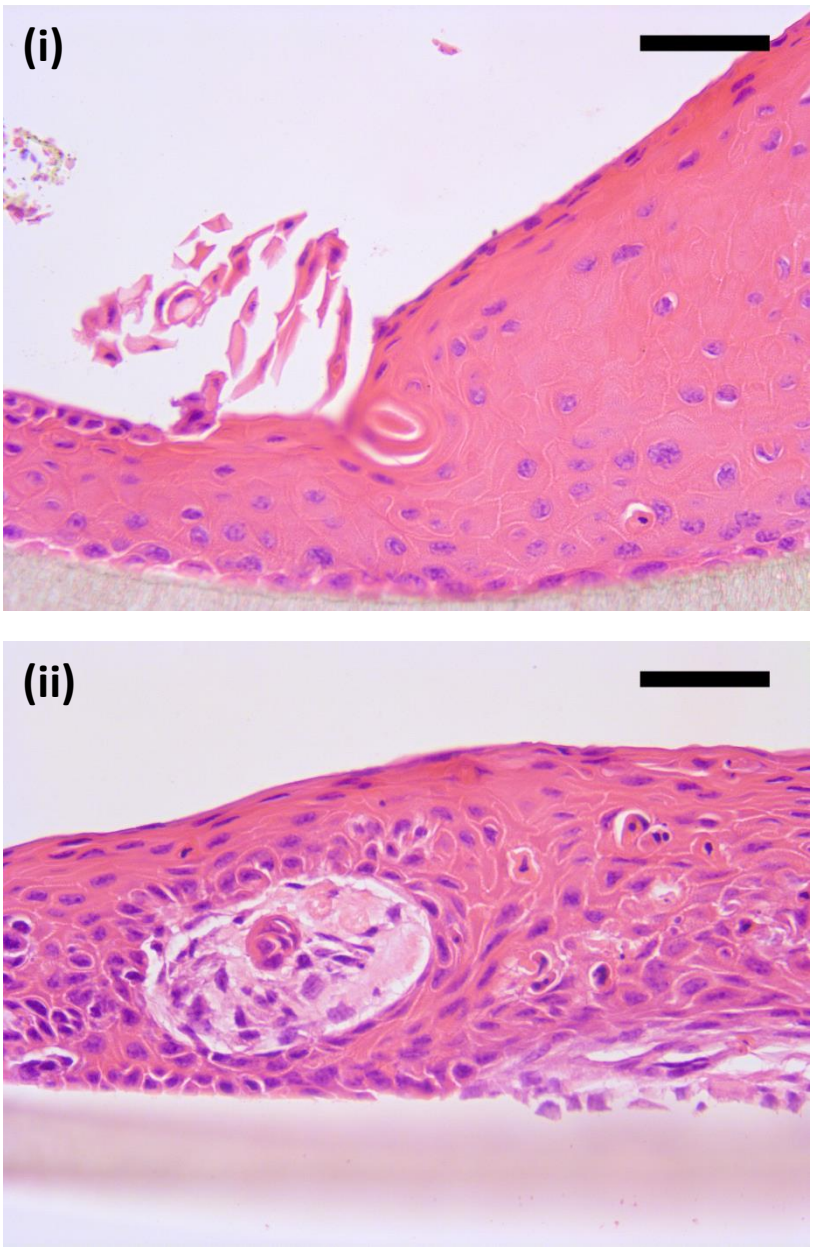

Fig 7.1 ALI epithelial cell cultures grown in the absence of either EGF or RA.
Image (i) shows a 14 day post-ALI culture grown without RA. Image (ii) shows a 14 day post-ALI culture grown without EGF. Scale bar represents 50µm.

Table 7.2 Gel-based peptide matches and EmPAI scores for the reference isolate PH202. Values are the maximum from redundant MASCOT matched proteins within a single replicate. EmPAI and peptide numbers were then averaged between the indivual values for each replicate.

		PH202			
		Gel Slice		Whole Lane Section	
Gi Number	Name	EmPAI #	Peptides #	EmPAI #	Peptides #
gi|493293655	Bam A / YaeT	1.17	68	0.6	42
gi|493291552	BamD / ComL	0	0	0.49	11
gi|261311737	Bor / Iss_1	0	0	0.3	5
gi|493293858	Bor / Iss_2	0	0	0.32	3
gi|224552355	CpxD	1.2	32	0.67	13
gi|261312441	FhaC	0.05	2	0	0
gi|525775788	fHbp_1	0.28	12	0.51	10
gi|493291535	FhuE			0.04	2
gi|493292841	FrpB	3.08	136	1.67	77
gi|757543197	HbpA	0.6	48	0.43	25
gi|493293182	Hly	0	0	0.53	7
gi|493292227	HmbR2	0.42	27	0.14	10
gi|493291030	HxuB / CcmD	0.26	18	0.15	7
gi|749034389	HxuC	0.04	3	0.24	9
gi|493294116	Hypothetical Protein 2	3.4	84	4.11	58
gi|493292739	IgA1_1	0	0	0.02	4
gi|528875644	IgA1_2	0	0	0.08	9
gi|493294120	IgA1_3	0		0.03	7
gi|452085966	LamB	0.66	20	0.33	12
gi|493290743	LemA			0.59	10
gi|493292674	LpoA	0.17	7	0.19	8
gi|493291784	LppB	0.07	2	0.27	5
gi|493290356	LptD	0.39	20	0.22	13
gi|493290706	LptE / RlpB	0.4	7	0.24	4
gi|261311127	Mam7 / PqiB	0	0	0.03	3
gi|493291152	MltA	0.08	6	0	0
gi|493294648	MltB	0.08	3	0	0
gi|493293125	MltC	0.26	12	0.19	6
gi|493293267	NanH	0.12	9	0.15	7
gi|493291640	NlpC/P60	0.16	2	0	0
gi|589590796	NlpE	0.23	1	0	0
gi|493293971	OapA	0.07	4	0.07	3
gi|493292204	Omp 18/16	1.25	16	1.41	19
gi|261308954	Omp P1	1.27	54	1.7	52
gi|261310065	Omp P2 Like	2.89	72	3.37	70
gi|493292126	Omp P4	0.69	8	1.16	15
gi|493294930	OmpA	2.85	98	2.66	112
gi|493290729	OmpH	0.23	6	0	0
gi|493290329	PalA	1.73	66	1.54	34
gi|493290796	Pcp	1.29	8	1.29	15
gi|261308934	PilA	0.23	1	0	0
gi|493291432	PlpA	2.16	39	1.04	17
gi|61396521	PlpB	0.81	17	0.37	7
gi|294071	PlpC	0.23	9	0.23	6
gi|78098845	PlpE	0.86	29	0.4	10
gi|493292120	PotD / Lpp38	0	0	0.18	3
gi|493291782	Putative Lipoprotein 1	0.33	6	0.37	4
gi|493290543	Putative Omp 1	1.19	66	0.75	27
gi|493290756	Putative Omp 2	1.27	41	0.71	20
gi|493295535	Ssa1	0.79	65	0.74	61
gi|261309846	Tam A / YtfM	0	0	0.14	8
gi|61743089	TbpA	0.28	22	0.22	20
gi|61743088	TbpB	0.05	1	0.1	5
gi|493291409	TolC	2.05	101	1.7	47
gi|493294752	YadA-like	0	0	0.28	23
gi|493293041	YajG	0	0	0.54	6

Table 7.3 Gel-free proteomic EmPAI values for 74 matched OMPs

Values are the maximum value amongst redundant protein matches from each replicate. Replicate averages were taken for each bacterial isolate resulting in the EmPAI numbers below.

		Average EmPAI #							
Gi Number	Protein Name	PH2	PH8	PH202	PH278	PH292	PH296	PH344	PH588
gi|472258490	BamA/ YaeT	1.54	1.45	1.42	1.68	1.61	1.96	0.9	1.53
gi|472258736	BamD / ComL	0.9	0.77	1.38	1.04	0.92	0.84	0.56	0.18
gi|472258252	BamE	0	0	0	0.26	0.26	0	0	0
gi|472257997	Bor / Iss_2	0.63	0.49	0.5	0.5	0.52	0.88	0.68	0.93
gi|472258883	BtuB	0	0	0	0	0	0.22	0.21	0
gi|472259234	CcmD/ HxuB	0	0.14	0.18	0	0.26	0.06	0	0.08
gi|493293918	CirA domain containing protein	0.04	0	0	0	0.14	0.08	0.04	0
gi|472257917	FhaB	0	0.16	0	0.01	0.11	0	0.09	0
gi|472257918	FhaC / ShlB	0.21	0.25	0	0.15	0.3	0	0.16	0
gi|472258899	FhuA	0	0	0	0	0.16	0	0	0
gi|472258286	FhuE	0	0	0.05	0	0	0	0	0
gi|472259454	FrpB / FetA	0.24	0.24	1.5	0.47	1.1	0.78	0.21	0.28
gi|472259236	HbpA	0.05	0.23	0.22	0.22	0.23	0.24	0.09	0.27
gi|472257276	Hly	1.03	0.73	0.71	0.54	0.98	1.15	0.35	0.89
gi|472257384	HmbR2.1	0.13	0	0.22	0	0.04	0.05	0	0.05
gi|472259021	HmbR2.2	0	0	0	0	0	0	0.07	0
gi|472257086	Hsf	0	0.05	0	0	0	0.02	0	0
gi|525964212	HxuC	0	0.22	0.32	0.16	0.92	0.2	0	0.4
gi|472257682	hypothetical protein / NlpE	0.44	0.54	0.44	0.59	0.88	0.6	0.24	0.4
gi|472257232	Hypothetical protein 1	0.29	0.29	0.39	0.3	0.4	0.17	0.38	0.4
gi|472259029	Hypothetical protein 3	0	0	0	0	0.19	0	0.22	0
gi|472257912	Hypothetical protein 4	0	0	0	0	0	0.15	0	0
gi|261311542	IgA1_4	0	0	0	0	0	0	0.05	0
gi|472258914	IgA1-3	0	0.02	0.11	0.14	0	0.15	0	0.07
gi|472258914	IgA1-3 Like	0	0	0.22	0.3	0	0.35	0	0
gi|472257424	LamB	0	0	0.08	0.07	0	0	0	0.08
gi|472258478	LemA	0.24	0.17	0.19	0.54	0.52	0.31	0.19	0.62
gi|472258343	LolB	0	0.14	0.16	0	0.14	0	0.24	0.16
gi|472257273	LpoA	0.21	0.27	0.33	0.32	0.4	0.32	0	0.1
gi|472257142	LppB / NlpD	0.3	0.36	0.41	0.6	0.4	0.33	0.22	0.46
gi|472257731	LptD	0.33	0.39	0.66	0.88	0.4	0.59	0.28	0.54
gi|472258510	LptE / RlpB	0.87	1.25	0.82	1.48	1.46	1.84	1.76	0.57
gi|472257325	Mam7 / PqiB	0	0.12	0.08	0.09	0	0.04	0.07	0.08
gi|472258419	MltA	0.29	0	0.25	0.23	0.19	0	0.13	0.09
gi|472257942	MltB	0	0	0	0	0	0	0.13	0
gi|472259387	MltC	0.21	0.25	0.32	0.51	0.59	0.4	0.39	0.37
gi|472258277	NanH	0.31	0.56	0.41	0.79	0.37	0	0	0.23
gi|472257959	NlpC / P60	0	0	0.19	0	0	0	0	0.2
gi|472257163	OapA	0.16	0.12	0.1	0.16	0.13	0.23	0.12	0.21
gi|472258540	Omp P1	0.35	0.38	0.43	0.4	0.46	0.55	0	0.48
gi|472257001	Omp P2	0.6	0.37	0	0	0	0.26	0.17	0.43
gi|472258334	Omp P2-like	0.08	0.14	0.26	0.28	0.22	0.19	0.22	0.39
gi|472257701	Omp P6 / Pal	1.86	1.6	2.35	1.59	2.19	2.55	1.76	3.45
gi|472256940	OmpA	0.66	0.83	1.56	0.76	0.96	0.79	1.02	1.08
gi|472258491	OmpH	0.34	0.24	0.26	0.35	0.32	0.34	0.21	0.18
gi|472258662	OmpP4	2.28	2.03	1.11	1.53	0.95	2.56	1.15	1.51
gi|472257617	OmpW	0	0.14	0	0	0	0.35	0.14	0
gi|472257023	Pcp	0.5	0.22	0.39	0.32	0.24	0.24	0.25	0.41
gi|472258517	PilA	0	0	0	0	0	0	0	0.23
gi|472258802	PlpA	1.76	1.87	2.21	2.45	2.01	2.91	0.99	2.41
gi|472258801	PlpB	0.78	0.87	0.69	0.75	0.56	0.85	0	0.8
gi|472258800	PlpC	0.55	0.44	0.27	0.41	0.55	0.51	0.26	0.52
gi|472258068	PlpD	0.77	1.1	0	0	0	1.59	0.41	1.18
gi|472257531	PlpE	1.98	0.76	0.79	0.46	1.04	0.92	0	1.54
gi|472258667	PotD / Lpp38	0.46	0.62	0.68	0.64	0.43	1.29	0	1.56
gi|472257084	Putative Autotransporter Adhesin	0	0	0	0	0	0.06	0	0
gi|472257144	Putative Lipoprotein 1	0.19	0.19	0.2	0.2	0.21	0.21	0.19	0.22
gi|472256984	Putative Omp 2	0.09	0.12	0	0.09	0	0.29	0.09	0
gi|472259196	Putative Omp 3	0	0	0.09	0	0	0	0	0
gi|493293240	Putative Omp 4	0.19	0.19	0.2	0.2	0.21	0.21	0.19	0.22
gi|472256848	Putative Omp1	0.24	0.12	0.17	0.13	0.18	0.13	0.13	0.14
gi|472256863	RlpA	0	0.14	0.16	0	0	0	0	0.16
gi|472258673	Ssa1	1.88	0.89	0.75	0.27	0.74	1.39	1.28	1.23
gi|757542574	TadG-like	0	0	0.05	0	0	0	0	0
gi|472258140	TamA / YtfM	0.18	0.1	0.25	0.25	0.07	0.05	0	0.21

Table 7.3 Continued

Gi Number	Protein Name	Average EmPAI #							
		PH2	PH8	PH202	PH278	PH292	PH296	PH344	PH588
gi|472257461	TbpA	0.32	0.32	0.22	0.14	0.35	0.34	0.03	0.29
gi|472257460	TbpB	0.26	0.45	0.39	0	0.23	0.17	0	0.25
gi|472258822	TolC	0.31	0.24	0.44	0.44	0.43	0.25	0.24	0.27
gi|472259186	VacJ	0.63	0.4	0.14	0.48	0.51	0.78	0.27	0.49
gi|472256811	Wza	0.44	0.49	0.48	0.26	0.49	0.49	0.2	0.74
gi|472256991	WzzB	0	0	0	0	0	0.12	0	0
gi|472258161	Yad-A like	0	0	0.3	0.1	0.6	0	0	0
gi|472257680	YajG	0.81	0.9	1.16	0.81	1.37	1	0.45	0.88
gi|472257571	Ydcf domain containing protein	0.08	0.08	0.04	0.15	0.09	0.11	0	0

Table 7.4 Gel-free proteomic peptide matches for 74 matched OMPs
Values are the maximum value amongst redundant protein matches from each replicate. Replicate averages were taken for each bacterial isolate resulting in the peptide numbers below.

		Average Peptide #							
Gi Number	**Protein Name**	**PH2**	**PH8**	**PH202**	**PH278**	**PH292**	**PH296**	**PH344**	**PH588**
gi|472258490	BamA/ YaeT	68	66	56	73	71	83	37	60
gi|472258736	BamD / ComL	10	11	13	14	11	11	7	6
gi|472258252	BamE	0	0	0	2	2	0	0	0
gi|472257997	Bor / Iss_2	4	4	3	4	4	5	4	4
gi|472258883	BtuB	0	0	0	0	0	7	7	10
gi|472259234	CcmD/ HxuB	0	6	4	0	8	2	0	7
gi|493293918	CirA domain containing protein	8	0	0	0	6	6	2	0
gi|472257917	FhaB	0	27	0	19	24	0	14	10
gi|472257918	FhaC / ShlB	7	10	0	6	9	0	7	10
gi|472258899	FhuA	0	0	0	0	8	0	0	0
gi|472258286	FhuE	0	0	1	0	0	0	0	0
gi|472259454	FrpB / FetA	11	10	56	19	43	28	10	11
gi|472259236	HbpA	3	8	10	8	8	8	3	9
gi|472257276	Hly	10	8	6	5	7	10	2	5
gi|472257384	HmbR2.1	7	0	9	0	4	5	0	2
gi|472259021	HmbR2.2	0	0	0	0	0	0	7	10
gi|472257086	Hsf	0	8	0	0	0	8	0	0
gi|525964212	HxuC	0	11	9	9	10	9	0	19
gi|472257682	hypothetical protein / NlpE	3	4	3	3	4	4	2	2
gi|472257232	Hypothetical protein 1	6	5	4	6	5	5	5	5
gi|472259029	Hypothetical protein 3	0	0	0	0	4	0	1	0
gi|472257912	Hypothetical protein 4	0	0	0	0	0	5	0	0
gi|261311542	IgA1_4	0	0	0	0	0	0	3	3
gi|472258914	IgA1-3	0	5	12	14	0	17	0	8
gi|472258914	IgA1-3 Like	0	0	9	9	0	10	0	0
gi|472257424	LamB	0	0	3	1	0	0	0	0
gi|472258478	LemA	1	2	1	3	4	4	1	5
gi|472258343	LolB	0	2	2	0	2	0	2	3
gi|472257273	LpoA	9	9	8	10	13	8	0	6
gi|472257142	LppB / NlpD	6	9	9	12	9	7	7	8
gi|472257731	LptD	12	17	21	29	18	23	10	18
gi|472258510	LptE / RlpB	8	10	6	10	10	11	9	9
gi|472257325	Mam7 / PqiB	0	14	18	15	0	13	14	13
gi|472258419	MltA	5	0	4	4	4	0	3	3
gi|472257942	MltB	0	0	0	0	0	0	11	11
gi|472259387	MltC	6	9	10	12	13	8	7	8
gi|472258277	NanH	14	23	13	36	12	0	0	10
gi|472257959	NlpC / P60	0	0	1	0	0	0	0	2
gi|472257163	OapA	5	5	4	4	3	5	8	7
gi|472258540	Omp P1	19	21	17	18	24	25	0	26
gi|472257001	Omp P2	12	8	0	0	0	6	5	7
gi|472258334	Omp P2-like	4	5	7	5	6	7	6	9
gi|472257701	Omp P6 / Pal	58	89	77	94	85	122	34	96
gi|472256940	OmpA	54	45	73	55	56	49	68	56
gi|472258491	OmpH	4	3	5	4	6	4	4	4
gi|472258662	OmpP4	24	24	12	14	14	29	16	26
gi|472257617	OmpW	0	1	0	0	0	2	1	1
gi|472257023	Pcp	4	2	3	2	2	2	1	3
gi|472258517	PilA	0	0	0	0	0	0	0	0
gi|472258802	PlpA	48	62	58	66	62	84	14	58
gi|472258801	PlpB	9	9	8	8	8	7	0	9
gi|472258800	PlpC	11	9	5	7	10	10	3	8
gi|472258068	PlpD	10	14	0	0	0	18	6	12
gi|472257531	PlpE	29	12	13	7	18	16	0	19
gi|472258667	PotD / Lpp38	7	12	11	11	8	17	0	19
gi|472257084	Putative Autotransporter Adhesin	0	0	0	0	0	4	0	0
gi|472257144	Putative Lipoprotein 1	1	2	2	2	1	2	2	2
gi|472256984	Putative Omp 2	3	3	0	2	0	5	5	5
gi|472259196	Putative Omp 3	0	0	1	0	0	0	0	0
gi|493293240	Putative Omp 4	1	2	2	2	1	2	2	2
gi|472256848	Putative Omp1	7	5	6	5	7	3	4	7
gi|472256863	RlpA	0	3	2	0	0	0	0	4
gi|472258673	Ssa1	125	52	50	19	37	74	83	70
gi|757542574	TadG-like	0	0	2	0	0	0	0	0
gi|472258140	TamA / YtfM	7	5	7	7	3	2	0	9

Table 7.4 continued.

		Average Peptide #							
Gi Number	**Protein Name**	**PH2**	**PH8**	**PH202**	**PH278**	**PH292**	**PH296**	**PH344**	**PH588**
gi|472257461	TbpA	16	26	17	11	24	19	4	12
gi|472257460	TbpB	10	15	11	0	8	11	0	13
gi|472258822	TolC	7	7	9	10	7	5	6	5
gi|472259186	VacJ	6	4	3	5	5	7	3	6
gi|472256811	Wza	7	9	10	5	6	8	6	8
gi|472256991	WzzB	0	0	0	0	0	3	0	0
gi|472258161	Yad-A like	0	0	23	13	32	0	0	0
gi|472257680	YajG	7	8	9	8	10	9	6	7
gi|472257571	Ydcf domain containing protein	4	6	2	8	5	6	0	0